HANDBOOK OF POLYCARBONATE SCIENCE AND TECHNOLOGY

PLASTICS ENGINEERING

Founding Editor

Donald E. Hudgin

Professor
Clemson University
Clemson, South Carolina

1. Plastics Waste: Recovery of Economic Value, *Jacob Leidner*
2. Polyester Molding Compounds, *Robert Burns*
3. Carbon Black-Polymer Composites: The Physics of Electrically Conducting Composites, *edited by Enid Keil Sichel*
4. The Strength and Stiffness of Polymers, *edited by Anagnostis E. Zachariades and Roger S. Porter*
5. Selecting Thermoplastics for Engineering Applications, *Charles P. MacDermott*
6. Engineering with Rigid PVC: Processability and Applications, *edited by I. Luis Gomez*
7. Computer-Aided Design of Polymers and Composites, *D. H. Kaelble*
8. Engineering Thermoplastics: Properties and Applications, *edited by James M. Margolis*
9. Structural Foam: A Purchasing and Design Guide, *Bruce C. Wendle*
10. Plastics in Architecture: A Guide to Acrylic and Polycarbonate, *Ralph Montella*
11. Metal-Filled Polymers: Properties and Applications, *edited by Swapan K. Bhattacharya*
12. Plastics Technology Handbook, *Manas Chanda and Salil K. Roy*
13. Reaction Injection Molding Machinery and Processes, *F. Melvin Sweeney*
14. Practical Thermoforming: Principles and Applications, *John Florian*
15. Injection and Compression Molding Fundamentals, *edited by Avraam I. Isayev*
16. Polymer Mixing and Extrusion Technology, *Nicholas P. Cheremisinoff*
17. High Modulus Polymers: Approaches to Design and Development, *edited by Anagnostis E. Zachariades and Roger S. Porter*
18. Corrosion-Resistant Plastic Composites in Chemical Plant Design, *John H. Mallinson*
19. Handbook of Elastomers: New Developments and Technology, *edited by Anil K. Bhowmick and Howard L. Stephens*
20. Rubber Compounding: Principles, Materials, and Techniques, *Fred W. Barlow*

21. Thermoplastic Polymer Additives: Theory and Practice, *edited by John T. Lutz, Jr.*
22. Emulsion Polymer Technology, *Robert D. Athey, Jr.*
23. Mixing in Polymer Processing, *edited by Chris Rauwendaal*
24. Handbook of Polymer Synthesis, Parts A and B, *edited by Hans R. Kricheldorf*
25. Computational Modeling of Polymers, *edited by Jozef Bicerano*
26. Plastics Technology Handbook: Second Edition, Revised and Expanded, *Manas Chanda and Salil K. Roy*
27. Prediction of Polymer Properties, *Jozef Bicerano*
28. Ferroelectric Polymers: Chemistry, Physics, and Applications, *edited by Hari Singh Nalwa*
29. Degradable Polymers, Recycling, and Plastics Waste Management, *edited by Ann-Christine Albertsson and Samuel J. Huang*
30. Polymer Toughening, *edited by Charles B. Arends*
31. Handbook of Applied Polymer Processing Technology, *edited by Nicholas P. Cheremisinoff and Paul N. Cheremisinoff*
32. Diffusion in Polymers, *edited by P. Neogi*
33. Polymer Devolatilization, *edited by Ramon J. Albalak*
34. Anionic Polymerization: Principles and Practical Applications, *Henry L. Hsieh and Roderic P. Quirk*
35. Cationic Polymerizations: Mechanisms, Synthesis, and Applications, *edited by Krzysztof Matyjaszewski*
36. Polyimides: Fundamentals and Applications, *edited by Malay K. Ghosh and K. L. Mittal*
37. Thermoplastic Melt Rheology and Processing, *A. V. Shenoy and D. R. Saini*
38. Prediction of Polymer Properties: Second Edition, Revised and Expanded, *Jozef Bicerano*
39. Practical Thermoforming: Principles and Applications, Second Edition, Revised and Expanded, *John Florian*
40. Macromolecular Design of Polymeric Materials, *edited by Koichi Hatada, Tatsuki Kitayama, and Otto Vogl*
41. Handbook of Thermoplastics, *edited by Olagoke Olabisi*
42. Selecting Thermoplastics for Engineering Applications: Second Edition, Revised and Expanded, *Charles P. MacDermott and Aroon V. Shenoy*
43. Metallized Plastics: Fundamentals and Applications, *edited by K. L. Mittal*
44. Oligomer Technology and Applications, *Constantin V. Uglea*
45. Electrical and Optical Polymer Systems: Fundamentals, Methods, and Applications, *edited by Donald L. Wise, Gary E. Wnek, Debra J. Trantolo, Thomas M. Cooper, and Joseph D. Gresser*
46. Structure and Properties of Multiphase Polymeric Materials, *edited by Takeo Araki, Qui Tran-Cong, and Mitsuhiro Shibayama*
47. Plastics Technology Handbook: Third Edition, Revised and Expanded, *Manas Chanda and Salil K. Roy*
48. Handbook of Radical Vinyl Polymerization, *Munmaya K. Mishra and Yusuf Yagci*
49. Photonic Polymer Systems: Fundamentals, Methods, and Applications, *edited by Donald L. Wise, Gary E. Wnek, Debra J. Trantolo, Thomas M. Cooper, and Joseph D. Gresser*
50. Handbook of Polymer Testing: Physical Methods, *edited by Roger Brown*

51. Handbook of Polypropylene and Polypropylene Composites, *edited by Harutun G. Karian*
52. Polymer Blends and Alloys, *edited by Gabriel O. Shonaike and George P. Simon*
53. Star and Hyperbranched Polymers, *edited by Munmaya K. Mishra and Shiro Kobayashi*
54. Practical Extrusion Blow Molding, *edited by Samuel L. Belcher*
55. Polymer Viscoelasticity: Stress and Strain in Practice, *Evaristo Riande, Ricardo Díaz-Calleja, Catalina Salom, Margarit Prolongo, and Rosa Masegosa*
56. Handbook of Polycarbonate Science and Technology, *edited by Donald G. LeGrand and John T. Bendler*

Additional Volumes in Preparation

Handbook of Polyethylene: Structures, Properties, and Applications, *Andrew J. Peacock*

Handbook of Polyolefins, Second Edition, Revised and Expanded, *edited by Cornelia Vasile*

Supramolecular Polymers, *edited by Alberto Ciferri*

HANDBOOK OF POLYCARBONATE SCIENCE AND TECHNOLOGY

edited by

DONALD G. LEGRAND
General Electric Company
Schenectady, New York

JOHN T. BENDLER
South Dakota School of Mines and Technology
Rapid City, South Dakota

MARCEL DEKKER, INC. NEW YORK • BASEL

ISBN: 0-8247-9915-1

This book is printed on acid-free paper.

Headquarters
Marcel Dekker, Inc.
270 Madison Avenue, New York, NY 10016
tel: 212-696-9000; fax: 212-685-4540

Eastern Hemisphere Distribution
Marcel Dekker AG
Hutgasse 4, Postfach 812, CH-4001 Basel, Switzerland
tel: 41-61-261-8482; fax: 41-61-261-8896

World Wide Web
http://www.dekker.com

The publisher offers discounts on this book when ordered in bulk quantities. For more information, write to Special Sales/Professional Marketing at the headquarters address above.

Current printing (last digit):
10 9 8 7 6 5 4 3 2 1

PRINTED IN THE UNITED STATES OF AMERICA

To our wives, Kathryn and Julie, for their patience and understanding

Preface

The idea of producing a book on polycarbonates was inspired by three independent events. The first was an interview with Joe Hogan of GE Plastics that was published in *R&D* magazine; the second, a reference in the *R&D* article to one of the coeditors; and the last, a telephone call from Russell Dekker to propose editing such a book. A preliminary survey of the literature showed that considerable research on almost every aspect of polycarbonates had been carried out and that a large number of patents had been issued. As a result, the need became apparent for a book that addresses and summarizes both the methods of syntheses and the physical properties of polycarbonate resins, and that also illustrates current methods of fabrication and significant applications.

It has been almost 40 years since two—now classic and out-of-print—books were written on this subject. During this time, there has been progress in several different areas pertaining to the syntheses of the material. A significant amount of research has been carried out in an effort to understand polycarbonate properties utiizing novel experimental, theoretical, and modeling techniques, and much of this work has been discussed at technical meetings and published. Many new applications, formulations, and methods of fabrication have also been discovered and patented. The scope of the present book has been limited by a desire to cover in detail the topics that are the best understood, and that would likely be useful in future studies of properties and applications of polycarbonates.

The book begins with Chapter 1 on historical background. Chapter 2 describes various methods of syntheses, followed by Chapter 3 on molecular modeling. Chapter 4 describes NMR studies that have helped to elucidate some of the molecular motions that occur. Chapter 5 describes other polycarbonates such as the spirobis-indanes.

Chapters 6, 7, 8, and 9 deal with the physical properties of these materials. The focus is on mechanical, optical, thermal and rheological properties.

Chapters 10, 11, 12, and 13 address physical and chemical aging and degradation of polycarbonates. Crystallization is included in this section because it can be induced by long-term thermal aging or chemical degradation.

Chapters 14, 15, and 16 describe formulations of commercial products, fabrication methods, and secondary finishing operations.

Finally, Chapter 17 addresses more recent polycarbonate applications.

We wish to express our thanks to Russell Dekker, who approached us about writing this book, to Joe Hogan and Patricia Keenan for their support, and to Ray Naar, Niles Rosenquist, YeeGang Lin, Wie Pan, and many others who helped by reviewing the chapters. Of course, thanks are due the contributors to the book who made it a reality, to Connie Vanbockern who helped us with the typing, and to our production editor, Kathleen Baldonado, without whose perseverance the book would not have been completed.

Donald G. LeGrand
John T. Bendler

Contents

Contributors

Lorene Erb Baccaro, M.B.A. Commercial Technology, General Electric Plastics, Pittsfield, Massachusetts

John T. Bendler, Ph.D. Department of Chemistry and Chemical Engineering, South Dakota School of Mines and Technology, Rapid City, South Dakota

E. E. Bostick, Ph.D. Lexan Technology, General Electric Plastics, Mt. Vernon, Indiana

Michael C. Burrell, Ph.D. Corporate Research and Development, General Electric Company, Schenectady, New York

Herbert S.-I. Chao, Ph.D. Corporate Research and Development, General Electric Company, Schenectady, New York

James L. DeRudder, Ph.D. Lexan Technology, General Electric Plastics, Mt. Vernon, Indiana

Arnold Factor, Ph.D. Corporate Research and Development, General Electric Company, Schenectady, New York

Mary F. Garbauskas, Ph.D. Materials Characterization Technology, General Electric Silicones, Waterford, New York

Paul T. Inglefield, Ph.D. Carlson School of Chemistry, Clark University, Worcester, Massachusetts

Alan A. Jones, Ph.D. Carlson School of Chemistry, Clark University, Worcester, Massachusetts

Therese C. Jordan, Ph.D. Corporate Research and Development, General Electric Company, Schenectady, New York

Patricia Keenan Marketing Department, General Electric Plastics, Atlanta, Georgia

Joseph A. King Jr., Ph.D. Product Management and Capital Markets, General Electric Financial Assurance, Richmond, Virginia

Donald G. LeGrand, Ph.D. Corporate Research and Development, General Electric Company, Schenectady, New York

Gregory B. McKenna, Ph.D. Polymers Division, National Institute of Standards and Technology, Gaithersburg, Maryland

Paul A. O'Connell, Ph.D. Polymers Division, National Institute of Standards and Technology, Gaithersburg, Maryland

Andrew J. Poslinski, Ph.D. Engineering Mechanics Laboratory, Corporate Research and Development, General Electric Company, Schenectady, New York

William D. Richards, Ph.D. Polymer Materials Laboratory, Corporate Research and Development, General Electric Company, Schenectady, New York

John Schmidhauser, Ph.D.* Corporate Research and Development, General Electric Company, Schenectady, New York

Michael F. Shlesinger, Ph.D. Physical Sciences Division, Office of Naval Research, Arlington, Virginia

Allan R. Shultz, Ph.D. Department of Chemistry, Virginia Polytechnic Institute and State University, Blacksburg, Virginia

Paul D. Sybert, Ph.D. Advanced Lexan Platform Group, General Electric Plastics, Mt. Vernon, Indiana

* *Current affiliation:* Elf Atochem North America, King of Prussia, Pennsylvania.

1

Introduction and Historical Background

E. E. Bostick
General Electric Plastics, Mt. Vernon, Indiana

I. INTRODUCTION

The discovery, invention, and development of aromatic polycarbonates has closely followed and been stimulated by developments in aromatic polyesters such as polyethylene terephthalate [1–4]. As will be stated later, there was a span of 50 years between early published findings and the actual discovery of useful thermoplastic aromatic polycarbonates. There were many factors possible to account for the low level of activity such as lack of perceived need for high-temperature resistance in applications, shortage of suitable commercially feasible monomers, and absence of process technology to fabricate useful parts. As it turned out, all of these factors were converging when D. W. Fox and H. Schnell, who were working independently toward different goals, discovered the polycarbonate of bisphenol A and both recognized the unique properties of this most interesting polymer [4,5].

II. EARLY CHEMISTRY

A. Aliphatic Polyesters and Polycarbonates

Aliphatic polyesters were first published by Lourenco [6] in 1863. Reaction products from succinic acid and ethylene glycol were described. Thirty years later Vorlander [7] prepared polyesters from fumaric and maleic acid and ethylene glycol. Hofmann [8] prepared and introduced polymers from adipic acid or

methyl adipic acid and ethylene glycol or 1,2-propanediol in 1917 as substitutes for natural fats and waxes. The intended use gives an idea that these materials were low molecular weight and possessed no structural properties. These polyesters later found use in coatings and polyurethanes by O. Bayer [9] but have never found use as load-bearing materials.

Some years later, W. H. Carothers and his colleagues [10–12] conducted an extensive study on aliphatic and aliphatic aromatic polyesters. Polyesters of malonic acid, succinic acid, adipic acid, sebacic acid, maleic acid, fumaric acid, and phthalic acid were obtained when reacted with ethylene glycol, 1,3-propanediol, 1,6-hexanediol, and/or 1,10-decanediol. Most of these products were low-melting, viscous liquids or microcrystalline wax-like solids with melting points below 100°C.

This group also prepared so-called superpolyesters and superpolycarbonates that were film and fiber formers, but once again the melting points and thermal resistance were low. None of these polyesters or corollary polycarbonates has become a standalone, commercially significant thermoplastic.

B. Aromatic Polyesters and Polycarbonates

The earliest significant report of the synthesis of aromatic polycarbonates was by Einhorn [13] who reacted hydroquinone, resorcinol, and catechol with phosgene in pyridine solution to obtain linear polymers from hydroquinone and resorcinol and a cyclic carbonate from catechol. Hydroquinone yielded an insoluble crystalline powder that melted above 280°C. Resorcinol polycarbonate resin was an amorphous material that melted with decomposition at 190–200°C. Later, in 1902, Bischoff and Hedenstroem [14] reported the synthesis of these same polymers by transesterification with diphenyl carbonate.

Nothing was reported in connection with aromatic polycarbonates for the next 50 years.

Activity in aromatic acid aliphatic diol or polyol polyesters did proceed. The most significant report was that of the Whinfield and Dickinson invention of polyethylene terephthalate [3]. In fact, D. W. Fox [1] was looking for a more hydrolytically stable alternate to polyethylene terephthalate for use as a magnet wire insulation varnish when he discovered bisphenol A polycarbonate (BPA-PC). H. Schnell [15] reported a definite goal in achieving properties similar to polyethylene terephthalate while leading the research at Farben Fabricken Bayer. It is certainly interesting that they were actively conducting independent research in this field at the same time and discovered the same polymer. It is even more interesting that the unique and commercially valuable properties of this polymer have not been offset by any other feasible aromatic diol. The foundation of the polycarbonate engineering thermoplastic resin industry rests on BPA-PC.

III. BISPHENOL A CHEMISTRY AND DEVELOPMENT

Access to a high-quality purified monomer feedstock such as BPA has been and continues to be critical to the development and continued growth of polycarbonate resins as premier engineering thermoplastic resins of choice. Therefore, it is appropriate to briefly cover BPA research and commercial development during the same time frame. A. Baeyer [16] reported results of acid-catalyzed condensation of phenol with aldehydes and ketones in 1872. Later, in 1891, Dianin [17] condensed phenol with acetone to make BPA. Almost 60 years later, J. E. Janson [18] was granted a patent on the use of an ionizable sulfur compound as a promoter and accelerator with acid catalysis. This acceleration was very important during the commercialization of BPA.

BPA prepared for use in the manufacture of linear polycarbonates must be of highest purity to achieve the highest quality polycarbonate with respect to color and performance. In this connection, Kissinger and Wynn [19] have been allowed a process patent for fractional crystallization of crude BPA to yield a product of the highest purity without the use of water, organic solvents, extraction, or distillation. This innovation, along with acidic ion exchange resins in fixed or fluid beds, has advanced the commercial manufacture of BPA to a very accessible position.

IV. PROCESS HISTORY

A. Polymerization

The original discovery of BPA-PC was by transesterification of BPA monomer with diphenyl carbonate [4,5]. However, equipment limitations at that time prevented scale-up and commercialization of resin from melt processes. The first solvent system scaled up was pyridine as both solvent and acid acceptor in a system reaction of BPA with phosgene and a monofunctional phenol as molecular weight regulator [20]. Supply and economics of pyridine as a reaction solvent limited its growth.

Reaction of BPA, phosgene, and monohydric phenols in methylene chloride solution in contact with an aqueous solution of sodium hydroxide became the process of choice by one of the major producers early on [21]. Triethylamine was the catalyst of choice. An alternate process employing lime as the acid acceptor has been used extensively [22].

Processes for manufacture of BPA-PC resin have evolved and been modernized extensively during the past 35 years that significant production has been carried out. Both batch and continuous polymerization systems are now utilized. As it turns out, the original melt polymerization process is receiving attention and development facilitated by modern melt polymerization equipment and the

need to reduce or eliminate volatile organic chemical emission into the environment.

B. Polymer Recovery

The original solution polymerization processes yielded a resin solution of varying degrees of purity and quality. One of the first resin isolation processes was to simply add a nonsolvent until the polymer precipitated partially or entirely. Different purification schemes such as filtration through beds or columns of natural or synthetic zeolites, charcoal, activated carbons, silica gels, or other adsorbents have been used. Washing in plate columns or centrifuges has been extensively used in purification of polycarbonate resin solutions prior to nonsolvent precipitation, gelling and crushing, or steam precipitation. Resins are also recovered from these purified solutions by vacuum extrusion in devolatilizing extruders. All of these processes have one common goal—the attainment of a very pure water-white resin so as to receive maximum properties and performance from the resin.

V. PRODUCT COMMERCIALIZATION AND HISTORY

Polycarbonates derived from BPA and terminated with monofunctional phenols are essentially linear polymers. The properties that differentiate these thermoplastic resins are inherent toughness, transparency, broad temperature resistance, good electrical properties, high index of refraction, ease of colorability and compounding, and general structural properties suitable for engineering and durable goods applications. A very large, diverse, and important market has been developed for these materials. Every person on earth is affected by some or many applications of BPA-PC resins produced by several major firms on a global basis. Markets range from architectural to automotive, digital recording, electrical, electronic, and safety. The markets have been built in large part by replacing conventional wood, metal, glass, and other materials of less capability.

BPA polycarbonates are typical aromatic polyesters with respect to flame resistance. In order to enhance flame resistance early on, copolymers with tetrabromo BPA/BPA were introduced [23]. Although other more sophisticated systems have been discovered, these copolymers are still in use.

Although linear polymers of various molecular weights and with various monofunctional phenol end-groups predominate in the products offered to the marketplace, there are needs for resins with non-Newtonian, shear-dependent, viscoelastic flow properties. This is particularly true for extrusion and extrusion blow-molding processes.

Low-level copolymers with trifunctional and tetrafunctional monomers and BPA provide the desired flow characteristics. Incorporation of these monomers began over 30 years ago [24] and has evolved to meet product application needs, particularly in parts requiring extrusion blow molding, i.e., water bottles and large hollow shapes [25].

In order to achieve even higher levels of heat resistance, much work has been done to copolymerize difunctional aromatic carboxylic acids with BPA [26,27]. Increased heat resistance with retention of clarity and practical toughness has been obtained. Other approaches to include different structures of biphenols have been and are in development. Details of these activities are beyond the scope of this chapter and will be properly addressed elsewhere.

For a material development that many felt would not be commercially feasible in the early stages, BPA-PC has been extremely successful. From a very modest beginning of a market and capacity of less than 10 million pounds in 1960, steady growth has developed to more than 2.5 billion pounds of capacity and demand worldwide. Over the years many have estimated that the polycarbonate market is mature. On the contrary, there are major new opportunities appearing now with no valid evidence of a slowdown.

REFERENCES

1. W. F. Christopher and D. W. Fox, *Polycarbonates*, Reinhold, New York, 1962, pp. 2–4.
2. H. Schnell, *Chemistry and Physics of Polycarbonates*, Interscience, New York, 1964, p. 3.
3. J. R. Whinfield and J. T. Dickson, Br. Pat. 578,079 (1946); J. R. Whinfield, *Nature 158*, 930 (1946); *Endeavor 11*:29 (1952).
4. D. W. Fox (to General Electric Co.), Aust. Pat. 221,192 (1959).
5. Belg. Pat. 532,543 to Farbenfabricken Bayer AG (1954).
6. M. A. Lourenco, *Ann. Chem. Phys. 67*:257 (1863).
7. D. Vorlander, *Annählen 280*:167 (1894).
8. F. Hofmann (to I. G. Farbenindustrie A. G.), Ger. Pat. 318,222 (1917).
9. O. Bayer, et al. *Annählen 549*:286 (1941).
10. W. H. Carothers and J. A. Arvin, *J. Am. Chem. Soc. 51*:3560 (1929).
11. W. H. Carothers and J. W. Hill, *J. Am. Chem. Soc. 54*:1559, 1566, 1579 (1932).
12. W. H. Carothers and F. J. Vannatta, *J. Am. Chem. Soc. 52*:314 (1930).
13. A. Einhorn, *Annählen 300*:135 (1898).
14. C. A. Bischoff and A. V. Hedenstroem, *Berichte 35*:3431 (1902).
15. H. Schovell, *Ang. Chemi. 68*:633 (1956).
16. A. Baeyer, *Berichte 5*:25–26 (1872, ibid., 280–282).
17. Dianin, *Berichte 25*:344 (1892).
18. J. E. Jansen, U.S. Pat. 2,468,982 (1949).

19. G. M. Kissinger and Nicholas P. Wynn, U.S. Pat. 5,362,400 (1994).
20. D. W. Fox, U.S. Pat. 3,144,432 (August 11, 1964).
21. H. Schnell, Ludwig Bottenbruch, and Heinrich Krimm, U.S. Pat. 3,028,365 (April 3, 1962).
22. H. E. Munro, U.S. Pat. 3,290,409 (December 6, 1966).
23. J. K. S. Kim, U.S. Pat. 3,311,589 (August 1, 1967).
24. M. Kramer, Ger. Pat. (DOS) 1,595,762 (September 9, 1965).
25. T. J. Hoogeboom, U.S. Pat. 3,816,373 (June 11, 1974).
26. Chemische Werke Albert, Fr. Pat. 1,177,517 (June 25, 1957).
27. E. P. Goldberg, U.S. Pat. 3,031,331 (August 22, 1957).

2
Synthesis of Polycarbonates

Joseph A. King, Jr.
General Electric Financial Assurance, Richmond, Virginia

I. HISTORICAL EVOLUTION

The development of polycarbonate thermoplastic resins evolved as a subset of general polyester chemistry. Since Einhorn's initial solution preparation of resorcinol- and hydroquinone-derived polycarbonates in 1898 [1], research has focused on efficient resin preparation and material properties. This seminal synthetic work used phosgene in a pyridine solution. Einhorn's phosgene procedure was followed in 1902, by the development of a melt transesterification method. Using diphenyl carbonate (DPC) as a phosgene synthon, Bischoff and v. Hedenstroem produced the same materials obtained by Einhorn [2]. Due to the poor solubility of these early resins, the general difficulty in their manipulation (processing), and the limited methods of material characterization available, interest in aromatic polycarbonates waned.

By the early 1930s, interest in general polycarbonates was renewed. Carothers and van Natta demonstrated the preparation of low-melting, low molecular weight microcrystalline aliphatic polycarbonates using two synthetic approaches [3]: (a) transesterification of aliphatic dihydroxylic compounds with diethyl carbonate and (b) ring opening polymerization of cyclic carbonates of aliphatic dihydroxylic compounds. The transesterification work was extended by Peterson to make low-melting, high molecular weight films and fibers using 1,6-hexanediol and dibutyl carbonate [4]. By 1941, the first commercially viable polycarbonate was introduced by the Pittsburgh Plate Glass Company (PPG); this material was a liquid casting resin intended for use as a surface coating in fiber or optical applications. This crosslinkable resin—designated CR-39—is derived from the allyl ester of diethylene glycol carbonate; peroxide-initiated reaction produces a scratch-resistant, colorless (transparent) plastic.

The evolution of the field continued with the reexamination of the aromatic derivatives. Following in the footsteps of Whinfield and Dickson's work with aromatic polyesters in 1946 [5], Schnell et al. [6] prepared linear, high-melting, high molecular weight aromatic polycarbonates derived from 4,4′-dihydroxydiphenylalkane monomers in 1954. These aromatic polycarbonates could be prepared by either a two-phase interfacial method—a modified Schotten-Baumann reaction—or via a melt (monomers as solvent) transesterification process using diphenyl carbonate [7]. In contrast to the aliphatic polycarbonates, these aromatic polycarbonates were unique in that they could be made into transparent (colorless) structures exhibiting excellent long-term mechanical properties.

Prior to the Whinfield and Schnell disclosures, polyesters and polycarbonates were commonly believed to be either liquids or low-melting solids. However, major differences exist between these two types of materials. Whinfield's aromatic polyesters exhibited limited solubility in common organic solvents. They tended to crystallize, becoming translucent and brittle with a concomitant loss of mechanical properties. In contrast, the aromatic polycarbonate resins exhibited good solubility in organic solvents. Furthermore, the polycarbonates retained their amorphous internal structure, transparency, and long-term mechanical properties after molding.

The excellent properties of the aromatic polycarbonates—particularly for those derived from 2,2-bis(4-hydroxyphenyl)propane (bisphenol A or BPA)—precipitated a large amount of research into these materials. By 1959, Fox of the General Electric Company (GE) had initiated studies similar to those in progress at the Bayer AG laboratories in Uerdingen [8]. These concurrent efforts resulted in the commercialization of BPA-derived polycarbonate processes by Farbenfabriken Bayer AG (Uerdingen, Germany) in the fall of 1958, Mobay Chemical Company (New Martinsville, West Virginia; now Bayer America) in early 1960, and GE (Mt. Vernon, Indiana) by late 1960.

Due to the large number of concurrent research efforts oriented to commercialization of BPA-based amorphous polycarbonates, a number of technology infringement disputes arose. After protracted litigation, Farbenfabriken Bayer AG was awarded the initial U.S. patent on these materials [9]; their basic process claimed an interfacial method. Bayer AG's initial U.S. issue was followed shortly by GE's basic coverage of the melt transesterification process [10].

In the mid 1960s, GE reexamined and piloted both a DPC-based transesterification process and the phosgene-based interfacial method. This work led GE to abandon its initial homogeneous phosgene-pyridine "lime" process in favor of the interfacial technology. A similar pilot evaluation by Farbenfabriken Bayer AG indicated that the interfacial process produced better quality material than their current transesterification technology. By the 1970s, all commercial BPA polycarbonate homopolymer (BPA-PC) was produced via an interfacial technology.

The industrial predisposition toward the interfacial production of commercial BPA-PC persists today with three notable exceptions. Since the early 1980s, the Chinese government has operated a commercial transesterification (melt) process in Shanghai; their material suffers a number of the earlier melt process deficiencies, most notably poor resin color. The second is a new, high-technology transesterification process developed by GE Plastics Japan, a joint venture of the General Electric Company, Mitsui Petrochemical Industries, and Nagase. The GE Plastics Japan 35,000 ton/year capacity process went on-line in Chiba, Japan in the spring of 1993. The new melt process produces a virgin BPA polycarbonate resin with lower residual inorganic contaminant levels and inherently better melt stability than the traditional interfacial processes [11]. This new melt resin exhibits superior transparency and color (YI < 1) than the early melt materials while retaining all of the desirable BPA-PC mechanical properties. The third is a 150,000 ton/year melt plant in Cartagena, Spain run by G.E. Plastics. It went into operation in the spring of 1999. The Spain plant is based on the Chiba experience.

Given the long history and extensive work involved in the evolution of the field of polycarbonates, the purpose of this chapter is not to review all aspects of the properties, synthesis, and methods of characterization related to resin production. A number of excellent reviews already address these subjects. Most notably, the reader should be aware of the reviews by Schnell [12], Vernaleken [13], Fox [14], Lapp [15], Serini [16], Clagett and Shafer [17], and Freitag [18]. Although major efforts for polycarbonate copolymer production exist, only a few specific systems will be mentioned. The focus of the present section is to outline and critique a few of the synthetic trends in engineering thermoplastics related to aryl polycarbonates with particular emphasis on the BPA-PC homopolymer. Copolymer production generated by reactive blending, coextrusion, and/or compatibilizing materials (e.g., grafting) will not be discussed; a historical overview of commercial alloys and blends may be found in a recent work by Utracki [19].

II. COMMERCIAL POLYCARBONATE PRODUCTION

To date, only two commercial production methods have been demonstrated to produce high-quality resin and remain economically viable. These processes are the two-phase interfacial (phosgene) and the melt transesterification (DPC) processes mentioned previously. All other potentially useful methods are merely direct variations on or simple combinations of these two main procedures. The spin-off process technologies include (a) the simple oligomer approach (Asahi Chemical Industries Co. Ltd., Bayer AG., Daicel Chemical Industries Ltd., Idemitsu Petrochemical Co. Ltd., Nippon GE Plastics K.K., Mitsui Petrochemical Industries K.K., and Teijin Ltd.); (b) the "crystalline" oligomer approach (Asahi

Chemical Industries Co. Ltd., Daicel Chemical Industries Ltd., and Teijin Ltd.); and (c) the "cyclic oligomer" polymerization process (GE Plastics, Bayer AG/Miles Inc. or Bayer America). These newer oligomer approaches all require multiple condensation reaction stages in order to produce high molecular weight materials. This multistep polymerization requirement, coupled usually with an intermediate isolation step, makes these oligomeric processes inherently more expensive.

Although empirically well understood, both of the principal synthetic approaches and their process derivatives continue to be areas of active research. Much of the work is oriented towards computational modeling for process simulation. Toward this end, a number of studies have developed accurate mathematical derivations of the incremental kinetic expressions and process parameter dependencies in simplified model systems. The following summaries update the earlier reviews on these commercial processes [18,20].

A. Interfacial Technology

The basic process is outlined in Scheme 1. The BPA is initially introduced into the reactor in methylene chloride along with a monohydroxylic phenol (end-capper) to control the polymer molecular weight. Phosgene is added as a gas-liquid (bp 4°C) into this solution. Concomitant with the phosgene addition, aqueous sodium hydroxide (caustic) is added to scavenge the HCl produced; this aqueous caustic addition generates a two-phase liquid–liquid system. At high pH (9–12), low organic phase volume, and high BPA concentration, the system also contains a third (solid) phase consisting of the mono/dianion of BPA (pK_{a1} = 9.59; pK_{a2} = 10.2; 40°C) [21]. After reaction is complete, the organic phase is washed a number of times with aqueous acid and water to remove the residual base and salts. The polycarbonate resin is collected via solvent exchange (e.g., chlorobenzene) followed by evaporation of the solvent, by direct steam precipitation, or by its precipitation from antisolvent addition (e.g., MeOH), followed by filtration and drying.

Due to the low reaction temperature of this synthetic procedure (40°C), the average molecular weight of the polymer is the result of a kinetic distribution. This type of nonequilibrium distribution necessitates the final material to be completely passivated by end-capping (~100%) and melt-stabilized. These precautions are necessary to prevent a lowering of molecular weight as indicated by changes in gel permeation chromatography (GPC), melt flow index (MFI), and intrinsic viscosity (IV) on processing or extrusion; once in the neat, molten state, an unstabilized resin tends to redistribute itself towards a thermodynamic product.

Since the early work of Schnell [12], the mechanistic assumption has been that the reaction takes place at the liquid–liquid interface and involves the addi-

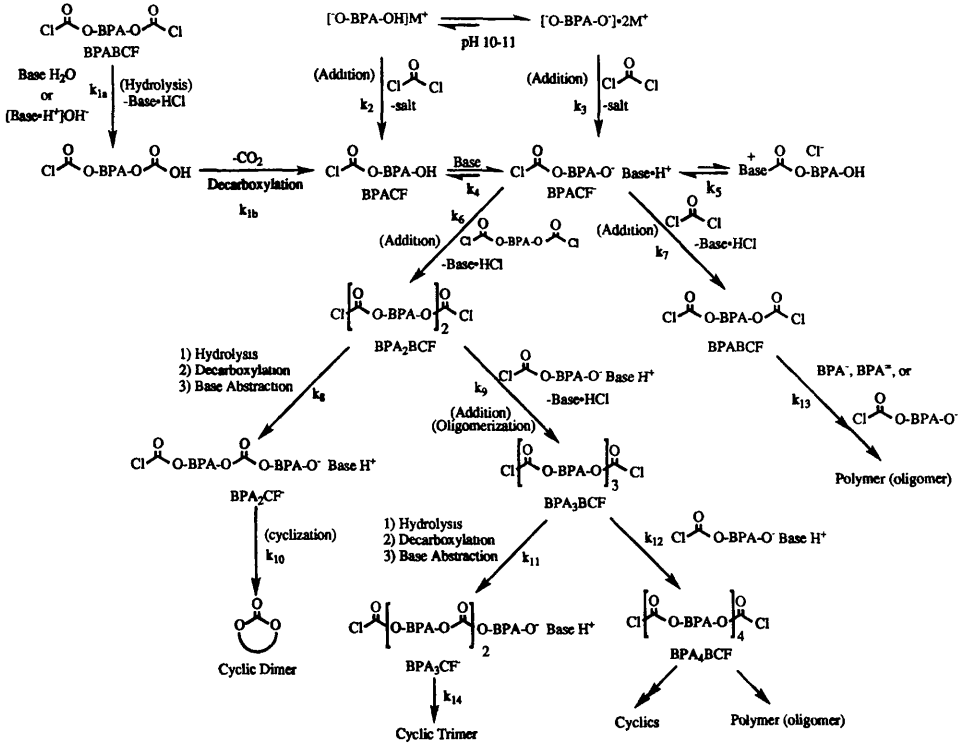

Scheme 1 General BPA polycarbonate (BPA-PC) formation steps in interfacial synthesis.

tion of BPA or its corresponding anion to an acylammonium species. Due to the complexity of this multiphase system, accurate experimental confirmation of the mechanism for each of the incremental steps is still wanting. Model systems and computer reaction simulations are currently attempting to confirm the dominant mechanistic contributions and pathways. King and Bryant [22,23] have prepared a variety of model acylammonium compounds in order to facilitate study of the putative condensation reaction steps. Their analysis of the triethylammonium carbophenoxy model salt indicates it to be quite stable. Its x-ray data indicate the carbonyl moiety to be sterically unencumbered, i.e., open toward nucleophilic addition, and of normal bond length (1.180 Å) compared to either BPA bischloroformate (1.177 Å) or phosgene (1.180 Å). These putative condensation reaction intermediates also contribute to the unwanted carbamate end-group formation. Modeling of this carbamate side reaction indicates it to follow first-order reaction

kinetics based on the intermediate acylammonium salt concentration [24]. Studies are underway to determine the bimolecular rate constants for the addition to these acylammonium species [25].

Recently, detailed computational kinetic rate analyses of the interfacial process have appeared. The published work relates to the production of polymer in both batch and semibatch/semicontinuous processes [26,27]. The dominant variables that influence the resin composition are the linear velocity, liquid–liquid volume ratio, aqueous pH, and phosgene/BPA ratio. Modeling of a Stockmayer distribution of BPA-PC oligomers based on a Monte Carlo method has received some attention [28]. Although the continuous production of the BPA-PC homopolymer is known, no process rate work has been published [29].

B. Transesterification (Melt or Solventless) Process

The process involves the base-catalyzed condensation polymerization of DPC (bp 312°C/760 torr) with BPA (bp 208°C/2 torr, 250°C/12.8 torr, or 287°C/50 mm Hg) The general reaction is shown in Scheme 2. The reaction is run at sufficiently high temperature (150–350°C) such that the starting monomers, oligomers, and final polymer remain molten throughout the course of the reaction. The reactor pressure is staged throughout the course of the reaction to allow the efficient removal of phenol (bp 180°C); the pressure ranges from 150–200 torr initially to 0.1–1 torr in the later stages of conversion. Using this methodology, the BPA-PC resin is prepared without any additional solvent, drying step, or phosgene. When the process is properly designed and engineered, the quality of the final resin is directly related to the quality of the starting monomers. Thus, the amount of residual contaminants in the final resin is highly controllable.

Based on experimental observation, the tacit mechanistic assumption is that a simple phenoxy anion addition to a carbonate linkage is involved in the oligomer/polymer production steps. Once the phenoxy-based anion adds to a carbonate group (e.g., DPC) a phenoxide anion is liberated. Phenol distills from the melt after the liberated phenoxide anion exchanges a proton with another hydroxy end-group or BPA; proton exchange is extremely rapid and the equilibrium constant for the reaction of phenoxide with BPA is roughly unity. The conversion of the monomers to BPA-PC is driven by the constant removal of phenol from the melt. This removal of phenol from the reaction solution is mandatory

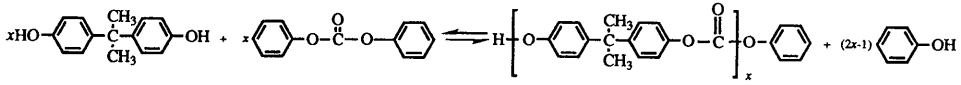

Scheme 2 General "melt" BPAPC synthesis.

for the production of high molecular weight polymer. Based on evaluation of the published data (and patent claims), this simple base-catalyzed condensation process is the most effective and commonly used approach. The catalyst loading necessary to effect efficient conversion to polymer is in the 10–250 ppb range [11].

Detailed mechanistic examinations of both the batch [30] and semibatch [31] processes have been published by Choi et al. Both works are substantial improvements over the earlier efforts of Losev et al. [32]. The model condensation steps are predicated on base-catalyzed reactions. Choi's more recent process model accounts for the evaporative loss of DPC during each phase of the multistage polycondensation in the melt process [31]. The earlier work assumed that only phenol was removed from solution during the transesterification reaction; this leads to inaccurate rate expressions due to a poor control of the DPC/BPA ratio and improper mass balance at each stage of the reaction. His work indicates that efficient condensation polymerization requires the proper maintenance of the ratio of reactive end-groups. This end-group dependence becomes particularly important during the later stages of the semibatch process. Furthermore, in order to compensate for the loss of DPC from solution during the low-pressure polycondensation stages, their results indicate that the addition of a slight excess of DPC is beneficial; the advantage of using an excess of DPC has been known since the early 1960s [10,12,14].

With the advent of high-quality, high molecular weight BPA-PC melt resin a commercial reality, current research focus has been directed to catalyst improvement. Catalyst systems other than alkali metal hydroxides (e.g., NaOH) have been investigated; they range from fluoride [33], carboxylate [34], and phosphonium [35] salts to neutral amines [36], phosphite [37], and guanidine [38] systems. However, except in very special circumstances or applications, alkali metal hydroxides (e.g., NaOH) are still the catalysts of choice.

The principal product advantage of the melt transesterification approach is its production of a resin having a most probable (''thermodynamic'') molecular weight distribution. Thus, under normal processing conditions, the anhydrous resin exhibits no tendency toward redistribution (i.e., a change in molecular weight, MFI, or IV). This distribution allows the resin to have extremely high OH end-group concentrations, which allow easy copolymer elaboration. Furthermore, the process yields a final resin that is contaminated neither with residual solvent (plasticization) nor with high salt concentrations (e.g., NaCl). Because the process is solventless, monomers of limited or no appreciable solution solubility and thermotropic liquid crystalline polycarbonates [39] can easily be prepared or incorporated into resins via a melt route. This thermodynamic material distribution coupled with the solventless, nonphosgene nature of the process makes the melt approach highly desirable from both a processing and an environmental viewpoint [40].

C. General Redistribution Method

The general redistribution method is merely the opposite path from the melt synthetic process mentioned previously. Various lower molecular weight polycarbonate resins can be produced from existing higher polycarbonate materials via incorporation of monomeric or oligomeric materials [41]. This process is amenable to both extrusion and melt equilibration reactors, e.g., in a Helicone. Since the material is equilibrated, the final molecular weight of the resin is determined by the numerical weight average (wt%) of the added components plus that of the initial polycarbonate resin. A catalyst is necessary for efficient (rapid) redistribution. During a redistribution process, the number and type of end-groups present within the system are conserved. The extreme of this methodology is the complete reversion of the initial polycarbonate back to monomeric materials; this latter process is the basis of a number of resin recycling efforts [42].

D. Simple Oligomer or Multistage Method

BPA-PC oligomers are produced by a melt transesterification or an interfacial process [43]; the interfacial method usually requires a large amount of end-capper (e.g., phenol or *p*-substituted phenols) to keep the chains short. The oligomer molecular weights produced in this process range from 800 to 12,000 (M_w). These oligomers can be used as a blend stock for alloying and copolymer production or polymerized/copolymerized in the melt to produce higher molecular weight polycarbonate materials.

The potential advantages of such oligomeric materials are their (marginally) improved miscibility with a variety of resins relative to a high molecular weight polycarbonate, lower melt viscosity, ease of preparation, and (possibly) added flexibility in end-capping % (e.g., % hydroxyl end-group) for copolymer alloying.

E. "Crystalline" Oligomer Approach

BPA-PC oligomers are generated via either an interfacial or a transesterification process and subsequently injected into a solvent to induce precipitation; injection into a solvent (e.g., acetone) results in their partial crystallization upon oligomer precipitation. After their isolation and drying, these oligomers can be further polymerized to produce high molecular weight BPA-PC via a melt transesterification process or solid state polymerization. This process is essentially the same as the simple oligomer approach but with a change in the oligomer isolation procedure.

Since all low molecular weight BPA-PC oligomeric materials (IV $< \sim 0.35$ dL/g) are known to produce a crystalline precipitate under the process conditions

(e.g. [14]), it is not surprising that the isolated powders are found to exhibit high crystallinity [12]. These isolated materials are intermediate between the starting monomers and traditional polycarbonate resin grades in terms of ease of manipulation and processing.

The crystalline oligomers would be used for the same applications as the noncrystalline (simple) oligomeric materials. Their principal use would be as a feedstock for melt polycarbonate or copolymer production; a secondary use would be as a low molecular weight blending or compounding resin. Any advantage due to the crystalline nature of these oligomers (e.g., hydrolytic stability and solvent resistance) will be lost on processing since the materials will revert to an amorphous, glassy structure on melting. As with the multistaged approach mentioned previously, except for the crystalline oligomer's unique application to solid state polymerization, the principal use of this technology is to skirt existing process patents.

An inverted variant of this "crystalline" approach is the *solid state polymerization* method (e.g., Iyer et al. [44,45]). Using this approach, one first prepares the low molecular weight linear oligomers (IVs; η = 0.26–0.35 dL/g; T_g = 120–135°C) using a melt process. After isolation, a basic catalyst (e.g., an alkali hydroxide, phenoxide, or BPA dialkali salt) is blended into this "prepolymer." After thermal/vacuum conditioning, the prepolymer is heated to 210–250°C in stages while under vacuum (<1 torr); this temperature range is above the T_g but below the T_m, hence the name "solid state" polymerization. After prolonged heating (4–8 h) high molecular weight polymer (IVs; η = 0.44–0.81 dL/g; T_g = 151–159°C; T_m = 254–271°C) with high crystallinity (26–43%) is obtained. The initial crystallinity of the starting oligomer is assumed to contribute to or induce further crystallinity in the product [44]. Bayer AG has been active in this area as well [46].

The solid state polymerization stage suffers the same kinetic limitations (mass transport) as the later stages of the traditional melt technology. A high concentration of hydroxylic end-groups (many as their anion) are required to undergo reasonable polymer build and exchange rates. However, this process has none of the transport/surface renewal advantages of the traditional melt process. Due to the static nature of the prepolymer glass during the final polymerization stage, encounter group problems (diffusion limitations) and phenol-DPC removal rates are much lower than in a melt. This procedure generates a "living" resin since the catalyst is unquenched in the final product. Due to the long heated residence time with high catalyst loading (up to 300 ppm wt%), the potential for base-induced crosslinking (due to Fries product, branched or gel formation) and degradation is quite high. Due to the crystallinity, the materials are translucent to opaque and densification occurs. Color-body formation may be an occasional problem.

During solid state polymerization high crystallinity in the product would

be anticipated. The percent crystallinity usually tracks the catalyst loading, which functions as the nucleating agent [44,47]. Thermal annealing at these polymerization temperatures should induce quite rapid crystallization. The literature reports that polyarylcarbonates undergo crystallization at 180°C over 8 days [48]. If the crystallization rate can be approximated by a simple Arrhenius rate expression, then 8 days/180°C ≈ 1–2 h/230–250°C. In fact, experimental work by Bailly et al. [49] and Gallez et al. [50] indicates that the rate of crystallization with phenoxide anions is on the order of tens of minutes at 230°C. The rate of BPAPC crystallization can also be accelerated by the presence of plasticizers [49–51]; smaller oligomers, phenol, and DPC might function in this capacity under the prepolymer conditioning. An additional contribution to the observed crystallinity might come from the oligomeric materials themselves. As produced, the prepolymer oligomers have high crystallinity (20–30%), which may increase in proportion to the catalyst loading or their conditioning, prior to polymerization; this conditioning stage is at 210°C (2–6 h). Since low molecular weight BPA-PC crystallizes more rapidly than higher molecular weight material, this latter rationale would explain the narrow crystalline composition range usually observed (26–38%).

The advantage of a high crystallinity BPA-PC material would be to increase the tensile heat distortion temperature and its solvent resistance while decreasing the gas permeability [14] and increasing embrittlement [52]. In order to retain these desirable properties, the solid state BPA-PC would have to be used like a thermoset resin. One would anticipate densification of the resin as crystallinity increases plus overall loss of material volume and mass due to the expulsion of phenol and DPC. Normal secondary melt processing such as injection molding and extrusion will convert these materials to the normal glassy polycarbonate resin.

F. "Cyclic" Oligomer Technology

Cyclic oligomers are synthesized using an initial interfacial preparation of the cyclic BPA-PC oligomers followed by their isolation (Scheme 3). Catalyst-initiated polymerization of the anhydrous cyclic oligomeric powder in the melt can then be used to produce high molecular weight resin. These materials were originally discovered by Schnell and Bottenbruch in 1962 [53]. Their work demonstrated that Lewis acid catalysts could be used effectively to produce very high molecular weight resin from a variety of tetrameric oligomers. This preliminary work was extended by Moody in 1964 [54] and Prochaska between 1965–1969 [55]. The basic interfacial technology for this process was further developed by Horbach [56] and Weirauch [57] at Bayer AG in the late 1970s. More recently, the application of the interfacial approach was developed as a commercial process

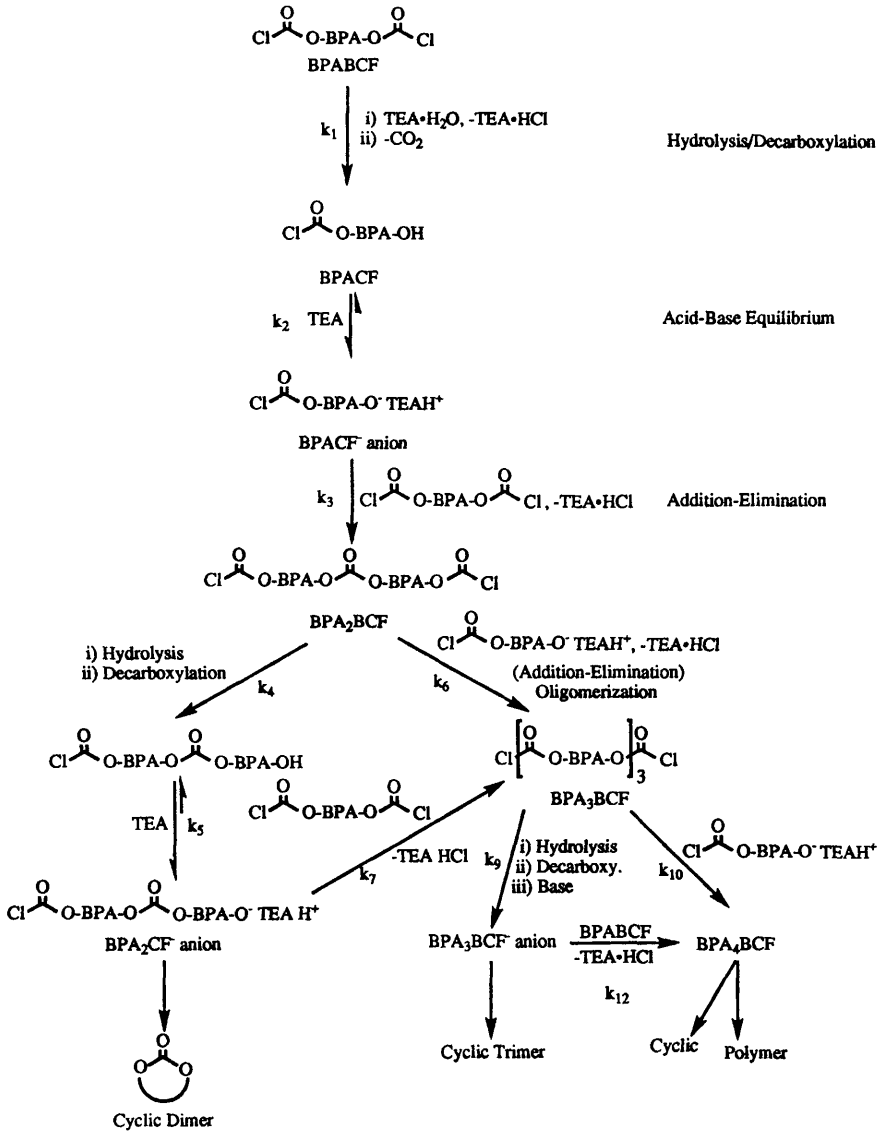

Scheme 3 General "cyclic" oligomer formation steps.

by the General Electric Company [58–60]. Work in this general area has resurfaced at Bayer AG recently [61].

In the current cyclics process, the oligomers are prepared interfacially at a lower pH (3–7) than the usual interfacial process (9–12); this minimizes any base-initiated ring opening hydrolysis resulting in linear oligomerization. Unlike the standard interfacial process, no end-capping agents are used because they would promote the formation of linear material. The cyclic oligomers range from 2 to 20 monomer units in length, the bulk of the composition usually being the dimer-heptamer cyclic oligomers. The molecular weight range is usually M_w = 1300–1700 with $M_w/M_n < 2$ (1.3–1.5).

Since an interfacial synthesis generates a kinetic distribution of products, the cyclic oligomers themselves represent a kinetically distributed material. Nested in this process is a second kinetically selective distribution process for the generation of cyclic oligomers vs. linear material. This latter selectivity is obtained by controlling the reaction conditions such that the *monomer* concentrations are in constant high dilution in the reaction phase; this original type of *Ziegler-Ruggli dilution* approach [12] was renamed the "pseudo-high dilution" method by Brunelle [59]. The traditional *Ziegler-Ruggli* dilution approach is quite effective for small cyclic oligomer synthesis; this is the result of the addition of the aryloxy anion monomers to either the chloroformate anions or linear oligomeric chloroformates being rate limiting. Thus, the intramolecular cyclization of aryloxy anion-chloroformate–derived species can be favored over intermolecular condensations by simple control of the monomer addition rates (concentrations), liquid phase ratios, added base, and temperature. Although quite high concentrations of the cyclic oligomers are present in solution by the end of the reaction (20–40 wt%), these oligomers are known to be stable to the reaction conditions. This kinetic stability results from the intermolecular rate of addition of an anionic species to the carbonate bond being 10^4–10^7 times slower than the corresponding addition to a chloroformate-derived species.

To gain insight into the formation of cyclic oligomers, efforts have been made to simulate the existing experimental data [62]. This work has had limited success since the model can be parameterized to simulate any specific oligomer distribution but lacks any predictive value. The principal cause of this weakness is that to date accurate, experimentally derived rate data and kinetic expressions for cyclic oligomer formation are still lacking. As a result, the mechanism for the incremental condensation steps is simply assumed to be that of the traditional interfacial process [12]. Recently, Aquino et al. have endeavored to clarify a number of the reactions related to carbonate bond formation [25,63].

For the polymerization of cyclic oligomers, a variety of catalyst initiators work well in the melt. The most effective catalysts are simple bases. Their mechanism of initiation involves anionic (base) addition to the carbonate bond. The mechanism of propagation involves a phenolic anion (end-group) addition similar

to that indicated in the melt polymerization process; the addition of (acidic) melt stabilizers is often required to prevent premature polymerization in the melt. In general, the ring opening of the cyclic BPA oligomers generates a "living" polymer system with M_w = 202,500 and M_n = 45,410 [64]; molecular weights (M_w) as high as 700,000–1,000,000 can be obtained by using low initiator levels. The base-initiated activation energy for cyclics polymerization is roughly 12.5 kcal mol [65]; this activation energy value is comparable to that observed in simple carbonate transesterification [66].

Although the overall reaction to form linear polycarbonates is only mildly exothermic (0.4 kcal mol [64]), less than 0.5% cyclic material remains at the end of the polymerization. The polymerization (redistribution) to linear material is driven entropically, coupled to the small exothermicity of the cyclic dimer and trimer ring openings.

The principal advantages of the cyclic oligomers derives from their low viscosity in the melt (T_g = 149°C; mp ~ 200°C; 170 poise at 200°C; 6 poise at 250°C) and their ability to rapidly form very high molecular weight resin without the evolution of volatile materials (e.g., phenol or DPC). The cyclic oligomers have potential use in applications where higher resin flow and surface wetting (lower surface tension/energy) are required in comparison to normal polycarbonate grades. Once applied, the cyclic materials can be command-cured in either the liquid or solid (glassy) state to form the final high molecular weight resin; this technology is similar to that used for epoxy resin and pre-preg applications. Furthermore, their direct use in injection molding applications where high flow and concomitant rapid polymerization were required would be an excellent fit for this technology.

III. DIRECT COPOLYMER PRODUCTION

Over the past 45 years during which interest in aryl polycarbonates was renewed, literally hundreds of monomer and copolymer systems have been evaluated. Only those materials will be discussed that have had a sustained research effort due to their current or potential commercial viability; a few of the commercial copolymers, such as the polyester carbonates and optical materials, will be dealt with in separate chapters. Within this framework, all of the reaction processes common to polycarbonate homopolymers (e.g., interfacial, melt, etc.) have been tried for most of the copolymer systems. In general, the most consistent preparative success has been in condensation polymerizations involving monomers of similar intrinsic reactivity (e.g., HO-Ar-OH with HO-Ar′-OH). Largely disparate monomer–monomer intrinsic reactivities lead to copolymer blockiness or low-to-variable copolymer production.

A. General Synthetic Preparation: Aryl-aryl Copolymers

A variety of aryl-aryl copolycarbonates have been prepared. These copolymers demonstrate either improved melt flow properties [67] or hydrolytic stability [68,69] as their primary goal. Resorcinol incorporation into the normal BPA-PC backbone greatly improves its overall flow properties [67]; a melt synthetic approach is preferred but interfacial or "cyclic" methods work just as well.

Polymer hydrolytic and solvent stability are usually important considerations in engineering thermoplastic applications. For BPA-PC, hydroquinone and its derivatives offer the potential for improved hydrolytic stability with minimum monomer expense [68,69]. The incorporation of the simple biphenols such as 4,4′-biphenol improve hydrolytic stability as well. As with the resorcinol above, a melt approach is preferred. This preference is a logical extension of what one is trying to achieve with a solvent-resistant material—limited or no solubility. A melt synthetic approach circumvents any monomer–polymer solubility problems.

B. Enhanced Weathering, Thermal Stability, and Flame Retardancy of Novel Copolymers

The addition of copolymers to polycarbonate for the simple improvement of its weatherability, thermal and photochemical stability are constantly being sought. Towards these goals, heteroatom incorporation into the polycarbonate backbone—particularly silicon and sulfur—is an area of active research. The direct substitution of these heteroatoms into BPA-PC structure generally improves both chemical resistance and flame retardancy (FR) of the resin. Due to their potential importance as substitutes for halogens and phosphorus-containing PC resins and copolymers, a few of these materials will be discussed briefly.

Copolymers of BPA-PC and polydimethylsiloxane (PDMS) have been examined intensively since their accidental discovery in the early 1960s by the General Electric Company; attempts to lower the melt viscosity of BPA-PC during extrusion led to the addition of silicone fluids as internal lubricants. The coextrusion of silicone fluids with BPAPC resulted in copolymer production. The improved FR, UV and hydrolytic stability of these materials has made them of interest. Newer methods of preparation include direct cocondensation between the respective monomers as well as via cyclic PC oligomers with dimethylsiloxane cyclic tetramer (D_4 [70]).

The solvent resistance and weatherability of these materials has been examined in detail. One simple indicator of a polymer's resistance to a given solvent is manifested by the liquid's ability to wet the resin surface. The surface wettability of BPA-PC-PDMS blends is similar to that of pure PDMS even at low concentrations of the block copolymer [71]. The wettability was shown to be insensitive

to PDMS block length when the block length was greater than 20 units. More recently, Chen et al. [72] studied multiblock copolymers of these materials in order to evaluate PDMS block size on surface segregation. Using an ESCA analysis of the surface (27 Å), Chen studied PDMS block lengths of 2–40 units and found that their surface concentrations of the PDMS greatly exceeded their bulk concentrations; ESCA depth profiling of each material indicated this effect as well. For a given bulk loading of PDMS, there was an increase in its surface concentration with increasing block length; this is similar to the earlier observations by LeGrand and Gaines [71]. In all cases, annealing enhanced the PDMS percentage at the surface of the resins.

Copolymer systems of BPA and bis(*p*-hydroxyphenyl)dimethylsilane (BPSi) have been prepared using an interfacial synthesis [73,74]. These materials exhibit increased flame resistance (increased oxygen index) and char residue with increasing BPSi monomer content vs. BPA homopolymer. These materials show great improvement in their weathering behavior (UV stability, yellowness index, and % haze) due to lower UV absorptivity, higher water repellency, and a lower number of side chain photooxidation reactions. Their general optical behavior has been examined [75]. A number of patents have been issued in this area; see, for example, Davis et al. [76], Evans and Carpenter [70], Lewis [77], Lewis and Bunelle [78], Lucarelli et al. [79], Yokoyama et al. [80], Umeda et al. [81], and Rich et al. [82].

Due to the possibility for enhanced chemical resistance and FR properties, substitution of the carbonate oxygen atoms by sulfur atoms has been investigated. Polythio-, polydithio-, and polytrithiocarbonate analogs of BPA-PC have been prepared and characterized. The polythiocarbonates from thiophosgene and BPA [83,84] and the polydithiocarbonate of phosgene plus 4,4′-isopropylidenedibenzenethiol (BTA [85]), and polytrithiocarbonate from BTA with carbon disulfide [86] were originally prepared some time ago. However, extensive reexamination of these materials have recently been published [87–89]. These more current works report improved general (interfacial) syntheses and include better material characterization. Although high molecular weight polymers (M_w = 40,000–170,000) are now easily produced, their thermogravimetric analyses indicated that the substitution of any of the oxygen atoms by sulfur atoms leads to a lower overall thermal stability than the parent BPAPC. These thio-containing polymers range in color from light yellow to dark orange. Thus, as is often the case, improvement in one desirable resin property with a change in monomer composition comes at the expense of another property. These thio-substituted materials did show better chemical resistance than the BPAPC homopolymer, but no new FR work was reported.

One other FR monomer has had a long and favored history in BPAPC chemistry. This monomer is tetrabromobisphenol A (TBBPA). At relatively low

bromide loadings, copolymers of BPA-TBBPA show substantially enhanced FR properties over the parent BPAPC polymer. Current work by Gu and Wang [90] and Marks et al. [91] exemplifies this interest.

IV. CONCLUSIONS

Although work in the field of aryl polycarbonates is into its fifth decade, much research is still necessary to fully develop our understanding of this industrially important material. A number of efficient, synthetic methodologies have evolved into commercially viable processes that allow great flexibility in the large-scale preparation of BPAPC resins. Convenient quantities of a variety of modified resins are available for study. As part of these preparative developments, a variety of improved homo- and copolymers, blends, and alloys are being sought for evaluation and potential future commercialization.

REFERENCES

1. A. Einhorn, *Annählen 300*:135 (1898).
2. C. A. Bischoff and A. v. Hedenstroem, *Berichte 35*:3431 (1902).
3. W. H. Carothers and F. J. van Natta, F. J. *J. Am. Chem. Soc. 52*:314 (1930).
4. W. R. Peterson, U.S. Pat. 2,210,817 (1940) assigned to E. I. du Pont de Nemours & Co.
5. J. R. Whinfield and J. T. Dickson, Br. Pat. 578,079 (1946); J. R. Whinfield, *Nature 158*:930 (1946).
6. H. Schnell, L. Bottenbruch, and H. Krimm, Belg. Pat. 532,543 (1954) assigned to Farbenfabriken Bayer AG.
7. H. Schnell, *Angew. Chem. 68*:633 (1956); H. Schnell *Ind. Eng. Chem. 51*:157 (1959).
8. D. W. Fox, Aust. Pat. 221,192 (1959) assigned to the General Electric Company.
9. H. Schnell, L. Bottenbruch, and H. Krimm, U.S. Pat. 3,028,365 (1962) assigned to Farbenfabriken Bayer AG.
10. D. W. Fox, U.S. Pat. 3,153,008 (1964) and D. W. Fox U.S. Pat. 3,148,172 (1964) both assigned to the General Electric Company.
11. T. Sakashita and T. Shimoda, Eur. Pat. A3511168 (1988); Eur. Pat. A360578 (1988); U.S. Pat. 5,026,817 (1991); U.S. Pat. 5,276,129 (1994); U.S. Pat. 5,306,801 (1994); T. Sakashita, T. Shimoda, and T. Nagai, U.S. Pat. 5,276,109 all assigned to GE Plastics Japan Ltd.
12. H. Schnell, *The Chemistry and Physics of Polycarbonates*, Wiley-Interscience, New York, 1964, p. 1.
13. H. Vernaleken, Polycarbonates, in *Interfacial Synthesis, Vol. 2, Polymer Applications and Technology* (F. Millich and C. E. Carrahers, eds.), Marcel Dekker, New York, 1977, p. 65.

14. D. W. Fox, Polycarbonates, in *Kirk-Othmer Encyclopedia of Chemical Technology*, Vol. 18, 3rd ed. John Wiley and Sons, New York, 1982, p. 479.
15. M. Lapp, *Plaste und Kautschuk 37*:361 (1990).
16. V. Serini, Polycarbonates, in *Ullmann's Encyclopedia of Industrial Chemistry*, 5th ed. (B. Elvers, S. Hawkins, and G. Schulz, eds.), VCH, New York, 1992, A21, p. 207.
17. D. C. Clagett and S. J. Shafer, Polycarbonates, in *Comprehensive Polymer Science; The Synthesis, Characterization, Reactions, and Applications of Polymers*, Vol. 5 (G. Allen and J. C. Bevington, eds.), Pergamon Press, Oxford, 1989, p. 345.
18. D. Freitag, G. Fengler, and L. Morbitzer, *Angew. Chem. Int. Ed. Engl. 30*:1598 (1991).
19. L. A. Utracki, *Polym. Eng. Sci. 35*:2 (1995).
20. D. Freitag, U. Grigo, P. R. Müller, and W. Nouvertnè, *Encycl. Polym. Sci. Eng. 11*: 648 (1988).
21. P. G. Kosky, J. M. Silva, and E. A. Guggenheim, *Ind. Eng. Chem. Res. 30*:462 (1991).
22. J. A. King, Jr., and G. L. Bryant, Jr. *Acta. Cryst. C47*:2249 (1991).
23. J. A. King, Jr., and G. L. Bryant, Jr. *J. Org. Chem. 57*:5136 (1992).
24. P. G. Kosky and E. P. Boden, *J. Polym. Sci. 28*:1507 (1990).
25. E. Aquino, W. J. Brittain, and D. J. Brunelle, *Polym. Inte. 33*:161 (1994); E. C. Aquino, W. J. Brittain, and D. J. Brunelle, *J. Polym. Sci. A: Polym. Chem. 32*:741 (1994).
26. P. L. Mills, *Ind. Eng. Chem. Process Des. Dev. 25*:575 (1986); P. L. Mills, *Chem. Eng. Sci. 41*:2939 (1986).
27. J.-T. Gu and C. S. Wang, *J. Appl. Polym. Sci. 44*:849 (1992).
28. S. Munjal, *Polym. Eng. Sci. 34*:93 (1994).
29. H. H. M. van Hout, M. H. Oyevaar, and B. J. Held, U.S. Pat. 5,210,172 (1993) assigned to the General Electric Company.
30. S. N. Hersh and K. Y. Choi, *J. Appl. Polym. Sci. 41*:1033 (1990).
31. Y. Kim and K. Y. Choi, *J. Appl. Polym. Sci. 49*:747 (1993).
32. I. P. Losev, O. V. Smirnova, and Y. V. Smurova, *Polym. Sci. USSR 5*:662 (1963).
33. S. Kühling, W. Alewelt, H. Kauth, and D. Freitag U.S. Pat. 5,314,985 (1994); S. Kühling, W. Alewelt, H. Kauth, and D. Freitag, Eur. Pat. Appl. 93108043.6 Pub. Number 0 571 869 A1 (1993) both assigned to Bayer AG.
34. S. Sivaram, J. C. Sehra, V. S. Iyer, I. S. Bhardwaj, and S. Satish, U.S. Pat. 5,288,838 assigned to the Council of Scientific & Industrial Research, New Delhi, India.
35. J. A. King, Jr, and P. J. McCloskey, U.S. Pat. 5,412,061 (1995) assigned to the General Electric Company; S. Sivaram, J. C. Sehra, V. S. Iyer, I. S. Bhardwaj, U.S. Pat. 5,288,838 (1994) assigned to the Council of Scientific & Industrial Research, New Delhi, India.
36. J. A. King, Jr., and K. Brouwer, U.S. Pat. 5,362,840 (1994); J. A. King, Jr., and K. Brouwer, U.S. Pat. 5,373,083 (1994) both assigned to the General Electric Company.
37. M. Yokoyama, J. Takano, and K. Takakura, U.S. Pat. 5,250,655 (1993) assigned to Mitsubishi Petrochemical Company Ltd.
38. J. A. King, Jr., U.S. Pat. 5,319,066 (1994) assigned to the General Electric Company;

S Kühling, H. Kauth, and W. Alewelt, U.S. Pat. 5,418,316 (1995) assigned to Bayer AG.
39. S.-J. Sun and T.-C. Chang, *J. Polym. Sci. A: Polym. Chem. 31*:2237 (1993).
40. T. J. Cavanaugh and E. B. Nauman, The future of solvents in the polymer industry, *TRIP 3*:48 (1995).
41. A. J. Campbell, D. D. Dardaris, G. R. Faler, P. J. McCloskey, and T. L. Evans, U.S. Pat. 5,414,057 (1995); J. A. King, Jr., P. J. McCloskey, and D. D. Dardaris, U.S. Pat. 5,459,226 both assigned to the General Electric Company.
42. See, for example: H.-J. Buysch, N. Schön, and S. Kühling, U.S. Pat. 5,266,716 (1993); H. Kauth, S. Kühling, W. Alewelt, and D. Freitag, U.S. Pat. 5,373,082 (1994); H.-J. Buysch, N. Schön, and S. Kühling, U.S. Pat. 5,391,802 (1995) assigned to Bayer AG.
43. S. Kühling, H. Kauth, and W. Alewelt, U.S. Pat. 5,340,905 (1994); S. Kühling, H. Kauth, and W. Alewelt, U.S. Pat. 5,399,659 (1995) both assigned to Bayer AG; H. E. Tuinstra and H. D. Myers, U.S. Pat. 5,336,750 (1994) assigned to The Dow Chemical Company; T. Yamoto, Y. Oshino, Y. Fukuda, T. Kanno, and T. Kuwana, U.S. Pat. 5,418,314 (1995); Y. Oshino and T. Kanno, Eur. Pat. Appl. 0 620 240 A2 (1994); Y. Okano, M. Taniganwa, and Y. Fukuda, Eur. Pat. Appl. 0 622 418 A2 (1994) all assigned to Daicel Chemical Industries Ltd.
44. V. S. Iyer, J. C. Sehra, K. Ravindranath, and S. Sivaram, *Macromolecules 26*:1186 (1993).
45. S. Sivaram, J. C. Sehra, V. S. Iyer, K. Ravindranath, U.S. Pat. 5,266,659 (1993) assigned to the Council of Scientific & Industrial Research, New Delhi, India.
46. U. Westeppe, D. Freitag, G. Fengler, and U. Grigo, DE Pat. 39 41 014 A1 (1991); P. Tacke, D. Freitag, G. Fengler, and U. Grigo, DE Pat. 40 38 788 A1 (1991); P. Tacke, C. Wulff, D. Freitag, U. Grigo, and G. Fengler, DE Pat. 40 38 967 A 1 (1991) all assigned to Bayer AG.
47. R. Legras, J. P. Mercier, and E. Nield, *Nature 304*:432 (1983).
48. G. Kampf, *Kolloid Z. 172*:50 (1960).
49. C. Bailly, M. Daumerie, R. Legras, and J. P. Mercier, *J. Polym. Sci. B: Polym. Phys. Ed. 23*:751 (1985); C. Bailly, M. Daumerie, R. Legras, and J. P. Mercier, *J. Polym. Sci.: Polym. Phys. Ed. 23*:493 (1985).
50. F. Gallez, R. Legras, and J. P. Mercier, *Polym. Eng. Sci. 16*:276 (1976).
51. R. Legras, C. Bailly, M. Daumerie, J. M. Dekoninck, J. P. Mercier, V. Zichy, and E. Nield, *Polymer 25*:835 (1984).
52. K. Varadarajan and R. F. Boyer *J. Polym. Sci. B: Polym. Phys. Ed. 20*:141 (1982).
53. H. Schnell and L. Bottenbruch, *Die Makrom. Chem. 57*:1 (1962) and H. Schnell and L. Bottenbruch, Belg. Pat. 620,620 (1962); Ger. Pat. 1,229,101 (1966); U.S. Pat. 3,386,954 (1968) all assigned to Farbenfabriken Bayer AG.
54. L. S. Moody, U.S. Pat. 3,155,683 (1964) assigned to the General Electric Company.
55. R. J. Prochaska, U.S. Pat. 3,220,980 (1965); U.S. Pat. 3,221,025 (1965); U.S. Pat. 3,274,214 (1966); U.S. Pat. 3,422,119 (1969) all assigned to the General Electric Company.
56. A. Horbach, *Polym. Prep. 21*:185 (1980).
57. K. Weirauch, A. Horback, and H. Vernaleken, U.S. Pat. 4,229,948 (1981) assigned to Farbenfabriken Bayer AG.

58. D. J. Brunelle, T. L. Evans, M. A. Vallance, K. R. Stewart, T. G. Shannon, D. A. Williams, D. J. Patterson, N. R. Rosenquist, and W. Hilakos, U.S. Pat. 4,749,583 (1988) assigned to the General Electric Company.
59. D. J. Brunelle, E. P. Boden, and T. G. Shannon, *J. Am. Chem. Soc. 112*:2399 (1990); D. J. Brunelle, T. L. Evans, and E. P. Boden, *Indian J. Technol. 31*:234 (1993).
60. D. J. Brunelle and T. G. Shannon, *Macromolecules 24*:3035 (1991).
61. H. Keul, F. Diesel, H. Hooker, E. Leis, H.-J. Burst, and N. Schooner, *Makromol. Chem. Rapid Commun. 12*:133 (1991).
62. P. G. Kosky, *J. Polym. Sci. A: Polym. Chem. 29*:101 (1991).
63. E. Aquino, W. J. Brittain, and D. J. Brunelle, *Macromolecules 25*:3827 (1992); E. Aquino, W. J. Brittain, and D. J. Brunelle, *Polym. Prep. 34*:865 (1993); E. Aquino, W. J. Brittain, and D. J. Brunelle, *Polym. Int. 33*:161 (1994).
64. T. L. Evans, C. B. Berman, J. C. Carpenter, D. Y. Choi, and D. A. Williams, *Polym. Prep. 30*:573 (1989).
65. K. R. Stewart, *Polym. Prep. 30*:575 (1989).
66. J. E. Bartmess, R. L. Hays, and G. Caldwell, *J. Am. Chem. Soc. 103*:1338 (1981).
67. P. C. Raymond III, U.S. Pat. 5,336,751 (1994); T. Sakashita, T. Shimoda, and T. Nagai, U.S. Pat. 5,384,388 (1995) both assigned to the General Electric Company.
68. T. Sakashita, T. Shimoda, and K. Kishimura U.S. Pat. 5,286,834 (1994); T. Sakashita, T. Shimoda, and K. Kishimura, U.S. Pat. 5,401,826 (1994); T. Sakashita, T. Shimoda, and T. Nagai, U.S. Pat. 5,405,933 (1995); T. Sakashita, T. Shimoda, K. Kishimura, and S. Uchimura, U.S. Pat. 5,418,315 all assigned to the General Electric Company.
69. D. J. Brunelle, *TRIP 3*:154 (1995).
70. T. L. Evans and J. C. Carpenter, U.S. Pat. 4,920,183 (1990) assigned to the General Electric Co.
71. D. G. LeGrand and G. L. Gaines, Jr., *Polym. Prep. 11*:442 (1970).
72. X. Chen, H. F. Lee, and J. A. Gardella, Jr., *Macromolecules 26*:4601 (1993).
73. A. Factor and P. T. Engen, *J. Polym. Sci. A: Polym. Chem. 31*:2231 (1993).
74. A. Factor, *Die Angew. Makromol. Chem. 232*:27 (1995).
75. D. G. LeGrand, *Structure and Properties of Polymer Films* (R. W. Lenz and R. S. Stein, eds.), Plenum Publishing, New York, 1973, p. 81.
76. G. Davis, B. McGrath, and K. Snow, U.S. Pat. 5,025,074 (1991); G. Davis, B. McGrath, and K. Snow, U.S. Pat. 5,039,772 (1991) assigned to the General Electric Company.
77. L. N. Lewis, U.S. Pat. 5010148 (1991) assigned to the General Electric Company.
78. L. N. Lewis and T. Bunelle, U.S. Pat. 4,954,549 (1990) assigned to the General Electric Company.
79. M. A. Lucarelli, J. W. Raleigh, and K. A. Schryer, U.S. Patent 5,401,578 (1995) assigned to the General Electric Company.
80. M. Yokoyama, K. Takakura, and J. Takano, U.S. Patent 5,391,691 (1995) assigned to Mitsubishi Petrochemical Co., Ltd.
81. T. Umeda, A. Nodera, and K. Hashmoto, U.S. Patent 5,449,710 (1995) assigned to Idemitsu Petrochemical Co.
82. J. D. Rich, P. D. McDermott, G. Davis, P. Policastro, K. Regh, P. Hernandez, and T. Guggenheim, U.S. Pat. 4,945,147 (1990); J. D. Rich, P. D. McDermott, G. Davis,

P. Policastro, K. Regh, P. Hernandez, and T. Guggenheim, U.S. Pat. 4,945,148 (1990) assigned to the General Electric Co.
83. G. L. Brode and T. L. Pickering, U.S. Pat. 3,640,965 (1968) assigned to Union Carbide Corp.
84. F. N. Jones and S. Andreades, *J. Org. Chem. 34*:3011 (1969).
85. F. J. Williams, U.S. Pat. 4,024,162 (1974); F. J. Williams, U.S. Pat. 3,933,862 (1974) both assigned to the General Electric Co.
86. K. Soga, H. Imamura, M. Sato, and S. Ikeda, *J. Polym. Sci. A: Polym. Chem. Ed. 14*:677 (1976).
87. M. Bandiera, C. Berti, P. Manaresi, E. Marianucci, F. Pilati, and M. Poloni, *Makromol. Chem. 194*:2453 (1993).
88. L. M. Leung, W. H. Chan, and S. K. Leung, *J. Polym. Sci. A: Polym. Chem. 31*: 1799 (1993).
89. G. Montaudo, C. Puglisi, C. Berti, E. Marianucci, and F. Pilati, *J. Polym. Sci. A: Polym. Chem. 27*:2277 (1989); G. Montaudo, C. Puglisi, C. Berti, E. Marianucci, and F. Pilati, *J. Polym. Sci. A: Polym. Chem. 27*:2657 (1989).
90. J.-T. Gu and C.-S. Wang, *J. Appl. Polym. Sci. 50*:149 (1993); J.-T. Gu, W.-C. Luo, and C.-S. Wang, *Die Angew. Makromol. Chem. 208*:65 (1993).
91. M. J. Marks, S. L. Brewster, and J. K. Sekinger, *J. Appl. Polym. Sci. 52*:1809 (1994).

3

Quantum Molecular Orbital Calculations, Levy-Stable Distributions, and Molecular Relaxation in Polycarbonate

John T. Bendler
South Dakota School of Mines and Technology, Rapid City, South Dakota

Michael F. Shlesinger
Office of Naval Research, Arlington, Virginia

I. MOLECULAR STRUCTURE CALCULATIONS FOR POLYCARBONATE

A. Introduction and Early Studies

It has long been thought likely that the exceptional ductility of bisphenol A polycarbonate (BPA-PC) (Fig. 1) is in some way linked to specific intramolecular motions of the polymer chain. Direct evidence for rapid and extensive solid state motion in glassy polycarbonate is seen in the large, low-temperature, dynamic mechanical loss peak found at $-100°C$ at 1 Hz [1,2]. This glassy state loss peak is frequently called the γ process (e.g. [3]) since between it and the higher temperature glass transition at T_g (i.e., the α process) is found a smaller intensity β process at a temperature T_β whose magnitude and position are sensitive to the thermal and mechanical history of the sample. The temperature T_γ of the loss peak maximum and the intensity of the γ process, on the other hand, are quite insensitive to thermal and mechanical history. Furthermore, the unperturbed chain dimensions of BPA-PC in solution are independent of temperature [4], suggesting

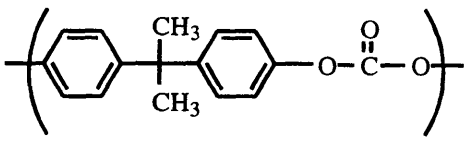

Figure 1 Molecular structure of bisphenol A polycarbonate (BPA-PC).

that free rotational statistics are obeyed and that intrasegmental rotational barriers are minimal.

The first conformational analysis of BPA-PC was undertaken by Williams and Flory [5] for the purpose of interpreting the dilute solution chain properties [4]. Williams and Flory reasoned that the (planar) carbonate groups should be perpendicular to the planes of the adjoining phenyl rings and that in the trans-trans chain configuration essentially free rotation would be possible at both the ring–carbonate and ring–isopropylidine connections. Force field methods led to an estimate of 1.3 kcal/mole for the relative cis-trans energy difference in solution. On this basis, Williams and Flory concluded that the polymer would be found chiefly in the trans-trans configuration and, assuming free rotation about the virtual bonds of length 7.02 Å, they found excellent agreement with experiment. A more quantitative conformational analysis of BPA-PC using 6–12 van der Waals atom–atom potentials for the carbon, hydrogen, and oxygen nonbond interactions was carried out by Tonelli [6]. From these calculations, Tonelli concluded that the largest conformational barrier occurring in the molecule was 1.0 kcal/mole, and that not only did the virtual bonds undergo free rotation but that the chemical bond rotations themselves were near to having unhindered (intramolecular) rotational freedom. Tonelli went on to discuss the probable connection between the rotational mobility of the isolated chain and the low-temperature toughness of the glassy bulk polymer [6].

Though the force field modeling methods had helped to clarify the conformational possibilities for the polycarbonate molecule, there were a number of unresolved issues that prompted efforts to use quantum Self Consistent Field (SCF) molecular orbital (MO) approaches [7,8]. The most serious technical problem was the lack of reliable forcefield parameters for molecules containing oxygen [7]. Some of the difficulty concerned the lone pair electrons whose behavior during a dihedral rotation could not be accurately modeled with atom-based central force parameters. Difficulties in parameterization were also due to the great flexibility of the oxygen–carbon bond, which caused its hybridization to vary with changes in steric nonbond interactions, especially when bonded to an aromatic ring. Questions arose [8] as to the accuracy of the Williams and Flory prediction that BPA-PC would be entirely trans-trans inasmuch as the single-crystal x-ray data sug-

gested a cis-trans arrangement in the solid. Also, efforts to understand and control the photostability of the polymer as it related to the photo-Fries rearrangement plus the questionable assignment of the first excited singlet state to an $n \rightarrow \pi^*$ transition required a clearer picture of the conformational preferences at the carbonate–phenyl ring linkage [8]. These early quantum calculations were semiempirical (MNDO) [9] and focused mostly on the two model compounds diphenyl carbonate (DPC) and 2,2-diphenyl propane (DPP), shown in Fig. 2. These semiempirical SCF calculations confirmed that the trans-trans form of the aromatic carbonate is most stable, but also showed that the cis-trans was not much higher in energy (0.1–0.5 kcal/mole), with a barrier of approximately 3.0 kcal/mole for interconversion between cis and trans [7,8]. The carbonate was predicted to be perpendicular to the aromatic rings, and aromatic ring rotation across the isopropylidine group in DPP was clearly cooperative, with one ring driving the other as it rotated. The barrier in DPP from MNDO was 3.5 kcal/mole, and both the DPC and DPP barriers were in reasonable agreement with dilute solution nuclear magnetic resonance (NMR) studies of segmental mobility in BPA-PC [10].

At about the same time that these early theoretical quantum studies of BPA-PC were being carried out, new experimental findings were announced that dramatically heightened the significance of a clear understanding of the monomer level geometry and conformational freedom of the polymer [11,12]. First was the discovery from solid state NMR studies that the phenyl rings in BPA-PC, as well as chloral PC, undergo 180° flips in the glassy state with a rate and activation energy very near to that of the mechanical γ process. (These and other NMR results in polycarbonate research are reviewed and discussed in detail in Chapter 4 of this volume.) Surprising features of the ring motions revealed unambiguously in the NMR experiments included (a) that complete 180° flips of the aromatic backbone rings could occur in the bulk polymer glass hundreds of degrees below the macroscopic T_g with a motional dynamics reflecting almost perfectly that of the bulk dielectric-mechanical γ-relaxation process; and (b) that the ring motions were occurring with little or no change in the 1,4-phenylene axis. The second

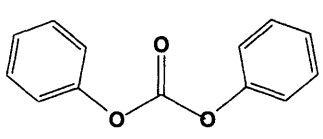

Diphenyl Carbonate (DPC)

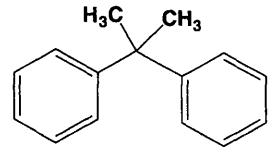

Diphenyl Propane (DPP)

Figure 2 Structures of diphenyl carbonate (DPC) and diphenyl propane (DPP), model compounds of BPA-PC often used for molecular calculations.

important experimental information was a detailed single-crystal x-ray structure of DPC [12,13] showing that the carbonate group was not perpendicular to the aromatic rings, as MNDO suggested, but was at an angle of 55–65°.

Since it was otherwise well known that semiempirical methods, especially MNDO, tended to exaggerate dihedral distortions in oxygen-bonded aromatic systems, efforts soon followed to refine the semiempirical quantum SCF findings by undertaking more time-consuming, but hopefully more accurate, ab initio calculations for both DPC and DPP [13,14]. These early ab initio calculations used the minimal STO-3G basis set and predicted a carbonate/ring dihedral angle much nearer to the x-ray result (66°), a cis-trans energy bias over trans-trans of 1.5 kcal/mole, and a barrier for cis-trans interconversion slightly greater than 5 kcal/mole [14]. Full-geometry optimization was not employed for these Gaussian '80 calculations, because computer speeds and memories were limited by today's standards and it was assumed that carbons and hydrogens in the meta and para positions to the carbonate–ring linkage would not adjust significantly to carbonate rotations. While it is true that the absolute movements of these distant atoms are small, even small displacements play a role in determining the minimum energy carbonate position since the total barrier to carbonate rotation is actually much smaller than was assumed at that time.

B. High-Level MO Calculations and a New Proposed Mechanism for the Gamma Process

Fortuitously as it turns out, these early nonoptimized ab initio results for DPC [14] agreed so well with available information at that time that it was not thought critical to extend or confirm them using larger basis sets or post-Hartree-Fock methods. Attempts were made to run a 3-21G* minimization for DPC on a CRAY 1S, but when convergence was not reached after 45 cpu hours the effort was abandoned.

The first high-level ab initio calculations directed at the carbonate–ring conformational questions were performed by Laskowski et al. [15] and Jaffe et al. [16], though the main carbonate model compound they studied, in contrast to earlier workers, was phenyl formate (PF), shown in Fig. 3. Other models such as monophenyl carbonate were studied by these authors, but to a lesser degree because the goal of quantifying the influence of basis set size required a prohibitive amount of cpu time and memory for complete geometry optimization for the larger molecules.

Since phenyl formate is considerably smaller than DPC, it was possible for Laskowski et al. to systematically study the influence of basis set size on the conformational properties as determined by ab initio calculations [15,16]. It was also possible to examine in an approximate way the role of electron correlation using MP2 post-Hartree-Fock methods for the SCF geometry. They found that,

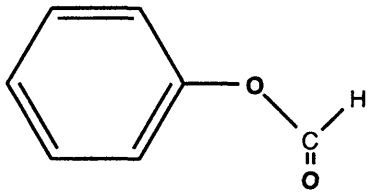

Figure 3 Phenyl formate PC model compound [17].

indeed, the structural and energetic parameters for PF depended strongly on the basis set employed and concluded that one needed to go to 6-31G* for PF to ensure agreement with experiment and to eliminate artifacts introduced by smaller basis sets. Ironically, the carbonate–ring dihedral, which was predicted to be 58° with STO-3G [14], became 0° using 4-31G, 90° with 6-31G* with polarization functions on oxygen only, and, finally, 64° for 6-31G* with polarization functions on both oxygen and carbon. The experimental x-ray results for single-crystal DPC show 45° for this dihedral angle [12,13]. Thus the success of the STO-3G calculations in fitting to experiment in retrospect is seen as largely fortuitous. Significant discrepancies between the STO-3G bond angles and bond distances and experiment had been neglected or overlooked. The high-level SCF MO calculations of Laskowski et al. [15] and Jaffe et al. [16] showed clearly that the carbonate rotational barrier was very shallow, and the barrier was the result of a delicate balance between the tendency of the carbonate unit to share nonbonded electrons with the aromatic ring (as in phenol, for example) and steric repulsion effects between the carbonyl oxygen and the ortho hydrogens of the ring.

Most recently, Sun et al. [17,18] reported an extensive series of ab initio calculations for small-molecule analogs of BPA-PC. In addition to HF/6-31G*, they have compared calculations using MP2/6-31G*, MP2/6-311G**, and density functional theory (DFT). Their overall purpose was to have a detailed structural, energetic, and electronic database from which a so-called ab initio force field parameterization could be developed. Changes in geometrical parameters from one conformation to another were noted, strongly suggesting that molecular flexibility will need to be a fundamental ingredient of any reliable BPA-PC force field. While each of the four high level methods above gave different results for geometries, energies and partial atomic charges, *differences* between conformations were found not to be sensitive to the method used, and therefore many of their reported results are for the most economical approach, namely, HF/6-31G* [18]. Again, because of time and memory constraints, Sun et al. performed most of their high-level optimized computations on the BPA-PC model compound monophenyl carbonate (MPC) shown in Fig. 4.

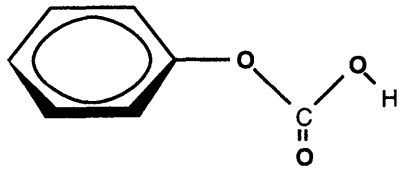

Figure 4 Monophenyl carbonate PC model compound [18].

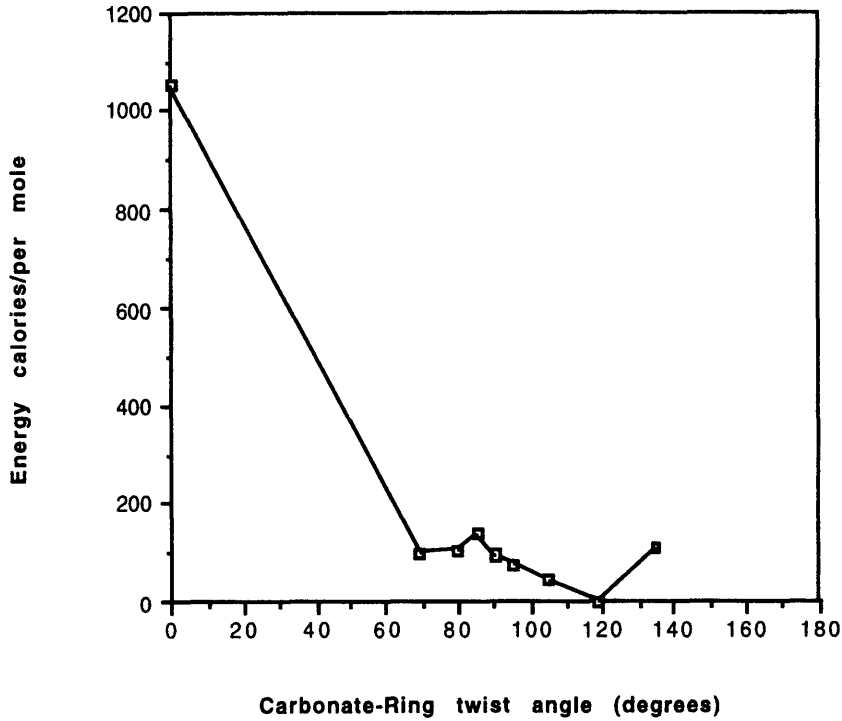

Figure 5 Hartree Fock energies calculated for diphenyl carbonate with full-geometry optimization using Gaussian '94 and the 6-31G** basis set. The low-energy conformation is "anti" and the higher energy one is "syn" (the same as found in single crystal x-ray studies).

The results of Sun et al. [18] for MPC are very similar to those of Jaffe et al. [16] for PF, the primary difference being the energy penalty for having the carbonyl in the plane of the aromatic ring. Jaffe et al. reported 0.72 kcal/mole for PF, whereas Sun et al. found 1.01 kcal/mole, in each case comparing the coplanar conformation to the minimum energy conformation. The minimum energy conformations found by both groups (for PF and MPC) are nearly identical. Sun et al. found a carbonate/ring twist angle of 63.5° for MPC using HF/6-31G*, whereas Jaffe et al. reported an angle of 64.0°, again with HF/6-31G* (i.e., with polarization functions on both carbons and oxygens). Sun et al. emphasize the large variations in bond angle and distances found with changes in conformations but conclude, as did Laskowski et al. [15] and Jaffe et al. [16], that ring rotations across the carbonate unit are not correlated because energy differences between specific conformations did not seem to depend on whether or not a second phenyl group was attached to the carbonate.

One of us has recently carried out high-level ab initio calculations for PF, MPC, and DPC using the 6-31G** basis set, and the details are reported separately [19]. The geometries and energies for PF and MPC are very similar to those previously reported [15–18], while full optimization for DPC gives a twist angle of 69° compared to 64° for MPC. The major difference, however, is that the phenyl ring–carbonate torsional energy surface shows two unequal minima, as illustrated in Fig. 5.

The barrier separating the two minima is very small, less than 40 cal/mole, and the energy difference (in vacuum) is about 50 cal/mole. Figure 6a shows the ab initio DPC geometry at the local minimum corresponding to a twist angle of 69.0° and Fig. 6b shows the geometry of the molecule at the lowest energy mini-

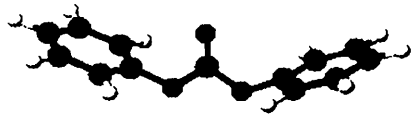

(a)

(b)

Figure 6 (a) DPC with 69 degree ring twist. (b) DPC with 119 degree ring twist.

mum of 119.0°. Also, it should be noted that in the lowest energy conformation (Fig. 6b) the two aromatic rings in DPC are on different sides of the carbonate plane. It has recently been proposed [19] that the low-temperature γ process in BPA-PC corresponds to carbonate rotational transitions between the two conformational energy minima seen in Fig. 5 at twist angles of 69° and 119°. Though this transition occurs with a very small activation energy in vacuum (corresponding to the ab initio calculations for isolated DPC molecules), in agreement with the observations of Sun et al., there are also large geometrical changes leading to intramolecular and intermolecular hindrances that will increase the barrier in the bulk polymer.

II. KOHLRAUSCH RELAXATION IN GLASSY POLYCARBONATE

A. Background

A principal objective in understanding the molecular nature of local motions in BPA-PC is the possibility that such understanding can provide insight into the origins of the exceptional ductility and toughness of this glassy polymer. However, interpretation of experiments such as dynamic mechanical spectroscopy, NMR, and dielectric relaxation, which directly probe local motions in glassy polymers, necessarily confront the fact that multiple relaxation times and highly dispersive dynamics are one of the prominent hallmarks of glassy state behavior. Whether the glass is polymeric or nonpolymeric, simple exponential relaxation such as follows from Kramers' model of thermally activated jumps over uniform barriers [20] is never observed in real glasses. Our interest lies in relaxation laws for glassy materials. We will particularly focus on a model (Fig. 7) of mobile defects inducing relaxation upon encountering a frozen-in part of a system. The release of a frozen-in dipole is reflected through dielectric relaxation, and the release of a frozen-in configuration is reflected through mechanical relaxation. Our defects will alternate between being trapped and being mobile. The inhomogeneous environment of the glass induces a probability distribution of escape times for the defects from traps. One might assume that a wide variety of escape time distributions are possible for the defects and this will induce a wide distribution of relaxation laws. We will find a simpler situation. The crucial quantity we calculate is the mean time $\langle t \rangle$ that a defect spends in a trap. If this is finite, diffusive behavior ensues and an exponential relaxation occurs. If the mean time is infinite (actually $\langle t \rangle$ greater than the duration of the experiment), then in our model subdiffusive defect motion produces stretched exponential relaxation.

B. Debye Relaxation

Debye considered the relaxation of spherical dipolar molecules in a fluid. An electrical field can align the dipolar molecules. When the field is turned off the

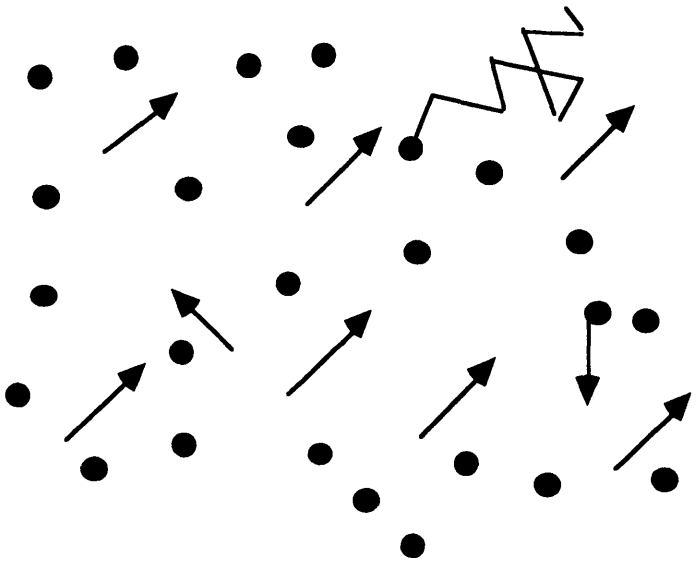

Figure 7 The arrows represent dipoles, all but two of which are frozen in and pointing to the northeast. These two dipoles are assumed to have interacted with defects that caused them to change their direction. As time progresses more dipoles will reorient and the material's total dipole moment will relax toward zero (no preferred direction). A possible path is shown for one of the defects. A defect waits a random time between jumps.

dipoles undergo rotational Brownian motion and their orientations are randomized via impacts with the fluid particles. If an individual dipole moment is denoted by $\mu(t)$, then the normalized dipole-dipole moment correlation function $\phi(t)$ is given by

$$\phi(t) = \frac{\langle \mu(t)\mu(0) \rangle}{\langle \mu^2(0) \rangle} \tag{1}$$

Debye found that at time t after the field is turned off the $\phi(t)$ behaved as

$$\phi(t) = \exp(-t/\tau_D) \tag{2}$$

where

$$\tau_D = \frac{4\pi R^3 \eta}{k_B T}$$

where R is the radius of the spherical dipole, η is the viscosity of the fluid, k_B is Boltzmann's constant, and T is the temperature in Kelvins.

The relaxation function $\phi(t)$ is related to the dielectric $\varepsilon(\omega)$ by

$$\frac{\varepsilon(\omega) - \varepsilon(\infty)}{\varepsilon(\infty) - \varepsilon(0)} = \varepsilon'(\omega) + i\varepsilon''(\omega) = \int_0^\infty \exp(i\omega t) \frac{d\phi(t)}{dt} dt \tag{3}$$

where ε' and ε'' are the real and imaginary parts of the dielectric constant. For Debye's case,

$$\varepsilon'(\omega) = \frac{1}{1 + (\omega\tau)^2} \quad \text{and} \quad \varepsilon''(\omega) = \frac{\omega\tau}{1 + (\omega\tau)^2} \tag{4}$$

A plot of ε' vs. ε'' as ω varies from zero to infinity describes a semicircle of radius 1/2 centered about $\varepsilon' = 1/4$. This type of graph is called a Cole-Cole plot. A good example of Debye relaxation and a semicircular Cole-Cole plot is *i*-butyl bromide at 25°C, with a $\tau_D = 5.3 \times 10^{-11}$ s.

Plots of experimental data for more complex polar fluids and glassy materials showed considerable deviations from semicircular behavior. Analysis of these deviations became a topic of intense interest.

C. Stretched Exponential Relaxation

The focus of dielectric relaxation changed from frequency to time [from $\varepsilon(\omega)$ to $\phi(t)$] with the work of Williams and Watts [21]. They inverted dielectric data to find $\phi(t)$. Surprisingly, all of the data they analyzed fit a single simple law, the stretched exponential:

$$\phi(t) = \exp[-(t/\tau)^\beta] \tag{5}$$

where $\beta < 1$ (Fig. 8). Polyethyl acrylate was a polymeric material for which they found a good stretched exponential fit. Polycarbonate is another example of this nonexponential behavior. This law was actually introduced in 1854 by Rudolf Kohlrausch to study the loss of charge in Leyden jars. We will now derive Eq. (5) from the mobile defect model and explore the temperature dependence of β and τ.

The mobile defect model posits that defects can move (perhaps with encapsulated free volume) and induce relaxation in a frozen-in part of a glass upon this encounter. Because of the inhomogeneous nature of a glassy material a distribution of escape times for a defect from a site is needed. We denote by $\psi(t)$ the probability density for a defect to remain at a site for a time t.

Let us consider the case of a lattice with V sites and N mobile defects. Let us further assume there is a frozen-in dipole at the origin. We start an experiment at $t = 0$ measuring dielectric relaxation. Our relaxation function, $\phi(t)$, is the probability that by time t the dipole has not been visited by a defect. We write:

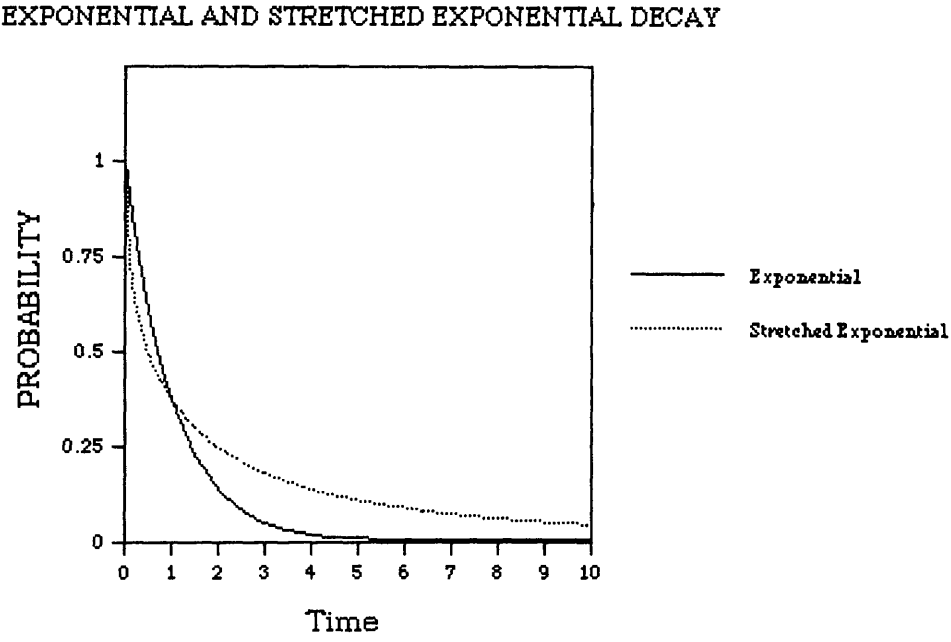

Figure 8 The exponential decay (single time scale) compared to a stretched exponential decay for $\beta = 1/2$. The stretched exponential decay is initially faster, but is slower after the 1/e decay of the exponential.

$$\phi(t) = \left[1 - V^{-1} \sum_{\ell'} \int_0^t F(\ell', \tau) d\tau\right]^N \tag{6}$$

where F is the first passage time probability for a defect that began at ℓ' to reach the origin at time τ. The sum is over all lattice sites, and $1/V$ is the probability of starting at any lattice site. The term in brackets is 1 minus the probability that a defect reaches the dipole and causes relaxation to occur. This is also the probability that relaxation did not occur. It is raised to the Nth power to account for none of the N defects having reached the dipole by time t. We take the limit $N \to \infty$, and $V \to \infty$, with $N/V = c$, where c is the defect concentration. In this limit the expression for $\phi(t)$ becomes

$$\phi(t) = \exp\left[-c \sum_{\ell'} \int_0^t F(\ell', \tau) d\tau\right] \tag{7}$$

where now the term in brackets is the flux of defects into the dipole. This is precisely the type of expression Smoluchowski would write for this process. We now note a symmetry. If we start a defect at the origin and then let it random-walk for a time t, it will visit a number of distinct sites, which we denote $S(t)$. Conversely, we could start walkers at any of these sites and they could reach the origin by time t. Therefore, $cS(t)$ is the flux of defects into the origin, so we can rewrite Eq. (7) as

$$\phi(t) = \exp[-cS(t)] \tag{8}$$

The form of $S(t)$ will depend on the form of $\psi(t)$, the pausing time density of a single walker. If $\psi(t)$ has a finite first moment, $\langle t \rangle \equiv \int_0^\infty t\psi(t)dt$, then, in 3D, $S(t) \approx t/\langle t \rangle$, and we have simple exponential relaxation. If $\psi(t) \approx t^{-1-\beta}$ with $\beta < 1$, then it can be shown [22] that $S(t) \approx t^\beta$, and we find stretched exponential behavior:

$$\phi(t) = \exp(-ct^\beta) \tag{9}$$

Note how the stretched exponential arises as a probability limit distribution. Other mechanisms and approaches for deriving the stretched exponential have also been explored [23]. This type of derivation was first given in another context by Hamill and Funabashi [24] and in the present form and context by Shlesinger and Montroll [25]. Note that the theory is asymptotic and is not applicable for very early times (high frequencies). Initially, defects jump quickly over the smaller barriers and the relaxation begins with an exponential decay. Fast-moving defects soon find themselves trapped by higher barriers and the relaxation slows and changes to stretched exponential.

D. Temperature Dependence

To determine the possible effects of temperature on relaxation we must more closely examine the nature of $\psi(t)$, the waiting time distribution between jumps.

1. The Exponent

Assume that the defect is presented with a barrier of height Δ. The waiting time density then takes the form:

$$\psi(t) = \lambda \exp(-\lambda t) \tag{10}$$

where

$$\lambda = \nu \exp(-\Delta/k_B T)$$

A distribution of barrier heights, $f(\Delta)$, induces a distribution of rates, $\rho(\lambda)$, via

$$\rho(\lambda)d\lambda = f(\Delta)d\Delta \tag{11}$$

If $f(\Delta) = \exp(-\Delta/\Delta_0)$ which also equals $(\lambda/\nu)^{kT/\Delta_0}$, then $\rho(\lambda) = \lambda^{-1}(kT/\Delta_0)(\lambda/\nu)^{kT/\Delta_0}$. The waiting time density function averaged over all barrier heights takes the form:

$$\psi(t) = \int_0^\infty \lambda \exp(-\lambda t)\rho(\lambda)d\lambda \approx t^{-1-\beta} \tag{12}$$

with

$$\beta = kT/\Delta_0 \tag{13}$$

when β is less than 1. If β is greater than 1 (when $kT > \Delta_0$), then one can analyze the general behavior of $\psi(t)$ using Laplace transforms. In this case,

$$\psi^*(s) \equiv \int_0^\infty \psi(t) \exp(-st)dt \approx 1 - s\langle t\rangle \frac{1}{1 + s\langle t\rangle} \tag{14}$$

which implies that

$$\psi(t) \approx \frac{1}{\langle t\rangle} \exp(-t/\langle t\rangle) \tag{15}$$

which leads to an exponentially decaying relaxation function. As an example, in a-Si:H, stretched exponential relaxation is found with a $\beta = \beta(T)$ with a linear temperature dependence. The introduction of infinite mean waiting times for transport in amorphous glasses was first made by Scher and Montroll [26] and applied to stretched exponential relaxation by Bendler and Shlesinger [27].

2. Concentration

We can rewrite the stretched exponential in Eq. (9) in the form of Eq. (5) when we make the identification:

$$\tau = c^{-1/\beta} \tag{16}$$

i.e., the time scale depends on the concentration of defects. In our model, if we lower the temperature, the only way we can lower the entropy is to form defect clusters. We assume a lattice gas model with two species, defects and vacancies (no defect). The defects are also assumed to interact through an attractive potential. As the temperature is lowered a phase transition occurs characterized by a correlation length ξ, which grows as the temperature falls. For a lattice gas there is a critical temperature T_c at which ξ diverges as

$$\xi \approx (T - T_c)^{-1/2} \tag{17}$$

We now assume that single defects are significantly more mobile than defect clusters and that we need only consider in Eq. (8) c_1, the number of single defects. Likewise, we calculate the time scale as

$$\tau = c_1^{-1/\beta} \tag{18}$$

The number of single uncorrelated defects is given by

$$c_1 = c(1 - c)^{V_\xi} \tag{19}$$

where c is the probability that a site contains a defect and V_ξ is a correlation volume that grows as ξ^3. Equation (18) says that a defect is uncorrelated and single if it exists (probability c) and none of its neighbors within a correlation volume are other defects. We can rewrite Eq. (19) as

$$c_1 \approx c \exp([\ln(1 - c)]/(T - T_c)^{3/2}) \tag{20}$$

or, using Eq. (18),

$$\tau \approx \exp\left(\frac{T^*}{T - T_c}\right)^{3/2} \tag{21}$$

where T^* is a constant put in for dimensional considerations. If the exponent were 1 instead of 3/2, Eq. (21) would be called the Vogel-Fulcher law. This law [29,30] was empirically determined in the 1920s. Our Eq. (21) has been found in several cases which have been examined in detail to give a better fit than the Vogel-Fulcher law [28,31].

E. Conclusions

We have shown that a mobile defect model leads to stretched exponential relaxation in a glassy material. Even though each jump of a defect is Arrhenius, the averaging over all configurations leads to a jump waiting time density with an infinite mean waiting time. Note that we only need a Poisson distribution of barrier heights to induce the algebraic distribution of waiting times. The model of parallel relaxation pathways (any defects can initiate the relaxation) gives a sharper law for the dielectric relaxation. The relaxation is faster than the motion of any defect and arises out of possible contributions for all of the defects.

We have not said much about identifying possible defects, but candidates range from vacancies to conformational changes. Polycarbonate is the best studied material in this regard [32] where a cis-trans conformation change has been shown capable of transporting along these polymeric chains. The temperature dependence of mobile conformations (defects) has been investigated using NMR and the mobile population was found to follow a Vogel-Fulcher type of law.

The mobile defect theory makes separate predictions about the relaxation

law and the behavior of time scales. It is possible for our theory to find stretched exponential behavior and an Arrhenius law for the time scale. We only get a Vogel-Fulcher type of law if a lattice gas phase transition occurs, which depends on an attractive interaction between defects. In α-SiO_2 defects repel and one can find stretched exponential behavior with an Arrhenius law. Polycarbonate is again a good example of both stretched exponential and Vogel-Fulcher behavior. We envision that defects relax a glassy material. As the temperature is lowered rigid regions grow in number and size as not enough defects are available to relax the entire material. At the glass transition rigidity percolates but the mobile defect population is not zero, so some relaxation still takes place. All single defects would vanish at T_c, so T_g is higher than T_c in our theory, which is in agreement with all experiments.

REFERENCES

1. K. H. Illers and H. Breuer, *Kolloid-Z. 176*:110 (1961).
2. N. G. McCrum, B. E. Read, and G. Williams (eds.), *Anelastic and Dielectric Effects in Polymeric Solids*, John Wiley and Sons, New York, 1967, pp. 242–246.
3. A. F. Yee and S. A. Smith, *Macromolecules 14*:54 (1981).
4. G. C. Berry, H. Nomura, and K. G. Mayhan, *J. Polym. Sci. Part A-2 5*:1 (1967).
5. A. D. Williams and P. J. Flory, *J. Polym. Sci. Part A-2 6*:1945 (1968).
6. A. E. Tonelli, *Macromolecules 5*:558 (1972).
7. J. T. Bendler, *Ann. N.Y. Acad. Sci. 371*:299 (1981).
8. D. T. Clark and H. S. Munro, *Polym. Degrad. Stabil. 4*:83 (1982).
9. M. J. S. Dewar and W. Thiel, *J. Am. Chem. Soc. 99*:4899 (1977).
10. J. F. O'Gara, S. G. Desjardins, and A. A. Jones, *Macromolecules 14*:64 (1981).
11. P. T. Inglefield, A. A. Jones, R. P. Lubianez, and J. F. O'Gara, *Macromolecules 14*: 288 (1981).
12. B. Erman, D. C. Marvin, P. A. Irvine, and P. J. Flory, *Macromolecules 15*:664 (1982).
13. J. T. Bendler and M. F. Garbauskas, *AIP Conference Proceedings 137* (Y. Rabin, ed.), 1985, pp. 227–239. See also D. J. Brunelle and M. F. Garbauskas, *Macromolecules 26*:2724 (1993).
14. A. A. Jones, J. F. O'Gara, P. T. Inglefield, J. T. Bendler, A. F. Yee, and K. L. Ngai, *Macromolecules 16*:658 (1983).
15. B. C. Laskowski, D. Y. Yoon, A. D. McLean, and R. L. Jaffe, *Macromolecules 21*: 1629 (1988).
16. R. L. Jaffe, D. Y. Yoon, and A. D. McLean, *Computer Simulation of Polymers*, Prentice-Hall, Englewood Cliffs, NJ, 1991, pp. 1–14.
17. H. Sun, S. J. Mumby, and J. R. Maple, *J. Am. Chem. Soc. 116*:2978 (1994).
18. H. Sun, S. J. Mumby, J. R. Maple, and A. T. Hagler, *J. Phys. Chem. 99*:5873 (1995).
19. J. T. Bendler, *Computational and Theoretical Polymer Science 8*:83 (1998).
20. H. A. Kramers, *Physica 7*:284 (1940).

21. G. Williams and D. C Watts, *Trans. Faraday Soc. 66*:80 (1970).
22. M. F. Shlesinger, *J. Stat. Phys. 10*:421 (1974).
23. J. Klafter and M. F. Shlesinger, *Proc. Natl. Acad. Sci. USA 83*:848 (1986).
24. W. H. Hamill and K. Funabashi, *Phys. Rev. B16*:5523 (1977).
25. M. F. Shlesinger and E. W. Montroll, *Proc. Natl. Acad. Sci. USA 81*:1280 (1984).
26. H. Scher and E. W. Montroll, *Phys. Rev. B12*:2455 (1975).
27. J. T. Bendler and M. F. Shlesinger, *Macromolecules 18*:55 (1985).
28. J. T. Bendler and M. F. Shlesinger, *J. Stat. Phys. 53*:531 (1988).
29. H. Vogel, *Zeit. Phys. 22*:645 (1921).
30. G. Fulcher, *J. Am. Chem. Soc. 8*:339 (1925).
31. J. J. Fontanella, M. C. Wintersgill, C. S. Coughlin, P. Mazaud, and S. G. Greenbaum, *J. Polym. Sci. 29*:747 (1991).
32. K. L. Li, P. T. Inglefield, A. A. Jones, J. T. Bendler, and A. D. English, *Macromolecules 21*:2940 (1988).
33. J. J. Fontanella, M. C. Wintersgill, and J. J. Immel, *J. Chem. Physics,* In press (1999).

4

Polycarbonate Dynamics by Nuclear Magnetic Resonance

Paul T. Inglefield and Alan A. Jones
Carlson School of Chemistry, Clark University, Worcester, Massachusetts

I. INTRODUCTION

The power of nuclear magnetic resonance (NMR) spectroscopy lies in the ability to observe structure and dynamics at the level of chemical bonds. The primary interactions influencing NMR spectra, such as shielding, dipolar interactions and quadrupolar interactions, are all short range. Thus one can monitor structure over length scales of a few chemical bonds or one can monitor molecular motion occurring over this same length scale.

Motions over this length scale, referred to as local motions in synthetic polymers, can have a significant influence on important technological properties. This is especially true for polycarbonate where it has long been recognized that motions are present in the bulk material and are linked to the impact resistance of glassy polycarbonate [1].

In the last 20 years major developments have taken place in NMR instrumentation and techniques that have allowed the probing of local motions in polymers. In the 1970s the development of multinuclear high-resolution liquids experiments provided the opportunity for structurally specific investigations of local motions [2]. The major breakthrough that stimulated the rapid development of the field of polymer solid state NMR was the development of high-resolution magic angle spinning by Schaefer et al. [3]. A few years later, Spiess [4] continued the development of polymer solid state NMR spectroscopy with the introduction of one- and two-dimensional deuterium experiments. The developers of these

techniques applied them to polycarbonate as a good example of what NMR could contribute to addressing important questions in polymer science. Many other investigators also studied polycarbonate with a wide variety of NMR experiments making it one of the best studied systems. In spite of the generation of new insights and a considerable database on motion in polycarbonate, questions remain and NMR experiments on this material continue.

II. SOLUTION RELAXATION STUDIES

A classical way to study the dynamics of a polymer system is to monitor the changes in motion caused by structural variation of the repeat unit [1]. This approach has been applied to solution spin-lattice relaxation studies of various structural analogs of polycarbonate [5–12] where it is an especially valuable approach because of the structural specificity of NMR spectroscopy. Thus if several different motions are occurring within the polymeric repeat unit each one can be individually monitored by high-resolution NMR experiments and the effect of structural changes on each motion can be considered.

Another piece of information available from a dilute solution NMR study is knowledge of the intramolecular barriers. In studies on bulk polymers, both intramolecular and intermolecular effects are significant and a change in repeat unit structure can alter both of these factors complicating subsequent interpretation. In solution, intramolecular effects dominate, so that changes in structure can be directly connected with variations in specific local motions.

In polycarbonate, several local motions are possible given the structure of the repeat unit. The motions are methyl group rotation, phenylene group rotation, and segmental motion. Methyl group rotation is of little general interest since it is not considered to lead to any important mechanical relaxation. Therefore, attention has centered on the other two motions. The time scale, temperature dependence, amplitude, and geometry of phenylene group motion and segmental motion can each be separately identified since a number of different nuclei in the repeat unit provide complementary information. The dominant relaxation mechanism for both carbon and proton relaxation times in solution is the dipole-dipole mechanism and the orientation of the dipolar vector relative to the local motion allows for differential relaxation effects at different locations in the repeat unit.

In Fig. 1, a series of structures of polycarbonates are listed which have been studied by solution NMR experiments. The polycarbonate listed as chloral-PC is the simplest system to explain how phenylene group rotation can be separately determined from segmental motion [6]. In Fig. 2, the orientation to the

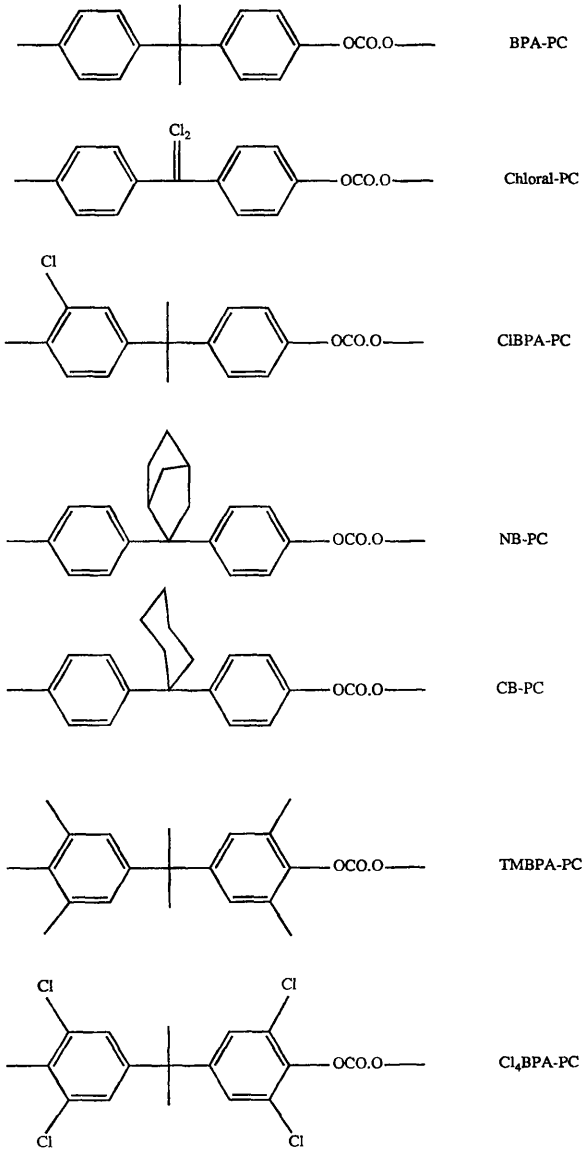

Figure 1 Repeat unit structures for the related polycarbonates studied by solution state NMR.

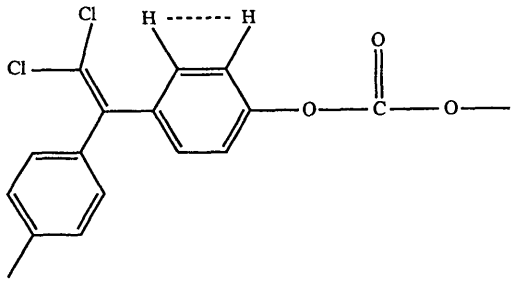

Figure 2 Repeat unit structure for chloral polycarbonate (chloral-PC) showing the principal dipolar interactions.

proton-proton dipolar interaction is shown and it is parallel to the polymer backbone. The only motion that can relax this dipolar interaction is segmental motion (motion that causes reorientation of the polymer backbone) so the time scale of segmental motion can be determined from proton spin-lattice relaxation experiments on the phenylene protons. Measurements can be made as a function of Larmor frequency by varying the static field strength so that information on the shape of the correlation function vs. time or, equivalently, which frequencies are present in the spectral density can be determined.

If attention is shifted to the protonated phenylene carbons, the low natural abundance of ^{13}C precludes the existence of any dipolar interactions except those with protons. Here the dipolar interaction (C-H) makes an angle of 60° with the C_1C_4 axis as shown in Fig. 2, so that both segmental motion and phenylene group rotation affect it and therefore contribute to the carbon-13 spin-lattice relaxation time of these nuclei. Since a description of segmental motion has already been determined from the proton relaxation data and the mathematical descriptions for the combined effects of both motion are known, these relaxation times can be used to establish the time scale and geometry of phenylene group motion.

To quantitatively interpret spin-lattice relaxation times, it is convenient to express these observables in terms of the spectral densities. For carbon-13 spin-lattice relaxation, the equation is as follows [13]:

$$\frac{1}{T_1} = \sum_i \gamma_C^2\gamma_H^2\hbar^2 J_1(\omega_0)/20r_j^6 + 2\sum_j 3\gamma_C^2\gamma_H^2\hbar^2 J_1(\omega_C)/40r_j^6 + \sum_j 3\gamma_C^2\gamma_H^2\hbar^2 J_2(\omega_2)/10r_j^6 \quad (1)$$

where $\omega_0 = \omega_H - \omega_C$ and $\omega_2 = \omega_H + \omega_C$. The Larmor frequency for carbon is ω_C whereas the Larmor frequency for protons is ω_H. The gyromagnetic ratios are γ_C for carbon and γ_H for hydrogen. The carbon–hydrogen internuclear distance is r. Similar expressions for proton-proton relaxation are well known. The spectral density is J and for segmental motion the description most commonly applied is the Hall-Helfand [7,14] function.

$$J(\omega) = 2\{[(\tau_0^{-1})(\tau_0^{-1} + 2\,\tau_1^{-1}) - \omega^2]^2 + [2(\tau_0^{-1} + \tau_1^{-1})\,\omega]^2\}^{-1/4} \times \cos[1/2 \arctan\{2(\tau_0^{-1} + \tau_1^{-1})\,\omega/[(\tau_0^{-1})(\tau_0^{-1} + 2\tau_1^{-1}) - \omega^2]\}] \tag{2}$$

In this function the correlation time for single-bond conformational transition is τ_0 and the correlation time for cooperative or correlated conformational transitions is τ_1. To reasonably determine both correlation times, measurements should be made at several field strengths corresponding to different Larmor frequencies.

The effects of an anisotropic internal rotation in combination with segmental motion are easily incorporated. The spectral density equations for the model combining segmental motion with phenylene group rotation about the C_1C_4 axis can be written as [7]:

$$J(\omega) = AJ_a(\tau_0, \tau_1, \omega) + BJ_b(\tau_{bo}, \tau_1, \omega) + CJ_c(\tau_{co}, \tau_1, \omega) \tag{3}$$

where

$$A = (3\cos^2\Delta - 1)^2/4$$
$$B = 3(\sin^2 2\Delta)/4$$
$$C = 3(\sin^2\Delta)/4$$

For a twofold jump:

$$\tau_{bo}^{-1} = \tau_0^{-1} + \tau_{np}^{-1}$$
$$\tau_{co}^{-1} = \tau_0^{-1}$$

For stochastic diffusion:

$$\tau_{bo}^{-1} = \tau_0^{-1} + \tau_{np}^{-1}$$
$$\tau_{co}^{-1} = \tau_0^{-1} + (\tau_{np}/4)^{-1}$$

The form of the J_a, J_b, and J_c was the same as in Eq. (2) with τ_0 replaced by τ_0, τ_{bo}, and τ_{co}, respectively. The correlation time for internal rotation of the phenyl group is τ_{np}.

A restricted anisotropic rotational diffusion model developed by Gronski [8,15,16] had also been combined with the Hall-Helfand segmental motion corre-

lation function. The composite spectral density for this situation can be written as

$$J(\omega) = \left\{A + \frac{B}{\ell^2}[(1 - \cos\ell)^2 + \sin^2\ell] + \frac{C}{4\ell^2}[(1 - \cos 2\ell)^2 + \sin^2 2\ell]\right\} J^{01}(\omega) + \frac{B}{2}\sum_{n=1}^{\infty}\left[\left(\frac{1 - \cos(\ell - n\pi)}{\ell - n\pi} + \frac{1 - \cos(\ell + n\pi)}{\ell + n\pi}\right)^2 + \left(\frac{\sin(\ell - n\pi)}{\ell - n\pi} + \frac{\sin(\ell + n\pi)}{\ell + n\pi}\right)^2\right] J^{\lambda_n}(\omega) + \frac{C}{2}\sum_{n=1}^{\infty}\left[\left(\frac{1 - \cos(2\ell - n\pi)}{2\ell - n\pi} + \frac{1 - \cos(2\ell + n\pi)}{2\ell + n\pi}\right)^2 + \left(\frac{\sin(2\ell - n\pi)}{2\ell - n\pi} + \frac{\sin(2\ell + n\pi)}{2\ell + n\pi}\right)^2\right] J^{\lambda_n}(\omega)$$

where

$$J^{\lambda_n}(\omega) = 2\{[(\tau_0^{-1} + \lambda_n)(\tau_{01}^{-1} + \tau_1^{-1} + \lambda_n) - \omega^2]^2 + [2(\tau_{01}^{-1} + \lambda_n)\omega]^2\}^{-1/4} \otimes \cos\left[\frac{1}{2}\tan^{-1}\frac{2(\tau_{01}^{-1} + \lambda_n)\omega}{(\tau_0^{-1} + \lambda_n)(\tau_{01}^{-1} + \tau_1^{-1} + \lambda_n) - \omega^2}\right]$$

and

$$J^{01}(\omega) = 2\{[\tau_0^{-1}(\tau_{01}^{-1} + \tau_1^{-1}) - \omega^2]^2 + [2\tau_{01}^{-1}\omega]^2\}^{-1/4} \times \cos\left[\frac{1}{2}\tan^{-1}\frac{2\tau_{01}^{-1}\omega}{\tau_0^{-1}(\tau_{01}^{-1} + \tau_1^{-1}) - \omega^2}\right]$$

with

$$\tau_{01}^{-1} = \tau_0^{-1} + \tau_1^{-1}$$
$$\lambda_n = (n\pi/\ell)^2 D_{\parallel}$$

where $D_{\parallel}$ is the diffusion constant for restricted diffusion and ℓ is the angular amplitude of the restricted diffusion. Here restricted anisotropic rotational diffusion is characterized by two parameters in lieu of the correlation times, $D_{\parallel}$ and

ℓ. If the restricted rotation was a harmonic well, ℓ should be proportional to $T^{1/2}$ and D should be proportional to T.

The application of the preceding interpretational equations to dilute solution spin relaxation measurements on a series of structurally related polycarbonates has produced a reasonable picture of local dynamics reflecting intramolecular barriers and constraints. For bisphenol A polycarbonate (BPA-PC) itself at a concentration of 10 wt% in tetrachloroethane, segmental motion, phenylene group rotation, and methyl group rotation all occur on a time scale of tenths of nanoseconds [7]. This is an ideal time scale for most commercial NMR spectrometers because the inverse of the correlation times for these motions is comparable to the Larmor frequency and variation of the Larmor frequency provides details on the shape of the correlation function. The Hall-Helfand function has proven successful in interpreting segmental motion in these systems with correlated motions having the shorter correlation time and thus dominating relaxation. Phenylene group motion occurs in a fourfold [17] or higher symmetry potential and is treated as stochastic diffusion in the comparisons made here. Methyl group rotation occurs in a threefold potential according to the interpretation developed in these studies. As concentration of BPA-PC is raised, segmental motion and phenylene group rotation slow but methyl group motion is little affected. Thus, although all three motions have very similar times scales in dilute solution only segmental motion and phenylene group motion may be cooperative under these conditions.

The effects of structural variation on segmental motion are summarized in Table 1. Substitution on either the phenylene rings or on the isopropylidene

Table 1 Segmental Motion in Dissolved Polycarbonates

		Apparent activation energy (kJ/mole)		Arrhenius prefactor ($\tau_\infty \times 10^{14}$S)		
Polymer	T_g (°C)	Cooperative segmental (τ_1)	Single backbone rotation (τ_0)	Cooperative segmental (τ_1)	Single backbone rotation (τ_0)	Ref.
BPA-PC	150	19	16	28	1003	7
Chloral-PC	164	17	18	94	409	7
ClBPA-PC	146	23	20	10	130	11
CB-PC	185	17	22	150	50	12
TMBPA-PC	203	23	34	11	3	10
Cl_4BPA-PC	225	23	34	20	3	11
NB-PC	232	24	30	6	17	9

unit slows segmental motion. The activation energy for the correlation time for single-bond rotation in the Hall-Helfand function, τ_0, in dilute solution generally correlates with an increase in glass transition temperature of the bulk polymer as shown in Table 1. The exception, CIBPA-PC, probably reflects poor packing in the bulk which is caused by the asymmetrical substitution of the repeat unit [11].

The effects of structural variation on phenylene group motion is considerably more complicated as seen in Table 2. Substitution can fundamentally change the motion. In BPA-PC and in chloral-PC, phenylene group rotation can be described as complete anisotropic rotation by stochastic diffusion. Substitution on the phenylene group or on the isopropylidene group changes the dominant motion contributing to spin-lattice relaxation from complete anisotropic rotation to restricted anisotropic rotation. Phenylene group motion has generally been correlated with the γ relaxation in bulk polycarbonates by solid state NMR experiments [1,4,5–12]. Those polymers where restricted rotation is seen to dominate contributions to solution T_1 values are generally also seen to have a higher temperature for the γ or low-temperature loss peak in the bulk polymer. The exception to this parallel is NB-PC, which is thought to pack very poorly in the bulk leading to high free volume and thus a low temperature for the γ loss peak [9]. In this case the intramolecular barrier is not the determining factor for the bulk relaxation behavior but rather the intermolecular barriers.

For CB-PC [12], there is also a bulky substituent on the isopropylidene unit much like NB-PC. However, the cyclohexyl group in CB-PC is flexible whereas the norbornyl group in NB-PC is a rigid, fused ring. Good packing with little free volume occurs in CB-PC leading to a higher temperature for the γ loss peak in combination with intramolecular effects slowing phenylene group motion. Poor packing in NB-PC apparently more than compensates for the increase in intramolecular barriers in this system.

The cyclohexyl ring in CB-PC also has an asymmetrical influence on the two phenylene rings in the repeat unit. The cyclohexyl group essentially lies over one of the two phenylene rings and that ring is found to undergo restricted rotation while the other ring undergoes complete anisotropic rotation only slightly slower than that of the rings in BPA-PC. At room temperature in solution slow conformational interchange occurs within the cyclohexyl group, leading to only a single resonance for each carbon in the two types of phenylene rings. Nevertheless, a difference in the dynamics must be considered to produce a satisfactory interpretation.

In CIBPA-PC only one chloro group is introduced on one of the two rings. At lower temperatures the two rings are seen to be inequivalent [11] and both undergo restricted diffusion on the time scale of the spin-lattice relaxation experiment. At higher temperatures, the dominant motion becomes complete anisotropic rotation but it is slower than in BPA-PC. In this case substitution on one

of the two rings slows motion of both rings, indicating cooperativity of phenylene group rotation across the isopropylidene unit.

In those cases where complete anisotropic rotation occurs, an apparent activation energy is given for the motion. This apparent activation energy includes the intramolecular barrier height as well as contributions from solvent viscosity. According to Kramers' theory [18,19] the effects of viscosity can be removed if the temperature dependence of the solvent viscosity is known. However, Ediger et al. [20] have shown that at least in some polymer systems the Kramers theory does not apply and thus the effects of solvent viscosity are not easily eliminated. The apparent activation energies are likely to be higher than the intramolecular barriers by 5 or 10 kJ/mole and this should be considered when making comparisons of the measured quantities with calculated barriers. In bulk systems, the barriers appear to be much higher than the values obtained from dilute solution. This indicates that intermolecular effects are very important in bulk systems and the availability of values for the intramolecular barriers allows for a more precise analysis of the relative roles of the two factors.

III. SOLID STATE RELAXATION STUDIES

Most attempts to study dynamics by NMR in polycarbonate have been made on the sub–glass transition relaxation referred to as the γ relaxation, which occurs at $-100°C$ and a frequency of 1 Hz in BPA-PC. The presence of this significant relaxation below T_g has long been considered a key part of the high impact resistance displayed by polycarbonate. Before high-resolution solid state NMR spectroscopy, only speculation was possible on the repeat unit level motions associated with the γ process.

The first solid state NMR experiment that provided structurally specific information on the nature of the motions in glassy polycarbonate came from wide-line proton measurements on chloral-PC. This system fortuitously has only phenylene protons with the major dipolar interaction parallel to the chain backbone as shown in Fig. 2; thus it offers the prospect of structurally specific information in contrast to most polymers where several chemically distinct protons are present with overlapping wide-line resonances. One of the motions proposed for the γ relaxation was rotation of the whole BPA unit [1]. This motion would partially average the dipolar interaction indicated in Fig. 2 but the observed proton spectrum showed that this interaction was not averaged until the glass transition was reached. Thus the proposed motion could be ruled out for the γ transition based on this structurally specific proton experiment. The proton spectra did show the presence of considerable motion but the only allowed geometry for this motion is rotation about the C_1C_4 axis of the phenylene group.

Solid echo deuterium line shapes indicated that the motion consisted of π flips or jumps between two minima separated by 180°. Carbon-13 chemical shift anisotropy line shapes on an isotopically enriched sample indicated the same geometry of motion. Several other geometrical factors could be identified from these line shapes. First was the presence of fairly large-amplitude oscillation about the same C_1C_4 axis extending over an angular range of 30–40° at room temperature. Second, the π flips were not precise 180° jumps but occurred over an angular range comparable to the range of the librational motion. Other line shape experiments confirmed this geometrical description of motion including carbon-13 proton dipolar experiments. Two-dimensional deuterium NMR experiments emphasized the presence of a wide distribution of π flip-jump angles. To date this is the sole large-amplitude motion identified in polycarbonates.

The time scale of the π flip motion was also linked with the γ or low-temperature loss peak in polycarbonate. The first NMR experiments demonstrating this linkage were proton $T_{1\rho}$ experiments on chloral-PC. Again the fortuitous structure of chloral-PC with only a single kind of proton present allowed for more definitive proton information than is typically possible in a synthetic polymer.

Proton $T_{1\rho}$ experiments were conducted over a 200° range with a characteristic frequency of 44 kHz. The best quantitative interpretation of the relaxation times was produced using the stretched exponential or Kohlrausch-Williams-Watts function. This is one of the earliest applications of this function to NMR data. It allowed not only for a quantitative interpretation of the time and temperature dependence of the NMR data; but once the correlation times and apparent activation energy were obtained, the breadth and temperature of relaxation occurring at the mechanical frequency of 1 Hz could be calculated. A good match was obtained between the relaxation at 1 Hz calculated from NMR data and the observed mechanical response of bulk polycarbonate. This quantitative linkage of time scales left little doubt that π flips are associated with the principle sub–glass transition relaxation in polycarbonate.

A similar quantitative interpretation was developed for BPA-PC itself. The NMR data consisted of proton T_1 and $T_{1\rho}$ on BPA-PC d_6 (deuterated methyl groups) as well as carbon-13 T_1 and carbon-13 chemical shift line shape collapse data. All measurements were made over a 200° range. The stretched exponential form was employed:

$$\phi(t) = \exp -(t/\tau_p)^{\alpha} \tag{4}$$

where the correlation times τ_p were given an Arrhenius dependence. The value of α was found to be 0.15, which corresponds to a distribution of exponential correlation that extends over several decades. The apparent activation energy obtained is 46 kJ/mole, which is consistent with the value obtained form mechanical data [1]. The Arrhenius prefactor is 7×10^{-17} s. The activation energy in the bulk is over twice as much as the value obtained in solution (Table 2), demonstrat-

ing the importance of intermolecular contributions to the barrier to phenylene group motion. Furthermore, the fundamental geometry of the motion changes from fourfold or higher symmetry to twofold in the bulk. The twofold character must arise from the intermolecular interactions of the surrounding matrix.

The angular amplitude of the librational motion is given by L where

$$L = 6.67T^{1/2} - 68.4$$

and T is temperature. Ring flips are allowed to occur any where within the range of angles given by L around to the two minima. The time scale of libration is given by a rotational diffusion constant $D_{\parallel}$ that has the temperature dependence

$$D_{\parallel} = (1.47 \times 10^6 T - 2.2 \times 10^7)^{-1}\ \mathrm{s}^{-1}$$

The contribution of this librational motion to spin-lattice relaxation is governed by the same equations developed by Gronski [15,16] and presented in the section on solution relaxation, except that here they were combined with the Kohlrausch-Williams-Watts correlation function instead of the Hall-Helfand correlation function.

The equation used to predict the temperature and breadth of the mechanical response of polycarbonate based on the stretched exponential function is

$$G(\omega)^{\text{loss}} = \frac{\langle \sigma(0)^2 \rangle}{kT} \int_0^\infty \sin(\omega t)[-\phi'(t)]\,dt \tag{5}$$

and a comparison of the predicted response and the observed response is shown in Fig. 3. One should bare in mind that the amplitude of the mechanical response is set to match the observed result and the NMR-based correlation function only predicts the temperature and breadth of the loss peak for a particular frequency corresponding to the mechanical experiment.

Figure 4 is a relaxation map for polycarbonate including mechanical, dielectric, and NMR relaxation data. This figure indicates the connection between all of these experiments on the low-temperature, γ, transition.

Another extremely important aspect of the information available from NMR is the heterogeneous nature of the relaxation in glassy polycarbonate. By heterogeneous it is meant that the correlation time for phenylene group flips varies for different spatial locations in the sample. Mechanical and dielectric response as well as proton NMR experiments cannot distinguish between heterogeneous relaxation and nonexponential homogeneous relaxation. Nonexponential homogeneous relaxation would occur if all phenylene groups regardless of spatial location had the same relaxation behavior but it was described by a nonexponential function. For instance, the Hall-Helfand correlation function used to described segmental motion in solution is a nonexponential, homogeneous description of

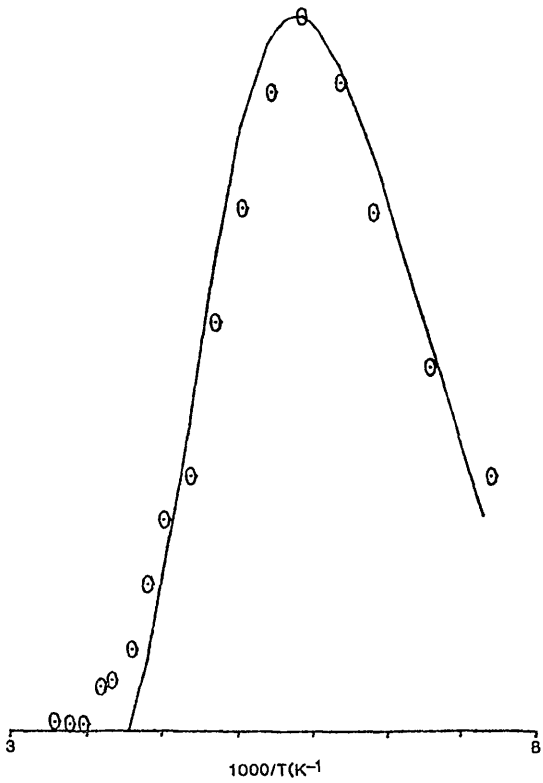

Figure 3 A comparison of the experimental mechanical response with that predicted by NMR for BPA-PC. The points are the mechanical data and the solid line is the simulation based on NMR parameters.

motion. The first experiments that clearly identified the heterogeneous nature of the relaxation in glassy polymers including polycarbonate are the carbon-13 $T_{1\rho}$ of Schaefer et al. [3]. The heterogeneous nature of the relaxation is seen as nonexponential behavior in logarithmic plots of intensity vs. spin lock time. Proton experiments of the same type are more nearly exponential because of rapid proton spin diffusion. The heterogeneous character of glassy polymer dynamics is even more striking in the solid echo deuterium line shapes where fast and slow relaxation are obviously superimposed [4]. Figure 5 shows how a composite line shape for fast and slow π-flip processes arises. The heterogeneous distributional character of these lines shapes is very useful in quantitatively determining the breadth of the distribution of motional rates.

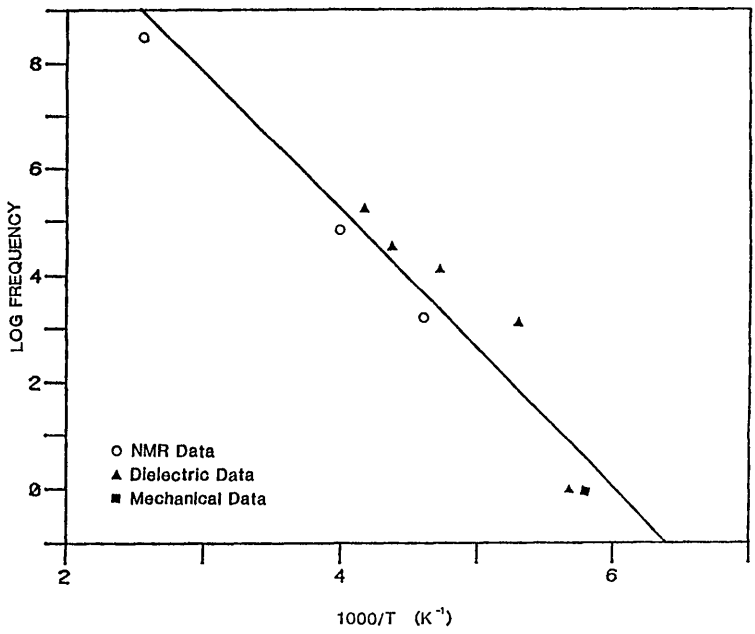

Figure 4 Relaxation map for BPA-PC showing mechanical, dielectric, and NMR data.

The Kohlrausch-Williams-Watts correlation function is readily applied in a heterogeneous form as a sum of exponentials although the physical basis of the derivations of this function for glasses leads to a homogeneous description. The appearance of homogeneous or heterogeneous behavior in an experiment partially reflects the rate of exchange of spatial environments vs. the time scale of the experiment in question. For the NMR experiments discussed here the spatial environments do not exchange on the same time scale though this question has been directly probed in a three-dimensional solid state line shape experiment by Spiess.

Henrichs has investigated the intermolecular influence on the π-flip motion by considering low molecular weight model compounds. For this system, two crystalline forms were produced. In one form π flips were observed over a range of temperatures but in the other form no flips occurred on the NMR time scale. This type of experiment clearly indicates the dominant role intermolecular interaction can play on the rates of motion.

Motion of other parts of the repeat unit of polycarbonate have also been investigated by NMR. Spiess has obtained deuterium line shape data on the methyl groups of the BPA unit. The methyl groups rotate at lower temperatures

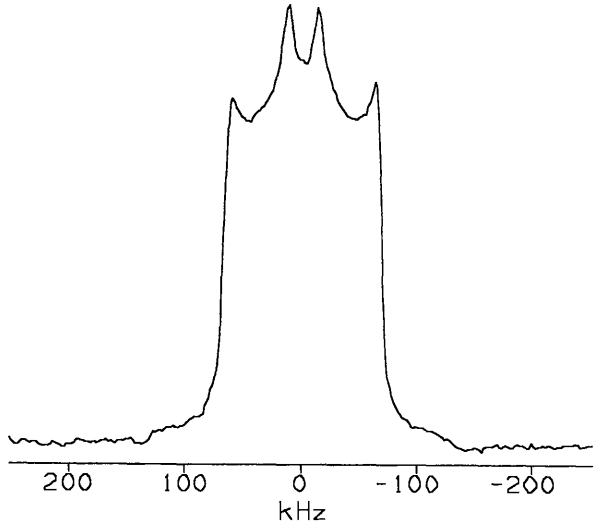

Figure 5 Deuterium NMR line shape for chloral-PC showing the presence of both slow and fast motional components.

than the phenylene groups. Methyl group rotation has a heterogeneous character in the glass but a narrower distribution is observed than for the phenylene groups. This implies less coupling of methyl group rotation to the surrounding matrix than is the case for phenylene groups. Methyl group rotation occurs at a different time scale than is associated with the γ transition and does not coincide with an important mechanical response of the bulk polymeric glass.

Henrichs performed carbon-13 chemical shift anisotropy line shape studies on polycarbonate labeled at the carbonate unit. Surprisingly, almost no line shape collapse of the carbonate carbon resonance occurs in spite of the presence of a significant dielectric loss, which one would assume arises form carbonate motion. The carbonate unit can undergo motion librational motion as large as $\pm 20°$ before significant line shape collapse would be observed.

Similar librational motion of the order of $\pm 10°$ has been reported in the BPA unit for motions other than around the C_1C_4 axis of the phenylene groups. Motions of this amplitude are reported in many glassy polymers but they have a modest effect on NMR line shapes.

Essentially all locations in the repeat unit of BPA-PC have been probed by NMR line shape experiments. The only large-amplitude motion identified is π flips of the phenylene group, but this motion is considered to be an unlikely source of the large mechanical and dielectric response observed in polycarbonate.

The motion would not be very mechanically active since the position of the phenylene group is nearly unchanged before and after the π flip. This motion is coincident in time with the mechanical response so it must either be involved in the mechanically active motion or be a monitor of the motion responsible for the mechanical response.

This leaves the somewhat unsatisfying situation that NMR experiments have not clearly identified the motion responsible for mechanical and dielectric relaxation in the best studied polymer system. It seems that π flips are an unlikely source of the mechanical relaxation and the carbonate unit is hardly seen to move at all. This has led to alternative proposals for the source of the mechanical and dielectric relaxation.

The first of these is a defect diffusion model involving cis-trans isomerization of the carbonate unit. Unfortunately, the very concept of a defect that might only exist at the level of a couple of percentage points makes it unlikely to be observed in an NMR line shape experiment, and indeed no confirmatory experimental information is available for the presence of the defect. A second proposal is that the mechanically and dielectrically active motion is a coupled librational motion of the carbonate unit and the BPA unit. Again, NMR line shape experiments cannot really provide any confirmation because the librational effects are so small. For instance, no time scale or even any more than an upper bound on the amplitude of the carbonate unit can be made from the available NMR data. The last proposal for the mechanically active motion is an intermolecular motion. Clearly intermolecular interactions are very important to the intramolecularly defined motions such as π flips. However, no NMR experiment has yet directly detected intermolecular motion so as to define an amplitude or time scale though such motions seem quite reasonable. The concept of intermolecular and intramolecular cooperativity is attractive in the discussions of motions leading to mechanical or dielectric response but the cooperativity either along the chain or between chains remains to be experimentally characterized. Thus the somewhat unsatisfying situation remains that NMR relaxation, dielectric response, and mechanical response in BPA-PC are not clearly linked with a verifiable molecular level model.

Other approaches to the link of mechanical behavior to NMR relaxation have been made. A direct mechanical-NMR experiment has been carried out by Spiess and coworkers. A sample of deuterated BPA-PC was placed under a tensile stress of 50 MPa, which produces 3% strain, and under these conditions a two-dimensional solid state deuterium line shape experiment was performed. A modest change in the π-flip process in the form of a broader distribution of flip angles was observed. The change shows at least some linkage of mechanical deformation to the flip process but the change in dynamics was quite small, i.e., close to detectable limits. The conclusion drawn remains unchanged in that π flips must

be linked with the process responsible for mechanical relaxation but they themselves are not the process.

The rate of phenylene flip motion did not change under strain but in spin-lattice relaxation experiments performed on polycarbonate under hydrostatic pressure produced by a gas T_1 shifted by a factor of 2–5 at 2500 bar. Spin-lattice relaxation depends on both high-frequency libration and the flip process, making it difficult to assign the change in T_1 to the flip process alone. Values for an activation volume reflecting all processes involved in T_1 was determined as a small fraction of the repeat unit volume.

Many of the structural variations of polycarbonates shown in Fig. 1 and studied in solution have also been studied in the bulk. Carbon-13 magic angle spinning studies of Cl_4BPA-PC, NB-PC, and chloral-PC have been performed as have deuterium line shape studies on tetramethylbisphenol-1-polycarbonate (TMBPA-PC). Chloral-PC is rather similar to BPA-PC as one would expect from the solution results and from mechanical results. In TMBPA-PC and in Cl_4BPA-PC, π flips slowed in the glassy state relative to BPA-PC. Spiess reports a shift of the flip process to higher temperature based on one- and two-dimensional deuterium line shape experiments, which is consistent with mechanical and solution NMR results. NB-PC displays anomalous carbon-13 $T_{1\rho}$ values in the sense that it is very similar to BPA-PC but is brittle. Of course, the mechanical data are also anomalous since a low-temperature loss peak is present much like that in BPA-PC. The solution data indicate that phenylene motion should be hindered in the bulk so this system is intriguing. The survey of structural analogs by solid state NMR does not add sufficient information to identify the molecular source of the mechanical response and experiments on other structural variations continue in the hope that one of these studies will generate the key piece of information to solve the mechanical puzzle.

Another way to modify the low-temperature loss peak or γ transition in polycarbonate is to add low molecular weight diluents. The loss peak is significantly depressed by the addition of 10 or 15 wt% of the appropriate diluent such as the classic antiplasticizer di-*n*-butylphthalate. The proton $T_{1\rho}$ minimum corresponding to the γ transition of the polycarbonate shows a suppression at low concentrations of diluent corresponding to antiplasticization. At higher concentrations the motion of the polymer is enhanced and the diluent itself also enjoys rotational freedom leading to a plasticization effect. The relative levels of antiplasticization and plasticization in polycarbonate upon addition of diluent have been interpreted with a lattice model that focuses on nearest-neighbor contacts.

Deuterium solid echo line shapes have also been used to study polycarbonate motion in the presence of diluent. Again, antiplasticization is observed as a slowing of phenylene flip motion and the distribution of correlation times describing the flip process is seen to broaden. All of these antiplasticization experi-

ments confirm the connection between the flip process and the γ transition but go no further in identifying the exact nature of the molecular processes leading to mechanical response.

ACKNOWLEDGMENT

This work was carried out with the support of National Science Foundation Grant DMR9303193.

REFERENCES

1. A. F. Yee and S. A. Smith, *Macromolecules 14*:54 (1981).
2. F. Heatley, *Prog. Nucl. Magn. Reson. Spectrosc. 13*:47 (1979).
3. J. Schaefer, E. O. Stejskal, and R. Buchdahl, *Macromolecules 10*:384 (1977).
4. H. W. Spiess, *Colloid Polym. 261*:193 (1983).
5. A. A. Jones and M. Bisceglia, *Macromolecules 12*:136 (1979).
6. J. F. O'Gara, S. G. DesJardins, and A. A. Jones, *Macromolecules 14*:64 (1981).
7. J. J. Connolly, E. Gordon, and A. A. Jones, *Macromolecules 17*:722 (1984).
8. M. F. Tarpey, Y.-Y. Lin, A. A. Jones, and P. T. Inglefield, *ACS Symp. Ser. 247*:67 (1984).
9. J. J. Connolly and A. A. Jones, *Macromolecules 18*:906 (1985).
10. A. K. Roy and A. A. Jones, *J. Polym. Sci. B: Polym. Phys. 23*:1793 (1985).
11. J. A. Ratto, P. T. Inglefield, R. A. Rutowski, K.-L. Li, A. A. Jones, and A. K. Roy, *J. Polym. Sci. B: Polym. Phys. 25*:1419 (1987).
12. J. Zhao, A. A. Jones, P. T. Inglefield, and J. T. Bendler, *Polymer 39*:1339 (1998).
13. D. Doddrell, V. Glushko, and A. Allerhand, *J. Chem. Phys. 56*:3683 (1972).
14. E. Helfand, Z. R. Wasserman, and T. A. Weber, *Macromolecules 13*:526 (1980).
15. W. Gronski and N. Murayama, *Makromol. Chem. 179*:1529 (1978).
16. W. Gronski, *Makromol. Chem. 180*:1119 (1979).
17. P. Tekley, *Macromolecules 19*:2544 (1986).
18. H. A. Kramers, *Physica 7*:284 (1940).
19. W. H. Stockmayer, *Pure Appl. Chem. Macromol. Chem. 8*:379 (1973).
20. W. Zhu, D. J. Gisser, and M. D. Ediger, *J. Polym. Sci. B: Polym. Phys. 32*:2251 (1994).

5
Nonbisphenol A Polycarbonates

John Schmidhauser*
General Electric Company, Schenectady, New York

Paul D. Sybert
General Electric Plastics, Mt. Vernon, Indiana

I. AROMATIC POLYESTER CARBONATES

Polyester carbonates find use in applications that require higher heat distortion temperatures than can be obtained from bisphenol A polycarbonate (BPA-PC). The resins are used in high-end automotive reflectors where the heat buildup in the reflector assembly would cause distortion of the reflector and beam pattern with polycarbonate. Because of the resin's combination of clarity, toughness, heat resistance, and flame retardancy (FR) performance, polyester carbonates and their blends have been used in fire helmets and face shields where, in addition to being able to withstand higher temperatures, the resins also exhibit toughness at both temperature extremes. Polyester carbonate and its blends are also used in medical applications that require steam sterilization.

High-heat aromatic polyester carbonates are derived from BPA, isophthaloyl chloride, terephthaloyl chloride, and phosgene. Bayer AG, Dow Chemical, General Electric, and Mitsubishi Chemical Industries, Ltd. first commercialized or marketed experimental resin based on these compositions in the late 1970s and early 1980s. The incorporation of the aromatic ester group increases the glass transition temperature (T_g) without significantly decreasing the ductility of the resins. The resins maintain excellent clarity. The monomers are commercially available at a reasonable price, and the resins can be prepared by processes that are compatible with existing PC facilities.

---

* *Current affiliation:* Elf Atochem North America, King of Prussia, Pennsylvania.

The polyester carbonates have been prepared using aromatic acid and acid chlorides with phosgene and BPA in both homogeneous and interfacial polymerizations. The homogeneous reactions are typically performed with an organic chlorinated solvent and a tertiary amine, normally pyridine [1,2]. The procedures using the phosgenation of the aromatic diacids [3–5] were shown [2] to give less than quantitative incorporation of the ester into the polymer backbone. In the interfacial reaction, BPA is allowed to react with the acid chloride using a tertiary amine or a phase transfer catalyst. Phosgene is then added to complete the polymerization [6–10]. The molecular weight (MW) of the resins has been controlled by the addition of monophenols [11], chloroformates [11], carboxylic acids [12], acid chlorides [12], and amines [13].

Other solution polymerizations have been performed using the less expensive aromatic diacids. The diacids have been reacted with phosgene and BPA at a low pH or, alternately, the diacids have been allowed to react with the bischloroformates of BPA at a pH of 7–8 in the presence of a tertiary amine followed by polymerization at pH 13 [14]. Both polymerization methods significantly reduce the raw materials costs of the resins.

Melt transesterification polymerizations have included the reaction of BPA with diphenyl phthalates [15–17] and diphenyl carbonate or dimethyl terephthalate with polycarbonate [18]. The evaporative extrusion of solutions of aromatic polyarylates and polycarbonates has also been used to prepare polyester carbonates [17,19].

Table 1 Properties of Polyester Carbonates

Property	Test method	Lexan PPC 4501 Resin	Lexan PPC 4701 Resin
Tensile strength, at yield, psi (MPa)	ASTM D-638	9500 (66)	9500 (66)
Elongation at break, %	ASTM D-638	122	78
Flexural modulus, 0.125″ psi (MPa)	ASTM D-790	294,000 (2,000)	338,000 (2,300)
Izod impact, notched, 0.125″ ft-lb/in. (J/m)	ASTM D-256	10 (530)	10 (530)
DTUL, 66 psi, 0.250″ °F (°C)	ASTM D-648	320 (160)	345 (174)
DTUL, 264 psi, 0.250″ °F (°C)	ASTM D-648	305 (152)	325 (163)
CTE, flow X E-5, −40 to 200°F in./in.-F(m/m-C)	ASTM E-831	5.1 (9.2)	4.8 (8.1)

Data obtained from Lexan Resin Data Sheet, GE Plastics.

Table 2 Other Polyester Carbonates

	Monomers	Properties	Ref.
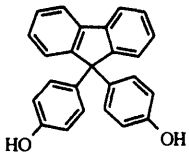	+ ICl + $COCl_2$	High heat	33
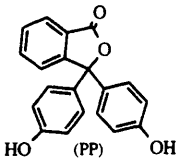	+ TCl + $COCl_2$	High heat	33
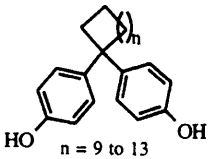	+ ICL/TCl + $COCl_2$	High heat	24,26, 27
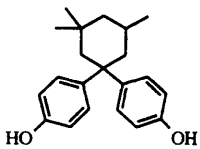	+ ICl + $COCl_2$	High heat T_g 256°C	35
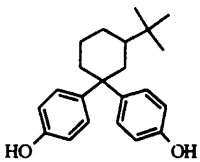	+ ICl + $COCl_2$	High heat T_g 303°C	36
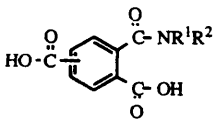	+ BPA + $COCl_2$	High heat, higher Modulus	37,38
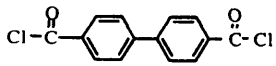	+ BPA + $COCl_2$	High heat, nonyellowing	39
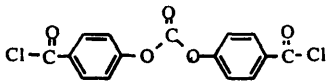	+ PP + $COCl_2$ or BPA	High heat improved ductility	40

ICL, isophthaloyl chloride; TCL, terephthaloyl chloride.

The properties of the polyester carbonates prepared from BPA and iso- and terephthaloyl chloride have been well documented in the literature [2,20–25]. These compositions are typically amorphous. As the ester content is increased, the distortion temperature under load (DTUL) and T_g increases while the melt flow decreases. At a constant ester content, the T_g and the thick section impact strength increases as the iso/tere ratio is decreased. At high iso/tere ratios, the resistance to edge cracking is increased. Typical properties for polyester carbonates are listed in Table 1.

A variety of bisphenols have been copolymerized with iso- and/or terephthaloyl chlorides to increase the T_g of the resins; selected examples are listed in Table 2. In addition, polyester carbonates have been prepared from 4,4′-diphenyldicarboxylic acid chlorides or bis(4-chloroformylphenyl carbonate) in place of iso/terephthaloyl diacid groups (Table 2). The polymers based on 4,4′-diphenyldicarboxylic acid chlorides have shown increased resistance to yellowing on exposure to UV radiation as compared to the corresponding polyester carbonate prepared from terephthaloyl chloride. Finally, dihydroxydiphenyl sulfide has been copolymerized with iso/terephthaloyl chlorides to produce nonhalogen FR polyester carbonates [26] and polyester carbonate blends [27]. Phosphorous comonomers have been added to increase the thermal oxidative stability of the resins.

Polyester carbonates of BPA and iso/terephthalate typically form miscible blends with BPA polycarbonate. These blend DTULs, melt flows, and ductilities between those of polycarbonate and polyester carbonate homopolymers [28,29]. Blends [30,31] of polyester carbonates and polyesterimides, polyamides, and polyimides are typically phase-separated. By controlling the comonomer composition, the continuous phase, ductility, DTUL, and solvent resistance can be controlled. The addition of bromine-containing copolycarbonates can been used to prepare FR blends with low smoke generation [32].

II. SILOXANE-BISPHENOL COPOLYCARBONATES

Extensive research has been done in the last few years on the preparation and use of siloxane-polycarbonate block copolymers. Among other properties, the siloxane block affords a low T_g (−123°C [41]), neutral FR, excellent thermal stability, and good weathering properties. Polycarbonate siloxane block copolymers were first prepared by Vaughn in the mid-1960s [42,43].

Since Vaughn's work, several methods have been developed to functionalize and incorporate the siloxane block into the copolymer (Fig. 1). In most processes, a cyclic siloxane is equilibrated with an acid or base catalyst and the appropriate difunctional siloxane or silane to give the α, ω-difunctionalized siloxane fluid. The length of the siloxane block is controlled by the ratio of cyclic

siloxane to difunctional siloxane or silane [44]. In solution and interfacial polymerizations, the functionallized siloxane fluids are then capped with the desired phenolic or acid chloride groups. The phenol- or acid chloride–terminated siloxane blocks are then added to the interfacial polymerization with the bisphenol and phosgene. Monofunctional siloxane blocks have been prepared from the reaction of 4-acetoxystyrene with α-hydro-ω-methylpolydimethylsiloxane and a platinum catalyst. This hydride terminated fluid was prepared by ring opening polymerization of the cyclic siloxane with lithium trimethylsilylate followed by capping with dimethylchlorosilane [45].

A phosgeneless process was developed whereby BPA-terminated PC oligomers were allowed to react in solution with α,ω-dichlorosiloxane fluid in the presence of a tertiary amine [46]. The PC oligomers were prepared from the reaction of BPA with cyclic polycarbonate or with polycarbonate homopolymer in solution [46] or with homopolycarbonate in the melt [47].

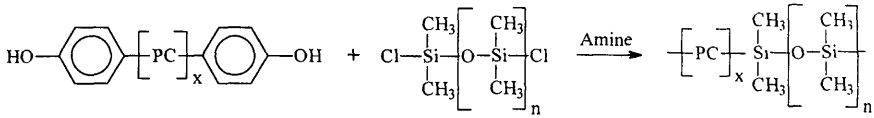

Siloxane block copolymers have been prepared in the melt by the extrusion of functionalized siloxanes with high molecular weight polycarbonates. Both secondary amine–terminated [48] and carboxylic acid–terminated [49] siloxanes have been used (Fig. 2).

Using the synthetic approaches described above, a variety of other block copolymers have been prepared for specific applications (Table 3). The siloxane blocks have been polymerized with a variety of high-heat monomers to increase the ductility and FR of the resins while maintaining significant high-heat performance of the resin. The preparation of tetrabromobisphenol A–siloxane block copolymers has been used to prepare halogenated FR resins with good ductility. Terpolymers were prepared from bisphenol-terminated siloxanes, bisphenol A, and aliphatic diacids to produce resins with high melt flow and good ductility.

Several examples of polysiloxane-polyester carbonate copolymers have been disclosed. The siloxane block copolymers with high isophthalate/terephthalate ratios were shown to have increased resistance to stress cracking when exposed to gasoline [50]. Block copolymers with terephthaloyl chloride gave increased low-temperature ductility [51]. In a separate example, polysiloxane-polyester carbonate copolymers were found to exhibit non-Newtonian melt flow in addition to increased low-temperature ductility [52].

The siloxane-polycarbonate block copolymers prepared from BPA-terminated siloxane blocks have been extensively studied [53–58]. The properties can be varied from a gum to a thermoplastic to a thermoplastic elastomer, depending on the comonomer block lengths and the siloxane content. The clarity and me-

chanical properties of these resins are controlled by the formation and size of the domains. Depending on the domain size the resins are transparent, translucent, or opaque. These resins have been used as impact modifiers, adhesion layers for bullet resistant laminates [59], contact lenses [60], and gas-permeable membranes.

The enhanced ductility obtained by the incorporation of siloxane blocks into polycarbonate was first documented in the mid-1970s. Increasing the siloxane content from 0 to 25 wt% decreased the ductile/brittle transition from −15°C to −110°C in BPA copolycarbonates [57]. The results of this study have been applied to numerous other poly- and copolycarbonates (Table 3). The preparation of siloxane block copolymers of the bisphenol of fluorenone increased the notched Izod strength from 0.5 to 2 ft-lb/in. Typically, the high-heat copolymer prepared from BPA and the bisphenol from 3,3,5-trimethylcyclohexane-1-one gives resins with low notched Izod strengths and brittle failures. The preparation of these resins containing only 5 wt% of a siloxane block increases the Izod impact strength four- to fivefold and gives ductile failures [61].

For increased utility, polysiloxane-polycarbonates were prepared and used as impact modifiers in blends with other homo- and copolycarbonates. Because these block copolymers are stable up to 400°C under a nitrogen atmosphere [62], they afford the best low-temperature ductility along with the best thermostability of any impact modifier for polycarbonates.

The addition of these block copolymers to polycarbonate blends was found to increase the low-temperature ductility and decrease the loss of impact on heat aging. For even greater ductility, blends of polycarbonate, polycarbonate-siloxane block copolymers and EPDM or acrylates were prepared [63].

A synergistic flame retardancy effect was reported for block copolymers prepared from bisphenol-terminated siloxanes and the bisphenol of fluorenone. At 15 to 25 wt% siloxane, the resins had oxygen indices and char yields that were greater than either of the homopolymers [57,64]. This synergism was subsequently reported in 1,1-dichloro-2,2-bis(4-hydroxyphenyl)ethylene-based copolymers [65]. Following these results, extensive research was directed at the preparation and optimization of the nonhalogen FR properties in siloxane-BPA block copolycarbonates.

The incorporation of 3 wt% of siloxane into BPA polycarbonate by melt extrusion afforded compositions that were V-0 at 1/8 in., whereas the control was V-2 according to UL 94 testing [48]. Additionally, these compositions show excellent retention of ductility on heat aging. ABA-Triblock copolymers prepared from siloxane containing monophenols also gave improved nonhalogen FR compositions. These interfacially prepared polymers gave a UL-94 rating of V-0 at 1/16 in. thickness [5]. (A polycarbonate control failed this test because of the flaming drips produced by the first application of the flame.) In a separate example, a copolycarbonate obtained using 2.2 mol% (based on BPA) of 1,2-bis(4-

benzoylchloro)-1,1,2,2-tetramethyldisiloxane failed the UL-94 test because of flaming drips on the first application of the flame. However, compounding this resin in an extruder with 5 wt% of hexaphenyldisiloxane afforded a resin that passed the test with a V-0 rating at 1/16 in. thickness [66]. The replacement of the polycarbonate with siloxane-polycarbonate copolymers in PC/ABS blends has led to V-0 ABS blends that do not contain halogen [67]. In addition, these blends had increased ductility at low temperature.

III. HIGH-T_g POLYCARBONATE

Increasing the heat resistance properties of polycarbonates continues to be a very active area for research. Restricting the rotational mobility of the bisphenol phenylene rings can have a marked effect on the heat properties of the resulting polymers (Fig. 3). When substituents are placed at the ortho positions on the phenylene rings they sterically interact with the carbonate carbonyl oxygen. One substituent on each bisphenol ring (as in 3,3′-disubstituted bisphenols) gives a single barrier to rotation and lowers the polycarbonate T_g. In contrast, two substituents on each aromatic ring (3,3′,5,5′-tetra-substituted bisphenols) gives a double barrier to rotation and increases the polymer's T_g values. The chain packing and chain mobility properties of a series of these ortho-substituted polycarbonates have been analyzed by experimental and computer modeling methods and related to the thermal properties [74]. 3,3′,5,5′-Tetramethylbisphenol **1** polycarbonate (TMBPA-PC) is by far the most widely studied member of this class of polymers [75]. While the reduced impact strength of this polymer has limited its commercial utility, it has been the subject of numerous physical and chemical studies.

Replacing the mobile isopropylidene group joining the BPA phenylene rings with a rigid group is another means of increasing polycarbonate heat resistance. An extreme example of this approach is the spirobiindane bisphenol **2**, where the spiro-fused structure prevents any phenylene ring rotation and the resulting polycarbonate has a T_g of 230°C [76]. Spirodilactam bisphenol **3** has a similar structured subunit connecting the phenylene rings and its PC also exhibits high-heat properties (T_g = 223°C) [77]. The monoindane bisphenol **4** can be used to prepare high-T_g polymers, although the fact that this polycarbonate decomposes at a lower temperature than a structurally related nonfused-ring bisphenol with much lower T_g illustrates that a high T_g may not necessarily be accompanied by an increased processing window [78]. Finally, bisphenols based on the rigid adamantane skeleton are found to possess high T_g values [79], as illustrated by the polycarbonate of 1,3-bis(4-hydroxyphenyl)-5,7-dimethyladamantane **5** with a T_g of 243°C [80].

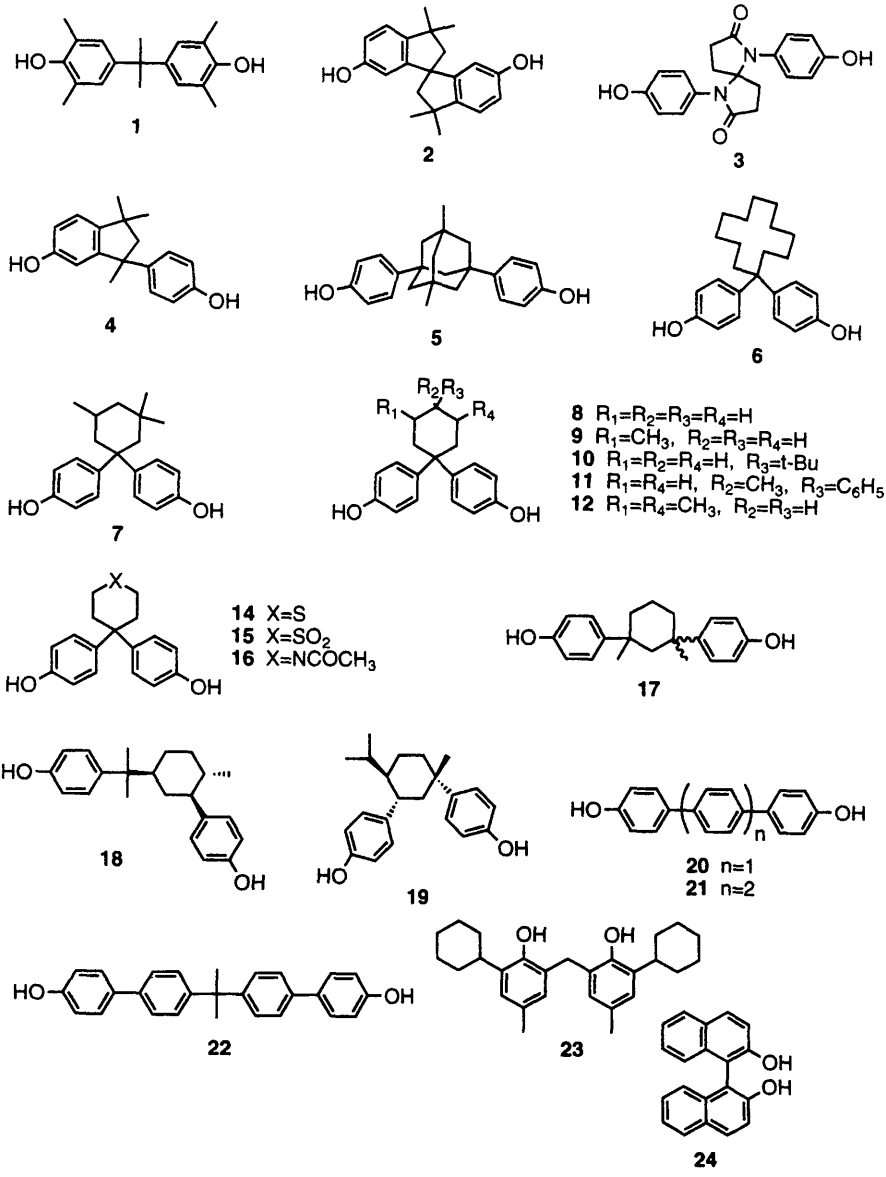

Figure 3 Bisphenols for high-heat polycarbonates.

The motion of the bisphenol phenylene rings may also be restricted by steric interaction with a substituent on the central carbon atom. Bisphenols derived from large-ring aliphatic ketones, such as cyclododecanone **6**, have been known to give polycarbonates with high T_g values [81]. An important new example based on medium-ring cycloaliphatic-based monomers involves the bisphenol of 3,3,5-trimethylcyclohexane **7**. One of the methyl groups at the 3 position of the cyclohexyl ring must have an axial orientation, thereby impeding the rotational mobility of one phenylene ring. The polycarbonate of this bisphenol has a T_g of 239°C [82–85], nearly 60°C higher than that of the polycarbonate of unsubstituted cyclohexyl bisphenol **8** (T_g = 180°C). The structural properties of this polycarbonate have been studied by molecular modeling [86] and attempts have been made to relate the polymer structure to its mechanical and thermal properties [82]. In fact, placement of a variety of substituents at different positions of the aliphatic ring of the bisphenol of cyclohexane leads to a substantial increase in polycarbonate T_g. Specific examples include polycarbonates of the bisphenol of the following cyclohexane derivatives: 3-methyl **9** (T_g = 207°C) [88], 4-*t*-butyl **10** (T_g = 221°C) [89], 4-methyl-4-phenyl **11** (T_g = 199°C) [90], 3,5-dimethyl **12** (T_g = 229°C) [91], and decalin derivative **13** (T_g = 242°C) [92]. Early studies found that bisphenols containing rigid and planar substituents can be used to prepare high-T_g polycarbonates [93]. There has been a resurgance in studies using the bisphenol of 9,9-fluorene [94–96], due in part to an improved synthesis of the bisphenol monomer [97].

Derivatives of cyclohexyl bisphenols where one aliphatic carbon atom has been replaced by a heteroatom (S or N) **14–16** are also found to have high T_g values compared to the unsubstituted cyclohexyl bisphenol polycarbonate [98]. Polycarbonate of cyclohexyl bisphenol where the two phenyl rings are attached to different ring carbons are also found to exhibit high thermal properties. For example, polycarbonates based on the isomeric 1,3-dimethyl-1,3-(4-hydroxyphenyl)cyclohexane monomers **17** have T_g values as high as 195°C [99]. The main two products from the acid-catalyzed reaction of phenol with a wide variety of cyclic monoterpenes were found to be cyclohexane bisphenol derivatives **18** and **19** [100]. Once again, polycarbonates with high T_g values (**18**—PC T_g = 200°C, **19**—PC T_g = 250°C) can be prepared from these bisphenols [101–103].

Increasing the repeat length of the PC monomer can be another method for giving materials with enhanced thermal properties. Copolymerization of 4,4′-bishydroxyter- or quaterphenyls (**20** or **21**) into polycarbonates is reported to give products with slightly elevated T_g values [104]. Similar increases in T_g are found in polycarbonates containing the dihydroxybisbiphenol of acetone (BBPA) **22** [105]. Finally, high T_g polycarbonates of *ortho,ortho*-biphenyls **23** [106] of binaphthyls **24** [107] are prepared by anionic ring opening polymerization of cyclic carbonate monomers.

IV. OPTICAL MATERIALS

Bisphenol A polycarbonate is currently the material of choice for many optical applications such as lenses and CDs. The utility of this material, due to a combination of properties such as high physical strength, low water absorption, high transparency, and good flowability, is detailed in a separate chapter. However, several material properties of BPA-PC such as birefringence and refractive index are not ideally suited to demanding future optical applications such as in erasable/rewritable optical data storage disks. Therefore, numerous polycarbonates based on monomers other than BPA have been prepared and their optical properties have been investigated.

The mechanism of optical anisotropy in BPA-PC was investigated by studying as-molded and annealed samples using a rotating analyzer birefringence measuring system [108]. This study concluded that the optical anisotropy relates to the molecular orientation of the constructive units, particularly the polarizing phenyl groups all located in the polymer backbone. Therefore, while the birefringence of BPA-PC can be minimized ($D \sim 20$ nm at 30°) by processing conditions, a polycarbonate with a modified molecular structure must be used to achieve lower birefringence properties.

A number of polymers with phenyl rings out of the plane of the PC backbone have been investigated (Fig. 4). The spirobiindane bisphenol (SBI) is an outstanding example of using structural modification to minimize polymer birefringence [109]. The spiro-fused structure rigidly holds the two phenyl rings perpendicular to each other, so that polymers consisting of mostly SBI monomer and the balance BPA can be prepared with zero orientational birefringence.

Efforts to reduce polycarbonate birefringence by modifying the bisphenol structure have been reviewed [110–113]. In one detailed study the bisphenol of acetophenone was found to have roughly 50% reduced birefringence compared to BPA-PC (stress-optical constant of 1.8×10^{-9} Pa^{-1} vs. 3.6×10^{-9} Pa^{-1}) [114–116]. The structurally similar benzyl-substituted bisphenol PC has a stress-optical constant that is higher than that of BPA-PC. Molecular mechanics calculations suggest that the phenyl group in the side chain adopts an orientation parallel to the polymer backbone, leading to a higher optical anisotropy [112]. Further illustrating the subtlety of the polymer structure–property relationship, polymers based on the bisphenol of dibenzyl ketone [118] or the bisphenol of 4-phenylbutan-2-one [119] each have lower photoelastic coefficients (46 and 41.5 Brewsters, respectively) compared to BPA-PC (73 Brewsters).

Other polymers with aromatic substituents have been prepared for optical applications, including those based on the following bisphenols: 4-methyl acetophenone bisphenol (optical elasticity coefficient = 43 Brewsters) [120], 9,9-bis(4-hydroxyphenyl) fluorene [121–123], bis(4-hydroxyphenyl)anthracene and

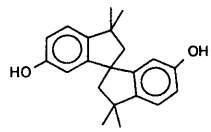

1

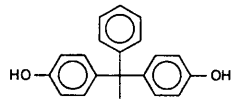

2

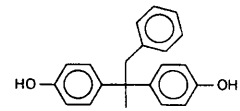

3

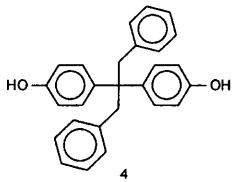

4

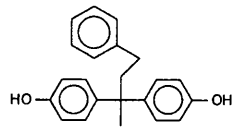

5

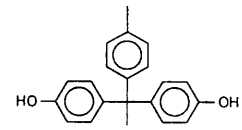

6

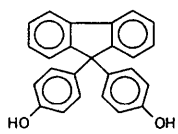

7

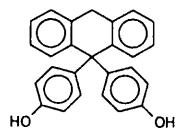

8

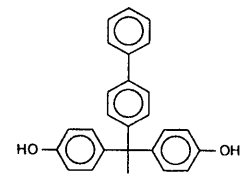

9

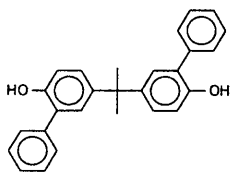

10

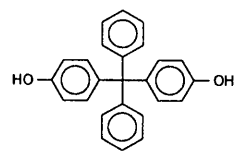

11

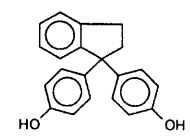

12

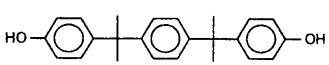

13

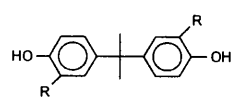

14, R = Me
15, R = *i*-Pr
16, R = cyclohexane
19, R = *t*-butyl

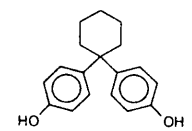

18

Figure 4 Bisphenols for polycarbonate for optical applications.

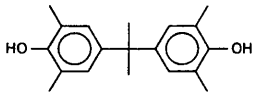

17

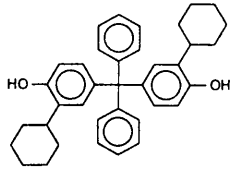

20

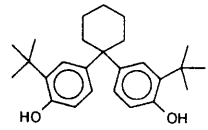

21

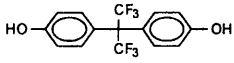

22
23 = d_8

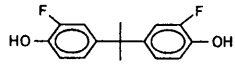

24

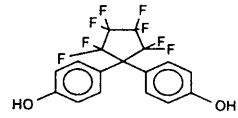

25

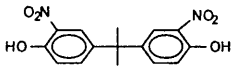

26

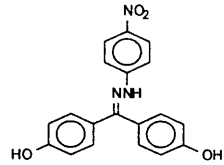

27

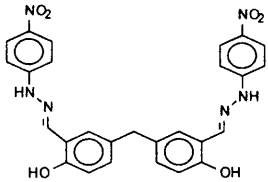

28

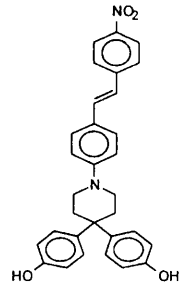

29

its derivatives [124], 1-(4-biphenyl)-1,1-(4-hydroxyphenyl)ethane [125], 3,3′-diphenyl BPA [126,127], 4,4′-dihydroxytetraphenylmethane [128], and the bisphenol of indanone [129]. Finally, 1,1-bis(4-hydroxyphenyl)-*p*-diisopropylbenzene and its meta isomer have been copolymerized by themselves or with other bisphenol comonomers to prepare polycarbonates for optical disk applications [130].

Numerous alkyl-substituted bisphenols have been used to prepare polycarbonates with improved optical properties. Aliphatic groups do not contribute to birefringence, so that increasing the aliphatic content of a polycarbonate is another approach to minimizing this polymer property. Other benefits imparted by incorporating aliphatic groups into polycarbonates include lower moisture absorption and in some cases improved melt flow. Bisphenols used to prepare these materials include 3,3′-dimethyl BPA (optical elastic modulus = 41 Brewsters) [131], 3,3′-diisopropyl BPA [132], 3,3′-dicyclohexyl BPA (optical elastic modulus = 29 Brewsters) [133], 3,3′,5,5′-tetramethyl BPA (birefringence = 2 nm and 0°, 8 nm at 30°) [134], and the bisphenol of cyclohexane [135]. A series of patents describes polycarbonate copolymers containing two or more of these aliphatic-substituted bisphenols, and several examples include, in addition, 3,3′-di-*tert*-butyl BPA [136]. Polycarbonates prepared from bisphenols that have substituents on both the central carbon atom and the ortho positions of the aromatic rings can possess very low photoelastic coefficients, as illustrated by PCs of 1,1-diphenyl-1,1-bis(3-cyclohexyl-4-hydroxyphenyl)methane [132] and 1,1-bis(4-hydroxy-3-*tert*-butylphenyl)cyclohexane [138] (photoelastic coefficient or 9 and 23 Brewsters, respectively).

The aliphatic content of polycarbonate can be increased by using monomers that contain long-chain hydrocarbon segments [139] or aliphatic spiro-ether segments [140]. In a similar manner, polycarbonate-ester copolymers can be prepared from bisphenols and aliphatic diacids. For example, a copolymer of dodecanedioic acid, phosgene, and the 9,9-bisphenol of fluorene possess outstanding optical properties (photoelasticity = 11 Brewsters) [141]. Copolycarbonates between a series of bisphenols and tetramethylcyclobutane diol have been prepared as another technique to learn the polycarbonate polarizability, although cloudiness from partial crystallization would limit their utilization in optical application [142,143].

In some optical applications, such as optical guides and claddings, it is desirable to have a material with a low refractive index. It is well established that fluorine atom substituents can contribute to a low molar refraction. Not surprisingly, a number of fluorinated bisphenols have been used to prepare polycarbonates, including hexafluoro-BPA, either as a homopolymer [144] or as a copolymer with 9,9-bis(4-hydroxyphenyl)fluorene, perdeuteriohexafluoro-BPA [145], and 3,3′-difluoro-BPA [146]. Polycarbonates prepared from 1,1-bis(4-hydroxy-

phenyl)octafluorocyclopentane have heat properties comparable to those of BPA-PC, but a much lower refractive index [147].

Nonlinear optic materials (NLOs) are a class of materials that change the frequency of the light they transmit and thereby fill applications where optical signals drive, e.g., integrated circuits or fiberoptic communication networks. Bisphenols that have been used to prepare polymers with these properties include 3,3′-dinitro-BPA [148] and aryl hydrazones, such as the 4-nitrohydrazones of 4,4′-dihydroxybenzophenone or of 5,5′-methylene bissalicylaldehyde [149]. Preparations of polycarbonates containing bisphenols substituted with NLO functional groups such as pyrazolines, benzidines, hydrazones, and carbazoles have been described. Finally, copolymers of 4,5-bis(4-hydroxyphenyl)-2-(4-nitrophenyl)oxazole have been prepared by ring opening polymerization of substituted cyclic polycarbonate oligomers [150].

V. MATERIALS FOR GAS TRANSPORT APPLICATIONS

The gas transport properties of a polycarbonate can determine whether that material is suitable for use in varied applications ranging from gas or moisture barriers with low permeabilities to gas separation membranes with high permeabilities and gas pair selectivities. However, general relationships between polymer structures and these gas transport properties have not existed. As a consequence, a large number of structurally different polycarbonates have been prepared both in trial-and-error attempts to obtain materials with desired transport properties and to parameterize potentially predictive structure–property models. For example, one early study included the helium and carbon dioxide permeabilities of four different polycarbonates [151]. In a more recent study [152,153], 24 structurally different polycarbonates were prepared and their oxygen permeabilities were found to vary by nearly a factor of 200 between the least and the most permeable materials.

Attempt to prepare polycarbonates with gas barrier (low permeability) properties have achieved only limited success. While materials based on monomers with polar functionality such as cyanobisphenol **1** and ester bisphenol **2** have oxygen permeabilities 25 times lower than BPA-PC [154], they are still only considered moderate barrier materials, comparable with PET polyester. Another approach to preparing barrier polycarbonates involved the use of compact bisphenol monomers that have minimal free volume in the glass, such as 3,3′-dihydroxydiphenyl ether **3** [155]. Polycarbonates with improved moisture barrier properties have been prepared from bisphenols that have large hydrocarbon substituents such as phenyl groups on either the aromatic rings, bisphenol **4** [156] or in place of the geminal dimethyl groups, bisphenol **5** [157].

While glassy polymers such as polycarbonates generally have lower gas permeabilities than rubbery polymers, they exhibit much higher separation selectivies to relevant gas pairs such as N_2/O_2, CO_2/CH_4, and H_2/CH_4. This property, along with their inherent toughness and thermal resistance properties, has created much interest in the use of polycarbonate as gas separation membrane materials. The gas transport properties of polymeric materials, including structurally varied polycarbonates, have been the subject of several recent review articles [158–161].

Studies of series of bisphenol polycarbonates where substituents on both the aromatic ring and the central carbonate have been systematically changed have begun to shed light on the relationship between polymer structures and gas transport properties. Most significantly, sterically large substituents that inhibit either polymer segmental motion and/or polymer interchain packing give materials with high gas permeabilities. Elucidating a relationship between polymer structure and gas pair selectivity has proven to be more problematic, and most polycarbonates follow the general rule that higher gas permeability is accompanied by lower gas separation selectivity properties [162].

The effects of placing substituents on the aromatic ring of the bisphenol A repeat unit is considered first. Placing one methyl group at the ortho position of each polycarbonate phenol ring reduces the oxygen permeability of the polymer by a factor of 5, while the tetramethyl bisphenol A (TMBPA) **6** polycarbonate (two methyl groups on each aromatic ring) has an oxygen permeability four times greater than the unsubstituted PC [152,153]. The gas separation coefficients for a series of three tetra-substituted aromatic polycarbonates have been measured [163]. While the tetrachloro- (**7**) and tetrabromobisphenol (**8**) A polycarbonates have lower gas permeabilities than TMBPA-PC (**8**), the high gas selectivites of particularly the tetrabromo material (TBBPA-PC) have lead to extensive investigation of its use as a gas separation membrane material. For example, patents have detailed the use of this material in N_2/O_2 separation systems (PO_2 = 1.4 Barrer, PO_2/PN_2 = 7.4) [164,165] and for H_2 recovery (PH_2 = 5 Barrer, PH_2/PCH_4 = 25) [166]. A number of reports supply information that is pertinent for the use of TBBPA-PC in membrane applications. Very high molecular weight polymer (IV up to 0.9, MW > 200,000), which would have improved toughness, can be prepared in a two-step process where first TBBPA is reacted with phosgene to form oligomeric chloroformates, which are subsequently condensed by the addition of an amine catalyst, 4-diethylaminopyridine [167,168]. The polymer separation membrane films can be fabricated by casting a polymer solution onto an antisolvent, and to aid in the choice of solvent/nonsolvent systems the solubility properties of TBBPA-PC in over 100 organic liquids have been determined [169]. Finally, methods to crosslink TBBPA-PC illustrate another approach to increasing the toughness of gas separation membranes [170,171].

A number of studies have investigated the changes in polymer gas transport properties that accompany replacement of the geminal dimethyl groups of the BPA monomer with different substituents. Polycarbonates containing sterically compact substituents such as norbornane **9**, cyclohexyl **10**, dichlorovinylidene (BPC) **11** [172], or phenyl **12** [173] exhibit transport properties similar to those of BPA-PC. In contrast, polymers containing large or motion-restricting substituents such as trifluoromethyl (as in HFBPA (**13**) [174,175], trimethylcyclohexyl [176], phenolphthalein [177], or fluorenone [173] typically exhibit higher gas permeabilities with lower gas pair selectivities compared to BPA-PC. The spirobiindane bisphenol PC is different that the other substituted materials in that the two aromatic rings are joined as spiro-fused indane groups, giving a rigid, helically twisted conformation in which the carbonate links are held out of plane to each other. This open, rigid structure gives both high O_2 permeability (7.0 Barrer) and high O_2/N_2 selectivity (5.1) [178].

There are indications that gas transport effects caused by placing substituents on both the aromatic ring and the central carbon atom of the bisphenol monomer are roughly additive. For example, placing a single methyl group on each aromatic ring lowers the oxygen permeability of the polymer regardless of the structure of the substituent on the central carbon atom [152,153]. Conversely, very high gas permeabilities and gas pair selectivities are obtained for "hybrid" materials that combine the structural features of the tetra-substituted aromatic bisphenol rings with the large bistrifluoromethyl groups at the central carbon, illustrated by the polycarbonates of tetramethylhexafluorobisphenol (TMHFBP-PC) (PO_2 = 32 Barrer, PO_2/PN_2 = 4.1) [174], and tetrabromhexafluorobisphenol (PO_2 = 9.7 Barrer, PO_2/PN_2 = 5.4) [179].

Gas separation membranes that can function in high-pressure and high-temperature environments are necessary for some applications. Therefore, the performances of some of the substituted PC materials have been evaluated under these extreme conditions. Gas transport properties of TMBPA-PC and TMHFBP-PC have been evaluated up to 200°C [180], and the effects of different thermal annealing histories on TMBPA-PC's properties have been reported [181]. Conditioning TMBPA-PC or HFBPA-PC to CO_2 pressures up to 900 psi leads to a volume dilation and increases in gas permeability and solubility properties [182].

Another method for modifying a gas separation membrane material involves adding a second polymeric component, so that gas transport properties between blends of substituted polycarbonates and other polymers have been reported. For example, a comparison between blends and random copolymer of BPA-PC and TMBPA-PC found that the copolymers have lower gas permeability, diffusion, and solubility properties than the blends [183]. Gas transport properties for miscible blends of TMBPA-PC with styrene/acrylonitrile copolymers [184] and with polystyrene [185] have been reported. Finally, the effects of high-

pressure carbon dioxide conditioning on the transport properties of BPC-PC and polymethyl methacrylate have been investigated [186].

VI. HIGH-MELT-FLOW POLYCARBONATES

The balance of melt flow and other physical properties must be optimized to function in some end users' applications. Several approaches have been taken to achieve this, including variations of the MW of the resin, improved end-capping agents, addition of plasticizers, blending of high- and low-viscosity resins, and modification of the polymer backbone. Typically, the addition of plasticizers will decrease the ductility or the retention of ductility of polycarbonate and may cause plate-out problems. The preparation of blends of polycarbonate with high-flow non-PC resins typically causes a loss in clarity. In cases where the end-user has needed either extremely high flow or high flow and good ductility, especially with clarity, the suppliers have turned to the modification of the polymer backbone. Several methods have been used to accomplish this:

Modification of the bisphenol
Incorporation of aliphatic diacids
Incorporation of aliphatic diols
Incorporation of siloxane blocks (see Section II)

Extensive research has been done on the modification of the bisphenol vs. the T_g of the resin [187,188]. This work is illustrated with high-viscosity polyester carbonates (Table 4). The resins were prepared with 50 mol% isophtha-

Table 4 Modification of the Bisphenol in Aromatic Polyester Carbonates for Improved Melt Flow[a]

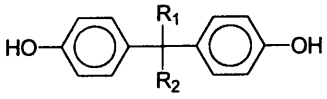

Bisphenol			
R^1	R^2	T_g	KI[b] (300°C)
CH_3^-	CH_3^-	171	24,620
H^-	$CH_3(CH_2)_{10}^-$	53	—
H^-	CH_3^-	155	18,840

[a] Polymer composition: isophthaloyl chloride and phenol were 50 and 2.1 mol% of the bisphenol used.
[b] KI = Kasha index (see Ref. 3).
Data taken from Ref. 200.

loyl chloride (based on the bisphenol). The resin prepared with BPA has a T_g of 170°C and has a low melt flow (high KI). The use of 1,1-bis(4-hydroxyphenyl)ethane in place of BPA depresses the T_g by 10% and increases the melt flow by 20%. The use of a bisphenol with a long-chain aliphatic group, 1,1-bis(4-hydroxyphenyl)dodecane, dramatically decreases the T_g to an unacceptable level (53°C). Thus, the structure of the bisphenol along with the amount copolymerized with BPA can be used to balance the T_g and melt flow of the resin.

The melt flow has been increased, with some loss in the T_g, by the copolymerization of various aliphatic dicarboxylic diacids with BPA [189,190]. The incorporation of ~10 mol% of the diacid gives greater than two times the melt flow of the polycarbonate control without sacrificing the ductility of the resin (Table 5). These resins are claimed to have excellent clarity. In another comparison, stearic acid end-groups were used to depress the T_g of the resin (Table 5). This method was successful at increasing the melt flow, but at the expense of the ductility of the resin [189].

The incorporation of 10–25 mol% of resorcinol into BPA polycarbonate increases the melt flow by 20–40% at similar intrinsic viscosities [191]. The increase in melt flow is accompanied by a 5–10°C decrease in the DTUL.

The incorporation of aliphatic diols has been used to decrease the T_g and increase the melt flow of the copolycarbonates. For example, 2,2-dimethylpro-

Table 5 Incorporation of Aliphatic Dicarboxylic Acid in BPA Polycarbonate for Improved Flow and Ductility[a]

IV (dL/g)[b]	T_g (°C)	MFI[c]	Notched Izod[d]
0.48	124	46	704
0.48[e]	149	18	728
0.48[f]	126	34	64
0.51	124	32	781
0.52[e]	149	11	770
0.53	123	27	772
0.53	131	19	96
0.62	127	13	883
0.63[e]	150	5	875

[a] Copolymers contain 10 mol% of dodecanedioic acid. End-cap level was adjusted to obtain the various intrinsic velocities (IVs).

[b] Intrinsic viscosity in methylene chloride.

[c] Melt flow index at 300°C (g/10 min).

[d] Notched Izod strength at room temperature measured according to ASTM D-256 (J/M).

[e] Control-polycarbonate homopolymer.

[f] Stearic acid end-capped BPA polycarbonate homopolymer.

Data taken from Ref. 189.

panediol has been incorporated into polyester carbonates through the bischloroformate of the diol [192]. The melt index increased by ~35% with the incorporation of 4 mol% of the diol without loss in the ductility of the resin (Table 6). The increase in melt flow was accompanied with a slight loss in the DTUL (7°C).

A second method to incorporate the aliphatic diols into the polymer backbone is by the reaction of the diol with an alkyl hydroxybenzoate to form a bishydroxy ester.

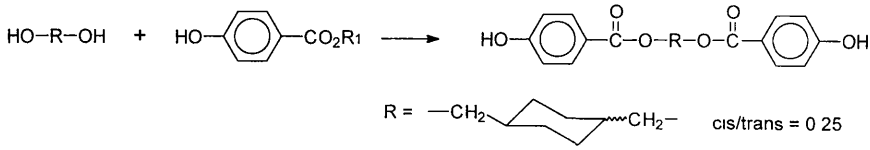

The incorporation of ~20 mol% of butanediol (through the butanediol bischloroformate) along with the bishydroxy ester in BPA polycarbonate decreased the T_g from 150°C to 122°C.

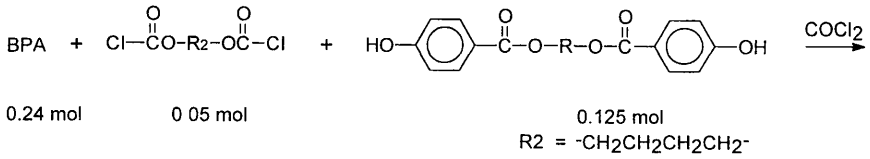

The melt flow decreased dramatically: the KI [3] of the homopolymer = 9220 as compared to a KI of 425 for the copolymer [193].

Block copolymers increase the melt flow of polycarbonates while maintaining or improving the ductility of the resins. The incorporation of hydroxy-

Table 6 Use of Aliphatic Diols to Increase the Melt Flow of Polyester Carbonates[a]

Diol content[b]	IV[c]	Melt index[d]	NI[e]	DTUL[f]
0	0.53	0.73	6.5	163
2	0.52	0.80	6.5	163
4	0.53	0.99	6.5	156

[a] BPA polyester carbonate composition: 52.4 mol% terephthaloyl chloride, 9.5 mol% isophthaloyl chloride, 5 1 mol% *p-tert*-butyl phenol.
[b] Diol = 2,2-dimethyl propane diol. Content in mol% of BPA monomer.
[c] The intrinsic viscosity measured in methylene chloride at 25°C (dL/g).
[d] The melt index was obtained according to ASTM D-1238 (modification O).
[e] Notched Izod at room temperature according to ASTM D-256
[f] The heat distortion temperature (°C) under load was obtained according to ASTM D-648.
Data taken from Ref 192.

Table 7 High-Flow Polybutadiene-b-Polycarbonate Copolymers

Wt% butadiene	Notched Izod impact (ft-lb/in.) 1/8″	1/4″	KI[a]	T_g (°C)	DTUL (°C)
0	18	2.1	6390	149	132
5	17	8	2700	148	123

[a] KI = Kasha index (see Ref. 3).
Data obtained from Ref. 10.

[194–197] or acyl chloride-[198] terminated butadiene or isobutylene blocks gave resins with greater than twice the melt flow and with better thick-section ductility (Table 7). These resins have excellent retention of ductility on heat-aging as compared to the homopolymer control [194]. Although no loss in the polycarbonate T_g was noted, the DTUL did decrease slightly. The lack of loss in the T_g was believed to be due to good phase separation of the PC block from that of the polybutadiene or polyisobutylene block. Another soft block used for this purpose was polycaprolactone [199].

The use of the above technology to incorporate low levels of flexible groups into the polymer chain has led to the commercialization of high-flow ductile resins (Table 8). At the same ductility significantly higher flow can be obtained. As with the resins above, some loss in DTUL is sacrificed for the improved flow. These resins are especially useful in thin-walled or complex, difficult-to-fill parts.

Table 8 Comparison of High-Flow Resins vs. Standard Polycarbonate Resins

Resin	Resins with the following notched Izod values (ft-lb/in.) 12	13	16	17
MFI (g/10 min, 300°C, 1.2 kg):				
Lexan SP resins	48	22	16	10
Lexan resins	25	18	11	9
DTUL (264 psi, °F):				
Lexan SP resins	225	228	230	232
Lexan resins	260	265	270	270

Data obtained from the Lexan Polycarbonate Resin Property Guide, GE Plastics. Registered Trademark of General Electric Company.

VII. FLAME RESISTANT POLYCARBONATE

Halogenated bisphenol polycarbonates have superior ignition resistance properties. By far the most frequently cited examples involve 3,3′,5,5′-tetrabromobisphenol A 1 (TBBPA) PCs and co-PCs. New processes to prepare high molecular weight TBBPA PCs have been described in the Gas Transport Materials section. Copolymers of BPA and TBBPA can have six types of endgroups, the concentrations of which vary depending upon the polymerization method of preparation. These endgroup compositions have been correlated with copolymer isolation and processing properties [201]. Oligomeric TBBPA PC can serve as an intermediate to high MW polymer or as a flame retardant additive to polymer formulations. Details of an HPLC analytical method to characterize mixtures of these oligomers have been reported [202]. Treating BPA with two equivalent of bromine in N_2-sparged methylene chloride solution gives the 3,5-dibromo BPA monomer **2** with 96% selectivity [203]. Properties of this bisphenol's polycarbonate, prepared by a two step polymerization process, have been compared to those of BPA PC and a 50/50 BPA/TBBPA coPC.

Polycarbonates based on the 1,1-dichloro-2,2-bis(4-hydroxyphenyl)ethylene monomer **3** (bisphenol C) are recognized to be highly flame-resistant, with an oxygen index of 56 for the homo-PC compared to 26 for BPA-PC [204]. The mechanism of char formation in this family of polycarbonates has been extensively studied [205]. Fluorinated bisphenols can also be used to prepare flame-retardant (V-O) polycarbonates [206].

Nonhalogenated heteroatom-containing comonomers can also impart flame-retardant properties in polycarbonates. For example, siloxane copolymers are generally flame-resistant (see separation section). However, one study of siloxane copolymers with inherently flame-retardant bisphenol comonomers found one example (bisphenol of fluorenone **4**) where the siloxane and the bisphenol exhibited synergistic flame retardancy and one example (bisphenol C) where the siloxane actually lowered the PC's flame resistance [65]. Sulfur-containing bisphenols can improve flame resistance, and a new process to prepare high molecular weight co-PCs with up to 80 mol% sulfonyl diphenol **5** has appeared [207]. Bisphenols that combine both sulfur and halogen substituents such as BIs (3,5-dibromo-4-hydroxysulfide) can be used in small amounts to give flame-retardant polymers (10%, V-O) [208].

The addition of phosphorous compounds as additives or comonomers is a general method to make flame-retardant polymer compositions [209] and this strategy has been successfully used with polycarbonates. Various bisphenol carbonate/phosphonate polymers have been prepared [210]. In addition, various phosphorus-substituted dihydroxy aromatic compounds have been used as comonomers to form polycarbonates. Examples include bis(4-hydroxyphenyl)phenyl (or methyl) phosphine oxide (**6** or **7**) [211], bisphenols with a phosphine oxide

substituted on the aliphatic group joining the bisphenol aromatic rings, e.g., **8** [212], and polycarbonates containing phosphine oxide– [213,214] or bisphosphine oxide– [215] substituted hydroquinones, **9** or **10**.

The flame retardancy of polycarbonates can be increased by using monomers with minimal aliphatic content and maximum aromatic content. For example, using either 4,4′-dihydroxybiphenyl **11** [216] or hydroquinone **12** [217] as a comonomer increases the flame resistance of the PC. Copolycarbonates based on phenolphthalein **13** exhibit improved heat resistance, high flame resistance, and high char yield [218]. The mechanism of thermal degradation of phenolphthalein polycarbonates has been studied [219]. In addition, pyrolysis studies of homopolymers of eight phenolphthalein derivatives, including phthalimides and chloro- and bromophenolphthalein derivatives, have been reported [220]. Finally, pyrolysis studies of copolycarbonates of BPA with phenolphthalein or 4,5,6,7-tetrabromophenolphthalein bisphenol **14** correlate comonomer content with oxygen index and char yield [221].

VIII. ELECTROPHOTORESPONSIVE MATERIAL APPLICATIONS

Polycarbonate has been widely used as a matrix material in electrophotoresponsive applications. These organic photoconductors have become the preferred photoreceptor for many plain paper copiers and laser printer systems. Currently, most organic photoconductors consist of a thin charge generator layer (CGL) covered by a thicker charge transport layer (CTL). The CTL is a mixture of the matrix resin and the actual charge transport material (CTM). CTMs are a family of electron donor molecules that are responsible for hole transport to the outermost layer of the system where surface charge is neutralized to form an electrostatic image that is developed by a thermoplastic toner. To provide good charge mobility the CTL can contain up to equal amounts of the CTM and the binder resin. Therefore, the binder resin must possess a combination of properties to function in this application including miscibility and compatibility with the CTM, high carrier mobility, transparency, adhesion to the CGL, solubility (for processing by film coating), and durability. Aromatic polycarbonates are the most suitable binder resins, and polymers based on monomers other than BPA have shown some advantages for use in these applications.

The service lifetime of an organic photoconductor correlates with its abrasion resistance since each printing cycle brings the surface of the CTL in contact with paper and machine components. Polycarbonate prepared from the bisphenol of cyclohexane (BPZ, Fig. 5) **1** has been widely used as a matrix material due to its superior abrasion resistance compared to BPA-PC [222–224]. Recently, other polycarbonates have been demonstrated to exhibit excellent wear resistance.

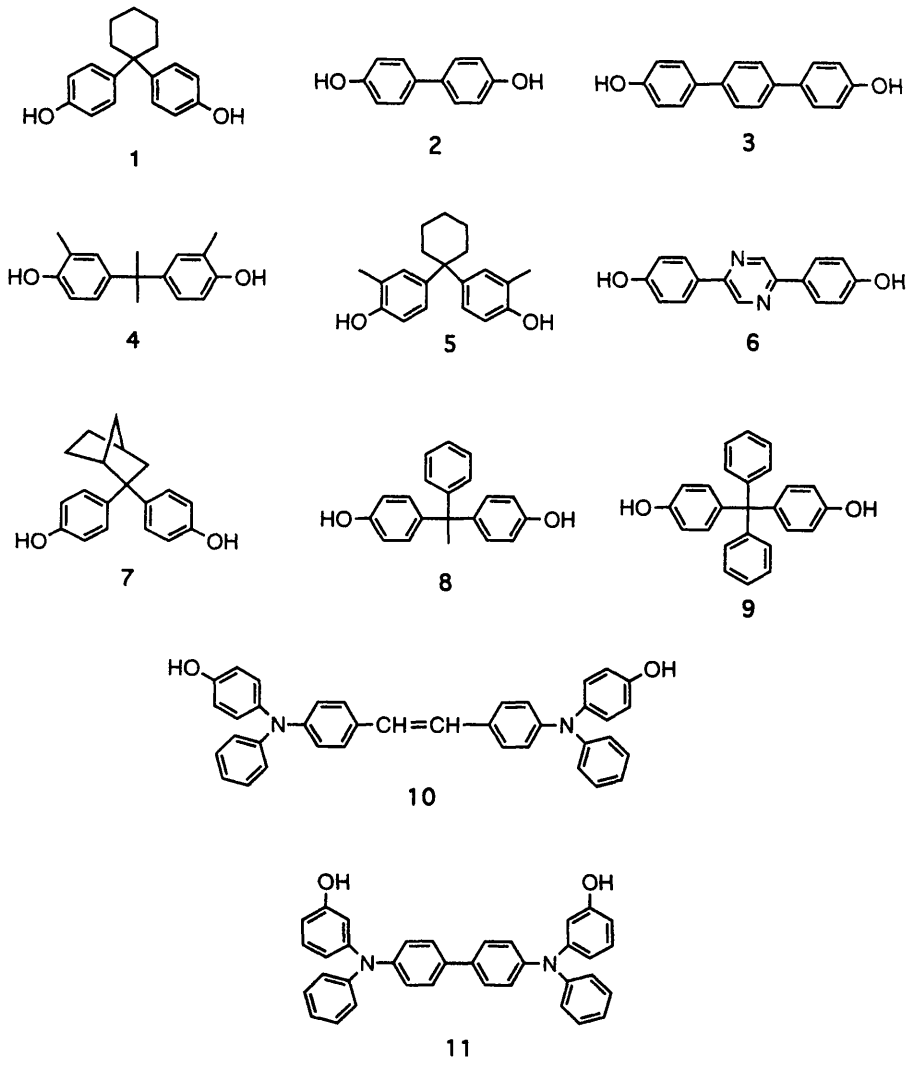

Figure 5 Bisphenols for polycarbonates for electroresponsive applications.

For example, a copolymer of BPA (85%) and 4,4′-dihydroxybiphenyl **2** (15%) abrades at roughly half the rate of BPZ-PC when each is doped with 50% of a hydrazone CTM [225]. Copolymers of 4,4′-dihyhdroxy-*p*-terphenyl **3** are also claimed to exhibit improved abrasion resistance [226].

A detailed comparison between the mechanical properties of BPA-PC, BPZ-PC, and the PC of 3,3′-dimethyl-BPA (DMBPA) **4**, each doped with series of diphenyl hydrazone derivatives, demonstrated that DMBPA-PC has the best abrasion resistance [227]. The authors found a correlation between abrasion resistance and the strength and position of the sub-T_g dynamic mechanical relation, as materials with a mechanical transition nearer to the photoconductor use temperature showed improved toughness.

Other bisphenol comonomers used to increase toughness and abrasion resistance of photoconductor CTLs include 1,1-bis(4-hydroxy-3-methylphenyl)-cyclohexane **5** [228], 2,5-bis(4-hydroxyphenyl)pyrazine **6** [229], norbornyl bisphenol **7** [230], and the bisphenol of acetophenone **8** [231] and hexafluoro-BPA **9** [232]. Finally, copolymers of BPA and hydroxyphenyl-terminated dimethyl siloxane oligomers (see separate section) are reported to give photoreceptors with superior surface mechanical strength, wear resistance, and lubricity [233,234].

A high charge transportability in a CTL is desirable, especially for high-speed or continuous (belt) copying as this minimizes residual photoreceptor surface potential between exposure and development cycles and maintains image quality. While charge mobility is not limiting in older amorphous selenium photoreceptors, the electron mobility of an organic CTL is dependent on both the CTM dopant and the matrix resin. For example, 4,4′-dihydroxytetraphenylmethane **9** copolymers give a higher electron mobility than BPA-PC (both doped with a bistriarylamine CTM) for a range of applied electronic fields [225,235].

Imperfect compatibility between the photoactive dopant and the polycarbonate matrix can lead to material degradation and accompanying deterioration of copier image quality. One approach to resolving this issue involves the preparation of a copolymer between the matrix monomer, typically BPA, and a photoactive dihydroxyaryl comonomer. For example, dihydroxybisarylamines such as **10** [225] and **11** [236] have been polymerized with BPA at 10–20 mol% and these nondispersible CTMs have performed comparably to dopant/matrix systems with excellent durability.

IX. LIQUID CRYSTALLINE POLYCARBONATES

The incorporation of mesogenic monomers into the polycarbonate chain can give rise to resins with anisotropic melt (ligand crystalline) properties. A study [237,238] of the monomer structure vs. the mesophase stability indicates the following order of stabilities:

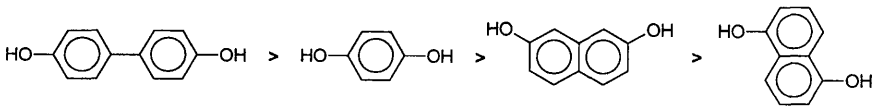

A proper balance of the mesogenic and nonmesogenic monomer is necessary to prepare a melt-stable polymer. For example, the biphenol homopolymer does not melt below its decomposition temperature (450°C) [239]. However, at low biphenol/BPA ratios, tough transparent resin are obtained that are not thermotropic (Table 9) [240]. When the biphenol/BPA ratio was increased from ~60:40 to 70:30 thermotropic resins were obtained [241]. These resins were insoluble in methylene chloride and displayed anisotropic melts above 270°C. In place of biphenol, dihydoxyterphenyl and dihydoxyquaterphenyls have been polymerized with BPA to form anisotropic resin [242].

To increase the decomposition temperature of the resins and to increase the stability of the nematic melt, BPA was substituted with 4,4′-dihydroxydiphenyl ether. The resins have been prepared both by melt [243] and by interfacial polymerizations (Table 9) [244]. A detailed study of the nonmesogenic monomer and the stability of the nematic phase in the biphenol copolymers has shown that the nonmesogenic monomers that are more linear produce the most stable nematic phases [245]. Thus, the nonmesogenic monomers with bond angles $\geq 120°$ gave stable nematic melts, whereas less linear monomers gave isotropic melts (Table 10). In addition to flexible nonlinear comonomer, substituted hydroquinones [231,245,246] and resorcinol [237] have been used to decrease the melt temperature.

Interestingly, anisotropic melts could be obtained from nonlinear groups,

Table 9 Liquid Crystalline Copolycarbonates Based on Biphenol

Nonmesogenic monomers	Mol% mesogenic monomer	T_g(°C)	Thermotropic?	Ref.
BPA	0	148	No	4
〃	10	151	〃	4
〃	15	153	〃	4
〃	20	158	〃	4
〃	30	160	〃	4
〃	60	165	Yes	5
〃	60	170	〃	5
〃	70	180	〃	5
Diphenyl ether	50	—	〃	8
〃	75	—	〃	8
〃	70	154	〃	7

Table 10 50:50 Mol% Copolycarbonates with Biphenol

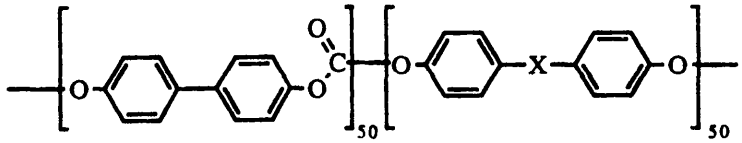

X	hinh[a]	T_g[b]	T_t[c]	Bond angle of X[d]
Ether	1.38	110	390–410	123
Ketone	0.33	95	300–330	121
Sulfide	1.16	130	Isotropic	100–110
Sulfone	0.42	170	Isotropic	100–110
Isopropylidene	1.20	160	Isotropic	100–110

[a] Measured with c = 2 g/L at 20°C in methylene chloride/trifluoroacetic acid.
[b] By differential scanning colorimetry at 20°C/min.
[c] By optical microscopy with cross-polarizers at 20°C/min.
[d] Bond angles from model compounds (in degrees). From Ref. 253–255.
Source: Ref 245.

such as resorcinol and 2,7-naphthalenediol. Although the carbonate group is also nonlinear, the combination of the carbonate group with these bent phenols appears to be self-correcting to give an extended chain conformation [238].

Other mesogenic monomers have included hydroquinone, 2,7-dihydroxynaphthalene, and 1,5-dihydroxynaphthalene [237]. Polyester carbonate LCPs have been prepared by the copolymerization of biphenol with *p*-hydroxybenzoic acid [11], 2-hydroxy-6-naphthoic acid [247], 4-hydroxydiphenyl-4-carboxylic acid [247], and 4-carboxy-*N*-hydroxyphenyl phthalimide [248]. In addition, several series of thermotropic polycarbonates have been prepared with flexible spacers [249–251].

Finally, a series of polycarbonates with stilbene-based monomers was prepared and studied by differential calorimetry, polarized microscopy, and x-ray diffractions. Methyl-1-substituted stilbenes (T_m 118–144°C, T_c 87–136°C) gave polymers with LC properties, whereas ethyl-substituted stilbenes gave amorphous polymers [252].

X. WEATHERABILITY

Small-molecule UV stabilizers are typically added to commercial formulations to improve the properties of polycarbonates in sunlight or ultraviolet (UV) light environments. An alternative approach to UV stalizilization involves incorporat-

ing into the polymer a comonomer that contains the UV-stabilizing functionality. For example, copolycarbonates that contain benzotriazolylbisphenols **1** [256,257] or triols **2** [258] exhibits less change in yellowness index than polycarbonate formulations containing an equivalent amount of monomeric UV additive (Fig. 6).

The weathering behavior of different polycarbonates has been studied to give insight into the structural characteristics of BPA-PC that account for its

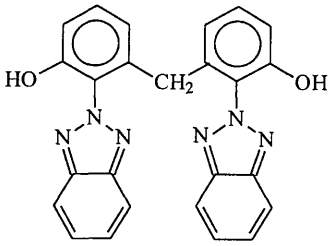

1

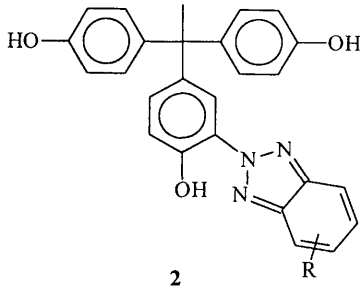

2

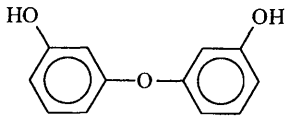

3

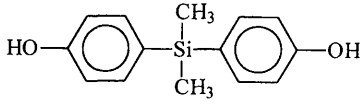

4

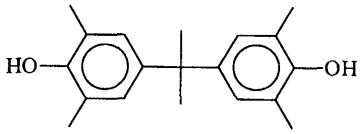

5

Figure 6 Bisphenols for polycarbonates for weatherable applications/studies.

photo-yellowing properties. The polycarbonate of a bisphenol devoid of aliphatic methyl groups, 3,3′-dihydroxyphenyl ether **3** (T_g = 71°C), was found [259] to photo-yellow at a rate three to four times faster than BPA-PC. These results are interpreted to suggest that ring oxidation is an important source of yellowing. This conclusion was corroborated by a related study [260] where the PC of bis(4-hydroxyphenyl)dimethylsilane **4** (T_g = 117°C), a material with lower UV absorbency and higher water repellancy that BPA-PC, was found to exhibit less change in yellowness index and % haze when compare to BPA-PC in a weathering study.

Mechanistic studies have demonstrated that the photo-Fries rearrangement (carbonyl migration to give an *ortho*-hydroxy aromatic ester) is responsible for color development in sun-exposed polycarbonate. A recent study [261] found that TMBPA-PC **5** does not undergo photo-Fries reaction, since all bisphenol ortho positions are occupied by methyl groups. However, the presence of the methyl groups does lead to a faster rate of photo- and thermooxidation for TMBPA-PC compared to BPA-PC.

REFERENCES

1. D. C. Prevorsek and Y. Kesten, Bisphenol-A/terephthalate/carbonate melt processable copolymers, U.S. Pat. 4,156,069 (1979).
2. D. C. Prevorsek, B. T. Debonna, and Y. Kesten, Synthesis of poly(ester carbonate) copolymers, *J. Polym. Sci. Polym. Chem. Ed. 18*:75 (1980).
3. E. P. Goldberg, Process for preparing copolyester comprising reacting a carbonyl halide with a dicarboxylic acid and a dihydroxide compound in the presence of a tertiary amine, U.S. Pat. 3,030,331 (1962).
4. E. P. Goldberg, S. F. Strause, and H. E. Munro, *Polym. Preprints 5*:233 (1964).
5. E. P. Goldberg, Carbonate-carboxylate copolesters of dihydric phenols and difunctional carboxylic acids, U.S. Pat. 3,169,121 (1965).
6. R. L. Markezich and C. B. Quinn, Process for producing copolyester-carbonates, U.S. Pat. 4,238,597 (1980).
7. J. E. Kochanowski, Method of preparing polyester carbonate, U.S. Pat. 4,286,083 (1981).
8. K. Kohyama, K. Sakata, and K. Ono, Method for preparation of aromatic polyester-carbonate, U.S. Pat. 4,429,103 (1984).
9. H. Mori, K. Kohyama, K. Nakamura, and S. Nakama, Method for manufacture of aromatic polyestercarbonate, U.S. Pat. 4,252,939 (1981).
10. H. Mori, K. Kohyama, K. Nakamura, S. Sakata, and A. Matsuno, Process for producing an aromatic polyestercarbonate, U.S. Pat. 4,369,303 (1983).
11. P. Tacke, D. Freitag, W. Novertne, L. Bottenbrunch, and M. P. R., Aromatic polester carbonates and their use in injection molding, Ger. Offen. 3,007,934:Eur. Pat. 36,080; (p 181) (CA 95:204,9089y) (1981).
12. N. R. Rosenquist, Benzoate ester terminated polyester-carbonate, U.S. Pat. 4,330,663 (1982).

13. V. Mark, Amide and carbamate terminated copolyester-carbonates, U.S. Pat. 4,506,064 (1985).
14. P. Tacke, Interfacial process for the production of fully aromatic polyester carbonate from alkali salt of aromatic dicarboxylic acid and bis-chlorocarbonic ester of diphenol, U.S. Pat. 4,569,984 (1986).
15. H. Schnell, V. Bollert, and G. Fritz, PPCs by melt, Ger. Pat. 1,495,626 (1960).
16. M. Matzener and L. M. Maresca, PPCs by melt, Eur. Pat. 79,075 (1981).
17. D. Freitag, L. Bottenbruch, and M. Schmidt, Aromatic polyester carbonate with high notched impact strength, Ger. Pat. (DOS) 3,223,980 (1982); CA 100:104098n.
18. W. J. Jackson Jr., and W. R. Darnell, Process for the preparation of polyestercarbonates and polyester-carbonates, U.S. Pat. 4,360,648 (1982).
19. D. Freitag, L. Bottenbrunch, and M. Schmidt, Aromatic polyester carbonates having high notched impact strength and a process for the production thereof, U.S. Pat. 4,533,702 (1985).
20. C. P. Bosnyak, J. N. Hay, I. W. Parsons, and R. N. Haward, Relations between structure and properties in bisphenol A polyester carbonates, *Polymer 21*:1448 (1980).
21. C. P. Bosnyak, J. N. Hay, I. W. Parsons, and R. N. Haward, Synthesis and properties of some poly(bisphenol A isoterephthalate), *Polymer 23*:608 (1982).
22. K. F. Miller and E. L. Belfoure, Copolyestercarbonates, U.S. Pat. 4,506,065 (1985).
23. K. F. Miller and W. Hilakos, Copolyestercarbonates, U.S. Pat. 4,465,820 (1984).
24. H. Marton, S. E. Bales, R. A. Bubeck, T. A. Dodds, and D. R. Near, Polycarbonate copolymers break new ground, *Plastics Eng. (June)*:49–52 (1986).
25. D. Freitag, U. Grigo, P. R. Muller, and W. Nouvertne, Polycarbonates in, *Encyclopedia of Polymer Science and Engineering*, 2nd ed., Vol. 11 (J. Kroschwitz, ed.), pp. 692–694.
26. V. Mark, Flame retardant copolyester-carbonate compositions, U.S. Pat. 4,477,632 (1984).
27. V. Mark, Flame retardant polycarbonate compositions, U.S. Pat. 4,430,485 (1984).
28. E. L. Belfoure and K. F. Miller, Compositions, U.S. Pat. 4,469,850 (1984).
29. K. F. Miller and E. L. Belfoure, Copolyester-carbonate blends, U.S. Pat. 4,436,879 (1984).
30. C. H. Quinn, Polyester-carbonate resin blends, U.S. Pat. 4,430,484 (1984).
31. P. D. Sybert and R. H. Glaser, Ductile blends of polyester-carbonate or polyarylates and polyetherimide resins, U.S. Pat. 5,387,639 (1995).
32. H. L. Curry, Polycarbonate/polyphthalate carbonate blends exhibiting good flame resistance, U.S. Pat. 4,923,933 (1990).
33. B. T. Debona and D. C. Prevorsek, Melt processable poly(ester carbonate) with high glass transition temperature, U.S. Pat. 4,310,652 (1981).
34. V. Mark and C. V. Hedges, Polyestercarbonates exhibiting improved heat resistance from cycloalkylidene diphenol, U.S. Pat. 4,554,330 (1985).
35. V. Serine, D. Freitag, U. Grigo, and U. Westeppe, Polyesters and polyester-carbonates from cycloalkylidenediphenols, Eur. Pat. Appl. EP 443058 A1; CA: 116:21704 (1991).
36. V. Serini, D. Freitag, and U. Grigo, Cycloalkylidenediphenol-based polyester-poly-

carbonates and their blends, Eur. Pat. Appl. EP 469,404 A2; CA: 116:236365 (1992).
37. N. R. Rosenquist, Polyestercarbonate from amide substituted aromatic dicarboxylic acid, U.S. Pat. 4,622,379 (1986).
38. N. R. Rosenquist, Composition, U.S. Pat. 4,727,184 (1988).
39. S. E. Bales, K. A. Burdett, and G.-S. J. Lee, Blend of copolyestercarbonate polymer derived from diaryl dicarboxylic acid, U.S. Pat. 5,045,610 (1991).
40. D. J. Swart and J. S. Kelyman, Alternating copolyestercarbonate resin, U.S. Pat. 4,105,633 (1978).
41. C. E. Weir, W. H. Leser, and J. H. Wood, Siloxane T_g, *J. Res. Natl. Bur. Stand. 44*:367 (1950).
42. H. A. Vaughn, Jr., LR, U.S. Pat. 3,189,662.
43. H. A. Vaughn, Jr., LR, U.S. Pat. 3,419,634.
44. G. E. Niznik and D. G. LeGrand, The effect of the end capping ratio on the properties of block copolymers, *J. Polym. Sci.: Polym. Sympo. 60*:97 (1977).
45. G. C. Davis, B. E. McGrath, and K. M. Snow, Flame retardant organopolysiloxane-polycarbonate triblock copolymers, U.S. Pat. 5,025,074 (1991).
46. T. L. Evans and J. C. Carpenter, Method for making silicone-poly(arylcarbonate) block copolymers, U.S. Pat. 4,920,183 (1990).
47. N. R. Rosenquist, Process for the manufacture of polycarbonate-oligomers without solvent, U.S. Pat. 5,344,908 (1994).
48. E. N. Peters, Process for making poly(carbonate-siloxanes) via alkyl amino terminated silicones, U.S. Pat. 5,194,524 (1993).
49. C. M. Hawkins and R. R. Gallucci, Polycarbonate-silicone block copolymer compositions, U.S. Pat. 4,994,532 (1991).
50. V. Serini, D. Rathamann, L. Morbitzer, and D. Freitag, Thermoplastic polyester carbonate-polysiloxane block copolymers, U.S. Pat. 5,126,495 (1992).
51. PPCSi, *Eur. Pat. EP368-104-A* (1988).
52. J. F. Hoover and P. D. Sybert, Terepolymers having aromatic polyester, polysiloxane and polycarbonate segments, Eur. Pat. Appl. EP 626,416: CA: 122:315411b (1994).
53. H. A. Vaughn, Jr., *J. Polym. Sci. B7*:569 (1969).
54. H. A. Vaughn, Jr., The synthesis and properties of alternating block polymers of dimethylsiloxane and bisphenol-A carbonate, *Polym. Lett. 7*:569 (1969).
55. R. P. Kambour, Microdomains in alternating block polymers of dimethylsiloxane and bisphenol-A carbonate, *Polym. Lett. 7*:573 (1969).
56. R. P. Kambour, Structure and properties of alternating block polymers of dimethylsiloxane and bisphenol-A carbonate, in *block copolymers*, Plenum Press, New York, 1970, pp. 263–276.
57. R. P. Kambour, D. Faulkner, E. E. Kampf, S. Miller, G. E. Niznik, and A. R. Shultz, Toughness enhancement by introduction of silicone blocks into polycarbonates of bisphenol acetone and bisphenol fluorenone, in *Toughness and Brittleness of Plastics* (R. D. Deanin and A. M. Crugnola, eds.), American Chemical Society, 1976.
58. D. G. LeGrand, Mechanical and optical studies of poly(dimethylsiloxane) bisphenol-A polycarbonate copolymers, *Polym. Lett. 7*:579 (1969).
59. R. E. Molari, Jr., Laminates, U.S. Pat. 4,123,588 (1978).

60. Ophthalmic formed bodies comprised of siloxane and polyestercarbonates, Ger. Pat. DE 4113292-A: Derwent Abstract 92-366908/45 (1991).
61. D. Freitag, U. Westeppe, A. Jung, P. Horlacher, G. Weymans, U. Grigo, L. Morbitzer, and K. Idel, Polydiorganosiloxane/polycarbonate block cocondensates based on certain dihydroxydephenylcycloalkanes, U.S. Pat. 5,109,076 (1992).
62. G. R. Grubbs, M. E. Kleppick, and J. H. Magill, *J. Appl. Polym. Sci. 27*:601 (1982).
63. W. Paul, H.-J. Kress, W. Stix, C. Lindner, D. Neuray, and W. Nouvertne, Thermoplastic moulding compositions based on polysiloxane/polycarbonate block copolymers, U.S. Pat. 4,569,970 (1986).
64. R. P. Kambour, W. V. Ligon, and R. R. Russell, Enhancement of the limiting oxygen index of an aromatic polycarbonate by the incorporation of silicone blocks, *J. Polym. Sci.: Polym. Lett. Ed. 16*:327 (1978).
65. A. Factor, K. N. Sannes, and A. M. Colley, The effect of flame resistant hard segments on the flammability and physical properties of polydimethylsiloxane based multiblock copolymers, *J. Fire Flamm. 12*:101 (1981).
66. G. C. Davis and L. N. Lewis, Flame retardant, halogen free aromatic polycarbonate copolymer blends, U.S. Pat. 4,996,255 (1991).
67. W. Paul, W. Nouvertne, H. Lower, M. Witman, and U. Grigo, Polydiorganosiloxane/polycarbonate block copolymers, U.S. Pat. 4,732,949 (1988).
68. R. P. Kambour, J. E. Corn, S. Miller, and G. E. Niznik, Tough, transparent heat- and flame-resistant thermoplastics via silicone block-modified bisphenol fluorenone polycarbonate, *J. Appl. Polym. Sci. 20*:3275 (1976).
69. P. Horlacher, V. Serini, D. Freitag, U. Grigo, K.-J. Idel, and U. Westeppe, Polysiloxane-polycarbonate block copolymers based on certain dihydroxydiphenylcycloalkanes, U.S. Pat. 5,068,302 (1991).
70. P. D. Sybert, Copoly(aromatic sulfone carbonate-aromatic alkylcarbonate)-polysiloxane block copolymer, U.S. Pat. 5,011,899 (1991).
71. O. Masaya and O. Ryozo, TB50 XT??, Jpn. Kokai Tokkyo Koho JP 06,329,781: CA: 123:10252f (1994).
72. O. Masaya and O. Ryozo, 105B XT??, Jpn. Kokai Tokkyo Koho JP 06,298,922: CA: 122:291822h (1994).
73. J. F. Hoover and L. P. Fontana, Terpolymer having aliphatic polyester, polysiloxane and polycarbonate, U.S. Pat. 5,608,026 (1997).
74. J. T. Bendler and J. C. Schmidhauser, Conformation and chain-packing properties of ortho-substituted aromatic polycarbonates, *Polym. Prepr. (Am. Chem. Soc., Div. Polym. Chem.) 36*:55 (1995).
75. V. Serini, D. Freitg, and H. Vernaleken, Polycarbonates from *o,o,o′,o′*-tetramethylsubstituted bisphenols, *Angew. Makromol. Chem. 55*:175 (1976).
76. G. R. Faler and J. C. Lynch, Preparation of spirobiindanediol polycarbonates with high glass temperature and low birefringence by interfacial polymerization, Eur. Pat. Appl. EP 287,887 (1988).
77. P. C. Wang, Polycarbonate containing spiro dilactam segment, U.S. Pat. 4,906,725 (1990).
78. L. H. Tagle and F. R. Diaz, Thermogravimetric analysis of polymers with indanic structure, *J. Thermal Anal. 38*:2385 (1992).

79. G. Sh. Papava, N. S. Gelashvili, C. A. Beridze, and P. D. Tsiskarishvili, *Svobsch. Akad. Navk Grut. SSR. 88:597 (1977)* (Chem. Abstr. 88:170527).
80. T. Tokuda, Heat-resistant transparent aromatic polycarbonates, Jpn. Kokai Tokkyo Koho JP 05078467 (Chem. Abst. 119:118131).
81. V. Mark and C. V. Hedges, Polycarbonate exhibiting improved heat resistance from cycloalkylidenediphenol, U.S. Pat. 4,638,027 (1991).
82. D. Freitag and U. Westeppe, A new principle for polycarbonates with superior heat resistance, *Makromol. Chem., Rapid Commun. 12*:95 (1991).
83. D. Freitag, G. Fengler, and L. Morbitzer, Routes to new aromatic polycarbonates with special material properties, *Angew. Chem. Int. Ed. Engl. 30*:1598 (1991).
84. V. Serini, D. Freitag, U. Westeppe, K. Idel, U. Grigo, C. Casser, K.-C. Paetz, and M. Hajek, Polycarbonate of alkyl cyclohexylidene bisphenol, U.S. Pat., 5,010,162 (1991).
85. V. Serini, D. Freitag, U. Westeppe, K. Idel, U. Grigo, C. Casser, K.-C. Paetz, and M. Hajek, Polycarbonate of cycloalkylidene bisphenol, U.S. Pat. 5,010,163 (1991).
86. K. Sommer, Correlation between chemical primary structure and property phenomena of polycondensates, *Adv. Mater. (Weinheim. Fed. Repub. Ger.) 3*:590 (1991) (Chem. Abstr. 117:27641f).
87. G. Weymans, K. Berg, L. Morbitzer, and U. Grigo, Influence of chemical structure on the mechanical properties of modified polycarbonates, *Angew. Makromol. Chem. 162*:109 (1988).
88. V. Serini, D. Freitag, U. Westeppe, K. Idel, and U. Grigo, (Alkylcyclohexylidene) bisphenol polycarbonates with good processability, Ger. Offen. DE 3,926,768 (1991).
89. V. Serini, D. Freitag, U. Westeppe, K. Idel, U. Grigo, C. Casser, K. C. Paetz, and M. Hajek, Polycarbonates from (alkylcyclohexylidene)diphenols, Eur. Pat. Appl. EP 374,656 (1991) (Chem. Abstr. 114:63021).
90. U. Westeppe, G. Fengler, C. Casser, M. Hajek, D. Freitag, and H. Waldmann, Process of preparation of bis(4-hydroxyphenyl)cycloalkanes and their use for the preparation of polycarbonates, Ger. Offen. DE 4,003,437 (1991) (Chem. Abstr. 115:231851).
91. V. Serini, D. Frietag, K. J. Idel, U. Westeppe, U. Grigo, and K. C. Paetz, Polycarbonates from polysubstituted cyclohexylidenediphenols, Eur. Pat. Appl. EP 374,623 (1990) (Chem. Abst. 113:232295).
92. V. Serini, U. Westeppe, G. Fengler, M. Hajek, C. Casser, and H. Waldmann, Bicycloalkylidene diphenols for use in polycarbonates, Ger. Offen. DE 4,031,756 (1992) (Chem. Abstr. 117:90993).
93. P. W. Morgan, Aromatic polyesters with large cross-planar substituents, *Macromolecules 3*:536 (1970).
94. R. Okumura, M. Nakae, and K. Hara Heat-resistant plastic molding for automobile lamp lends, Jpn. Kokai Tokkyo Koho JP 07,268,089 (1994) (Chem. Abst. 124: 58708).
95. J. O. Osby and J. K. Sekinger, Interfacial polymerization process for preparing polycarbonate from a bishydroxyphenylfluorene, U.S. Pat. 5,412,064 (1995).
96. T. Sakashita, K. Nagai, and T. Shimoda, Heat-resistant transparent copolycarbo-

nates with good color and compositions and manufacture thereof, Jpn. Kokai Tokkyo Koho JP 06,192,411 (1994) (Chem. Abst. 122:56864).

97. S. L. Brewster, K. S. Clement, V. R. Duruasula, H. A. Nguyen, P. M. Puckett, W. F. Richey, E. L. Tasset, and M. E. Walters, Chlorination of acidic proton-containing compounds which can delocalize electron density of conjugate base by contacting with perchloro alkane and aqueous base solutions in presence of tetraalkylonium hydroxide phase transfer catalyst to produce gem-chloro compounds, U.S. Pat. 5,387,725 (1995).
98. J. C. Schmidhauser, Polycarbonates from heterocyclic bis(4-hydroxyphenyl) cycloalkanes, U.S. Pat. 5,300,622 (1994).
99. J. C. Schmidhauser, Polycarbonate from 1,3-bis(4-hydroxyphenyl)-1,3-dialkylcyclohexanes, U.S. Pat. 5,281,688 (1994).
100. J. C. Schmidhauser, G. L. Bryant, Jr., P. E. Donahue, M. F. Garbauskas, and E. A. Williams, Products from the acid-catalyzed reaction of cyclic monoterpenes and phenol, *J. Org. Chem. 60*:3612 (1995).
101. J. C. Schmidhauser, Substantially pure bisphenols and polymers comprising bisphenols, U.S. Pat. 5,480,959 (1996).
102. Y. Inui, S. Kishimoto, A. Motoyama, T. Oowaki, and Y. Hashimoto, Heat-resistant and transparent polycarbonates with good melt flow and modability, Jpn. Kokai Tokkyo Koho JP 06329780 (Chem. Abstr. 123:33918).
103. M. Yokoyama, H. Yoshitoku, and J. Takano, Polycarbonates having limonene-phenol adduct units with good heat resistance and fluidity, Jpn. Kokai, Tokkyo Koho JP 05132551 (Chem. Abstr. 120:9661).
104. H. Miyashita, H. Kahiwabara, T. Saito, H. Kadomachi, and D. Kishimoto, Bisphenol polycarbonates containing polyphenyls for high heat deformation temperature, Jpn. Kokai, Tokkyo Koho JP 04,525,263 (1992) (Chem. Abstr. 119:9799a).
105. J. T. Bendler, J. C. Schmidhauser, and K. L. Longley, Polycarbonate from bis[4′-(4-hydroxyphenyl)-phenyl]alkanes, U.S. Pat. 5,281,689 (1994).
106. H. Keul, F. Deisel, H. Hoecker, E. Leitz, N. Schoen, and G. Sylvester, Preparation of statistical copolycarbonates of *o*- and *p*-bisphenols, Ger. Offen. DE 4,109,278 (1992) (Chem. Abstr. 118:255549h).
107. T. Takata, H. Matsuoka, and T. Endo, Synthesis and anionic ring-opening polymerization of a novel aromatic cyclic carbonate having binaphtyl structure, *Chem. Lett*: 2091 (1991).
108. S. Shirouzu, K. Shigematsu, S. Sakamoto, T. Nakagawa, and S. Tagami, Refractive index ellipsoids of a polycarbonate magnetooptical memory disk substrate, *Jpn. J. Appl. Phys. Part 1 28*:797 (1989).
109. G. R. Faler and J. C. Lynch, Method for preparing spirobiindane polycarbonates, U.S. Pat. 4,950,731 (1990).
110. H. Yoshioka, Special plastics for optical disks. Polycarbonate, *Purasuchikkusu 38*: 14 (1987).
111. G. Koempf, D. Freitag, and W. Witt, Polycarbonate and light: use of polycarbonates in optical application areas, *Angew. Makromol. Chem. 183*:243 (1990).
112. G. Koempf, D. Freitag, G. Fengler, and K. Sommer, Polymers for electrical and optical data storage, *Polymers for Advanced Technologies*, Vol. 3, 1992, p. 169.

113. H. Yoshioka, Optical materials with low double refraction, *Purasuchikkusu 43*:42 (1992).
114. T. Nakagawa, K. Shigematsu, and S. Shiromizu, Aromatic polycarbonates for optical devices, Jpn. Kokai Tokkyo Koho JP 61,255,929 [86,255,929] (1986).
115. H. Masayoshi, S. Mukai, H. Urabe, S. Yoshida, and M. Nukii, Polycarbonates, Jpn. Kokai Tokkyo Koho JP 62 45,623 [87 45,623] (1987).
116. M. Hasuo, S. Mukai, H. Urabe, S. Yoshida, and M. Nukii, Polycarbonate and optical disc substrate, U.S. Pat. 4,734,488 (1988).
117. G. H. Werumeus Buning, R. Wimberger-Friedl, H. Janeschitz-Kriegl, and T. M. Ford, Optical anisotropy of polycarbonates, Integr. Fund. Polym. Sci. Tech., 405 (1988).
118. T. Nakagawa and K. Shigematsu, Heat-resistant and transparent polycarbonates for optical devices and their preparation, Jpn. Kokai Tokkyo Koho JP 63 95,228 [88 95,228] (1988) (Chem. Abstr 109:129888).
119. T. Nakagawa and K. Shigematsu, Bisphenols for polymers and manufacturing the same, Jpn. Kokai Tokkyo Koho JP 63 68,534 [88 68,534] (1988) (Chem Abstr. 110:95965).
120. T. Nakagawa and K. Shigematsu, Manufacture of aromatic polycarbonates, with good heat resistance and low optical elasticity, Jpn. Kokai Tokkyo Koho JP 63 68,632 [88 68,632] (1988) (Chem Abstr. 109:55492).
121. T. Tajima, H. Miwa, and R. Sudo, Optical disks containing polycarbonate substrates and their manufacture, Jpn. Kokai Tokkyo Koho JP 02,304,741 [90,304,741] (1990).
122. T. Tokuda and H. Takemoto, Scratch-resistant aromatic polycarbonate substrates for photocards, Jpn. Kokai Tokkyo Koho JP 06 25,399 [94 25,399] (1994) (Chem. Abstr. 121:37304).
123. M. Nishiguchi and T. Tokuda, Aromatic polycarbonate copolymer, a process for its preparation, and a plastic optical waveguide using the polymer, Eur. Pat. Appl. EP 608,493 (1994) (Chem. Abstr. 122:82341).
124. T. Tajima, H. Miwa, and R. Sudo, Optical disks containing polycarbonate substrates and their manufacture, Jpn. Kokai Tokkyo Koho JP 02,304,742 [90,304,742] (1990).
125. K. Shigematus and T. Nakagawa, Manufacture of heat-resistant polycarbonates with good mechanical properties, Jpn. Kokai Tokkyo Koho JP (Chem. Abstr. 109: 7157).
126. K. Shigematsu, T. Nakagawa, and S. Sakamoto, Polycarbonates, Eur. Pat. Appl. EP 249,963 (1987) (Chem. Abstr. 109:55870).
127. H. Sakamoto, K. Shigematsu, S. Shiromizu, and S. Tagami, Manufacture of aromatic polycarbonates, Jpn. Kokai Tokkyo Koho JP 01,155,301 [89,155,301] (1989) (Chem. Abstr. 112:21451).
128. H. Sakamoto, K. Shigematsu, and S. Shiromizu, Manufacture of optical disk substrates by injection molding, Jpn. Kokai Tokkyo Koho JP 02 16,121 [90 16,121] (1990) (Chem. Abstr. 112:243163).
129. H. Ozawa, H. Tsuboi, T. Enomoto, and M. Okita, Molded part for optical devices, Jpn. Kokai Tokkyo Koho JP 61,148,401 [86,148,401] (1986) (Chem. Abstr. 106: 166296).

130. T. Sugano and I. Takahashi, Aromatic polycarbonates for laser-sensitive optical disks, Jpn. Kokai Tokkyo Koho JP 63,223,034 [88,223,034] (1988) (Chem. Abstr. 110:115578).
131. T. Kakagawa, S. Shiromizu, and H. Sakamoto, Manufacture of aromatic polycarbonates for optical recording materials, Jpn. Kokai Tokkyo Koho JP 62,185,709 [87,185,709] (1987).
132. T. Kanno, A. Izuka, T. Katsuki, I. Takahashi, and K. Sasaki, Polycarbonate and optical disk therefrom, Eur Pat. Appl. EP 262,557 (1988) (Chem. Abstr. 109: 74809).
133. H. Sakamoto, T. Nakagawa, and K. Shigematsu, Polycarbonates of cyclohexyl-substituted bisphenols for use as optical materials, Jpn. Kokai Tokkyo Koho JP 01 20,228 [89 20,228] (1989) (Chem. Abstr. 111:79559).
134. T. Kawaki, Y. Kijima, and K. Hasawara, Tetramethylbisphenol A polycarbonate compositions for optical materials, Jpn. Kokai Tokkyo Koho JP 01,315,445 [89,315,445] (1989) (Chem. Abstr. 113:7622).
135. M. Arii, Polymer optical waveguide materials and applications, *Oputoronikusu 111*: 81 (1991) (Chem. Abstr. 116:107096b).
136. See, for example, K. Sasaki, I. Takahashi, and T. Sugano, Aromatic polycarbonate terpolymers for laser-sensitive optical disks, Jpn. Kokai Tokkyo Koho JP 63,199,729-34 (1988) (Chem. Abstr. 110:31538–43).
137. T. Suzuki and K. Shigematsu, 1,1-Diphenyl-1,1-bis(3-cyclohexyl-4-hydroxyphenyl)methane and its manufacture, Jpn. Kokai Tokkyo Koho JP 01 70,426 [89 70,426] (1989) (Chem. Abstr. 111:215076).
138. I. Takahashi and T. Sugano, 1,1-Bis(4-hydroxy-3-tert-butylphenyl)cyclohexane containing polycarbonates for optical disks, Jpn. Kokai Tokkyo Koho JP 01 60,626 [89 60,626] (1989) (Chem. Abstr. 111:175708).
139. T. Tokuda and S. Kaneyuki, Modification of aromatic polycarbonates for optical materials, Jpn. Kokai Tokkyo Koho JP 06228296 (1994) (Chem. Abstr. 122: 161769).
140. M. Masumoto, S. Kanayama, T. Asoh, and T. Kawahigashi, Polycarbonate resin from bis(hydroxybenzoyl oxy-tetra oxa Spiro) compound, U.S. Pat. 5,021,541 (1991).
141. T. Tokuda and S. Kaneyuki, Modification of aromatic polycarbonates for optical materials, Jpn. Kokai Tokkyo Koho JP 06,228,296 (1994) (Chem. Abst. 122: 161769).
142. W. H. Daly and B. R. Hahn, Synthesis of optically isotropic materials, *Polym. Prepr. (Am. Chem. Soc. Polym. Chem. Div.) 30*:337 (1989).
143. C. C. Geiger, J. D. Davies, and W. H. Daly, Aliphatic-aromatic copolycarbonates derived from 2,2,4,4-tetramethyl-1,3-cyclobutanediol, *J. Polym. Sci. A: Polym. Chem. 33*:2317 (1995).
144. M. Nishiguchi and T. Tokuda, Bisphenol AF polycarbonate, a method for producing the same, and a plastic optical waveguide using the same, Eur. Pat. Appl. EP 596,391 (1994) (Chem. Abstr. 121:181111).
145. S. Imamura and T. Izawa, Polycarbonates for optical fiber communication materials and sealing insulating materials, Jpn. Kokai Tokkyo Koho JP 04 13,720 [92 13,720] (1992) (Chem. Abstr. 117:71243).

146. M. Nishiguchi and T. Tokuda, Transparent and heat-resistant aromatic polycarbonates, Jpn. Kokai Tokkyo Koho JP 06,322,093 [94,322,093] (1994) (Chem. Abstr. 122:266391).
147. W. Ebert, M. Negele, and G. Fennhoff, Aromatic polycarbonate containing a special fluorine-containing bisphenol component, U.S. Pat. 5,155,205 (1992).
148. R. J. Gulotty and S. E. Bales, Nitro-containing polycarbonate compositions with nonlinear optical activity, U.S. Pat. 5,037,935 (1991).
149. S. E. Bales, D. J. Brennan, R. J. Gulotty, A. P. Haag, and M. N. Inbasekaran, Nonlinear optical arylhydrazones and nonlinear optical polymers thereof, U.S. Pat. 5,208,299 (1993).
150. C. Moore and W. J. Brittain, Synthesis of polycarbonates containing nonlinear optical chromophores, *Polym. Prepr. (Am. Chem. Soc. Div. Polym. Chem.) 36*:47 (1995).
151. L. A. Pilato, L. M. Litz, B. Hargitay, R. C. Osborne, A. G. Farnham, J. H. Kawakami, P. E. Fritze, and J. E. McGrath, Polymers for permselective membrane gas separations, *Polym. Prepr. (Am. Chem. Soc. Div. Polym. Chem.) 16*:42 (1975).
152. J. C. Schmidhauser and K. L. Longley, The effect of bisphenol monomer structure on the gas permeability of aromatic polycarbonates, *J. Appl. Polym. Sci. 39*:2083 (1990).
153. J. C. Schmidhauser and K. L. Longley, Gas transport through bisphenol-containing polymers, *ACS Symp. Ser. 423*:159 (1990).
154. J. C. Schmidhauser and K. L. Longley, Thermoplastic polycarbonate composition having improved oxygen barrier properties from diester diol, U.S. Pat. 5,110,897 (1992).
155. G. Weymans, U. Grigo, K. Berg, and F. J. Mais, Films of 3,3′-oxydiphenol polycarbonates, Ger. Offen. DE 3,823,305 (1990) (Chem. Abstr. 112:200202).
156. K. Shigematsu and S. Sakamoto, Preparation of aromatic polycarbonate films, Eur. Pat. Appl. EP 329,991 (1989) (Chem. Abstr. 112:78229).
157. T. Nakagawa and H. Sakamoto, Polycarbonates with reduced moisture permeation, Jpn. Kokai Tokkyo Koho JP 63,223,033 [88,223,033] (1988) (Chem. Abstr. 110: 174003).
158. W. J. Koros and G. K. Fleming, Membrane-based gas separation, *J. Membrane Sci. 83*:1 (1993).
159. S. A. Stern, Polymers for gas separations: the next decade, *J. Membrane Sci. 94*: 1 (1994).
160. R. E. Kesting and A. K. Fritzsche, *Polymeric Gas Separation Membranes*, John Wiley and Sons, New York, 1993.
161. Yu. P. Yampol'skii and N. A. Plate, Is it possible to predict transport properties of polymers on the basis on the chemical structure of the chains. A review, *Polym. Sci. (Russian) 36*:1599 (1994).
162. L. M. Robeson, Correlation of separation factor versus permeability for polymeric membranes, *J. Membrane Sci. 62*:165 (1991).
163. N. Muruganandam, W. J. Koros, and D. R. Paul, Gas sorption and transport in substituted polycarbonates, *J. Polym. Sci. B: Polym. Phys. 25*:1999 (1987).
164. J. Anada, D. C. Feay, S. E. Bales, and T. O. Jeanes, Semipermeable gas separation

membranes from polycarbonates containing tetrahalobisphenols, Eur. Pat. Appl. EP 242,147 (1987).
165. E. S. Sanders, Jr., D. O. Clark, J. A. Jensvold, H. N. Beck, and G. G. Lipscomb II, Process for preparing membranes of tetrahalobisphenol A polycarbonates for separating oxygen from nitrogen, U.S. Pat. 4,772,392 (1988).
166. E. S. Sanders, Jr., and D. C. Overman III, Selective hydrogen separation from gas mixtures using semipermeable membranes consisting predominantly of polycarbonates derived from tetrahalobisphenols, U.S. Pat. 5,000,763 (1991).
167. T. H. Ho, F. B. Kassell, C. I. Kao, and J. L. Aguilar, Two-stage-catalytic production of high molecular weight polyhalobisphenol polycarbonates, U.S. Pat. 4,784,156 (1988).
168. J. T. Gu, W. C. Luo, and C. S. Wang, The interfacial polycondensation of tetrabromobisphenol A polycarbonate. I. Model reaction and mechanism studies, *Angew. Makromol. Chem. 208*:65 (1993).
169. H. N. Beck, Solubility characteristics of tetrabromobisphenol-A polycarbonate in various liquids, *Ind. Eng. Chem. Res. 31*:2628 (1992).
170. T. L. Parker, E. S. Sanders, W. E. Mickols, S. M. Jordan, and T. O. Jeanes, A crosslinked semipermeable gas separation membrane from a reaction product of a thermoformable, thermosettable aromatic polycarbonate, polyestercarbonate, and/or polyester and an epoxy resin, Eur. Pat. Appl. EP 489,417 (1992) (Chem. Abstr. 118:40476).
171. J. A. Jensvold, S. R. Chary, W. S. Jacks, H. R. Keller, T. L. Parker, and D. Reddy, Gas-separation membranes having improved selectivity and recovery and their manufacture, *PCT Int. Appl. WO 94 12,269* (1994) (Chem. Abstr. 122:292733).
172. J. S. McHattie, W. J. Koros, and D. R. Paul, Effect of isopropylidene replacement on gas transport properties of polycarbonates, *J. Polym. Sci. B: Polym. Phys. 29*: 731 (1991).
173. M. Aguilar-Vega and D. R. Paul, Gas transport properties of polycarbonates and polysulfones with aromatic substitutions on the bisphenol, *J. Polym. Sci. B: Polym. Phys. 31*:1599 (1993).
174. M. W. Hellums, W. J. Koros, G. R. Husk, and D. R. Paul, Fluorinated polycarbonates for gas separation applications, *J. Membrane Sci. 46*:93 (1989).
175. T. O. Jeanes, Gas separation membranes from bisphenol AF-based polycarbonates or polyester-polycarbonates, *Eur. Pat. Appl. EP 316,960* (1989) (Chem. Abstr. 112: 21967).
176. M.-B. Hagg, W. J. Koros, and J. C. Schmidhauser, Gas sorption and transport properties of bisphenol-I polycarbonate, *J. Polym. Sci. B: Polym. Phys. 32*:1625 (1994).
177. P. Tacke, U. Westeppe, D. Freitag, and G. Weymans, Permeable polycarbonates resistant to heat distortion, *Ger. Offen. DE 3,922,496* (1991) (Chem. Abstr. 114: 248023).
178. M. W. Hellums, W. J. Koros, and J. C. Schmidhauser, Gas separation properties of spirobiindane polycarbonate, *J. Membrane Sci. 67*:75 (1992).
179. M. W. Hellums, W. J. Koros, G. R. Husk, and D. R. Paul, Gas transport in halogen-containing aromatic polycarbonates, *J. Appl. Polym. Sci. 43*:1977 (1991).

180. L. M. Costello and W. J. Koros, Effect of structure on the temperature dependence of gas transport and sorption in a series of polycarbonates, *J. Polym. Sci. B: Polym. Phys. 32*:701 (1994).
181. M. B. Moe, W. J. Koros, and D. R. Paul, Effects of molecular structure and thermal annealing on gas transport in two tetramethyl bisphenol-A polymers, *J. Polym. Sci. B: Polym. Phys. 26*:1931 (1988).
182. S. M. Jordan, G. K. Fleming, and W. J. Koros, Permeability of carbon dioxide at elevated pressures in substituted polycarbonates, *J. Polym. Sci. B: Polym. Phys. 28*:2305 (1990).
183. C. K. Kim, M. Aguilar-Vega, and D. R. Paul, Dynamic mechanical and gas transport properties of blends and random copolymer of bisphenol-A and tetramethyl bisphenol-A polycarbonate, *J. Polym. Sci. B: Polym. Phys. 30*:1131 (1992).
184. J. S. Chiou and D. R. Paul, Gas permeation in miscible homopolymer-copolymer blends. II. Tetramethyl bisphenol A polycarbonate and a styrene/acrylonitrile copolymer., *J. Appl. Polym. Sci. 34*:1503 (1987).
185. N. Muruganandam and D. R. Paul, Gas sorption and transport in miscible lends of tetramethyl bisphenol a polycarbonate and polystyrene, *J. Polym. Sci. B: Polym. Phys. 25*:2315 (1987).
186. P. C. Raymond and D. R. Paul, Kinetics of carbon dioxide conditioning of copolymers and blends containing methyl methacrylate (MMA) units, *J. Polym. Sci. B: Polym. Phys. 28*:2213 (1990).
187. D. G. Freitag, U. Grigo, P. R. Muller and W. Nouvertne, Polycarbonates, in *Encyclopedia of Polymer Science and Engineering*, 2nd ed., Vol. 11 (J. Kroschwitz, ed.), pp. 692–694.
188. H. Schnell, Chemistry and physics of polycarbonates, in *Polymer Reviews*, Vol. 9, Interscience, New York, 1964.
189. L. P. Fontana, K. F. Miller, A. A. Claesen, P. W. van Es, T.O.N. de Vroomen, C. B. Quinn, and R. W. Campbell, Phenolic compound end capped polyester carbonate, U.S. Pat. 5,321,114 (1994).
190. L. P. Fontana and P. W. Buckley, Preparation of polyestercarbonate from aliphatic dicarboxylic acid, US Pat. 5,025,081 (1991).
191. T. Sakashita, T. Nagai, and T. Shimoda, Copolymerized polycarbonates, Eur. Pat. Appl. 92303160.3: Publ. 508 774 A2 (1992).
192. N. R. Rosenquist, Copolyester-carbonates containing aliphatic diol co-monomers, U.S. Pat. 4,381,358 (1983).
193. V. Mark, Copolyester-carbonate resins, U.S. Pat. 4,504,649 (1985).
194. V. Mark and E. N. Peters, Polycarbonate exhibiting improved impact properties, U.S. Pat. 4,628,081 (1986).
195. V. Mark and E. N. Peters, Polycarbonate exhibiting improved impact properties containing divalent residue of polymerized alkadiene monomer, U.S. Pat. 4,728,716 (1988).
196. V. Mark and E. N. Peters, Polycarbonate exhibiting improved impact properties containing divalent residue of polymerized, partially hydrogenated conjugated alkadiene monomer, U.S. Pat. 4,677,183 (1987).
197. V. Mark and E. N. Peters, Polyestercarbonate containing divalent residue of polymerized alkadiene monomer, U.S. Pat. 4,871,830 (1989).

198. E. N. Peters, Telechelic polyisobutylene and block copolymer derivatives, U.S. Pat. 4,845,158 (1989).
199. T. Tokuda, I. Furukawa, and M. Miyauchi, Substituted phenols as modifiers for aromatic polycarbonates and polycarbonate-polyester and polyarylates, Eur. Pat. Appl. EP 622,393 (1994).
200. V. Mark and C. V. Hedges, Copolyester-carbonate compositions exhibiting improved processability.
201. M. J. Marks and J. K. Sekinger, Effects of chain end group composition and concentration on the properties of bisphenol A tetrabromobisphenol A copolycarbonates, *J. Polym. Sci. A: Polym Chem 32*:1885 (1994).
202. J. T. Gu and C. S. Wang, HPLC analysis of tetrabromobisphenol A polycarbonate oligomers. Its application in interfacial phosgenation reaction, *Polym. Bull. (Berlin) 25*:583 (1991).
203. M. J. Marks and J. K. Sekinger, Synthesis and properties of 2,2′-dibromobisphenol A polycarbonate, *Polymer 36*:209 (1995).
204. A. Factor and C. M. Orlando, Polycarbonates from 1,1-dichloro-2,2-bis(4-hydroxyphenyl)ethylene and bisphenol A: a highly flame-resistant family of engineering thermoplastics, *J. Polym. Sci.: Polym. Chem. Ed. 18*:579 (1980).
205. A. Factor, Char formation in aromatic engineering polymers, *ACS Symp. Ser. 425*: 274 (1990).
206. V. Mark and C. V. Hedges, Flame-retardant aromated polycarbonate compositions made from fluorinated diphenols, PCT Int. Appl. WO 82/2402 (Chem. Abstr. 97: 217318).
207. R. L. Price, M. W. Witman, and S. Krishnan, Process for the preparation of copolycarbonates of sulfonyl diphenol, U.S. Pat. 4,535,143 (1985).
208. S. Krishnan and A. L. Baron, Fire retardant polycarbonates with improved critical thickness, Eur. Pat. Appl. EP 31958 (1981) (Chem. Abstr. 96:53178).
209. S. Maiti, S. Banerjee, and S. K. Palit, Phosphorus-containing polymers, *Prog. Polym. Sci. 18*:227 (1993).
210. K. Fuhr, F. Muller, K. H. Ott, J. Schoeps, H. Peters, and W. Ballas, Flame-resistant thermoplastic polycarbonate molding compounds, U.S. Pat. 5,137,953 (1992).
211. S. Hashimoto, I. Furukawa, and T. Kondo, Synthesis and properties of phosphorus-containing polycarbonates, *J. Polym. Sci.: Polym. Chem. Ed. 12*:2357 (1974).
212. K. Zander, J. Kirsch, M. Hajek, H. Waldmann, and C. Casser, Synthesis and properties of bis(hydroxyalkoxy)diphenylalkanes and -cycloalkanes, DE Offen. 4138244A1 (1993).
213. A. Udea, T. Matsumoto, T. Imamaura, and K. Tsujimoto, Flame resistant polyester from diaryl-di(hydroxyalkylene oxy)aryl phosphine oxide, U.S. Pat. 5,003,029 (1991).
214. G. C. Davis, C. A. A. Claesen, and E. M. A. Gijzen, Phosphine oxide substituted polycarbonate, U.S. Pat. 5,194,564 (1993).
215. G. C. Davis, Polycarbonate compositions comprising bisphophine oxide monomer, U.S. Pat. 5,312,890 (1994).
216. T. Sakashita, T. Shimoda, and K. Kishimura, Diphenol comonomer in flame-retardant aromatic polycarbonates, Eur. Pat. Appl. EP 544,407 (1993).

217. H. O. Krabbenhoft, E. J. Pearce, D. J. Brunelle, and D. K. Bonauto, Solvent- and fire-resistant bisphenol A (BPA) polycarbonate blends, U.S. Pat. 5,162,458 (1992).
218. J. M. Baggett, Phenolphthalein-dihydroxy aromatic compound polycarbonates, U.S. Pat. 4,210,741 (1980).
219. M. S. Lin, B. J. Bulkin, and E. M. Pearce, Thermal degradation study of phenolphthalein polycarbonate, *J. Polym. Sci. A: Polym. Chem. 19*:2773 (1981).
220. M. S. Lin and E. M. Pearce, Polymers with improved flammability characteristics. I. Phenolphthalein-related homopolymers, *J. Polym. Sci. A: Polym. Chem. 19*:2659 (1981).
221. M. S. Lin and E. M. Pearce, Polymers with improved flammability characteristics. II. Phenolphthalein-related copolycarbonates, *J. Polym. Sci. A: Polym. Chem. 19*: 2151 (1981).
222. M. Kato, Y. Nishioka, and Y. To, Organic composite electrophotographic photoreceptor containing polycarbonate binder, Jpn. Kokai Tokkyo Koho JP 63,261,266 [88,261,266] (1988).
223. T. Yoshiaki, N. Hiroyuki, and M. Katumi, Photoreceptor having polycarbonate layers and process for the preparation thereof, U.S. Pat. Re. 33,724 (1991).
224. Y. Sato and S. Mayama, Carrier for electrophotography, and two-component type developer having the carrier, Eur. Pat. Appl. EP 631,199 (1994).
225. S. Sakamoto and H. Morishita, Materials for electrophotographic photoreceptors, *Idemitsu Giho 36*:224 (1993).
226. T. Nagao, H. Sakamoto, and H. Morishita, Polycarbonate copolymers and manufacture thereof and electrophotographic photoreceptors using the same, Jpn. Kokai Tokkyo Koho JP 05,163,339 [93,163,339] (1993).
227. R. E. Cais, M. Nozomi, M. Kawai, and A. Miyake, Antiplasticization and abrasion resistance of polycarbonates in the charge-transport layer of an organic photoconductor, *Macromolecules 25*:4588 (1992).
228. S. Otsuka, Y. Rin, S. Mayama, H. Urabe, and R. Kojika, Electrophotographic photoreceptors using a polycarbonate resin as a binder resin for charge-transporting layer, Jpn. Kokai Tokkyo Koho JP 01,312,548 [89,312,548] (1989).
229. T. Nagao, H. Sakamoto, H. Morishita, and H. Myamoto, Polycarbonates, manufacture thereof, electrophotoreceptors using same, Jpn. Kokai Tokkyo Koho JP 06,56,982 [94,56,982] (1994).
230. L. E. Contois, High resolution heterogeneous photoconductive compositions and method of preparing, U.S. Pat. 4,350,751 (1982).
231. S. Kanayama, N. Ogawa, and J. Tajima, Electrophotographic photosensitive material, PCT Int. Appl. WO 95 08,138 (1995).
232. Y. Yoshihara and T. Kimura, Electrophotographic photoreceptor with fluoropolymer-containing layer, Jpn. Kokai Tokkyo Koho JP 63 65, 451 [88 65, 451] (1988) (Chem. Abstr. 109:240 602).
233. N. Ootani and T. Sakakibara, Carrier member for transferred toner image-receiving sheet used in electrostatographic copiers, Jpn. Kokai Tokkyo Koho JP 06 19,337 [94,19,337] (1994).
234. H. Myamoto, H. Sakamoto, H. Morishita, and T. Nagao, Abrasion-resistant polycarbonates, manufacture thereof, and electrophotographic photoreceptors using the same, Jpn. Kokai Tokkyo Koho JP 06,136,108 [92,136,108] (1992).

235. I. Takegawa, K. Mashimo, Y. Sakaguchi, and M. Takemoto, Electrophotographic photoreceptor with copolymerized polycarbonate resin, U.S. Pat. 5,141,832 (1992).
236. J. F. Yanus, J. W. Spiewak, D. S. Renfer, and W. W. Limburg, Arylamine carbonate polymer, U.S. Pat. 5,028,687 (1991).
237. S.-J. Sun and T.-C. Chang, Studies on the thermotropic liquid crystalline polycarbonates. II. Synthesis and properties of fully aromatic liquid crystalline polycarbonates, *J. Polym. Sci. A: Polym. Chem. 31*:2237–2243 (1993).
238. S.-J. Sun and T.-C. Chang, Studies on the thermotropic liquid crystalline polycarbonates. III. Synthesis and properties of fully aromatic liquid crystalline polycarbonates, *J. Poly. Sci. A: Polym. Chem. 31*:2711 (1993).
239. H. R. Kricheldorf and D. Jubbers, Synthesis of thermotropic aromatic polycarbonates by means of bis(trichoromethyl)carbonate, *Makromol. Chem. Rapid Commun. 10*:383–386 (1989).
240. T. Nakagawa, Polycarbonate copolymer and its manufacturing method, Kokai Pat. SHP 62[1987]-227927 (1987).
241. T. Toshioka, Method to produce aromatic polycarbonates, Jap. Pat. Appl. disclosure S,61-264020 (1986).
242. LCPs from Dihydroxyterphenyls *JO 3250-023-A* (1990).
243. G. H. Riding, Liquid crystalline polycarbonate from dihydroxy biphenyl and dihydroxy diphenyl ether, U.S. Pat. 5,102,975 (1992).
244. P. Pakull, D. Freitag, V. Eckhart, K-J Idel, H.R. Kricheldorf, and D. Lubbers, Copolycarbonate from mixture of polyarylene diol. U.S. Patent 5,084,550 (1992).
245. H. R. Kricheldorf and D. Lubbers, Polymers of carbonic acid. 3. Thermotropic polycarbonates derived from 4,4′-dihydroxybiphenyl and various diphenols, *Macromolecules 23*:2656 (1990).
246. D. N. Schissel, Anisotropic melt-forming copolycarbonate from 4′4-dihydroxy biphenyl and methyl hydroquinone, U.S. Pat. 4,831,105 (1989).
247. A. Takahashi, H. Inada, and S. Matsumura, Aromatic polyester carbonate and production thereof, Derwent 89-216505/30, Jap. Pat. JO 1153-720-A (1989).
248. S. Murakami and T. Tomioka, (4-Carboxy-*N*-hydroxyphenyl phthalimide LCPs) resin composition, Derwent 88-032038/05, Jap. Pat. JP-133827 (1986).
249. M. Sato, K. Kurosawa, K. Nakatsuchi, and Y. Ohkatsu, Synthesis and liquid crystalline properties of thermotropic homo- and copolycarbonates, *J. Polym. Sci. A: Polym. Chem. 26*:3077 (1988).
250. M. Sato, K. Nakatsuchi, and Y. Ohkatsu, New liquid-crystalline polycarbonates from diols containing a biphenol ring sequence as central core, *Makromol. Chem. Rapid Commun. 7*:231 (1986).
251. C. De Backer, M. Van Beylen, R. Ottenburgs, and C. Samyn, Synthesis and liquid-crystalline properties of thermotropic homopolycarbonates, *Macromol. Chem. Phys. 196*:1495 (1995).
252. A. L. Bluhm, P. Cebe, H. L. Schreuder-Gibson, J. T. Stapler and W. Yeomans, Synthesis of stilbene-based polycarbonates, *Mol. Cryst. Liq. Cryst. 239*:123 (1994).
253. S. C. Abrahams, *O. Rev. Chem. Soc. 10*:407 (1956).
254. E. B. Fleischer, N. Sung, and S. Hawkinson, Bond angles of non-mesogenic, *J. Phys. Chem. 72*:4311 (1968).

255. H. G. Norment and J. L. Karlee, Bond angles for non-mesogenic bisphenols, *Acta Cryst. 15*:873 (1962).
256. S. Kanayama, T. Uemura, T. Takada, H. Ohtaki, and M. Masumoto, UV-absorbing polycarbonate resins, *Gosei Jushi 39*:50 (1993).
257. M. Masumoto and S. Kanayama, Self-antioxidant and weather-resistant copolycarbonates and preparation, Jpn. Kokai Tokkyo Koho JP 03 39,326 [9139,326] (1991).
258. N. Ogawa, T. Takata, and S. Kanayama, Bisphenol polycarbonates and their manufacture, Eur. Pat. Appl. EP 614,926 (1994) (Chem. Abstr. 122:266370).
259. A. Factor, J. C. Lynch, and F. H. Greenberg, The synthesis, characterization, and weathering behavior of polycarbonates derived from 3,3′-dihydroxydiphenyl ether, *J. Polym. Sci. A: Polym. Chem. 25*:3413 (1987).
260. A. Factor and P. T. Engen, The synthesis, characterization, and weathering behavior of polycarbonates derived from bis(*p*-hydroxyphenyl)dimethylsilane (BPSi), *J. Polym. Sci. A: Polym. Chem. 31*:2231 (1993).
261. A. Rivaton and J. Lemaire, Photo-oxidation and thermo-oxidation of tetramethylbisphenol-A polycarbonate, *Polym. Degrad. Stabil. 23*:51 (1988).

6

Mechanical Properties of Polycarbonates

Donald G. LeGrand
General Electric Company, Schenectady, New York

I. INTRODUCTION

The investigation of different polycarbonate structures has focused on specific properties, e.g., high heat distortion temperature (HDT), hydrolytic and ultraviolet (UV) stability, permeability, and flammability. However, most work has been performed on the polycarbonate of diphenylol-2,2′-propane, better known as bisphenol A polycarbonate or, more briefly, as BPA-PC because of its unusual ductility [1–18].

The mechanical properties of polycarbonates and other amorphous thermoplastics are a function of their molecular structure, molecular weight, end-groups, methods of fabrication, secondary finishing operations including annealing, and physical aging [1–136]. In the latter case, the primary distinction between annealing and physical aging is that the former is done to relieve residual internal stresses and strains whereas the latter is a naturally occurring process. This process goes on between the glass transition of a material and its low-temperature γ peak according to Struik [20,60,125].

Early studies of the stress relaxation, creep, and dynamic mechanical behavior of BPA-PC were conducted under both tension and torsion for two different molecular weight materials [23]. In the same time period, Izod impact, yield stress, and density were done on samples with different molecular weights and annealed at several temperatures below T_g for varying lengths of time [3]. The dynamic mechanical studies suggested the presence of three transitions that were denoted α, β, and γ where the α peak was assigned to the glass transition and the β to the presence of residual stresses in the sample [28]. The γ transition was

interpreted as consisting of three peaks on the basis of dielectric, broad-line NMR, and the mechanical data and was proposed to involve internal motions of the BPA-PC monomer.

The primary objective of many of these early studies was to explain the unusual ductility of BPA-PC. Many investigators believed that the low-temperature γ transition was responsible for its ductility, but other thermoplastics with similar low-temperature transitions do not have similar ductility [16,19]. Excess free volume and the presence of residual stresses have also been proposed to explain this ductility.

There are many different aspects in terms of the mechanical properties that need to be addressed in order to have a complete understanding of the behavior of polycarbonates. As a result, their properties will be discussed on the basis of data from several different mechanical test methods. However, as a basis for this discussion, the first section will examine a model that has been used to interpret some of these data. It should be noted that other models have been proposed and used to interpret the same or similar data.

II. MODELING

The earliest models to interpret and extrapolate mechanical data were based on several models that had been developed for metals. In general, they were founded on the basis of the classic Kelvin-Voigt and Maxwell models, which are illustrated in Fig. 1. These models were empirical in the sense that they only involved the assumption of elasticity, anelasticity, and plasticity. However, they had lim-

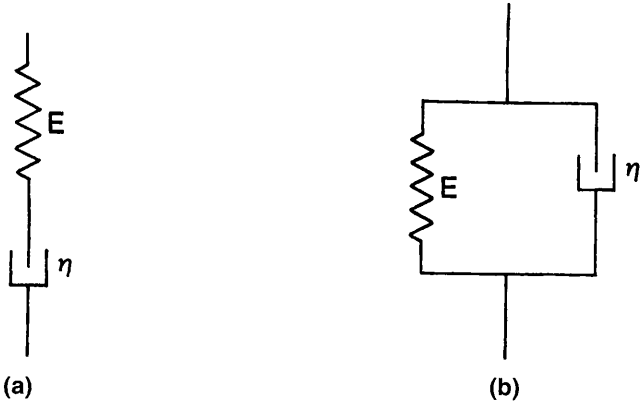

Figure 1 (a) Kelvin-Voigt model. (b) Maxwell model.

ited use in providing a fundamental explanation of the properties, particularly the phenomenon of physical aging.

As a consequence, subsequent models tended to focus on the use of the concept of free volume because of the classic studies of Kovacs [104], who studied the volume relaxation behavior of a polymer glass as it was subjected to different thermal histories. These studies demonstrated that if a polymer glass was brought the same temperature below T_g by different thermal histories, then the volume relaxation behavior was dependent on the path of the thermal history. Differential scanning calorimetry (DSC) studies by Petrie and coworkers supported the work of Kovacs by showing that thermal history had an important effect on the DSC response, in particular at the T_g [105].

The idea that defects exist in amorphous polymer glasses is more recent and is based in part on the same concept as in crystals. The primary difficulty is that early ideas behind these defects focused on similarities with crystals, resulting in large-scale Volterra dislocations that encompassed the sample cross-section. More recently, such defects have focused on conformational states that might coexist within a given polymer chain. In the case of BPA-PC, cis, trans, and trans, trans sections have been predicted on the basis of light scattering data as well as quantum field calculations. It is believed, although not experimentally verified, that the thermal quenching of BPA-PC captures some of the higher energy cis, trans conformers and that these serve as the nuclei for local internal deformation [14]. This model has led to the development of another set of equations that have been used to describe the response of BPA-PC to a variety of mechanical test conditions as will be discussed later in this chapter [33]. Clearly, it should be understood that these alternative equations provide a different insight into the basic understanding of how this material and other glassy polymers might respond to mechanical deformation.

Alternative methods of analysis and a more detailed discussion of this model can be found in Chapter 3 on molecular modeling and Chapter 10 on physical aging.

The procedures for analyzing data obtained from either stress relaxation or creep experiments have been based primarily on two different assumptions. In the first case, it is assumed that the amorphous polymer glass that is subject to either constant strain or stress will ultimately be converted to the melt state, i.e., it will undergo flow like a liquid. There is nothing in the laws of physics to support this assumption. In the second case, it is assumed that the glass will remain a glass unless it is chemically or biologically degraded. As a result of different assumptions, the equations that have been used to analyze the data have a different from as given below.

$$J(t) = J^* \phi(t) \tag{1}$$

$$J(t) = J1 + J2\ \phi(t) \tag{2}$$

In Eq. (1), J^* is the compliance when $t = 0$ and $\phi(t)$ is an increasing function of time. In the case of the second equation, $J1$ is equal to the zero time compliance, $J2$ contributes to the change in the compliance between $t = 0$ and $t = \eta$ as the function $\phi(t)$ increases. Clearly, at infinite time, Eq. (2) predicts that $J(t)$ will be equal to $J1 + J2$ whereas Eq. (1) predicts that it will become infinite. In the case of stress relaxation, the equations will be given by

$$E(t) = E^* \phi(t) \tag{3}$$

$$E(t) = E_1 + \Delta E \phi(t) \tag{4}$$

which when t goes to infinity, $E(t) = 0$ in Eq. (1) or $E(t) = E_1$ in Eq. (4).

The critical issue in the use of either set of equations or any other equation is not whether the data can be fitted by the equation but rather whether the model from which they have been formulated can satisfy the underlying physics and provide predictions that can be used to further test the model. If the equations are empirical, then their primary use must be considered as either a time-dependent strain or stress calculator and clearly can be useful in engineering applications where one is concerned about dimensional instabilities including failure.

III. DYNAMIC MECHANICAL ANALYSIS

The first dynamic mechanical data on polycarbonate were reported by Illers and Bruer [27]. This work followed the earlier dielectric work of Krum and Muller who studied both stretched and annealed samples [26]. These works were quickly followed by a series of papers by several investigators in which the origins of the various transitions were addressed [28–30]. Wada and colleagues reported on mechanical dispersions in polycarbonate in the early 1960s and Reding and associates gave a detailed discussion on polycarbonates in the same time frame [43,44]. In 1981, Yee and Smith presented a systematic study of the dynamic mechanical response of a number of different polycarbonate structures [19]. This study was seminal in its presentation because it set the stage for work that has focused on the β and γ transitions. Othmezouri-Decerf provided an interpretation of the linear response of glassy polycarbonate in the nonlinear range [34]. Yee and coworkers continued their studies in the 1990s and provided new data on the origin of the low-temperature transition [36,37]. They proposed that it involves a motion of two consecutive monomers. This interpretation is based on studying copolymers containing various size block units [37]. Studies of the γ transition have been presented by other investigators who proposed a different model. The molecular dynamics of the β process has been discussed by Havriliak and Shortridge [39].

Similar studies of a variety of copolymers of BPA-PC with other comonomers have been presented [41]. It should be noted that there is still a need for an experimental method and a molecular theory that can elucidate the ductile behavior of this material. Other studies have been reported in Refs. 38–41.

IV. STRESS RELAXATION

In the early 1950s, Tobolosky and McCloughin studied the stress relaxation of poly(methyl methacrylate) (PMMA) and noted that the rate of relaxation was dependent on its history [46]. This work was the earliest work on polymer glasses that indicated that thermal history could have an effect even though it had been known for some time that the mechanical and optical properties of inorganic glasses could be altered by thermal annealing. In fact, the Kohlrauch-Williams-Watts (KWW) equation was used to describe the rates of change in these materials.

In general, it can be stated that most aromatic polycarbonates exhibit similar stress relaxation behavior. Typical tensile data are shown in Fig. 2a at three different temperatures as a function of log time for samples with the same thermal history; the coefficient temperature variations are shown in Fig. 2b. Similar data are presented in Fig. 3 for the same strain level and temperature but different thermal histories, and in Fig. 4 for the effect of strain on annealed samples at room temperature. It should be noted that all of the data in Fig. 3 and 4 were taken at least 60°C below the T_g of BPA-PC. Evaluation of these data by Eq. (3) and data for other polycarbonates indicates that the primary effects of strain level, temperature, and thermal history are in the variation of coefficients E_1 and E_0 rather than τ or β. These results suggest that the underlying morphology and topology of the amorphous chains are more critical in determining the amount of relaxation than the rate of relaxation. This hypothesis is in agreement with some of the modeling work of Sutter and his colleagues which starts with a primitive cell structure and then increases the size of the test specimen by increasing the number of cells [47,47a]. Bendler has carried out similar work using the idea of local defects in structure [48,66]. These defects act as stress concentrators and are the initiation sites for initial response. As the sample is stressed the size of the site increases until macroscopic deformation is attained.

In 1965, Tobolosky and his colleagues reported the first study of the stress relaxation of BPA-PC from below the glass transition up into the melt for two different molecular weights [23]. They also reported the glass transitions, thermal coefficients of expansion, and volume–temperature for these two materials. They used these latter data to perform a time–temperature superposition of the data. In 1972, Yannas et al. studied the stress relaxation of this material at room temper-

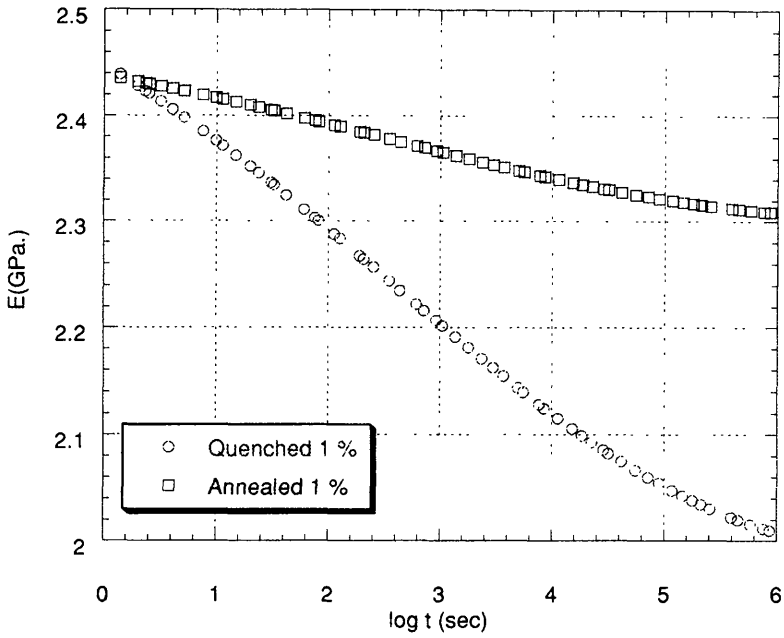

Figure 3 Comparison of the tensile stress relaxation modulus at room temperature for quenched and annealed BPA-PC samples.

ature as a function of strain level in order to determine its transition from a linear to a nonlinear response [24]. Similar work was reported by Litt and Torp who studied both the strain and temperature dependence relaxation phenomenon [22]. Matsuoka et al. also studied the relaxation of this material [50]. The cryogenic relaxation was studied by Hong and Brittain who noted the existence of a peak below the gamma transition [49]. The first detailed studies of the effects of thermal history, strain, and temperature were reported in the 1980s by LeGrand, Olszewski and Bendler [51–53]. Subsequent work by these investigators compared creep and stress relaxation on samples with the same thermal history as a method of testing their model, which has been described earlier [53]. Other

Figure 2 (a) Tensile stress relaxation modulus as a function of log time for thermal quenched BPA-PC at a 1% strain. (b) A plot of the variation of E_i and ΔE with temperature for quenched BPA-PC samples at a 1% strain.

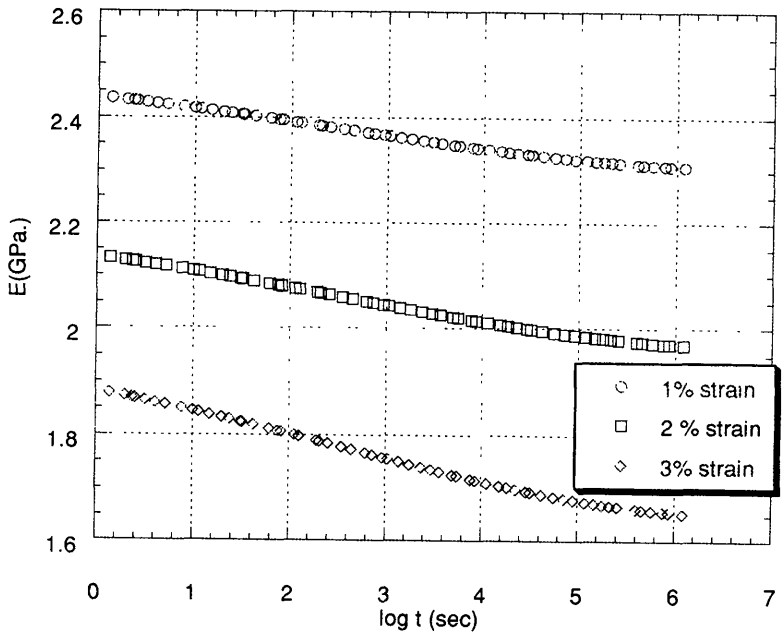

Figure 4 Effect of strain level on the tensile stress relaxation modulus for annealed BPA-PC samples.

investigators reported similar data but the method used to analyze the data was different [54]. These methods and an application of them is provided at the end of this section.

Yee and colleagues described the use of a tickle experiment to follow structural changes that occur in BPA-PC during stress relaxation and focused their attention on changes in the exponent, β, and the relaxation time, τ [54]. A careful examination of their procedure indicates that they assumed the quantity t/τ. Furthermore, their method of analysis involves other assumptions, i.e., that the material will be converted at infinite time to a liquid and that the response from the tickle can be analyzed independently. As a result, while the values of β which are derived from this approach are similar to that of other methods, the values of τ as a function of both strain and temperature history appear physically unreasonable. In fact, the magnitudes of τ derived by their procedure invalidate the assumptions used to derive them, i.e., $t/\tau = 1$ where t is the experimental time.

Empirical horizontal and vertical shifting of either creep or stress relaxation data obtained as a function of aging time, temperature, or constant stress/strain may be useful in correlating large amounts of experimental data. This is one

method of predicting the long-term behavior for many engineering applications and does not require significant knowledge of material behavior.

V. CREEP

The investigation of the creep behavior of polycarbonates was initiated in the early 1960s by Lai and Findley who did combined tension–torsion experiments in the nonlinear range [29]. They analyzed their data using an empirical equation proposed by Marin and Pao which had been previously used on a variety of other materials. Subsequent work by Mindel and Brown in the 1970s and the works of Struik indicated that the material was undergoing an aging process [20,30,31,60]. These works have been followed by more recent work of Matsumoto and others [130]. Read et al. have provided a detailed time–temperature–compliance picture for this material [64]. The analysis of these data has been performed by assuming two different models for the behavior. The algorithm that is proposed for one model assumes that a polymer glass under a constant stress will ultimately behave as a liquid, whereas the algorithm for the other model assumes that there will be a limiting compliance at infinite time. This phenomenon has been discussed by Chai and McCrum [61]. As an illustration of these different approaches, creep data on BPA-PC have been analyzed.

VI. STRESS–STRAIN

The first detailed study of the temperature dependence of strain–strain behavior of polycarbonate was reported by Ekvall and Low [67]. Their study was conducted on films rather than injection-molded samples. They observed that the material underwent shear yielding similar to that observed in some metals and that at very low temperatures the samples underwent a ductile-to-brittle transition. Mears and Pae studied the deformation and fracture of this material as a function of hydrostatic pressure and demonstrated that brittle fracture was suppressed by the application of pressure [68]. Wu and Turner reported on the strain response to complex stress histories but failed to take into account thermal and processing histories in their work [69]. They determined the thermal activation parameters for the large strain deformation of polycarbonate, whereas Yee and Detorres examined how a sudden change in strain rate would effect the yield process and found that the yield stress increased if the strain rate was decreased [76]. They interpreted this in terms of the Robertson model of yielding [84]. LeGrand [3] and Haward [70] reported on the effects of thermal annealing on yield behavior. Bauwens attempted to correlate the yield processes above and below the glass transition using a modified Eyring model [77], whereas Heymans proposed a

model to explain the development of orientation at large strains [79]. Titomanlio and Rizzo studied the large strain compressive behavior of BPA-PC [74]. Brown and Windle presented a model to interpret the stress–orientation–strain in amorphous glassy polymers [72]. The large strain–stress behavior at high temperatures were reported by Nied et al. [75]. The effects of thermal pretreatment on the fracture behavior in medium strain rate tensile experiments have been reported by Paakkonen [78].

VII. IMPACT

The impact behavior of BPA-PC has long intrigued investigators because it was the first high-temperature amorphous thermoplastic to exhibit ductile behavior in a notched Izod impact test. The first reports of this in the technical literature were in 1967 by Golden et al., who focused on the effect of thermal pretreatment on the strength of BPA-PC and in a second paper on the effects of molecular weight and strain rate [1,2]. Subsequently, LeGrand reported on the combined effects of molecular weight, annealing times, and annealing temperatures [3]. The data were correlated by an empirical equation that would be used to predict the influence of these various parameters [3,10]. A model based on the work of Robertson was proposed and assumed that annealing altered the concentration of conformers [3]. This model has been further advanced in the work of Bendler and Shlesinger [14]. LeGrand as well as Key and Katz [5] noted that a critical flaw was formed at the tip of the notch in notched samples [3]. Locati and Tobolosky discussed this toughness in light of its low-temperature transition, which was discussed earlier [4].

There are at least two reasons to believe that the notched Izod impact value is not a consequence of the low-temperature transition. The first is that the dynamic mechanical response of many of the different polycarbonate structures as well as other aromatic polymers exhibits a low-temperature γ transition. Second, thermal annealing of BPA-PC causes little change in the low-temperature transition but does result in a loss in notched Izod impact strength. It should be noted that in the absence of a notch even well-annealed samples of BPA-PC are quite ductile unless there has been extensive chemical degradation.

Broutmann and Krishnakumar proposed that the toughness of polycarbonate was due to the residual stresses in its surface and demonstrated an enhanced toughness as a result of cold rolling [6,7]. Paravin and Williams reported on the ductile-to-brittle transition in polycarbonate [8], whereas Mills discussed the mechanism of brittle fracture in this material [11]. Ryan presented an extensive study of the impact and yield properties as a function of strain rate, molecular weight, thermal history, and temperature similar to previous works [10]. Bendler and Shlesinger presented a model that can be used to explain the molecular weight

dependence on the rate of thermal aging [14]. Bubeck et al. examined the effects of copolymerization on the ductility of BPA-PC [16]. Most recently, Chang and Hsu have discussed the precrack hystersis energy in regard to ductile-to-brittle transition [15].

Other models that have been discussed involve both free volume and coupling. An early model used to explain this was based on the concept of free volume and assumed that the amount of free volume was related to ductility. In more recent times, this model has been expanded to include fluctuations in free volume. A critical question in this model is the definition of free volume, i.e., is it the difference between the hard core and the glass or the liquid volume and the glass? Another model, i.e., the coupling model, was proposed some 15 years ago and involves the idea of cooperative interactions between primary species and their surroundings. As noted by Hutchinson, this model is not thermorheologically simple and as a result is distinctly different from other models [132].

VIII. THERMAL RECOVERY

The early observation that glassy polymers such as polystyrene and PMMA exhibited brittle fracture when tested in tension suggested that the mechanism of failure involved the fracture of chemical bonds as discussed in some of the early works of Berry [83]. In contrast to the behavior of these materials, BPA-PC underwent extensive uniaxial deformation. The mechanism of this large-scale deformation was initially thought to occur via a mechanism similar to that for polymer melts because it was proposed that during yielding and cold drawing the sample's temperature was increased above the glass transition. Subseqent work demonstrated that the temperature rise was insufficient to convert the material from a glass to a melt [84]. At the time Andrews and coworkers reported that hot-drawn samples of polystyrene would undergo partial shrinkage if heated to their glass transition [85]. LeGrand reported that while cold-drawn samples underwent complete recovery, hot-drawn samples exhibited only partial recovery in accordance with the data on polystyrene [86].

These early studies have been followed by a number of other studies, but in general the results are the same [87–94]. The primary conclusion of these studies is that the large-scale yielding of this polymer glass is similar to the stretching of a rubber and that little if any disentanglement of the chains occurs during or after the deformation [94]. In contrast, large-scale deformation of this material well above its glass transition must involve some disentanglement because full recovery is not observed. Most recently, it has been observed that residual strains in samples that have undergone stress relaxation or creep well below the glass transition exhibit a series of transitions but in all cases total recovery [94].

IX. RESIDUAL STRESSES

The effects of residual stresses in polycarbonate were first discussed by Litt and Koch [96] and by So and Broutmann [97] in terms of impact. Later studies by So and Broutmann examined their effect on mechanical properties in general. Much work has focused on the mechanisms of the development of these stresses, their measurement, and their distribution [6,7,97]. The effect of residual stresses on the viscoelastic and aging properties of polycarbonate have been reported [98–109].

X. PHYSICAL AGING AND ANNEALING

Currently, at least four different models have been proposed to explain physical aging and these models are based on different assumptions [110–136]. In general, most theoretical work has focused on volumetric and DSC data rather than mechanical and dielectric data. In fact, the early volumetric and DSC data of Kovacs and Petrie [104,105] and the more recent work of Hodge [106] have served as the primary database for model development and/or testing. This circumstance has changed and thermorheologically simple models to describe these latter properties are being investigated [107–109].

The early works of Tobolosky and McCloughlin [46] provided the first evidence of the influence of thermal history on stress relaxation behavior of glassy polymers. Polycarbonates are no exception and are influenced by thermal history as discussed in earlier parts of this chapter as well as in other chapters. It is unfortunate that the terms *physical aging* and *annealing* may be used to describe the same effects depending on the objectives of the work. For example, thermal annealing below the glass transition is known to reduce residual stresses and at the same time to alter a number of the mechanical properties of the material. Is this reduction in residual stress a part of the physical aging process? Are the changes in mechanical properties due to physical aging or are they independent of the annealing process? Some of the answers to these questions are dependent on the objectives of the investigation, whereas others are clearly a matter of semantics.

Struik was probably the first investigator to identify the changes in the properties of amorphous polymers as physical aging and who proposed that the process would occur between the glass transition and the low-temperature γ transition [20,60,125]. Subsequently, Guerdoux and Marchal discussed physical aging in the region of the γ transition whereas Bubeck et al. reported on changes in the yield and deformation of polycarbonates that were caused by physical aging [126,129]. A series of papers by Smith and associates reported on the effects of both tensile and compressive strains on the physical aging process [119–124]. Matsumoto discussed the effects of physical aging on the creep response of poly-

carbonate and time–temperature [130]. The influence of physical aging on the macroradical reactivity in polycarbonate was studied by Bartos et al. [128].

XI. CRAZING AND CRACKING

Crazing and cracking of amorphous thermoplastics are known to occur as a result of several different circumstances including mechanical fatigue, exposure to simple organic liquids, and exposure to everyday environments [137–142]. In many of these cases, specific chemicals such as gasoline or alkaline detergent solutions may be the cause of both crazing and cracking as a result of the presence of large residual stresses. Annealing as discussed earlier, alternative processing conditions, and tool design can minimize such problems.

A detailed study of the effect of strain on crazing of polycarbonate in the presence of different organic liquids on compression-molded samples was undertaken by Kambour et al. using Bergen jigs [137,139–141]. Attempts to correlate these results with the solubility parameter of the liquids, the amount of liquid absorption, and the depression of the glass transition have been discussed. Miller et al. presented data with respect to gasoline as well as several other organic liquids [138]. Mechanisms by which crazes are formed in glassy polymers have been proposed by Gent [143] and by Argon and Hannosh [151]. Sternstein et al. discussed the inhomogeneous deformation and yielding of polymers in terms of local complex stress fields [157]. Detailed reviews of crazing have been presented by Kambour [137,147] as well as by Rabinowitz and Beardmore [148] and more recently by Kramer [142].

Crazing and cracking have also been observed when BPA-PC is exposed to elevated temperatures in the presence of moisture. In many cases, the sites where the crazes and cracks were initiated appear to be near or at contaminant particles. Addition of some organic compounds appears to retard but not stop these effects from occurring. It is believed that the additives may be acting as both physical and chemical stabilizers. In the former case the additive may be absorbed on the surface of the contaminant particle and reduce local stresses around the particle, whereas in the latter case it chemically interacts with the material.

The fact that crazing can be initiated during mechanical fatigue at both low and high stresses and that the type of craze is dependent on the magnitude of the stress field clearly implies that mechanisms of craze initiation might differ. These results are similar to the combined effects of temperature- and solvent-induced crazing, i.e., thermochemical crazing. It seems possible that one mechanism can be associated with the presence of particulate matter and another with effects of the environment in a number of amorphous and semicrystalline polymers.

Plummer and Donald studied the structure and crazing of ultrathin films of BPA-PC in the electron microscope [159], whereas Verheulpen-Heymans and Bauwens studied the growth of crazes during low-stress creep [145]. Takemori studied the formation of crazes druing mechanical fatigue at both low and high stress levels [161–165]. More recently, LeGrand reported on the thermochemical crazing as a function of thermal quenching temperature, molecular weight, and organic liquids [153].

A primary mechanism of crazing might involve contaminants while the other mechanism might be associated with an intrinsic crazing mechanism such as the types proposed by Gent and Argon. This possibility might be an explanation for Kambour's difficulty in correlating his solvent stress crazing and cracking data with the solubility parameters of liquid, i.e., the presence of particulate matter could enhance the local strain and stress and cause crazing to occur at lower strains and stresses. Obviously, this hypothesis can be tested by comparing materials that have been contaminated with materials that have prepared and tested in an ultraclean and ultrapure environment. In the case of BPA-PC, the testing of materials prepared by the melt process provides one possible approach since in theory these materials are the cleanest in terms of contaminants.

Electron microscopy has been used extensively by Kramer and Donald to study the formation and morphology of crazes. Much of their work has been predicated on the assumption that ultrathin films prepared from polymer solutions are the same as macroscopic samples.

XII. FATIGUE

Thermoplastics such as BPA-PC because of their ductility can exhibit two distinct modes of crack propagation [162]. The first is a craze-dominated subcritical discontinuous crack growth mode at low stresses yielding a short fatigue life. The alternate mode is a shear fracture mode that yields a long fatigue life at high stresses. These two different modes of failure are dependent on the balance of temperature and stress level. Other factors such as physical aging, frequency, and both thermal and mechanical history can also affect this behavior [160].

XIII. POSITRON ANNIHILATION AND THERMALLY STIMULATED CURRENT

The use of thermally stimulated current and positron annihilation to investigate residual free volume and electric charges in polycarbonate has been the subject of several papers in recent years. A number of investigators have reported on the effects of thermal treatment on the thermally stimulated discharge current and

the dielectric relaxation [167,168,174]. More recent work has been reported by Bernes and others [175–177].

In the case of positron annihilation, the primary objectives have been to determine if and how free volume changes occur as a result of tensile deformation, thermal aging, and physical aging [169–172]. A recent article by Hutchinson gives an excellent critique of the studies and their conclusions [132]. In the case of polycarbonate, it is argued that PC ductility is related to PC free volume.

XIV. COPOLYMERS AND BLENDS

As noted in earlier chapters, a number of different copolymers containing either alternating and/or random blocks of BPA-PC with other comonomers have been studied. Early work by Goldberg involved the use of polyethylene glycols, whereas that of Vaughn focused on the incorporation of dimethyl silicone blocks [178–190]. The mechanical properties of the latter materials were reported by Kambour and LeGrand [178–190]. Copolymerization of BPA-PC with aspriobindane was patented by Faler and coworkers. Yee, Smith, Bubeck et al. discuss the mechanical properties of several different BPA-PC copolymers and note that mechanical impact properties are dependent on thermal aging and molecular structure [19,40,41].

Much work has been done with blending BPA-PC with other polymers such as polybutylene terephthalate, polystyrene, etc., and in many cases an impact modifier has been added to recover impact strength [193].

REFERENCES

1. J. H. Golden, B. L. Hammant, and E. A. Hazell, The effect of thermal pretreatment on the strength of polycarbonate, *J. Appl. Polym. Sci. 11*:1571 (1967).
2. J. H. Golden, B. L. Hammant, and E. A. Hazell, Effects of molecular weight and strain rate on the flexural properties of polycarbonate, *J. Appl. Polym. Sci. 12*:557 (1968).
3. D. G. LeGrand, Crazing, yielding, and fracture of polymers 1. Ductile-brittle transition in polycarbonate, *J. Appl. Polym. Sci. 13*:2129 (1969).
4. G. Locati and A. V. Tobolosky, Studies of the toughness of polycarbonate of bisphenolo A in light of its secondary transition, ONR Tech. Rep. 115, Feb. 1969.
5. P. L. Key and Y. Katz, On the pop-in mode of fracture, *Int. J. Frac. Mech. 5*:63 (1969).
6. L. J. Broutmann and S. M. Krishnakumar, Impact strength of polymers. 1. The effect of thermal treament and residual stress, *Polym. Eng. Sci. 16*:74 (1976).
7. L. J. Broutmann and S. M. Krishnakumar, Cold rolling of polymers. 2. Toughness enhancement in amorphous polycarbonate. *Polym. Eng. Sci. 14*:249 (1974).

8. M. Paravin and J. G. Williams, Ductile-brittle transition in polycarbonate, *Int. J. Frac. 11*:963 (1975).
9. G. P. Marshall and J. G. Williams, *J. Mater. Sci. 8*:138 (1973).
10. J. T. Ryan, Impact and yield properties of polycarbonate as a function of strain rate, molecular weight, thermal history, and temperature, *Polym. Eng. Sci. 18*:264 (1978).
11. N. J. Mills, The mechanism of brittle fracture in notched impact tests of polycarbonate, *J. Mater. Sci. 11*:363 (1976).
12. G. L. Pittman, I. M. Ward, and R. A. Duckett, *J. Mater. Sci. 13*:2092 (1978).
13. U. Biskup, D. Rathmann, and P. TAcke, *Die Angewandte Makromol. Chem. 144*: 11 (1986).
14. J. T. Bendler and M. F. Shlesinger, Defect-diffusion models of relaxation, *J. Mol. Liq. 36*:37 (1987).
15. F. C. Chang and H. C. Hsu, Effect of polycarbonate molecular eight on precrack hystersis energy in determining its ductile-brittle transiton, *J. Appl. Polym. Sci. 43*: 1025 (1991).
16. R. A. Bubeck, P. B. Smith, and S. E. Bales, in *Order in the Amorphous State of Polymers* (S. K. Keinath, R. L. Miller, and J. K. Rieke, eds.), Plenum Press, New York, 1987.
17. F. C. Chang and L. H. Chu, Co-existence of ductile, semi-ductile, and brittle failures of polycarbonate, *J. Appl. Polym. Sci. 44*:1615 (1992).
18. A. Kim, A. Chudnosky, and C. P. Bosnyak, Effects of weathering, scale and rate of loading on polycarbonate fracture toughness, *J. Appl. Polym. Sci. 51*:1841 (1994).
19. A. F. Yee and S. A. Smith, Molecular structure effects on the dynamic mechanical spectra of polycarbonates, *Macromolecules 14*:54 (1981).
20. L. C. E. Struik, Physical aging, in *Encyclopedia of Polymer Science and Engineering*, Vol. 1, John Wiley and Sons, New York, 1985.
21. D. G. LeGrand, Annealing, in *Encyclopedia of Polymer Science and Engineering*, Vol. 2, John Wiley and Sons, New York, 1985.
22. M. H. Litt and S. Torp, Strain and temperature dependence of relaxation phenomena in polycarbonate, *J. Appl. Phys. 44*:4282 (1973).
23. J. P. Mercier, J. J. Aklonis, M. Litt, and A. V. Tobolosky, Visco-elastic behavior of the polycarbonates of bisphenol-A, *J. Appl. Polym. Sci. 9*:447 (1965).
24. V. Yannas, N. H. Sung, and A. C. Lunn, Transition from linear to nonlinear viscoelastic behavior. II. Stress relaxation of polycarbonate, *J. Macromol. Sci.-Phys. B5*: 487 (1971).
25. V. Yannas and M. J. Doyle, Comparison of optical and mechanical limits of linear relaxation behavior in glassy polycarbonate, *J. Polym. Sci A-2 10*:159 (1972).
26. F. Krum and F. H. Muller, Vorbehandlung und dielektrisches verhalten hochpolymerer, *Kolloid Zeit. 164*:81 (1959).
27. K. Illers and H. Bruer, *Kolloid Zeit. 176*:110 (1961).
28. D. G. LeGrand and P. F. Erhardt, Dynamic mechanical properties of polymers, *Appl. Polym. Sci. 13*:1707 (1969).
29. J. S. Y. Lai and W. N. Findley, Combined tension–torsion experiments on polycarbonate in the non-linear range, *Polym. Sci. Eng. 9*:373 (1969).
30. M. J. Mindel and N. Brown, *J. Mater. Sci. 8*:863 (1973).

31. M. J. Mindel and N. Brown, *J. Mater. Sci. 9*:1661 (1974).
32. R. E. Robertson, *Appl. Polym. Sci. 7*:201 (1968).
33. A. D. Williams and P. J. Flory, Analysis of the random configuration of the polycarbonate of diphenylol-2,2′-propane, *J. Polym. Sci. A-2 6*:1945 (1968).
34. J. Othmezouri-DeCerf, Interpretation of the linear response of glassy polycarbonate deformed in the non-linear range, *Polym. Rep. 29*:641 (1988).
35. J. Othmezouri-DeCerf, *Polymer 29*:2463 (1988).
36. J. T. Jho and A. F. Yee, *Macromolecules 24*:1905 (1991).
37. C. Xiao and A. Yee, *Macromolecules 25*:6800 (1992).
38. C. Xiao and A. Yee, *Polym. Prepr. 33*:100 (1992).
39. S. Havriliak, Jr., and T. J. Shortridge, Molecular dynamics of the beta process in the polycarbonate of bisphenol-A, *Polymer 31*:1782 (1990).
40. R. A. Bubeck, S. E. Bales, and H. D. Lee, *Polym. Eng. Sci. 24*:1142 (1984).
41. R. A. Bubeck, P. B. Smith, and S. E. Bales, Molecular origins of deformation behavior and physical aging of polycarbonates, in *Order in the Amorphous State of Polymers* (S. E. Keinath, R. L. Miller, and J. A. Rieke, eds.), Plenum Press, New York, 1987.
42. H. J. Kolman, K. Ard, and C. L. Beatty, Variation of dynamic mechanical properties as a result of deformation, *Polym. Eng. Sci. 22*:950 (1982).
43. K. Arisawa, H. Hirose, M. Iskikawa, T. Harada, and Y. Wada, Mechanical dispersions in polycarbonate, *Jpn. Appl. Phy. 2*:695 (1963).
44. F. P. Reding, J. A. Faucher, and R. D. Whitman, *J. Polym. Sci. 54*:556 (1961).
45. L. E. Nielsen, *Mechanical Properties of Polymers*, Reinhold, New York, 1962.
46. J. R. McLoughlin and A. V. Tobolosky, The viscoelastic behavior of polymethyl methacrylate, *J. Colloid Sci. 7*:555 (1952).

46a. J. R. McLoughlin and A. V. Tobolosky, Effect of rate of cooling on stress relaxation of polymethyl methacrylate, *J. Poly. Sci. 7*:658 (1951).

47. A. A. Gusev, M. M. Zehnder, and U. W. Suter, Elasticity of solid polymers as a result of thermal motion, *Macromolecules 27*:615 (1994).

47a. D. N. Theodorou and U. W. Suter, Atomistic modeling of mechanical properties of polymeric glasses, *Macromolecules 19*:139 (1986).

48. J. T. Bendler, Levy (stable) probability densities and mechanical relaxation in solid polymers, *J. Stat. Phys. 36*:625 (1984).
49. J. Hong and J. O. Brittain, On the cryogenic relaxation in polycarbonate, *J. Polym. Sci.: Polym. Letts. 19*:295 (1981).
50. S. Matsuoka, H. E. Bair, S. S. Bearder, H. E. Kern, and J. T. Ryan, *Polym. Eng. Sci. 18*:1073 (1978).
51. D. G. LeGrand, W. V. Olszewski, and J. T. Bendler, Anelastic and plastic response of polymers, *Ann. NY Acad. Sci. 484*:307 (1986).
52. D. G. LeGrand, W. V. Olszewski, and J. T. Bendler, Anelastic behavior of bisphenol-A polycarbonate, *J. Polym. Sci. B: Polym. Phys. 25*:1149 (1987).
53. D. G. LeGrand, W. V. Olszewski, and J. T. Bendler, Strain, birefringence, and volume relaxation and recovery in polymer glasses, *Thermochim Acta 166*:105 (1990).
54. A. F. Yee, R. J. Bankert, K. L. Ngai, and R. W. Rendell, Strain and temperature accelerated relaxation polycarbonate, *J. Polym. Sci. B: Polym. Phys. 26*:2463 (1988).

55. J. M. Alberdi, A. Alegria, E. Macho, and J. Colmenero, Viscosity and relaxation times temperature behavior above the glass transtion in some glassy polymers, *Polym. Bull. 18*:39 (1987).
56. F. J. Horth, K. J. Kuhn, J. Mertes, and G. P. Hellmann, *Polymer 33*:1223 (1992).
57. F. J. Horth, K. J. Kuhn, J. Mertes, and G. P. Hellmann, On the mechanical γ-relaxation modes of polycarbonate, *Polymer 33*:1223 (1992).
58. N. G. McCrum, B. E. Read, and G. Williams, *Anelastic and Dielectric Effects in Polymeric Solids*, John Wiley and Sons, London, 1967.
59. D. G LeGrand, Relaxation of residual thermal stresses and strains: effects on tensile stress relaxation and creep, *J. Rheol. 39*:437 (1995).
60. L. C. E. Struik, Physical aging in amorphous polymers and other materials. Amsterdam: Elsevier, 1978.
61. C. K. Chai and N. G. McCrum, The freezing-in of non-equilibrium values of the limiting compliances as a mechanism of physical aging, *Polymer 21*:706 (1980).
62. G. B. McKenna, Glass formation and glassy behavior, in *Comprehensive Polymer Science: Polymer Properties*, Vol. 2 (C. Booth and C. Price, eds.), Pergamon Press, Oxford, 1989, pp. 311–362.
62a. G. B. McKenna, On the physics required for prediction of the long term performance of polymers and their composites, *J. Res. Natl. Inst. Stand. Tech. 99*:169 (1994).
62b. W. Waldron, Jr., G. B. McKenna, and M. M. Santore, The nonlinear visco-elastic response and apparent rejuvenation of an epoxy glass, *J. Rheol. 39*:471 (1995).
63. D. S. Matsuoka, Time–temperature superposition and physical aging in amorphous polymers, *Polym. Eng. Sci. 22*:1313 (1988).
64. M. A. Hussain, J. T. Bendler, and D. G. LeGrand, Asymptotic and approximate solution for mechanical relaxation, creep and recovery in glassypolymers, *Comput. Eng. 2*:73 (1990).
64a. B. E. Read, P. E. Tomlins, and G. D. Dean, Physical ageing and short-term creep in amorphous and semicrystalline polymers, *Polymer 31*:1204 (1990).
65. B. E. Read, Analysis of creep and physical aging in glassy polymers, *J. Noncryst. Solids 131*:408 (1991).
66. J. T. Bendler and M. F. Shlersinger, Defect diffusion models of relaxation, *J. Mol. Liq. 36*:37 (1987).
67. R. A. Ekvall and J. R. Low, Jr., Temperature dependence of tensile properties of polycarbonate films, *J. Appl. Polym. Sci. 8*:1677 (1964).
68. D. R. Mears and K. D. Pae, Deformation and fracture of polycarbonate under high pressure, *Polym. Lett. 7*:349 (1969).
69. W. Wu and A. P. L. Turner, Thermal activation parameters for large strain deformation of polyethylene and polycarbonate, *J. Polym. Sci. 13*:19 (1975).
70. R. N. Haward, The effect of chain structure on the annealing and deformation behavior of polymers, *K. Zeit. Zeit. Polym. 258*:42 (1980).
71. C. J. G. Plummer and A. M. Donald, *J. Polym. Sci: B: Polym. Phys. 27*:325 (1989).
72. D. J. Brown and A. H. Windle, Stress-orientation-strain relationships in noncrystalline polymers. 1. Strategy for a model, *J. Mater. Sci. 19*:1997 (1984).
73. N. Heymanns, *Polymer 87*:2009 (1987).

74. G. Titomanlio and G. Rizzo, Compressive large deformation viscoelastic behavior of a polycarbonate, *Polymer 21*:461 (1980).
75. H. F. Nied, V. K. Stokes, and D. A. Ysseldyke, High-temperature large-strain behavior of polycarbonate, polyetherimide, and poly(butylene)terephthalate, *Poly. Sci. Eng. 27*:101 (1987).
76. A. F. Yee and P. de Detorres, The effect of sudden strain–rate change on the yield behavior of bisphenol-A polycarbonate, *Polym. Eng. Sci. 14*:691 (1974).
77. J. C. Bauwens, Attempt to correlate the yield processes above and below the glass transition in glassy polymers, *Polymer 25*:1523 (1984).
78. E. J. Paakkonen, Effect of thermal pretreatment on the fracture behavior of polycarbonate in medium strain rate tensile tests, *J. Appl. Polym. Sci. 42*:453 (1991).
79. N. Heymans, Development of orientation in glassy polycarbonate at high strains, *Polymer 28*:2009 (1987).
80. S. Turner, The strain response of plastics to complex stress histories, *Polym. Eng. Sci. (October)* 306 (1966).
81. O. A. Hasan and M. C. Boyce, Energy storage during inelastic deformation of high polymers, *Polymer 34*:5085 (1993).
82. D. L. Goble and E. G. Wolff, Strain-rate sensitivity index of thermoplastics, *J. Mater. Sci. 28*:5986 (1993).
83. J. Berry, Brittle behavior of polymeric solids in *Fracture Processes in Polymeric Solids* (Bernard Rosen, ed.), Wiley-Interscience, New York, 1964.
84. R. Robertson, Temperature rise for yielding, *J. Appl. Poly. Sci. 7*:443 (1963).
85. R. A. Andrews, *J. Appl. Phys. 26*:1091 (1955).
86. D. G. LeGrand, Crazing, yielding, and fracture of polymer. II. Studies of the retraction of crazed and drawn films, *J. Appl. Polym. Sci. 16*:1367 (1972).
87. T. E. Brady and G. S. Y. Yeh, *J. Polym. Sci. B: Polym. Phys. 10*:731 (1972).
88. T. Kato and N. Yanagihara, Multiple molecular relaxations of hot-drawn and quenched polymers above their glass transition, *J. Appl. Polym. Sci. 26*:2139 (1981).
89. G. Rizzo and G. Spadaro, Deformation recovery behavior of a solid polymer after tensile yielding, *Polym. Eng. Sci. 24*:1429 (1984).
90. T. Pukula and M. Trznadel, *Polymer 26*:1011 (1985).
91. M. Trznadel and M Kryszewski, Shrinkage and related relaxation of internal stresses in oriented polymers, *Polymer 29*:418 (1988).
92. M. Trznadel, T. Pakuta, and M Kryszewski, *Polymer 29*:619 (1988).
93. M. Trznadel, The influence of internal stress relaxation on the induction effect of shrinkage in oriented polycarbonate, *J. Macromol. Sci.-Phys. B28*:285 (1989).
94. D. G. LeGrand and J. T. Bendler, *J. Polym. Sci.* (submitted).
95. M. Washer, Effect of physical ageing on enthalpy relaxation and isothermal contraction in bisphenol-A polycarbonate, *Polymer 26*:1546 (1985).
96. M. H. Litt and P. Koch, Cold flow of glassy polymers. I. Effect of internal stress, *Polym. Lett. 5*:251 (1967).
97. P. So and L. Broutman, Residual stresses in polymers and their effect on mechanical behavior, *Polym. Eng. Sci. 16*:785 (1976).
98. J. R. Saffel and A. H. Windle, The influence of thermal history on the internal stress distribution in sheets of PMMA and polycarbonate, *J. Appl. Polym. Sci. 25*: 1117 (1980).

99. N. J. Mills, Residual stresses in plastics, rapidly cold from the melt, and their relief by sectioning, *J. Mater. Sci. 17*:558 (1982).
100. H. T. Pham, C. P. Bosnak, and K. Sehanobish, Residuals stress in injection molded reactangular bars, *Polym. Eng. Sci. 33*:1634 (1993).
101. S. Lee, J. de la Vega, and D. C. Bogue, *J. Appl. Polym. Sci. 31*:2791 (1986).
102. M. Trznadel, T. Pakula, and M. Kryszewski, The influence of internal stresses on viscoelastic and thermal properties of oriented and aged glassy polymers, *Polymer 29*:619 (1988).
103. D. G. LeGrand, *J. Rheol. 39*:437 (1995).
104. A. J. Kovacs, *Fortschr. Hochpolym. Forsch. 3*:394 (1963).
105. S. E. B. Petrie, *J. Polym. Sci. A-2 10*:1255 (1972).
106. I. M. Hodge, Enthalpy relaxation and recovery in amorphous materials, *J. Noncrys. Solids 169*:211 (1994).
107. J. M. Caruthers and R. E. Cohen, Consequence of thermorheological complexity in viscoelastic materials, *Rheo. Acta 19*:606 (1980).
108. W. Busko and V. K. Stokes, *Polym. Eng. Sci. 35*:1–14, 15–34 (1995).
109. A. A. M. Flaman and B. Veltman, *Rheol. Acta 26*:129 (1988).
109a. A. A. M. Flaman, Buildup and relaxation of molecular orientation in injection molding. I. Formulation, *Polym. Eng. Sci. 33*:193 (1993).
110. J. M. Crissman and G. B. McKenna, Physical and chemical aging in PMMA and their effects on creep and creep rupture behavior, *J. Polym. Sci. B: Polym. Phys. 28*:1463 (1990).
111. D. G. LeGrand, Annealing, in *Encyclopedia of Polymer, Science and Engineering*, Vol. 2, John Wiley and Sons, New York, 1985.
112. C. Bauwens-Crowet and J. C. Bauwens, *Polymer 31*:646 (1990).
113. C. Bauwens-Crowet and J. C. Bauwens, Rejuvenation and annealing effects on the loss curve of polycarbonate. 1. Structural temperature dependence, *Polymer 31*:248 (1990).
114. C. Bauwens-Crowet and J. C. Bauwens, The relationship between the effect of thermal pretreatment and the viscoelastic behavior of polycarbonate in the glassystate, *J. Mater. Sci. 14*:1817 (1979).
115. J. Bartos, F. Szocs, M. Klimova, and J. Muller, *Polymer 33*:3861 (1992).
116. J. Bartos, J. Muller, and J. H. Wendorff, Physical ageing of isotropic and anisotropic polycarbonate, *Polymer 31*:1678 (1990).
117. D. G. Powell, Annealing with infrared radiation to improve the quality of molded polycarbonate parts, Antec 1993, June, p. 923.
118. A. Golden and H. H. Golden, *J. Macromol. Sci. Rev. Macromol. Chem. C3*:49 (1969).
119. B. Haidar and T. L. Smith, *Polymer 31*:1904 (1990).
120. B. Haidar and T. L. Smith, History and temperature dependent yield phenomenon of polycarbonate related to its rate of physical ageing, *Polymer 32*:2594 (1991).
121. T. Ricco and T. L. Smith, Rejuvcntation and physical ageing of a polycarbonate film subject to finite tensile strains, *Polymer 26*:1979 (1985).
122. T. Ricco and T. L. Smith, *J. Polym. Sci. B: Polym. Phys. 28*:513 (1990).
123. T. L. Smith, T. Ricco, G. Levita, and W. K. Moonan, Rejuvenation and physical

ageing of polycarbonate at constant strains in simple tension and compression, *Plastics Rubber Proc. Appl. 6*:81 (1986).
124. T. L. Smith, G. Levita, and W. K. Moonan, Reversal and activation of physical aging by applied deformations in simple compression and tension, *J. Polym. Sci. B: Polym. Phys. 26*:875 (1988).
125. L. C. E. Struik, *Polym. Eng. Sci. 18*:799 (1978).
126. L. Guerdoux and E. Marchal, Physical aging of PMMA and polycarbonate in the region of the secondary relaxation, *Polymer 22*:1199 (1981).
127. L. B. Liu, A. F. Yee, and D. W. Gidley, *J. Polym. Sci. B: Polym. Phys. 30*:221 (1992).
128. J. Bartos, F. Szocs, M. Klimova, and J. Muller, Study of the influence of physical aging and rejuvenation on macroradical reactivity in polycarbonate, *Polymer 33*: 722 (1992).
129. R. A. Bubeck, S. E. Bales, and H. D. Lee, Changes in yield and deformation of polycarbonates caused by physical aging, *Polym. Eng. Sci. 24*:1142 (1984).
130. D. S. Matsumoto, Time–temperature superposition and physical aging in amorphous polymers, *Polym. Eng. Sci. 28*:1313 (1988).
131. L. C. E. Struik, Effect of thermal history on secondary relaxation processes in amorphous polymers, *Polymer 28*:57 (1987).
132. J. M. Hutchinson, Physical aging of polymers, *Prog. Polym. Sci. 20*:703 (1995).
133. C. M. Agrawal, K. J. Agrawal, and A. J. Hill, Physical properties of aged polycarbonate as a function of the cooling rate, *J. Mater. Sci. Lett. 8*:1414 (1989).
134. A. J. Hill, K. J. Heater, and C. M. Agrawal, The effects of physical aging in polycarbonate, *J. Polym. Sci. B: Polym. Phys. 28*:387 (1990).
135. J. S. Royal and J. M. Torkelson, Physical ageing effects on molecular-scale polymer relaxations monitored with mobility-sensitive fluorescent molecules, *Macromolecules 26*:5331 (1993).
136. M. R. Tant and G. L. Wilkes, An overview of the nonequilibrium behavior of polymer glasses, *Polym. Eng. Sci. 21*:874 (1981).
137. R. P. Kambour, Structure and properties of crazes in polycarbonate and other glassy polymers, *J. Polym. Sci. 2*:143 (1964).
138. G. W. Miller, S. A. D. Visser, and A. S. Morecroft, *Polym. Eng. Sci. 11*:73 (1971).
139. R. Kambour, E. E. Romagosa, and C. C. Gruner, *Macromolecules 5*:7 (1972).
140. R. Kambour, E. E. Romagosa, and C. C. Gruner, *Macromolecules 7*:248 (1974).
141. S. A. White, S. R. Weissman, and R. Kambour, *J. Appl. Polym. Sci. 27*:2675 (1982).
142. E. J. Kramer, *Adv. Polym. Sci. 52/53*: 1–56 (1983).
143. A. N. Gent, Hypothetical mechanism of crazing in glassy plastics, *J. Mater. Sci. 5*:925 (1970).
144. H. L. Heiss, The classification of solvents for bisphenol A polycarbonate, *Polym. Eng. Sci. 19*:625 (1979).
145. N. Verheulpen-Heymans and J. C. Bauwens, Effect of stress and temperature on dry craze growth kinetic during low-stress creep of polycarbonate, *J. Mater. Sci. 11*:1 (1976).
146. M. Dettenmaier, *Adv. Polym. Sci. 52/53*:57–104 (1983).
147. R. Kambour, *J. Polym. Sci. Macromol. Rev. 7*:1 (1973).
148. S. Rabinowitz and P. Beardmore, *CRC Rev. Macromol. Sci. 1*:1 (1972).

149. M. Dettenmaier, and H. H. Kausch, *Polymer 21*:1232 (1980).
150. G. L. Pittman, I. M. Ward, and R. A. Duckett, *J. Mater. Sci. 13*:2092 (1978).
151. A. S. Argon and J. G. Hannosh, *Phil. Mag. 36*:1195 (1977).
152. A. A. Griffith, *Phil. Trans R. Soc. London A221*:163 (1921).
153. D. G. LeGrand, Thermochemical stress crazing and cracking of thermoplastics, *J. Appl. Polym. Sci. 52*:1933 (1994).
154. M. Ishikawa and H. Takahasi, Crazing mechanism based on plastic instability, *J. Mater. Sci. 26*:1295 (1991).
155. W. Doll and L. Konczol, Micromechanics of fracture under static and fatigue loading: optical interferometry of crack tip craze zones, *Adv. Polym. Sci. 2*:137 91/92 (1992).
156. H. R. Brown, V. R. Deline, and P. F. Green, Evidence for the cleavage of polymer chains by crack propagation, *Nature 341*:221 (1989).
157. S. S. Sternstein, L. Ongchin, and A. Silverman, Inhomogeneuous deformation and yielding of glasslike high polymers, *Appl Polym. Symp. 7*:175 (1968).
158. R. P. Kambour and E. A. Farraye, Crazing beneath notches inducitle polymer: a materials correlation, *Polym. Commun. 25*:357 (1984).
159. C. J. G. Plummer and A. M. Donald, The deformation behavior of polyethersulfone and polycarbonate, *J. Polym. Sci. B: Polym. Phys. 27*:325 (1989).
160. J. M. Schultz, Fatigue behavior of engineering polymers in *Fatigue of Engineering Plastics* (R. W. Hertzberg and J. A. Manson, eds.), Academic Press, New York, 1980, p. 295.
161. M. T. Takemori, Fatigue fracture of polycarbonate, *Polym. Eng. Sci. 22*:937 (1982).
162. M. T. Takemori, Shear and craze competition in subcritical fatigue crack growth: fatigue lifetime inversions, *Polym. Eng. Sci. 27*:46 (1987).
163. M. T. Takemori, *Polym. Eng. Sci. 22*:937 (1982).
164. M. T. Takemori, and D. S. Matsumoto, *J. Polym. Sci. B: Polym. Phys. 20*:297 (1982).
165. M. T. Takemori, *J. Mater. Sci. 17*:2547 (1982).
166. M. Y. Ruan, H. Moaddel, A. M. Jamieson, R. Simha, and J. D. McGervey, Positron annihilation life-time studies of free volume changes in polycarbonate under static tensile deformation, *Macromolecules 25*:2407 (1992).
167. J. E. Kluin, Z. Yu, S. Vleeshouwers, J. D. McGervey, A. M. Jamieson, and R. Simha, Temperature and time dependence of free volume in bisphenol A polycarbonate studied by positron lifetime spectroscopy, *Macromolecules 25*:5089 (1992).
168. Y Aoki and J. O. Brittain, Thermally stimulated discharge current studies on the effect of thermal treatment on the strength of polycarbonate, *J. Appl. Poly. Sci. 20*: 2879 (1976).
169. A. J. Hill, I. M. Katz, and P. L. Jones, Isothermal volume relaxation in aged polycarbonate measured by positron annihilation spectroscopy, *Polym. Eng. Sci. 30*:762 (1990).
170. A. J. Hill and C. M. Agrawal, Positron lifetime spectroscopy characterization of thermal history effects on polycarbonate, *J. Mater. Sci. 25*:5036 (1990).
170a. D. M. Bigg, A review of positron annihilation lifetime spectroscopy as applied to the physical aging of polymers, *Polym. Eng. Sci. 36*:737 (1996).

171. A. J. Hill, K. J. Heater, and C. M. Agrawal, The effects of physical aging in polycarbonate, *J. Polym. Sci. B: Polym. Phys. 28*:387 (1990).
172. J. S. Royal and J. M. Torkelson, *Macromolecules 25*:4792 (1992).
173. T. Pakula and M. Trznadel, Thermally stimulated shrinkage forces in oriented polymers. 1. Temperature dependence, *Polymer 26*:1011 (1985).
174. M. Kryszewski, M. Zielinski, and S. Sapieha, Analysis of relaxation processes in methyl acrylate polymers by thermally stimulated discharge, *Polymer 17*:212 (1976).
175. A. Bernes, D. Chatain, and C. Lacabanne, *Polymer 33*:4682 (1992).
176. B. B. Sauer and P. Avakian, *Polymer 33*:5128 (1992).
177. Y. Aoki and J. O. Brittian, Isothermal and nonisothermal dielcetric relaxation studies on polycarbonate, *J. Polym. Sci. B: Polym. Phys. 14*:1297 (1976).
178. H. A. Vaughn, Jr., *J. Polym. Sci. B7*:569 (1969).
179. H. A. Vaughn, Jr., The synthesis and properties of alternating block polymers of dimethylsiloxane and bisphenol-A carbonate *Polym. Lett. 7*:569 (1969).
180. R. P. Kambour, Microdomains in alternating block polymers of dimethylsiloxane and bisphenol-A carbonate, *Polym. Lett. 7*:573 (1969).
181. R. P. Kambour, Structure and properties of alternating block polymers of dimethylsiloxane and bisphenol-A carbonate, in *Block Copolymers*, 1970, Plenum Press, New York, 1970, pp. 263–276.
182. R. P. Kambour, D. Faulkner, E. E. Kampf, S. Miller, G. E. Niznik, and A. R. Shultz, Toughness enhancement by introduction of silicone blocks into polycarbonates of bisphenol acetone and bisphenol fluorenone, in *toughness and brittleness of Plastics* (R. D. Deanin and A. M. Crugnola, eds.), American Chemical Society, 1976.
182a. D. G. LeGrand, Mechanical and optical studies of poly(dimethylsiloxane) bisphenol-A polycarbonate copolymers, *Polym. Lett. 7*:579 (1969).
183. R. P. Kambour, J. E. Corn, S. Miller, and G. E. Niznik, Tough, transparent heat- and flame-resistant thermoplastics via silicone block–modified bisphenol fluorenone polycarbonate, *J. Appl. Polym. Sci. 20*:3275 (1976).
184. G. E. Niznik and D. G. LeGrand, The effect of the end capping ratio on the properties of block copolymers, *J. Polym. Sci.: Polym. Symp. 60*:97 (1977).
185. P. Horlacher, V. Serini, D. Freitag, U. Grigo, K.-J. Idel, and U. Westeppe, Polysiloxane-polycarbonate block copolymers based on certain dihydroxydiphenylcycloalkanes, U.S. Patent 5,068,302 (1991).
186. G. C. Davis, B. E. McGrath, and K. M. Snow, Flame retardant organopolysiloxane-polycarbonate triblock copolymers, U.S. Patent 5,025,074 (1991).
187. T. L. Evans and J. C. Carpenter, Method for making silicone-poly(arylcarbonate) block copolymers, U.S. Patent 4,920,183 (1990).
188. N. R. Rosenquist, Process for the manufacture of polycarbonate-oligomers without solvent, U.S. Patent 5,344,908 (1994).
189. E. N. Peters, Process for making poly(carbonate-siloxanes) via alkyl amino terminated silicones, U.S. Patent 5,194,524 (1993).
190. C. M. Hawkins and R. R. Gallucci, Polycarbonate-silicone block copolymer compositions, U.S. Patent 4,994,532 (1991).
191. V. Serini, D. Rathamann, L. Morbitzer, and D. Freitag, Thermoplastic polyester carbonate-polysiloxane block copolymers, U.S. Patent 5,126,495 (1992).

192. J. F. Hoover and P. D. Sybert, Terepolymers having aromatic polyester, polysiloxane and polycarbonate segments, Eur. Pat. Appl. EP 626,416; *CA 122:315411b* (1994).
193. P. D. Sybert, Copoly(aromatic sulfone carbonate-aromatic alkylcarbonate)–polysiloxane block copolymer, U.S. Patent 5,011,899 (1991).
194. D. S. Parker et al, Toughening mechanisms in core-shell rubber modified polycarbonate, *Polymer 31*:2267 (1990).
195. H. J. Sue, J. Huang, and A. F. Yee, Interfacial toughening mechanism in an alloy of polycarbonate/polyethylene, *Polymer 33*:4868 (1992).
196. S. Wu, Chain structure, phase morphology, and toughness in polymers and blends, *Polym. Eng. Sci. 30*:753 (1990).

7

Optical Properties of Polycarbonates

Donald G. LeGrand
General Electric Company, Schenectady, New York

I. INTRODUCTION

The general principles of geometrical and physical optics are given in several textbooks. The former is useful in the design of lenses, refractors, and optical wave guides, whereas the latter involves wave equations and is useful in a variety of applications including birefringence, diffraction, and scattering.

General reviews of the optical properties of polymers can be found in Volume 10 of the *Encyclopedia of Polymer Science and Engineering* and a brief review of the properties of polycarbonates in Volume 11, whereas applications such as optical data storage are discussed in Chapters 3 and 14, and in Volume 11 of the above-mentioned encyclopedia. Other information pertaining to the optical properties of polymers is given in Refs. 1–4.

The physical phenomena that describe the propagation of electromagnetic radiation through matter are absorption, refraction, reflection, scattering, and birefringence in the case of oriented or stressed materials [5,6]. A comprehensive account of these properties in polymers is outside the focus of this chapter, which deals with polycarbonates and their copolymers.

A brief outline of the basis for these phenomena will be given and data presented as appropriate. In particular, some of the effects of molecular structure, molecular weight, copolymerization with other monomers, and deuteration on the refractive index and on the static and time-dependent birefringence will be reviewed. The effect of perdeuteration on near-infrared spectra and on neutron scattering will also be addressed.

II. ORDER IN POLYCARBONATES

Questions as to whether order exists in amorphous polymers were raised in the late 1960s [7–9]. This question was investigated in the case of bisphenol A polycarbonate (BPA-PC) by the use of light scattering and neutron scattering, whereas for other amorphous materials, the stress–optical coefficient was determined [10–16]. For example, Dettenmaier and Kausch measured the angular dependence of the depolarized light scattering from BPA-PC over the temperature range 50–240°C. They concluded that there was no evidence for ordering. Additional small-angle neutron scattering studies using deuterated polycarbonate with five different molecular weights dispersed in protonated polycarbonate were conducted by Ballard et al. The results of these studies indicated that the molecules were in the form of random coils in agreement with Flory's theory [17]. The results of a number of theoretical calculations were also reported. Finally, wide-angle neutron scattering studies by Cervinka et al. suggested that one possible model that was consistent with the wide-angle neutron scattering data involved three parallel segments, each of two monomer units in a trans-trans configuration. This hypothesis was based on computer modeling studies in which computed curves were compared to experimental scattering curves. Measurement of the temperature dependence of the stress–optical coefficient of several amorphous polymers by Stein and Hong did not support the concept of long-range ordering in amorphous polymers but did not rule out short-range ordering in these materials. At this point, it is believed by most investigators that long-range order does not exist in BPA-PC.

III. REFRACTIVE INDEX

While the definition of refractive index can be easily given in terms of the ratio of the velocity of light in vacuum to that in a medium and the term birefringence as the difference in refractive index between any two of the principal axes of the optical ellipsoid, the underlying physical causes for the change in velocity or velocities is best understood in terms of Maxwell's equations.

A classical expression for the refractive index that was first derived by Lorenz is called the Lorentz-Lorenz equation, given by:

$$\frac{n^2 - 1}{n^2 + 2}\frac{M}{\rho} = \frac{4}{3}\pi N_{av}\alpha \tag{1}$$

where n is the refractive index, M the molecular weight, ρ the density, N_{av} Avagadro's number, and α the polarizability.

This equation was derived by assuming that the incoming radiation field interacts with the electron clouds surrounding the atoms to create induced dipoles [18,19] where the induced moment is given by

$$m_i = \mathbf{E}\alpha \tag{2}$$

where $\mathbf{E}$ is a field vector and α is the polarizability tensor for the ith species. The radiation from these dipoles gives rise to a secondary field similar to a scattered field in the forward and backward direction which interacts with the incoming radiation. The scattered field in the forward direction lags the incident field by 180°, and by summing the scattered field in the forward direction with the incident field there is an apparent slowing down of the total field. A similar argument is used for the scattered field in the backward direction. It is obvious that for a constant $\mathbf{E}$, the larger the values of α, the greater the value of the moments. As a result, the total field undergoes a slowing down and the material exhibits a larger refractive index. It should be noted that the degree of interaction is dependent on the wavelength of the radiation because not all of the electrons respond to the same degree. A more general form of Eq. (1) is given by:

$$\frac{n^2 - 1}{n^2 + 2}\frac{M}{\rho} = \frac{4}{3}\pi \sum N_i \alpha_i \tag{3}$$

where

$$\alpha_i = \frac{C_i \lambda_i^2 \lambda^2}{\lambda^2 - \lambda_i^2} \tag{4}$$

Substitution of Eq. (4) into Eq. (3) indicates that the refractive index will be dispersive. This dispersion is normally described in terms of an Abbe number (ν), defined as

$$\nu_D = \frac{n_D - 1}{n_F - n_C} \tag{5}$$

An early evaluation of the refractive index of BPA-PC was done and a more complete evaluation of the refractive index of BPA-PC at room temperature from the vacuum ultraviolet to the infrared using data obtained by several different optical methods has been reported [20]. The effects of molecular weight and moisture have been measured [21]. The effect of temperature on the refractive index has been investigated [22,23]. These investigators also evaluated the thermooptical coefficient which is the change in refractive index with temperature. It is a function of the density and the polarizability of the material as expressed in the Lorenz-Lorentz equation. Early work demonstrated that the molar refraction of several polymers was independent of the state of the material. Changes in the polarizability of organic polymers have been shown to be due primarily

Table 1 Optical Properties of Several Polymers Including Glass

Thermoplastic	Refractive index	$dn/dT \times 10^{-4}$	Stress–optical coefficient	Strain–optical coefficient
PVC	1.528			
PE	1.53			
PMMA	1.490	1.24	−11	−0.01
PS	1.591	1.35	10	0.03
PPO	1.59			
PC	1.585	1.39	111	0.15
Glass	1.54			0.14

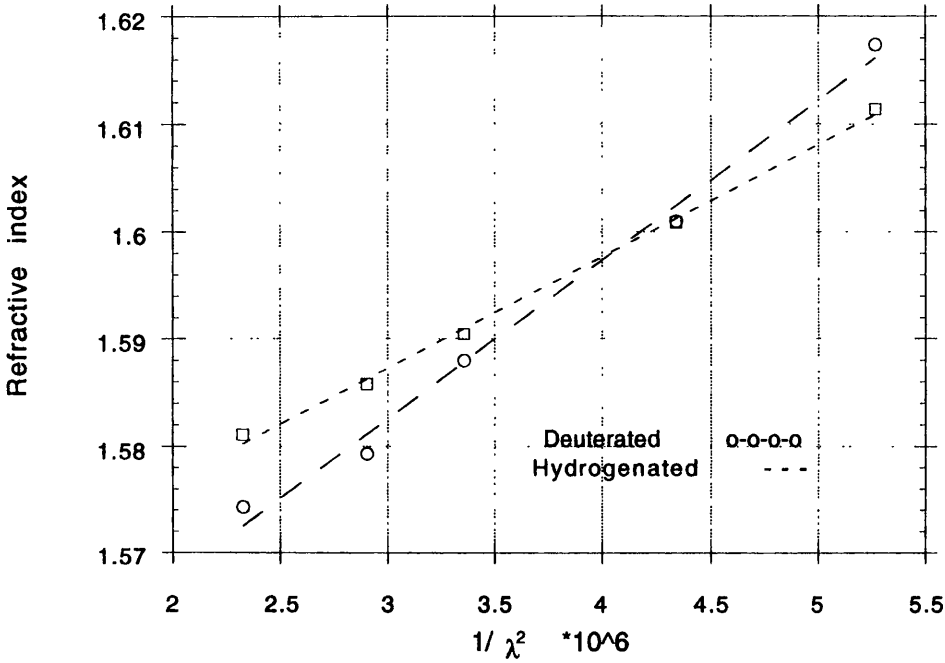

Figure 1 Comparison of the index of refraction of perdeuterated and hydrogenated BPA-PC as a function of the reciprocal of the wavelength squared.

to changes in intermolecular rather than intramolecular bonding, i.e., the temperature dependence of bond distances rather than changes in local atomic polarizabilities [23]. In the case of anisotropic samples, shrinkage and expansion strains may be superimposed on the isotropic strains and give rise to apparent changes in the local polarizability either positive or negative. Such effects may be important in the case of refractive index measurements, photon correlation spectroscopy, and Raman spectroscopy. With this assumption, the thermooptical coefficient is given as

$$\frac{dn}{dT} = -\frac{(n^2 + 2)(n^2 - 1)}{6n}\alpha_T \tag{6}$$

where n is the average refractive index and α_T is the bulk thermal coefficient of expansion. Typical values are listed in Table 1. The refractive index data in the visible range can be easily fitted to the Cauchy equation, which is given by

$$n = A + \frac{B}{\lambda^2} + \frac{C}{\lambda^4} \tag{7}$$

The refractive index of perdeuterated BPA-PC has been measured and is compared with nondeuterated polycarbonate in Fig. 1. The refractive indices of some other polymers have been measured and are presented in Table 1 [22,23]. In general, polymers containing aromatic groups tend to have high refractive indices. The stress–optical coefficients and strain–optical constants in the melt and glass for some of these polymers are listed in Table 1. The large strain–optical coefficient in BPA-PC has been explained in terms of its molecular structure and, in particular, the response of the phenyl rings and the large angular correlation between neighboring chains.

The optical properties of BPA-PC copolymers with polydimethyl siloxane blocks, polyester blocks, as well as a number of other comonomers have been evaluated and are listed in Table 2. In many cases, the refractive indices of the

Table 2 Refractive Indices of Polycarbonate Copolymers

Name	Composition (%)	Refractive index for NaD
BPAC	100	1.5875
PDMS-BPAC	25:75	1.5518
	50:50	1.518
	75:25	1.46
PDMS	100	1.425
PEC	100	1.606

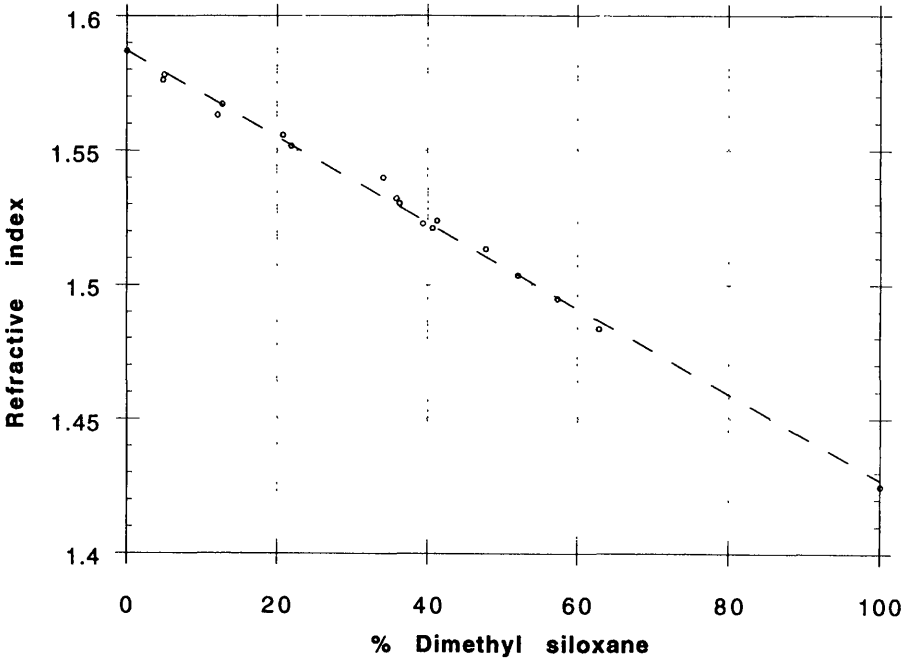

Figure 2 The refractive index of copolymers BPA-PC and polydimethyl siloxane copolymers as a function of % dimethyl siloxane.

copolymers are nominally the weight fraction sum of the refractive indices of the individual comonomers. This is illustrated in Fig. 2.

IV. REFLECTION AND TRANSMISSIVITY

The reflection of light from the surface of polycarbonates is governed by the refractive index of the material, the angle of incidence and the state of polarization of the radiation, and any birefringence in the surface if it is optically smooth. In these cases, the Fresnel equations for the amplitudes of the reflected and refracted waves for isotropic samples are

$$E'_p = E_p \frac{n_2 \cos \theta - n_1 \cos \theta''}{n_2 \cos \theta + n_1 \cos \theta''} \tag{8a}$$

$$E'_n = E_n \frac{n_1 \cos \theta - n_2 \cos \theta''}{n_1 \cos \theta + n_2 \cos \theta''} \tag{8b}$$

and for the refracted waves:

$$E_p'' = E_p \frac{2n_1 \cos \theta}{n_1 \cos \theta'' + n_2 \cos \theta} \tag{9a}$$

$$E_n'' = E_n \frac{2n_1 \cos \theta}{n_2 \cos \theta'' + n_1 \cos \theta} \tag{9b}$$

where n_1 is the refractive index of the top layer and n_2 is the refractive index of the substrate [5]. The angles of incidence and refraction are θ and θ''. The intensity of the reflected waves for these two different planes of polarization are

$$R_p = \left| \frac{\tan (\theta - \theta'')}{\tan(\theta + \theta'')} \right|^2 \tag{10a}$$

$$R_n = \left| \frac{\sin (\theta'' - \theta)}{\sin (\theta'' + \theta)} \right|^2 \tag{10b}$$

In the case of rough or scratched surfaces, the amount of reflected light will depend in part on the type and magnitude of the roughness. The addition of particulate matter to polycarbonate may alter the reflectance as a consequence of differences in refractive index and of surface roughness.

In the case of injection-molded or extruded polymers, which nominally contain a thin skin on the surface, these formulas are modified in accordance to the theory of Drude who proposed the existence of a transition layer [18]. Drude's equations were derived from the Maxwell electromagnetic relations using the boundary conditions for the tangential components of the electrical and magnetic fields. Under these conditions, the light reflected for waves polarized parallel and perpendicular to the plane of incidence consists of two terms and are expressed as

$$r_s = \frac{\cos \theta - (n_o^2 - \sin^2 \theta)^{1/2}}{\cos \theta + (n_o^2 - \sin^2 \theta)^{1/2}} \tag{11a}$$

$$r_p = \frac{n_e n_o \cos \theta - (n_e^2 - \sin^2 \theta)^{1/2}}{n_o n_e \cos \theta + (n_e^2 - \sin^2 \theta)^{1/2}} \tag{11b}$$

where n_o and n_e are the ordinary and extraordinary rays. In the case of aromatic polymers such as BPA-PC as well as other polymers, these equations indicate that the light incident on their surfaces not only will become polarized but can lead to development of surface colors as a consequence of birefringence in the surface layer.

The amount of light transmitted through polycarbonate is a function of several parameters as indicated above [5,22]. Aside from the classical Fresnel relationships between refractive indices and the angles of incidence as discussed earlier, one has to consider the effects of additives such as dyes and pigments

and that of unknown contaminants. Measurement of transmissivity as a function of thickness will immediately indicate the magnitude of this effect in a given polycarbonate sample but may not identify the cause.

V. NEAR-INFRARED

The use of polymers as optical fibers in local area networks (LANs) has been cited as one of the potential areas for growth in the near future [25,26]. In this application, the transmission of light in the fiber is governed by classical absorption, reflection from the boundaries, and scattering. In the case of scattering, the scattering term may be due to frozen-in thermal fluctuations, contaminants, or additives. In the case of absorption, it has been suggested that vibrational harmonics, also called Urbach tails, which occur in the near-infrared, contribute to the absorption process and that this loss can be suppressed by replacement of hydrogen atoms by deuterium [27–31]. This hypothesis has been tested and the results are presented in Fig. 2. These data clearly demonstrate that replacement of the hydrogen atoms by deuterium has shifted these bands to much longer wavelengths.

VI. BIREFRINGENCE

Cold- and hot-drawn bars, extruded sheet and film, blow-molded bottles, and injection-molded dogbones of polycarbonates are optically anisotropic and behave optically like uniaxial or biaxial crystals as indicated earlier. The optical axis is frequently parallel to the drawing, extrusion, or flow direction and the refractive index depends on the direction of the plane of polarization with respect to this axis [5]. When light is plane-polarized with the electrical vector vibrating parallel to the optical axis the refractive index, $n_{\parallel}$, is either a maximum or minimum, and when the electrical vector is perpendicular to the optical axis, the refractive index is either a minimum or a maximum. The difference between these two refractive indices is equal to the birefringence or double refraction. It is given by

$$\Delta_{\gamma} = n_{\parallel} - n_{\perp} \tag{12}$$

The first detailed study of the relationship between polymer structure, mechanical properties, and birefringence was done by Stein and Tobolosky [32]. Their work focused on polyvinyl chloride and other plasticized polymers. The birefringence and stress–optical properties of BPA-PC were first reported by Ito whose interest was in its use as model for photoelastic and photoplastic studies [33]. Subsequently, this material was studied in the glassy state by Brinson and LeGrand

and in solution by Champion et al. [33–38]. In the latter case, a magnetic field was used to induce birefringence. In the latter 1960s, Flory and coworkers reported on analysis of the random configuration of this material [39–41]. Several calculations of the theoretical optical anisotropy and birefringence of this BPA-PC have been reported and in 1982 William and Flory published the results of calculation on the optical anisotropy for both model compounds and the polymer [41]. All of these calculations used values for the bond polarizabilities that are based on the early data of Bunn and Daubeny [41a] for the C-H bond and neglect any changes in the local internal field due to orientation. Stein and coworkers and LeGrand attempted to take this effect into account by the use of two simple models [42,43]. In the 1980s the primary focus was on the experimental evaluation of the intrinsic birefringence and was performed on cold- and hot-drawn polycarbonate. The birefringence of the samples was measured. The orientation function for the samples was evaluated by four different methods: infradichroism, wide-angle x-ray scattering, sonic modulus, or by computing the orientation function from the degree of elongation [44–52].

In the 1980s, the measurement and calculation of the birefringence in molded plaques, compact discs (CDs), and magneto-optic discs (MOs) became the subjects of most interest because of the effect of residual birefringence on the quality of the laser signal, i.e., the beam becomes elliptically polarized during passage through and reflection from the metalized surface [53–61]. This effort has led to the development of several modified optical techniques for measuring detailed differences in the birefringence in CDs and MO disks. Some of them are available as commercial apparatus while others are primarily being used as research and development tools [62,63]. Fewer studies of the birefringence of BPA-PC in the melt are found in the early literature due to its higher T_g and its relatively large stress–optical coefficient [64]. More recently, several authors have investigated the birefringence in the melt [64–82].

There has been a renewed interest in the optical properties of a number of different polycarbonate structures with a particular emphasis on the magnitude of the birefringence [83,84]. For example, substitution of the gem dimethyl groups with phenyl groups reduces the stress–optical coefficient from 4400 to 640 Brewsters [53]. However, the ductility of the material is loss and the glass transition is increased. Copolymerization of BPA-PC with spirobiindane has been shown to reduce the birefringence and has been patented [83]. The formation of a terpolymer using the SBI and BPA monomers with dimethyl siloxanes has been shown to reduce the birefringence while enhancing ductility [84]. The effects of processing on the birefringence in polycarbonates has been further studied in the 1990s. Hot and cold drawing, extrusion, blow molding, and injection molding cause birefringence (see Chap. 5), but the distribution, magnitude, and type of birefringence are quite different. For example, in hot and cold drawing the orientation tends to be uniaxial and homogeneous throughout the samples, whereas

in the case of injection molding and extrusion there tends to be more orientation at the surface, i.e., a highly oriented skin, than in the core and depending on the flow geometry may be biaxial. Early studies by LeGrand [47] and Robertson [44] on hot- and cold-drawn samples and extruded sheet, and more recent studies by White [65] and Flannan [74] on compact disks have provided an indepth visualization of how the melt must have flowed in the various applications.

The small strain–optical coefficient of amorphous polymer glasses is not a parameter that can be calculated a priori because the magnitude and sign of this parameter is dependent on the changes that occur in the orientation of the monomeric unit, internal changes in conformation, as well as changes in the bond length and bond angles in the unit. Gurnee [46] has proposed one method that involves the use of the differential of the Lorentz-Lorenz equation and is given by

$$\Delta n = C_1\varepsilon_1 + C_2\varepsilon_2 \tag{13a}$$

$$\nu = -\frac{\varepsilon_2}{\varepsilon_1} \tag{13b}$$

$$\Delta n = (C_1 - C_2\,\nu)\varepsilon_1 \tag{13c}$$

where C_1 are constants, ν is Poisson's ratio, and ε_1 is the strain along the x axis [72]. One notes that this equation predicts that all strain–optical coefficients will be positive if the expression in parentheses is positive and will depend on the refractive index of the material. This expression can be used to obtain an equation for the stress–optical coefficient by assuming a linear correlation between the stress and strain. The result is given by

$$k = \frac{4\pi}{45}\frac{(n^2 + 2)^2}{n}\frac{N_c P}{M_n E}(1 + \nu)(\delta_1 - \delta_2) \tag{14}$$

The limitation of this expression is that it predicts a dependence of the stress–optical coefficient in the glass on the optical anisotropy of the monomer or the statistical segment. This is not observed. In fact, most glassy polymers when deformed appear to exhibit a positive birefringence in accordance with the initial conclusions of Gurnee except for PMMA as shown in Table 3.

The large strain–optical coefficient of BPA-PC is explained in terms of the molecular structure. BPA-PC contains phenyl rings in the backbone of the chain and there is a large angular correlation between neighboring chains. Therefore, it is easy to cooperatively displace the phenyl groups.

The evaluation of the optical anisotropy of BPA-PC carbonate and its analogs was carried out both theoretically and experimentally by several investigators in the solid state and in solution as discussed earlier. Critical issues with the theoretical calculations were the values of the principal polarizabilities of the carbon–carbon bond, the influence of the internal field in highly oriented struc-

Table 3 Refractive Indices and Strain–Optical Coefficients for Glass and Glassy Polymers

Material	Refractive index	Strain–optical coefficient
PMMA	1.49	−0.01
PS	1.58	0.03
PPO	1.58	0.14
PC	1.58	0.15
Glass	1.54	0.14

tures, and, finally, the geometry of a highly oriented sample in the amorphous state. On the experimental side, questions in regard to the materials tested in terms of additives, molecular weight, end-groups, and thermal or processing history have frequently been ignored or not discussed in the references. Recent work has provided more information but not necessarily everything.

A number of copolymers have been synthesized and evaluated in terms of their birefringence and refractive indices. These results have been presented in Chap. 5, which deals with copolymers.

VII. TIME-DEPENDENT BIREFRINGENCE

As indicated earlier, the measurement of the time-dependent birefringence of BPA-PC was first done in the early 1970s in the glass and in the transition zone between the glass and the melt [33]. In these early studies the focus was on the correlation between the mechanical and optical properties. Two different models were proposed to interpret these data [33,34]. In more recent times, measurements of the birefringence during stress relaxation and during dynamic tensile straining have been reported. These data have been interpreted using a modified stress–optical rule that is derived from two equations involving the complex dynamic tensile moduli and the complex strain–optical coefficients. These equations are as follows:

$$E' = E'_R + E'_G \tag{15a}$$

$$O' = C_R E'_R + C_G E'_G \tag{15b}$$

$$E'' = E''_R + E''_G \tag{15c}$$

$$O'' = C_R E''_R + C_G E''_G \tag{15d}$$

where O' and O'' are the in-phase and out-of-phase strain–optical coefficients. At all temperatures near 148°C, O' is nominally constant, whereas at higher temperatures up to 170°C O' is positive and increases as a function of frequency. In contrast, O'' initially decreases as a function of frequency at lower temperatures whereas at higher temperatures it increases [76]. Earlier work by these same investigators measured birefringence during stress relaxation and computed the strain–optical coefficient.

$$\Delta = C_m \varepsilon_m + C_g \varepsilon_g \tag{16}$$

If $C_m = C_g$, then

$$\Delta = C_{g,m} (\varepsilon_m + \varepsilon_g) \tag{17}$$

VIII. INFRARED ABSORPTION AND DICHROISM

Early studies of the infrared spectrum and dichroism of BPA-PC were performed by Krimm et al. [85,86]. The focus of these studies was to develop an assignment

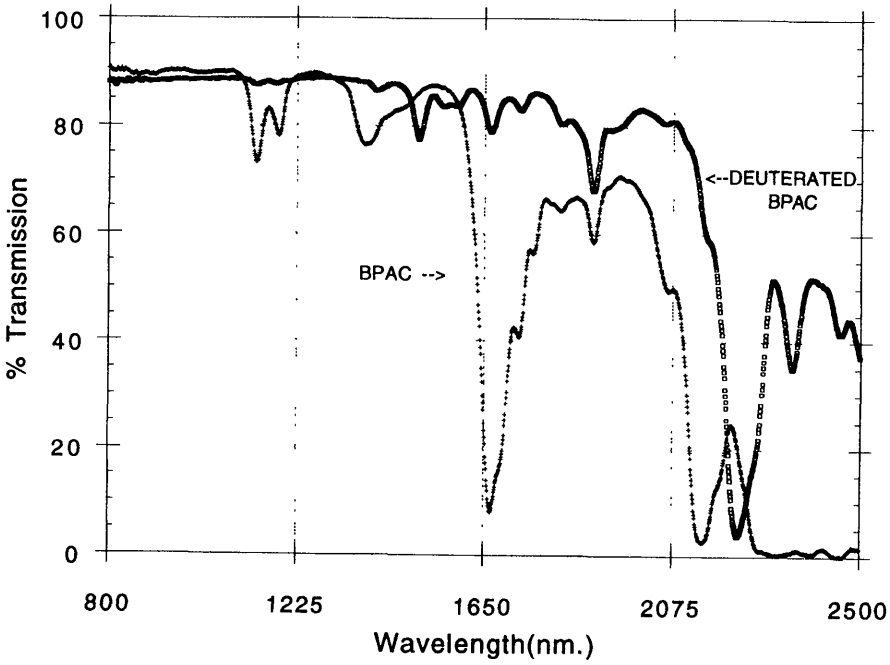

Figure 3 Near-infrared spectra of perdeuterated and hydrogenated BPA-PC as a function of wavelength.

of the bands to various vibrational modes of the groups in the material and also to aid in the definition of the crystal structure. The infrared spectra of polycarbonates exhibit very strong absorptions at 1235 and 1770 cm that are associated with C=O vibration. There is also a strong band at 1220 cm associated with a C—O mode. A band that has been identified with crystallinity is located at 725 cm, whereas terminal —OH groups have an absorption at 1383 cm.

Later work by Jansson and Yannas investigated the use of infrared dichroism as a method of determining the mechanism of orientation at small strains [87]. They measured the dichroism of bands at 889, 1363, and 3063 cm. They noted negligible dichroism up to about 0.6% strain at 23°C.

Measurements of the near-infrared spectra of perdeuterated and hydrogenated polycarbonate as shown in Fig. 3 and for cold-drawn samples in Fig. 4 indicate that these vibrational bands are shifted by the substitution of deuterium for hydrogen but that orientation does not alter these bands. These results suggest that perdeuterated BPA-PC would exhibit a higher degree of light transmission because the Urbach tails have been shifted to longer wavelengths.

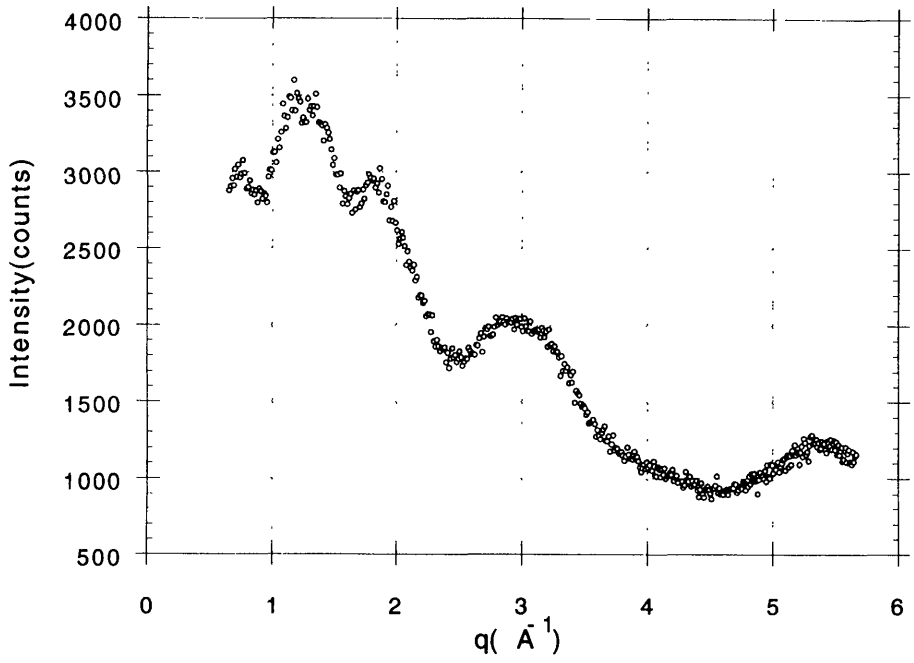

Figure 4 Neutron scattering from perdeuterated BPA-PC as a function of q^{-1}.

IX. SCATTERING

The use of scattering techniques to probe the structure of polycarbonates has been performed using light, x-rays, and neutrons. Perdeuterated samples were used in the case of neutrons. A typical neutron scattering curve for such materials is shown in Fig. 3 [12–15]. In the case of x-rays, the scattering curves from amorphous and crystalline samples are reported in Chapter 13.

The use of light scattering as a tool in the study of polycarbonates has focused on two different areas of scattering. The first is the classical method of light scattering, which is described in terms of the Rayleigh-Einstein-Debye theories of scattering, i.e., thermal and concentration fluctuations. This method has been used to determine the molecular weight of the material in solution and the optical anisotropy of the correlated segments in the chain [39]. The early work of Debye and Bueche reported that scattering occurred from PMMA and from polystyrene [88]. More recent work has shown scattering from BPA-PC.

A second type of scattering that has been used to study polycarbonate and other polymers is photon correlation spectroscopy. The use of photon correlation spectroscopy was introduced and applied by Patterson in the late 1970s and early 1980s to investigate the short-time relaxation processes in a number of amorphous and semicrystalline polymers [89]. Both longitudinal and transverse Brillouin peaks were observed in the case of BPA-PC and were observed over the entire range of temperature from 60°C to 240°C [90]. A change in the slope of these waves was observed near the glass transition. A critical problem in many of these studies has been the issues of additives and the presence of birefringence due to residual orientation and stresses as pointed out by Patterson.

X. CONCLUSIONS

The use of polycarbonates as glazing materials and both ophthalmic and automotive lenses has occurred because of its transparency, ductility, and high heat distortion temperature, as described in other chapters. Possible use as an optical fiber for local area networks (LANS) is currently under investigation. One of the primary deficiencies of most polycarbonates have been their optical sensitivity in terms of both orientational and stress birefringence vs. their degree of ductility. Current work is expected to mitigate or eliminate these problems.

REFERENCES

1. L. R. Treolar, *The Physics of Rubber Elasticity*, 2nd ed., Oxford University Press, New York, 1967.

2. D. J. Williams, ed., *Nonlinear Optical Properties of Organic and Polymeric Materials*, ACS Sym. 233, Washington, DC, 1983.
3. J. A. Emerson and J. M. Torkelson (eds.), *Optical and Electrical Properties of Polymers*, Materials Res. Soc., 1991.
4. G. A. Lindsay and K. D. Singer (eds.), *Polymers for Second-Order Nonlinear Optics*, ACS Symp. 601, Washington, DC, 1995.
5. B. Rossi, *Optics*, Principles of Physics Series, Addison-Wesley, Reading, MA, 1957.
6. P. Drude, *Theory of Optics*, Longmans, Green, New York, 1902.
7. G. S. Y. Yeh and P. H. Geil, *J. Macromol. Sci.-Phys. B1*:251 (1967).
8. R. E. Robertson, *J. Chem. Phys. 69*:1575 (1965).
9. K. Neiki and P. H. Geil, *J. Macromol. Sci. Phys. B8*:295 (1973).
10. W. Frank and H. A. Stuart, *Koll. Zeit. 225*:1 (1968).
11. M. Dettenmaier and H. H. Kausch, Light scattering of bisphenol A polycarbonate in the amorphous state and at the beginning of thermal crystallization, *Colloid Polym. Sci. 259*:209 (1981).
12. M. Dettenmaier and E. W. Fischer, Untersuchungen zu den Anistorpie- and Dichtefluktuationen in PMMA, *Koll. Zeit. fur Polym. 251*:922 (1973).
13. D. G. H. Ballard, A. N. Burgess, P. Chesire, E. W. Janke, A. Nevin, and J. Schelten, Small-angle neutron scattering study of amorphous polycarbonate, *Polymer 22*:1353 (1981).
14. L. Cervinka, E. W. Fischer, K. Hahn., B. Z. Jaing, G. P. Hellmann, and K.-J. Kuhn, On the intermolecular order in amorphous polycarbonate. Neutron scattering results and model calculations, *Polymer 28*:1287 (1987).
15. C. Lamers, O. Scharpf, W. Schweika, J. Batoulis, K. Sommer, and D. Richter, Short range order in amorphous polycarbonates, *Physica B180/181*:515 (1992).
16. R. S. Stein and S. D. Hong, The stress-optical coefficient and amorphous order, *J. Macromol. Sci.-Phys. B-122*:125 (1976).
17. P. J. Flory, *Principles of Polymer Chemistry*, Cornell University Press, Ithaca, NY, 1953.
18. W. Kauzman, *Quantum Chemistry*, Academic Press, New York, 1957.
19. H. A. Lorentz, *Theory of Electrons*, 2nd ed., Dover, New York, 1952.
20. H. R. Phillips, D. G. Legrand, and H. S. Cole, The optical properties of bisphenol-A polycarbonate, *Polym. Eng. Sci. 27*:1148 (1987).
21. Lexan Resin Optical Properties, General Electric Company, Lexan Products Division, Pittsfield, MA (1986).
22. R. M. Waxler, D. Horowitz, and A. Feldman, Optical and physical parameters of Plexiglas and Lexan, *Appl. Optics 18*:101 (1979).
23. P. Michel, J. Dugas, J. M. Cariou, and L. Martin, Thermal variation of refractive index of PMMA, PS, and PMP4-1, *J. Macromol. Sci. Phys. B25*:379 (1986).
24. G. Beaucage, R. Composto, and RS Stein, Ellipsometric study of the glass transition and thermal expansion of thin polymer films *J. Polym. Sci. B: Polym. Phys. 31*:319 (1993).
25. Y. Takezawa, N. Takeetani, S. Tanno, and S. Ohara, *J. Appl. Polym. Sci. 46*:1835 (1992).
26. Y. Takezawa, N. Takeetani, S. Tanno, and S. Ohara, Light absorption due to higher harmonics of molecular vibrations in transparent amorphous polymers for plastic optical fibers, *J. Polym. Sci. B: Polym. Phys. 30*:379 (1992).

27. L. H. Garcia-Rubio, Refractive index effects on the absorption spectra of macromolecules, *Macromolecules 25*:2608 (1992).
28. E. Marquez, V. R. Bhethanabotla, and L. H. Garcia-Rubio, Conformational effects on the absorption spectra of macromolecules, *Macromolecules 26*:479 (1993).
29. F. Urbach, *Phys. Rev. 92*:1324 (1953).
30. L. Ferrari and G. Russo, Urbach tails in chalcogenideds: a self consistent approach, *Phil. Mag. B 63*:501 (1991).
31. C. Bosio and W. Czaja, Urbach tails in the absorption spectra of amorphous and crystalline SiO, *Phil. Mag. B 63*:7 (1991).
32. R. S. Stein and A. V. Tobolosky, "An investigation of the relationship between polymer structure and mechanical properties Part I. Relationship between structure, mechanical properties and birefringence," *Tex. Res. Journal 18*:201 (1948).
33. K. Ito, New model materials for photoelasticity and photoplasticity, Exp. Mech. pg. 1, Dec. 1962.
34. D. G. LeGrand, Rheo-optical properties of polymers VI. Dynamic birefringence, *J. Polym. Sci., A: 2*:931 (1964).
35. B. E. Read, *Polymer 3*:143 (1962).
36. H. F. Brinson, An interpretation of inelastic birefringence Exper. Mech. pg. 467, Oct. 1971.
37. J. V. Champion, R. A. Desson, and G. H. Meeten, Conformation of polycarbonate by flow and magnetic birefringence, *Polymer 15*:301 (1974).
38. D. G. LeGrand, Optical anisotropy of the statistical segment in block copolymers, in Structure and Properties of Polymers, ed. R. S. Stein and R. Lenz, Plenum Publishers, NY 1972.
39. A. D. William and P. J. Flory, Analysis of the random configuration of polycarbonate of diphenylol-2,2′-propane, *J. Poly. Sci. A-2 6*:1945 (1968).
40. B. Erman, D. C. Marvin, P. A. Irvine, and P. J. Flory, Optical anisotropies of model analogues of polycarbonates, *Macromol. 15*:664 (1982).
41. B. Erman, D. Wu, P. A. Irvine, D. C. Marvin and P. J. Flory, Optical anisotropy of the polycarbonate of diphenylolpropane, *Macromol. 15*:670 (1982).
41a. C. W. Bunn and R. de P. Daubeny, *Trans. Far. Soc. 50*:1173 (1954).
42. D. G. LeGrand, The effect of the internal field on birefringence in oriented polymers, *Macromolecules 3*:674 (1970).
43. Y. Shindo and R. S. Stein, *J. Polym. Sci. A-2 7*:2115 (1969).
44. R. E. Robertson and R. J. Buenker, *J. Polym. Sci. A-2*:4889 (1964).
45. M. Pick and R. Lowell, Photoelasticity of glassy polymers, *Polymer 20*:1448 (1978).
46. E. F. Gurnee, Theory of orientation and double refraction in polymers, *J. Appl. Phys. 25*:1232 (1954).
47. D. G. LeGrand, Crazing, yielding, and fracture of polymers II. Studies of the retraction of crazed and drawn films, *Jpn. Appl. Polym. Sci. 16*:1367 (1972).
48. H. J. Biangardi, Calculation of the intrinsic birefringence of amorphous polyethylene terephthalate, from wide angle x-ray scattering, *J. Polym. Sci. B: Polym. Phys. 18*: 903 (1980).
49. H. J. Biangardi, Determination of the orientation distribution function of amorphous polymers by x-ray scattering measurements, *Macromol. Chem. 183*:1785 (1980).

50. M. S. Wu, Intrinsic birefringence of amorphous poly(bisphenol-A carbonate), *J. Appl. Polym. Sci. 32*:3263 (1986).
51. M. Takeshima and N. Funakoshi, Molecular orientation distribution in injection-molded discs, *J. Appl. Polym. Sci. 32*:3457 (1986).
52. H. Saito and T. Inoue, Chain orientation and intrinsic anisotropy in birefringence-free polymer blends, *J. Polym. Sci. B: Polym. Phys. 25*:1627 (1987).
53. S. Shirouzu, K. Shigematsu, S. Sakamoto, T. Nakagawa, and S. Tagami, Refractive index anisotropies of constructive unit in polycarbonates, *Jpn. J. Appl. Phys. 28*: 801 (1989).
54. S. Shirouzu, K. Shigematsu, S. Sakamoto, T. Nakagawa, and S. Tagami, Refractive index ellipsoids of a modified polycarbonate magneto optical memory disk substrate, *Jpn. J. Appl. Phys. 28*:1629 (1989).
55. W. Siebourg, H. Schmid, F. M. Rateike, S. Anders, U. Grigo, and H. Lower, Birefringence—an important property of plastic substrates for magneto-optical storage disks, *Polym. Eng. Sci. 30*:1133 (1990).
56. R. Wimberger-Friedl and R. D. H. M. Hendriks, The measurement and calculation of birefringence in quenched polycarbonate specimens, *Polymer 30*:1143 (1989).
57. S. Anders, H. Schmid, and K. Sommer, Birefringence in optical information storage discs made of polycarbonate, *Kunstoffe 79*:55 (1989).
58. R. Wimberger-Friedl, Analysis of the birefringence distribution in compact discs of polycarbonate, *Polym. Eng. Sci. 30*:813 (1990).
59. J. S. Machell, J. Greener, and B. A. Contestable, Optical properties of solvent-cast films, *Macromolecules 23*:186 (1990).
60. Y. Shindo, M. Saito, Y. Iwatsucka, and H. Hasegawa, Residual birefringence of amorphous polymer for optical disk substrates, *J. Appl. Sci. 43*:767 (1991).
61. K. Yoon and K. K. Wang, Birefringence measurements of injection-molded disks, Antec, May 1991, Montreal, Canada, p. 333.
62. K. Shigematsu, S. Shirouzu, S. Sakamoto, T. Nakagawa, and S. Tagami, Refractive index ellipsoids of a polyformal magneto-optical memory disk substrate, *Jpn. J. Appl. Phys. 30*:1724 (1991).
63. K. Shigematsu, S. Shirouzu, S. Sakamoto, T. Nakagawa, and S. Tagami, Optical anisotropies in modified polycarbonates, *Jap. J. Appl. Phys. 30*:1720 (1991).
64. D. Freitag, G. Fengler, and L. Morbitzer, *Angew. Chem. Int. Ed. Eng. 30*:1598 (1991).
65. J. Wu and J. L. White, Study of birefringence character of injection- and compression-molded polycarbonate and its interpretation, *Polym. Eng. Sci. 31*:652 (1991).
66. D. LeGrand, Optical anisotropy of the statistical segment in block copolymer, in *Structure and Properties of Polymer Films* (R. W. Lenz and R. S. Stein, eds.), Plenum Press, New York, 1972.
67. T. Hovatter, D. LeGrand, W. Morris, R. Lillquist, and B. McKinley, Replitech, San Jose, 1995.
68. T. Hovatter and M. Niedmeyer, Replitech, San Jose, 1996.
69. D. G. LeGrand, Rheo-optical properties of polymers. VI. Dynamic birefringence, *J. Polym. Sci. A-2*:931 (1964).
70. T. Inoue, H. Okamoto, and K. Osaki, *Macromolecules 25*:7069 (1992).

71. T. Nagai, Y. Kimizuka, K. Neto, and J. Seto, Melt viscosity and flow birefringence of polycarbonate, *J. Appl. Polym. Sci. 44*:1171 (1992).
72. E. Hwang, T. Inoue, and K. Osaka, Viscoelasticity of some engineering plastics analyzed with the modified stress-optical rule, *Polym. Eng. Sci. 34*:135 (1994).
73. E. J. Hwang, T. Inoue, and K. Osaki, Viscoelasticity and birefringence of bisphenol A polycarbonate, *Polymer 34*:1661 (1993).
74. A. A. M. Flaman, Buildup and relaxation of molecular orientation in injection molding. I. Formulation, *Polym. Eng. Sci. 33*:193 (1993).
75. A. A. M. Flaman, Buildup and relaxation of molecular orientation in injection molding. II. Experimental verification, *Polym. Eng. Sci. 33*:202 (1993).
76. R. Wimberger-Friedl, The peculiar rheo-optical behavior of bisphenol-A polycarbonate and polmethylmethacrylate, *Rheol. Acta 30*:329 (1991).
77. R. Wimberger-Friedl and J. G. deBruin, The time-dependent stress-optical behavior of polycarbonate in the glass transition region, *Rheol. Acta 30*:419 (1991).
78. G. R. Faler and J. C. Lynch, U.S. Patent 4,950,731 (Aug. 21, 1990).
79. G. F. Faler, D. M. Dardaris, and D. G. LeGrand, U.S. Patent 4,895,919 (Jan. 23, 1990).
80. R. Wimberger-Friedl and J. G. deBruin, Birefringence inpolycarbonate: molecular orientation induced by cooling stresses. I. Free quenching, *J. Polym. Sci. B: Polym. Phys. 31*:1041 (1993).
81. R. Wimberger-Friedl, Molecular orientation induced by cooling stresses. Birefringence in polycarbonate. III. Constrained quench and injection molding, *J. Polym. Sci. B: Polym. Phys. 32*:595 (1994).
82. G. D. Shyu and A. I. Isayev, Residual birefringence in amorphous plastics products, SPE 51st Annual Technical Conference, New Orleans, 1993, p. 1673.
83. T. Bouchard, W. V. Olszewski, and D. G. LeGrand, Nondestructive evaluation of residual stresses and orientation in polycarbonate resin, SPE 44th Annual Technical Conference, Boston, 1986, p. 393.
84. J. F. Rudd and E. F. Gurnee, Photoelastic properties of polystyrene in the glassy state. II. Effect of temperature, *J. Appl. Phys. 28*:1096 (1957).
85. S. Krimm, The crystal structure of poly(bisphenol-A carbonate), *J. Polym. Sci. 61*: S10 (1962).
86. C. Y. Liang and S. Krimm, *J. Mol. Spectrosc. 3*:554 (1959).
87. J. F. Jansson and I. V. Yannas, Infrared dichroism of glassy polycarbonate at small strains, *J. Polym. Sci. B: Polym. Phys. 15*:2103 (1977).
88. P. Debye and A. M. Bueche, *J. Appl. Phys. 20*:518 (1949).
89. G. D. Patterson, Brillouin scattering from polymer films, *J. Polym. Sci. B: Polym. Phys. 14*:143 (1976).
90. G. D. Patterson, Brillouin scattering from amorphous bisphenol-A polycarbonate, *J. Polym. Sci. B: Polym. Phys. 14*:741 (1976).

8

PVT, Specific Heat, and Thermal Transitions

Allan R. Shultz
Virginia Polytechnic Institute and State University, Blacksburg, Virginia

I. PRESSURE–VOLUME–TEMPERATURE RELATIONS

Polycarbonates can exist as equilibrium amorphous liquids, as two-phase crystal solids/liquids, as nonequilibrium glasses, or as nonequilibrium crystal/glass solids. Polycarbonates containing aromatic groups in their backbone units are normally found to be glassy solids or mixed glass/crystal solids at room temperature. Of the aromatic polycarbonates, bisphenol A polycarbonate (BPA-PC) is by far the one of greatest technological importance and therefore the best characterized with respect to structure–property relationships.

Pressure–volume–temperature (PVT) relationships are of fundamental importance in describing the physical behaviors of materials. For polycarbonates in their equilibrium liquid states PVT relationships can be expressed as equations of state that permit derivation of several thermodynamic functions. For nonequilibrium, glassy polycarbonates PVT observations can be made and reported, but the volume is not a unique function of temperature and pressure. The effects of the history of formation and subsequent regimens on the physical "state" of the glass can, however, yield valuable information. Expression of PVT data for polymers in their glassy condition by empirical equations of state is useful as long as one recognizes that different glasses might differ somewhat in the characteristic parameters obtained.

An examination of volume–temperature studies of polycarbonates (especially BPA-PC) at atmospheric pressure will be presented. PVT studies of crystal/liquid, glassy, and equilibrium liquid polycarbonates will then be reviewed. PVT data for equilibrium liquid BPA-PC and three other aromatic polycarbonates have

been represented by empirical equation fits. Finally, brief reference will be made to recent fitting of these data to theoretical equations of state.

A. Volume–Temperature Studies at Atmospheric Pressure

High molecular weight BPA-PC is normally a clear, amorphous, nonequilibrium solid (i.e., a glass) at temperatures below 140°C. At higher temperatures it exists in an amorphous, viscous-liquid state. If BPA-PC is isolated from solution by casting a film or by precipitation by a nonsolvent it can contain low to moderate amounts of crystallinity. Crystallization from its melt at temperatures between its glass transition and melting temperatures requires very long times and is often the result of concurrent chain scission to lower average molecular weight. Solid BPA-PC obtained by cooling its melt under ordinary conditions is a noncrystalline, glassy solid.

Dilatometric measurements on a Lexan BPA-PC resin (General Electric Co.) were published in 1962 [1,2]. For this BPA-PC a glass transition temperature of 141°C was found as the intersection of straight lines drawn through the lower temperature and higher temperature v_{sp}, T data points. Although the BPA-PC was melt-pressed into a sheet from which the dilatometric sample was cut, there remained (or developed) a very low degree of crystallinity that disappeared at 220°C [2]. A specific volume for the BPA-PC of 0.836 $cm^3\ g^{-1}$ at 20°C, and cubical expansion coefficients of 0.00020 (20–120°C), 0.00059 (150–220°C), and 0.00060 (220–280°C) K^{-1} were reported.

When a glass is formed without imposition of external stresses its expansion upon heating is isotropic. The linear thermal expansion coefficient of a glassy BPA-PC sample stretched along one axis was found to be less along the stretch axis than perpendicular to it [3]. Also, thermal conductivity along the stretch axis increased.

For partly crystalline films of BPA-PC cast from CH_2Cl_2 melting tempera tures, T_m, of 233–239°C (optical microscope) and specific volumes at 20°C, v^{20}, of 0.826–0.807 $cm^3\ g^{-1}$ (density gradient column) were found [4]. Films of a lower molecular weight polymer, intrinsic viscosity $[\eta] = 0.30$, exhibited T_m = 185–200°C and a $v^{20} = 0.802\ cm^3\ g^{-1}$ for the most highly crystallized film was reported in the same study. Correlation of the heat of fusion of BPA-PC with its specific volume as determined in a density gradient column was reported in 1970 [5]. Dilatometric measurements of BPA-PC crystallization rates for 200–1000 h in the temperature range 170–205°C revealed a maximum crystallinity of 33% achieved at 205°C crystallization temperature [6].

Modification of an Instron tensile tester to follow linear expansion of polymers with temperature increase permitted T_g determinations of BPA-PC and other polymers that compared well with the T_g values determined by other

methods [7]. This is a forerunner of present day thermomechanical analysis (TMA).

Measurements of thermal expansion and heat capacity of BPA-PC in the 60–280 K range found the specific heat increasing nearly linearly with increasing temperature, but the expansion coefficient not increasing linearly [8]. These data showed a decrease in the Gruneisen constant with increasing temperature.

Several studies examined volume–temperature–time phenomena of BPA-PC in the region of its glass transition temperature [9–11,13,14]. A study of T_g as a function of cooling rate (0.031–10 K/min) found T_g elevation with increasing cooling rate in substantial agreement with elevations determined by other means [9]. A mechanical deformation rate effect on the measured glass transition temperature of BPA-PC of ~3 K elevation of T_g for each order of magnitude increase in frequency in dynamic mechanical analysis was cited. Volume relaxation was found to correlate well with enthalpy relaxation [10]. The time dependence of free volume and enthalpy of BPA-PC in the glass transition region could be rationalized [11] in terms of the Williams-Landel-Ferry (WLF) model of relaxation time/temperature correspondence (cf. Ref. 12). Anomalous relaxation behavior below T_g was observed for glasses formed under pressure. Density fluctuations in poly(methyl methacrylate) (PMMA) and BPA-PC were measured as functions of temperature during constant heating, cooling, and isothermally employing small-angle x-ray scattering techniques [13]. Specific volumes of the PMMA were measured under similar isothermal regimens. Both the density fluctuation and the specific volume of PMMA decreased with isothermal annealing time in a 20–40° region around T_g. At lower temperatures the specific volume continued to decrease linearly with decreasing temperature but the density fluctuation showed no further change. The investigators interpreted the density fluctuations in terms of a free volume consisting of holes having a distribution of sizes. A study of the dependence of relaxation times of glassy BPA-PC, polyvinyl chloride, and polystyrene on their specific volumes following complicated thermal conditionings showed that specific volumes could pass through maxima during isothermal holds [14]. Mechanical creep properties changed in a manner consistent with a log time scale shift determined by the instantaneous specific volumes of the glasses. A more thorough discussion of volume–temperature–time phenomena is to be found in Chapter 10, which deals with physical aging.

At this point some comments should be made concerning the effects on T_g of polymer average molecular weight, molecular weight distribution, and long-chain branching. A four-variable equation was constructed to describe the T_g of polydisperse, randomly branched polymers and applied to BPA-PC [15]. Gel permeation chromatography, viscometry and differential scanning calorimetry (DSC) were employed to characterize the branched polymer and T_g. The author cited the usefulness of specific volume measurements in determining thermal

expansion coefficients, glass transition temperatures, and degrees of crystallinity [16,17]. Reference was also made to a study of v^{23} of linear BPA-PC as a function of molecular weight [18]. It was there found that the specific volume of glassy BPA-PC at 296 K (23°C) was linearly related to the reciprocal number-average molecular weight of the polymer, in agreement with the Fox and Flory findings for liquid polystyrene [19] and the essentially concurrent findings of Ueberreiter and Kanig [20]. The excess specific volume of finite chain length polymers over that of "infinite chain length" polymers is proportional to the number of chain ends per unit mass in the former. The Fox and Flory relation can therefore be written as

$$v^T = v_\infty^T + A_1 M_n^{-1} \tag{1}$$

where v^T, v_∞^T, and A_1 are for a linear, glassy polymer of number-average molecular weight M_n at temperature T, respectively, the specific volume, the specific volume of the polymer at "infinite molecular weight," and a constant. For polydisperse, linear BPA-PC values of v_∞^{23}°C and A_1 were found to be 0.8338 $cm^3\ g^{-1}$ and 27.15 $cm^3\ mol^{-1}$ [18] and 0.8331 $cm^3\ g^{-1}$ and 27.17 $cm^3\ mol^{-1}$ [15]. For long-chain branched molecules there are more chain ends per number-average molecule and therefore larger A_1. Empirical correction for this fact for pregelation and postgelation polymers was attempted [15,21]. It should be possible to calculate exactly the end-unit concentrations in given random long-chain branched polymers and thereby from observed A_1 gain information on the effects of branch unit volume and chain mobility restrictions.

The effect of molecular weight on the specific volumes of glassy and liquid linear polymers is, of course, important principally for low M_n. The v^{23} of M_n = 40,000, 20,000, 10,000, 5000, and 2500 g mol^{-1} BPA-PC are calculated according to [18] to be 0.8345, 0.8352, 0.8365, 0.8392, and 0.8447 $cm^3\ g^{-1}$, respectively. Increased compressibility and thermal expansivity should be found as M_n is decreased.

The specific volume at 296 K as a function of M_n for 2,2-(4-hydroxyphenyl)-1,1-dichloroethylene polycarbonate (BPC-PC) has also been reported and found to obey Eq. (1) [22].

Linear expansion dilatometry was used to follow volume relaxation during secondary transitions in polymer samples quenched from above their glass transitions to 93 K [23]. Volume relaxation rates showed secondary peaks similar to those of mechanical damping during heating.

Dilatometric measurements of thermal expansion of BPA-PC, and tetramethyl-, tetrachloro-, and tetrabromo-substituted BPA-PCs, have been used to interpret structural effects on CO_2, CH_4, O_2, N_2, and He sorption at 35°C and 1–20 atm pressure [24]. Permeabilities were found to be increased by tetramethyl substitution but were decreased by tetrachloro and tetrabromo substitutions.

Strain-gauge dilatometry has become a useful method of correlating isothermal dilation under tensile stress with deformation mechanisms in polymers and polymer blends [25–29]. The major toughening mechanism for poly(butylene terephthalate) (PBT) and for PBT/BPA-PC blends each toughened by core/shell impact modifier was found to be shear deformation [25]. Low-temperature brittleness resulted from a decreased capability of the matrix to undergo shear deformation. Tensile dilatometry detected increased internal cavitation of the impact modifier particles in this instance. The toughened blend had greater impact toughness at low temperatures than the toughened PBT. This is believed due to the presence of the partially miscible BPA-PC in the interlamellar regions of the PBT spherulites providing slippage capability. Study of a similar ternary blend suggested that the partially miscible BPA-PC in the matrix tended to coat the rubber particles and facilitate shear yielding, but both tensile dilatometry and light scattering indicated the presence of void formation by internal cavitation of the rubber particles [28]. Advantages of measuring the transverse and axial strain rate ratio during creep of BPA-PC was pointed out in a time-dependent stress dilatometry study [29].

Physical aging of BPA-PC by isothermal annealing of isotropic and cold-drawn (anisotropic) samples has been studied by a combination of dilatometry, electron spin resonance spectroscopy, and x-ray scattering [30]. The dilatometry and x-ray scattering analyses permit interpretation of mobility changes in terms of changes in free volume and free volume distribution.

B. Pressure–Volume–Temperature Studies

An early application of PVT measurements on BPA-PC involved determination of the heat of fusion of BPA-PC through observation of its melting point as a function of pressure [31]. A pressure range of 100–2200 atm and a temperature range of 235–310°C were spanned. The use of the Clausius-Clapeyron equation, of v vs. T relations at atmospheric pressure [2], of crystal density by x-ray crystallography [32], of a $T_m^\circ = 253$°C [33], and of an assumption that the expansion coefficient of the crystals equaled that of the glass, the $dT_m/dP = 0.042$°C atm^{-1} in the limit of 1 atm pressure yielded a heat of fusion $H_f = 34.6$ cal g^{-1}. This was in good agreement with a finding of $H_f = 32$ cal g^{-1} obtained from a study of melting point depressions by dibenzyl ether and di-*n*-butyl phthalate [34]. The authors reported a compressibility, β, as a function of temperature to be consistent with an average β previously found along a 300-atm isobar [35].

PVT measurements on a BPA-PC (Lexan 101 injection-molded resin, General Electric Co.) over a pressure range of 100–1800 kg cm^{-2} and a temperature range of 30–340°C were made by Zoller [36]. Figure 1 presents some of the isobars that were obtained from cross-plots of the original isothermal data. The

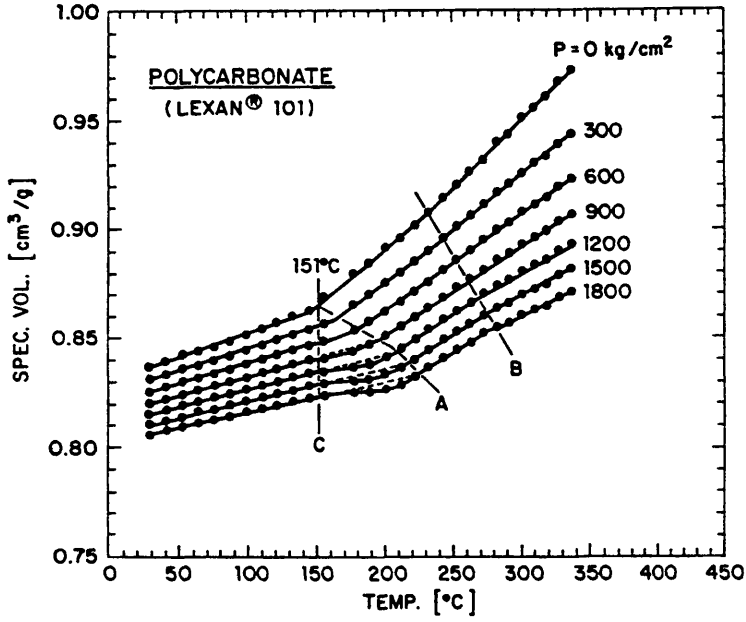

Figure 1 Selected isobars in the PVT relation of BPA-PC. (From Ref. 36.)

$v(0, T)$ isobar was obtained by extrapolation of the isothermal data to zero pressure. Below 151°C (line C) the polymer is a glass at all pressures. Line A connects the loci of glass transition temperatures $T_g(P)$, which are the intersections of the lower temperature glassy and higher temperature equilibrium melt $v(P, T)$ vs. T isobaric lines. At the higher pressures, one notes (between lines C and A) that the glasses formed from the pressured melts are denser than the original glass would have been if heated isobarically into the same temperature region. Line B connects the loci of melting points of a very small amount of crystallinity originally present or formed during the isothermal pressure cycles. A measured specific volume, v, at 22°C and atmospheric pressure was 0.836 $cm^3\ g^{-1}$, which is in good agreement with the $v = 0.836\ cm^3\ g^{-1}$ at 20°C previously reported [2]. The $v(0, T) = [0.8302 + 2.20 \times 10^{-4} \cdot T(°C)]\ cm^3\ g^{-1}$ extrapolated isobar has a slope approximately 10% lower than the $2.4 \times 10^{-4}\ cm^3\ g^{-1}\ deg^{-1}$ reported in the earlier study [2].

Three empirical, or semiempirical, equations useful in fitting polymer melt PVT data are available. These are the longstanding Tait equation [37] and, more recently, the Hartmann-Haque (HH) equation [38] and the Sun-Song-Yan equation [39].

The Tait equation may be written as

$$V(P, T) = V(0, T) \cdot \{1 - C \ln[1 + P/B(T)]\} \tag{2}$$

where for polymers a "universal" value of $C = 0.0894$ [40] is usually employed. The volume–temperature isotherm at zero pressure, $V(0, T)$, has been variously expressed by

$$V(0, t) = a_0 + a_1 \cdot t + a_2 \cdot t^2 \tag{3}$$

$$V(0, t) = b_0 \exp(b_1 \cdot t) \tag{4}$$

$$V(0, T) = c_0 \exp(c_1 \cdot T^{3/2}) \tag{5}$$

and the Tait parameter, $B(T)$, by

$$B(t) = B_0 \exp(-B_1 t) \tag{6}$$

In Eqs. (3)–(6) t is °C and T is K.

Zoller [36] fitted PVT data for the glassy BPA-PC to the Tait equation, Eq. (2), employing $C = 0.0894$ and Eq. (3) and Eq. (6) for $V(0, T)$ and $B(T)$, respectively. With P in bar and setting $a_2 = 0$, the parameters were found to be $a_0 = 0.8302$ (cm^3 g^{-1}); $a_1 = 2.20 \times 10^{-4}$ (cm^3 g^{-1} °C^{-1}); $B_0 = 3878$ (bar); $B_1 = 2.609 \times 10^{-3}$ (°C^{-1}). A fit of the melt PVT data to the Tait equation employing $C = 0.0894$ and Eq. (5) and Eq. (6) for $V(0, T)$ and $B(T)$, respectively, yielded $c_0 = 0.73565$ (cm^3 g^{-1}); $c_1 = 1.859 \times 10^{-5}$ (K$^{-3/2}$); $B_0 = 3100$ (bar); $B_1 = -4.078 \times 10^{-3}$ (°C^{-1}).

In an extensive review of equations of state for 43 homopolymer and 13 copolymer liquids, Rodgers [41] reported the Tait equation parameters [Eqs. (2), (3), and (6)] for three polycarbonates, tetramethyl bisphenol A polycarbonate (TMBPA-PC), hexafluorobisphenol A polycarbonate (HFBPA-PC), and bisphenol chloral polycarbonate (BPC-PC), computed by Kim [42] (see Fig. 2 for the chain unit structures of these three polymers). The temperature and pressure ranges covered were TMBPA-PC (218–290°C, 0–1600 bar); HFBPA-PC (159–280°C, 0–2000 bar); BPC-PC (155–284°C, 0–2000 bar). These Tait characteristic parameters are listed in Table 1.

The HH equation is expressed in reduced variables as

$$\tilde{P}\tilde{v}^5 = \tilde{T}^{3/2} - \ln \tilde{v} \tag{7}$$

where $\tilde{P} = P/B_0$, $\tilde{T} = T/T_0$, and $\tilde{v} = v/v_0$. The characteristic reference parameters B_0, T_0, and v_0 are determined by fitting PVT data to Eq. (7).

Using the Kim [42] data for TMBPA-PC, HFBPA-PC, and BPC-PC, and PVT data generated for BPA-PC from the Tait equation fit [36], Rodgers calculated the characteristic reference parameters for the HH equation [Eq. (7)].

A comprehensive liquid polymer PVT database has been reported by Wohlfarth [43] and application of an all-variables method [44] permitted computation

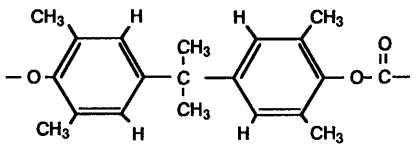

TMBPA PC

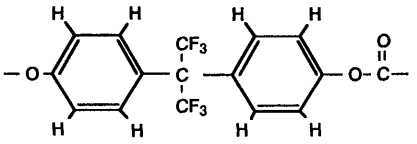

HFBPA PC

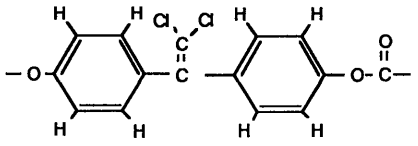

BPC PC

Figure 2 Chain unit structures of three polycarbonates.

and error assessment of HH equation-of-state parameters for 105 polymer samples, which included BPA-PC.

A review of theoretical equations of state for polymers was published in 1974 by Curro [45]. Application of these equations, and other theoretical equations of state derived since that review to polycarbonate PVT data, will now be mentioned.

Table 1 Tait Equation of State Parameters for Three Polycarbonate Liquids

Polymer	a_0 (cm^3/g)	$a_1 \times 10^4$ ($cm^3/g°C$)	$a_2 \times 10^7$ ($cm^3/g°C^2$)	B_0 (bar)	$B_1 \times 10^3$ ($°C^{-1}$)
TMBPA-PC	0.8497	5.073	3.832	2314	4.242
HFBPA-PC	0.6111	4.898	1.730	2366	5.156
BPC-PC	0.6737	3.634	2.370	3634	4.921

Source: Ref 41, table VIII.

Zoller [36] fitted his PVT data for BPA-PC to the Simha-Somcynsky (SS) hole theory cell model equations [46,47]. The same data were later examined [48] in the Flory-Orwoll-Vrij (FOV) cell model [49]. Using data calculated from the Tait equation fit [36] of BPA-PC PVT data, Wohlfarth determined the characteristic parameters for the chain-of-rotators (COR) [50] equation of state.

The most complete exposition of theoretical equations of state application to polycarbonate PVT data has been provided by Rodgers [41]. Characteristic parameters for five theoretical equations of state (and for the semiempirical HH [38] equation of state; see Table 2) were calculated and tabulated for BPA-PC Tait-generated data of Zoller [36], and the TMBPA-PC, HFBPA-PC, and BPC-PC PVT data of Kim [42]. The theoretical equations of state were the FOV cell model [49], the Prigogine cell model (CM) [51,52], the Dee and Walsh modified cell model (MCM) [53], the Sanchez-Lacombe (SL) lattice fluid model [54,55], and the Simha-Somcynsky hole theory cell model [46,47]. In addition to tabulating the characteristic parameters, comparison was made of the average difference between experimental and calculated specific volumes for the 56 polymers. In a subsequent examination of off-lattice van der Waals equations of state, Brannock and Sanchez [56] calculated characteristic parameters for these 56 polymers in the context of a generalized Flory [57] + van der Waals equation of state.

The various theoretical equations of state provide insight into the correlation of their characteristic parameters with molecular parameters employed in the models. The reader is encouraged to examine the basic assumptions of the theoretical models to assess the role of polymer molecular geometries and chain statistics in determining PVT behavior.

The characteristic parameters determined by Rodgers [41] for four polycarbonates in two of the theoretical equations of state will here be reproduced. The two equations of state are:

Flory-Orwoll-Vrij Cell Model

$$\tilde{P}\tilde{v}/\tilde{T} = \tilde{v}^{1/3}(\tilde{v}^{1/3} - 1)^{-1} - (\tilde{T}\tilde{v})^{-1} \tag{8}$$

Table 2 Hartmann-Haque Equation of State Characteristic Parameters

	For P = 0–500 bar			For full range of P		
Polymer	B_0 (bar)	T_0 (K)	v_0 (cm^3/g)	B_0 (bar)	T_0 (K)	v_0 (cm^3/g)
BPA-PC	37480	1450	0.7398	36440	1502	0.7474
TMBPA-PC	27760	1414	0.7990	29070	1430	0.8010
HFBPA-PC	29270	1271	0.5707	29200	1306	0.5758
BPC-PC	37130	1475	0.6302	36410	1520	0.5356

Source: Ref. 41, table XIV

Table 3 Flory-Orwoll-Vrij Equation of State Characteristic Parameters

	For P = 0–500 bar			For full range of P		
Polymer	P^* (bar)	T^* (K)	v^* (cm^3/g)	P^* (bar)	T^* (K)	v^* (cm^3/g)
BPA-PC	6659	8481	0.7179	6710	8039	0.7070
TMBPA-PC	5155	8286	0.7755	5142	8156	0.7720
HFBPA-PC	5488	7614	0.5575	5427	7360	0.5521
BPC-PC	6438	8576	0.6610	6110	8287	0.6065

Source: Ref. 41, table IX.

Prigogine "Square-Well" Cell Model

$$\tilde{P}\tilde{v}/\tilde{T} = \tilde{v}^{1/3}(\tilde{v}^{1/3} - 0.8909)^{-1} - 2\tilde{T}^{-1}(1.2045\tilde{v}^{-2} - 1.011\tilde{v}^{-4}) \quad (9)$$

In each equation, $\tilde{P} = P/P^*$, $\tilde{T} = T/T^*$, and $\tilde{v} = v/v^*$. The characteristic parameters P^*, T^*, and v^* are shown in Tables 3 and 4.

Approaching PVT data from the viewpoints of the various models permits rational description of phase equilibria behavior of mixtures. For instance, interpretation of a lower critical solution temperature type of phase boundary in TMBPA-PC/polystyrene mixtures in terms of PVT data within the framework of the SL theory permitted estimation of interaction parameters for the polymer pair [58]. Also, the use of the SL theory to treat the "equilibrium" Henry's law component in the sorption of gases in glassy polycarbonates was found to be advantageous [59]. Polymer blend studies using empirical PVT relations can also yield interesting structural information. The compressibility of BPA-PC/PMMA mixtures containing 1–40 wt% PMMA was found to be less than the compressibility of pure BPA-PC and PMMA [60]. This suggests that the "free volume"

Table 4 Prigogine Equation of State Characteristic Parameters

	For P = 0–500 bar			For full range of P		
Polymer	P^* (bar)	T^* (K)	v^* (cm^3/g)	P^* (bar)	T^* (K)	v^* (cm^3/g)
BPA-PC	7389	4972	0.7843	7747	4969	0.7835
TMBPA-PC	5543	4877	0.8492	6094	4875	0.8473
HFBPA-PC	5811	4488	0.6108	6207	4525	0.6116
BPC-PC	7361	4981	0.6656	7621	5046	0.6676

Source: Ref. 41, table X.

in the mixtures is less than that which would result from additivity of the pure polymer "free volume" contributions. Isothermal compressibility data in combination with light scattering data have led to an interpretation that the isothermal compressibility of glassy BPA-PC and PMMA is dominated thermodynamically by the dynamic density fluctuation still present in the glasses [61,62].

II. SPECIFIC HEAT AND MELTING PHENOMENA OF BPA-PC

Specific heat data for BPA-PC were examined by Gaur et al. [63]. It is recommended that the reader consult this paper for references to 13 specific heat studies. Of the 13 published studies they chose 3 as the best reliable sources of data and compiled a table of specific heats calculated from them [63,64]. Adiabatic calorimetric data of Dainton, et al. [65] and of O'Reilly et al. [66] were chosen for the temperature ranges 10–110 K and 120–560 K, respectively. Heat pulse data of Cieloszyk et al. [67] were chosen for the 0–4 K region.

Specific heat data from 110 to 400 K for a solution-precipitated Lexan polycarbonate powder and for a solution-crystallized powder coincided in a nearly straight line plot of C_p vs. T. Figure 3 presents C_p, T data from 370 to 560 K for the precipitated powder (first run) and for the same sample (second run) after cooling from its melt to 320 K at $-15°$/h [66]. The powder exhibited an upward drift in C_p beginning in the neighborhood of 410 K, which apparently was the result of a glass transition ΔC_p partially compensated by a concurrent crystallization exotherm. A melting endotherm began in the 450–460 K region and ended at 520 K. The heats of fusion of this solution-precipitated and of a solution-crystallized BPA-PC were 5.54 and 7.74 cal g^{-1}, respectively. Using 32 cal g^{-1} as the heat of fusion of pure crystal [34], these powder samples were 17% and 24% crystalline. The second run revealed a well-defined specific heat increase in the glass transition region with a ΔC_p of 0.25 J g^{-1} K^{-1} at T_g and no evidence of a melting endotherm. The C_p vs. T relations derived from these data, expressed in terms of C_p (J mol^{-1} K^{-1}) per mole of chain unit (254.29 g/mole), for the amorphous glassy and liquid BPA-PC are [63]:

$$C_p = \exp[0.043659(\ln T)^3 - 0.660333(\ln T)^2 + 4.2605(\ln T) - 5.19373] \qquad \text{range 120–418 K.} \tag{10}$$

$$C_p = 0.579\,T + 237.08 \qquad \text{range 418–560 K} \tag{11}$$

From these relations and the previously cited data [65,67], Table 5 was compiled [63,64]. A slightly different C_p vs. T relation for the melt has been determined and recommended [68]. This is

$$C_p = 0.559T + 249.17 \qquad \text{range 424–600 K} \tag{12}$$

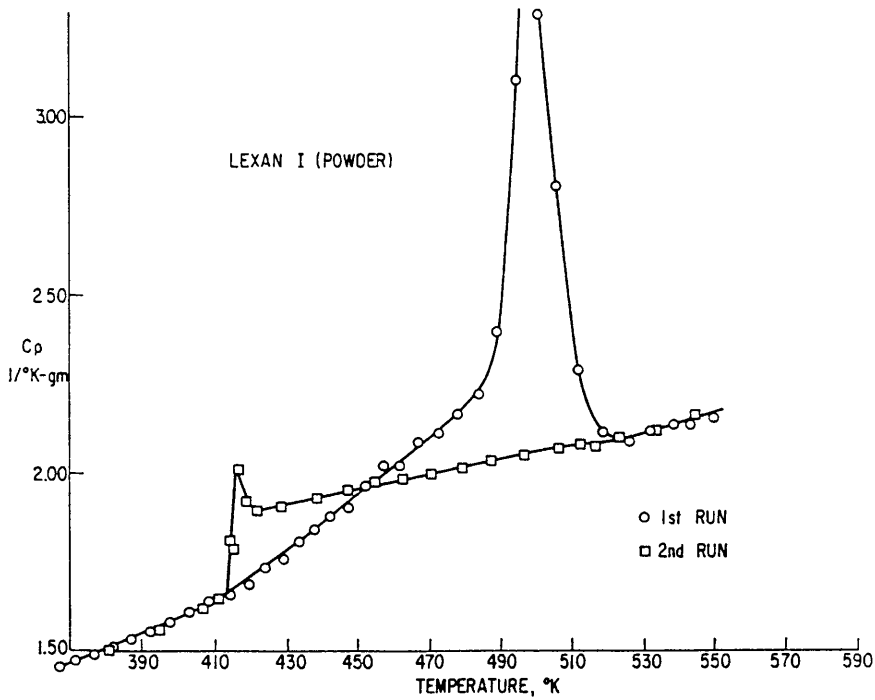

Figure 3 Heat capacity of Lexan polycarbonate powder. (From Ref. 33.)

There have been attempts to deduce conformational specific heats by examining specific heats of glassy and liquid polymer [69,70]. Also a structural unit contribution additivity scheme for specific heat calculation has been advanced for solid [71] and liquid [68] polymers.

Melting temperatures, T_m, for BPA-PC have been reported in the range of 494–526 K. The melting temperature is, of course, dependent on the conditions of crystallization and degree of perfection of the crystals. Crystals obtained by slow crystallization from solution have exhibited the highest melting temperature. The *equilibrium* melting temperature and heat of fusion have been calculated to be $T_m^\circ = 568$ K and $H_f^\circ = 33.6$ kJ mol^{-1}(31.6 cal g^{-1}) [72,73].

Crystallization, crystal structure, and effects of crystallinity on physical properties of BPA-PC are discussed in Chapter 12.

Some further sources of information concerning the specific heat of BPA-PC are available to the reader [74–83]. Specific heat effects in BPA-PC produced

Table 5 Heat Capacity C_p(J mol^{-1} K^{-1}) of BPA-PC (Based on Gram Mole of Chain Unit: 254.29 g)

T(K)	C_p	T(K)	C_p	T(K)	C_p	T(K)	C_p
10	5.95	150	158.8	290	296.7	430	486.0
20	25.38	160	168.7	300	306.8	440	491.8
30	39.85	170	178.5	310	316.9	450	497.6
40	52.46	180	188.3	320	327.1	460	503.4
50	63.75	190	198.0	330	337.4	470	509.2
60	73.72	200	207.8	340	347.7	480	515.0
70	82.62	210	217.6	350	358.1	490	520.8
80	91.39	220	227.3	360	368.5	500	526.6
90	100.4	230	237.1	370	379.1	510	532.4
100	109.7	240	247.0	380	389.7	520	538.2
110	118.8	250	256.8	390	400.3	530	543.9
120	128.9	260	266.7	400	411.1	540	549.7
130	139.0	270	276.7	410	421.9	550	555.5
140	148.9	280	286.7	420	480.3	560	561.3

Source: Ref. 63, table 3.

by deformation, stress, measurement rate, or annealing below T_g (physical aging) have also been reported [84–110]. Although, as remarked above, the subject of crystallinity in BPA-PC will be discussed in detail elsewhere, the reader is here alerted to some calorimetric determinations of T_m and BPA-PC crystal phenomena [111–116].

III. THERMAL TRANSITION ANALYSES OF POLYCARBONATE SYSTEMS

Calorimetric determinations of glass transitions, T_g, and melting temperatures, T_m, have proven to be extremely useful in analyzing polymer systems. Adiabatic calorimetry can be employed for this task, but it requires fairly large samples and is time consuming. Differential scanning calorimetry (DSC) and differential thermal analysis (DTA) are rapid and relatively simple procedures for measuring T_g, T_m, and the associated specific heat or latent heat changes in small polymer samples. The following sections will describe some research in which DSC was employed to characterize BPA-PC and two statistical copolymers, and will make reference to published research on polycarbonates, carbonate copolymers, and polycarbonate blends to assist readers in their search for pertinent literature.

A. Glass Transition Temperatures of Polycarbonates

Glass transition temperatures can be determined by many experimental methods such as dilatometry, DSC, thermooptical analysis (TOA), torsion pendulum, dynamic mechanical analysis, dielectric spectroscopy, etc. There will be no attempt to list here the T_g values for the numerous polycarbonates that have been synthesized. T_g values for 48 polycarbonates have been tabulated in the *Polymer Handbook* [117] and in a 1988 review [118]. The review is also a very good source of patent, commercial, and scientific information concerning polycarbonates. The reader is encouraged to examine the calorimetric and other studies on polycarbonates cited in the two references [117,118]. An early attempt to correlate the T_g of a polycarbonate with its unit structure was made in 1966 [119].

Reported glass transition temperatures for TMBPA-PC, HFBPA-PC, and BPC-PC (see Fig. 2 for unit structures) are 480 K [120], 449 K [121], and 441 K [122], respectively.

B. Glass Transition Temperatures of BPA-PC

Glass transition temperatures of BPA-PC have been reported to lie in the range 414–423 K [123]. Commonly accepted values have been 418 K [117] or 419 K [118]. T_g values of 419–420 K were found using DSC at 10° min^{-1} heating rate and defining T_g as the temperature at which one-half the specific heat increase in the glass transition region had occurred (midpoint T_g) [124]. Using the same DSC technique and heating rate a higher T_g = 424 K was found for two BPA-PC samples with average molecular weights that lie within a common range for commercial materials [68]. Our experience in determining T_g by the DSC midpoint method at 20° min^{-1} heating rate does indicate a slightly higher T_g for BPA-PC than those often reported in literature using various experimental approaches.

One expects the T_g of a polymer to decrease linearly with M_n^{-1} from the $T_{g\infty}$ of the infinite molecular weight polymer according to the Fox-Flory relation [125]:

$$T_g = T_{g\infty} - K/M_n \tag{13}$$

A study of BPA-PC glass transition temperatures by DSC (extrapolated to zero heating rate) as a function of reciprocal viscosity–average molecular weight revealed a linear dependence of T_g on M_v^{-1} and yielded an ultimate T_g of 436.9 K (163.5°C) in the limit of infinite M_v [126]. It should be remarked in passing that although extrapolation to a zero heating rate may remove some artifacts in DSC measurements, a T_g observation at near-zero heating rate is conceptually impossible. The polymer would approach its equilibrium, nonglassy state during the measurement.

Measurement of intrinsic viscosities in chloroform at 25°C and weight-

average molecular weights (light scattering) of four commercial BPA-PC resins yielded an intrinsic viscosity–gram molecular weight relation [127]:

$$[\eta] = 2.85 \times 10^{-3} M_w^{0.746} \tag{14}$$

where the units of $[\eta]$ are $cm^3\ g^{-1}$ and of M_w are g $mole^{-1}$.

Using this relation for M_w for three commercial BPA-PC resins a plot of T_g (midpoint, 20° min^{-1} heating rate) vs. M_w^{-1} yielded an ultimate T_g = 433.4 K (160.2°C) and a slope -2.71×10^5 K g $mole^{-1}$ [128]. Since T_g values in the region of 160°C have been observed for very high molecular weight BPA-PC obtained from ring opening polymerizations [129], these findings [128] or the findings of Dobkowski [126] appear to be substantiated.

Blends of BPA-PC with BPA diphenylcarbonate and with BPA (biscumylphenyl) carbonate have been treated as bimodal homopolymer blends and a T_g–M_n^{-1} relation involving the number–average molecular weights of the components, the ratio of free volume expansion for the individual chain ends, the product of the ratios of densities of the individual components and of their chain-end free volumes, and the weight fraction compositions of the blends [130]. The coefficient of M_n^{-1} for the pure polycarbonate was calculated to be -2.15×10^4 K g $mole^{-1}$. Agreement between this coefficient and the -2.71×10^5 K g $mole^{-1}$ (based on a mole of weight-average molecules) [128] would require that M_w/M_n for the polycarbonate samples of that study be 12.6. This is much larger than the actual M_w/M_n of those samples. The cause of this discrepancy is not at present understood.

C. Thermal Analyses of Copolymers

Thermal analyses of statistical, block, and graft copolymers will now be considered. DSC is the major experimental method employed. For amorphous copolymers a single T_g is the criterion normally used to indicate a homogeneous, single-phase system. When the addition of monomers during copolymerization is nonstatistical or when oligomeric species are employed as reactive monomers, phase separation can occur. Similar phase separation can also occur in graft copolymers. Two T_g values indicate phase separation. In the case of two phases the displacement of the T_g values from those of the individual unit homopolymers can sometimes be used to estimate the average block or graft masses. The magnitudes of the specific heat change at the two transition temperatures may also, in some instances, permit calculation of the weight fractions of the phases.

1. Statistical Copolymers

Amorphous statistical copolymers are expected to exist as single-phase materials having glass transition temperatures lying between those of the homopolymers

formed from the individual comonomers [131]. The simplest approximation of the T_g–composition relationship is given by the Fox equation [132] as applied to copolymers:

$$1/T_g = w_1/T_{g1} + w_2/T_{g2} \tag{15}$$

where T_g is the copolymer glass transition temperature, w_1 and w_2 are the weight fractions of units 1 and 2, and T_{g1} and T_{g2} are the glass transition temperatures of homopolymers composed of units 1 and 2, respectively.

The glass transition temperatures of statistical copolycarbonates synthesized from mixtures of BPA and BPC (bisphenol-chloral) have been found to obey the additivity approximated by Eq. (15) [126]. In these copolymerizations essentially statistical distribution of the counits is probable, but this is not proven because the BPA-PC and BPC-PC homopolymers are miscible [122].

A T_g–composition study of statistical copolycarbonates of BPA and SBI (6,6′-dihydroxy-1,1′-spirobiindane) [133] revealed deviation from the simple Fox-Flory relationship. Data were taken on Lexan 141 polycarbonate (0/100, 149.7), and three copolymers A (35/65, 187.7), B (50/50, 200.0), and C (72/28, 213.0). The quantities in parentheses are the molar ratios of the copolymer units, SBI carbonate and BPC carbonate, and the observed T_g values (DSC midpoint, 20° min) in °C. The data were fit to an empirical extension of the Fox-Flory relation yielding

$$1000/T_g = 2.3651 - 0.5578w + 0.20479w^2 \tag{16}$$

with w representing the weight fraction of SBI carbonate units. Extrapolation to $w = 1.000$ gives $T_g = 497.0$ K (223.8°C) for BPC-PC homopolymer.

A statistical copolycarbonate of BPA and bis(4-hydroxyphenyl)phenyl phosphine oxide having 50 wt% of the latter carbonate unit has been found to have a T_g of 186°C and much improved fire resistance relative to BPA-PC [134].

2. *Block Copolymers*

There have been many studies of carbonate block copolymers. The majority have focused on poly(BPA carbonate-bl-dimethyl siloxane) [135–147]. Early controlled syntheses and measurement of mechanical loss peak temperatures revealed that these block copolymers were phase-separated into microdomains [135–140]. The upper T_g was found to be related to the average block length of the BPA carbonate blocks [140]. Subsequent mechanical, morphological, and calorimetric examinations of these block copolymers are in essential agreement with the early microdomain phase structure description. Research on poly(BPF carbonate-bl-dimethyl siloxane), where BPF is bisphenol fluorenone, has also been reported [142].

Other carbonate block copolymers that have been examined are poly(BPA

carbonate-bl-aryl sulfone) [148], poly(aryl carbonate-bl-arylene ether sulfone) [149], poly(BPA carbonate-bl-oxyethylene) [150,151], and poly(BPA carbonate-bl-BPA terephthalate) and poly(BPA carbonate-bl-BPA isophthalate) [152,153]. Multiblock copolymers poly(styrene-bl-BPA carbonate) and poly(methyl methacrylate-bl-BPA carbonate) have been prepared from macroinitiators and analyzed by DSC [154].

IV. THERMAL ANALYSES OF POLYCARBONATE BLENDS

Polycarbonate blends have been analyzed by several techniques. Among these techniques thermal analysis has proven to be quite useful. In particular, the observation of glass transition behavior in amorphous blends has been utilized. The blends may consist of a polycarbonate mixed with a low molecular weight diluent or of a polycarbonate mixed with one or two other polymers. Polycarbonate–low molecular weight diluent (sometimes called a plasticizer or additive) blends may be homogeneous or separated into two phases. The former system will exhibit a single glass transition intermediate between the T_g values of the polycarbonate and the diluent; the latter will exhibit two T_g values. If the polycarbonate is crystallizable, its melting point depression by the diluent can be employed to determine the heat of fusion of the polycarbonate. In binary or ternary blends of a polycarbonate with other polymers DSC may detect one, two, or three distinct glass transitions. The observed T_g values and the specific heat steps at T_g can be used to estimate the compositions and magnitudes of the separated phases. If one polymer in the blend is partially crystallizable the kinetics of its crystallization, the amount of crystallinity, and the T_g of the amorphous phase are diagnostic elements.

Chapter 14 describes some blends of commercial importance. We will here make reference to blend studies that are to be found in the scientific literature.

A. Blends with Small-Molecule Diluents

BPA-PC blends with low molecular weight diluents can be analyzed by DSC using T_g–composition data by considering the T_g as a function of blend weight fraction composition and of the T_g of both the polymer and the diluent [155]. Calorimetric analyses have been used to examine BPA-PC blends with additives and fillers [156], with liquid crystals [157,158], with surface plasticizers [159], with ultraviolet light stabilizers [160], and with carbon dioxide [161]. Melting point depression was utilized in BPA-PC blends with dibenzyl ether and di-*n*-butyl phthalate [34] and with tricresyl phosphate [162] to determine a heat of fusion [162]. Acetone sorption and polymer crystallization in BPA-PC have been examined [163].

B. Binary and Ternary Polymer Blends

DSC measurements on BPA-PC and on PMMA were published in 1975 [164]. Calorimetric research on blends of BPA-PC with PMMA has been reported [165–168]. BPA-PC and PMMA are only partially miscible and their blends normally exhibit two phases characterized by two T_g values that are displaced toward each other from those of the individual polymers. Low molecular weight PMMA is soluble in BPA-PC at low concentrations. Addition of certain salts increases the miscibility of BPA-PC and PMMA [168]. BPA-PC blends with methyl methacrylate–based copolymers have been examined by DSC [169,170]. Cyclohexyl methacrylate and other comonomers promote increased miscibility.

Numerous investigations of BPA-PC blends with polyesters exist [171–186]. DSC T_g data show that BPA-PC blends with poly(butylene terephthalate) are partially miscible [171,178], with PET are two-phase up to 60–70% PET then single phase [172], with copolymers and terpolymers from 1,4-cyclohexanedimethanol/terephthalic acid/isophthalic acid are miscible and amorphous [173] and ester interchange must be suppressed [176]. Blends with poly(ε-caprolactone) are miscible at lower temperatures but exhibit lower critical solution temperature (LCST) behavior and are phase-separated at elevated temperatures [174,177]. TMBPA-PC blends with aliphatic polyesters have also been examined by DSC [187].

Other BPA-PC blends that have been examined by calorimetry include blends with BPC-PC [122], poly(styrene-co-vinylphenyl hexafluorodimethyl carbinol) [188], poly(2,6-dimethyl-1,4-phenylene oxide) [189], polyurethane-polyureas [190], polystyrene [191], acrylonitrile-butadiene-styrene (ABS) terpolymer [180], nitrile copolymers [192], poly(styrene-co-acrylonitrile) and (acrylonitrile-styrene-acrylate) terpolymer [193], nylon 6 [194], TMBPA-PC [195], poly(hydroxyether of phenolphthalein) [196], poly(styrene-co-maleic anhydride) and SMA/methyl methacrylate-butadiene-styrene elastomer ternary blend [197], poly(styrene-co-acrylonitrile)/aliphatic polyester ternary blend [198], and polysulfone and poly(ether imide) [199]. There is also reported research on interpenetrating networks containing aliphatic carbonate units [200] and on ternary blends of TMBPA-PC, polystyrene, and poly(2,6-dimethyl-1,4-phenylene oxide) [201].

V. THERMAL ANALYSES OF LIQUID CRYSTAL POLYCARBONATES

From 1979 forward publications concerned with thermal analyses of carbonate polymers and copolymers that exhibit liquid crystalline character have appeared. Since thermal analysis is naturally an important technique for evaluating the phase behavior of such polymers, the reader's attention is directed to some studies

in this area [202–208]. Direction to other liquid crystalline polymer research can be found in these publications.

REFERENCES

1. K.-H. Hellwege, W. Knappe, and W. Wetzel, Specific heats of polyolefines and some other high polymers in the temperature range 30 to 180°C, *Kolloid.-Z. 180*(2): 126 (1962).
2. K.-H. Hellwege, J. Hennig, and W. Knappe, The thermal expansion of some partly crystalline high polymers in the temperature range −60 to +300°C, *Kolloid-Z. 186*(1):29 (1962).
3. K.-H. Hellwege, J. Hennig, and W. Knappe, *Kolloid-Z. 188*:121 (1963).
4. Z. Sobiczewski and M. Wajnryb, Measurements of polymer density in a gradient column, *Polimery 8*(2):69 (1963).
5. J. P. Mercier and R. Legras, Correlation between the enthalpy of fusion and the specific volume of crystallized polycarbonate of bisphenol A, *J. Polym. Sci. B: 8*(9):645 (1970).
6. B. V. Falkai and W. Rellensmann, Crystallization of polycarbonates. II. Dilatometric investigation of bisphenol A polycarbonate, *Makromol. Chem. 88*:38 (1965).
7. E. C. Rothstein and D. Spechler, Rapid determination of thermal expansion and apparent second-order transition temperature of polymer films, *Polymer Eng. Sci. 6*(2):112 (1966).
8. V. N. Beilinson, V. I. Ovcharenko, V. P. Popov, and V. A. Pervakov, Thermal expansion and heat capacity of polycarbonate in the 10–300 K range, *Ukr. Fiz. Zh. (Russ. Ed.) 27*(7):1107 (1982).
9. H. J. Bittrich, H. J. Schad, and H. Tanneberger, Study of the volume–temperature–time relations of amorphous polymers in the glass transition region, *Acta Polym. 33*(12):736 (1982).
10. H. J. Bittrich, R. Hofmann, H. J. Schad, and H. Tanneberger, Study of the volume-temperature time relations of amorphous polymers in the glass transition region. 2. Volume relaxation in the glass transition region, *Acta Polym. 34*(3):153 (1983).
11. H. Tanneberger, H. J. Bittrich, and U. J. Steinau, Secondary volume effects in amorphous polymers, *Wiss. Z. Tech. Hochsch. "Carl Schorlemmer", Leuna-Merseburg 26*(3):472 (1984).
12. L. C. E. Struik, *Physical Aging of Amorphous Polymers and Other Materials*, Elsevier, Amsterdam, 1978.
13. J. J. Curro and R.-J. Roe, Isothermal relaxation of specific volume and density fluctuation in PMMA and BPA PC, *Polymer 25*(10):1424 (1984).
14. L. C. E. Struik, Dependence of relaxation times of glassy polymers on their specific volume, *Polymer 29*:1347 (1988).
15. Z. Dobkowski, Influence of molecular weight distribution and long-chain branching on the glass transition temperature of polycarbonate, *Eur. Polym. J. 18*(7):563 (1982).

16. D. W. Van Krevelen, *Properties of Polymers* 2nd ed., Elsevier, Amsterdam, 1976. Chapter 4.
17. B. Wunderlich, *Macromolecular Physics*, Vol. 1, Academic Press, New York, 1973.
18. Z. Dobkowski and D. Grzelak, *Polimery 28*:44 (1983).
19. T. G Fox and P. J. Flory, Second-order transition temperatures and related properties of polystyrene. I. Influence of molecular weight, *J. Appl. Phys. 21*:581 (1950).
20. K. Ueberreiter and G. Kanig, *Z. Naturforsch. 6A*:551 (1951).
21. Z. Dobkowski, Dependence of polymer specific volume on molecular characteristics, *Eur. Polym. J. 20*(4):399 (1984).
22. Z. Dobkowski and D. Grzelak, Specific volume of bisphenol C-2 polycarbonate, *Eur. Polym. J. 20*(11):1045 (1984).
23. L. C. E. Struik, Volume relaxation and secondary transitions in amorphous polymers, *Polymer 28*(11):1869 (1987).
24. N. Muruganandam, W. J. Koros, and D. R. Paul, Gas sorption and transport in substituted polycarbonates, *J. Polym. Sci. B: Polym. Phys. 25*(9):1999 (1987).
25. M. E. J. Dekkers, S. Y. Hobbs, and V. H. Watkins, Toughened blends of poly(butylene terephthalate) and BPA polycarbonate. Part 2. Toughening mechanisms, *J. Mater. Sci. 23*(4):1225 (1988).
26. G. Levita, A. Lazzeri, E. Butta, and V. Frosini, Tensile and volumetric deformations in polymeric materials, *Mater. Eng. (Modena, Italy) 1*(1):233 (1990).
27. M. E. J. Dekkers, S. Y. Hobbs, and V. Watkins, Morphology and deformation behavior of toughened blends of poly(butylene terephthalate), polycarbonate, and poly(phenylene ether), *Polymer 32*(12):2150 (1991).
28. M. Okamoto, Y. Shinoda, T. Kojima, and T. Inoue, Toughening mechanism in a ternary polymer alloy: PBT/PC/rubber system, *Polymer 34*(23):4868 (1993).
29. M. Delin, R. W. Rychwalski, J. Kubat, M. J. Kubat, H. Bertilsson, and C. Klason, Volume changes during flow of solid polymers, *J. Non-cryst. Solids 172-174 (Pt. 2)*:779 (1994).
30. J. Bartos, J. Mueller, and J. H. Wendorff, Physical aging of isotropic and anisotropic polycarbonate, *Polymer 31*(9):1678 (1990).
31. L. D. Jones and F. E. Karasz, Heat of fusion of Lexan polycarbonate, *Polym. Lett. 4*:803 (1966).
32. R. Bonart, *Makromol. Chem. 92*:149 (1966).
33. J. M. O'Reilly, F. E. Karasz, and H. E. Bair, *Thermal Analysis of High Polymers (J. Polym. Sci. C 6)* (B. Ke, ed.), Interscience, New York, 1964, p. 109.
34. P. L. Wineman, General Electric Co., Pittsfield, Mass., private communication.
35. M. M. Martynyuk and V. K. Semenchenko, *Kolloidn. Zh. 26*:83 (1964).
36. P. Zoller, A study of the pressure-volume-temperature relation-ships of four related amorphous polymers: polycarbonate, polyarylate, and polysulfone, *J. Polym. Sci. B: Polym. Phys. 20*:1453 (1982).
37. P. G. Tait, *Phys. Chem. 2*:1 (1888).
38. B. Hartmann and M. A. Haque, Equation of state for polymer liquids, *J. Appl. Polym. Sci. 30*:1553 (1985).
39. Z. Sun, M. Song, and Z. Yan, A new isothermal equation of state for polymers, *Polymer 33*:328 (1992).

40. V. S. Nanda and R. Simha, Equation of state and related properties of polymer and oligomer liquids, *J. Chem. Phys. 41*:1884 (1964).
41. P. A. Rodgers, Pressure-volume-temperature relationships for polymeric liquids: A review of equations of state and their characteristic parameters for 56 polymers, *J. Appl. Polym. Sci. 48*:1061 (1993).
42. C. K. Kim, Ph.D. thesis, University of Texas at Austin, 1992.
43. C. Wohlfarth, COR-eos and BH-eos parameters for polymer melts with the error in the all-variables method, *J. Appl. Polym. Sci. 48*:1923 (1993).
44. B. Hartmann, R. Simha, and A. E. Berger, PVT scaling parameters for polymer melts. II. Error in all variables, *J. Appl. Polym. Sci. 43*:983 (1991).
45. J. G. Curro, Polymeric equations of state, *J. Macromol. Sci.: Rev. Macromol. Chem. C11*:321 (1974).
46. R. Simha and T. Somcynsky, On the statistical thermodynamics of spherical and chain molecule fluids, *Macromolecules 2*:342 (1969).
47. R. Simha, Configurational thermodynamics of the liquid and glassy polymeric states, *Macromolecules 10*:1025 (1977).
48. P. Zoller, PVT Relationships and Equations of State of Polymers, in *Polymer Handbook*, 3rd ed. (J. Brandrup and E. H. Immergut, eds.), John Wiley and Sons, New York, 1989, pp. VI/475–483.
49. P. J. Flory, R. A. Orwoll, and A. Vrij, Statistical thermodynamics of chain molecule liquids. I. An equation of state for normal paraffin hydrocarbons, *J. Am. Chem. Soc. 86*:3507 (1964).
50. C. H. Chien, R. A. Greenkorn, and K. C. Chao, Chain of rotators equation of state, *AIChE J. 29*:560 (1983).
51. I. Prigogine, N. Trappeniers, and V. Mathot, Application of the cell method to r-mer liquids, *Disc. Faraday Soc. 15*:93 (1953).
52. I. Prigogine, A. Bellemans, and V. Mathot, *The Molecular Theory of Solutions*, North-Holland, Amsterdam, 1957.
53. G. T. Dee and D. J. Walsh, Equations of state for polymer liquids, *Macromolecules 21*:811 (1988).
54. I. C. Sanchez and R. H. Lacombe, An elementary molecular theory of classical fluids. Pure fluids, *J. Phys. Chem. 80*:2352 (1976).
55. I. C. Sanchez and R. H. Lacombe, An elementary equation of state for polymer liquids, *J. Polym. Sci. Polym. Lett. 15*:71 (1977).
56. G. R. Brannock and I. C. Sanchez, Off-lattice van derWaals equations of state for polymer liquids, *Macromolecules 26*:4970 (1993).
57. R. Dickman and C. K. Hall, Equation of state for chain molecules: continuous-space analog of Flory theory, *J. Chem. Phys. 85*:4108 (1986).
58. C. K. Kim and D. R. Paul, Interaction parameters for blends containing polycarbonates. 1. Tetramethyl bisphenol A polycarbonate/polystyrene, *Polymer 33*:1630 (1992).
59. S. S. Jordan and W. J. Koros, A free volume distribution model of gas sorption and dilation in glassy polymers, *Macromolecules 28*:2228 (1995).
60. S. Sato, S. Toda, T. Hayashi, T. Yoshinaga, and Y. Oyanagi, A study on equation of state and compressibility of amorphous polymer alloys, *Kobunshi Ronbunshu 52*:97 (1995).

61. T. Yamashita and K. Kamada, Quasi-static and dynamic density fluctuations in the glassy state. III. Isotropic scattering related to isothermal compressibility of glass and anisotropic scattering, *Jpn. J. Appl. Phys., Part 1 33*:220 (1994).
62. T. Yamashita, Quasi-static and dynamic density fluctuations in the glassy state, *Jpn. J. Appl. Phys., Part 1 33*:4025 (1994).
63. U. Gaur, S. F. Lau, and B. Wunderlich, Heat capacity and other thermodynamic properties of linear macromolecules. IX. Final group of aromatic and inorganic polymers, *J. Phys. Chem. Ref. Data 12(1)*:93 (1983).
64. B. Wunderlich, Heat Capacities of High Polymers, Part B: Data Tables for Solids and Liquids, *Polymer Handbook, 3rd ed.* (J. Brandrup and E. H. Immergut, eds.), John Wiley and Sons, New York, 1989, pp. VI-408–409.
65. F. S. Dainton, D. M. Evans, F. E. Hoare, and T. P. Melia, Thermodynamic functions of linear high polymers. Part VII-Lexan, *Polymer 3*:316 (1962).
66. J. M. O'Reilly, F. E. Karasz, and H. E. Bair, Thermodynamic properties of Lexan polycarbonate from 110-560°K, *J. Polym. Sci., Part C 6*:109 (1963).
67. G. S. Cieloszyk, M. T. Cruz, and G. L. Salinger, *Cryogenics 13*:718 (1973).
68. S. Z. D. Cheng and B. Wunderlich, Heat capacities and entropies of liquid, high-melting point polymers containing phenylene groups (PEEK, PC, and PET), *J. Polym. Sci. B: Polym. Phys. 24*:1755 (1986).
69. J. M. O'Reilly, Conformational specific heat of polymers, *J. Appl. Phys. 48*:4043 (1977).
70. R.-J. Roe and A. E. Tonelli, Contribution of the conformational specific heat of polymer chains to the specific heat difference between liquid and glass, *Macromolecules 11*:114 (1978).
71. B. Wunderlich and L. D. Jones, Heat capacities of solid polymers, *J. Macromol. Sci.-Phys. B3*:67 (1969).
72. B. Wunderlich, Equilibrium melting of flexible linear macro-molecules, *Polym. Sci. Eng. 18*:431 (1978).
73. B. Wunderlich, *Macromolecular Physics*, Academic Press, New York, Vol. 1 (1973), Vol. 2 (1976), and Vol. 3 (1980).
74. G. Peilstoecker, Temperature behavior of polycarbonates, *Kunstoffe 51*:509 (1961).
75. G. Peilstoecker, The temperature behavior of polycarbonate, *Br. Plastics 35*:365 (1962).
76. J. M. O'Reilly and H. E. Bair, Thermodynamic properties of bisphenol A polycarbonate, *J. Polym. Sci., Part C 6*:109 (1963).
77. M. Van de Voorde, Results of physical tests on polymers at cryogenic temperatures, *Cryogenics 16*:296 (1976).
78. G. Ya. Zemlyanoi and V. P. Dushchenko, Temperature dependence of the specific heat capacity of polycarbonate, *Vysokomol. Soedin., Ser. B 18*:752 (1976).
79. W. M. Prest, Jr., D. J. Luca, and F. J. Roberts, Jr., The capabilities and application of a computer controlled differential scanning calorimeter, *Therm. Anal. Polym. Charact., Sel. Pap. East. Anal. Symp., Meeting Date 1980*, E. A. Turi, Ed., Heyden, Philadelphia, Pa., 1981, pgs. 24–42.
80. B. K. Sharma, Evaluation of interchain heat capacity ratio and ultrasonic absorption in polymers from the lattice grueneisen parameter, *J. Phys. D 15*:1735 (1982).

81. B. K. Sharma, The Grueneisen parameter of polymers and evaluation of interchain specific heat and ultrasonic absorption, *Acoust. Lett. 6*:25 (1982).
82. Z. Dobkowski and B. Krajewski, Use of physicochemical methods in studies of polycarbonates, *Polimery (Warsaw) 27*:246 (1982).
83. Z. Dobkowski, Application of multimethod procedure for characterization of branched polydisperse polymers, *J. Appl. Polym. Sci. 28*:3105 (1983).
84. M. S. Ali and R. P. Sheldon, Structural changes in glassy polymers, *J. Appl. Polym. Sci. 14*:2619 (1970).
85. G. W. Miller, Thermal analyses of polymers. VII. Calorimetric and dilatometric aspects of the glass transition, *J. Appl. Polym. Sci. 15*:2335 (1971).
86. D. G. LeGrand, Yielding, crazing, and fracture of polymers. II.Retraction of crazed and drawn films, *J. Appl. Polym. Sci. 16*:1367 (1972).
87. A. Conde Cotes and J. A. Manson, Annealing of polycarbonate membranes in the glassy state, *Polym. Prepr. (ACS Div. of Polym. Chem.) 15(2)*:465 (1974).
88. G. A. Adam, A. Cross, and R. N. Haward, Effect of thermal pretreatment on the mechanical properties of polycarbonate, *J. Mater. Sci. 10*:1582 (1975).
89. M. S. Ali and R. P. Sheldon, Investigation into the effect of heating rate on the thermodynamic transition and glass transition endotherm, *Bangladesh J. Sci. Ind. Res. 12*:232 (1977).
90. I. W. Gilmour, A. Trainor, and R. N. Haward, The thermoelastic effect in glassy polymers, *J. Polym. Sci. B: Polym. Phys. 16*:1277 (1978).
91. H. J. Ott, Effect of previous thermal history on the enthalpy of amorphous thermoplastics, *Colloid Polym. Sci. 257*:486 (1979).
92. M. J. Richardson and N. G. Savill, What information will differential scanning calorimetry give on glassy polymers?, *Br. Polym. J. 11*:123 (1979).
93. F. R. Saffell, The effects of heating and cooling rate on the characteristics of the calorimetric glass transition for glassy polymers, *Thermochim. Acta 36*:251 (1980).
94. F. C. Chen, C. L. Choy, S. P. Wong, and K. Young, Kinetic nature of the glass transition II, *Polymer 21*:1139 (1980).
95. M. Yokouchi and Y. Kobayashi, Effect of heat pretreatment and strain rate on tensile properties of polycarbonate sheet, *J. Appl. Polym. Sci. 26*:431 (1981).
96. K. Varadarajan and R. F. Boyer, Effects of thermal history, crystallinity, and solvent on the transitions and relaxations in poly BPA carbonate, *J. Polym. Sci. B: Polym. Phys. 20*:141 (1982).
97. C. Bauwens-Crowet and J. C. Bauwens, Annealing of polycarbonate below the glass transition: Quantitative interpretation of the effect on yield stress and DSC measurements, *Polymer 23*:1599 (1982).
98. I. M. Hodge, Effects of annealing and prior history on enthalpy relaxation in glassy polymers. 4. Comparison of five polymers, *Macromolecules 16*:898 (1983).
99. W. M. Prest, Jr. and F. J. Roberts, Jr., Non-equilibrium processes in stressed polymeric glasses, *Contemp. Topics Polym. Sci. 4*:855 (1984).
100. R. A. Shanks and C. N. Smith, Differential scanning calorimetry of stressed polymers, *Br. Polym. J. 18*:72 (1986).
101. G. W. Adams and R. J. Farris, Latent energy of deformation of amorphous polymers. 1. Deformation calorimetry, *Polymer 30*:1824 (1989).

102. E. Oleynik, Plastic deformation and mobility in glassy polymers, *Prog. Colloid Polym. Sci. (Relax. Polym.) 80*:140 (1989).
103. S. N. Rudnev, O. B. Salamatina, V. V. Voennyi, and E. F. Oleynik, Plastic deformation kinetics for glassy polymers and blends, *Colloid Polym. Sci. 269*:460 (1991).
104. B. Moeginger and U. Fritz, Thermal properties of strained thermoplastic polymers, *Polym. Int. 26*:121 (1991).
105. Y. T. Liao, DSC heat capacity hysteresis of semicrystalline polymers, *J. Mater. Sci. Lett. 10*:706 (1991).
106. D. C. McHerron and G. L. Wilkes, Reversal of physical aging in glassy polymers by electron beam irradiation, *Polym. Prepr. (ACS, Div. Polym. Chem.) 33(1)*:1142 (1992).
107. K. M. Nairn, R. L. Walters, G. P. Simon, and A. J. Hill, DSC as a measurement technique for physical aging in polycarbonate, *Mater. Forum 16*:167 (1992).
108. S. R. Saucrbrunn, B. S. Crowe, and M. Reading, Modulated DSC, *Polym. Mater. Sci. Eng. 68*:269 (1993).
109. M. Reading, D. Elliott, and V. L. Hill, A new approach to the calorimetric investigation of physical and chemical transitions (Modulated DSC), *J. Therm. Anal. 40*: 949 (1993).
110. J. A. Koenen, Quantitative measurement of the heat exchange during deformation using an infrared camera, *Thermochim. Acta 247*:55 (1994).
111. B. von Falkai and W. Rellensmann, Crystallization of polycarbonates, *Makromol. Chem. 75*:112 (1964).
112. J. M. O'Reilly and F. E. Karasz, Specific heat studies of transition behavior in polymers, *Polym. Prepr. (ACS Div. Polym. Chem.) 6(2)*:731 (1965).
113. T. Hatakeyama, H. Kanetsuna, and E. Ito, Crystallization of polycarbonate in organic solvents, *Kobunshi Ronbunshu 31*:197 (1974).
114. E. Turska and H. Janeczek, Liquid-induced crystallization of a bisphenol A polycarbonate, *Polymer 20*:855 (1979).
115. R. Legras, C. Bailly, M. Daumerie, J. M. Dekoninck, J. P. Mercier, Mrs. V. Zichy, and E. Nield, Chemical nucleation, a new concept applied to the mechanism of action of organic acid salts on the crystallization of polyethylene terephthalate and bisphenol-A polycarbonate, *Polymer 25*:835 (1984).
116. C. Bailly, R. Legras, and J. P. Mercier, Crystallization of BPA PC induced by organic salts: chemical modification of the polymer. II. Model reactions, *J. Polym. Sci. B: Polym. Phys. Ed. 23*:355 (1985).
117. P. Peyser, Glass transition temperatures of polymers, *Polymer Handbook*, 3rd ed., (J. Brandrup and E. H. Immergut, eds.), John Wiley and Sons, Inc., New York, 1989, pp. VI/209–258. Based on a table by W. A. Lee and R. A. Rutherford, *Polymer Handbook*, 2nd ed., 1975.
118. D. Freitag, U. Grigo, P. R. Muller, and W. Nouvertne, Polycarbonates, in *Encyclopedia of Polymer Science and Technology*, 2nd ed. (J. I. Kroschwitz, exec. ed., H. F. Mark, N. M. Bikales, C. G. Overberger, and G. Menges, ed. bd.), John Wiley and Sons, New York, 1988, pp. 648–718.
119. A. N. Perepelkin and P. V. Kozlov, Effect of chemical structure on the glass transition temperature of polycarbonates, *Vysokomol. Soedin 8*:56 (1966).

120. V. Serini, D. Freitag, and H. Vernaleken, Polycarbonates from o,o,o',o'-tetramethylsubstituted bisphenols, *Angew. Makromol. Chem. 55*:175 (1976).
121. L. J. Garfield, Molecular motions in some polycarbonates, *J. Polym. Sci., Part C 30*:551 (1970).
122. A. Factor and C. M. Orlando, Polycarbonates from 1,1-dichloro-2,2-bis(4-hydroxyphenyl) ethylene and bisphenol-A: a highly flame-resistant family of engineering thermoplastics, *J. Polym. Sci. A: Polym. Chem. 18*:579 (1980).
123. D. W. Van Krevelen, *Properties of Polymers*, Elsevier, Amsterdam, 1976.
124. G. E. Wissler and B. Crist, Jr., Glass transition in semicrystalline polycarbonate, *J. Polym. Sci. B: Polym Phys. 18*:1257 (1980).
125. T. G Fox and P. J. Flory, Second-order transition temperatures and related properties of polystyrene. I. Influence of molecular weight, *J. Appl. Phys. 21*:581 (1950).
126. Z. Dobkowski, Measurement of the glass-transition temperature of polycarbonate by a calorimetric method, *Polimery (Warsaw) 23*:402 (1978).
127. J. C. Carnahan, P. E. Gundlach, R. B. Rohling, and S. R. Weissman, General Electric Corporate R&D, private communication, 1982.
128. A. R. Shultz and A. L. Young, General Electric Corporate R&D, unpublished data, 1990.
129. A. R. Shultz, General Electric Corporate R&D, unpublished data.
130. J. M. Pochan, D. F. Pochan, and J. F. Elman, Extension of the chain-end free volume theory for predicting the T_g-M_n^{-1} relationship for homopolymer bimodal blends, *Polymer 27*:747 (1986).
131. D. W. Van Krevelen, Relations for T_g of statistical copolymers. *Properties of Polymers*, 2nd ed., Elsevier, Amsterdam, 1976, Chap. 6.
132. T. G Fox, Influence of diluent and of copolymer composition on the glass transition temperature of a polymer system, *Bull. Am. Phys. Soc. 1*:123 (1956).
133. A. R. Shultz and A. L. Young, General Electric Corporate R&D, unpublished data.
134. D. M. Knauss, J. E. McGrath, and T. Kashiwagi, Copolycarbonates and poly(arylates) derived from hydrolytically stable phosphine oxide comonomers, *ACS Symp. Ser. (Fire and Polymers II) 599*:41 (1995).
135. E. P. Goldberg and E. J. Powers, Polycarbonate-siloxane copolymers, *J. Polym. Sci. B: Polym. Phys. 2*:835 (1964).
136. H. A. Vaughn, The synthesis and properties of alternating block polymers of dimethylsiloxane and bisphenol-A carbonate, *J. Polym. Sci. B: Polym. Phys. 7*:569 (1969).
137. R. P. Kambour, Microdomains in alternating block polymers of dimethylsiloxane and bisphenol-A carbonate, *J. Polym. Sci. B: Polym. Phys. 7*:573 (1969).
138. D. G. LeGrand, Mechanical and optical studies of poly(dimethyl siloxane) bisphenol-A polycarbonate copolymers, *J. Polym. Sci. B: Polym. Phys. 7*:579 (1969).
139. T. L. Magila and D. G. LeGrand, Physical properties of block copolymers of polydimethylsiloxane and polycarbonate, *Polym. Eng. Sci. 10*:349 (1970).
140. R. P. Kambour in *Block Polymers* (S. L. Aggarwal, ed.), Plenum Press, New York, 1970, p. 263. T_g of BPA-PC–PDMS block copolymer as a function of composition and block length, Fig. 7.
141. B. M. Beach, R. P. Kambour, and A. R. Shultz, Effect of short silicone blocks on the shear plasticity and low temperature toughness of BPA polycarbonate, I., *J. Polym. Sci. Polym. Lett. 12*:247 (1974).

142. R. P. Kambour, D. Faulkner, E. E. Kampf, S. Miller, G. E. Niznik, and A. R. Shultz, Toughness enhancement by introduction of silicone blocks into polycarbonates of bisphenol acetone and bisphenol fluorenone, *Adv. Chem. Series No. 154. Toughness and Brittleness of Plastics* (R. D. Deanin and A. M. Crugnola, eds.), Am. Chem. Soc., 1976, pp. 312–325.
143. M. R. Tant and G. L. Wilkes, Physical aging studies of styrene-butadiene and carbonate-siloxane block copolymers, Report, TR-2: Order No. AD-A079608 NITS 80:1684 (1980).
144. T. C. Ward, D. P. Sheehy, J. E. McGrath, and J. S. Riffle, Inverse gas chromatography studies of PDMS-PC copolymers and blends, *Polymer Preprints (ACS, Div. Polym. Chem.) 22(1)*:187 (1981).
145. M. R. Tant and G. L. Wilkes, Physical aging studies of styrene-butadiene and carbonate-siloxane block copolymers, *Polym. Eng. Sci. 21*:325 (1981).
146. T. C. Ward, D. P. Sheehy, J. E. McGrath, and J. S. Riffle, Inverse gas chromatography studies of poly(dimethylsiloxane)-polycarbonate copolymers and blends, *Macromolecules 14*:1791 (1981).
147. W. Maung and H. L. Williams, Damping modulus studies of poly(dimethylsiloxane)-bisphenol A polycarbonate block copolymers, *Polym. Eng. Sci. 25*:113 (1985).
148. J. E. McGrath, T. C. Ward, and A. J. Wnuk, Structure, morphology and properties of polycarbonate-polysulfone engineering thermoplastic block copolymers, *Soc. Plast. Eng., Tech. Pap. 24*:254 (1978).
149. T. C. Ward, A. J. Wnuk, E. Schori, R. Viswanathan, and J. E. McGrath, Poly(arylene ether sulfone)-Poly(aryl carbonate) block copolymers, *Adv. Chem. Ser. 176 (Multiphase Polym.)*:293 (1979).
150. T. Suzuki and T. Kotaka, Dielectric and mechanical relaxations in randomly coupled multiblock copolymers with varying block lengths: bisphenol A polycarbonate-poly(oxyethylene) system, *Macromolecules 13*:1495 (1980).
151. T. Suzuki and T. Kotaka, Morphological and physical properties of randomly coupled multiblock polymers: BPA PC-poly(oxyethylene) systems, *Polym. J. (Tokyo) 15*:15 (1983).
152. C. P. Bosnyak, I. W. Parsons, J. N. Hay, and R. N. Haward, Relations between structure and properties in bisphenol A polyester carbonates, *Polymer 21*:1448 (1980).
153. C. P. Bosnyak, J. N. Hay, I. W. Parsons, and R. N. Haward, Synthesis and properties of some poly(bisphenol A iso/terephthalate) co-polycarbonates, *Polymer 23*:609 (1982).
154. Y. Haneda, H. Terada, M. Yoshida, A. Ueda, and S. Nagai, Macro-azo-initiators composed of various polyesters: their syntheses, thermal properties, and application to block copolymerization, *J. Polym. Sci. A: Polym. Chem. 32*:2641 (1994).
155. L. J. Garfield and S. E. Petrie, Viscosity and T_g behavior of polymer-diluent systems, *J. Phys. Chem. 68*:1750 (1964).
156. B. Cassel, J. Hall, and D. Breakey, Use of thermal analysis methods for evaluating additives and fillers, *Soc. Plast. Eng., Tech. Pap. 24*:377 (1978).
157. T. Kajiyama, Y. Nagata, S. Washizu, and M. Takayanagi, Characterization and gas permeation of polycarbonate/liquid crystal composite membrane, *J. Membrane Sci. 11*:39 (1982).

158. L. A. Belfiore, Thermodynamic miscibility in polymer-liquid crystal blends, *Polym. Prepr. (ACS. Div. Polym. Chem.) 28(1)*:158 (1987).
159. A. R. Shultz, Characterization of plasticized surfaces, *Proc. IUPAC Macromol. Symp. IUPAC 28*:692 (1982).
160. A. R. Shultz, A. L. Young, S. Alessi, and M. Stewart, Glass transitions of poly(bisphenol-A carbonate)/ultraviolet light stabilizer blends by DSC and TOA, *J. Appl. Polym. Sci. 28*:1685 (1983).
161. J. S. Chiou, J. W. Barlow, and D. R. Paul, Plasticization of glassy polymers by carbon dioxide, *J. Appl. Polym. Sci. 30*:2633 (1985).
162. A. J. Çonix and L. Jeurissen, Plasticization of bisphenol A carbonate, *Advan. Chem. Ser. No. 48*:172 (1965).
163. R. P. Kambour and J. H. Dane, Kinetic and equilibrium phenomena in the system: acetone vapor and polycarbonate film, *J. Polym. Sci. A-2: Polym. Phys. 4*:327 (1966).
164. T. J. Gedemer, Characterization of poly(methyl methacrylate) and polycarbonate through differential scanning calorimetry, *Plast. Eng. 31*:28 (1975).
165. H. Polanska, T. Koomoto, and T. Kawai, Polycarbonate-poly(methyl methacrylate) blends. II. Mechanical properties, *Polimery (Warsaw) 25*:396 (1980).
166. Z. G. Gardlund, Thermal and dynamic mechanical analysis of polycarbonate/poly (methyl methacrylate) blends, *Polym. Prepr. (ACS. Div. Polym. Chem.) 23(1)*:258 (1982).
167. G. D. Butzbach and J. H. Wendorff, PC-PMMA blends: The role of molecular interactions on miscibility and antiplasticization, *Polymer 32*:1155 (1991).
168. J.-Y. Lai, S.-J. Huang, S.-L. Huang, and S. S. Shyu, Poly(methyl methacrylate)/polycarbonate membrane for gas separation, *Sep. Sci. Technol. 30*:461 (1995).
169. M. Nishimoto, H. Keskkula, and D. R. Paul, Miscibility of PC with methyl methacrylate-based copolymers, *Polymer 32*:1274 (1991).
170. C. C. Hung, W. G. Carson, and S. P. Bohan, Phase morphology of blends of polycarbonate with poly(methyl methacrylate-co-cyclohexyl methacrylate), and of polycarbonate with poly(methyl methacrylate) by solid-state NMR, DSC, and TEM, *J. Polym. Sci. B: Polym. Phys. 32*:141 (1994).
171. D. C. Wahrmund, D. R. Paul, and J. W. Barlow, Polyester-polycarbonate blends. I. Poly(butylene terephthalate), *J. Appl. Polym. Sci. 22*:2155 (1978).
172. T. R. Nassar, D. R. Paul, and J. W. Barlow, Polyester-polycarbonate blends. II. Poly(ethylene terephthalate), *J. Appl. Polym. Sci. 23*:85 (1979).
173. R. N. Mohn, D. R. Paul, and J. W. Barlow, Polyester-polycarbonate blends. III. Polyesters based on 1,4-cyclohexanedimethanol/terephthalic acid/isophthalic acid, *J. Appl. Polym. Sci. 23*:575 (1979).
174. C. A. Cruz, D. R. Paul, and J. W. Barlow, Polyester-polycarbonate blends. IV. Poly(epsilon-caprolactone), *J. Appl. Polym. Sci. 23*:589 (1979).
175. C. A. Cruz, D. R. Paul, and J. W. Barlow, Polyester-polycarbonate blends. V. Linear aliphatic polyesters, *J. Appl. Polym. Sci. 24*:2101 (1979).
176. W. A. Smith, J. W. Barlow, and D. R. Paul, Chemistry of miscible polycarbonate-copolyester blends, *J. Appl Polym. Sci. 26*:4233 (1981).
177. J. M. Jonza and R. S. Porter, Bisphenol A polycarbonate/poly(epsilon-caprolac-

tone) blends: melting point depression and reactivity, *Macromolecules 19*:1946 (1986).
178. S. Y. Hobbs, V. L. Groshans, M. E. J. Dekkers, and A. R. Shultz, Partial miscibility of poly(butylene terephthalate)/BPA polycarbonate blends, *Polym. Bull. 17*:335 (1987).
179. R. Kosfeld, F. Schubert, M. Hess, and W. Brostow, Structure and properties of blends of polycarbonate and poly(ethylene terephthalate-co-hydroxybenzoate). Phase diagram and mechanical behavior, *Mater. Res. Soc. Symp. Proc. (Polym. Based Mol. Compos.) 171*:183 (1990).
180. O. B. Salamatina, S. N. Rudnev, V. V. Voennyi, and E. F. Oleinik, Heat and stored energy of plastic deformation of solid polymers and heterogeneous blends, *J. Therm. Anal. 38*:1271 (1992).
181. J. S. Lee, H. J. Kim, and D. S. Lee, Thermal property and miscibility of polycarbonate/copolyester blends, *Polym. Bull. (Berlin) 30*:229 (1993).
182. M. Yang, M. Xu, R. Huang, and C. Zhang, Effect of mixing conditions on the compatibility of PC/PET blends, *Chengdu Keji Daxue Xuebao (2)*:31 (1993).
183. H. Yoon, Y. Feng, Y. Qiu, and C. C. Han, Structural stabilization of phase separating PC/polyester blends through interfacial modification by transesterification reaction, *J. Polym. Sci. B: Polym. Phys. 32*:1485 (1994).
184. H. Yang and W. Yetter, Miscibility studies of high T_g polyester and polycarbonate blends, *Polymer 35*:2417 (1994).
185. H. J. Radusch, R. Androsch, J. Vogel, and M. Stolp, Morphology-property relations of polymer blends based on technical and high temperature–resistant polymer blends, *Vortr. Poster—2nd Symp. Materialforsch.*, Vol. 3 (B. Vierkorn-Rudolph, D. Lillack, and H.-J. Clar, eds.), Forschungszentrum Juelich, Germany, 1991, p. 2551.
186. V. E. Reinsch and L. Rebenfeld, Crystallization processes in poly(ethylene terephthalate)/polycarbonate blends, *Mater. Res. Soc. Symp. Proc. (Crystallization and Related Phenomena in Amorphous Materials) 321*:543 (1994).
187. A. C. Fernandes, J. W. Barlow, and D. R. Paul, Blends containing tetramethylbisphenol-A polycarbonate: 2. Aliphatic polyesters, *Polymer 27*:1799 (1986).
188. S. P. Ting, E. M. Pearce, and T. K. Kwei, Compatibility studies of poly(styrene-co-vinylphenyl hexafluorodimethyl carbinol) with bisphenol A polycarbonate, poly(butyl methacrylate), and poly(2,6-dimethyl-1,4-phenylene oxide), *J. Polym. Sci. Polym. Lett. 18*:201 (1980).
189. J. R. Fried, G. A. Hanna, and H. Kalkanoglu, Compatibility studies of poly(2,6-dimethyl-1,4-phenylene oxide) blends, *MMI Press Sym. Ser. (Polym. Compat. Incompat.) 2*:237 (1982).
190. V. A. Kuz'mina, Yu. Yu. Kercha, V. A. Vilenskii, and V. V. Shevchenko, The effect of chain microstructure and polycarbonate additives on microphase separation in polyurethane ureylenes, *Kompoz. Polim. Mater. 18*:51 (1983).
191. W. N. Kim and C. M. Burns, Thermal behavior, morphology and the determination of the Flory-Huggins interaction parameter of polycarbonate-polystyrene blends, *J. Appl. Polym. Sci. 34*:945 (1987).
192. S. Percec and T. Hammond, Phase behavior of blend systems containing nitrile copolymers examined by solid-state NMR and DSC, *Polymer 32*:1252 (1991).
193. H. E. Bertilsson, J. Kubat, and E. Ribarits, Miscibility and phase behavior in

polycarbonate/poly(styrene-co-acrylonitrile) and polycarbonate/(acrylonitrile-styrene-acrylate) terpolymer blends, *Plast. Rubber Compos. Process. Appl. 19*:211 (1993).

194. M. Cortazar, J. I. Eguiazabal, and J. J. Iruin, A calorimetric study of the interchange reactions in bisphenol A polycarbonate/nylon 6 blends, *Br. Polym. J. 21*:395 (1989).
195. E. H. Hellmann, G. P. Hellmann, and A. R. Rennie, Solvent-induced phase separation in polycarbonate blends PC/TMPC, *Colloid Polym. Sci. 269*:343 (1991).
196. Q. Guo, J. Huang, T. Chen, and Z. Feng, Miscibility of poly(hydroxyether of phenolphthalein) with aromatic polyesters and polycarbonate, *Polym. Commun. 31*:240 (1990).
197. R. J. Chen and C. Feng, Rubber toughened polyblends of polycarbonate with styrene maleic-anhydride copolymer, *Polym. Networks Blends 3*:107 (1993).
198. V. S. Shaw, J. D. Keitz, D. R. Paul, and J. W. Barlow, Miscible ternary blends containing polycarbonate, SAN, and aliphatic polyesters, *J. Appl. Polym. Sci. 32*: 3863 (1986).
199. W. G. Kohlman and S. P. Petrie, Mechanical properties of polycarbonate-polysulfone and polycarbonate-poly(ether imide) blends, *Adv. Polym. Technol. 14*:111 (1995).
200. P. Zhou and H. L. Frisch, The effect of aging on the phase morphology of simultaneous interpenetrating polymer networks and their metastable isomers, *J. Polym. Sci. A: Polym. Chem. 31*:3479 (1993).
201. A. C. Su and J. R. Fried, A miscibility study of ternary blends of polystyrene, tetramethylbisphenol A polycarbonate, and poly(2,6-dimethyl-1,4-phenylene oxide, *J. Polym. Res. 1*:227 (1994).
202. A. Roviello and A. Sirigu, Mesophasic behavior of some polycarbonates of 4,4′-dihydroxy-alpha, alpha′-dimethylbenzalazine, *Eur. Polym. J. 15*:423 (1979).
203. T. Kobayashi, M. Sato, N. Takeno, and K. Mukaida, Synthesis and liquid crystallinity of thermotropic polycarbonate-polystyrene graft copolymers, *Eur. Polym. J. 28*: 1105 (1992).
204. A. L. Bluhm, P. Cebe, H. L. Schreuder-Gibson, J. T. Stapler, and W. Yeomans, Syntheses of new stilbene-based polycarbonates, *Mol. Cryst. Liq. Cryst. Sci. Technol. A 239*:123 (1994).
205. T. Hirata, M. Sato, and K. Mukaida, Thermotropic liquid-crystalline aromatic-aliphatic polyimides. 4. Poly(imide-urethane-carbonate)s based on pyromellitdiimide and 3,4-3′4′-biphenyldicarboximide, *Macromol. Chem. Phys. 195*:2267 (1994).
206. M. Sato, K. Muraki, and K. Mukaida, Thermotropic liquid crystalline semirigid polycarbonates based on diphenyl ether and benzophenone units, *Macromolecules 27*:4577 (1994).
207. Y.-Y. Cheng, P. Cebe, H. Schreuder-Gibson, A. Bluhm, and W. Yeomans, Crystallization of monotropic liquid crystalline polycarbonates based on a methylstilbene mesogen and a methylene-containing flexible spacer, *Macromolecules 27*:5440 (1994).
208. T. Zhang, M. H. Litt, and C. E. Rogers, Dipole-dipole interaction directed liquid crystalline polymers. I. Aliphatic poly (carbonate-sulfone)s based on 1,3-bis(3-hydroxypropylsulfonyl)propane, *J. Polym. Sci. A: Polym. Chem. 32*:2291 (1994).

9
Polycarbonate Melt Rheology

Therese C. Jordan and William D. Richards
General Electric Company, Schenectady, New York

I. INTRODUCTION

The rheological properties of a polymer melt are important to understand because, to a large extent, they determine the processing characteristics of the resin [1–4]. For example, the modeling of an injection molding process requires a knowledge of the shear rate and temperature dependence of the viscosity. For extrusion processes, the rheological properties of the resin determine the mixing dynamics, the pressure development at the die, and the degree of extrudate swell. For blow molding applications, the amount of parison sag is a function of the rheological properties.

The rheological behavior of a polymer melt also provides valuable insight into the resin's microstructural characteristics. The rheological properties are highly sensitive to such features as molecular weight, polydispersity, backbone stiffness, branching, and intermolecular associations. Thus, rheological measurements can serve as a useful tool to investigate these features.

In this chapter, the rheological properties of bisphenol A (BPA) polycarbonate resins will be discussed. The shear rate and temperature dependence of the viscosity will be described for resins that differ in molecular weight, polydispersity, and long chain branching. The optical characteristics of polycarbonate in flow will also be described, including the polymer's response to extensional and mixed shear/extension flow fields.

The rheological response of polycarbonate below the glass transition is discussed in detail in Chapter 11. For a description of rheological response close to or encompassing the glass transition region for polycarbonate, the reader is referred to a number of related monographs [5–10]. In the majority of these

studies the test procedures were geared to investigate creep and stress relaxation of the material in the glassy to rubbery transition zone. Additionally, several authors have also explored the dynamic mechanical properties in an oscillatory deformation mode [5,8,9]. Relaxation data taken at various temperatures have been superimposed using the principles of time–temperature superposition to create a master curve for a given material [7]. The features of a relaxation master curve are a glassy region ($E \sim 10^{10}$ dyne/cm^2), a transition region, a rubbery plateau ($E \sim 10^8$ dyne/cm^2), and a flow region. The majority of this chapter focuses on the flow region.

It is interesting to note that there are two different regimes of dynamics in and around the glass transition for high molecular weight polymer such as polycarbonate. Dynamic mechanical behavior in the region around and above the glass transition has been shown to exhibit two well-resolved dispersion regions related to the primary α relaxation (glass transition) and the much slower terminal zone relaxation (flow). Time–temperature superposition cannot simultaneously be applied to both processes. However, one can account for a coupling of the fast (segmental) and slow (diffusive) motions using a stretched exponential (Kolrausch-Williams-Watts function) [5,8,9]. The molecular level dynamics of these processes, discussed within the framework of free volume and local defects, is covered in Chapter 3.

The rheological properties of polycarbonate copolymers, blends, and filled systems are beyond the scope of this chapter. For an example of copolymer data the reader is referred to Ref. 11. For some examples of monographs on miscible and partially miscible blends the reader is referred to Refs. 12–19. An example of rheology of polycarbonate with rigid fillers is discussed explicitly elsewhere [20] and can be considered a general class of filled polymer rheology extensively covered in the literature [21].

II. LINEAR POLYCARBONATE

There have been numerous studies reported in the literature describing the rheological properties of linear BPA polycarbonate resins. In one of the earliest studies, Mercier et al. [7] measured the relaxation modulus in the temperature region surrounding the glass transition temperature. More recent studies have examined the dynamic rheological properties, transient properties, steady-state viscosity, and temperature dependence of the rheological properties [10,11,19,20,22–26].

In this section, the rheological properties of polycarbonate at temperatures far above the glass transition region are discussed. It is this temperature regime that is of primary importance for processing. By way of illustration, the rheological properties of a series of nine linear BPA polycarbonate resins ranging in

molecular weight from 16,600 to 35,500 g/gmol will be presented here. Some of the rheological properties of these resins have been described previously by Yoshimura and Richards [27]. A description of the resins is provided in Table 1. The molecular weights encompass the range typically available commercially. All of the resins have a similar polydispersity as indicated by the ratio $\overline{M}_w/\overline{M}_n$. The molecular weight values reported from gel permeation chromatography (GPC) measurements are based on polystyrene standards, as is common practice. The GPC values for $\overline{M}_w$ differ by about a factor of two from the $\overline{M}_w$ values determined by light scattering measurements.

The dynamic moduli, G' and G'', and the complex viscosity, $|\eta^*|$, of the highest molecular weight polycarbonate are shown in Figs. 1–3. The storage modulus, G', is a measure of the relative elasticity of the resin, whereas the loss modulus, G'', describes the extent to which the work of deformation is dissipated as heat [28]. As will be discussed in greater detail below, the complex viscosity often approximates the steady shear viscosity, $\eta(\dot{\gamma})$. The properties are presented as a function of frequency over a temperature range extending from approximately 50°C above the glass transition temperature, T_g, to the upper temperature typically encountered during processing. Time–temperature superposition [28] can be used to greatly expand the frequency range of the dynamic spectrum beyond the range accessible experimentally. By appropriate shifts along the axes, the moduli obtained at each temperature can be superposed to obtain master curves at any desired reference temperature. In Fig. 4, master curves of the dynamic properties at a reference temperature of 275°C have been generated from

Table 1 Polycarbonate Resins

Sample	IV[a] (dl/g)	$\overline{M}_w$ (light scattering)	$\overline{M}_w$ (GPC[a,b])	$\overline{M}_n$ (GPC[a,b])	$\overline{M}_w/\overline{M}_n$ (GPC[a,b])	MFI[c] (g/10 min)
PC63	0.63	35,500	72,600	28,100	2.6	3.2
PC58	0.58	32,000	66,100	25,400	2.6	4.9
PC55	0.55	29,000	62,000	25,400	2.4	6.5
PC54	0.54	27,900	60,600	24,400	2.5	7.4
PC51	0.51	26,300	57,000	23,900	2.4	9.2
PC49	0.49	27,400	54,500	22,700	2.4	11.2
PC45	0.45	21,200	49,800	20,400	2.4	16.2
PC43	0.43	22,700	46,900	18,400	2.5	20.9
PC35	0.35	16,600	35,800	13,900	2.6	78.0

[a] In methylene chloride.
[b] Based on polystyrene standards.
[c] ASTM Method D-1238, 1.2 kg weight, 300°C.

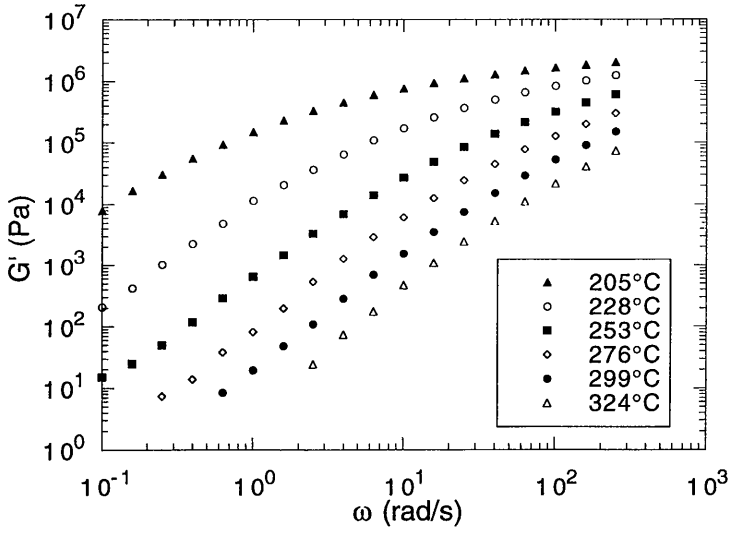

Figure 1 The storage modulus of PC63 over a temperature range of 205–324°C.

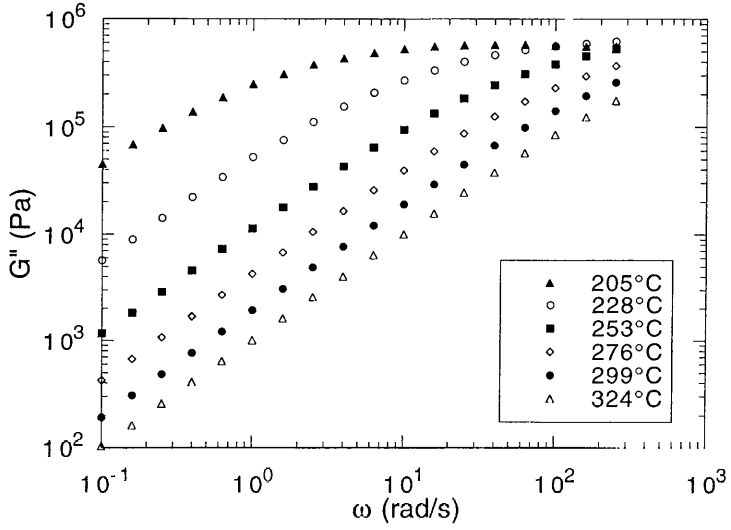

Figure 2 The loss modulus of PC63 over a temperature range of 205–324°C.

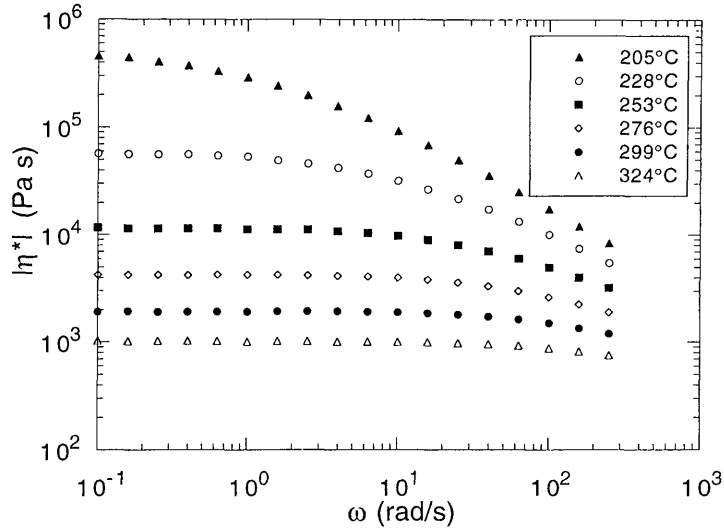

Figure 3 The complex viscosity of PC63 over a temperature range of 205–324°C.

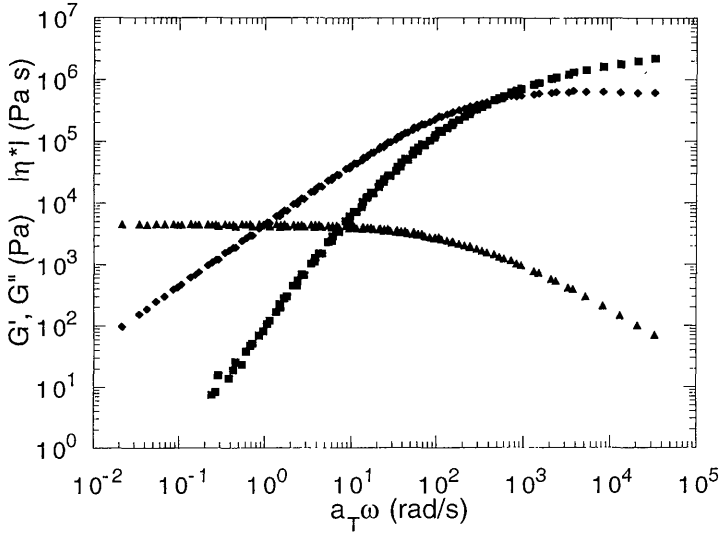

Figure 4 Master curves of the dynamic properties of PC63 at a reference temperature of 275°C.

the data presented in Figs. 1–3. In these plots, the reduced variables are as follows:

$$G'_p = G'(T_0\rho_0/T\rho) \tag{1}$$

$$G''_p = G''(T_0\rho_0/T\rho) \tag{2}$$

$$|\eta^*|_p = |\eta^*|(T_0\rho_0/a_T T\rho) \tag{3}$$

where T_0 is the reference temperature, T is the temperature at which the data were generated, and ρ_0 and ρ are the density at T_0 and T, respectively. The density of polycarbonate can be expressed as follows [29]:

$$\rho = \frac{10^3}{\exp(-0.307 + 1.86 \times 10^{-5}T^{3/2})} \tag{4}$$

where T is expressed in K, and ρ in kg/m^3. The factor a_T is the amount by which the dynamic data must be shifted along the frequency axis in order to obtain superposition and is a measure of the temperature dependence of the rheological properties.

The master curves span almost six decades of frequency. In the terminal or low-frequency region, G' and G'' approach slopes of 2 and 1, respectively, as is typical of linear polymers. At high frequencies, a plateau is observed in G'. The modulus in this region is referred to as the plateau modulus, G^0_N, and is dependent on the molecular entanglement density in the following manner [28]:

$$G^0_N = \rho RT/M_e \tag{5}$$

where M_e is the molecular weight between entanglements and R is the ideal gas constant. Because of the broad molecular weight distribution of this sample, a truly flat plateau in G' is not observed, and thus an accurate value for G^0_N cannot be determined directly. Methods for estimating the value of G^0_N have been described elsewhere [28]. For BPA polycarbonate G^0_N has been calculated to be 1.5 $\times$ 10^6 Pa at 150°C, which by Eq. (5) leads to a value of M_e of approximately 2500 [7,30].

The values of the shift factor, a_T, for PC63 are plotted as a function of temperature in Fig. 5. The nonlinearity of the data precludes the use of an Arrhenius expression to describe the temperature dependence of a_T over the broad temperature range of the measurements. The shift factor is more accurately described by the WLF equation [31]:

$$\log(a_T) = \frac{-C^0_1(T - T_0)}{C^0_2 + (T - T_0)} \tag{6}$$

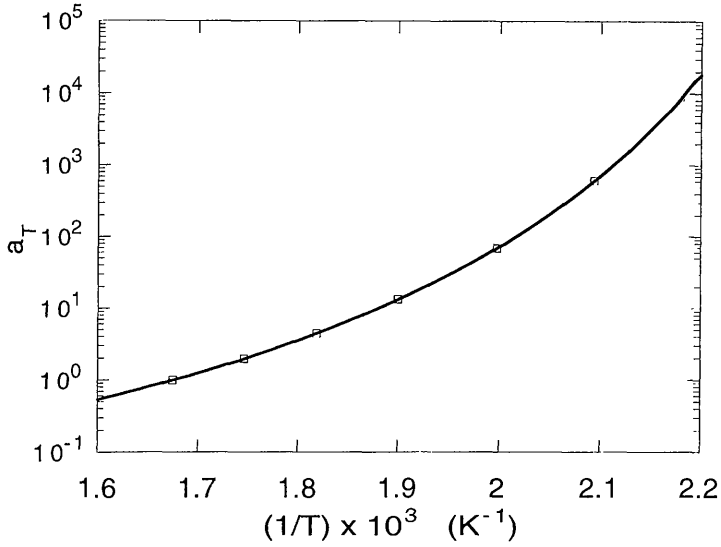

Figure 5 The shift factors, a_T, for PC63. The solid line represents the fit of the free volume–based description of the temperature dependence of a_T as defined by Eq. (7).

where C_1^0 and C_2^0 are empirical coefficients whose values are dependent on the choice of T_0. Alternatively, the following equivalent expression for a_T can be used [32]:

$$a_T = \exp\left(\frac{1}{\beta(T - T_\infty)} - \frac{1}{\beta(T_0 - T_\infty)}\right) \tag{7}$$

Equation (7) is derived from a free volume–based description of the temperature dependence of the linear viscoelastic properties. The parameters β is related to the thermal expansion coefficient of the fractional free volume, and T_∞, known as the Vogel temperature, is the temperature at which the free volume would approach zero in the absence of the glass transition. The term $\beta(T - T_\infty)$ is proportional to the fractional free volume. The parameters C_1^0 and C_2^0 are related to β and T_∞ in the following manner:

$$C_1^0 = 1/\beta(T_0 - T_\infty) \tag{8}$$

$$C_2^0 = T_0 - T_\infty \tag{9}$$

An advantage of using Eq. (7) is that the parameters β and T_∞, unlike C_1^0 and C_2^0, are both independent of the reference temperature, T_0.

The values of β and T_∞ can be determined from the best fit of Eq. (7) to the data using well-established procedures [33]. The ability of Eqs. (6) or (7) to describe the temperature dependence of a_T is shown in Fig. 5 for PC63. It is apparent that these expressions accurately represent the temperature dependence of the linear viscoelastic properties over the broad temperature range of the measurements. It has been found for these linear polycarbonate resins that β is independent of molecular weight with a value of $8.0 \times 10^{-4}\ K^{-1}$ while T_∞ decreases systemically with decreasing molecular weight. For polymers of sufficiently high molecular weight, the temperature dependence of a_T should be independent of molecular weight. However, as indicated in Table 1, the absolute molecular weights of typical commercial polycarbonate resins are relatively low. The free volume contributed by the ends of the polymer chains becomes significant at low molecular weights, and it is this increase in free volume with decreasing molecular weight that is responsible for the observed variation in the temperature dependence of a_T. It is expected that T_∞ will be a linear function of $1/\overline{M}_n$ [28] in the same manner that T_g is dependent on $1/\overline{M}_n$ as stated by the Fox-Flory equation [34,35]. For these polycarbonate resins, T_∞ and T_g can alternatively be expressed as a function of $1/\overline{M}_w$ since the polydispersity is independent of molecular weight. These relationships are shown in Fig. 6 for the resins listed in Table 1. Linear regression analyses of the two sets of data yield the following:

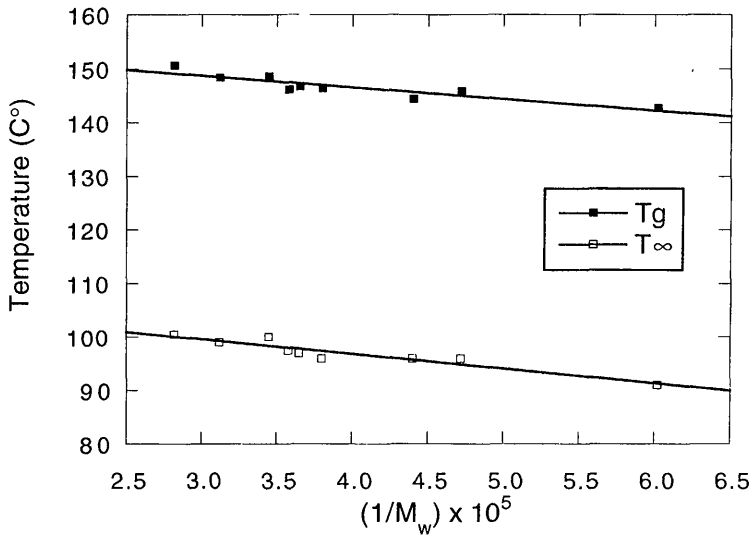

Figure 6 Molecular weight dependence of the glass transition temperature and the Vogel temperature for the nine polycarbonate resins.

$$T_g = 155 - 2.1 \times 10^5/\overline{M}_w \tag{10}$$

$$T_\infty = 108 - 2.8 \times 10^5/\overline{M}_w \tag{11}$$

It is noteworthy that T_∞ is approximately 50°C below the value of T_g over the full range of molecular weights, which is in the range determined for many other polymers [28].

Figures 7–9 show the G', G'', and $|\eta^*|$ master curves for several of the resins listed in Table 1. The low frequency limiting value of $|\eta^*|$ is equivalent to η_0, the zero shear rate viscosity obtained from steady-state shear viscosity measurements. For many polymers with flexible backbones, the frequency dependence of $|\eta^*|$ is often similar to that of the shear rate dependence of the steady shear viscosity, i.e.,

$$\eta(\dot{\gamma}) = |\eta^*(\omega)|_{\gamma=\omega} \tag{12}$$

This empirical rule is known as the Cox-Merz rule [36] and its applicability to linear polycarbonate resins is shown in Fig. 10 for PC51. The superposition of the two sets of data is very good except at low shear rates where errors in the capillary data are large due to the limitations of the transducer. Since the dynamic rheological properties can generally be measured more rapidly, with less error, and over a wider range of rates than steady shear rate viscosity measurements,

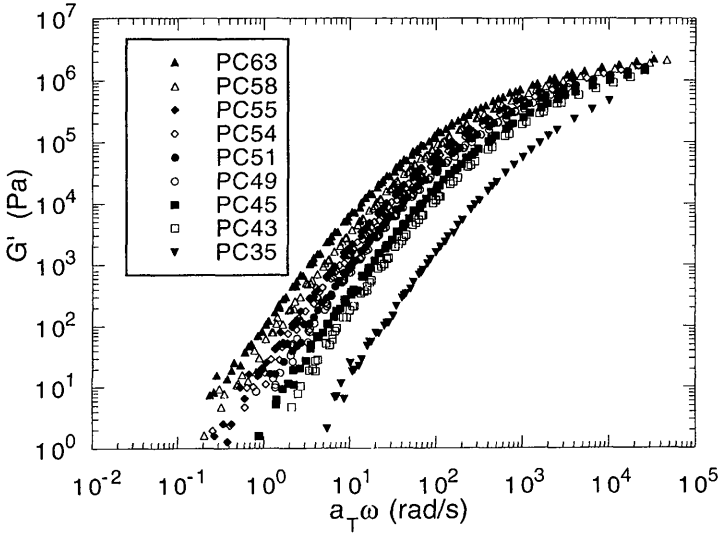

Figure 7 Storage modulus master curves at a reference temperature of 275°C.

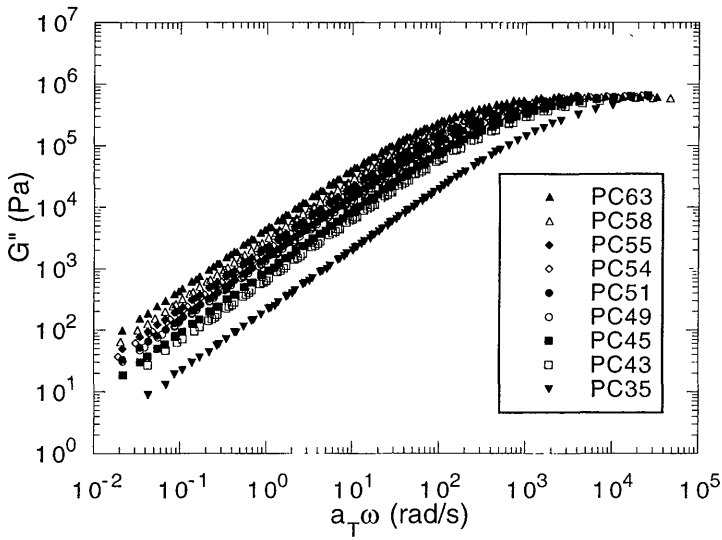

Figure 8 Loss modulus master curves at a reference temperature of 275°C.

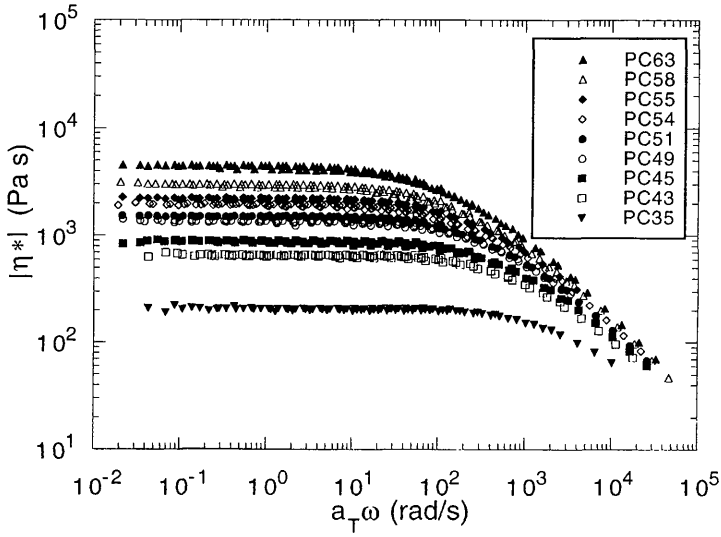

Figure 9 Complex viscosity master curves at a reference temperature of 275°C.

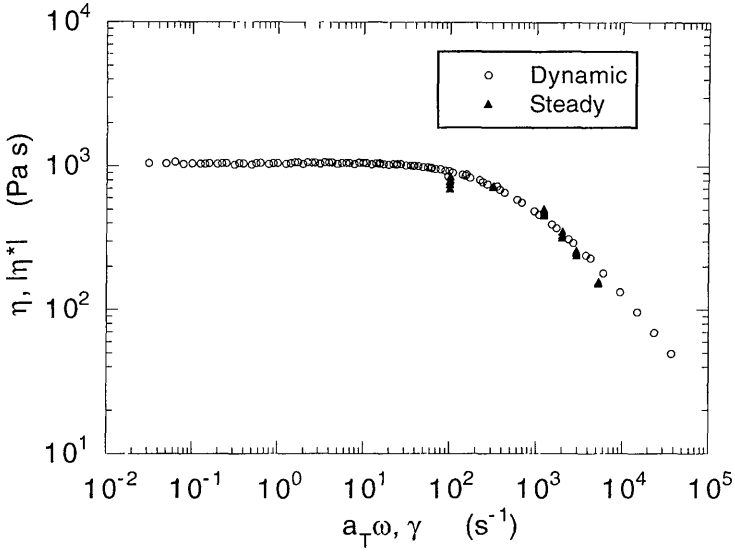

Figure 10 Comparison of steady-state viscosity and complex viscosity data for PC51 at 285°C.

the complex viscosity is often used as a substitute for the viscosity in steady flow. This practice has been used for the derivation of the viscosity model described below. Because of the equivalence of the two types of data for linear polycarbonate resins, this model for the complex viscosity should be valid for predicting steady shear viscosity as well.

III. A VISCOSITY MODEL FOR LINEAR POLYCARBONATE RESINS

Although it is possible to obtain rheological information for process modeling through interpolations and extrapolations from a large viscosity database, it is generally preferable to use a simple equation to define the viscosity. Many empirical equations have been proposed to describe the shear rate dependence of viscosity. A compilation of a number of these viscosity functions has been provided by Elbirli and Shaw [37]. By coupling these functions with an appropriate description of the viscosity temperature dependence, equations can be generated that completely describe the viscosity of a material as a function of temperature and shear rate.

Because the molecular weight distributions of linear polycarbonate resins do not vary significantly, the shapes of the viscosity–shear rate curves should be the same at all molecular weights. This similarity in shape is demonstrated in Fig. 11 where the normalized viscosity η/η_0 is plotted as a function of the normalized rate, $\lambda\omega$, for the samples listed in Table 1. The parameter λ, discussed in more detail below, is a characteristic relaxation time that is dependent on both molecular weight and temperature. By shifting the viscosity master curves appropriately along the viscosity and rate axes, excellent superposition of all data is obtained. Thus a viscosity model with a single set of parameters to describe the shape of the viscosity function can be used for all molecular weights. A modified Cross model [38] of the following form has been shown to accurately describe the shear rate dependence of the viscosity of polycarbonate resins [27,39]:

$$\eta = \eta_0[1 + (\lambda\dot{\gamma})^{0.8}]^{-1} \tag{13}$$

The limiting value of Eq. (13) at low shear rates is η_0, whereas at high shear rates the model reduces to the power law expression:

$$\eta = \eta_0(\lambda\dot{\gamma})^{n-1} \tag{14}$$

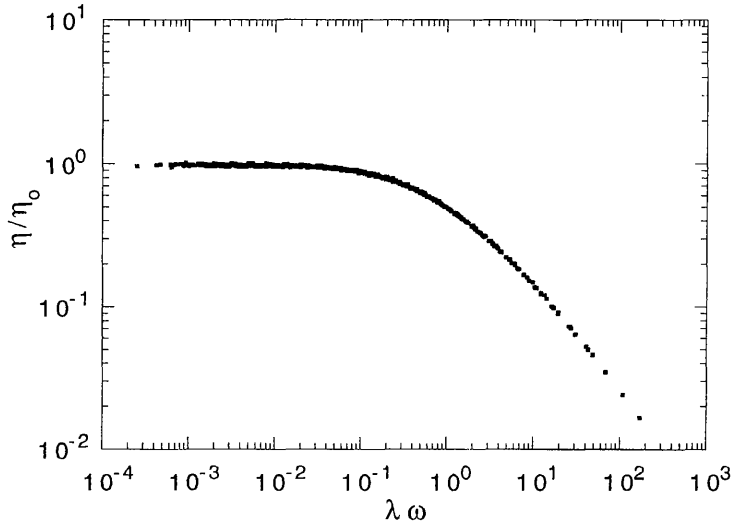

Figure 11 Reduced viscosity plotted as a function of reduced rate for all nine polycarbonate samples.

with the power law index n equal to 0.2. The ability of Eq. (13) to fit the viscosity master curve of PC63 is shown in Fig. 12. The agreement between the model and the data is excellent over the full six decades of rate.

The zero shear rate viscosity and the characteristic relaxation time are related in the following fashion [40]:

$$\eta_0 = k\rho T\lambda \tag{15}$$

with k being a constant. A plot of η_0 vs. $\rho T\lambda$ should be linear with a slope of k. Such a plot is shown in Fig. 13 using values of η_0 and λ determined from the best fits of Eq. (13) to the viscosity curves of the polycarbonate resins. Linear regression analysis yields a value of k equal to 1.5. Thus Eq. (13) can be reduced to the following simpler form:

$$\eta(\dot{\gamma}) = \frac{1.5\rho T\lambda}{[1 + (\lambda\dot{\gamma})^{0.8}]} \tag{16}$$

Only the parameter λ needs to be specified to fully describe the shear rate, temperature, and molecular weight dependence of η. The values of λ can be determined from the best fit of Eq. (16) to the viscosity master curves.

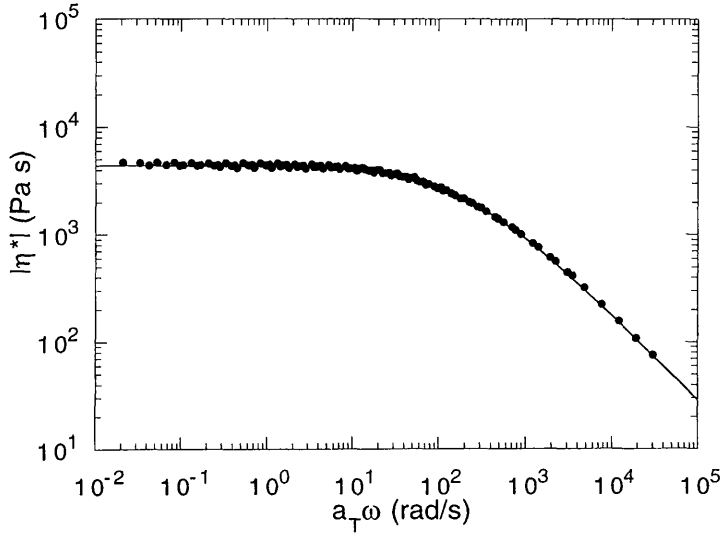

Figure 12 Comparison of the prediction of the viscosity model defined by Eq. (13) to the viscosity data of PC63 at a reference temperature of 275°C.

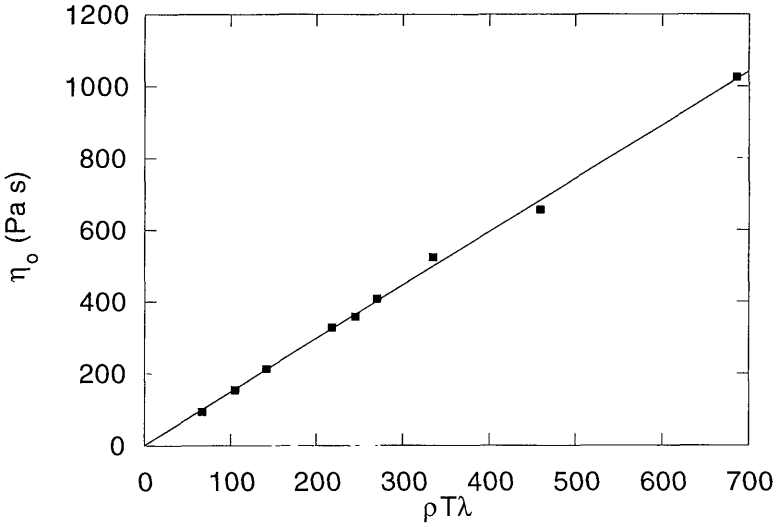

Figure 13 The zero shear rate viscosity as a function of ρTλ (ρ in kg/m^3, T in K, λ in s) for the nine polycarbonate samples. The solid line with a slope of 1.5 represents the best linear fit to the data.

From Eqs. (3) and (15), it is apparent that λ and a_T are related in the following manner:

$$a_T = \frac{\lambda}{\lambda_0} \tag{17}$$

where λ_0 is the characteristic relaxation time at the reference temperature. It follows from Eq. (7) that the molecular weight and temperature dependence of λ are described as follows:

$$\lambda(T, \overline{M}_W) = \lambda_b \exp\left[\frac{1}{\beta(T - T_\infty)}\right] \tag{18}$$

As indicated above, β has been found to have a value of $8.0 \times 10^{-4}\ K^{-1}$ for linear polycarbonate resins and T_∞ is specified by Eq. (11).

The accuracy with which Eq. (16) in combination with Eq. (18) describes the temperature and shear rate dependence of the viscosity of high and low molecular polycarbonate resins is shown in Figs. 14 and 15, respectively. For all molecular weights, the model fits the viscosity data with an error of less than 15% over the full temperature and shear rate range.

The parameter λ_b in Eq. (18) is dependent only on molecular weight. The

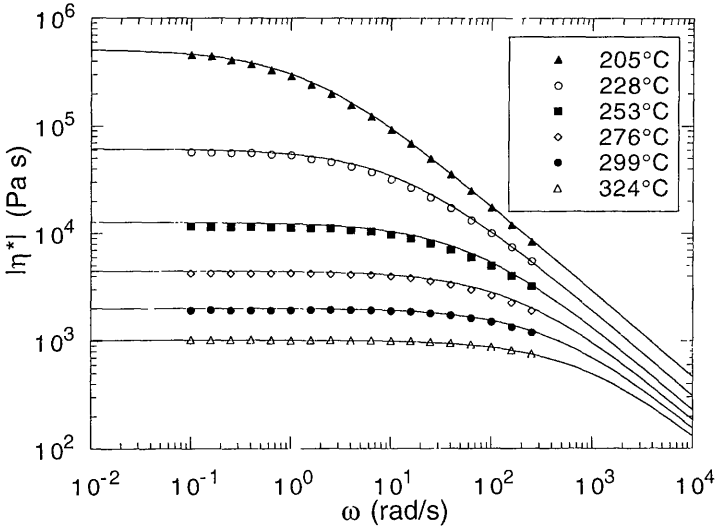

Figure 14 Comparison of the viscosity model predictions defined by Eq. (17) and (19) to the viscosity data of PC63. The solid lines represent the model.

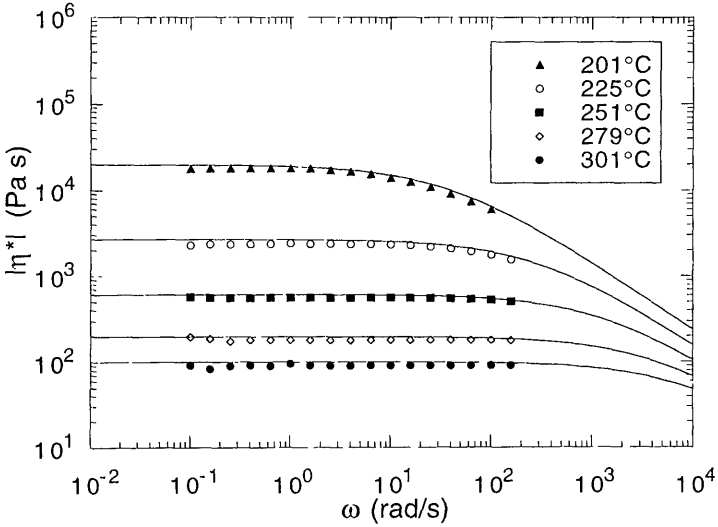

Figure 15 Comparison of the viscosity model predictions defined by Eqs. (17) and (19) to the viscosity data of PC35. The solid lines represent the model.

correlation between λ_b and $\overline{M}_w$ is shown in Fig. 16. Linear regression analysis yields the following relation:

$$\lambda_b = 1.4 \times 10^{-21}(\overline{M}_W)^{3.4} \tag{19}$$

The exponent 3.4 is in good agreement with the values found for many other polymers [32]. For the purposes of the viscosity predictions, λ_b can also be correlated to any measurements that are commonly used to provide an indication of polymer molecular weight. In Figs. 17–19, λ_b is shown as a function of the GPC values for $\overline{M}_W$, intrinsic viscosity, and melt flow index, respectively. In each case the relationship between λ_b and the corresponding measurement has the following form:

$$\lambda_b = bQ^a \tag{20}$$

where Q is the value of the measurement. The values for a and b determined from linear regression analyses for each type of measurement are provided in Table 2.

The viscosity model is now fully defined. If one of several commonly used measures of the relative molecular weight of a polycarbonate sample are known, Eq. (20) along with the values in Table 2 can be used to determine λ_b. The characteristic relaxation time is then described by Eq. (18), and the shear rate

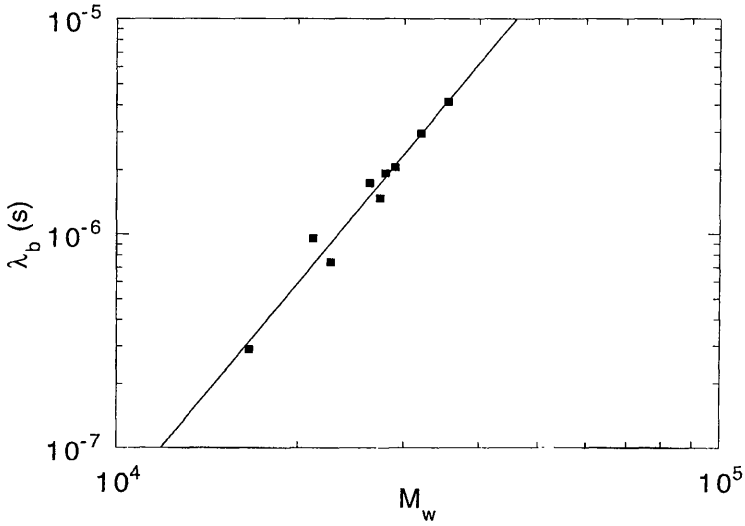

Figure 16 Molecular weight dependence of λ_b, with $\overline{M}_W$ determined from light scattering measurements. The solid line represents the best fit to the data and has a slope of 3.4.

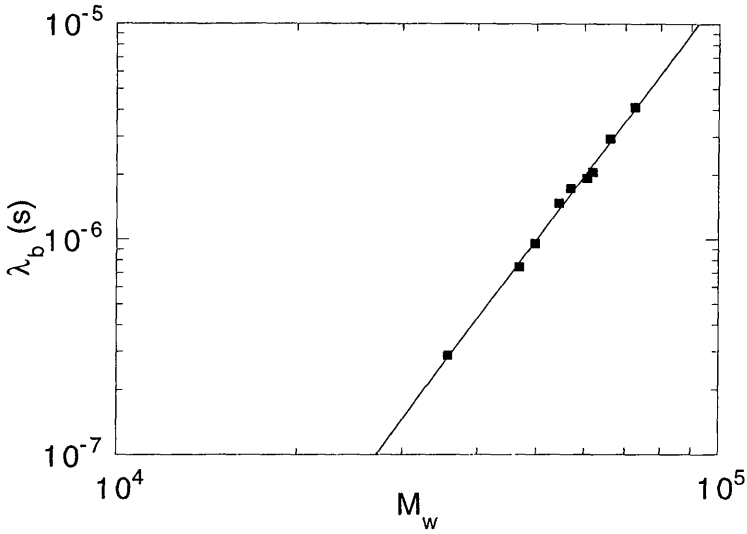

Figure 17 Dependence of λ_b on $\overline{M}_w$ as determined by GPC. The solid line represents the best fit to the data. The equation for the line is given in Table 2.

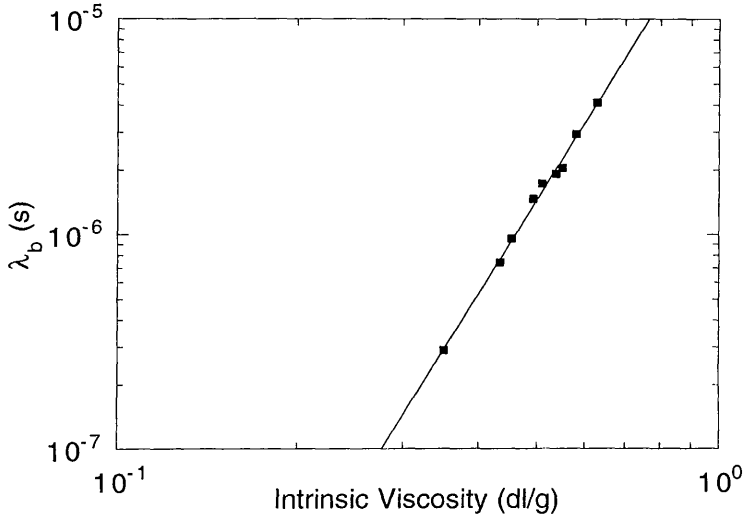

Figure 18 Dependence of λ_b on the resin intrinsic viscosity. The solid line represents the best fit to the data. The equation for the line is given in Table 2.

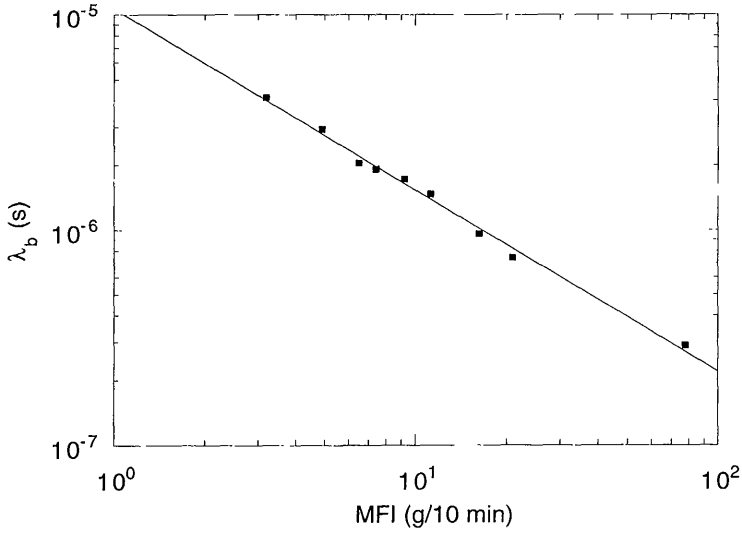

Figure 19 Dependence of λ_b on the melt flow index. The solid line represents the best fit to the data. The equation for the line is given in Table 2.

dependence of the viscosity by Eq. (16). While this model will not be valid for resins with a molecular weight distribution significantly different from that of the resins used in this study, it should be applicable to most commercially available linear polycarbonate resins.

IV. POLYDISPERSITY EFFECTS

The shear rate dependence of the viscosity of any polymer is influenced by its polydispersity. In fact, in some instances rheological techniques have been used

Table 2 Parameters for λ_b

Measurement	a	b	r^2
$\bar{M}_w$ by light scattering	3.40	1.41×10^{-21}	0.965
$\bar{M}_w$ by GPC	3.75	2.26×10^{-24}	0.995
Intrinsic viscosity	4.53	3.35×10^{-5}	0.995
Melt flow index	−0.84	1.07×10^{-5}	0.993

to determine molecular weight distribution, a particularly useful technique for insoluble polymers for which GPC is not practical [41–43]. It has been previously demonstrated that the breadth of the transition from Newtonian to power law dependence is a function of polydispersity for linear chain polymers such as polystyrene [41]. In contrast to these results, others have reported that when both long chain branching and polydispersity are present in polycarbonate, the influence of polydispersity is negligible [26,44–47]. Unfortunately, these two effects are difficult to separate in terms of their rheological ramifications, since both have the tendency to broaden the transition region. In the following section, we consider the effect of long chain branching on the rheology of polycarbonate melts.

In Fig. 20, the influence of polydispersity on the dynamic rheological properties can be seen for blends of high and low molecular weight polycarbonate. For the viscosity–frequency trace, it is the transition zone from Newtonian to power behavior that is most noticeably affected by differences in polydispersity. Broadening of the transition zone is seen when going from a polydispersity index of 2.6–3.0. A slower approach to Rouse-like terminal behavior ($G' \sim \omega^2$ and $G'' \sim \omega$) is exhibited for the broader molecular weight materials. While these effects are subtle, they are expected to be exaggerated as one goes to greater levels of polydispersity. Commercial polycarbonate materials typically vary in polydispersity between 2.5 and 2.8. Few observable differences in rheological behavior are exhibited in this range.

A molecular level explanation for the influence of polydispersity on rheology is an active area of research [48–52]. Most have relied on modifications to

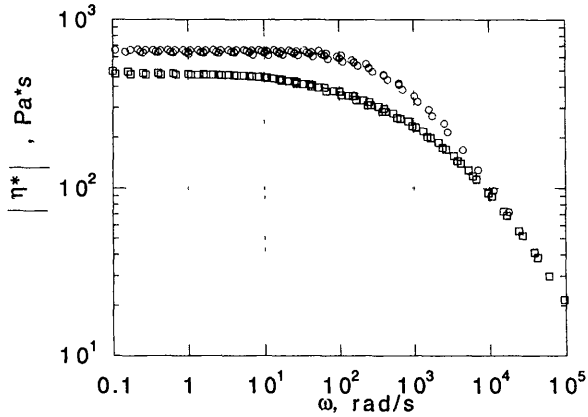

Figure 20 Influence of polydispersity on shape of viscosity curve. Polydispersity index of (○) 2.6 vs. 3.0 (□).

the well-known "reptation" theory wherein a polymer molecule is explained to relax via a slithering motion of the molecule through a tubelike region formed by the surrounding polymer molecules [53]. For the purposes of this work, it is sufficient to note that increasing the polydispersity of a blend increases the number of modes of molecular motion to the polymer melt and thereby a broadening of the low shear rate viscosity response.

V. BRANCHED POLYCARBONATE

Long chain branching in polycarbonate enhances melt elasticity at low shear rates and increases shear thinning at somewhat higher rates. These phenomena have been advantageous for blow molding applications where enhanced elasticity gives rise to good melt strength of a parison and shear thinning allows for ease of processing. Figure 21 shows the storage moduli of two branched series listed in Tables 3 and 4, corresponding to interfacially branched and linear/branched blends for Fig. 21a and b, respectively. These data, which are master curves obtained from time–temperature superposition shifted to 275°C, illustrate the enhancement in melt elasticity that arises from incorporating long chain branches into a polycarbonate molecule. Figures 22 and 23 show the influence of branching on loss modulus and complex viscosity for the same two series. Figure 23 illustrates the effect of branching on shear thinning characteristics. To examine the discrete effects arising from increasing levels of added branching agent vs. chain stopper, one needs to compare curves in Figs. 21–23a for samples Br-A, Br-B, and Br-C (for increasing levels of branching agent) and Br-B, Br-E, and Br-F or Br-C vs. Br-D (for increasing levels of chain stopper). Rheological consequences from these formulations arise through a variation of long chain architecture of the polycarbonate molecule (i.e., length and number of branches).

One method for characterizing the shear thinning behavior of branched materials is the utilization of a parameter referred to as R^* [15,55]. In this method, the temperature at which the melt has a viscosity of 2000 Pa · s at a shear rate of 100 s^{-1} is taken as the "optimum" processing temperature $T(R^*)$. R^* is then defined as the ratio of the viscosity at 1 s^{-1} to that at 100 s^{-1}. The R^* technique has shown significant utility in characterizing resins for blow molding applications by providing a single value as a descriptor of blow moldability. Materials with higher values for R^* tend to respond more favorably during blow molding. However, a more complete characterization of the rheology of branched materials is often desirable and may be accomplished by fitting viscosity–shear rate data to appropriate rheological models, as was illustrated in the previous section for the case of linear polymer melts.

The temperature and molecular weight dependence of branched polycarbo-

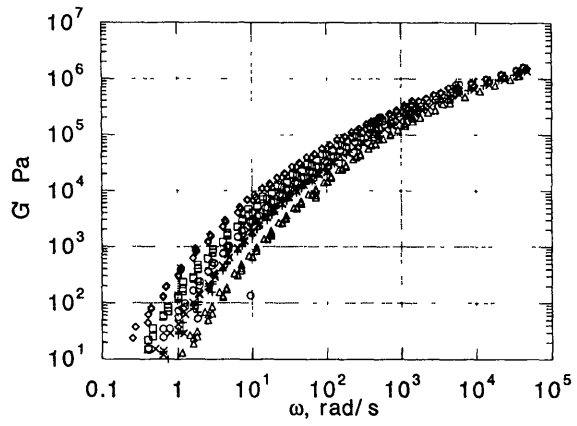

(a)

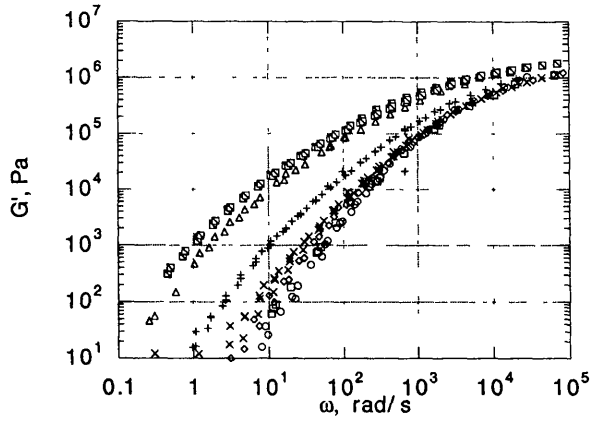

(b)

Figure 21 Storage modulus master curves shifted to 275°C for (a) interfacially branched polycarbonate series identified in Table 3. Symbols refer to samples Br-A (○), -B(❑), -C (◆), -D(×), -E (+), -F(Δ). For samples with same chain stopper levels and increasing level of branching agent, compare samples Br-A, -B, -C. For samples with same branching agent levels and increasing level of chainstopper, compare samples Br-B, -E, -F or Br-C, -D. (b) Blends of low molecular weight linear polymer and high molecular weight branched materials identified in Table 4. Symbols refer to samples LB-A (○), -B (❑), -C (◆), -D (×), -E (+), -F (Δ), -G (▣), corresponding to increasing levels of branched polycarbonate from LB-A to LB-G.

Table 3 Identification of Interfacially Prepared Branched Polycarbonates[a]

Sample ID	Chain-Stopper (mol%)	Branching agent (mol%)	Kash index
Br-A	5.0	0.5	2440
Br-B	5.0	0.6	3060
Br-C	5.0	0.7	4200
Br-D	5.5	0.7	2010
Br-E	6.0	0.6	1860
Br-F	6.5	0.6	1180

[a] Kash index correlated to zero-shear viscosity.

nate rheology has previously been investigated by others [56,57]. These authors found the zero-shear viscosity to be well described by:

$$\eta_0 = k\overline{M}_W^a \qquad k = 10^{(b/T+c)} \tag{21}$$

where $\overline{M}_W$ is the absolute weight averaged molecular weight determined via light scattering, T is in Kelvin, and a, b, and c are constants determined to be 5.14, 6830, and 31 for branched polycarbonate and 3.4, 5080, and 20.1 for linear polycarbonate. The 3.4 exponent for $\overline{M}_W$ for linear polycarbonate is consistent with vast empirical data on a number of different types of polymers. Of particular interest, however, is the greater than 3.4 power for branched polycarbonate. This steep molecular weight dependence has been noted in the past for branched polymer melts, particularly for materials where the number of monomer units between branch points, N, is large. For small N, randomly branched polymers have been

Table 4 Linear/Branched Blends vs. Apparent Weight and Number Averaged Molecular Weights (by GPC)

Sample ID	Composition (% branched component)	M_W	M_n
LB-A	0	35.2	12.2
LB-B	5	35.5	12.6
LB-C	10	38.4	13.5
LB-D	20	40.7	13.3
LB-E	40	46.3	14.5
LB-F	90	60.9	18.3
LB-G	100	63.9	19.2

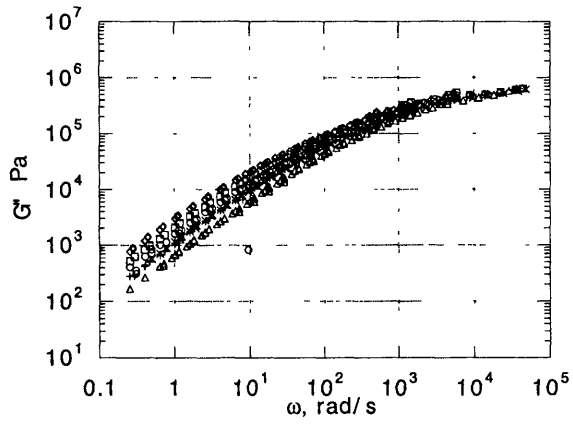

(a)

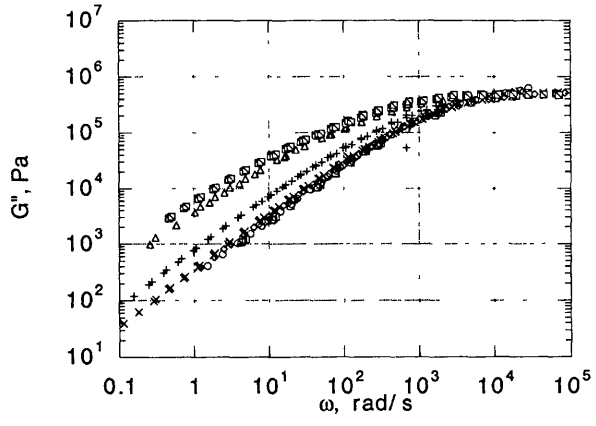

(b)

Figure 22 Loss modulus master curves shifted to 275°C for (a) interfacially branched polycarbonate series identified in Table 3 and (b) linear/branched blend series identified in Table 4. Symbols are the same as in Fig. 21.

seen to obey Rouse dynamics in the terminal (low-shear) regime. As N increases, the dependence of viscosity on molecular weight can be captured with a percolation model which provides a relationship between N and the exponent for $\overline{M}_w$. For the polycarbonate series previously studied, N was estimated to be between 250 and 450. This value is sufficiently large to accurately account for the 5.2 power on $\overline{M}_w$ [57].

The temperature dependence of rheological parameters (G', G'', $|\eta^*|$) for

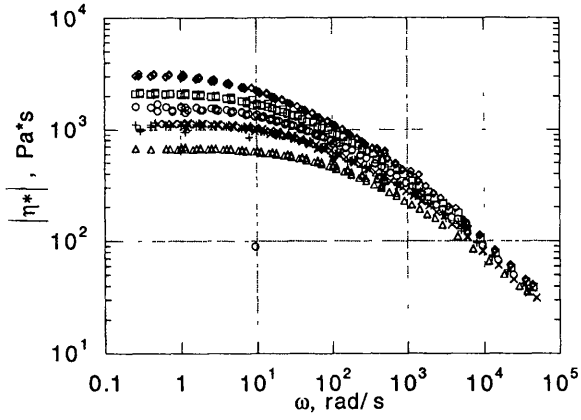

(a)

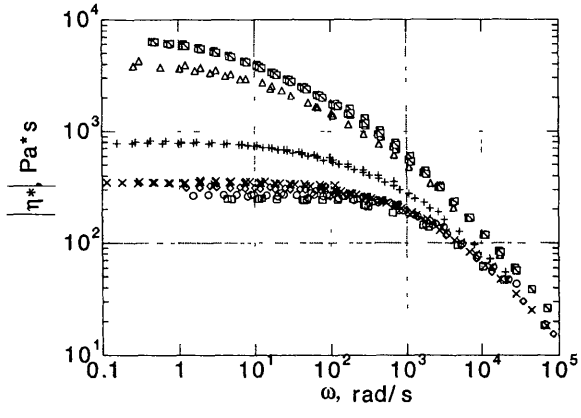

(b)

Figure 23 Complex viscosity master curves shifted to 275°C for (a) interfacially branched polycarbonate series identified in Table 3 and (b) linear/branched blend series identified in Table 4. Symbols are the same as in Fig. 21.

two branched polycarbonate resins (low and high molecular weight samples Br-B and LB-G, respectively) are illustrated in Figs. 24–26. Additional information on the influence of temperature on rheology may be obtained by plotting the horizontal shift factor a_T as a function of $1/T$. The shift factors utilized to obtain the master curves (in Figs. 21–23) are shown in Fig. 27 for the two aforementioned polycarbonate samples. A linear relationship for this plot indicates an Arrhenius temperature dependence, with an activation energy for flow given by

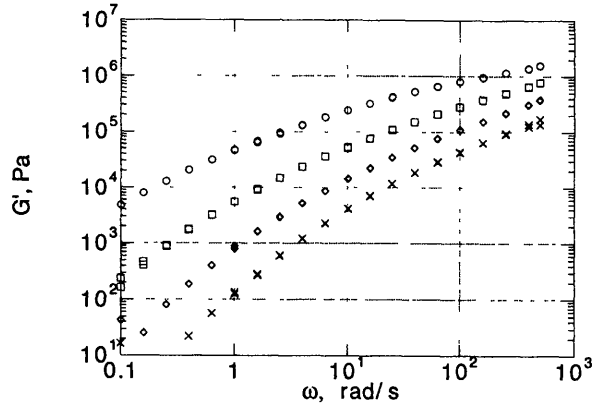

Figure 24 Storage modulus of (a) low molecular weight branched polycarbonate (sample Br-B in Table 3) as a function of temperature: (○) 200, (❑) 225, (◇) 250, (×) 275. (b) Commercial grade of branched polycarbonate (sample LB-G in Table 4) as a function of temperature (○) 180, (❑) 200, (◇) 225, (×) 250, (+) 300, (Δ) 320, (⊙) 340°C.

the slope. Over the temperature range studied, the rheology of branched polycarbonate is better explained by a WLF temperature dependence than an Arrhenius dependence, as evidenced by curvature in the a_T vs. $1/T$ plot. However, over a limited temperature range (200–275°C) a comparison of E_a is appropriate for samples Br-A through Br-F. These are listed in Table 5a. No significant influence of branching and chain stopper levels on the flow activation energy is observed. Similar values for E_a were also obtained for the linear/branched blends over the

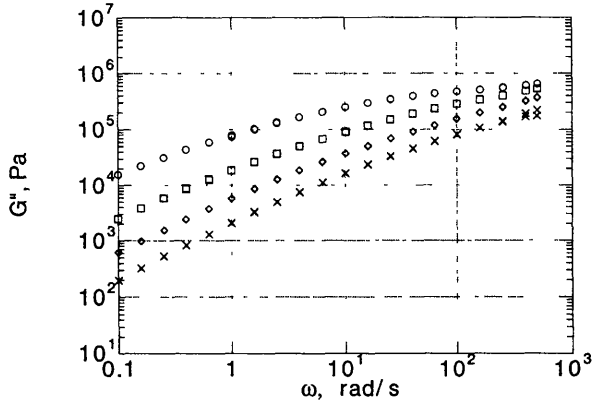

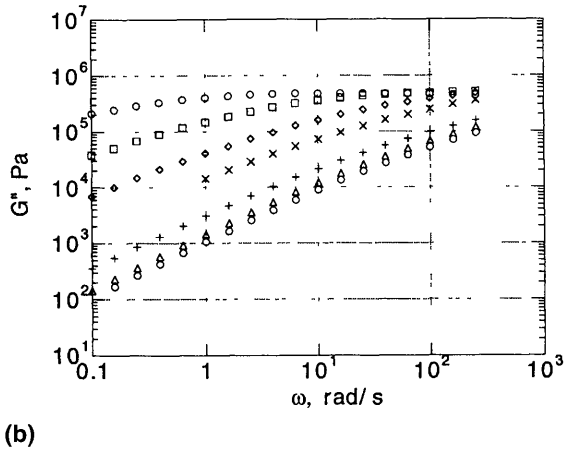

Figure 25 Loss modulus of (a) low molecular weight branched polycarbonate (sample Br-B in Table 3) as a function of temperature. (b) Commercial grade of branched polycarbonate (sample LB-G in Table 4). Symbols are the same as in Fig. 24.

full temperature range, albeit with substantially more scatter (Table 5b). Thus, the flow activation energy is appropriately 30–32 kcal/mol. This was somewhat higher than previously reported values for branched polycarbonate over a similar temperature range (26–27 kcal/mol) [57] and substantially higher than values reported for linear polycarbonate of 23–24 kcal/mol [57,58].

The shear rate dependence of viscosity can be described by a generalized Carreau model for branched polycarbonate:

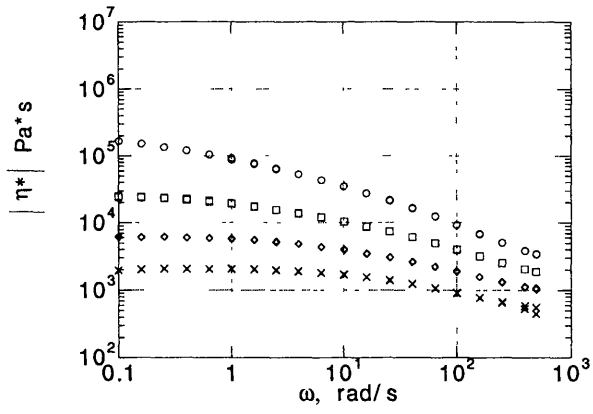

(a)

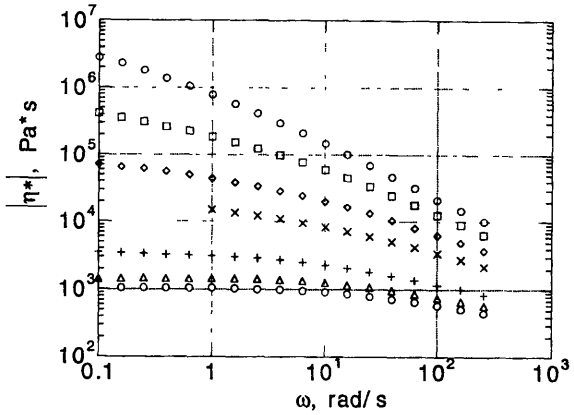

(b)

Figure 26 Complex viscosity of (a) low molecular weight branched polycarbonate (sample Br-B in Table 3) as a function of temperature. (b) Commercial grade of branched polycarbonate (sample G in Table 4) as a function of temperature. Symbols are the same as in Fig. 24.

$$\eta = \eta_0[1 + (\lambda\dot{\gamma})^{\alpha}]^{(n-1/\alpha)}$$

In order to account for the changes in shape of the viscosity curve for materials with different levels of branching, the parameters α and n were allowed to float when curve-fitting the viscosity–shear rate data to this model. In contrast to the previous results for linear polycarbonate melts, subsequent normalization along the viscosity and rate axes leads not to superposition of all samples

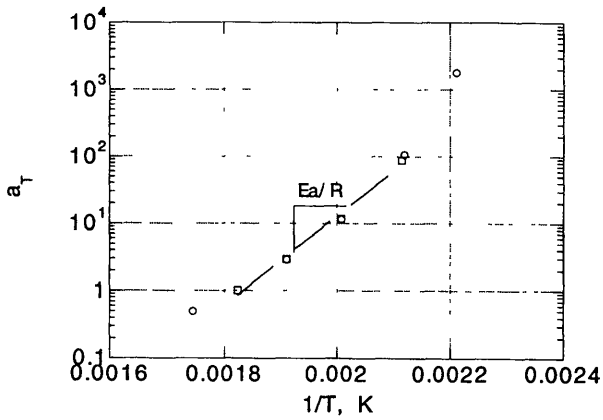

Figure 27 Horizontal shift factors (with a 275°C reference temperature) for sample Br-B in Table 3 (❑) and sample LB-G in Table 4 (○). The straight line through selected points is the best fit to an Arrhenius temperature dependence, over a limited temperature range, with the slope representing the flow activation energy.

Table 5 Constants to a WLF and Arrhenius Fit to the Viscosity Temperature Dependence of Branched Polycarbonates Listed in Tables 3 and 4

	Sample ID	WLF constant C1	WLF constant C2	Arrhenius activation energy, E_a (kcal/mol)
(a)	Br-A	3.28	201.1	32.4
	Br-B	3.33	204.3	32.5
	Br-C	2.84	185.7	32.5
	Br-D	3.71	216.5	32.8
	Br-E	3.47	212.3	31.4
	Br-F	2.91	193.6	30.4
(b)	LB-A	1.97	160.8	30.0
	LB-B	2.56	175.2	32.2
	LB-C	2.96	191.7	31.3
	LB-D	3.01	189.5	32.7
	LB-E	4.07	239.5	28.2
	LB-F	3.53	207	28.0
	LB-G	2.47	167.9	34.0

but to the appearance of enhanced shear thinning with increasing levels of branching. This is shown in Fig. 28 for interfacially prepared polycarbonate. The shape of the viscosity curve is altered by incorporation of long chain branches via higher levels of branching agent. Moreover, because of the steep molecular weight dependence of the low shear rate viscosity for branched polycarbonate, decreasing levels of chain stopper also have a dramatic effect on the rheology

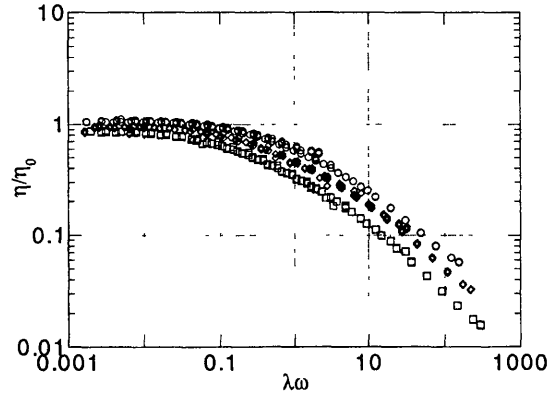

(a)

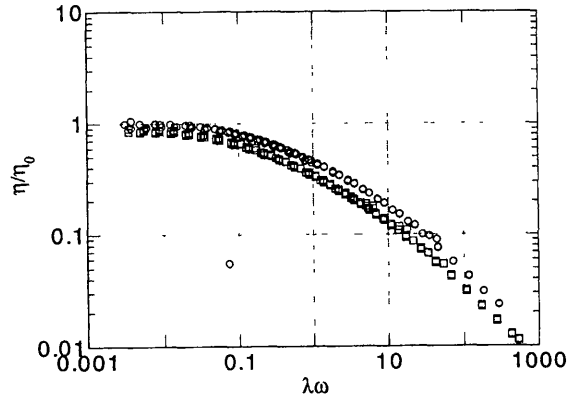

(b)

Figure 28 Reduced viscosity vs. reduced shear rate trace at 275°C for several interfacially branched polycarbonates (Table 3) for (a) 0.6 mol% branching agent and (○) 6.5, (◇) 6.0, and (❑) 5.0 mol% chain stopper. (b) 5 mol% chain stopper and (○) 0.5 and (❑) 0.7 mol% branching agent.

and alter the viscosity–rate trace in much the same way as increasing branching agent.

Values for the model parameters of branched polycarbonates are shown in Table 6. A monotonic increase in zero-shear viscosity, η_0, and a decrease in the transition breadth parameter, α, is observed as one goes to a more highly entangled branched melt. A decrease in α reflects the broadening of the transition zone when going to increasingly branched materials. The value for n, which dictates the slope of the power law region, did not deviate far from 0.2 for the linear/branched blends. This is consistent with the value obtained for linear polycarbonates, leaving α and η_0 as the two parameters of consequence for these systems. The value of n determined for the interfacially prepared polycarbonate was somewhat higher (0.3–0.4) and reflects the fact that the viscosity data obtained for these samples over a limited temperature range did not fully extend into the power law region.

Additional models that capture the viscosity–shear rate characteristics of branched polycarbonate have been described elsewhere [44–47]. With a slightly different functional dependence and one additional adjustable parameter, these authors essentially captured the same characteristics of enhanced zero-shear viscosity and broadening of the transition zone with increasing levels branching. They then correlated the exponential coefficients in their model to an independent

Table 6 Constants Determined by Fitting Viscosity Shear Rate Data to Generalized Carreau Model [Eq. (1)] (a) for Interfacially Prepared Polycarbonates at Reference Temperature 275°C and (b) for Linear Branched Blends at Reference Temperature 250°C

	Sample ID	η_0, Pa*s	(λ_0, s) $\times 10^3$	n	α
(a)	Br-A	1661 ± 44	7.7 ± 2.2	0.38 ± .04	0.57 ± .05
	Br-B	2459 ± 51	6.7 ± 1.5	0.30 ± .03	0.45 ± .02
	Br-C	3598 ± 80	12.6 ± 2.2	0.31 ± .02	0.44 ± .02
	Br-D	1194 ± 28	5.0 ± 1.6	0.36 ± .04	0.51 ± .04
	Br-E	1159 ± 22	5.5 ± 1.4	0.38 ± .04	0.57 ± .05
	Br-F	632 ± 10	4.3 ± 1.1	0.44 ± .04	0.71 + .06
(b)	LB-A	679 ± 5	1.01 ± .07	0.24 ± .01	0.84 ± .03
	LB-B	725 ± 4	0.94 ± .05	0.21 ± .01	0.75 ± .02
	LB-C	977 ± 8	1.24 ± .12	0.20 ± .02	0.69 ± .02
	LB-D	1183 ± 13	0.89 ± .10	0.12 ± .02	0.55 ± .02
	LB-E	2252 ± 21	2.24 ± .58	0.18 ± .05	0.50 ± .02
	LB-F	14391 ± 203	30.2 ± 4.7	0.25 ± .02	0.45 ± .01
	LB-G	22608 ± 421	15.8 ± 1.8	0.10 ± .01	0.37 ± .01

determination of degree of branching. This latter estimation was accomplished by comparison of the hydrodynamic volume in solution of branched vs. linear polymer molecules.

We found in the course of our studies with linear/branched blends that the branching parameter, as determined from hydrodynamic volume techniques, was indistinguishable between our samples. The low levels of branching in commercial polycarbonate is one explanation for this observation. Thus, in our lab, melt rheology appeared to be a far more sensitive indicator of level of long chain branching. We have used a process of fitting viscosity shear rate curves to a generalized Carreau model and a subsequent determination of α and η_0 as an indication of incorporation of branches into the main chain polymer. With appropriate calibration, this procedure alone serves the purpose of evaluating the effectiveness of a variety of synthetic techniques, branching agents, and process conditions on ability to incorporate long chain branches into the linear polymer molecule.

The effect of blending linear and branched polycarbonates on the zero-shear viscosity was explained by a logarithmic rule of mixing for the series described in Table 4. Following the procedures of Watanabe et al. [59], separable contributions to the zero-shear viscosity from the linear and branched molecules in the blend were examined independently. In Fig. 29, the contribution to the viscosity from branched polycarbonate in the blend is plotted as a function of composition. In the dilute regime, the viscosity was first order with concentration of branched component and indicated a region where the branched–linear entanglements

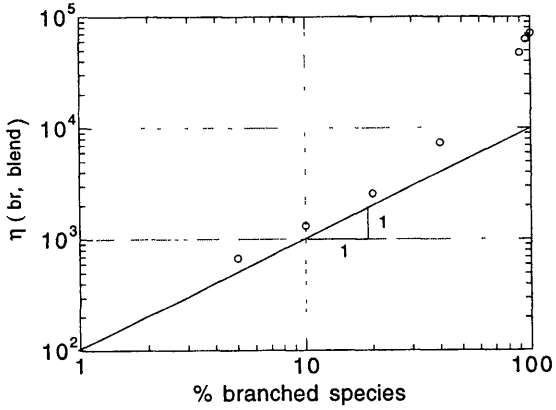

Figure 29 The zero-shear viscosity contribution from the branched species in linear/branched blends (Table 4) at 225°C.

dominated the rheological response. Deviation from a slope of 1 as upward curvature of this plot indicated an increasing importance of branched–branched interactions. Such a change in the nature of the interaction between entanglements appeared to occur at approximately 20% by weight of the branched component in the blend.

The molecular dynamics of branched polymers have been extensively investigated [60–71]. It is clear that the enhanced elasticity that accompanies long chain branching is a manifestation of decreased molecular mobility of highly entangled polymer molecules where the local environment is dominated by the branch points. It is generally accepted that the diffusive long-time motion (low shear rate) of entangled melts may be treated in an averaged way by defining a confining tube, whose radius is governed by the topological constraints on the molecule [72]. Taking into account local release of these topological constraints in polydisperse and branched melts complicates the mathematical treatment of dynamics of molecular motion. However, a simplified treatment for branched materials may be sought by assuming that the relaxation of stress in a deformed melt is governed by dynamics of sequential retraction of the branch arms along their contours in a "dilated" tube [68]. The results of such a treatment of long chain branching is to predict a decrease in the longest relaxation time (increase in zero-shear viscosity) with level of branching. The concept of tube dilatation also has the effect of adding modes of motion to the calculation of stress relaxation and allows for the observation that a trace of stress vs. time (or viscosity vs. shear rate) is broadened with branching or polydispersity. That is, the transition from zero-shear to power law behavior is expected to be sharpest for monodisperse linear melts and broadest for polymer melts with extensive long chain branching or broad molecular weight distribution. Experimental observations confirm these qualitative predictions, as illustrated in Fig. 28a and b.

McLeish et al. have considered a theoretical treatment of blends of well-entangled ($\gg M_e$) linear and branched molecules [63], predicting scaling laws for relaxation modulus based on considerations from reptation and tube dilatation models. They have addressed four distinct cases of relaxation dynamics, two of which apply when the reptation time of the linear molecule is less than the terminal relaxation time of the branch arm, the most realistic cases for the system of linear/branched described in Table 4. For both theoretical cases explored (dilute and concentrated solutions of branched in linear) a trace of modulus vs. frequency is expected to broaden as the quantity of branched component is increased. In the case of dilute branched in linear, a modified Rouse relaxation $G' \sim \omega^{3/2}$ is predicted in the terminal regime, as compared to $G' \sim \omega^2$ for purely linear chains. These qualities may be observed in Fig. 21b for the linear/branched blends investigated here.

VI. PRESSURE EFFECTS

Polymers in industrial processes such as injection mold filling often encounter very high pressures during injection and packing. Thus, an additional rheological consideration when modeling industrial processes is the influence of pressure on viscosity. Several authors have documented rheological ramifications for polycarbonate of increasing pressure even further by making use of a hydrostatic pressure rheometer capable of up to 25,000 psi [73,74]. In general, these authors found that an order of magnitude increase in hydrostatic pressure resulted in a corresponding order of magnitude increase in the apparent viscosity of the polymer. For more details the reader is referred to these works.

VII. OPTICAL PROPERTIES OF POLYCARBONATE MELT

Polycarbonate is widely used in optical data storage media such as compact disks. Residual birefringence in such media can interfere with the signal-to-noise ratio and other measures of performance. Birefringence occurs when light passes through anisotropic media and manifests itself as a nonzero transmittance when intercepting cross-polarized light. For more details on this property, see Chapter 7. Birefringence in molded parts is due in large part to the thermal quenching, which occurs during injection molding at fast cycle times. There is an effect from the flow-induced (orientational) birefringence that is unable to relax on the time scale of the cooling as well as a bond distortion (stress-induced birefringence) effect from tensile and compressive stresses in the glassy region of the part during the nonisothermal mold cooling process [25,75].

The quantitative application of flow birefringence in polymer melts is based on the anisotropic refractive index of a stretched polymer chain in flow. It has been frequently shown that for polymers that have been stretched to some distance that is less than their fully extended conformation, the principal axes of the refractive index tensor and stress tensor coincide and the refractive index difference is proportional to the stress difference. The relationship between stress and birefringence is termed the stress-optical rule and may be expressed simply as:

$$\tau_{12} = \frac{1}{2C}\Delta n \sin 2\chi \tag{22a}$$

$$(\tau_{11} - \tau_{22}) = \frac{1}{C}\Delta n \cos 2\chi \tag{22b}$$

where τ_{xy} is the shear stress, $(\tau_{xx} - \tau_{yy})$ is the first normal stress difference, C is the stress-optical coefficient (a material property), χ represents the average orientation angle of the anisotropy in the sample (extinction angle), and Δn is the flow birefringence (magnitude of the anisotropy), which may be determined experimentally with the measurable property of retardation, δ, given by:

$$\delta = \frac{2\pi d}{\lambda} \Delta n \tag{22c}$$

with d representing the thickness of the sample and λ the wavelength of light. The magnitude of birefringence of any flowing polymer melt may be determined by Eq. (22c). Depending on the measurement technique, χ is determined either simultaneously, along with retardation, or in a separate experiment. With δ and χ measured experimentally, the stresses in the melt can then be determined by Eqs. (22a) to (22c). The stress-optical coefficient for polycarbonate melt has been reported as being independent of molecular weight and a weak function of temperature. However, there is some variability in values reported in the literature ranging from 2.8–4.5 $\times$ 10^{-9} Pa^{-1} at 220°C [9,10,25,80].

In this chapter, we discuss two different techniques for studying flow birefringence behavior of polycarbonate with the primary goal of determining the local stress and orientation characteristics in complex flows. For quantitative analysis of birefringence the most advanced techniques are based on phase-modulated polarization and were pioneered by Frattini and Fuller [81]. In our studies we use an instrument modification to this approach after Kannan and Kornfield [82]. Specifically, we modify incoming circularly polarized light with an electro-optical modulator and analyze the light transmitted through the flowing melt with orthogonally crossed circularly polarized light. The fast response of the electro-optical modulator allows one to continuously phase-modulate the incoming polarization with a high-frequency linear ramp and is limited only by the rate at which one can generate and analyze such a signal. In practice we modulate at 200 kHz, a rate significantly faster than some of the first methods of modulation, but slow enough so as to eliminate artefacts to the polarization analysis which occur if the fall time of the linear ramp is a sufficiently large percentage of the input signal. Figure 32 is a schematic of the optical train used in this laboratory for phase-modulated flow induced birefringence measurement.

Analysis of the optical train is described in detail elsewhere [82]. The final result is shown in Eq. (23a):

$$I = 1/4*[1 + \cos(2\chi)\sin(\delta)\sin(\omega t) - \sin(2\chi)\sin(\delta)\cos(\omega t)] \tag{23a}$$

For convenience the components in front of the sin (ωt) and cos (ωt) are renamed as

$$R_1 = \cos(2\chi)\sin(\delta) \tag{23b}$$

$$R_2 = \sin(2\chi)\sin(\delta) \tag{23c}$$

Normalizing for I_{dc} and taking the measurable quantities in front of sin ωt and cos ωt components of the lock-in amp gives the following values for the retardation and orientation angle:

$$\delta = \text{sign}(R_1) * \sin^{-1}[\text{sqrt}(R_1^2 + R_2^2)] \tag{23d}$$

$$\chi = \tan^{-1}(R_2/R_1) \tag{23e}$$

Thus the birefringence and orientation angle may be measured simultaneously and used in Eqs. (22a) to (22c) to determine components of the stress tensor. In addition to the advantage of obtaining the two measurables simultaneously, this technique has the highest levels of spatial and temporal resolution (80 μm, 1 pt/μs) of any known flow birefringence technique.

To obtain a full-field image of orientation in a polymer melt at a point in time, one may utilize classical isochromatic/isoclinic techniques of flow induced birefringence [83]. If one wishes to determine local stress levels using this method it is necessary to perform two separate experiments with different optical configurations so as to obtain both χ and δ. The birefringence magnitude (retardation) is obtained using an isochromatic configuration. That is, monochromatic light (in our case, 546 nm with a mercury arc light source and green filters) is circularly polarized with a linear polarizer and quarter waveplate in series, sent through the sample, and then analyzed with orthogonally crossed circularly polarized light. Fringes (dark-field lines) are observed in this configuration and the intensity at any position in the flowing melt is given by:

$$I = \frac{I_0}{4} \sin^2 \frac{\delta}{2} \tag{24a}$$

where I_0 is the intensity of incident light and δ is the retardation. In practice, we determine the retardation at a position by counting the fringe "order," k, from the zero-order fringe, which is known from symmetry considerations to be the centerline in the steady-shear regions. The isochromatic fringes mark the positions where the retardation, δ, is $\pm k2\pi$ ($k = 0, 1, 2, \ldots$).

In order to evaluate the extinction angle, χ, the optical configuration is rearranged to observe isoclinic lines, superimposed on the isochromatic lines. In this instance quarter waveplates are removed so that linearly polarized light is used. The intensity of light is then described by:

$$I = \frac{I_0}{4} \sin^2(\chi - \theta) \sin^2 \frac{\delta}{2} \tag{24b}$$

where $(\chi - \theta)$ is the relative orientation of the optical axis of the sample to the orientation of the two polarizers. When this quantity is zero, light is extinguished and a black-line fringe is observed. Thus at any given position the extinction angle is determined by the rotation angle, θ, which causes a dark-field region.

When using a monochromatic light source in such an optical configuration, the isoclinic lines are distinguished from the isochromatic lines by rotating polarizers simultaneously. The isoclinic lines move and the isochromatic lines remain stationary.

VIII. APPARATUS—OPTICAL RHEOMETER

A schematic representation of the optical rheometer used to measure local rheological and orientational characteristics is shown in Fig. 30. Polymer is introduced as dried pellets into the 0.75-in. 3-zone single-screw extruder and is sent to a gear pump to regulate the flow (1.8 cm^3/rev capacity). A 3-way valve is installed to allow for bypass of the polymer through the main fluid delivery system. A static mixer at the entrance to the flow cell ensures a homogeneous melt stream in terms of composition and melt temperature. An adjustable ball valve at the exit of the flow cell allows for back-pressure adjustment. Pressure transducers are located at the exit to the extruder, the gear pump, and at the inlet and outlet regions of the flow cell. Temperature is controlled separately for the extruder, gear pump, valves, mixer, and flow cell. Thermocouples are placed at the inlet and outlet of the stainless steel flow cell.

A detailed sketch of the flow cell is shown in Fig. 31. Dimensions were chosen so as to accomplish a 4:1 contraction in pseudo-two-dimensional flow configuration. This is a common geometry for evaluation of constitutive equations and has been reviewed elsewhere [84,85]. The window material is a Pockels glass with Schott formulation SF57, with a stress-optical coefficient two orders of magnitude lower than most glasses at 2×10^{-14} Pa^{-1}, and allows for maximum signal attributed to the flowing polymer. Windows were optically polished and coated with antireflective coatings. Two-zone heating of the flow cell is accom-

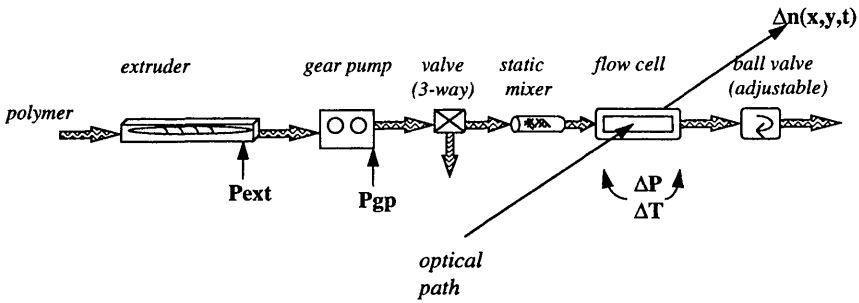

Figure 30 Schematic of optical rheometer. For description, see text.

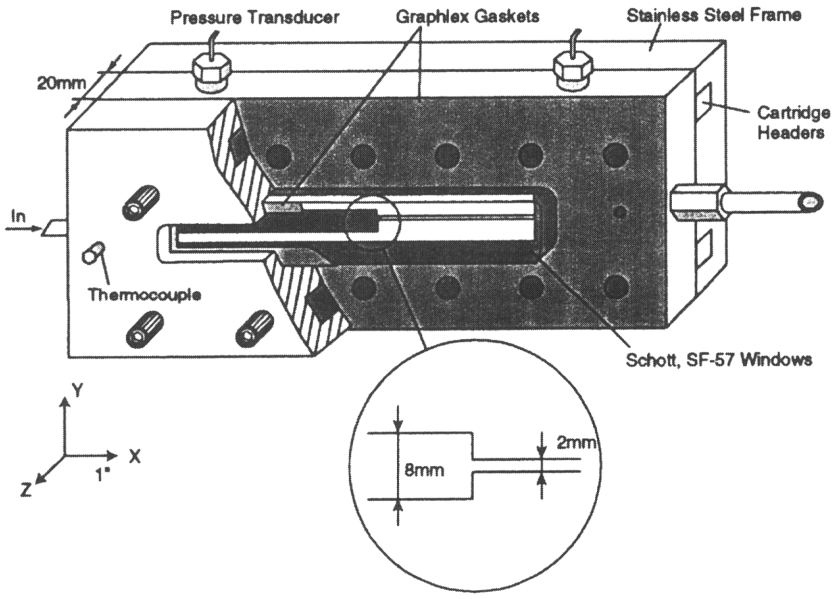

Figure 31 Schematic of flow cell. For description, see text.

plished with cartridge heater inserts. Insulation helps to minimize heat loss and temperature gradients.

Phase-modulated birefringence measurements are accomplished with the scheme discussed previously (see Fig. 32). Additionally, the optical rheometer is equipped with a video camera and digital image analysis system for viewing and analyzing full-field images of a flowing polymer melt. These are hooked up to a PC computer with a frame grabber on which is installed Optima's image analysis software. This image analysis system is used to view full-field birefringence images as well as flow visualization and particle tracking studies. The video analysis also lends itself to full-field illustrations of transients for buildup and relaxation of stress in shear startup and cessation studies. It provides a complementary method for the quantitative analysis of transients via pointwise measurement of birefringence using the phase-modulated technique. While beyond the scope of this chapter, such experiments have been conducted in this laboratory on various polycarbonates and will be documented elsewhere.

IX. RESULTS OF OPTICAL MEASUREMENTS

Figure 33a–c shows full-field birefringence images of two grades of polycarbonate flowing through a pseudo-two-dimensional planar contraction at a moderate

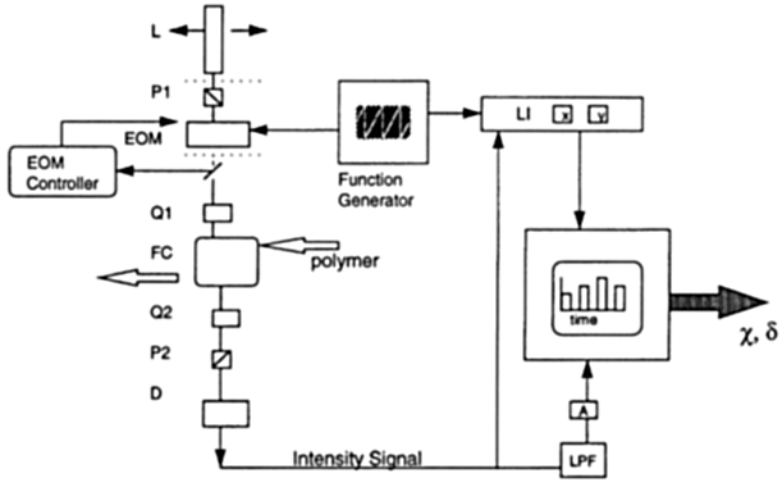

Figure 32 Schematic of polarization modulation scheme: 10mW He-Ne (L) at 632.8 nm sent through a polarized modulator (P1-EOM) and quarter wave plate (Q1). A non-polarizing beam-splitter cube is placed in-between the modulator and the quarter wave plate, sending a portion of the signal to a feature of the modulator which continually correct for drift. The light passes through a focusing lens before passing through the flow cell (FC) melt. The light transmitted through the melt is then sent through a second quarter waveplate (Q2) and polarizer (P2) oriented orthogonally to Q1 and detected with a photo diode (D). The signal is then sent to a lock-in amplifier to capture the in and out of phase components of the transmitted light.

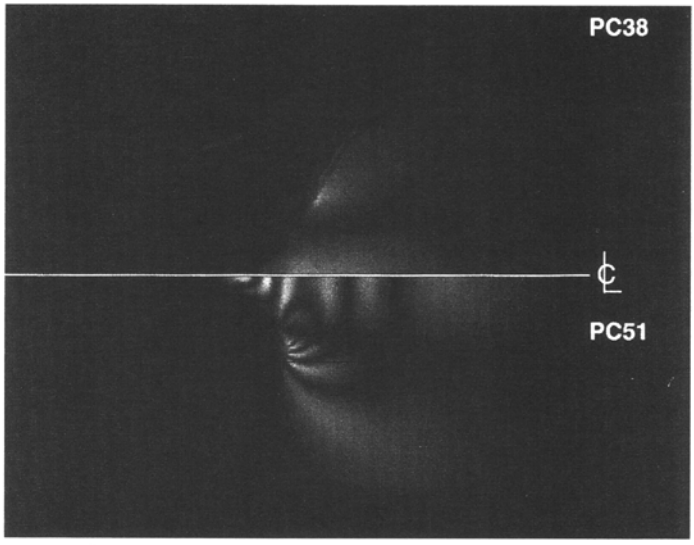

A

Figure 33 (A–C) Full-field isochromatic and isoclinic fringe patterns for a flowing polycarbonate melt. For full description, see text. Flow direction is right to left.

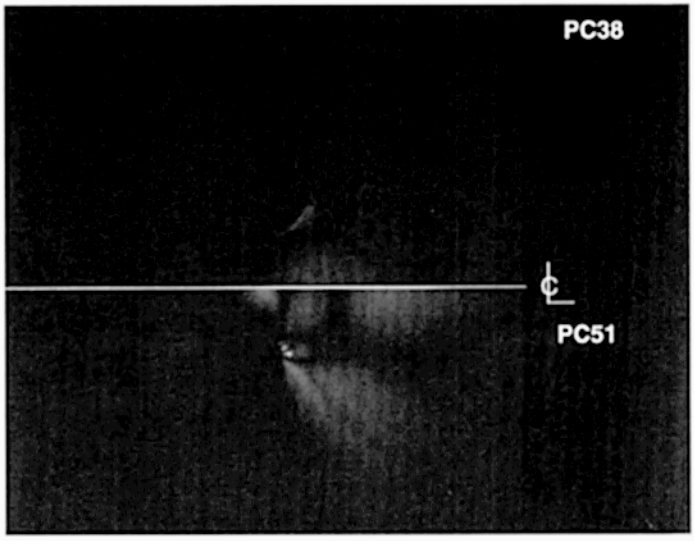

B

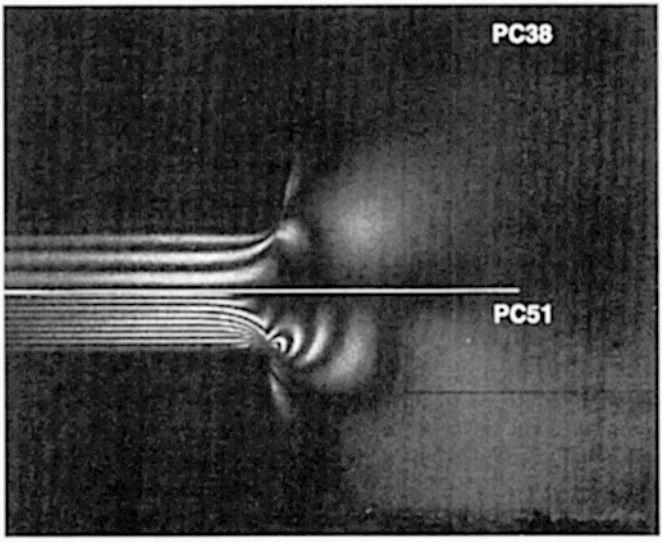

C

Figure 33 Continued

flow rate, 27 ml/min (refer to Table 1 for material designation). The isochromatic lines (fringes) in Fig. 33a ultimately give the magnitude of birefringence as a function of spatial position, whereas the isoclinic lines in Fig. 33b and c reveals the orientation angle. One of the most dramatic effects observed in these photographs is a high concentration of fringes near the entry corner, spreading apart as they emanate outward. Since local birefringence is measured by the number of "orders," the closely spaced fringes indicate a high retardation region and are a direct result of stress concentration near the entry corner. This effect is exaggerated in the higher molecular weight polycarbonate. Full-field pictorial representation of stresses may be achieved by combining magnitude and orientation information acquired by isochromatic/isoclinic or phase-modulated birefringence measurements. When coupled with local velocity measurements, they represent a powerful means of obtaining direct experimental verification of the validity of constitutive models of polymer flow. This is an active area of research for lower temperature melts and solutions flowing in complex geometries [54,76,78,79,84–91].

Spatially resolved stress fields in a flowing melt of PC38 were acquired at a flow rate of 9 ml/min using phase-modulated flow birefringence. A pictorial representation of stress magnitude and orientation was obtained for the full field (not shown). The results of several highly resolved line scans are shown in Figs. 34–36. These plots reveal quantitative information on the combined influences of extension, compression, and shear in complex geometry. Figure 34 shows lateral line scans upstream of the contraction, Fig. 35 shows axial line scans, and Fig. 36 shows lateral line scans downstream the contraction.

Fully developed flow regions are represented in Figs. 33, 34, and 36. Lateral

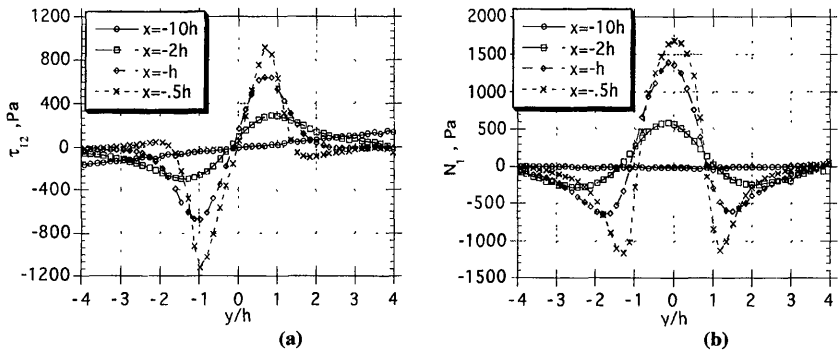

Figure 34 Lateral line scans upstream of contraction, encompassing fully developed flow regions, $x = -10$ h as well as centerline $y/h = 0$ and corner regions, for PC38 at 9 ml/min. (a) Shear stress. (b) First normal stress difference.

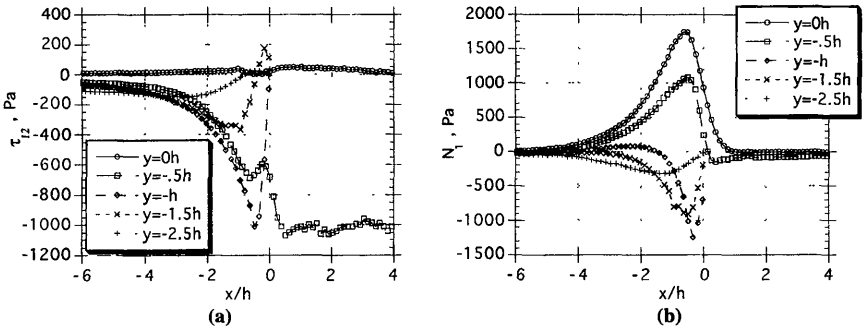

Figure 35 Axial line scans encompassing both shear and extensional flow regions with $x/h = 0$ the point of contraction and $y = 0$ h the centerline. Material is PC38 and flow rate is 9 ml/min. (a) Shear stress. (b) First normal stress difference.

line scans (Figs. 34 and 36) show nearly perfect symmetry for N_1 and negative symmetry for τ_{12}, with respect to the centerline. This is as expected from geometrical considerations and is verified in the full-field figures given in Fig. 33a, which shows that in the downstream (narrow slit) region, the zeroth order fringe is observed in the center of flow in the isochromatic configuration with multiple orders emanating outward symmetrically from this fringe with the maximum birefringence, consistent with maximum shear rate and shear stress, at the wall. (One can confirm the order of a particular fringe using polychromatic light in which case only the zeroth order fringe appears black.)

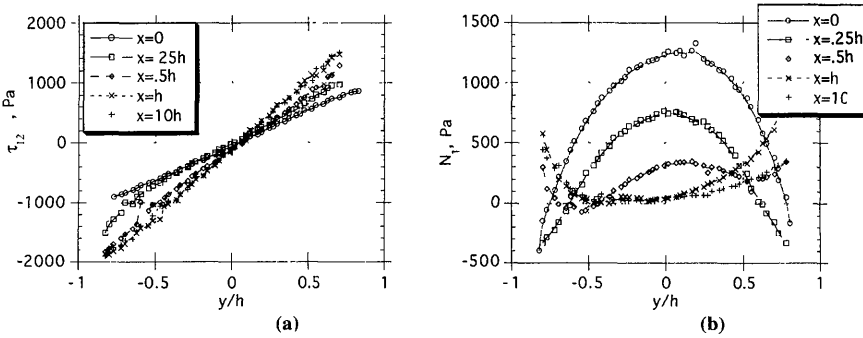

Figure 36 Lateral line scans downstream of the contraction for PC38 at 9 ml/min. Regions included are fully developed shear, $x = 10$ h and centerline $y/h = 0$. The point of contraction is $x = 0$ h. (a) Shear stress. (b) First normal stress difference.

Highly extensional flows are less studied than shear flows, in spite of their relevance to industrial processes such as injection molding, extrusion, blow molding, and fiber spinning. This is because it is often difficult to achieve a homogeneous extensional flow in a well-controlled manner. Spatially and temporally resolved flow birefringence represents a unique opportunity to study extensional flows as well as more complicated combinations of shear and extension.

Local extensional effects are illustrated in Figs. 34 and 35. Specifically, pure extension is seen at $y/h = 0$, as evidenced by zero-shear stress at all lateral positions (Figs. 34a and 35a) and a maximum in first normal stress difference (Figs. 34b and 35b). Also shown in Figs. 34b and 35b are the regions of compression near the corner, depicted by negative N_1. Steep gradients in shear and normal stress near the corner are thus a direct result of the confluence of compressive and extensive forces near the contraction. Ultimately, fully developed flow is recovered downstream of the contraction, once $x = h$. This is illustrated in Figs. 35 and 36 as a region of zero first normal stress difference along the centerline.

Directly along the centerline of flow one can examine the orientation and stresses arising exclusively from extension ($\tau_{11} - \tau_{11}$). The first normal stress difference along the centerline is shown in Figs. 37–39 for PC38, PC51, and LB-E, with the accompanying comparison from Newtonian calculations (FIDAP modeling software). Newtonian calculations accurately predict the rise in stress near the entry corner, especially for lower molecular weights. Slight overprediction of the stress maximum for the higher molecular weight materials is a result of deviation from Newtonian behavior. In all cases, extension of the molecules is not an instantaneous event, but starts as far back as to $x = -5\ h$, reaches a maximum at $x = -0.5$ h, and is fully relaxed by $x = h$ in the slit. An exception

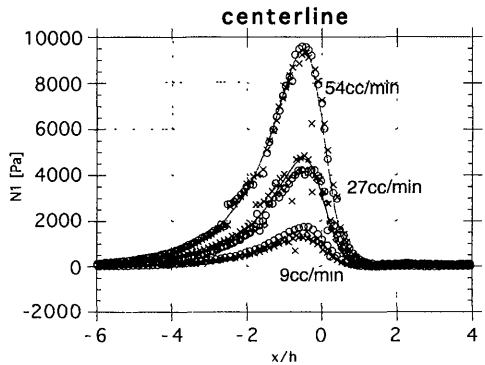

Figure 37 First normal stress difference along the centerline for PC38 and two other similar grades. Lines are Newtonian calculations, for three different flow rates.

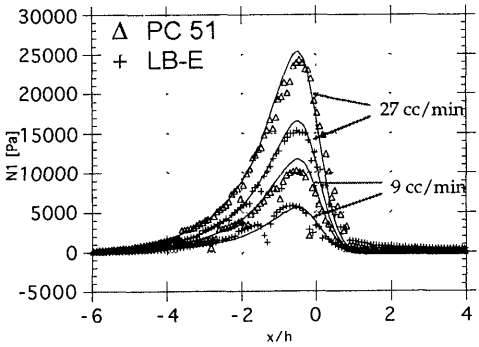

Figure 38 First normal stress difference along the centerline, PC51 and LB-E. Lines are Newtonian calculations, for two different flow rates.

to this relaxation behavior is seen for the linear-branched blend. Here relaxation from the extended state does not occur until $x = 2h$. Indeed, it is the relaxation of extensional stress that is least well predicted by Newtonian theory for all materials. This is seen most clearly in Fig. 39 where data for a range of molecular weights are compared. The downstream tail of all three sets of data are not well explained by the prediction. The linear/branched blend behavior is least well predicted using the Newtonian assumptions. The arrow in Fig. 39 points out the data for this blend, illustrating the preserved extended state, well beyond theoretical prediction. The extensional viscosity, η_e, is determined by dividing the peak

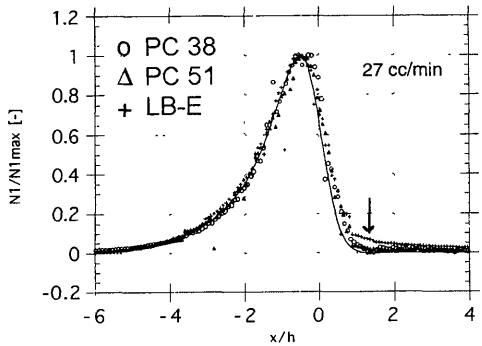

Figure 39 First normal stress difference along the centerline, scaled with the maximum value of N_1. Line is Newtonian calculation. Arrow points to relaxation behavior of LB-E.

in the extensional stress by the maximum expected strain rate. We find that Trouton's rule, which predicts that $\eta_e = 3 * \eta_s$ for Newtonian fluids, is slightly overestimated for PC38 (3.5–4.5 coefficient) using this technique.

REFERENCES

1. Z. Tadmor and C. Gogos, *Principles of Polymer Processing,* John Wiley and Sons, New York, 1979.
2. J. M. Dealy and K. F. Wissbrun, *Melt Rheology and its Role in Plastics Processing,* van Nostrand Reinhold, New York, 1990.
3. D. G. Baird and D. I. Collias, *Polymer Processing Principles and Design,* Butterworth-Heinemann, Boston, 1995.
4. S. Middleman, *Fundamentals of Polymer Processing,* McGraw-Hill, New York, 1977.
5. E. Macho, A. Alegria, and J. Colmenero, *Polym. Eng. Sci. 27:* 810–815 (1987).
6. J. P. Mercier and G. Groeninckx, *Rheo Acta 8:* 510–519 (1969).
7. J. P. Mercier, J. J. Aklonis, M. Litt, and A. V. Tobolsky, *J. Appl. Polym. Sci. 9:* 447–459 (1965).
8. A. Alegria, E. Macho, and J. Comenero, *Macromolecules 24:* 5196–5202 (1991).
9. R. Wimberger-Friedl and J. G. DeBruin, *Rheol. Acta 30:* 419–429 (1991).
10. R. Wimberger-Friedl, *Rheol. Acta 30:* 329–340 (1991).
11. R. A. Mendelson, *Polym. Eng. Sci. 23:* 79–85 (1983).
12. E. K. Borisenkova, *Int. J. Polym. Mater. 21:* 79–83 (1993).
13. M. G. Hansen and D. G. Bland, *Polym. Eng. Sci. 25:* 896–902 (1985).
14. J.-S. Wu, S-C, Shen, and F.-C. Chang, *J. Appl. Polym. 50:* 1379–1389 (1993).
15. N. A. Memon, *J. Appl. Polym. Sci. 54:* 1059–1072 (1994).
16. L. A. Utracki and P. Sammut, *Polym. Eng. and Sci. 30:* 1027–1040 (1990).
17. S. Kenig, *Polym. Adv. Technol. 2:* 201–207 (1991).
18. J.-C. Huang, H.-F. Shen, and Y.-T. Chu, *Adv. Polym. Technol. 13:* 49–55 (1994).
19. D. Beery, S. Kenig, A. Siegmann, and M. Narkis, *Polym. Eng. Sci. 32:* 14–19 (1992).
20. B. A. Knutsson, J. L. White, and K. B. Abbas, *J. Appl. Polym. Sci. 26:* 2347–2362 (1981).
21. S. A. Khan and R. K. Prud'homme, *Rev. Chem. Eng. 4:* 205–270 (1987).
22. P. Lomellini, *Makromol. Chem. 193:* 69–79 (1992).
23. C. J. Aloisio and V. W. Boehm, in *Rheology* (G. Astarita, G. Marrucci, and L. Nicolais, eds.), Plenum Press, New York, 1980, pp. 513–518.
24. H. T. Pham, C. P. Bosnyak, J. W. Wilchester, and C. P. Christenson, *J. Appl. Polym. Sci. 48:* 1425–1432 (1993).
25. T. Nagai, Y. Kimizuka, K. Nito, and J. Seto, *J. Appl. Polym. Sci. 44:* 1171–1177 (1992).
26. Z. Dobkowski, *Polym. Bull. 19:* 165–169 (1988).
27. D. K. Yoshimura and W. D. Richards, *ANTEC Proc.,* 1603–1606 (1990).
28. J. D. Ferry, *Viscoelastic Properties of Polymers,* John Wiley and Sons, New York, 1980.

29. P. Zoller, *J. Polym. Sci. Phys. Ed. 20:* 153–164 (1982).
30. S. M. Aharoni, *Macromolecules 19:* 426–434 (1986).
31. M. L. Williams, R. F. Landel, and J. D. Ferry, *J. Am. Chem. Soc. 77:* 3701–3707 (1955).
32. G. C. Berry and T. G. Fox, *Adv. Polym. Sci. 5:* 261–357 (1968).
33. G. C. Berry, *J. Phys. Chem. 70:* 1194–1198 (1966).
34. T. G. Fox and P. J. Flory, *J. Appl. Phys. 21:* 581–591 (1950).
35. T. G. Fox and S. Loshaek, *J. Polym. Sci. 15:* 371–390 (1955).
36. W. P. Cox and E. H. Merz, *J. Polym. Sci. 28:* 619–622 (1958).
37. B. Elbirli and M. T. Shaw, *J. Rheol., 22:* 561–570 (1978).
38. M. M. Cross, *J. Appl. Polym. Sci. 13:* 765–774 (1969).
39. C. A. Heiber and H. H. Chiang, *Rheol. Acta 28:* 321–332 (1989).
40. W. W. Graessley, *Adv. in Polymer Sci. 16:* 1–179 (1974).
41. W. H. Tuminello and N. Cudre-Mauroux, *Polym. Eng. Sci. 31:* 1496–1507 (1991).
42. W. H. Tuminello, T. A. Treat, and A. D. English, *Macromolecules 21:* 2606–2610 (1988).
43. W. H. Tuminello, in *Encyclopedia of Fluid Mechanics, Vol. 9, Polymer Processing and Flow Dynamics,* (N. P. Cheremisinoff, ed.), Gulf Publishing, Houston, 1990, pp. 209–243.
44. Z. Dobkowski, *Eur. Polym. J. 18:* 1051–1059 (1982).
45. Z. Dobkowski, *J. Appl. Polym. Sci. 28:* 3105–3121 (1983).
46. Z. Dobkowski and J. Brzezinski, *Eur. Polym. J. 17:* 537–540 (1981).
47. Z. Dobkowski, *Rheol. Acta 25:* 195–198 (1986).
48. T. C. B. McLeish, *Polym. 33:* 2852–2854 (1992).
49. M. Doi, W. W. Graessley, E. Helfand, and D. S. Pearson, *Macromolecules 20:* 1900–1906 (1987).
50. M. J. Struglinski and W. W. Graessley, *Macromolecules 18:* 2630–2643 (1985).
51. M. Rubinstein and R. H. Colby, *J. Chem. Phys. 89:* 5291–5306 (1988).
52. C. M. Ylitalo, J. A. Kornfield, G. G. Fuller, and D. S. Pearson, *Macromolecules 24:* 749–758 (1991).
53. P. G. deGennes, *Scaling Concepts of Polymer Physics,* Cornell University Press, Ithaca, NY 1979.
54. J. Schoonen, *Determination of Rheological Constitutive Equations Using Complex Flows,* PhD thesis, Eindhoven University of Technology, Eindhoven, The Netherlands, 1998.
55. T. Dunton, internal communication, GE CRD (1988).
56. M. G. Hansen and J. B. Jansma, *Polym. Prepr., ACS, Div. Polym. Chem. 20:* 157–159 (1979).
57. R. Colby, M. G. Hansen, A. R. Shultz, internal communication, 1981.
58. E. L. Kalinchev and M. B. Sakovtseva, *Int. Polym. Sci. Technol. 4* (8): T67–T69 (1977).
59. H. Watanabe, H. Yoshida, and T. Kotaka, *Macromolecules 21:* 2175–2183 (1988).
60. N. Clarke, T. C. B. McLeish, and S. D. Jenkins, *Macromolecules 28:* 4650–4659 (1995).
61. T. A. Yurasova, T. C. B. McLeish, and A. N. Semenov, *Macromolecules 27:* 7205–7211 (1994).

62. N. Clarke and T. C. B. McLeish, *J. Chem. Phys. 99:* 10034–10040 (1993).
63. T. C. B. McLeish and K. P. O'Connor, *Polymer 34:* 2998–3003 (1993).
64. N. Clarke and T. C. B. McLeish, *Macromolecules 26:* 5264–5266 (1993).
65. T. C. B. McLeish and K. P. O'Connor, *Makromol. Chem. Macromol. Symp. 56:* 127–134 (1992).
66. M. Rubinstein, S. Zurek, T. C. B. McLeish, and R. C. Ball, *J. Phys. 51:* 757–775 (1990).
67. R. C. Ball and T. C. B. McLeish, *Macromolecules 22:* 1911–1913 (1989).
68. T. C. B. McLeish, *Europhys. Lett. 6:* 511–516 (1988).
69. T. C. B. McLeish, *Macromolecules 21:* 1062–1070 (1988).
70. D. S. Pearson and E. Helfand, *Macromolecules 17:* 888–895 (1984).
71. G. Marrucci, in *Advances in Transport Processes, Vol. 5* (A. S. Mujumdar and R. A. Mashelkar, eds.), John Wiley, New York, 1984.
72. M. Doi and S. F. Edwards, *The Theory of Polymer Dynamics,* Oxford University Press, Oxford, 1986.
73. H. A. Lord, *Polym Eng. Sci. 19:* 469–473 (1979).
74. R. Staats-Westover, *Adv. Polym. Technol. 11:* 147–151 (1991).
75. R. Wimberger-Friedl and J. G. de Bruin, *J Polym. Sci. B Polym. Phys. 31:* 1041–1060 (1993).
76. R. G. Larson, *Constitutive Equations for Polymer Melts and Solutions,* Butterworths, Boston, 1988.
77. J. Greener, R. Kesel, and B. A. Contestable, *A. I. Ch. E. J. 35:* 449–458 (1989).
78. J.-M. Li and W. R. Burghardt, *J. Rheol. 39:* 743–766 (1995).
79. C. W. Macosko, M. A. Ocansey, and H. H. Winter, in G. Astarita, G. Marrucci and L. Nicolais, eds., *Proc. 8th Intl. Congr. Rheol.,* Naples, Italy, 3, Plenum Press, New York, 1980, pp. 723–728.
80. R. Wimberger-Friedl and J. G. de Bruin, *Rheol. Acta 30:* 419–429 (1991).
81. D. G. LeGrand, in *Structure and Properties of Polymer Films* (R. W. Lenz and R. S. Stein, eds.), Plenum Press, New York, 1973.
82. P. L. Frattini and G. G. Fuller, *J. Rheol. 28:* 61–70 (1984).
83. R. M. Kannan and J. A. Kornfield, *J. Rheol. 38:* 1127–1150 (1994).
84. H. Janeschitz-Kriegl, *Polymer Melt Rheology and Flow Birefringence,* Springer-Verlag, 1983.
85. D. L. Davidson, W. W. Graessley, and W. R. Schowalter, *J. Non-Newt. Fluid Mech. 49:* 317–344 (1993).
86. J. P. W. Baaijens. *Evaluation of Constitutive Equations for Polymer Melts and Solutions in Complex Flows,* PhD thesis, Eindhoven University of Technology, Eindhoven, The Netherlands, 1994.
87. J. van Aken and H. Janeschitz-Kriegl, *Rheo. Acta. 20:* 419–432 (1981).
88. G. H. McKinley, *Dynamics of Polymer Solutions,* PhD thesis, Massachusetts Institute of Technology, Cambridge, 1991.
89. D. V. Boger, *Ann. Rev. of Fluid Mech. 19:* 157–182 (1987).
90. D. V. Boger, M. J. Crochet, and R. A. Keiller, *J. Non-Newtonian Fluid Mech. 44:* 267–279 (1992).
91. C. D. Han and L. H. Drexler, *J. Appl. Polym. Sci. 17:* 2329–2393 (1973).

10

Large Deformation Response of Polycarbonate: Time–Temperature and Time–Aging Time Superposition

Paul A. O'Connell and Gregory B. McKenna
National Institute of Standards and Technology, Gaithersburg, Maryland

I. INTRODUCTION

There is currently increasing commercial interest in developing models that are able to predict material response to such industrial processes as injection molding, extrusion, blow molding, etc. Apart from the subsequent flow-induced characteristics from such processes, changes in the material in going from the melt to the glassy state can lead to changes in material dimension and stability that differ from those estimated from a thermoelastic analysis [1,2]. Furthermore, even in the glassy state the material may still evolve with time, leading to significant changes in material properties. As the models needed to adequately describe this complex behavior get increasingly sophisticated, there is a corresponding need for reliable material data to successfully implement them. In response to this need, ongoing work in this laboratory [3,4] has been aimed at developing an efficient methodology that reduces both the experimental time and complexity required to obtain accurate material parameters. As part of this work, a systematic study of one industrially important polymer (the polycarbonate Lexan LS) supplied by the General Electric Company [5] that is currently being evaluated in the context of the Thermoplastic Engineering Design program [6] has been carried out under a range of loading conditions and geometries in order to build a

comprehensive material database. This can then be used in a critical evaluation of proposed models of material behavior.

Here we examine time–temperature and time–aging time superposition behavior in polycarbonate. These are two techniques commonly used to predict the long-term material performance from relatively short-term tests.

A. Time–Temperature Superposition

Time–temperature superposition is widely used in the description of polymer behavior at temperatures above the glass transition temperature, T_g [7], whereby the viscoelastic response function changes with temperature by a shift in the time scale and the intensity by a vertical shift. This behavior can be understood in terms of a generalized Maxwell model [8] the basis of which is that the material response, such as the relaxation modulus $G(t)$, is governed by a number (n) of discrete relaxation mechanisms, each with a characteristic relaxation time $\tau_{n,I}$ at a temperature T:

$$G(T,t) = \sum_{n=1}^{I} b_{n,T} G_n e^{-(t/\tau_{n,I})} \tag{1}$$

where G_n are weighting parameters related to each element of the Maxwell model, and $b_{n,T}$ are temperature-dependent factors that have often been related to the plateau modulus in the melt state [7] but whose physical origin is less clear below the glass transition. On the assumption that the characteristic relaxation times all have the same temperature dependence, then a change in temperature from T_0 to T is manifested as a shift in the time scale by a temperature shift factor $a_I = \tau_{n,T0}/\tau_{n,T}$ (Fig. 1). Furthermore, for time–temperature superposition to be valid the $b_{n,T}$ must also each show the same temperature dependence. The change in the $b_{n,T}$ with temperature is often related to the change in the rubbery plateau modulus in the melt and results in an additional (small) vertical shift. Molecular theories of viscoelasticity [9] suggest that this vertical shift factor should be given by $T_0\rho_0/T\rho$ in changing from a temperature T (density ρ) to the reference temperature T_0 (density ρ_0), and indeed this has been demonstrated to be the case in several studies [10,11]. However, other studies [12] suggest that the vertical shift is based on a more complex mechanism, and this is especially so at temperatures close to T_g where large shifts have been observed. It should be noted that before the appearance of molecular theories for crosslinked networks [13,14] the data tended to be shifted empirically and the vertical shifts often went unnoticed or unreported [15,16]. Furthermore, it is only in the regions where the viscoelastic response is flat, i.e., deep in the rubbery and glassy phases, that the vertical shifts have a significant effect on the data reduction insofar as small changes in the vertical shift factor can lead to comparatively large changes in the time shift

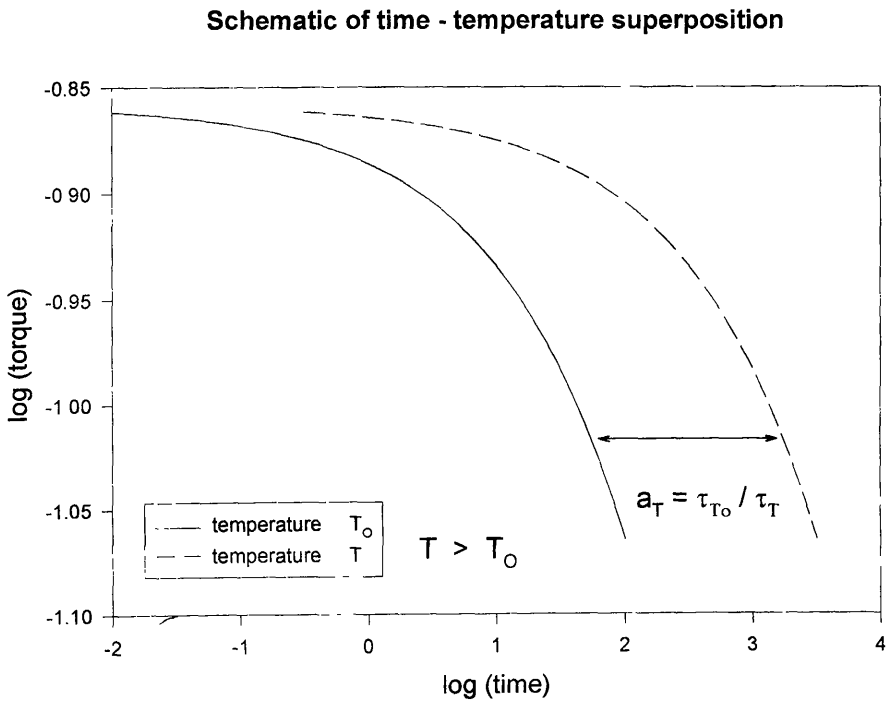

Figure 1 Schematic of time–temperature superposition.

factor. Note, however, that the physical origins of vertical shifts in the glassy state are unclear and deviations in the melt near to T_g from expectations of rubber elasticity are similarly not understood [12,27].

An often used, and computationally simpler, representation of the response function than that of the generalized Maxwell model is the stretched exponential of Kohlrausch-Williams-Watts (KWW) [17,18]:

$$M(t) = M_0 \, e^{-(t/\tau_0)^{\beta}} \tag{2}$$

where $M(t)$ is the torque response at time t, τ_0 a characteristic relaxation time, β a shape parameter for the relaxation curve, and M_0 is the zero time torque response. As before, a change in temperature from T_0 to T results in a change in the characteristic relaxation time leading to a temperature shift factor $a_T = \tau_{T0}/\tau_T$. Vertical shifts are seen as a temperature-dependent zero time torque response M_0.

A somewhat similar form for the relaxation response of polycarbonate has been proposed by LeGrand and Bendler [19]. In their work, the mechanical response was interpreted in terms of the motions of defects within a network, the analysis of which leads to the following equation for stress relaxation:

$$M(t) = M_1 + \Delta M\, e^{-(t/\tau_0)^{\beta}} \tag{3}$$

where, as before, $M(t)$ is the torque response at time t, τ_0 a characteristic relaxation time, β a shape parameter for the relaxation curve, and now M_g is the unrelaxed torque response and ΔM the difference ($M_g - M_r$) between the unrelaxed and relaxed (M_r) torque responses.

B. Time–Aging Time Superposition

When an amorphous polymer, initially in the melt regime, is cooled, the volume decreases and, at a characteristic temperature, the volume departs from equilibrium (Fig. 2). This temperature is what is generally referred to as the glass transition temperature (T_g) and is dependent on the rate of cooling. Upon further cool-

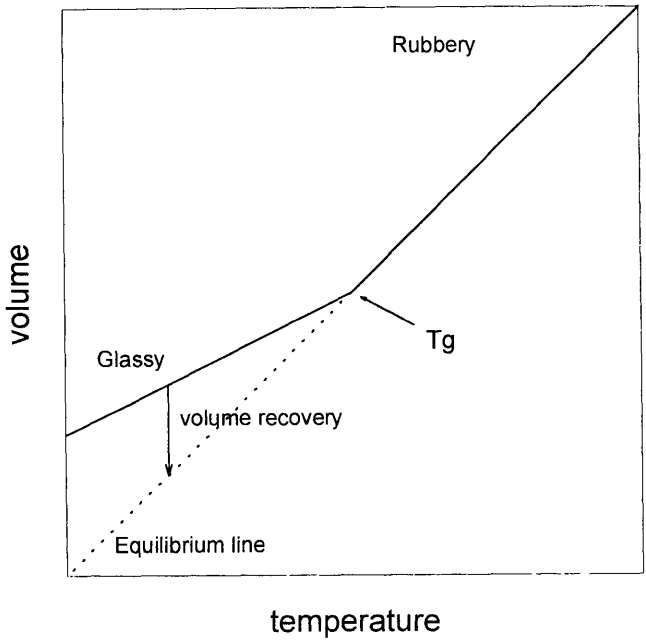

Figure 2 Schematic of the volume–temperature response of a polymer glass.

ing the material departs further from equilibrium. If the cooling is stopped and the material held isothermally it is observed that the volume recovers spontaneously toward equilibrium [20,21]. Associated with the changes in volume are changes in the mechanical, including viscoelastic, response of the polymer glass. These changes in properties that accompany the volume recovery have come to be known as physical aging [22]. As with a change in temperature, the volume evolution induces a change in molecular mobility, i.e., the time scale for the viscoelastic response. Here, though, we speak of responses at specific aging times rather than volumes. Time–aging time superposition principles can be applied in exactly the same manner as time–temperature superposition and have the possibility of use for the description of material response over time scales that would be impractical for material evaluation in an industrial environment.

It can be seen then that, if successful, the application of time–temperature and time–aging time superposition principles can be a powerful tool for the prediction of material response at long times from tests conducted over relatively short time scales.

The questions addressed in this paper are: Can time–temperature and time–aging time superposition principles be applied below T_g? If so, over what ranges of deformation and temperature are they valid? Furthermore, we explore the validity of the stretched exponential KWW [17,18] function and the modification due to LeGrand and Bendler [19] to fit the relaxation response of polycarbonate. To answer these questions, single-step stress relaxation experiments were carried out in torsion at temperatures from 30°C to 135°C. Strains were examined covering both the linear and nonlinear viscoelastic range, up to just below the yield point.

II. EXPERIMENTAL

The polycarbonate used in this study was supplied in the form of extruded rods of 25 mm diameter. Cylinders of the material were machined to a length of 50 mm and diameter 12 mm. A gauge section of 30 mm length and 4 mm diameter was machined in order to grip the samples in a special fixture for the torsion of solid samples [23]. In order to remove the effects of previous thermal and/or mechanical history, the samples were heated to 145°C for 1 h prior to testing. This is approximately 4°C above the measured T_g, as determined from differential scanning colorimetry (DSC) measurements at a heating rate of 10°C/min after slow cooling of the sample [4]. Observation of the samples through crossed polars subsequent to the heat treatment indicated no residual orientation

The torsion measurements were carried out on a Rheometrics RMS 7200 [5] load frame, modified in our laboratory with a computer-controlled servomotor. The torque force responses were measured with the original machine trans-

ducers with new excitation electronics. In addition, the sample and grips were housed within a heater chamber for temperature control. This allowed tests to be carried out from ambient to 135°C with a measured oven stability of better than ±0.1°C. The torque force relaxations were measured from nominal strains γ (based on the cylinder outer radius) from 0.0025 to 0.08:

$$\gamma = R\phi/L = R\psi \tag{4}$$

where ϕ = angle of twist, R the cylinder radius, L the length of the gauge section, and ψ the angle of twist per unit length.

In order to examine the effects of aging, a loading regime first proposed by Struik [22] was followed. In this, the strains are applied sequentially at aging times t_e that approximately double with each test. The duration of the applied strain, t_1, was such that the ratio t_1/t_e was constant at 0.10. The applied strains then are essentially "probes" into the material structure and are of a sufficiently short duration that aging effects do not significantly influence the measurements. By allowing the sample to recover for a time t_2 (= $9t_e$), the sample essentially "forgets" the effect of the previous loading cycle. In order to confirm that this loading regime is valid and that the sample really does forget the previous loading cycle, a number of tests were carried out where the sample was taken above T_g, cooled, and allowed to age for a given time at the appropriate test temperature and then a single probe strain applied. For most of the testing here the results from these tests agreed within experimental error to those found from sequential loading, indicating that the probe strains do not affect the subsequent viscoelastic response. It was noted, however, that at strains approaching the yield strain (the value of which decreased as temperature increased), the sequential loading procedure was not valid, and the material retained a memory of the previous probe. In these cases, tests had to be conducted by performing individual tests at each aging time on annealed samples with no previous strain history. Unless otherwise indicated, the results reported here are from tests where no memory effect was present, either because the sequential loading tests were equivalent to the individual ones or the full aging response was obtained from individual tests. Aging times from 0.5 to 18 h were examined.

III. ANALYSIS

Depending on the initial assumptions, two approaches can be taken in the analysis of superposition data. In the first approach, it is assumed that the superposition principle is valid and applicable, in which case the curves are shifted empirically to form the master curve. The question may then be asked as to what form this master curve takes.

Alternatively, in a second approach, it is assumed that the data obtained

for the relaxation response at each temperature or aging time is sufficient to determine accurately and fully the KWW parameters. If the KWW β is independent of temperature (aging time), then it follows that the first approach to the data analysis must also be valid and furthermore that the master curve constructed from the first approach will fit a KWW function. However, if the β value changes with temperature (aging time), it does not necessarily follow that time–temperature (time–aging time) superposition is not valid. Recourse needs to be made to the first approach above to establish this and it must be stated that the second method of analysis can lead to spurious interpretation of the physical meaning of, for example, the β term. Strictly then, in such a case, the KWW function should not be applied to any of the stress relaxation curves as it is not a valid description of the relaxation response. Preempting the results presented in the following sections, it appears that the KWW function is not valid over a wide range of reduced time scales. Nevertheless it is extremely useful for the description and reduction of data over limited time scales. Finally, the stress relaxation data as a function of temperature are examined using the LeGrand-Bendler [19] analysis and a comparison made with the results from the KWW analysis.

For pedagogical purposes, the following sections describe the data analysis with the assumption that the KWW function is valid, and defines the vertical and horizontal shifts in terms of KWW parameters. The first approach for the data analysis is semimanual and is described in the appropriate results section.

A. Time–Aging Time Analysis

Each stress relaxation curve was examined using the KWW function [17,18]:

$$M(t) = M_0 \, e^{-(t/\tau_0)^{\beta}} \tag{2}$$

where $M(t)$ is the torque response at time t, M_0 is the zero time torque response, τ_0 is a characteristic relaxation time, and β is a shape parameter for the relaxation curve.

For a given temperature and strain, and assuming that β is independent of aging time, it is possible to perform time–aging time superposition of the data by reducing the curves to a reference aging time via a shift along both the time and force axes (an additional proviso here is that the response be sufficiently "curved" to allow the distinction between the required vertical and horizontal shifts for superposition). The aging time shift factor a_{te} is then defined from the KWW function as

$$\log(a_{te}) = \log[\tau_0(t_e)/\tau(t_{ref})] \tag{5}$$

where $\tau_0(t_e)$ is the value of τ_0 in Eq. (5) at aging time t_e and $\tau^0(t_{ref})$ its value at the reference aging time. Having obtained the values of a_{te}, these are then analyzed in

the conventional manner of making plots of $\log(a_{te})$ vs. $\log(t_e)$, the slope of which has been defined as the shift rate, μ, by Struik [22] as:

$$\mu = d \log(a_{te})/d \log(t_e) \tag{6}$$

B. Time–Temperature Analysis

In a similar manner, stress relaxation curves at differing temperatures for a given strain and aging time can be superimposed by suitable shifts in the time and force axes to give a temperature shift factor defined by:

$$\log(a_T) = \log[\tau_0(T)/\tau_0(T_{ref})] \tag{7}$$

where $\tau_0(T)$ is the value of τ_0 in Eq. (2) at temperature T and $\tau_0(T_{ref})$ its value at the reference temperature T_{ref}.

C. Vertical Shifts in Time–Aging Time and Time–Temperature Superposition

Typically, when the results of both time–aging time and time–temperature superposition are reported in the literature, the required vertical shifts tend to be ignored or mentioned only in passing [7,12,24,27]. In particular, little attention is normally placed on the magnitudes of the vertical shifts. This may be due in part to the relatively small shifts observed compared to the corresponding large horizontal (time) shifts or because the nature of the shift is not clearly understood. However, deep in the glassy state where the material response is less pronounced, the application or not of vertical shifts can have a very significant effect on the temperature shift factors [7,24]. Data are presented subsequently to quantify these shifts and show that they are systematic in both temperature and aging time. The temperature and aging time vertical shifts may be defined by

$$\log(b_T) = \log [M_0(T,t_e)/M_0(T_{ref},t_e)] \tag{8}$$

and

$$\log(b_{te}) = \log[M_0(T,t_e)/M_0(T,t_{e,ref})] \tag{9}$$

where $M_0(T,t_e)$ is the zero time torque response at temperature T and aging time t_e. $M_0(T_{ref},t_e)$ is the zero time torque at aging time t_e and the reference temperature T_{ref} and $M_0(T,t_{e,ref})$ the zero time torque response at temperature T and the reference aging time $t_{e\,ref}$.

IV. RESULTS

A. Time–Aging Time Superposition

A typical set of stress relaxation curves as a function of aging time is shown in Fig. 3 (data for 4.5% strain at 70°C). As can be seen, the data for the longer aging times are shifted to the right on the time axis, i.e., the response is shifted to longer times. Because of the greater number of data points for the longest aging time, these data are generally used as the initial reference curve to determine τ_{ref}, $M_0(t_{e,ref})$, and β parameters. (The choice of the aging time to use as the reference curve is arbitrary, the only effect being a shift of the final master curve in the time axis.) Having determined the KWW parameters for this curve, we then take the second approach discussed above, i.e., each curve follows the same relaxation response (albeit shifted in time) and hence has the same shape parameter β. The β value then is held constant and the data at shorter aging times fitted to the KWW function by varying $\tau(t_e)$ and $M_0(t_e)$. The values of $\log(a_{te})$ and $\log(b_{te})$ can then be determined as discussed above. The assumption of a constant β value

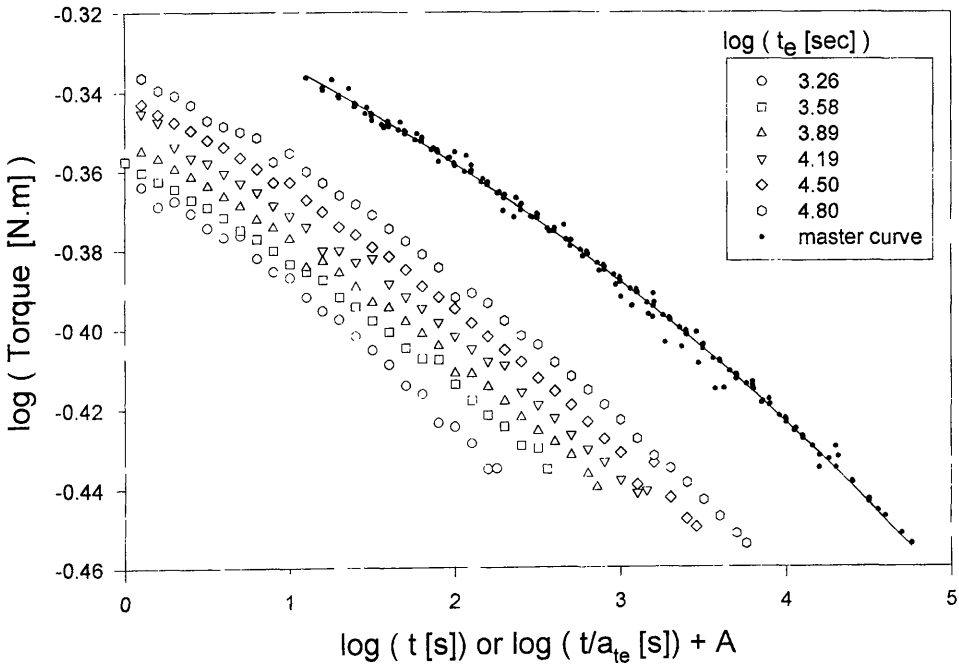

Figure 3 Stress relaxation response of polycarbonate at 4.5% strain and 70°C as a function of aging time.

can be validated by allowing the M_0, β, and τ parameters to vary for each relaxation curve; if this is carried out it is found that the β term is indeed essentially independent of aging time, with the proviso that this is true only over the time scale of these tests (Fig. 4). Application of the appropriate shift factor to the relaxation data results in a superposition of the data to form the time–aging time "master curve" (Fig. 3). (Note that the data for the master curve have been further offset by an arbitrary amount in the time direction for clarity.)

Figure 5 shows a plot of the $\log(a_{te})$ vs. $\log(t_e)$ values at 3.5% strain for 30°C and 110°C (note that the data are plotted as referenced to t_e = 1800 s). The data show good linearity, the gradient of which is the double logarithmic shift rate, μ.

Figure 6 illustrates the effect of both temperature and strain on the shift rate, μ, for temperatures up to 110°C and strains up to 7% (note that the data

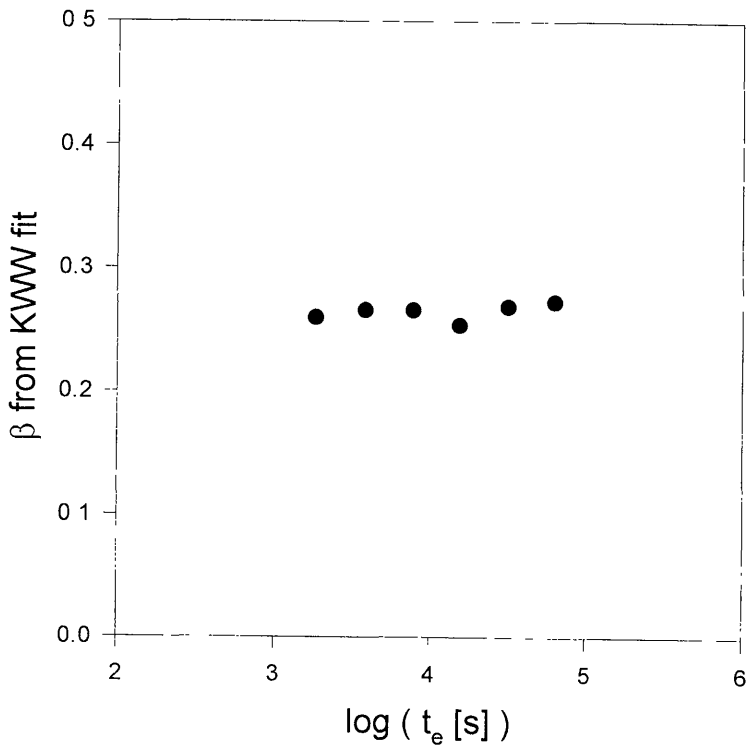

Figure 4 Variation of the KWW β parameter for polycarbonate as a function of aging time at 2% strain and 70°C.

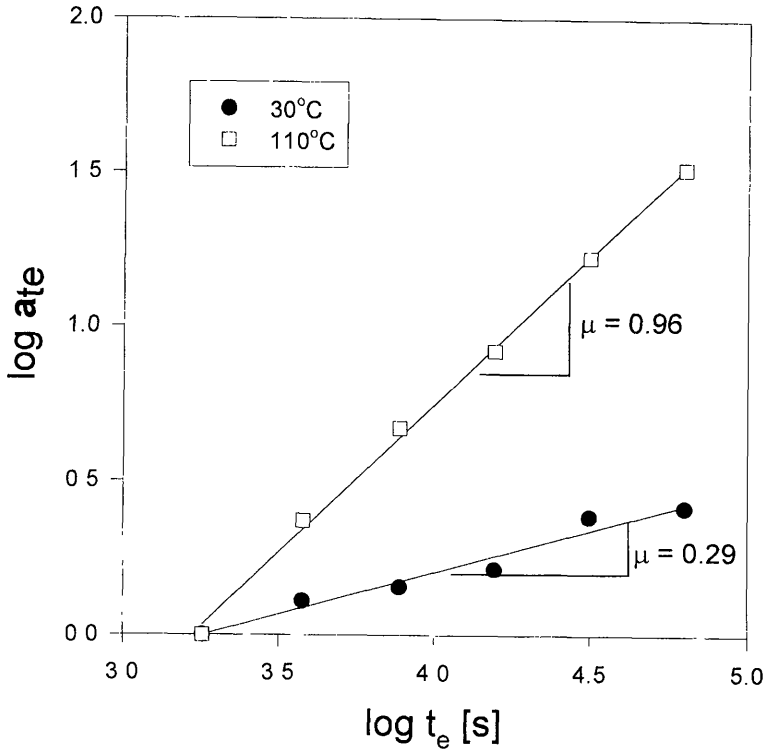

Figure 5 Double logarithmic representation of aging time shift factor vs. aging time for polycarbonate at 3.5% strain and temperatures of 30°C and 110°C.

marked with an asterisk are the results from tests conducted individually at each aging time). The error bars shown are the root mean square deviation from the average value. In the linear viscoelastic range at low strains (less than 2%) the shift rate is approximately constant at any given temperature. The small strain shift rate can be seen to increase slightly as the temperature increases.

As the strain is increased, i.e., as the material response moves into the nonlinear viscoelastic range, there is a systematic decrease in the shift rate with increasing strain. This strain dependence of the shift rate is seen to become progressively less pronounced at increasing temperatures, as evidenced by a leveling off of the curves. The temperature dependence of the shift rate then becomes an increasingly strong function of the temperature at higher strains. Significantly, the decreasing dependence of the shift rate on strain continues to such an extent that the shift rate is independent of strain at 110°C. This was an unexpected result

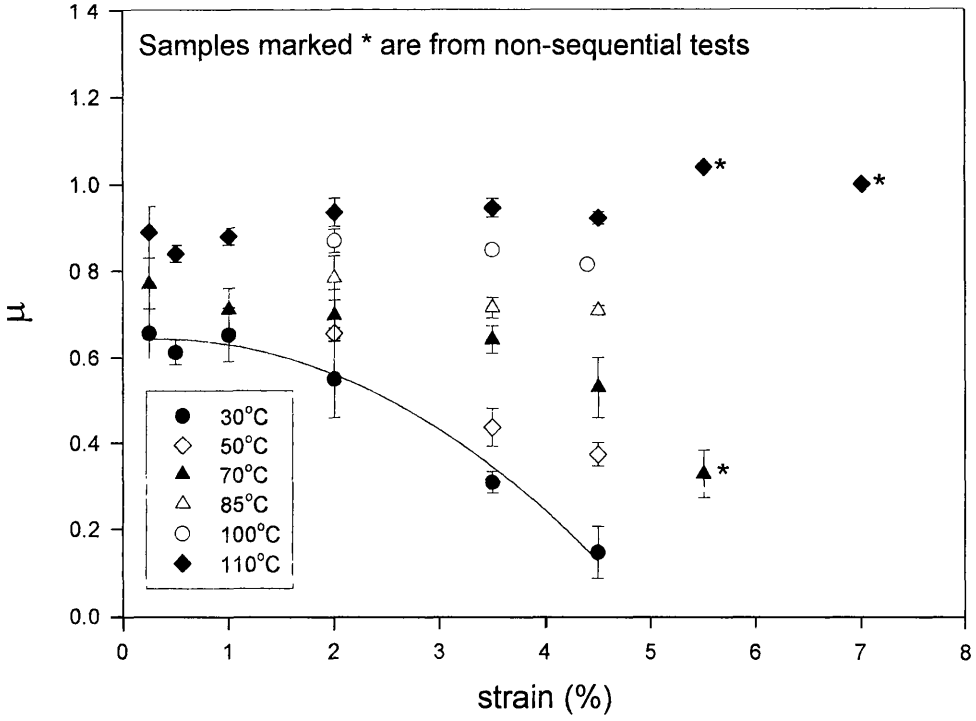

Figure 6 Aging time shift rate μ for polycarbonate as a function of strain and temperature.

and to our knowledge is the first time a strain-independent shift rate in the large deformation regime has been observed.

The effect of temperature on the shift rate is more clearly seen in Fig. 7 where μ values at three strains are plotted as a function of test temperature. Additional data at higher temperatures (up to 135°C and omitted for clarity from the previous figure) are also shown. At temperatures near T_g the shift rate reduces drastically at all strain levels (indeed by definition the shift rate is zero at T_g). The data show a (strain-independent) maximum at approximately 110–120°C and then a systematic decrease as the temperature is lowered to 30°C. As observed above, the temperature dependence of the shift rate is more pronounced at higher strains, shown here by the steeper slope at these strains. Lower strain data have been omitted, again for clarity, as the shift rate was shown to be virtually independent of strain below 2%.

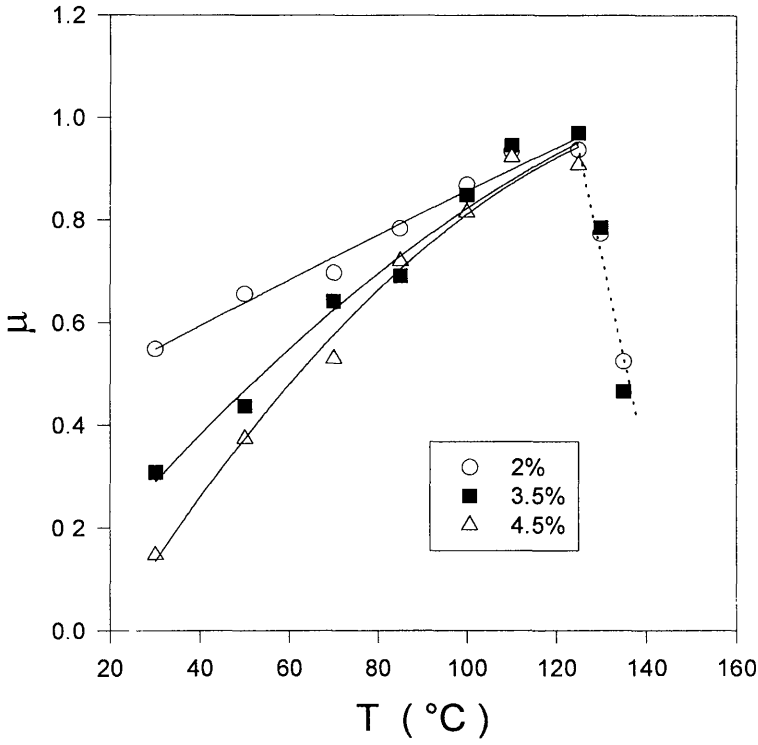

Figure 7 Aging time shift rate μ for polycarbonate as a function of temperature and strain.

These data are in contradiction to that presented by Struik [22] for polycarbonate where the shift rate remains constant at a value of approximately 1.2 down to temperatures of the order of −50°C. The reasons for such differences are unknown. We note, however, that the tests were performed in stress relaxation whereas those of Struik were performed in creep. Also, Sullivan [25] has reported shifts rates, μ, of approximately 0.75 for polycarbonate in the linear viscoelastic regime from creep experiments—a result in line with the results reported here.

Vertical Shifts

As with the horizontal (time) shifts, a plot of the vertical shifts [$\log(b_{te})$] as a function of $\log(t_e)$ yields a linear relationship, the gradient of which is denoted

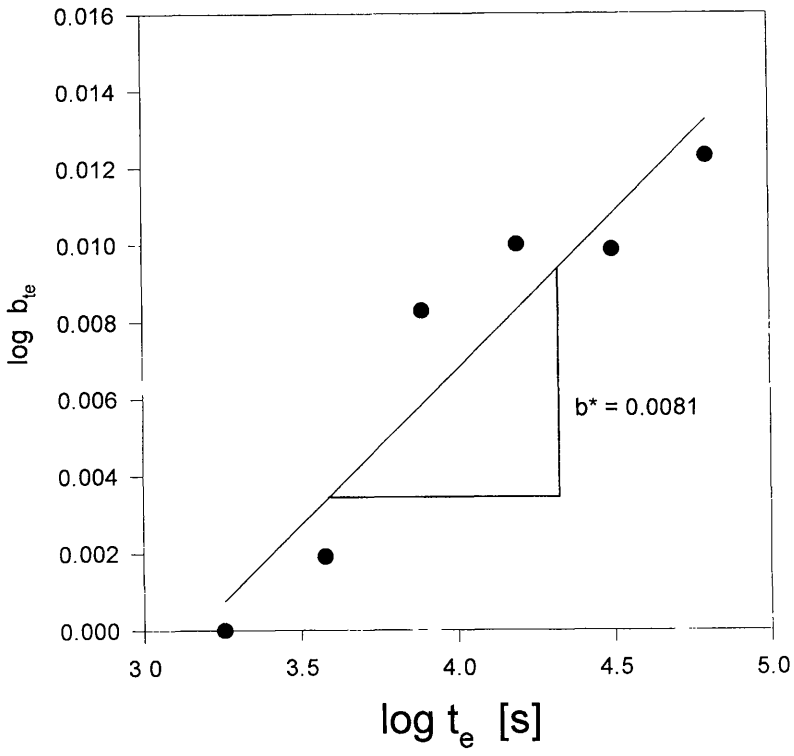

Figure 8 Vertical shift factor for polycarbonate as a function of aging time at 2.0% strain and 50°C.

by b^* (Fig. 8: data for 110°C and 3.5% strain). The variation of b^* with temperature and strain is shown in Fig. 9. Although there is a relatively large amount of scatter in the b^* values, there is no clear trend with either temperature or strain (as least up to the yield point of the material), giving an overall average value of approximately +0.008 over 0.5–18 h of aging. This implies that the zero time or intrinsic modulus is increasing by approximately 2% per decade of aging. This is perhaps not too surprising in considering that the underlying structure of the material must be changing as the material ages and densifies. The magnitude of the vertical shift rate is similar to that reported by Struik [22].

It was mentioned previously that at strains approaching the yield point the material starts to retain a memory of the previous loading cycles. Yield in the material was evidenced by a peak in the isochronal shear stress, $\sigma_s(t)$, as a func-

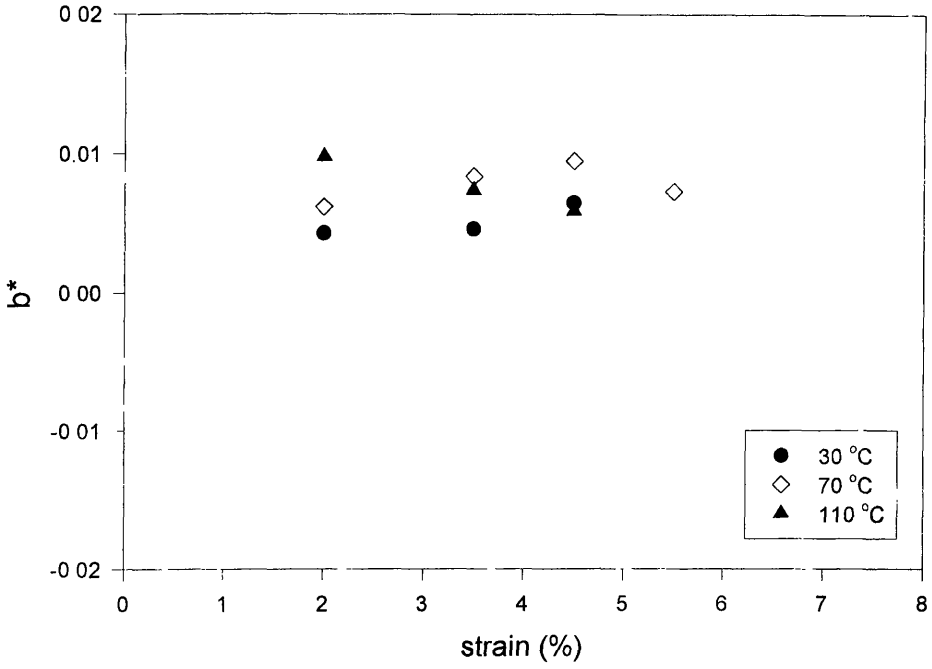

Figure 9 Vertical shift rate b^* for polycarbonate as a function of strain for three temperatures, as indicated.

tion of strain. Figure 10 portrays the 100-s values of the shear stress determined using the scaling approach of Penn and Kearsley [26]:

$$\sigma_s(t) = \frac{2\gamma}{4\pi\psi R^4}\left(3M(t) + \psi \cdot \frac{dM(t)}{d\psi}\right) \tag{10}$$

where the symbols are as defined previously and we note that the $dM(t)/d(\psi)$ is the derivative of the torque with respect to the angle of twist per unit length. Under such circumstances it was necessary to conduct the probe tests individually at each aging time, and it is these results that have been reported. It is interesting to note that for tests conducted sequentially at the large strains the data could still be reduced to form a master curve. In such a case, both the horizontal and vertical shifts were linear with aging time. Examples of the resulting μ and b^* values are listed in Table 1, along with the respective results from individual loading tests. It is clear from the results that when the strains get too large the

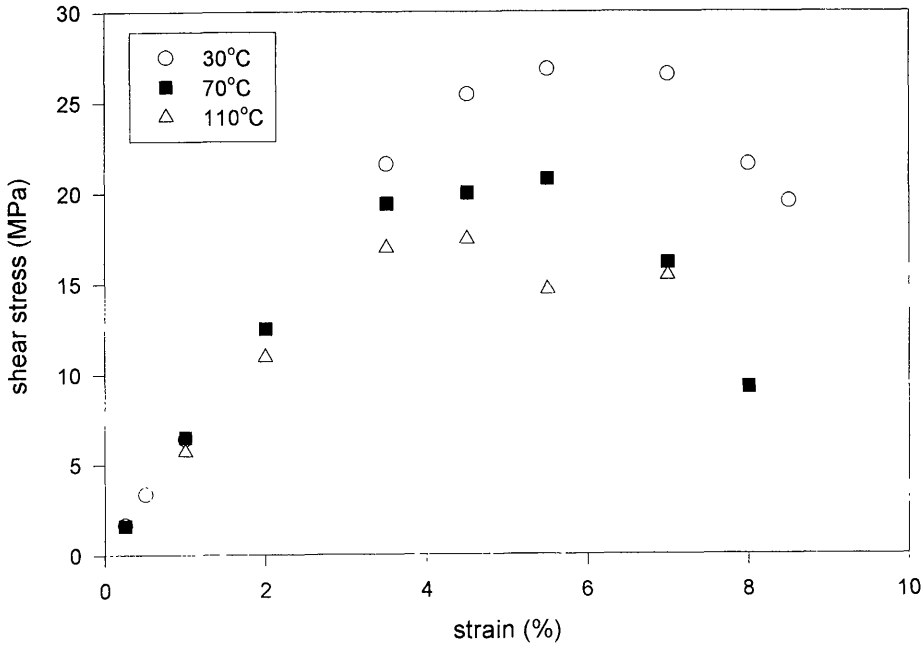

Figure 10 Isochronal (100 s) shear stress–strain response for polycarbonate for three temperatures, as indicated.

effect of the previous loading cycles is significant and can lead to an apparent increase in the shift rate, μ. More drastic is the change in b^* values from small positive values to somewhat larger negative values, an indication that the material is apparently softening at the longer aging times and after multiple sequential deformations. It is not clear at this point as to the significance of these observations. While they do raise interesting questions as to the effect of yield on the aging time response, further examination is beyond the scope of this chapter.

Table 1 Effect of Nonsequential Testing on Shift Rate (110°C, 7% Strain)

Test performed sequentially		Tests performed individually	
μ	b^*	μ	b^*
1.32	−0.023	1.01	0.002

B. Time–Temperature Superposition

Construction of a Master Curve

Time–temperature superposition is applied to data generated from tests carried out at a given strain and aging time. The data presented here are for 2% strain and an aging time of 64,800 s. The longest aging time was chosen as this gave the longest response time scale and consequently greater accuracy in the fitting procedures. Similarly, 2% strain was chosen as the strain most comprehensively covered in terms of the range and number of temperatures examined. Importantly, the aging results showed that the material response was virtually independent of strain to 2% strain. The same analysis as follows with the more limited dataset at 0.5% strain confirmed this to be the case.

As mentioned above, the "small" vertical shifts that are in general necessary to obtain good superposition of the data tend not to be emphasized. For clarity, Fig. 11 shows only a limited set of the data. The data have been shifted in time only and clearly demonstrate that good superposition is not obtained with horizontal shifts alone. However, as discussed in the next paragraph, use of vertical shifts does allow excellent superposition to be obtained.

It is assumed here that time–temperature superposition is valid and a master curve can be constructed. As was shown in the previous section, the KWW function adequately describes the relaxation response over the short time scales studied, and the function will again be used here. It should be made clear, however, that this is simply a convenient form with which to describe the data and with which to introduce some mathematical rigor in determining the appropriate shift factors. Importantly, it is not assumed that the parameters determined from a single curve at one temperature describe the response at all temperatures.

To determine the temperature shift factors a slightly different approach to that used for the aging time shift factors needed to be adopted, the reasons for which will be further elaborated in the following section. Importantly, as with the aging time data, both vertical and horizontal shifts were applied.

The highest temperature (say, $T1$) data were taken as the reference curve and the parameters (M_0, τ, and β) to fit to the KWW function determined. Keeping β constant, the KWW fit to the next lowest temperature ($T2$) was found, and hence the temperature shift factor determined for the temperature change $T1$–$T2$:

$$\log\,(a_{T1-T2}) = \log\,(\tau_{T2}/\tau_{T1}) \tag{11}$$

$$\log(b_{T1-T2}) = \log\,(M2_0/M1_0) \tag{12}$$

The $T2$ data were then refitted to the KWW function, this time allowing the β term to vary. Keeping this new β constant, the next lowest temperature ($T3$) data were fitted to the KWW function and the temperature shift factor determined for the temperature change $T2$–$T3$:

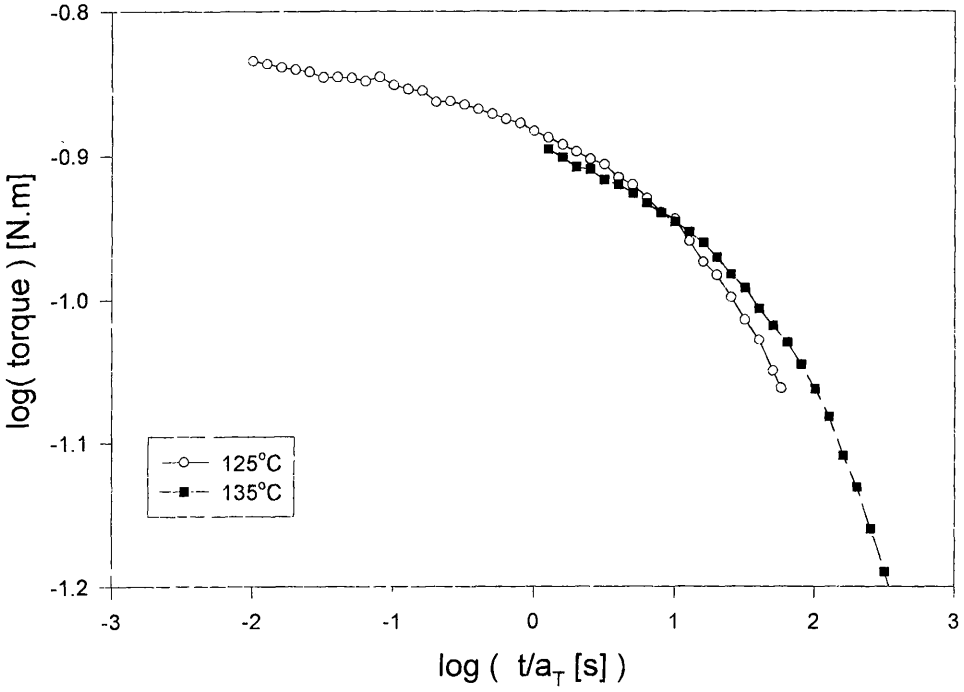

Figure 11 Application of time–temperature shifting for polycarbonate using no vertical shifts. The strain is 2% strain and a log [aging time (s)] of 4.80, showing that the curves do not superimpose.

$$\log (a_{T2-T3}) = \log (\tau_{T3}/\tau_{T2}) \quad (13)$$

$$\log(b_{T2-T3}) = \log (M3_0/M2_0) \quad (14)$$

By repeating this procedure for successively lower temperatures, it was possible to build up the overall time–temperature master curve from the individual shifts at neighboring temperatures. It should be emphasized that this procedure assumes that only at temperatures sufficiently close is it reasonable to impose the shape parameter determined from one curve onto an adjacent curve, and further that we are not imposing a single shape parameter onto the whole dataset. Also, each superposition is checked manually and the fit found to be at least as good as would be obtained empirically by eye.

The master curve constructed using the above procedure is shown in Fig. 12, from which it is evident that the data do appear to superimpose to form a master curve. The corresponding temperature shift factors, at 2% strain and an

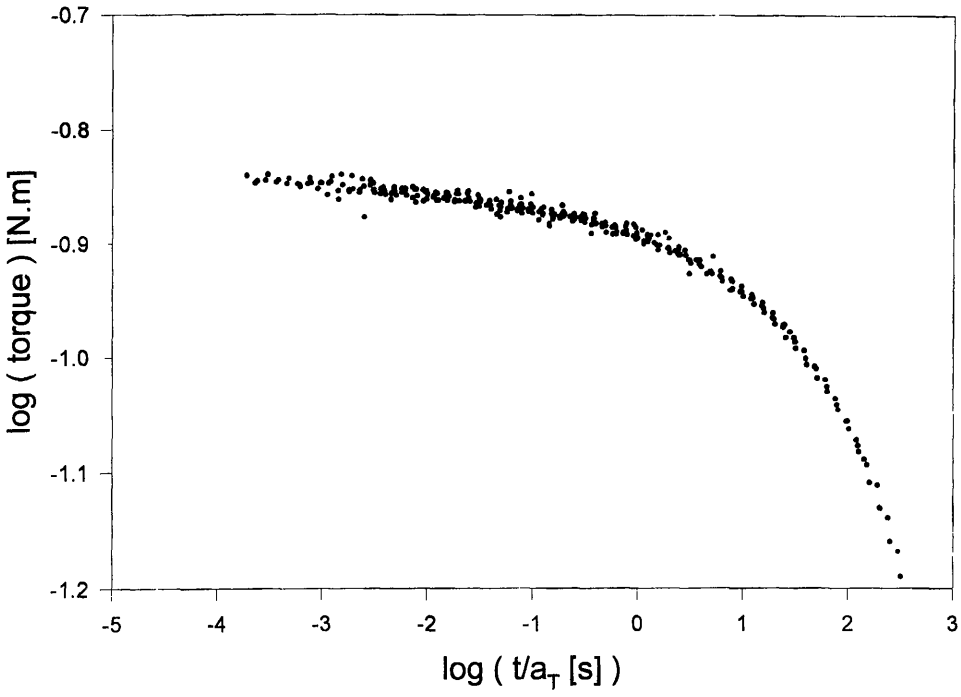

Figure 12 Time–temperature master curve for polycarbonate. The deformation is 2% and $\log(t_c/s) = 4.8$. The data are referenced to 135°C.

aging time of 64,800 s, are shown in Fig. 13. Also shown in Fig. 13 are the shift factors found from dynamic tests carried out on the same material in the temperature range 104–145°C [4], the latter data having been referenced to T_g. Since the choice of reference temperature is arbitrary, the relative shift factors remain the same regardless of the temperature chosen. The data in this study have been normalized to the dynamic data at a reference temperature of 110°C.

At temperatures just below T_g the temperature shift factor ($\log a_1$) rises rapidly with decreasing temperature, until about 20°C below T_g where the rate of increase begins to decrease. The rate then continues to decrease as the temperature is further reduced. This variation in the rate of change of the shift factor with temperature is significant, being about 50 times greater at 135°C than at room temperature.

The same general trends are observed at all other strains and aging times examined. The results from the time–aging time superposition can be used to make some qualitative observations about the effect of strain and aging time on

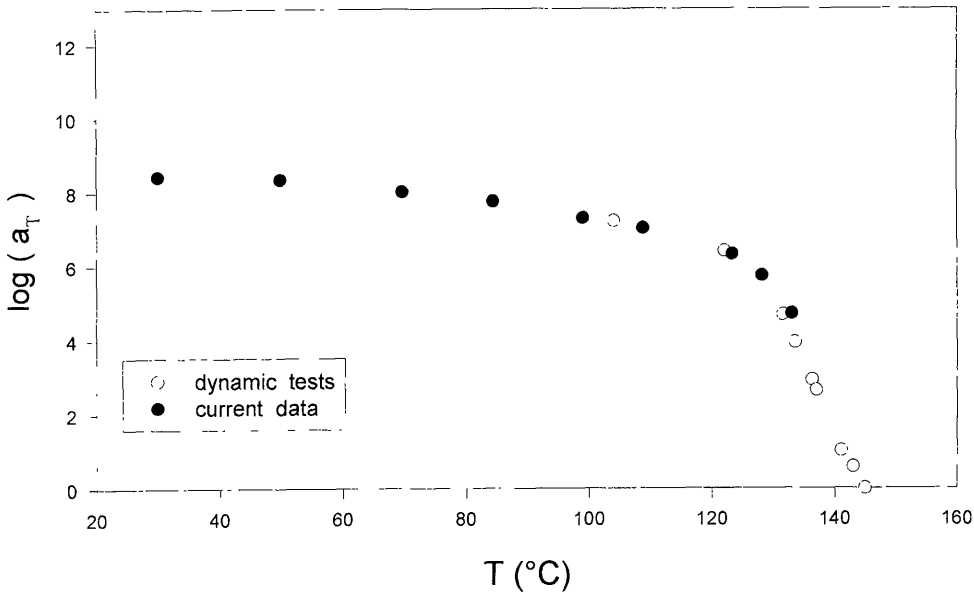

Figure 13 Temperature shift factors a_T for polycarbonate as a function of temperature at 2% strain and an aging time of 64,800 s (log t_e/s = 4.8).

the time–temperature superposition factors. Figure 14 shows a schematic of the torque response at two temperatures ($T_1 < T_2$) and two aging times ($t_{e1} < t_{e2}$). The temperature shift factors at aging times t_{e1} and t_{e2} are denoted by a_{T1} and a_{T2} and the aging time shift factors at temperatures T_1 and T_2 by a_{te1} and a_{te2}, respectively. We know from the μ variation that at a given strain the shift rate is reduced at the lower temperatures, i.e., the torque response curves are "bunched" closer together at the lower temperatures ($a_{te1} < a_{te2}$). Looking first at the longer aging time (t_{e2}), we can define a temperature shift factor a_{T2} for superposition. With reference to Fig. 14, if this shift factor is applied to the data at the shorter aging time (t_{e1}) it will not be sufficient for superposition and an additional shift will be required to obtain the correct shift factor (a_{T1}). We can say then that the relative time–temperature shift factor between any two temperatures will increase at shorter aging times. From Fig. 14:

$$a_{T1} = a_{T2} + (a_{te2} - a_{te1}) \tag{15}$$

i.e., the additional temperature shift factor required in going to a lower aging time is simply the difference in the aging time shift factors. Moreover, the difference in

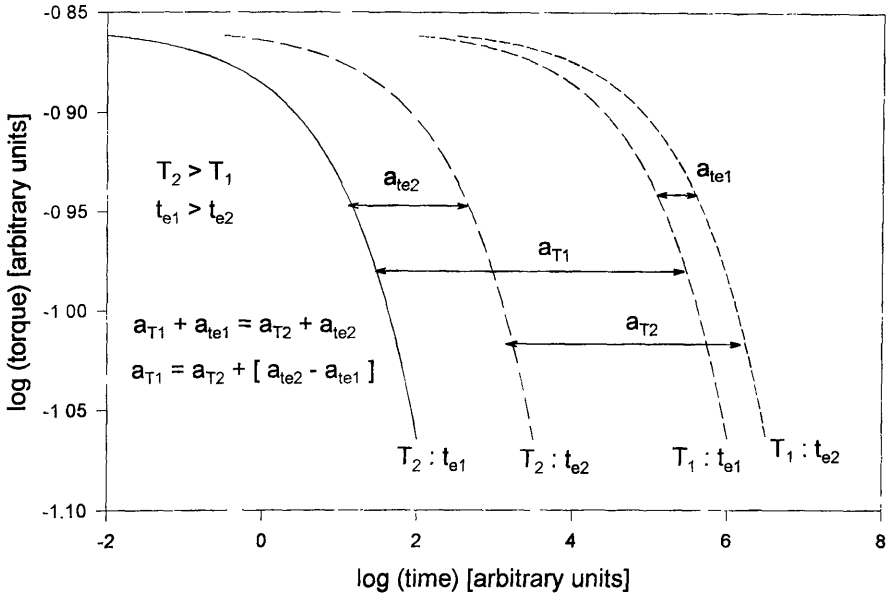

Figure 14 Schematic of the effect of temperature and aging time on the stress relaxation response. See text for discussion.

aging time shift factors at any two aging times is simply related to the difference in the μ values. Since the differences in the μ values at any two temperatures increase at increasing strain, then it is expected that the *relative temperature shift factor between any two temperatures at a given aging time should increase at increasing strain*. Table 2 lists the relative temperature shift factors for temperature changes of 30°C to 70°C and 70°C to 110°C at two aging times and strains

Table 2 Time–Temperature Shift Factors for the Temperatures Indicated as a Function of Applied Strain and Aging Time

Log [aging time(s)]	Temp. change	2%	3.5%	4.5%
3.26	30–70°C	0.50	1.42	2.13
3.26	70–110°C	1.46	1.89	2.09
4.8	30–70°C	0.41	1.16	1.91
4.8	70–110°C	1.00	1.20	1.63

of 2%, 3.5%, and 4.5%, from which it is seen that the above trends are clearly observed.

The vertical shift factors required for time–temperature superposition are shown in Fig. 15, referenced to 135°C. The trend is the same as that observed for the time shift factors, with a relatively rapid change at temperatures a little below T_g followed by a leveling off at temperatures far removed from T_g. Although the vertical shifts between adjacent temperature curves is small, over a broad temperature range the cumulative effect can be significant, in this case leading to a maximum vertical shift of approximately 25% over the temperature range 30–135°C. Note though that the vertical shifts are still small in comparison to the orders of magnitude by which the time scale is shifted. The shifts imply that the material is becoming intrinsically stiffer at lower temperatures. This may

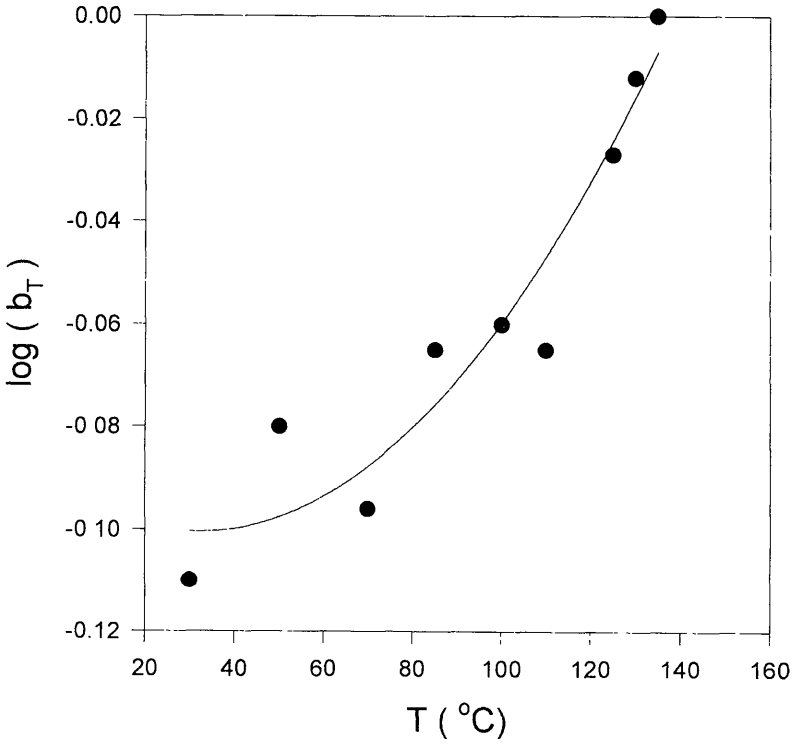

Figure 15 Vertical shift factor for polycarbonate from time–temperature superposition at 2% strain and a log [aging time (s)] of 4.80.

be reasonably expected since from thermal expansion effects alone the material will be denser at lower temperatures.

C. KWW Analysis of Temperature Data

In the following, we performed the KWW analysis in two ways. We first took the master curve obtained above and asked if it could be described by a KWW function. We then looked at the results from fitting KWW functions at each temperature and asked what the apparent change in KWW parameters would be as a function of temperature.

The time–temperature master curve of Fig. 12, determined using the "semimanual" method outlined above, is replotted in Fig. 16 and compared to a KWW

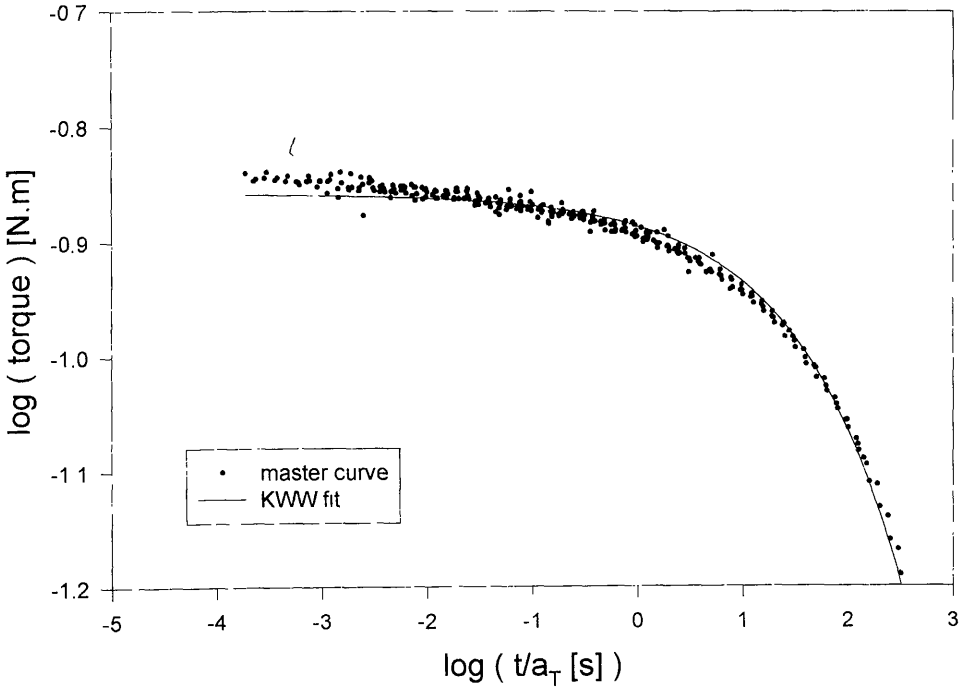

Figure 16 KWW fit to the time–temperature master curve for polycarbonate at 2% strain and a log [aging time (s)] of 4.80. Data referenced to 135°C. (See Table 3 for KWW parameter values.)

Table 3 KWW Parameters from Fit to the Time–Temperature Master Curve

KWW parameter	Value
M_0	0.139
τ	3.85×10^3
β	0.43

fit to these data (the fitting parameters are shown in Table 3). It is immediately clear that the KWW equation does not adequately describe the relaxation behavior over the whole range of data. This is surprising because the individual datasets at each temperature did appear to be described very well by the KWW equation. So, although the KWW expression will fit the data over a short time scale (approximately four decades), the error in the fit begins to show up when longer time scales are used (approximately seven decades).

The KWW equation was applied to the data at each temperature, with no restrictions on the parameters, and the resulting fitting parameters are shown in Table 4. The characteristic relaxation time, τ, decreases with increasing temperature, showing clearly that the relaxation response shifts to very much shorter time scales at higher temperatures. The zero time torque response, M_0, shows a systematic decrease with increasing temperature, possibly indicating an increase in the compliance of the material. However, since it was also found that the β

Table 4 KWW Fit Parameters to Relaxation Data at Each Temperature with No Restrictions on the Parameters

T (°C)	M_0 (N.m)	τ (s)	β
30	0.196	1.18×10^8	0.20
50	0.188	4.04×10^9	0.13
70	0.199	1.35×10^7	0.24
85	0.176	1.28×10^7	0.22
100	0.170	2.47×10^5	0.36
110	0.182	2.47×10^5	0.33
125	0.153	3.22×10^4	0.37
130	0.147	7.26×10^4	0.41
135	0.136	6.68×102	0.47

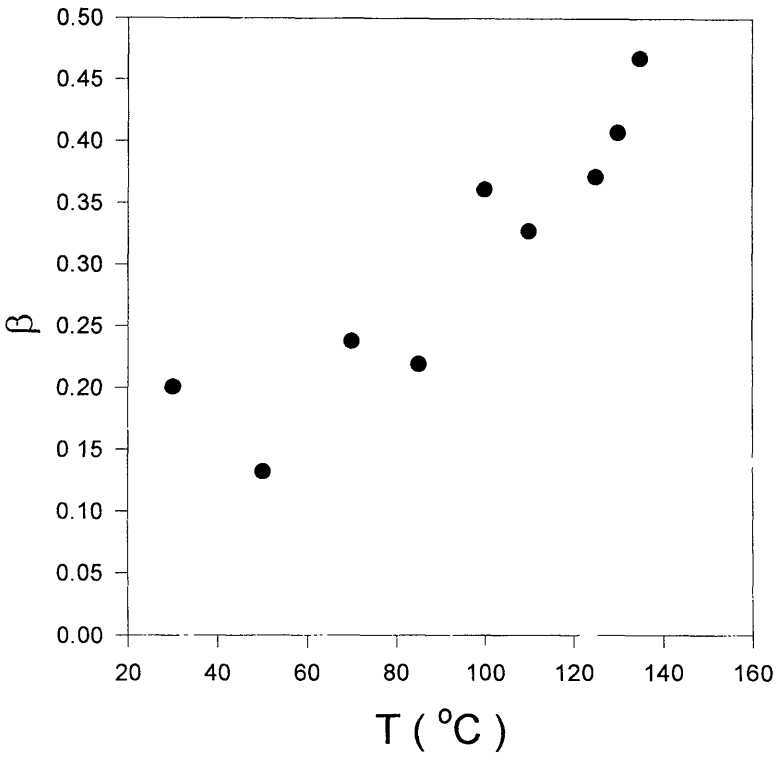

Figure 17 KWW β parameter as a function of temperature for polycarbonate at 2.0% strain and a log [aging time (s)] of 4.80.

term shows a systematic increase with increasing temperature (Fig. 17), then neither τ nor M_0 values at each temperature can be directly compared, since they are essentially derived from a different response curve. Furthermore, the variation in the β parameter with temperature, if taken literally and on the assumption that the master curve is described by a KWW function, implies that time–temperature superposition does not apply to these data. However, above we have shown that a very good master curve representation of the data can be obtained by using time–temperature superposition. We interpret the result of the present analysis to show that the KWW parameters are not strongly determined using the limited time window (which is typical of mechanical tests) available here. Further, it shows the danger of interpreting limited data in terms of the KWW parameters.

We also note that the master relaxation curve was not well described by a KWW function.

D. LeGrand–Bendler Analysis of Temperature Data

Here we follow the LeGrand-Bendler [19] approach to the analysis of relaxation data. The analysis was performed in much the same way as for the KWW analysis. The stress relaxation data at 2% strain and an aging time of 64,800 s were analyzed at each temperature using Eq. (3), with no restrictions placed on τ_0, β, M_r and ΔM. The resulting M_g and M_r values as a function of temperature are shown in Figs. 18 and 19, respectively. If the unrelaxed torque response, M_g (Fig. 18), is taken to be at least broadly related to the glassy modulus, then the data indicate a systematic decrease in the modulus with increasing temperature. This

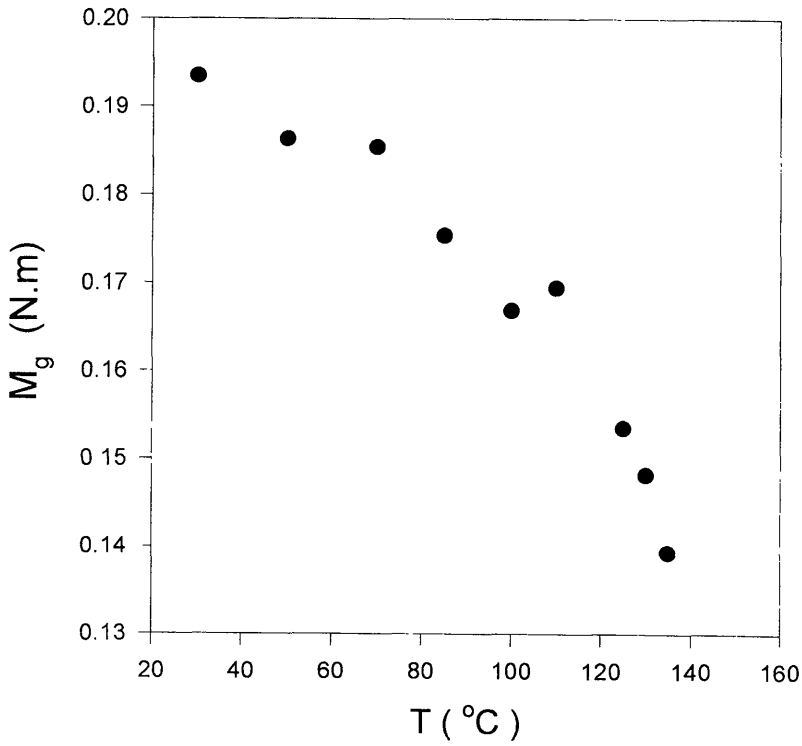

Figure 18 M_g for polycarbonate from the LeGrand-Bendler analysis.

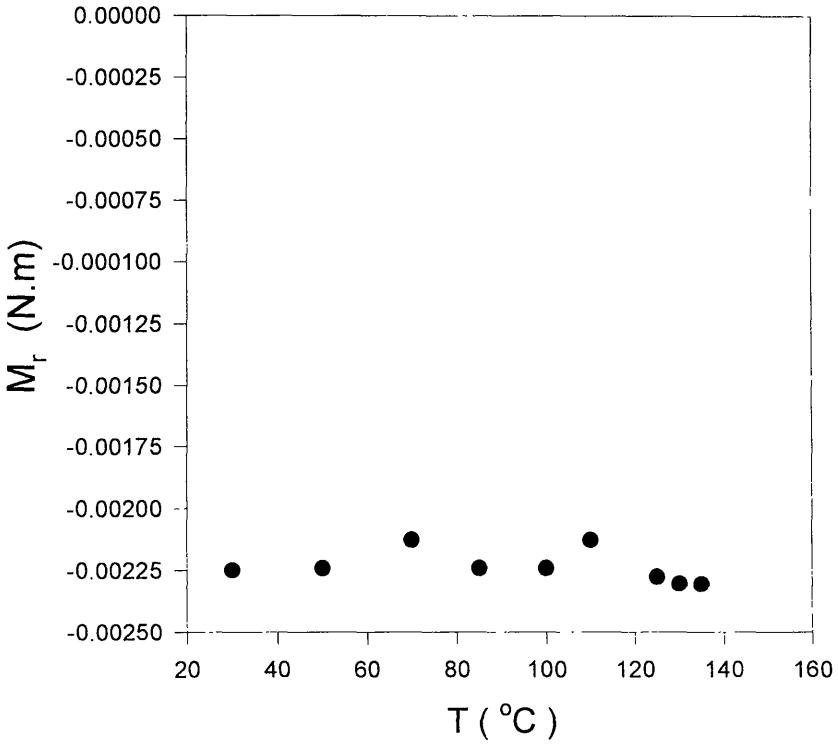

Figure 19 M_1 for polycarbonate from the LeGrand-Bendler analysis.

is consistent with the previous KWW analysis where the zero time torque response, M_0, was seen to decrease with increasing temperature (thus necessitating vertical shifts). The relaxed torque response, M_1, which may be taken to be related to the rubbery modulus, is small and relatively independent of temperature (see Fig. 19). The observation that the values are negative is physically inconsistent. However, since the rubbery modulus is expected to be approximately three orders of magnitude smaller than the glassy modulus, and these data are essentially obtained from extrapolation of the data far beyond the range of the experimental results, this result may be due to the data being insufficient to accurately determine M_r. The β values determined from both the KWW and LeGrand-Bendler analyses are shown in Fig. 20. The agreement between the two is very good, though this is perhaps not surprising since the very small magnitude of the M_1 term in the LeGrand-Bendler analysis means that it is dominated by what is essentially the KWW function. We do note that the prior analyses performed by Le-

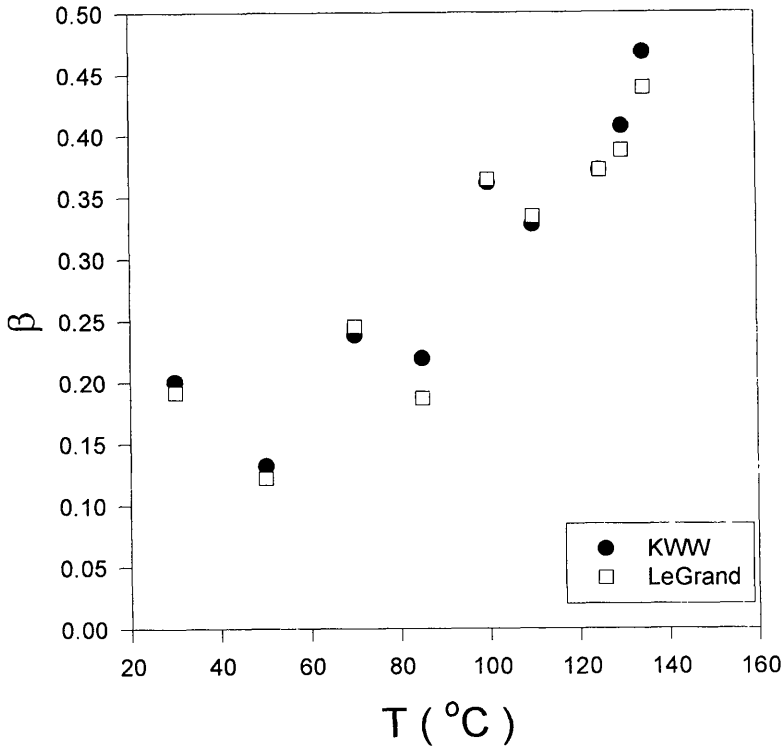

Figure 20 Comparison of β vs. T for polycarbonate from KWW and LeGrand-Bendler analyses at 2% strain and a log [aging time (s)] of 4.80.

Grand and Bendler [19] have considered uniaxial extension results rather than shearing results as was the case here. In this case, it is conceivable that the M_t term is related to a bulk relaxation rather than the rubbery plateau. This speculation requires further investigation.

V. CONCLUSION

Time–aging time superposition is valid for polycarbonate for temperatures from 30°C to 135°C and for strains covering the linear and nonlinear range up to the yield point. The KWW equation fits the data for time scales up to the order of

four decades and the β term appears to be relatively independent of aging time.

The aging behavior of this polycarbonate is significantly different from that reported by Struik. The aging time shift rate, μ, is found to be less than unity and nonconstant from 30°C to 135°C. In addition, while at lower temperatures μ is found to decrease with increasing strain, at higher temperatures it is found to be independent of strain. To our knowledge, this is the first report of such a result.

There is an indication that time–aging time superposition is applicable for strains above the yield point. This is true whether the sample is subjected to either a sequential or an individual loading history, though the apparent shift rate is different in each case.

Time–temperature superposition applies to polycarbonate at strains up to 4.5% torsion over the temperature range 30–135°C. The KWW function does not adequately describe the master curve. Furthermore, interpretation of individual KWW parameters obtained from data at each temperature leads to a spurious appearance of a temperature-dependent β and a breakdown of time–temperature superposition.

In addition to the change in time scale of the relaxation response at different temperatures and aging times, there is also a change in the zero time or intrinsic stiffness, with the material becoming inherently stiffer at lower temperatures and longer aging times. In all cases, the magnitude of the vertical shift is small in comparison to the shift in time scale. The vertical aging time shift appears to be independent of both temperature and applied strain level (within the scatter of the experimental results), yielding an increase in modulus of approximately 2% per decade of aging. The vertical temperature shifts follow closely the trend seen in the time–temperature shifts, with a relatively rapid change at temperatures a little below T_g and a gradual leveling off at temperatures far below T_g. The maximum vertical shift of approximately 25% should be compared to the corresponding time shift of approximately 10^4.

Application of the LeGrand-Bendler analysis gave the same qualitative and very similar quantitative results as those obtained from the KWW analysis. This was due to the very small magnitude of the M_r term we obtain from their model, and it remains to be seen as to which form is better suited for the description of the relaxation behavior.

Finally, it has been demonstrated that the use of reduced time concepts (aging time, temperature) shows promise as an efficient method of obtaining material parameters for polymer glasses in the nonlinear deformation range over a wide range of aging times and temperatures. However, the complicated temperature and aging shift dependences need to be mapped in some detail to obtain a full description of the behavior of the polycarbonate.

REFERENCES

1. W. C. Bushko and V. K. Stokes, *Polym. Eng. Sci, 35*(4): 291 (1995).
2. R. A. Malloy, *Plastic Part Design for Injection Molding*, Hanser Publishers, New York, 1994.
3. J. J. Pesce and G. B. McKenna, *Society of Plastic Engineers* Antec 1932 (1995).
4. J. Niemiec, C. Schultheisz, C. Shutte, and G. B. McKenna, *Society of Plastic Engineers* Antec 2402 (1995).
5. Certain commercial materials and equipment are identified in this chapter to specify adequately the experimental procedure. In no case does such identification imply recommendation or endorsement by the National Institute of Standards and Technology, nor does it necessarily imply that the product is the best available for the purpose.
6. *Natl. Thermoplastic Eng. Design Assoc. Newslett. 1*: 1 (1991).
7. J. D. Ferry, *Viscoelastic Properties of Polymers*, John Wiley and Sons, New York, 1980.
8. W. A. Findley, J. S. Lai, and K. Onaran, *Creep Relaxation of Nonlinear Viscoelastic Material*, North-Holland, New York (1976).
9. I. M. Ward, *Mechanical Properties of Solid Polymers*, John Wiley and Sons, New York, 1983.
10. I. L. Hopkins, *J. Appl. Phys. 24*: 1300 (1953).
11. W. Philippoff, *J. Appl. Phys. 25*: 1102 (1954).
12. D. J. Plazek and A. J. Chelko, *J. Polymer 18*: 15 (1977).
13. P. E. Rouse, *J. Chem. Phys. 72*: 3746 (1953).
14. J. G. Kirkwood, *J. Chem. Phys. 14*: 51 (1946).
15. H. Leaderman, *Elastic and Creep Properties of Filamentous Materials and Other High Polymers*, Textile Foundation, Washington, D.C., 1943.
16. F. H. Muller, *Kolloid-Z 114*: 2 (1949).
17. F. Kohlrausch *Pogg. Ann. Phys. 12*: 393 (1847).
18. G. Williams and D. C. Watts, *Trans. Faraday Soc. 66*: 80 (1970).
19. D. G. LeGrand, W. V. Olszewski, and J. T. Bendler, *Thermochem. Acta. 166*: 105 (1990).
20. A. J. Kovacs, *Fortschr. Hochpolym.-Forsch 3*: 394 (1964).
21. G. B. McKenna, *Glass formation and glassy behavior*, in *Comprehensive Polymer Science. Vol. 2. Polymer Properties* (C. Booth and C. Price, eds.), Pergamon Press, Oxford, 1989.
22. L. C. E. Struik, *Physical Ageing in Amorphous Polymers*, Elsevier, Amsterdam, 1978.
23. G. McKenna and A. Kovacs, *Polym. Eng. Sci. 24*: 1138 (1984).
24. H. Markovitz, Superposition in rheology. *J. Polym. Sci. Symp. 50*: 431 (1975).
25. J. L. Sullivan, Y. F. Wen and R. F. Gibson, Fundamental Aspects of Composite Viscoelastic Behavior, In: Use of Plastics and Plastic Composites: Materials and Mechanics Issues, ed. by V. K. Stokes, MD-vol. 46, ASME, New York (1993) pp 195–206.
26. R. W. Penn and E. A. Kearsley, *Trans. Soc. Rheol. 20*: 227–238 (1976).
27. R. Zorn, G. B. McKenna, L. Willner, and D. Richter, *Macromolecules 28*: 8552 (1995).

11
Annealing of Polycarbonates

Donald G. LeGrand
General Electric Company, Schenectady, New York

I. INTRODUCTION

When an amorphous polymer such as bisphenol A polycarbonate (BPA-PC) (1) is rapidly cooled from the liquid state into the glassy state, it is not at thermodynamic equilibrium but rather in a metastable condition. Such glasses contain excess volume as well as residual thermal and orientational strains and stresses (2–4). Annealing is one method whereby the residual strains, stresses, and orientation can be reduced or eliminated and has been defined as the tempering of materials by heat in the case of inorganic glasses and metals. In the case of thermoplastics, it is the process used to relax residual thermal stresses and to recover residual orientational strains (5–16). It is normally performed just below the glass transition temperature (T_g) of the material to reduce residual thermal strains and stresses and slightly above the glass transition temperature to remove orientation. Annealing is a secondary operation. Changes may also be observed in the volume and the thermal, mechanical, optical, and dielectric properties when samples are allowed to age at temperatures between the low-temperature β transition and the glass transition over long periods of time (15–24). These changes occur as a result of internal processes in the absence of external forces. This process is known as physical aging because of the changes in the physical properties (6). It is clear that the terms *annealing* and *physical aging* are being used to describe some of the same phenomena.

The purpose of this chapter is to outline the reasons behind the necessity for annealing; to examine the use of annealing as an operation that can be used after different methods of fabrication of engineering thermoplastics such as injection molding, extrusion, thermoforming, etc.; and to suggest alternative ways of

achieving the same goal by making changes in tool design, molding conditions, cycle times, packing pressures, and material selection including additives.

II. WHY ANNEAL?

There are several reasons for annealing injection-molded, blow-molded, or extruded parts made from BPA-PC. First, samples may exhibit crazing and/or cracking after standing only a short time at room temperature or after a long time under various environmental conditions in the field. Second, secondary finishing operations involving the application of organic and inorganic liquids may lead to either a delamination of a surface layer or to crazing and cracking. Finally, premature failures as a result of simple mechanical cycling as well as long-term thermal cycling in the presence of moisture may be reduced. There are also reasons for *not* annealing. First, annealing is a secondary finishing operation. Second, it requires an investment in equipment and space. Third, it requires time and people. Finally, annealing can reduce the impact performance of the material as well as its thermochemical shock resistance.

III. MACROSCOPIC PICTURE

Unlike metals, polymers are poor thermal conductors. As a result, if polymers are rapidly cooled from the melt into the glassy state, the properties at the surface will be different from those in the center (20–24). The asymmetry of these effects will depend on the geometry of the sample, whereas the magnitude will depend on the rate of cooling. As simple examples, consider the thermal quenching of a sphere, a cylinder, and a rectangle as shown in Fig. 1a–c. In the case of the sphere, there will be both radial and tangential thermal strains that will vary from the center to the boundary and will give rise to a radial (hydrostatic) stress that will vary from compressive at the boundary to tensile in the center. Similarly, the thermal strains in the cylinder will vary along the long axis of the cylinder except near the ends and again will vary from the center to the outer radius. In the case of the rectangle, one will have a varying thermal strain through the sample and at all edges and corners. A simple example for the case of the rectangle is shown in Fig. 2. In this example, it is assumed that the sample is composed of several plies of the same material and that initially each ply is not connected, but that the rate of thermal quenching is dependent on the position of the different plies, i.e., outside plies are cooled faster than internal plies. The overall effect as illustrated in Fig. 2 is that the plies have different lengths upon cooling from T_0 to T_g. If the plies are now made to be of the same length due to application of tensile stresses to the interior plies and compressive stresses to the exterior

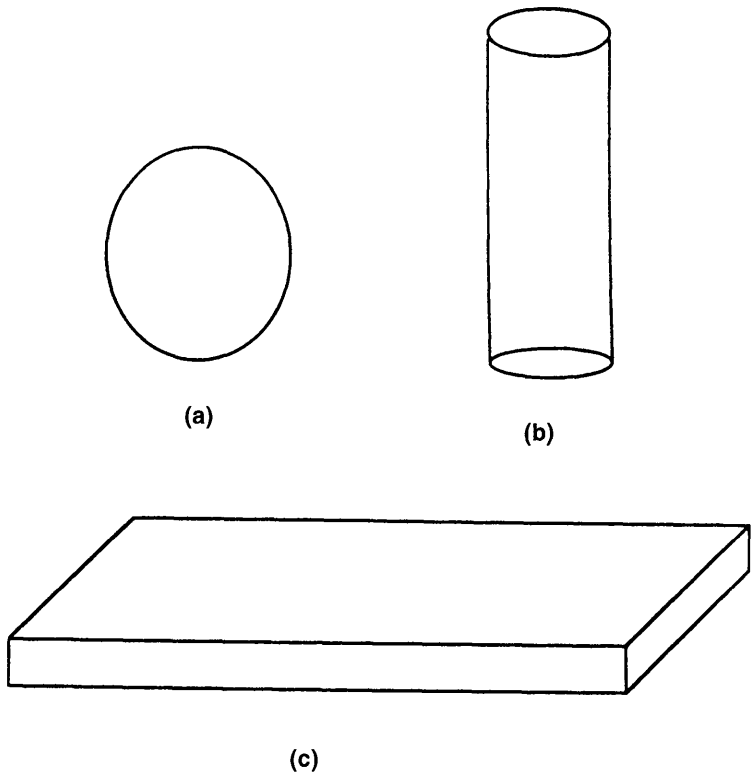

Figure 1 Effect of geometry of the part on the type of residual thermal strains and stresses that develop as a result of thermal quenching. (a) *Spherical geometry.* In this case, there will be radial gradient in the residual thermal strains and stresses. (b) *Cylinder.* In this case, the thermal strains along the major axis will be constant except near the ends of the cylinder and there will be gradient from the center to the outside. (c) *Rectangle.* in this case, the in-plane strains and stresses will be constant along the long axes except near the ends and will vary throughout the thickness.

plies until the structure is at mechanical equilibrium, then the overall stress distribution would be nominally parabolic if the material were perfectly elastic. Since BPA-PC is anelastic, there will be a partial relaxation of these stresses. If the part was fabricated by injection molding, then an oriented skin will be superimposed on the thermal strains. The process that causes this oriented skin has been called "fountain flow" and is illustrated in Fig. 3. The hot melt flows between the cold plattens of the mold, and as the outer surface of the melt contacts the wall it is frozen while the core of the melt flows between it. Another process

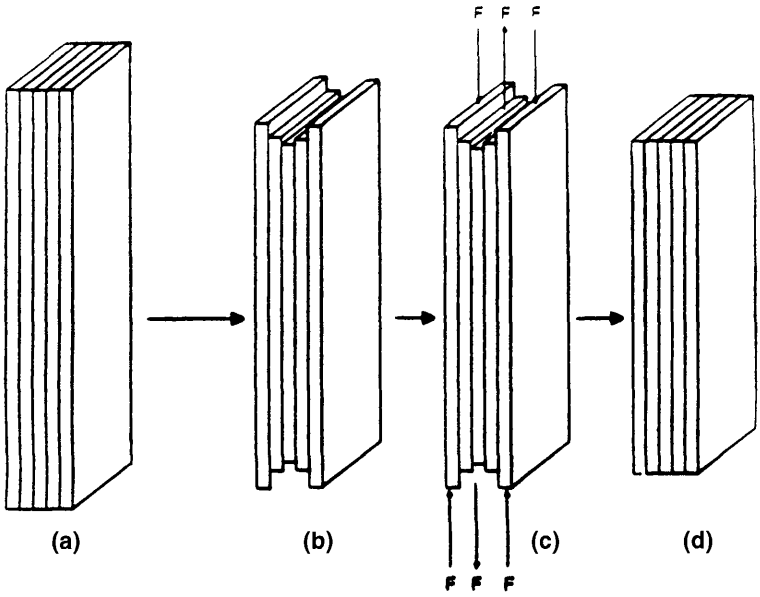

Figure 2 Schematic of the sample. (a) Sample at elevated temperature where $T_0 > T_g$. (b) Sample cooled to below its T_g in an unbonded configuration. (c) Forces applied to the plies to force them to be of equal length and in mechanical equilibrium. (d) Average length.

that occurs during the filling of the part and can cause orientation is extensional (or elongational) flow. This latter process occurs whenever the amount of surface area at the melt front is increasing, as illustrated in Fig. 4.

The effects of restraint by the mold as a result of packing pressure have been neglected in the preceding, i.e., it has been assumed that the part could

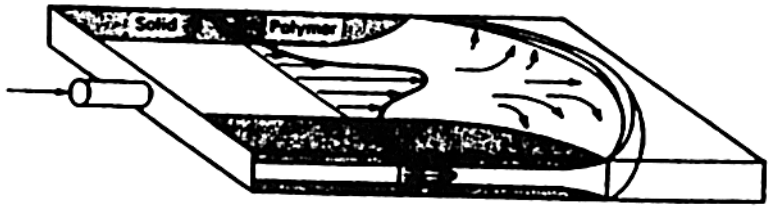

Figure 3 Schematic representation of the flow of a polymer melt between two parallel cold walls.

Figure 4 Schematic representation of elongational flow in a tool.

freely undergo dimensional changes (20). In the case of injection molding, the effect of packing pressure can lead to a significant change in the molding process in terms of both the physical and mechanical properties of the part for several reasons (27). First, the thermal history may be modified because pressure will increase the T_g of the material and may also change its thermal conductance of the material. Second, the volume of the pressurized melt in the core will be smaller whereas that of the glass in the outside layer will be larger. Third, upon release from the tool, the sample will initially want to expand and, depending on the temperature of the core and the packing pressure, can lead to an inversion of the overall residual thermal strains and stresses.

Chemical degradation of BPA-PC occurs by several mechanisms. The two mechanisms most commonly involved in practice are hydrolysis and photodegradation (28–31). In the former, long-term exposure of BPA-PC to moisture and heat in the presence of either acids or bases results in hydrolysis of the carbonate linkage (see Fig. 6, p. 261). This phenomenon has been shown to be accelerated by the presence of glass fibers and other fillers. Correspondingly, photodegradation can occur via photo-Fries rearrangement or by photooxidation. These latter processes can be partially inhibited by the use of surface coatings and the addition of photostabilizers.

IV. MOLECULAR PICTURE

At the molecular level, polymer molecules are thermally activated in the melt to rearrange in order to minimize the free energy of the system. This process occurs via several different mechanisms that may include changes in their configuration, conformation, and in the way that they pack. At short times during injection molding, bond bending and distortion can occur and lead to the storage of elastic

energy. If the sample is quickly cooled from the melt, then it is easy to visualize that some of the configurations and conformations that were present in the melt can get trapped in the glass if the rate of cooling is fast enough. The number of conformers that are trapped will depend on the energy wells in which they reside and the rate of quenching. In the case of BPA-PC, the cis-trans configuration is the preferred conformation at higher temperatures, i.e., the melt, whereas as the temperature is lowered the trans-trans conformation is the preferred one (32). One of the unique features of these different conformations is that the cis-trans conformer is shorter than the trans-trans conformer as illustrated in Fig. 5. This difference in conformation is believed to alter the packing volume and may be interpreted as an excess volume or free volume. As a result, when BPA-PC molecules are strained or stressed, one mechanism by which they can relieve the stress is to undergo a conformational change as illustrated in Fig. 5 for a single section

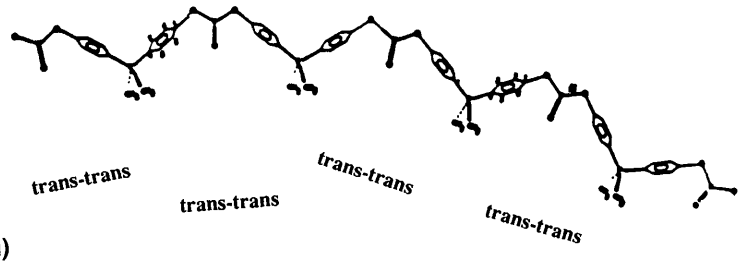

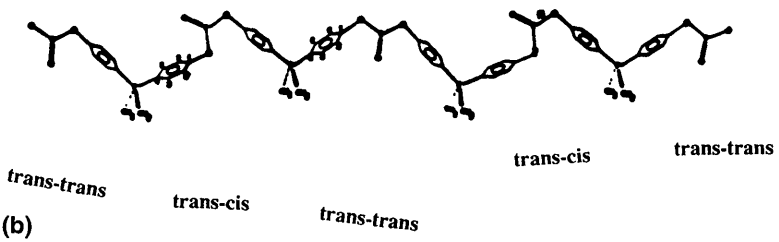

Figure 5 Two possible structures of BPA-PC. (a) The all-trans structure, which has been proposed to exist in the crystal; (b) a chain consisting of alternating units of cis-trans and trans-trans conformers.

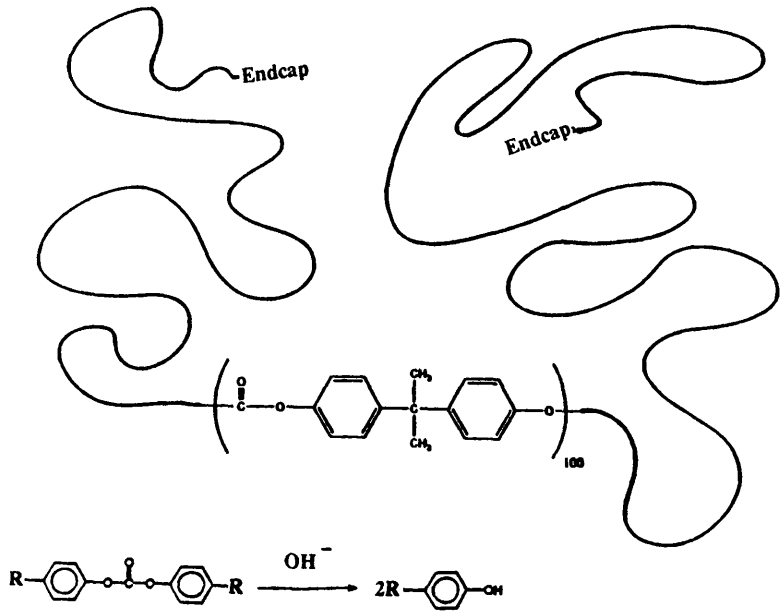

Figure 6 A picture of a section of a long-chain BPA-PC molecule that can undergo hydrolysis as a result of long-term exposure to temperature and moisture.

of a molecule where the length of the section is increased by the conversion of the cis-trans conformers to trans-trans conformers.

During annealing and physical aging, it is believed that the residual internal elastic strains undergo a relaxation process wherein they are partially converted to anelastic and plastic strains (33). This process can involve the relaxation of internal distortions in the chain and occur by the conversion of the cis-trans conformers to trans-trans conformers, which is the more stable form. Residual molecular orientation will be partially relaxed by heating near the glass transition temperature and totally relaxed by heating above the glass transition temperature.

V. METHODS OF ANNEALING

The most common methods of annealing BPA-PC have involved the use of liquid baths and air ovens. More recently, the use of infrared radiation has been patented and discussed as a new and novel technique (34,35). The use of liquid baths ensures a more rapid heating of the part because of the higher heat transfer than

in the case of a circulating air oven. Infraradiation will heat the part more quickly than either of the above, but since this technique depends on the absorption of the infraradiation, it will be limited to simple geometrical structures such as flat sheets or it will be necessary to set up a complex array of infraradiation devices to ensure uniform heating. One of the disadvantages of the liquid baths is that the choice of liquid is limited to high boilers that may be absorbed by the article during the annealing and ultimately be a contributing cause of failure.

One of the major questions in regards to annealing is, "How effective were the annealing conditions which were used?" Several techniques have been used to address this question. The molding shop will frequently use a solvent stress test wherein the article is immersed in or contacted with a mixture of simple organic liquids. The test mixture for BPA-PC consists of ethyl acetate with varying amounts of either methanol or hexane. The sample is placed in contact with the liquid for 1–3 min and is examined for crazes and cracks immediately after removal from the liquid mixture, 1 h later, and 24 h later. This test method has been in use for almost 30 years because of its simplicity. However, there is and has been a need to replace this method because tested parts cannot be recycled within the molding shop and the test results may not correlate with field problems. Alternative methods such as mechanical slicing, photoelastic stress analysis, x-ray diffraction, and sonic moduli have been actively investigated as possible tools. Each of these techniques has its limitations. Currently, new NDE methods such as impulse-stimulated scattering and polarized ultrasonic imaging are being investigated.

VI. TOOL DESIGN

One of major difficulties in the fabrication of BPA-PC by injection molding involves the design of the tool including the gates, the runners, and the sprue (25). Tool designs that increase the tendency for early failure include small runners that result in a loss in machine pressure being transmitted to the cavity and small gates that cause rapid gate freeze-off. Long flow distances and thin walls may give rise to excessive gases at the gas vents, loss of pressure at the end of flow, gradients in the skin thickness, and shear degradation. Finally, thick bosses, ribs, etc., can result in sink marks that can only be eliminated by applying excessive packing pressures. Deep vents can act as condensation traps for nonaqueous volatile compounds that may initiate crazing and cracking.

Current software that has been developed over the past 20 years in order to address how a mold fills has been based on the use of constitutive equations of state that simulate the properties of materials either under steady-state isothermal conditions and/or at small strains in simple shear, and further assumes no thermal- or shear-induced degradation of the material. Clearly, injection molding is

a transient process wherein the material is required to undergo significant deformation in complex flow geometries. As a result, there exists a need to investigate and evaluate the behavior of BPA-PC under such conditions.

VII. PROCESSING CONDITIONS

It has been clear for some time that the processing conditions can play an important role in the ultimate behavior of injection-molded and extruded BPA-PC. One of the more critical parameters is the melt temperature because of increased contraction during cooling, increased volatilization of low-boiling additives, and the possibility of both thermal degradation and shear degradation. Mold temperature and packing pressure are known to change both the magnitude and direction of the residual stresses, i.e., at low packing pressures a compressive stress is observed at the surface while the interior is in tension, whereas at high packing pressures a tensile stress exists at the surface while the interior is in compression (27). Low mold temperatures are also known to increase the skin thickness, to reduce flow, and can lead to early gate freeze-off. Low holding pressures and short holding times can cause increased core contraction during cooling.

The cycle time to produce a part is based on two factors that involve a compromise between business and technology. Long cycle times while reducing the level of residual internal stresses are not cost-effective, whereas short cycle times may lead to unstable products. As mentioned earlier, injection molding is a transient process.

VIII. MECHANICAL PROPERTIES

It has long been known that several of the mechanical and physical properties of BPA-PC are affected by annealing (5–16,33–38). Early work by Krumm and Muller indicated that there were changes in the dielectric response of thermally aged BPA-PC. Subsequent work by Golden and Hazell, LeGrand, and others demonstrated that annealing below the glass transition temperature caused the notched Izod impact strength to be reduced from 16 to 1–2 ft-lb per inch of notch with corresponding changes in the yield stress and the density. Struik observed changes in the creep behavior upon aging between the low-temperature β transition and the glass transition (18). More recently, it has been reported that annealing also results in changes in the relaxation moduli, in thermally activated recovery of residual internal strains, and in thermally stimulated relaxation and creep (33). It is important to point out that these effects are dependent on the molecular weight of the BPA-PC that is being used, its thermomechanical history, and the presence of additives and fillers. Long-term failure is due in part to the environ-

ment in which BPA-PC is used and in part to the presence of residual internal orientation and stresses. The presence of flaws such as nicks and scratches in the surface as well as defects such as gel particles and foreign heterogeneities within the material can locally enhance global stresses. Alteration of the residual stresses as a result of thermal cycling can lead to both physical aging (annealing) and to mechanical fatigue. Correspondingly, the sorption and desorption of moisture can lead to changes in the residual stresses and strains; if this sorption process occurs in the presence of acids or bases, then chemical degradation might occur. Crazing and cracking of BPA-PC as a result of contact with a variety of chemicals has long been recognized as intermolecular disruption of the polymer molecules. More recently, it has been reported that while thermal shocking of BPA-PC into water does not cause crazing or cracking, thermal quenching into a variety of simple organic liquids and solutions can lead to both crazing and cracking (19). Furthermore, it was observed that annealing caused the amount of crazing and cracking to increase.

IX. SUMMARY

The use of annealing as a method to reduce residual stresses, frozen-in orientation, and excessive dimensional changes in BPA-PC should be considered only after every effort has been made to optimize molding conditions and modifications in the design of the tool including the runner and the sprue. It should be understood that annealing might cause embrittlement and accelerate both mechanical and chemical failure.

REFERENCES

1. W. F. Christopher and D. W. Fox, *Polycarbonates*, Reinhold, New York, 1962.
2. R. Greiner and F. R. Schwarzl, *Rheol. Acta 23*:278 (1984).
3. M. Washer, *Polymer 26*:1546 (1985).
4. R. Wimberger-Friedl, G. Prast, A. V. Kurstjens, and J. G. Bruin, *J. Polym. Sci. B: Polym. Phys. 30*:83 (1992).
5. D. G. LeGrand, Annealing. In: Mark, Bikales, Overberger, Menges, eds. *Encyclopedia of Polymer Science and Engineering*, 2nd Ed. John Wiley & Sons, Inc., New York, 1985, vol. 2, p. 43.
6. L. C. E. Struik, *Internal Stresses, Dimensional Stabilities, and Molecular Orientation* in Plastics, John Wiley and Sons, Chichester, 1991.
7. D. G. LeGrand, XI Intern. Congress on Rheology, Brussels, Belgium, 1992.
8. J. Bartos, J. Muller, and J. H. Wendorf, *Polymer 32*:3861 (1990).
9. F. Krumm and F. H. Muller, *Kolloid Z. 164*:8 (1959).
10. K. H. Illers and H. Breuer, *J. Colloid Sci. 18*:1 (1963).

11. J. H. Golden, B. L. Hammant, and E. A. Hazel, *J. Polym. Sci. A2*:4787 (1964).
12. J. H. Golden, B. L. Hammant, and E. A. Hazel, *J. Appl. Polym. Sci. 11*:1571 (1967).
13. D. G. LeGrand, *J. Appl. Polym. Sci. 13*:2129 (1969).
14. R. J. Morgan and J. E. O'Neal, *J. Poly. Sci. Phys. Ed. 14*:1053 (1976).
15. A. J. Hill, K. J. Heater, and C. M. Agrawal, *J. Polym. Sci. B: Polym. Phys. 28*:387 (1990).
16. P. So and L. J. Broutman, *Polym. Eng. Sci. 16*:74 (1976).
17. N. G. McCrum, B. E. Read, and G. Williams, *Anelastic and Dielectric Effects in Polymeric Solids*, John Wiley and Sons, New York, 1967.
18. L. C. E. Struik, *Physical Aging in Amorphous Polymers and Other Materials*, Elsevier, Amsterdam, 1978.
19. D. G. LeGrand, *J. Appl. Poly. Sci.* (in press).
20. N. J. Mills, *J. Mater. Sci. 17*:558 (1982).
21. N. J. Mills, *Plastic Rubber Proc. Appl. 3*:181 (1981).
22. R. M. Shay and J. M. Caruthers, *Poly. Eng. and Sci. 30*:1266 (1990).
23. J. S. Yu, M. Lim, and D. M. Kaylon, *Polym. Eng. Sci. 31*:145 (1991).
24. A. Siegmann, A. Buchman, and S. Kenig, *Polym. Eng. Sci. 22*:560 (1982).
25. S. Middleman, Fundamentals of Polymer Processing, McGraw-Hill Book Co., New York, 1986.
26. A. A. M. Flaman, *Poly. Eng. Sci. 33*:193 (1993).
27. J. Greener, *Polym. Eng. Sci. 26*:534, 886 (1986).
28. A. Ram, O. Zilber, and S. Kenig, *Polym. Eng. Sci. 25*:577 (1985).
29. S. P. Petrie, A. T. DeBenedetto, and J. Miltz, *Polym. Eng. Sci. 18*:1200 (1978).
30. H. E. Bair, D. R. Falcone, and R. Merriweather, *J. Appl. Phys. 49*:4976 (1978).
31. M. Narkis, S. Chaouaat-Sibony, L. Nicholais, A. Apicella, and J. P. Bell, *Polym. Common. 26*:339 (1985) and references therein.
32. A. A. Jones, *Macromolecules 18*:902 (1985).
33. D. G. LeGrand, W. V. Olszewski, and J. T. Bendler, *Thermochimica Acta 166*:105 (1990).
34. D. G. Powell, ANTEC 93, p. 923.
35. K. Heidenreich, H. Depcik, and H. Radojewski, US Pat. 4,594,204, June, 1986.
36. J. F. Mandell, K. L. Mandell, and D. D. Huang, *Polym. Eng. Sci. 21*:1173 (1981).
37. J. R. McCloughlin and A. V. Tobolosky, *J. Polym. Sci. 7*:658 (1951).
38. W. Lethersich, *Proc. XI Cong. Pure Appl. Chem. 5*:591 (1947).

12

Degradation of Bisphenol A Polycarbonate by Light and γ-Ray Irradiation

Arnold Factor
General Electric Company, Schenectady, New York

I. INTRODUCTION

Bisphenol A polycarbonate (BPA-PC) is an important high-performance engineering thermoplastic well known for its combination of toughness, transparency, and heat resistance [1]. These properties make it an ideal material for use in demanding applications where it is exposed to external stresses such as ultraviolet (UV) light and sterilization by γ-ray irradiation. However, on extended exposure to these conditions BPA-PC slowly degrades, turning progressively more yellow and eventually leading to a decrease in its physical properties. Over the years there have been numerous studies of these degradative processes so as to better design more stable BPA-PC formulations. In this Chapter, the above chemistry will be reviewed, with special emphasis on correlating past work in these areas with more recent results.

II. PHOTODEGRADATION OF BPA-PC

A. Mechanisms of BPA-PC Photoaging

When unstabilized BPA-PC is exposed to UV light, such as that encountered during outdoor exposure, the surface of the resin will become yellow and often erode. The process is a surface phenomenon and generally extends only about

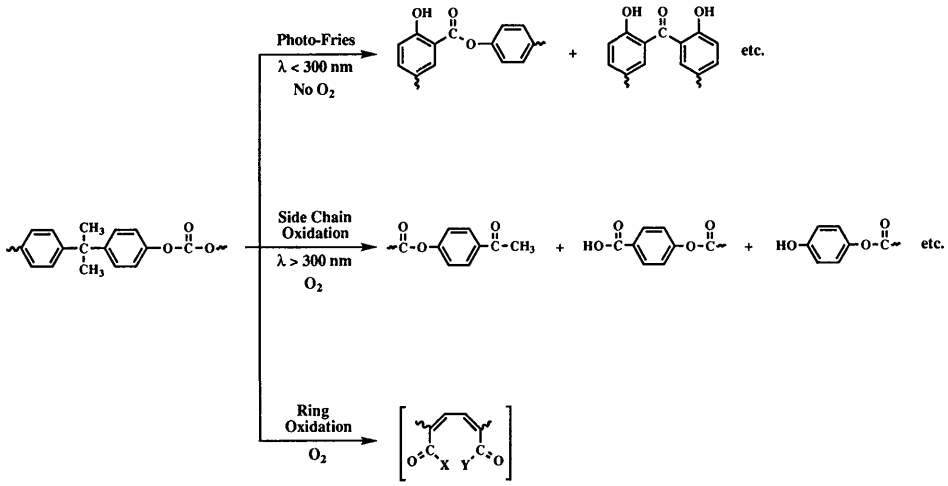

Scheme 1 The photochemistry of BPA-PC. (Reproduced from J. Kahovec ed., Macromolecules 1992, 345th IUPAC Int. Symp. on Macromolecules, Copyright 1993, pp. 517–526, with permission from International Science Publishers.)

25 μm into the exposed surface [2]. As indicated in Scheme 1, depending on the specific exposure conditions, the chemistry underlying these changes has been ascribed to three general processes: photo-Fries rearrangement and fragmentation/coupling reactions [3–7], side chain oxidation [2,8–16], and ring oxidation [8,9]. Recent spectral studies by Lemaire and coworkers [10,11] and Pryde [14] clearly illustrate that photo-Fries reactions are favored when light with $\lambda \leq 300$ nm is used, whereas photooxidation reactions were increasingly important as UV light of longer wavelengths was used. (A detailed description of the role of wavelength on the mechanism of BPA-PC photodegradation is given in Sec. II.C.) Nonetheless, the relative roles of each of the above reactions and the chemical nature of the compounds responsible for the observed color formation are not clear. To better answer these questions, we recently undertook a product study of an unstabilized sample of BPA-PC that had been exposed outdoors for 4 years in Florida. In this study, the weathered surface was removed by reductive cleavage with lithium aluminum hydride (LAH) and separately with lithium aluminum deuteride, and subsequently analyzed by tandem gas chromatography (GC/GC)–high-resolution mass spectroscopy (MS) [13]. In this way nearly 40 degradation products were characterized. The most important ones are listed in Fig. 1 and are grouped according to the most likely mechanism for their production. In order to analyze for higher molecular weight products, a direct-probe MS experiment

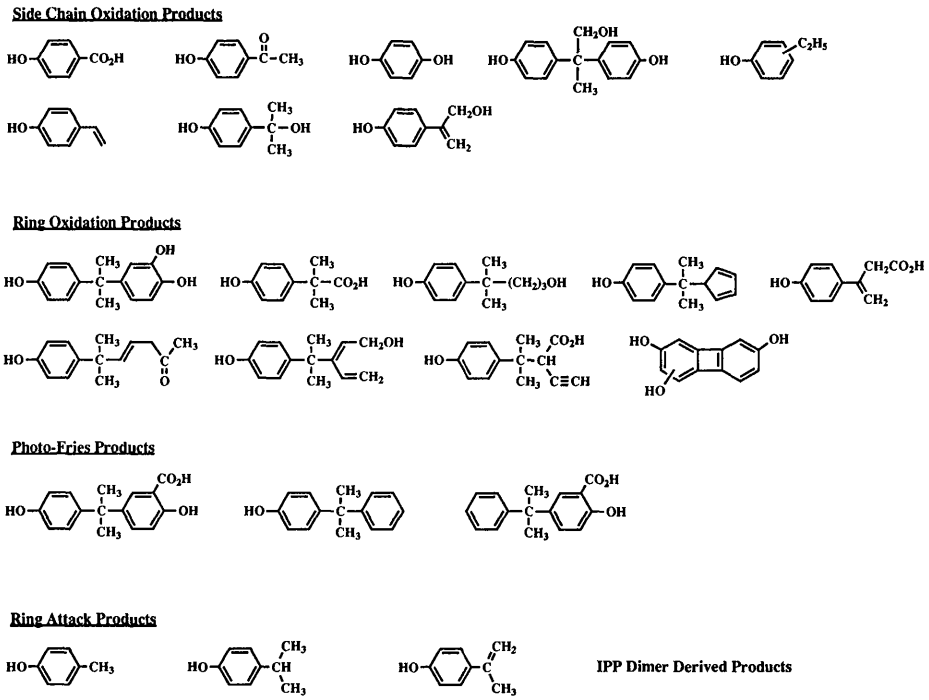

Figure 1 Key products identified by the tandem GC-GC/MS analysis of 4-year Florida-aged BPA-PC. (Reproduced from J. Kahovec ed. Macromolecules 1992, 345th IUPAC Int. Symp. on Macromolecules, Copyright 1993, pp. 517–526, with permission from International Science Publishers.)

was also carried out that revealed the presence of the BPA coupling products shown in Fig. 2. The production of these coupling products can best be rationalized by the occurrence of the photo-Fries fragmentation/coupling reactions illustrated in Scheme 2.

The results of these experiments indicate that the outdoor weathering of BPA-PC is quite complex and involves the operation of at least four processes: side chain oxidation, ring oxidation, photo-Fries rearrangement and fragmentation/coupling reactions, and ring attack reactions. Ring attack reactions were not previously reported and are thought to come about by a free radical reaction of phenolic end-groups with methyl radicals [13]. Most of the compounds found are not expected to be deeply colored; however, a few, such as the BPA resorcinol derivative listed in Fig. 1 and the ortho-coupled BPA products in Scheme 2, likely come from LAH reduction of highly colored *ortho*-quinone and *ortho*-

	m/e (daltons)	Empiracle Formulas	Proposed Structures
1	564.3	$C_{32}H_{48}O_3Si_3$	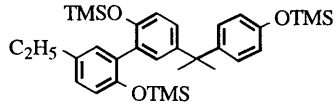
2	654.3	$C_{39}H_{54}O_3Si_3$	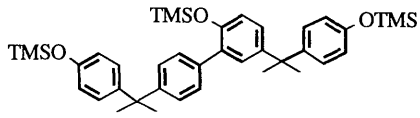
3	670.3	$C_{39}H_{54}O_4Si_3$	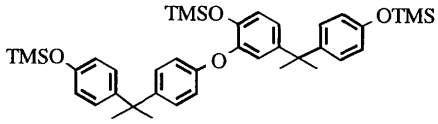
4	742.4	$C_{42}H_{62}O_4Si_4$	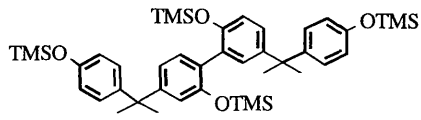
5	758.4	$C_{42}H_{62}O_5Si_4$	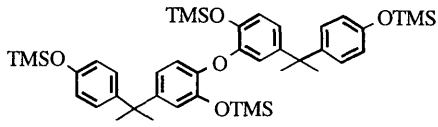

Figure 2 Direct probe MS analysis of the silylated $LiAlH_4$ reduction product from 4-year Florida-aged BPA-PC. (TMS stands for the $(CH_3)_3Si$ group.)

diphenoquinone structures. Even though the products of photo-oxidation predominate and the photo-Fries products constitute only a minor part of the product mixture from outdoor-weathered BPA-PC [2,13–15], the photo-Fries process likely plays a key role in the autocatalytic photooxidative process. During the initiation of the photodegradation process, the photo-Fries reactions are probably a major source of free radicals leading to photolabile oxidation products such as hydroperoxides and aromatic ketones, which in turn account for the final autocatalytic stage of BPA-PC photodegradation.

In an earlier study of BPA-PC photochemistry, Webb and Czanderna [12] found Fourier transform IR evidence for the presence of hydrogen bonding between free phenolic hydroxyl end-groups and the carbonyl of the carbonate group when the phenolic end-group concentration exceeded that of the water in the

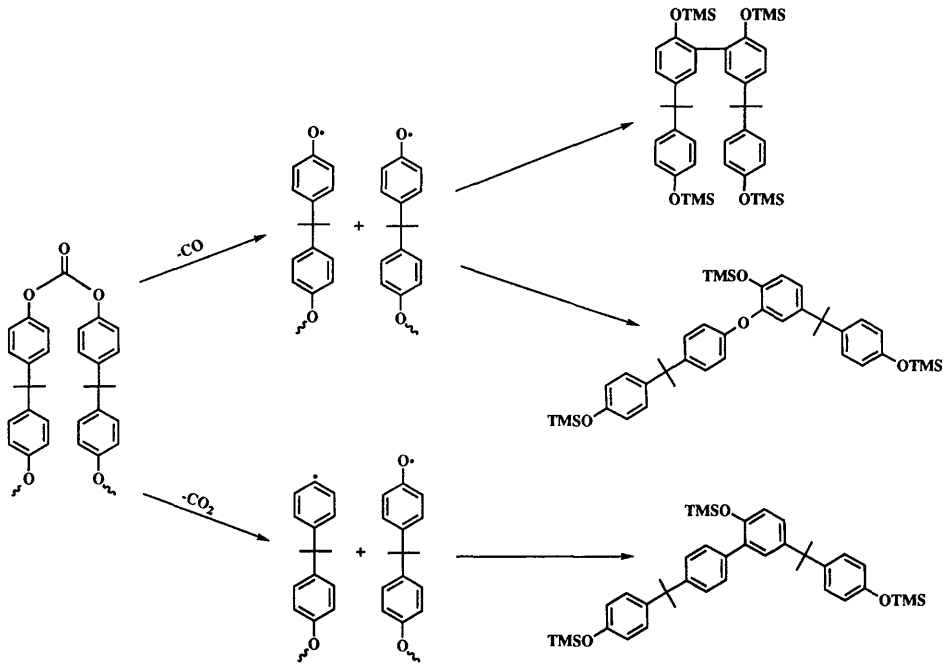

Scheme 2 Possible mechanism for the formation of higher molecular weight BPA-PC photoproducts. (TMS stands for the $(CH_3)_3Si$ group.) (Reproduced from J. Kahovec, ed. Macromolecules 1992, 345th IUPAC Int. Symp. on Macromolecules, Copyright 1993, pp. 517–526, with permission from International Science Publishers.)

polymer. They proposed that upon photolysis these hydrogen-bonded moieties underwent a hydrogen atom transfer reaction giving rise to reactive free radicals that led to crosslinking (Scheme 3). However, because commercial BPA-PCs are generally greater than 97% capped, this pathway probably does not play an important role in the early stages of BPA-PC photogradation. These reactions could very well be important in the later stages where, as shown by Moore [17], the concentration of phenolic end-groups becomes significant.

In recent publications by Hoyle and coworkers [18–20], fluorescence spectroscopy was used as an extremely sensitive tool for the detection of the primary products of the thermal degradation and photodegradation of BPA-PC. For example, short exposure in air to UV light having a λ_{max} of about 300 nm produced photo-Fries products such as salicylic acid and biphenolic species. Also, they found [18] that thermal treatment of BPA-PC in air or nitrogen at temperatures as low as 250°C gave rise to a structured fluorescence emission due mainly to the

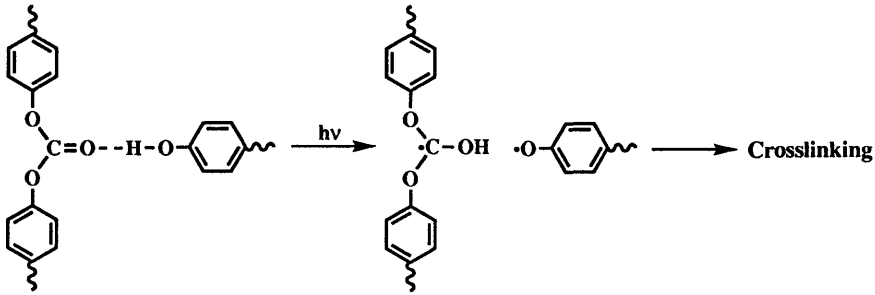

Scheme 3 Proposed photoreaction of hydrogen-bonded carbonate groups. (Reproduced from R. L. Clough, N. C. Billingham, and K. T. Gillen, eds. *Polymer Durability*, Advances in Chemistry Series *249*, Copyright 1996, pp. 59–76, with permission from the American Chemical Society.)

formation of dibenzofuran and phenyl-2-phenoxybenzoate. However, photolysis studies of representative BPA-PC thermal degradation products like dibenzofuran, BPA, and xanthone using broad-spectrum UV light with a λ_{max} of 305 nm showed that the presence of these structures in BPA-PC would not greatly affect the photodegradation of BPA-PC other than to form photoproducts that subsequently underwent photobleaching.

Finally, further proof of the occurrence of the photo-Fries process during outdoor exposure was provided by an experiment in which an unstabilized molded sample of BPA-PC was sealed under high vacuum (<0.13 Pa) in a Pyrex tube and exposed outdoors for 2.3 years in Schenectady, NY; after which time the sample was quite yellow with a change in yellowness index (ΔYI) of 31. Analysis by LAH reduction/GC-MS of the yellowed top surface revealed the presence of the following photo-Fries rearrangement and fragmentation/coupling products:

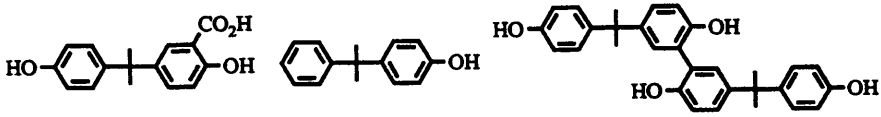

Note that as discussed before, the *ortho*-phenol coupling products, although not colored, can be easily oxidized to reactive *ortho*-diphenoquinones.

B. Source of Photoyellowing

From the previous research cited, we know that the photodegration of BPA-PC involves two major processes: the photo-Fries reaction and the oxidative attack

of the gem dimethyl groups and the aromatic groups of the BPA units. However, it is not known as to which of the two processes is the principal source of the yellow photoproducts found for BPA-PC. In an effort to shed more light on this question, the side chain free polycarbonate derived from 3,3′-dihydroxydiphenyl ether (BPO-PC) [21] and poly(oxycarbonyloxy-1,4-phenylenedimethylsilane-1,4-phenylene) (BPSi-PC) [22]—which is the polycarbonate based on bis(*p*-hydroxyphenyl)dimethyl silane—were prepared and evaluated in outdoor Florida exposure. Weathering of the side chain free BPO-PC showed that it photoyellowed about 3 times faster than BPA-PC; however, the importance of ring

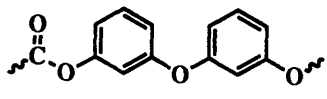

BPO-PC

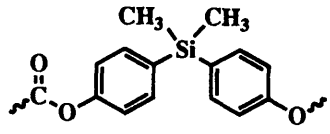

BPSi-PC

oxidation to photoyellowing was clouded because BPO-PC absorbed twice as much UV light as BPA-PC. In contrast, comparative weathering of BPSi-PC and BPA-PC films indicated that BPSi-PC was about five times more resistant to weathering than BPA-PC. This result can be attributed to the higher water repellency of BPSi-PC, the approximately 50% lower UV absorptivity, and the lower likelihood for side chain photooxidation in BPSi-PC because the oxidative cleavage/rearrangement reaction observed for the gem dimethyl groups in the BPA unit of BPA-PC is precluded. Even though this result is not definitive, it does suggest that side chain photooxidation rather than photo-Fries reactions or direct ring oxidation is the major source of BPA-PC photoyellowing. If this situation is the case, the actual compounds giving rise to color in BPA-PC are probably not the compounds produced by direct photooxidation of the geminal dimethyl groups in BPA but rather are the products resulting from further oxidation of these materials. This is because the products expected from the direct oxidation of these geminal dimethyl groups are not expected to be highly colored. For example, any phenolic compounds produced by side chain photooxidation probably would lead to highly colored ring oxidation products in secondary reactions.

C. Role of Wavelength of Light in the Photodegradation of BPA-PC

1. *Wavelength Sensitivity of the Photoaging of BPA-PC*

The most important principle involved in determining wavelength sensitivity in the photochemistry of any material is embodied in the First Law of Photochemistry [23]: "Only light which is absorbed by a molecule is effective in producing

a reaction which changes the molecule." Thus, to understand the photochemistry of BPA-PC, one must consider the UV-Vis absorption spectrum of BPA-PC shown in Fig. 3. As can be seen, the largest peak occurs at about 200 nm with a shoulder at about 222 nm which has been ascribed to an aromatic $\pi \rightarrow \pi^*$ transition. However, this absorption can be ignored for normal exposure conditions of BPA-PC where the most severe light source is usually sunlight, which on the surface of the earth does not extend below 290 nm [24]. The next strongest absorption peaks are at 264 and 272 nm, which have been ascribed to the $\pi \rightarrow \pi^*$ transition of the carbonate groups in the BPA-PC [7]. Gaussian analysis indicates that this absorption extends as far as 340 nm [7]. Studies have shown that this absorption is responsible for the photo-Fries rearrangement and fragmentation/coupling reactions [7]. As expected, these reactions predominate when BPA-PC is exposed to light of wavelengths less than 300 nm. Nonetheless, evidence for photo-Fries reactions has been found for samples exposed to the longer wavelengths of sunlight [13] presumably due to the above-mentioned tailing of the $\pi \rightarrow \pi^*$ absorption to wavelengths greater than 300 nm.

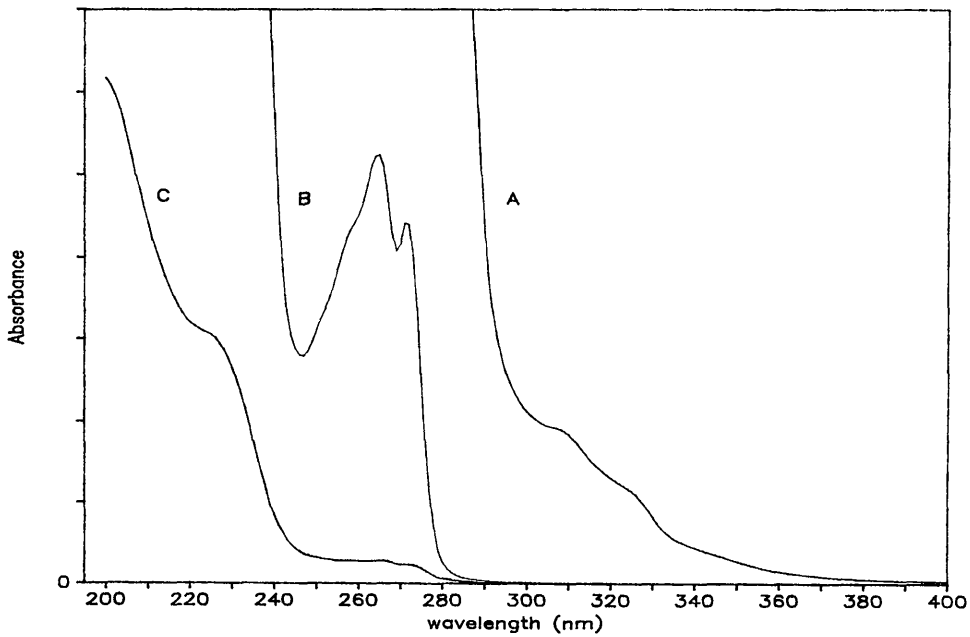

Figure 3 The UV absorption spectrum of BPA-PC (A, ~380 μM film; B, ~2 μM film; C, ~0.15 μM film).

Recent photophysical studies by Hoyle and coworkers [25] determined that BPA-PC has a short-lived π,π^* singlet excited state with an energy (E_S) of 102 kcal/mole and a lowest level π,π^* triplet energy state with an energy (E_T) of 80.5 kcal/mole.

Another important absorption that can often be observed in BPA-PC at about 287 nm is due to phenolic end-groups in the polymer. While, as previously discussed, studies by Webb and Czanderna [12] suggested that this absorption gives rise to reactive free radicals via a hydrogen atom transfer reaction, it is probably unimportant for most commercial BPA-PCs where the concentration of phenolic end-groups is negligible.

Lastly, as seen in Fig. 3 (curve A), the spectrum of a BPA-PC can have several faint absorption peaks at about 308 and 325 nm. These absorptions usually are not seen in the solution spectrum of BPA-PC that has not experienced any significant heat history and are due to minor amounts of BPA-PC thermal degradation products formed during melt processing. Gupta and coworkers [7] suggested that these bands were due to an unidentified ester and a salicylate group, respectively. In agreement, recent studies by Hoyle and coworkers [20] presented evidence that these peaks are due to the formation of dibenzofuran and phenyl 2-phenoxybenzoate groups. They found that thermal treatment of BPA-PC in either air or nitrogen at temperatures as low as 250°C gave rise to a structured fluorescence emission due mainly to the formation of these groups. Photolysis studies of representative BPA-PC thermal degradation products like dibenzofuran, BPA, and xanthone, a known thermal decomposition product of phenyl 2-phenoxybenzoate [26], with broad-spectrum UV light having a λ_{max} of 305 nm, showed that the presence of these structures in BPA-PC did not greatly affect the photodegradation of BPA-PC other than to form products that subsequently underwent photobleaching.

In addition to the peaks seen in Fig. 3, a weak broad-tail absorption of unknown origin is present in most thermally processed BPA-PC, which extends beyond 400 nm into the visible spectrum and which is the source of the slight yellow color observed in unstabilized and untinted BPA-PC. Since this tail absorption and subsequent yellow color is observed to increase with the severity of processing, its origin is no doubt due to small amounts of thermal and thermo-oxidative products formed during melt processing.

2. *Quantification of the Spectral Sensitivity of BPA-PC Photoaging*

There have been a number of studies made to quantify the spectral sensitivity of BPA-PC photoaging [27]. The most common way this was done was to measure BPA-PC's "activation spectrum," which identified the wavelengths in a specific light source responsible for damage to the material. In one case, the authors deter-

mined the "action spectrum" of BPA-PC, which was derived by normalizing the activation spectrum for the light intensity from a number of radiation sources. The action spectrum has the advantage of being independent of the spectral power distribution and thus represents the relative response of the material to the same radiant exposure in all actinic regions.

In the earliest study, Mullen and Searle [28] used spectrally dispersed light from a xenon arc lamp to determine the activation spectrum of a solution-cast film of BPA-PC, i.e., the wavelengths of light that caused the greatest increase in the UV absorption of BPA-PC. They found that the range of wavelengths causing photodegradation extended from 230 to 320 nm with the maximum changes occurring between 280 and 290 nm. The difference between this observed maximum and the approximately 270 nm predicted by the First Law of Photochemistry was explained by the occurrence of secondary photoreactions of longer wavelengths absorbing primary photoproducts.

In a similar study, Torikai et al. [29] reported the effects of monochromatic light of wavelengths 260, 280, 300, 320, 340, 400, and 500 nm on commercial BPA-PC films. They found that photodegradation and photo-Fries rearrangement of BPA-PC, as measured by changes in molecular weight and UV absorption, were caused by irradiation with 260–300 nm light, but not by irradiation at wavelengths greater than 320 nm. In agreement with the study by Mullen and Searle, the maximum rate of photo-Fries rearrangement were found to occur at approximately 280 nm, whereas that for main-chain scission occurred at 260 nm. In a related report from the same laboratory, Andrady et al. [30] obtain the action spectrum of a commercial BPA-PC film containing a UV screening agent by measuring the effect of monochromatic light of the above wavelengths on photoyellowing. They found that the extent of yellowing, when normalized for light intensity, decreased logarithmically with increasing wavelength from 280 to 340 nm. In contrast, with irradiation at 400 and 500 nm, the color of the sample was observed to decrease. From this they concluded that the photoyellowing of BPA-PC on exposure to a polychromatic light source such as sunlight is the net result of simultaneous yellowing and bleaching.

Finally, Andrady et al. [31] recently determined the activation spectra of extruded BPA-PC films based on both yellowing and increased UV absorption using the sharp-cut filter technique with either a borosilicate filtered xenon arc light source or Florida sunlight. With the xenon arc source they found that optical changes were caused by two distinctly separate actinic regions, one with wavelengths below 300 nm and the other extending from 310 to about 350 nm. This agrees with the earlier observation by Rivaton and coworkers [11] of increased UV tailing into the visible after prolonged exposure to monochromatic 365-nm light. In addition to observing photoyellowing, Andrady and coworkers found that unstabilized extruded BPA-PC film was photobleached both by a spectral band in the 300-nm region and by wavelengths longer than 380 nm due to the

destruction of trace amounts of the yellow-colored species in the film produced during melt processing. In contrast to the xenon arc results where two actinic regions were observed, with sunlight only the wavelength region between 310 and 350 nm was found to cause yellowing. This difference is no doubt due to the much smaller amount of energy below 300 nm available from sunlight.

In summary, the above studies of the spectral sensitivity of BPA-PC photoaging generally indicate that the greatest changes are brought about by the lowest wavelengths of light—from 230 to 350 nm—with the maximum effect at about 280 nm. In contrast, wavelengths above 380 nm caused the colored species in BPA-PC to photobleach.

Lastly, in a recent private communication, C. E. Hoyle described the results of his group's work on the effect of wavelength on the photochemistry of BPA-PC. Using fluorescence spectroscopy, as previously utilized in their work on non-wavelength-dependent studies of the photochemistry of BPA-PC [19,20], they found that 313 nm monochromatic light produced compounds containing salicylic acid, phenyl salicylate, and 2,2′-biphenol groups, whereas both 366 nm and 405 nm light gave only phenyl salicylate–and 2,2′-biphenol-containing products. Similarly, phenyl salicylate and 2,2′-biphenol groups were detected in BPA-PC exposed to natural sunlight. It was suggested that it might be possible that the photochemistry observed at these longer wavelengths, where BPA-PC does not normally absorb light, was due to either a nonallowed transition or the presence of BPA-PC aggregates that absorb light at these longer wavelengths. Such aggregates have previously been proposed to account for the effects of concentration and temperature on the fluorescence spectra of poly(ethylene terephthalate) [32].

3. *Significance of BPA-PC Wavelength Sensitivity on the Selection of UV Screening Agents and Accelerated Test Procedures*

An effective UV screening agent for a polymer must have the following characteristics: (a) It must have the ability to strongly absorb light in the wavelength regions that cause a material to degrade without itself being degraded; (b) It must possess little or no absorption in the visible region so as to impart little or no color to the polymer. (c) It must be unreactive to the polymer and have sufficient thermal stability to remain unchanged during the melt processing of the polymer. Based on the work reported in the previous section, and especially on the results of Andrady and coworkers [30,31], one would define an ideal UV screening agent for use of BPA-PC in sunlight as one that had the strongest absorption in the actinic 290- to 350-nm region of BPA-PC while having minimal absorption of light greater than 380 nm both to allow for photobleaching and to have a minimal effect on the color of the polymer. Examples of the absorption spectra of representatives from several common classes of commercial UV screening agents are

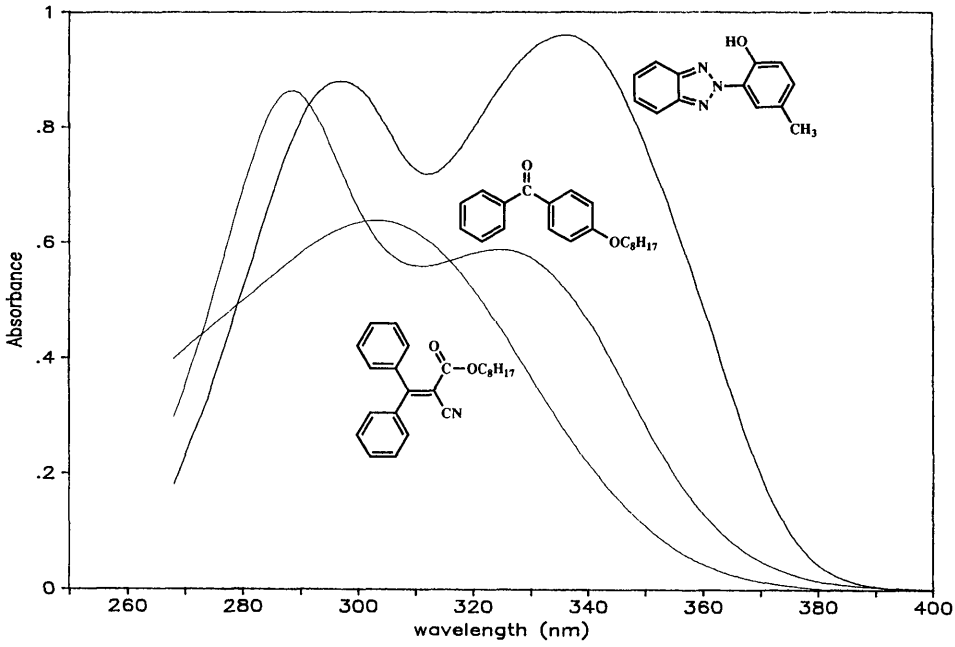

Figure 4 The UV spectra of representative UV screening agents (0.0015 wt/vol% in methanol).

shown in Fig. 4. As can be seen, the benzotriazole UV screening agents come closest to having the absorption characteristics described above. The combination of these absorption properties and their high thermal stability is why this class of UV screening agents is commonly used in BPA-PC.

4. *Significance of BPA-PC Wavelength Sensitivity on the Selection of Accelerated Test Procedures*

An important aspect of designing an accelerated UV test procedure for evaluation of the weathering behavior of a material is the selection of a light source that best simulates the wavelength distribution of the light to which the material is to be exposed. As previously discussed, this is especially important in the case of BPA-PC where the photodegradation mechanism is different at long- and short-wavelength UV irradiation. This is dramatically illustrated in a BPA-PC study by LeMaire and coworkers [33], wherein they simultaneously measured the photo-Fries reactions by UV spectroscopy and photooxidation by IR spectroscopy

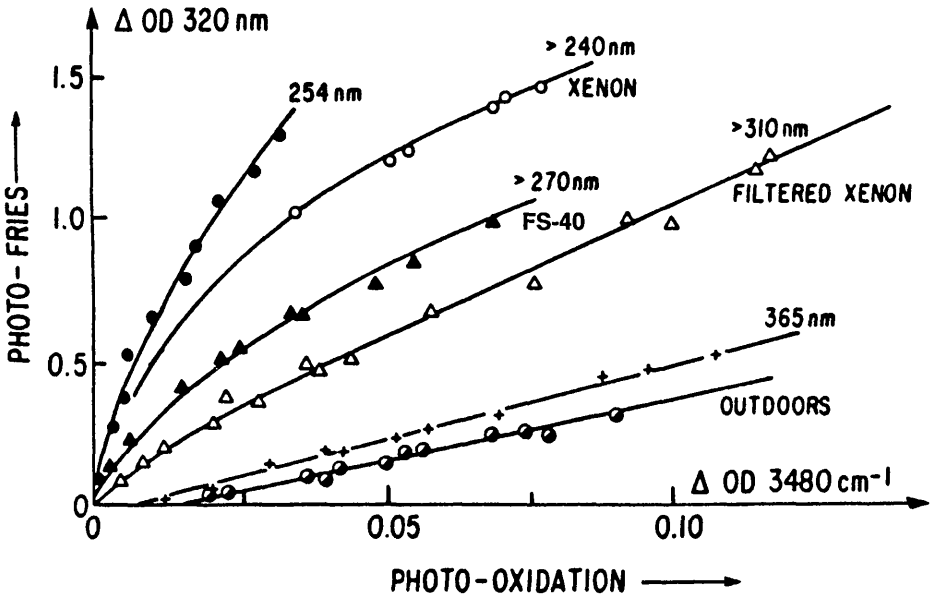

Figure 5 The effect of light source on the relative rates of photooxidation reactions (as measured by increased IR absorption at 3480 cm^{-1}) and photo-Fries reactions (as measured by increased UV absorption at 320 nm). (Data adapted from Ref. 33.)

for different light sources, as shown in Fig. 5. As expected from the above discussions, their results show that the light sources that gave the closest balance of photo-Fries and photooxidation reactions to sunlight were those possessing the longest wavelengths and that best matched the spectral distribution of sunlight in the 300 to 400 nm region.

III. CHEMISTRY OF γ-IRRADIATED BPA-PC

Because of its predominantly aromatic structure, BPA-PC is one of the most radiation-resistant commercial polymers. For this reason and because of its excellent physical properties, it has found numerous applications in medical devices that require sterilization by exposure to ^{60}Co γ-rays [34]. While BPA-PC generally shows good property retention after the 2.5–5.0 Mrad of γ-irradiation typically used for sterilization, the irradiated polymer takes on a moderately intense yellow color. Although there have been numerous studies on the chemistry involved when BPA-PC is exposed to ionizing radiation [3,35–42], the origin of

this color has not been satisfactorily explained. Various authors have ascribed the color in irradiated BPA-PC to substituted benzophenones [3], radical species [35,36], highly conjugated compounds [36], or rearranged isopropylidene radicals [38]. Davis and Golden [3] report that when BPA-PC is irradiated at 77 K with an electron beam, it acquires a green color due to free radicals. On exposure to oxygen, the color turns to amber-brown. UV analysis [39] indicated that this amber-brown color was associated with absorption maxima at 305 nm, with a shoulder at 320 nm. In a similar in vacuo x-ray irradiation study at 40°C, Barker and Moulton reported the appearance of adsorption maxima at 340 and 400 nm [40]. Subsequent aging in air caused the disappearance of the 400 nm peak that the authors ascribed to reactive radical species. Hama and Shinohara [35] observed the appearance of a similar dark green color and a strong electron spin resonance (ESR) signal when BPA-PC was exposed to 0.7 Mrad of γ-radiation in vacuum at 77 K. Exposure to visible light or warming caused a decrease in both the color and the ESR signal intensity. The authors ascribed the color to the presence of trapped electrons and positive radical ions. Later UV studies by Torikai et al. [36] showed that the green color produced by γ-irradiation of BPA-PC at 77 K under vacuum was due to a broad absorption band at about 415 nm that disappears when the sample is either warmed or exposed to visible light. They ascribed the green color to the presence of carbonate radical anions, e.g., $(ArO)_2\dot{C}\text{-}O^-$.

The only product studies on irradiated BPA-PC were done by Golden and coworkers on BPA-PC and model compounds irradiated with an electron beam [3,39,41,42]. Gas analysis of electron beam irradiation (1000 Mrad) of either BPA-PC or model compounds in vacuum showed the formation of the following gases: $CO > CO_2 \gg H_2 \gg CH_4 >$ benzene [41]. They suggested that the relatively low yields of H_2 and CH_4 found under these conditions indicated that the isopropylidene group is not as reactive as the carbonate group. The following is a list of products produced by the electron beam irradiation in a vacuum of the model compound, diphenyl carbonate [42]: CO, CO_2, phenol, diphenyl ether, biphenyl, 2-hydroxybiphenyl, 2-hydroxydiphenyl ether, 4-hydroxydiphenyl ether, 4-hydroxybiphenyl, phenyl salicylate, 2,2′-dihydroxybiphenyl, 2,4′-dihydroxybiphenyl, 2,2′-dihydroxybenzophenone, and 2,4′-dihydroxybenzophenone. The *G* values for these products, i.e., their yields per 100 eV of energy, were found to be constant up to a dose of 500 Mrad. The formation of these products was rationalized by the free radical process summarized in Scheme 4.

Recently, Ferain and Legras [43] studied the degradation of diphenyl carbonate by $^{40}Ar^{9+}$ 180-MeV heavy ions in vacuum in order to understand the chemistry of track formation in BPA-PC irradiated with heavy ions. Interestingly, they found the same degradation products as in the above electron beam study plus 4,4′-dihydroxybiphenyl, salicylic acid, phenyl benzoate, and 2-phenoxyphenyl benzoate. As with electron beam studies, the formation of these products can

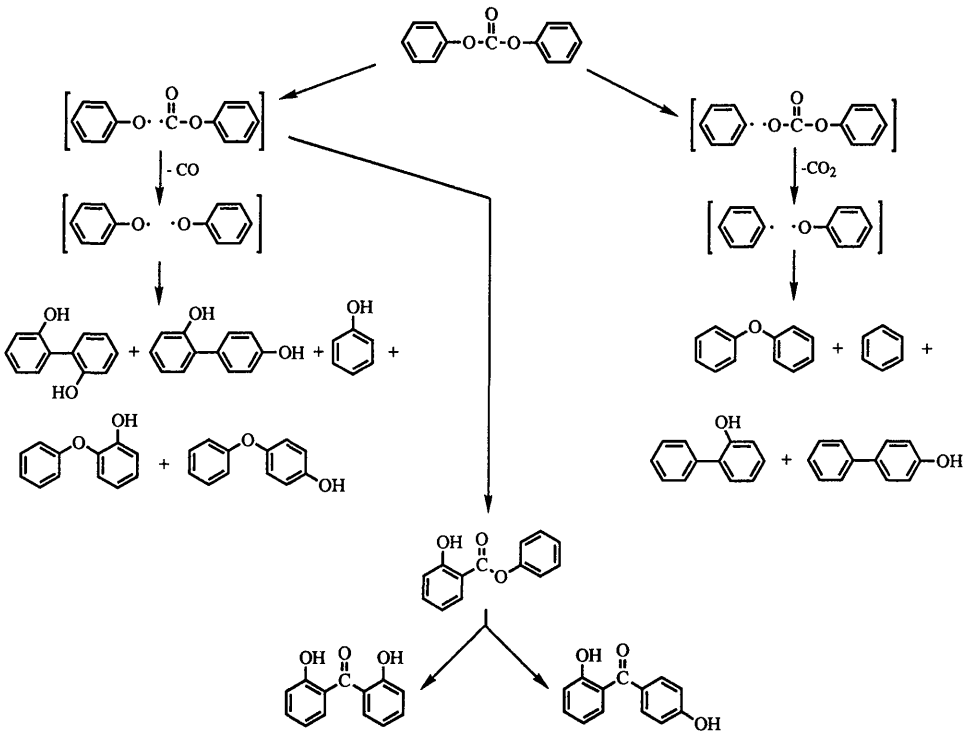

Scheme 4 Proposed mechanism for electron beam decomposition of diphenyl carbonate. (From Ref. 44. Copyright 1994 Elsevier.)

be explained by the free radical process postulated in Scheme 4 plus secondary reactions of phenyl salicylate.

In their review of the radiation chemistry of BPA-PC, Davis and Golden [3] imply that the chemistry involved during exposure of BPA-PC to high-energy ionizing radiation is independent of the kind of radiation used, i.e., γ-rays, electrons, etc. While this is generally true of other polymers, this has never been verified for BPA-PC by any detailed comparative product studies.

A. Product Studies of γ-Irradiated BPA-PC

Recently we completed a study undertaken to better define the chemistry involved when BPA-PC is exposed to sterilizing doses of ^{60}Co γ-rays [44]. Of special interest was the identification of the chemical species responsible for the yellow

color produced under these conditions in hopes of using this knowledge to develop more color-stable systems.

Samples of BPA-PC (film, injection-molded step chips, and powder) and a model compound, BPA-PC cyclic tetramer, were exposed to 10.5–10.8 Mrad of γ-irradiation from a ^{60}Co source. After irradiation, all of the powdered samples of BPA-PC and cyclic tetramer appeared light yellow when compared with nonirradiated control samples, although the extent of yellowing was difficult to quantify. Similarly, the samples of 1.0-mil and 10-mil BPA-PC films, and BPA-PC step chips were noticeably more yellow than their nonirradiated controls.

The IR spectra of the γ-irradiated BPA-PC films showed the appearance of an extended tail in the carbonyl peak at around 1750–1755 cm^{-1}. ^1H NMR spectra of γ-irradiated BPA-PC powder and cyclic tetramer (in $CDCl_3$) showed little change. Solutions of γ-irradiated BPA-PC and cyclic tetramer were shown to be slightly acidic by adding a small amount of methanol to the nuclear magnetic resonance (NMR) samples. In nonirradiated control samples, the methyl protons of the added methanol were split into a doublet by the OH proton, indicating slow exchange of the OH protons. However, in γ-irradiated samples, the methyl protons of the added methanol appeared as a singlet because they were no longer coupled to the OH proton, suggesting that the samples had become acidic enough to cause rapid exchange of OH protons.

As previously discussed, Davis and Golden [3] reported that new UV peaks appeared at 305 and 320 nm in electron beam–irradiated BPA-PC. They attributed the yellow color to tailing of the 320-nm peak into the visible region. In the present study, we also observed new peaks at 305 and 320 nm but, in addition, improved instrumentation and software for data manipulation allowed us to detect a smaller peak at about 360 nm that tails into the visible region and is the source of the observed yellow color. These three UV peaks were observed in all samples (analyzed in either the solid state or in solution) of γ-irradiated BPA-PC and cyclic tetramer with similar but somewhat variable relative intensities. Figure 6 shows typical *referenced* UV-Vis spectra for γ-irradiated BPA-PC and cyclic tetramer that were obtained by subtracting the spectra of the corresponding unirradiated samples.

HPLC/UV-Vis and HPLC/MS analysis of base-hydrolyzed cyclic tetramer provided information about the structure of the major products formed during γ-irradiation of BPA-PC. Figure 7 shows the HPLC/UV-Vis chromatogram of base-hydrolyzed γ-irradiated cyclic tetramer. Chromatograms of hydrolyzed γ-irradiated BPA-PC showed the same major products in similar relative abundances. Cyclic tetramer was chosen for closer study as a model for BPA-PC because it was purer, lacking phenolic chain stoppers and the trace impurities found in commercial BPA-PC.

The hydrolyzed solution of γ-irradiated cyclic tetramer giving the chromatogram in Fig. 5 was substantially separated from BPA using preparative

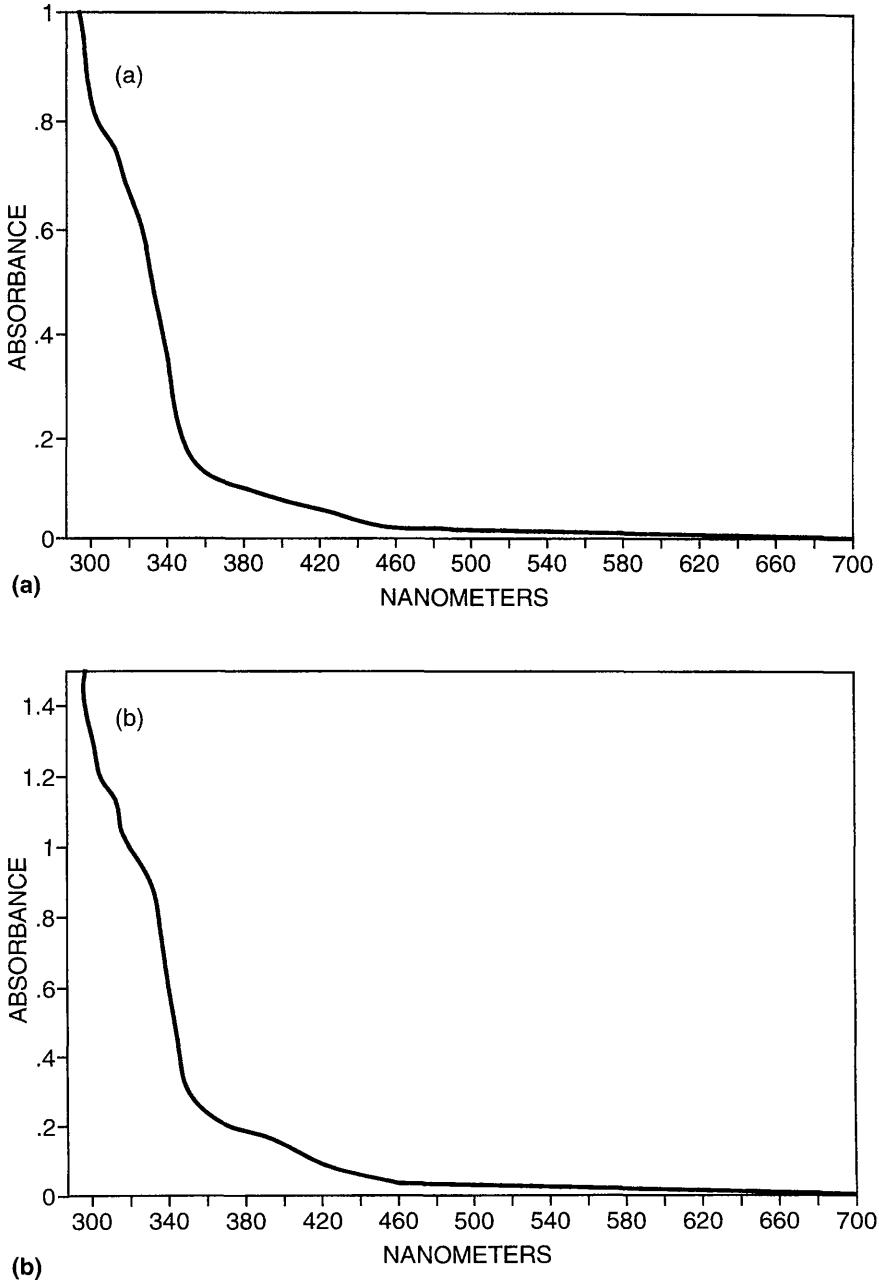

Figure 6 UV-Vis spectra of (a) γ-irradiated BPA-PC (10-mil film) and (b) γ-irradiated cyclic tetramer (0.206 M chloroform solution) referenced to unirradiated samples. (From Ref. 44, Copyright 1994 Elsevier.)

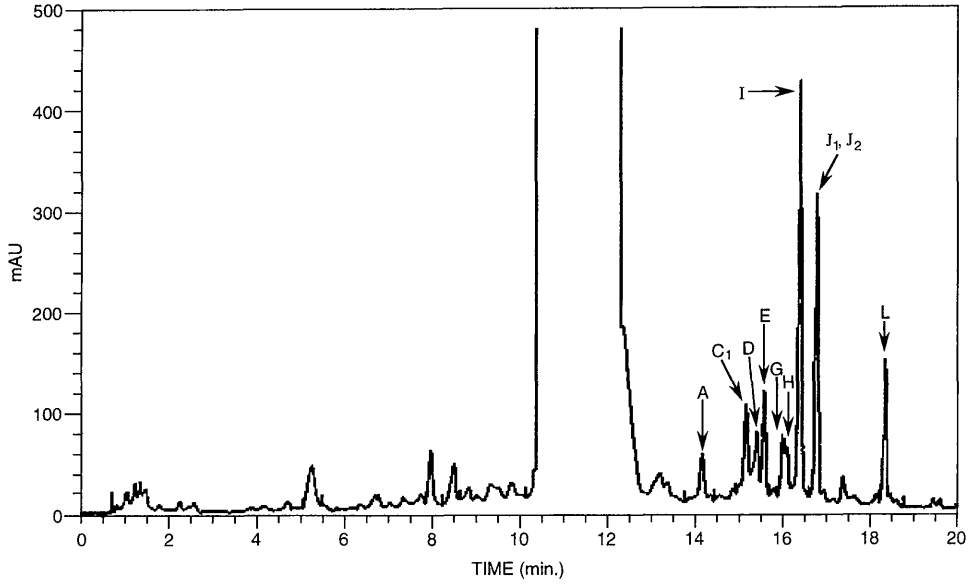

Figure 7 HPLC/UV-Vis chromatogram of base-hydrolyzed γ-irradiated cyclic tetramer (monitored at 260 nm). (From Ref. 44, Copyright 1994 Elsevier.)

HPLC and further analyzed by HPLC/MS. Some differences were observed when comparing the HPLC chromatogram before and after it was concentrated by preparative HPLC; however, most of the peaks in the HPLC/MS chromatogram did correspond with the peaks in the HPLC/UV-Vis chromatogram. Figure 8 shows the HPLC chromatogram after concentration by preparative HPLC and Fig. 9 summarizes the conclusions from the HPLC/UV-Vis and HPLC/MS experiments and shows the assigned structures when possible. In Fig. 9, numerical subscripts on the peak designations were used to indicate that a HPLC peak contained more than one compound. Unfortunately, the concentration of the materials giving rise to HPLC peaks eluting before BPA in Figs. 7 and 8 were too low to obtain usable mass spectra. The UV-Vis spectra obtained for these peaks generally showed λ_{max} values at 260–275 nm, suggesting that they are alkyl-substituted aromatic compounds.

As indicated in Fig. 9, most of the major products found in hydrolyzed γ-irradiated cyclic tetramer are similar to the products reported by Davis and Golden [3,42] in the model study of electron beam–irradiated diphenyl carbonate summarized in Scheme 4. The majority of these products arise from the recombination of phenyl and phenoxy radicals resulting from Fries-type free radical reac-

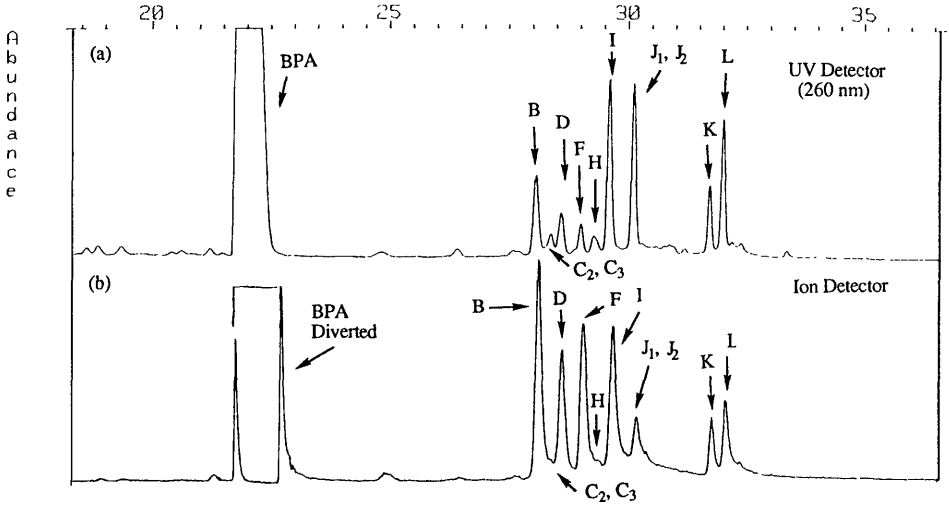

Figure 8 HPLC/MS chromatograms of base-hydrolyzed γ-irradiated cyclic tetramer after concentration by preparative HPLC. (a) 260-nm detector. (b) Ion detector. (From Ref. 44, Copyright 1994 Elsevier.)

tions. This indicates that as observed with electron irradiation, under γ-irradiation conditions the isopropylidene groups are not as reactive as the carbonate groups.

B. Attempts to Identify Color Bodies from γ-Irradiated BPA-PC

One of the most interesting results from the HPLC/UV-Vis analysis of both hydrolyzed γ-irradiated BPA-PC and cyclic tetramer was the discovery of colored products with UV peaks at 313 and 360 nm—very similar to the UV peaks observed in the original γ-irradiated BPA-PC polymer and cyclic tetramer (see Fig. 6).

A series of experiments were carried out to determine the relationship of the colored products observed in HPLC studies of hydrolyzed γ-irradiated BPA-PC tetramer to the yellow color observed in the untreated γ-irradiated polymer. Spectral studies indicate that the color of the γ-irradiated BPA-PC film was virtually unchanged when the film was dissolved in chloroform, demonstrating that the color bodies formed during γ-irradiation were unchanged when in solution. Spectral changes that occur upon hydrolysis of γ-irradiated cyclic tetramer are shown in Fig. 10. UV peaks at about 320 and 360 nm are still present after hydrolysis but have increased significantly in absorbance relative to nonhy-

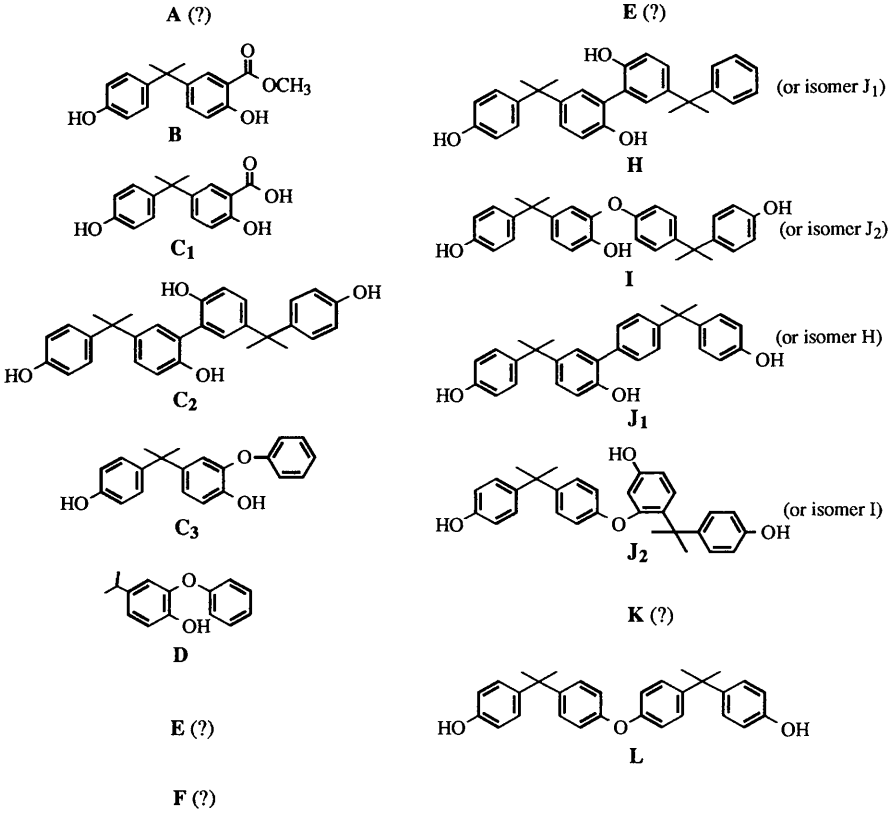

Figure 9 Products from the 10-Mrad γ-irradiation of BPA-PC cyclic tetramer (assigned structures based on UV and mass spectral data). (Reproduced from A. Factor, *Die Angewandte Makromolekulare Chemie 232*, Copyright 1995, pp. 27–43, with permission from Die Angewandte Makromolekulare Chemie.)

drolyzed γ-irradiated cyclic tetramer. The HPLC/UV-Vis and HPLC/MS analysis of hydrolyzed cyclic tetramer indicate that the approximately 320 nm peak is from BPA-salicylate (λ_{max} = 313 nm), i.e., peak C_1 in Fig. 9. HPLC/UV-Vis indicates two of the hydrolyzed products have UV peaks at about 360 nm. The UV-Vis spectra of these hydrolyzed products from γ-irradiated cyclic tetramer, with UV peaks at 313 and 360 nm, are shown in Fig. 11. Thus the evidence indicates that most of the yellow color in γ-irradiated BPA-PC is due to the compounds giving rise to peaks A and E in Fig. 9. Unfortunately, these compounds were not concentrated enough for direct HPLC/MS analysis and too labile to

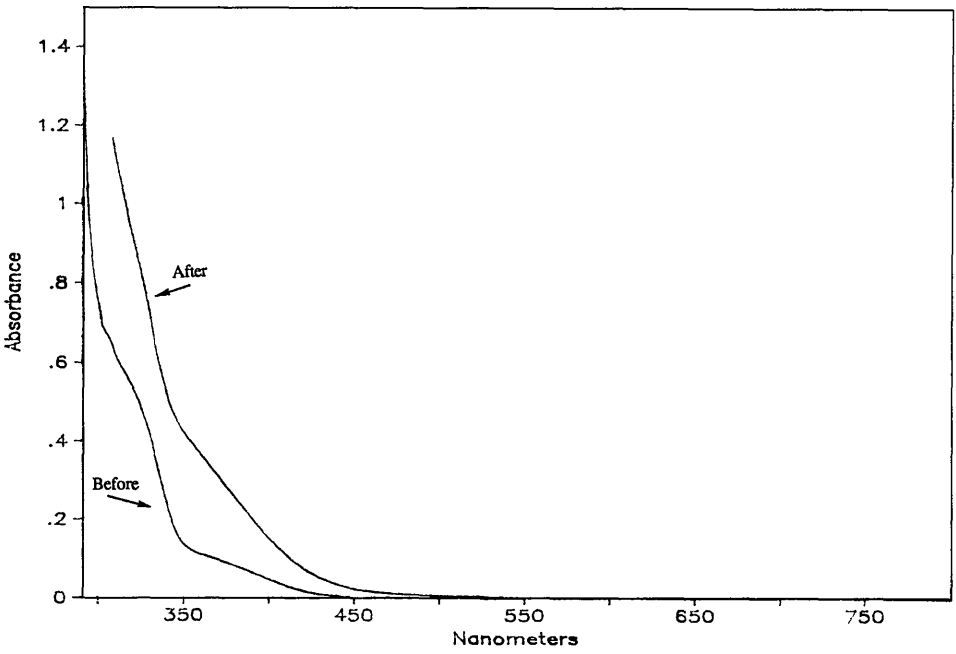

Figure 10 Comparison of the UV-Vis spectra of γ-irradiated cyclic tetramer before and after base hydrolysis as 0.111 M THF and THF/methanol/water solutions, respectively. (From Ref. 44. Copyright 1994 Elsevier.)

survive the preparative HPLC step required to prepare a high enough sample concentration for HPLC/MS analysis. A number of unsuccessful attempts to identify these materials were made using GC/MS of samples prepared both by base hydrolysis and by reductive cleavage with $LiAlH_4$ [13]. Finally, in an attempt to prepare high enough concentrations of peaks A and E for direct HPLC/MS analysis, a sample of BPA-PC cyclic tetramer was exposed to 100 Mrad of γ-irradiation—but again there were insufficient amounts present for identification by HPLC/MS.

While we were unsuccessful in actually identifying the yellow compounds giving rise to peaks A and E, one can speculate about BPA-PC-derived compounds that would display the observed thermal and photochemical instability and give rise to a broad absorption at about 360 nm. A possible identification would be the substituted benzophenone derivatives suggested by Davis and Golden [3,42]. However, one would expect these compounds to be stable enough to have been isolated and identified using the procedures described above. One

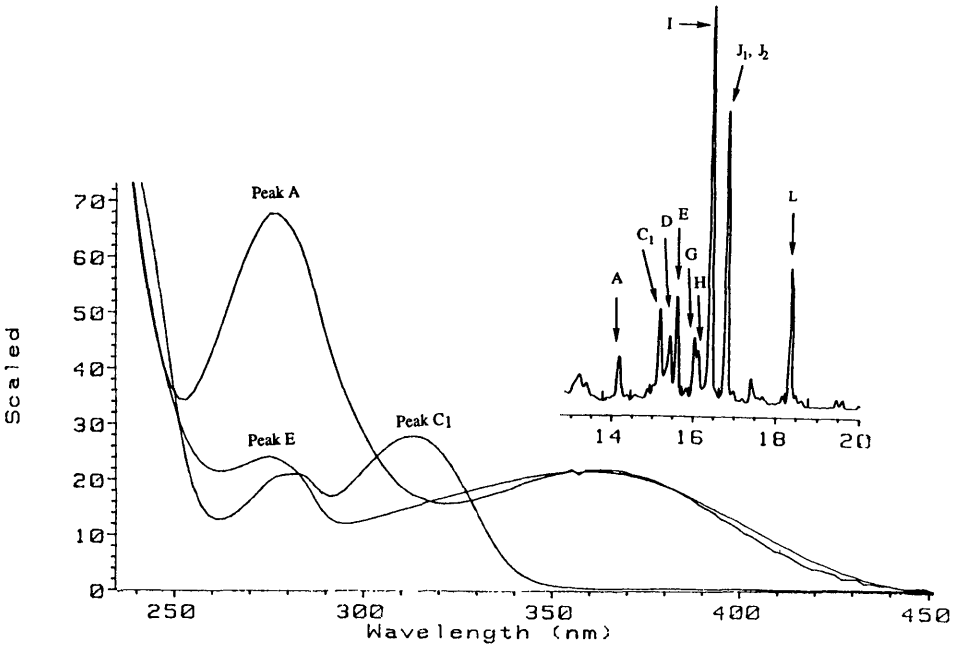

Figure 11 UV-Vis spectra of hydrolyzed products of γ-irradiated cyclic tetramer showing 315-nm and 360-nm peaks from HPLC/UV-Vis experiment (cf. Table 3). (Reproduced from A. Factor, *Die Angewandte Makromolekulare Chemie 232*, Copyright 1995, pp. 27–43, with permission from Die Angewandte Makromolekulare Chemie.)

class of compounds that possess both the appropriate UV absorption and high reactivity is the 1,2-benzoquinones (*ortho*-quinones). For example, red 1,2-benzoquinone (λ_{max} = 368 and 587 nm) rapidly reacts with water to form the yellow 2-hydroxy-1,4-benzoquinone (λ_{max} = 369 nm) [45]. In addition, this latter compound can be oxidized to a resinous dark brown acidic material refered to as humic acid [46]. Although we were never able to obtain rigorous proof for the presence of 1,2-benzoquinones in γ-irradiated BPA-PC, we recently obtained indirect evidence for their presence [47]. In work by Argyropoulos and coworkers [48], it was reported that *ortho*-quinone groups in wood pulp reacted with trimethyl phosphite to form unique cyclic phosphite esters whose presence could be detected by ^{31}P NMR. Application of this approach to BPA-PC and the BPA-PC cyclic tetramer that had been exposed to γ-rays gave rise to new ^{31}P NMR peaks at approximately −47.0 ppm. An identical peak was found when an authentic sample of 1,2-benzoquinone was treated with trimethyl phosphite, supporting the hypothesis that *ortho*-quinone groups are present in γ-irradiated BPA-PC.

IV. CONCLUSIONS

Exposure of BPA-PC in air to either UV light or high-energy irradiation leads to yellowing. The identified products from these processes, found in Fig. 1, 2 and 9, show many similarities. All show the occurrence of Fries-like reactions with the formation of salicylates and phenol coupling products. Products from side chain oxidation are found in the case of photoaging, such as *p*-hydroxyacetophenone, *p*-hydroxybenzoic acid, and *para*-quinone. While most of these products do not themselves absorb visible light and therefore do not contribute directly to color, many of them can be easily oxidized to highly colored species, as illustrated in Scheme 5. The fact that the UV-Vis spectra of yellowed BPA-PCs invariably show a broad tailing into the visible region but rarely show specific structure indicates that the color is due to the presence of a multitude of colored species rather than a few. No doubt the ring oxidation process, which would be increasingly favored by increasing the number of hydroxyl groups on the aromatic rings, will lead to a great number of highly unsaturated—and therefore highly colored—products. Unfortunately, except for a few of the products observed for photoaging shown in Fig 1, it has been very difficult to obtain any rigorous struc-

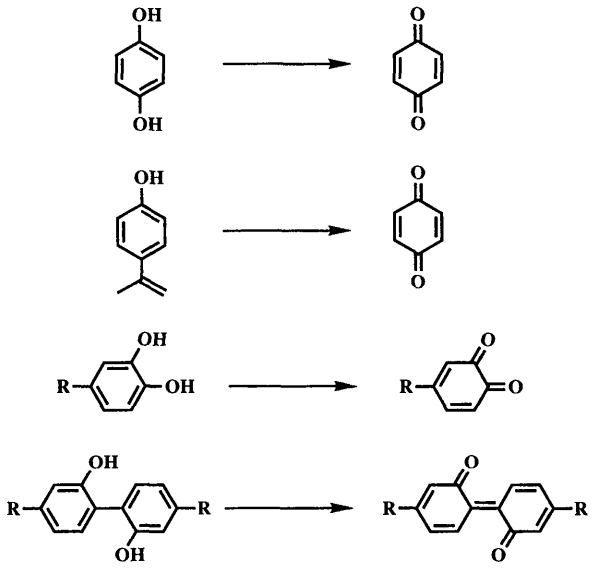

Scheme 5 Potential sources of color in degraded BPA-PC. (Reproduced from A. Factor, *Die Angewandte Makromolekulare Chemie 232*, Copyright 1995, pp. 27–43, with permission from Die Angewandte Makromolekulare Chemie.)

tural information about these compounds. Thus, while we presently have some insights as to the sources of color in degraded BPA-PC, rigorous proof of the actual structures of these compounds has as yet not been obtained.

REFERENCES

1. D. Freitag, U. Grigo, P. Mueller, and W. Nouvertne, Polycarbonates, in *Encyclopedia of Polymer Science and Technology*, Vol. 11 (H. F. Mark, N. M. Bikales, C. G. Overberger, and G. Menges, eds.), John Wiley and Sons, New York, 1987, p. 648.
2. A. Factor and M. L. Chu, The role of oxygen in the photo-aging of bisphenol-A polycarbonate, *Polym. Degrad. Stab.* 2:203 (1980).
3. A. Davis and J. H. Golden, Stability of polycarbonate, *J. Macromol. Sci.-Rev. Macromol. Chem. C3*:49 (1969).
4. D. Bellus, P. Hrdlovic, and Z. Manasek, Photoinitiated rearrangements in poly[2,2-propanebis(4-phenyl carbonate)], *Polym. Lett. 4*:1 (1966).
5. J. S. Humphrey, Jr., and R. S. Roller, Flash photochemical studies of diaryl carbonate esters: the mechanism of the photo-Fries rearrangement, *Mol. Photochem. 3*:35 (1971).
6. J. S. Humphrey, Jr., A. R. Shultz, and D. B. G. Jaquiss, Flash photochemical studies of polycarbonate and related model compounds, photodegradation vs. photo-Fries rearrangement, *Macromolecules 6*:305 (1973).
7. A. Gupta, A. Rembaum, and J. Moacanin, Solid state photochemistry of polycarbonates, *Macromolecules 11*:1285 (1978).
8. D. T. Clark and H. S. Munro, Surface aspects of the photodegradation of bisphenol A polycarbonate in oxygen and nitrogen atmospheres as revealed by ESCA, *Polym. Degrad. Stab. 4*:441 (1982).
9. D. T. Clark and H. S. Munro, Surface and bulk aspects of the natural and artificial photo-aging of bisphenol A polycarbonate as revealed by ESCA and difference UV spectroscopy, *Polym. Degrad. Stab. 8*:195 (1984).
10. A. Rivaton, D. Sallet, and J. Lemaire, The photochemistry of bisphenol-A polycarbonate reconsidered, *Polym. Photochem. 3*:463 (1983).
11. A. Rivaton, D. Sallet, and J. Lemaire, The photo-chemistry of bisphenol-A polycarbonate reconsidered. 2. FTIR analysis of the solid-state photo-chemistry in "dry" conditions, *Polym. Degrad. Stab. 14*:1 (1986).
12. J. D. Webb and A. W. Czanderna, End-group effects on the wavelength dependence of laser-induced photodegradation of bisphenol-A polycarbonate, *Macromolecules 19*:2810 (1986).
13. A. Factor, W. V. Ligon, and R. May, The role of oxygen in the photoaging of bisphenol A polycarbonate. 2. GC/GC/high-resolution MS analysis of Florida-weathered polycarbonate, *Macromolecules 20*:2461 (1987).
14. C. A. Pryde, Photoaging of polycarbonate: effects of selected variables on degradation pathways, in *Polymer Stabilization and Degradation* (P. P. Klemchuk, ed.), ACS Symposium Series No. 280, American Chemical Society, Washington, DC, 1985, p. 329.

15. H. S. Munro and R. S. Allaker, Wavelength dependence of the surface photooxidation of bisphenol A polycarbonate, *Polym. Degrad. Stab. 11*:349 (1985).
16. S. Pankasem, J. Kuczynski, and J. K. Thomas, Photochemistry and photodegradation of polycarbonate, *Macromolecules 27*:3773 (1994).
17. J. E. Moore, Differential UV spectroscopy as an aid in studying polycarbonate photodegradation, in *Photodegradation and Photostabilization of Coatings* (S. P. Pappas, and F. H. Winslow, eds.), ACS Symposium. Series No. 151, American Chemical Society, Washington, DC, 1981, p. 97.
18. I. B. Rufus, H. Shah, and C. E. Hoyle, Identification of fluorescent products produced by the thermal treatment of bisphenol-A-based polycarbonate, *J. Appl. Polym. Sci. 51*:1549 (1994).
19. C. E. Hoyle, H. Shah, and G. L. Nelson, Photochemistry of bisphenol-A-based polycarbonate: the effect of the matrix and early detection of photo-Fries product formation, *J. Polym. Sci. A: Polm. Chem. 30*:1526 (1992).
20. H. Shah, I. B. Rufus, and C. E. Hoyle, Photochemistry of bisphenol-A-based polycarbonate: early detection of photoproducts by fluorescence spectroscopy, *Macromolecules 27*:553 (1994).
21. A. Factor, J. C. Lynch, and F. H. Greenburg, The synthesis, characterization, and weathering behavior of polycarbonates derived from 3,3′-dihydroxydiphenyl ether, *J. Polym. Sci. A: Polym. Chem. 25*:3413 (1987).
22. A. Factor and P. T. Engen, The synthesis, characterization and weathering behavior of polycarbonate derived from bis (p-hydroxyphenyl) dimethylsilane (BPSi), *J. Polym. Sci. A: Polym. Chem. 31*:2231 (1993).
23. J. G. Calvert and J. N. Pitts, Jr., *Photochemistry*, John Wiley and Sons, New York, 1966, p. 19.
24. A. R. Webb, Solar ultraviolet radiation in southeast England: the case for spectral measurements, *Photochem. Photobiol. 54*:789 (1991).
25. I. B. Rufus, H. Shah, and C. E. Hoyle, Photophysical studies of bisphenol-A-based polycarbonate and diphenyl carbonate, *Polym. Prepr. 36*(1):389 (1995).
26. A. Davis and J. H. Golden, Thermal rearrangement of diphenyl carbonate, *J. Chem. Soc. (B)*:40 (1968).
27. A. L. Andrady, Wavelength sensitivity in polymer degradation, *Adv. Polym. Sci. 128*:48 (1997).
28. P. A. Mullen and N. D. Searle, The ultraviolet activation spectrum of polycarbonate, *J. Appl. Polym. Sci. 14*:765 (1970).
29. A. Torikai, T. Mitsuoka, and K. Fuekii, Wavelength sensitivity of photoinduced reaction in polycarbonate, *J. Polym. Sci. A: Polym. Chem. 31*:2785 (1993).
30. A. L. Andrady, K. Fueki, and A. Torikai, Spectral sensitivity of polycarbonate to light-induced yellowing, *J. Appl. Polym. Sci. 42*:2105 (1991).
31. A. L. Andrady, N. D. Searle, and L. F. E. Crewdson, Wavelength sensitivity of unstabilized and UV stabilized polycarbonate to solar simulated radiation, *J. Polym. Degrad. Stabil. 35*:238 (1992).
32. M. F. Sonnenschein and C. M. Roland, Absorption and fluorescence spectra of poly(ethylene terephthalate) dimers, *Polymer 31*:2023 (1990).
33. A. Rivaton, J.-L. Gardette, and J. LeMaire, Photoaging: evaluation of light sources, *Caoutchoucs et Plastiques 651*:81 (1985).

34. M. F. Sturdevant, Plastics in medicine, *Plastics Eng. (Jan.)*:27 (1991).
35. Y. Hama and K. Shinohara, Electron spin resonance studies of polycarbonate irradiated by γ-rays and ultraviolet light, *J. Polym. Sci. A-1, 8*:651 (1970).
36. A. Torikai, T. Murata, and K. Fueki, Radiation-induced degradation of polycarbonate: electron spin resonance and molecular weight measurements, *J. Polm. Deg. Stabil. 7*:55 (1984).
37. R. C. Giberson, Gamma-radiation effects on polycarbonate resin, *Mod. Plastics 39*: 143 (1962).
38. C. E. Lundy and S. Krishnan, The effects of gamma radiation on bisphenol A polycarbonate blends, 33rd IUPAC International Symposium on Macromolecules, Session 2.6.6, Montreal, July 8–13, 1990.
39. J. H. Golden and E. A. Hazell, Degradation of a polycarbonate by ionizing radiation, *J. Polym. Sci. A-1 1*:1671 (1963).
40. R. E. Barker and W. G. Moulton, Irradiation effects in Lexan resin, *J. Polym. Sci. 47*:175 (1960).
41. J. H. Golden, Degradation of polycarbonate. II. Effect of radiation on model compounds, *Macromol. Chem. 66*:73 (1963).
42. A. Davis and J. H. Golden, Radiolysis and photolysis of diphenyl carbonate, *J. Chem. Soc. (B)*:425 (1968).
43. E. Ferain and R. Legras, Heavy ion tracks in polycarbonate. Comparison with a heavy ion irradiated model compound (diphenyl carbonate), *Nucl. Instr. Method. Phys. Res. B 82*:539 (1993).
44. A. Factor, J. C. Carnahan, S. B. Dorn, and P. C. Van Dort, The chemistry of γ-irradiated bisphenol-A polycarbonate, *Polym. Degrad. Stabil. 45*:127 (1994).
45. S. Patai (ed.), *The Chemistry of the Quinoid Compounds,* John Wiley and Sons, New York, 1974.
46. W. Eller and K. Koch, Synthetic preparation of humic acid, *Chem. Ber. 53*:1469 (1920).
47. A. Factor and P. N. Donahue, The use of ^{31}P NMR to identify color bodies in γ-irradiated BPA-PC, *Polym. Degrad. Stabil. 57*:83 (1997).
48. D. S. Argyropoulos, C. Heitner, and F. G. Morin, ^{31}P NMR spectroscopy in wood chemistry. III. Solid state ^{31}P NMR of trimethyl phosphite derivatives of chromaphores in mechanical pulp, *Holzforschung 46*:221 (1992).

13
Polycarbonate Crystallinity

Mary F. Garbauskas
General Electric Silicones, Waterford, New York

I. INTRODUCTION

Bisphenol A polycarbonate (BPA-PC) [1] is an engineering thermoplastic that has many uses in building and construction, automotive, and consumer products. The material is usually extruded or injection-molded and, under these conditions, is totally amorphous. The rigidity of the polycarbonate chain, which results in a glass transition temperature within 100°C of the melting point, does not allow crystalline material to nucleate and grow as it cools from the melt. However, polycarbonate can be prepared under conditions that produce crystalline material. The preparation of this material and its properties is the subject of this chapter.

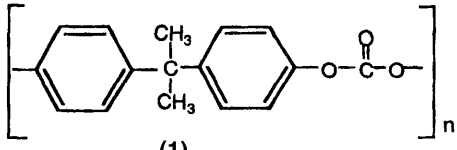

(1)

II. CRYSTAL STRUCTURE

The crystal structure of BPA-PC was first determined by Prietzschk [1] using highly oriented fibers of material that had been exposed to methylene chloride. The clear fibers turned white and opaque upon exposure to solvent vapors. The x-ray pattern indicated highly oriented, crystalline material. Based on the fiber diagram, the unit cell was determined to be orthorhombic, with a = 1.19 nm,

b = 1.01 nm, and c = 2.15 nm. The chains pack in the cell parallel to the c axis, with four chains per cell. This gives rise to an x-ray density of 1.30 g/cm^3.

By using fibers with high degrees of crystallinity, the two-phase structure consisting of crystalline and amorphous regions can be observed with small-angle x-ray scattering [2]. The long period is about 12 nm, consistent with that observed for other crystalline polymers.

III. MANIFESTATIONS OF CRYSTALLINITY

A. X-Ray Diffraction

The outward appearance of a transition from amorphous polycarbonate to crystalline material is generally a change in appearance from clear and colorless to opaque and white. The presence of crystallinity can be confirmed with a number of methods. One of these is x-ray diffraction (XRD), where, as implied above, the crystalline structure produces a coherent diffraction and hence relatively sharp diffraction lines in the wide-angle regime. An example of this can be found in Fig. 1. The diffraction pattern, collected with Cu radiation on a conventional powder diffractometer from an injection-molded bar of polycarbonate, is shown in Fig. 1a. A section of the same bar was soaked for 24 h in acetone and then dried. The diffraction pattern from this material is shown in Fig. 1b. The clear,

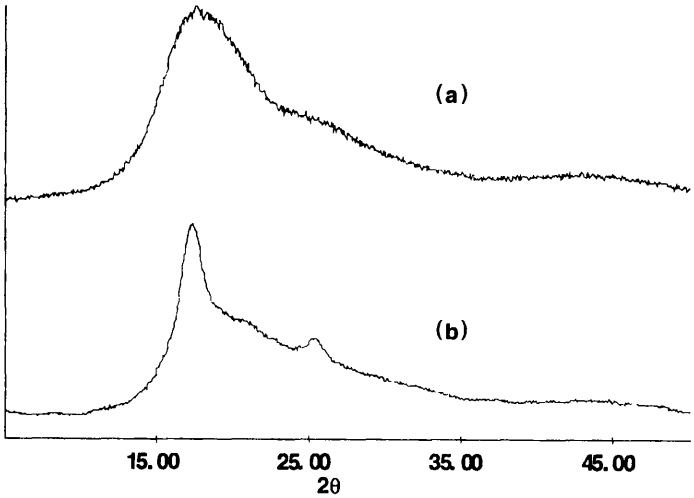

Figure 1 X-ray diffraction patterns using Cu Kα radiation of (a) an injection-molded polycarbonate bar and (b) a piece of same bar after soaking in acetone for 24 h.

transparent bar was transformed into a white opaque material. One can see that the broad bands characteristic of amorphous material have been converted to a series of sharper lines by the acetone treatment. These lines can be indexed according to the structure proposed by Prietzsck [1] and originate from material that has crystallized.

B. Differential Scanning Calorimetry

Another method that can be used to determine crystallinity is differential scanning calorimetry (DSC). When acetone-treated polycarbonate powder is run in a DSC, the first heat produces the lower curve shown in Fig. 2. In this scan there is a characteristic melting endotherm with an onset of 204.5°C, a peak temperature of 228.5°C, and a ΔH of 27 J/g. This corresponds to a material with a crystallinity

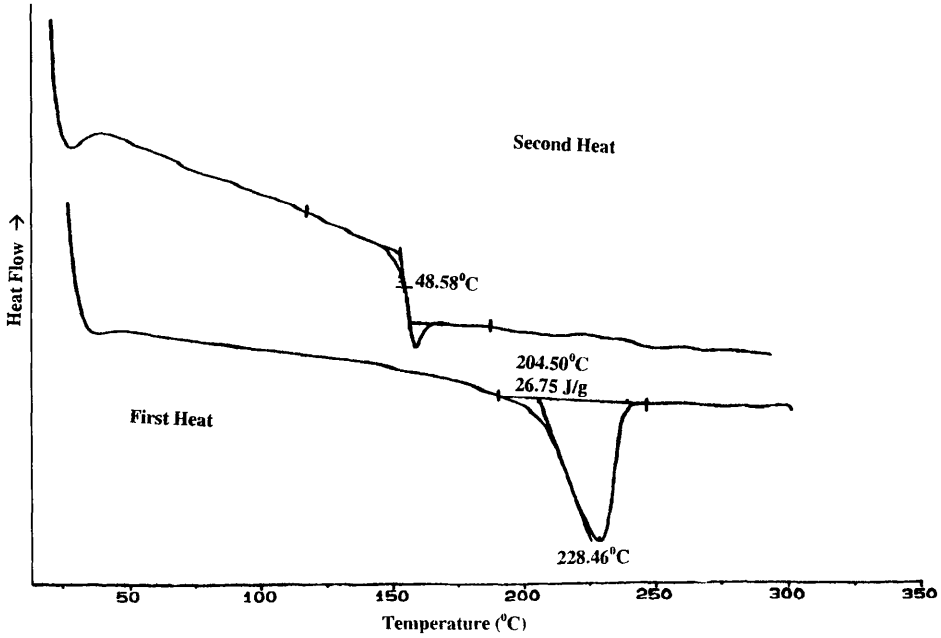

Figure 2 Differential scanning colorimetry curves obtained from samples of polycarbonate powder soaked for 24 h in acetone. The first heat (lower curve) contains a melting endotherm while the second heat (upper curve) contains only a glass transition temperature, indicating that crystallinity, induced via solvent treatment, is destroyed when the sample is remelted.

of approximately 20%, based on the heat of fusion of 133.8 J/g (32 cal/g) reported for polycarbonate crystal [3,4]. When the material is cooled and then remelted, the endotherm observed on the first heat is replaced by a glass transition with a half-height of ~148.5°C, as shown in the upper scan in Fig. 2. This latter trace is typical of amorphous polycarbonate and is evidence that the crystallinity produced by the solvent treatment is readily eliminated by further thermal treatment of the material [5]. Polycarbonate prefers the amorphous state to the crystalline state when being cooled from the melt under normal circumstances, and thus in most extrusion or injection-molded applications this polymer is almost exclusively amorphous.

C. Morphology

Another general indication that crystalline material has been formed is the appearance of spherulitic microstructures. A change in microstructure with annealing above the T_g of polycarbonate has been observed in polycarbonate [6–8]. Using electron microscopy, nodular units of about 12.5 nm can be observed, and these nodules enlarge upon annealing near T_g. Generally, the same microstructures are observed from films cast from solution, exposed to solvent vapors, or cast from the melt [7–9], although the crystallization takes place more slowly in films cast from the melt. The crystallization process appears to be associated with the formation of these nodules, which merge into patches to eventually form lamellar planar structures. In some instances, these structures are single crystals. Spherulitic structures eventually form from these planar structures. Under tensile deformation, the nodular structures appear to undergo rearrangements as shear occurs between them, suggesting that they may be related to some of polycarbonate's physical properties [6].

IV. PREPARATION OF CRYSTALLINE POLYCARBONATE

A number of methods can be used for the preparation of crystalline polycarbonate, including thermal annealing of specimens, treatments with solvents or vapors, additions of plasticizers or chemical nucleating agents, or mechanical methods. Each of these will be described separately.

A. Thermal Annealing

Crystallization of polycarbonate can be accomplished by annealing at approximately 190°C. The kinetics of the crystallization, however, are extremely slow; usually hundreds of hours is required to attain crystallinities of ~20% [10]. The crystallization process follows Avrami kinetics after an initial induction period.

The crystallization kinetics also depend on molecular weight and the previous treatment of the polymer [10,11].

B. Solvent Treatments

By far the most popular and effective method for causing polycarbonate to crystallize is to expose it to certain solvents or their vapors. Heiss [12] catalogued the effect of over 100 different solvents on polycarbonate. He classified the solvents into four categories:

Class I	Dissolved both amorphous and crystalline polycarbonate
Class II	Dissolved amorphous but not crystalline polycarbonate
Class III	Converted amorphous polycarbonate to crystalline polycarbonate with minimal dissolution
Class IV	No visible effect in 24 h

The experiments were performed on amorphous films prepared by extrusion or by casting from methylene chloride. The crystalline films for the tests were prepared by exposing the films to acetone vapors. It was also noted that after polycarbonate had been heat-aged for several days at 120°C, the material that resulted exhibited a melting endotherm rather than a glass transition temperature at 150°C. This material, which was still transparent and amorphous by x-ray examination, is more brittle than amorphous polycarbonate. This alternatively could be explained by solvent-induced "physical aging." Crystallization also occurred during solvent vapor penetration into the polycarbonate films [11,12]. Indeed, it was noted that as any solvent vapor penetrated polycarbonate, the successive stages listed in Table 1 were achieved.

The mechanism for the solvent-induced crystallization involves two main sequential processes, i.e., diffusion of the low molecular weight solvent into the interior of the polymer sample followed by crystallization of the polymer. In semicrystalline polymers, the crystallization process has been shown to occur

Table 1 Solvent Vapor Effect on Polycarbonate as a Function of Weight Change

ΔW (%)	Effect
5	Plasticization; T_g lowered to room temperature in some cases
10	Sample remains transparent; endotherm at ~150°C
20–60	Sample becomes opaque; melting endotherm at ~225°C
400	Solution occurs

Data from Ref. 12.

directly behind the penetration front moving through the polymer [14–16]. Benecki and Turska [17] have shown the existence of quite separate diffusion and crystallization fronts in polycarbonate with the magnitude of the separation dependent on the swelling liquid and the temperature of the process. The separation of the diffusion and crystallization fronts provides evidence for a crystallization induction period, which may be related to the gradual increase in the amount of trans-trans conformations of the polycarbonate chains, which must be assumed before crystallization can occur [18].

The kinetics of the crystallization of polycarbonate films is also controlled by the solvent used. Turska and Janeczek [19] used calorimetry to show that acetone-induced crystallization proceeds rapidly and terminates after 3–4 min, while carbon tetrachloride crystallization reaches a maximum in 2–5 min whereupon a very slow process takes place over several hours. A maximum crystallinity of 17% was reached for the carbon tetrachloride–crystallized material and 20% for the acetone-crystallized material.

C. Plasticizers

The use of plasticizers including tritolyl phosphate, pentaerythritol tetrabobanoate, and trimellitic acid–tridecyloctyl ester to aid in the crystallization of polycarbonate has been demonstrated [20,21]. The use of 10% trimellitic acid tridecyloctyl ester reduces the half-crystallization time at 170°C to 100 min from 300 h for unplasticized material. The crystallization still follows Avrami kinetics. It should be noted, however, that this time is still much less than for typical semicrystalline polyesters such as polyethylene terephthalate or polybutylene terephthalate, where half-crystallization times are on the order of seconds.

Another effective plasticizer is supercritical CO_2 [22]. Crystallization of polycarbonate occurs within 1 h of exposure at temperatures and pressures as low as 75°C and 100 atm. Optimum crystallization occurs at pressures of approximately 300 atm, with crystallization rates comparable to those of methylene chloride or acetone-induced crystallization. Crystallinities comparable to solvent-induced values (20%) are generally achieved, although the total crystallinity achieved is a function of CO_2 density, absolute pressure, and temperature. The plasticization occurs through a lowering of the polycarbonate T_g as CO_2 is absorbed by the polymer. Since the CO_2 can subsequently diffuse out of the material, the typical polycarbonate T_g of approximately 150°C can be recovered after ambient temperature and pressure have been restored.

D. Chemical Nucleation

Alkali metal salts of organic carboxylic acids are believed to react with molten polycarbonate to form ionic end-groups that act as nucleating agents. These com-

pounds have been classified as chemical nucleants because their action is believed to be different from that of heterogeneous nucleants such as talc or mica [23–26]. This phenomenon can be observed by mixing sodium *o*-chlorobenzoate and polycarbonate for several minutes at 270°C and then quenching the material to room temperature. DSC traces taken on this quenched material show a glass transition temperature of approximately 145°C followed by a crystallization exotherm at 212°C and a melting endotherm at 302°C. Once melted, the sample cannot be recrystallized and a second heat contains only the 145°C glass transition temperature. The initial crystallinity of this material is very high (about 50%) and single crystals have been observed in the electron microscope. It is well known that alkali metal salts of organic carboxylic acids are transesterification catalysts in polycarbonate.

Very-high-melting crystalline polycarbonate can also be obtained by vapor treatment followed by thermal annealing [27]. Acetone-treated polycarbonate film exhibited a melting endotherm at about 195°C. The melting temperature could be increased to 295°C with a crystallinity of 60% through a set of thermal annealing steps. Small-angle scattering experiments indicated an increase in lamellar thickness during the thermal annealing. The overall mechanism is believed to involve both a thickening of the crystalline lamellar and an increase in the crystal perfection during the course of the thermal anneal.

E. Chemical Structure Modification

The slow thermal crystallization rate of polycarbonate is attributed to the restricted rotational degrees of freedom, which produces a very rigid structure. In order to increase the flexibility, randomly dispersed flexible segments can be introduced into the polymer [28]. The synthesis of copolymers containing flexible repeat units, such as terephthalates, can be accomplished through a copolycondensation reaction. By introduction of small amounts of terephthalate units into the polymer chain, the rate of crystallization can be increased by a factor of 2–20. The mechanical properties of these materials reflect this increase in crystallinity, with an increase in the heat distortion temperature of about 35°C over that of amorphous samples. The elastic modulus also shows an increase.

Another copolymerization approach involves hydroquinone (HQ) and BPA from cyclic oligomers [29,30]. Use of the cyclic oligomer approach makes possible the synthesis of copolymers, which would be difficult to construct by more conventional routes. The solubility and melt-viscosity characteristics of the cyclics are generally different from those of the parent polymer, enabling the utilization of various procedures not possible in more conventional approaches. The copolymers synthesized by these procedures have unique properties. For instance, the polymer that results from a 60:40 HQ-BPA cocyclic is a semicrystalline material with a T_g of 154°C, a melting point of approximately 313°C (ΔH =

11.0 J/g), good impact properties, good solvent resistance, and high transparency. It is not yet apparent if this technology will have economically feasible applications.

F. Mechanical Methods

Highly crystalline fibers of polycarbonate can be prepared through dry spinning, wet spinning, melt spinning, or a special swelling-drawing process [2]. The latter process produces fibers with high degrees of crystallinity as deduced from density, birefringence, x-ray, and DSC measurements. These fibers also show an increase in tenacity due to the higher crystallinity and orientation.

Polycarbonate can also be made to crystallize by subjecting the material to high-pressure injection molding (up to 500 Mpa) [31]. When cylinders are injection-molded at 500 MPa, with a cylinder temperature of about 300°C and a 50°C mold temperature, a hazy region appears in the shear zone which occurs between the solidified material on the mold wall and the flowing material in the core of the part. X-ray and differential thermal analysis suggest that this material is crystalline polycarbonate. The position of the crystalline material in a layer about the shear zone suggests that shear stresses are important in producing this crystallization. The elastic modulus of these parts molded at 500 Mpa was around 20% higher than those molded at 150 MPa. In this case, the crystallization occurs during injection molding but does not occur uniformly throughout the part, indicating again that it is very difficult to force polycarbonate into a situation where crystallization is favored.

V. CONCLUSION

Crystalline polycarbonates that retain the desirable properties of polycarbonate, such as ductility and transparency, are currently unknown. Crystallinity in polycarbonate can be produced in a number of ways. However, the conventional applications of polycarbonate in extrusion and injection molding produce amorphous material. Using specialized approaches, crystalline material with better high-temperature mechanical properties can be achieved, but commercialization of these procedures is not yet feasible. In addition, unless dramatic increases in properties (such as modulus) can be demonstrated, the competition from other semicrystalline materials such as polyesters will make the search for routes to crystalline polycarbonate less attractive.

ACKNOWLEDGMENT

The author thanks L. L. McCraken for the differential scanning colorimetry on crystalline polycarbonate powder and S. Y. Hobbs for advice and discussion regarding this manuscript.

REFERENCES

1. V. A. Prietzschk, Die kristallstruktur des polycarbonats aus 4,4′-dioxydiphenyl-2,2-propan, *Kolloid Zh. 156*:8 (1958).
2. B. Falkai and G. Hinrichsen, Drawing behavior and mechanical properties of highly oriented polycarbonate fibers, *J. Polym. Sci. Polym. Symp. 58*:225 (1977).
3. L. D. Jones and F. E. Karasz, Heat of fusion of Lexan polycarbonate, *Polym. Lett. 4*:803 (1966).
4. J. P. Mercier and R. Legras, Correlation between the enthalpy of fusion and the specific volume of crystallized polycarbonate of bisphenol-A, *Polym. Lett. 8*:645 (1970).
5. J. M. O'Reilly, F. E. Karasz, and H. E. Bair, Thermodynamics of Lexan polycarbonate from 110–560°K, *J. Polym. Sci. C 6*:109 (1964).
6. S. H. Carr, P. H. Geil, and E. Baer, The development of spherulites from structural units in glassy poly(bisphenol-A-carbonate), *J. Macromol. Sci. Phys. B2*:13 (1968).
7. A. Siegmann and P. H. Geil, Crystallization of polycarbonate from the glassy state. I. Thin films cast from solution, *J. Macromol. Sci. Phys. B4*:239 (1970).
8. A. Siegmann and P. H. Geil, Crystallization of polycarbonate from the glassy state. II. Thin films melted and quenched, *J. Macromol. Sci. Phys. B4*:273 (1970).
9. R. E. J. Fryer, Spherulite crystallization in bisphenol-A-polycarbonate of varying molecular weight distribution, *J. Appl. Polym. Sci. 18*:2261 (1974).
10. E. Turska, W. Przygocki, and M. Maslowski, Crystallization kinetics of polycarbonates. I. *J. Polym. Sci. C 16*:3373 (1968).
11. G. V. Di Filippo, M. E. Gonzalez, M. T. Gasiba, and A. V. Muller, Crystalline memory on polycarbonate, *J. Appl. Polym. Sci. 34*:1959 (1987).
12. H. L. Heiss, The classification of solvents for bis-phenol-A polycarbonate, *Polym. Eng. Sci. 19*:625 (1979).
13. J. P. Mercier, C. Groeninckx, and M. Lesne, Some aspects of vapor-induced crystallization of polycarbonate of bisphenol A, *J. Polym. Sci. C 16*:2059 (1967).
14. A. B. Desai and G. L. Wilkes, Solvent induced crystallization of polyethylene terephthalate, *J. Polym. Sci. Polym. Symp. 46*:291 (1974).
15. P. J. Makarewicz, Y. Budnitsky, and G. L. Wilkes, Some mechanical property studies of unoriented polyethylene terephthalate crystallized by non-reactive environments, *Polym. Prepr. 17*:943 (1976).
16. P. J. Makarewicz and G. L. Wilkes, Diffusion studies of polyethylene terephthalate crystallized by nonreactive liquids and vapors. *J. Polym. Sci. B: Polym. Phys. 16*: 1529 (1978).

17. W. Benecki and E. Turska, Separation of the diffusion and crystallization fronts on swelling a bisphenol-A polycarbonate, *J. Appl. Polym. Sci. 25*:2653 (1980).
18. R. Bonart, Zur Kristallstrucktur der Polycarbonate aus 4.4′-dihydroxydiphenyl-2,2-propan, 4,4′-dihyroxydiphenylsulfid und 4,4′-dihydroxydiphenylmethan, *Makromol. Chem. 92*:149 (1966).
19. E. Turska and H. Janeczek, Liquid-induced crystallization of a bisphenol-A polycarbonate, *Polymer 20*:855 (1979).
20. F. Gallez, R. Legras, and J. P. Mercier, Crystallization of bisphenol-A polycarbonate. I. Influence of trimellitic acid tridecyloctyl ester on the kinetics of crystallization, *J. Polym. Sci. B: Polym. Phys. 14*:1367 (1976).
21. R. Legras and J. P. Mercier, Crystallization of bisphenol-A polycarbonate. II. Melting behavior and equilibrium melting temperature of the plasticized polymer, *J. Polym. Sci. B: Polym. Phys. 15*:1283 (1977).
22. E. Beckman and R. S. Porter, Crystallization of bisphenol A polycarbonate induced by supercritical carbon dioxide, *J. Polym. Sci. B: Polym. Phys. 25*:1511 (1987).
23. R. Legras, J. P. Mercier, and E. Nield, Polymer crystallization by chemical nucleation, *Nature 304*:432 (1983).
24. R. Legras, C. Bailly, M. Daumerie, J. M. Dekoninck, and J. P. Mercier, Chemical nucleation, a new concept applied to the mechanism of action of organic acid salts on the crystallization of polyethylene terephthalate and bisphenol-A polycarbonate, *Polymer 25*:835 (1984).
25. CH. Bailly, M. Daumerie, R. Legras, and J. P. Mercier, Crystallization of bisphenol-A polycarbonate induced by organic salts; physical aspects. I. Crystallization rate, melting behavior, and morphology, *J. Polym. Sci. B: Polym. Phys. 23*:751 (1985).
26. CH. Bailly, M. Daumerie, R. Legras, and J. P. Mercier, Crystallization of bisphenol-A polycarbonate induced by organic salts; chemical modification of the polymer I. Model reactions, *J. Polym. Sci. B: Polym. Phys. 23*:343 (1985).
27. J. Jonza and R. S. Porter, High melting bisphenol-A polycarbonate from annealing of vapor-induced crystals, *J. Polym. Sci. B: Polym. Phys. 24*:2459 (1986).
28. A. Conix and L. Jeurissen, Internal plasticization of bisphenol-A polycarbonate, *J. Polym. Sci. C 16*:3821 (1968).
29. D. J. Brunelle, Solvent-resistant polycarbonates, *Trends in Polymer Science 3*:154 (1995).
30. D. J. Brunelle, H. O. Krabbenhoft, and D. K. Bonauto, Preparation of crystalline and solvent resistant polycarbonates via ring-opening polymerization of cyclic oligomers, *Macromol. Symp. 77*:117 (1994).
31. K. Djurner, J-A. Manson, and M. Rigdahl, Crystallization of polycarbonates during injection molding at high pressures, *J. Polym. Sci. Polym. Lett. Ed. 16*:419 (1978).

14

Commercial Applications of Polycarbonates

James L. DeRudder
General Electric Plastics, Mt. Vernon, Indiana

Most materials either are specialty materials that find usage in small niche areas or commodity materials that have a few huge markets. This is as true for plastics as it is for other material systems. Whether we look at large-volume commodity plastics or low-volume specialty plastics, most tend to fit the 80:20 rule. That means that a relatively small volume of application usage accounts for 80% of the market volume. Whether it be polyolefins in garbage bags, packaging, and film applications; polyethylene terephthalate (PET) in bottle or fiber applications; or polyvinyl chloride (PVC) in pipe, siding, and lineals applications, most polymers are associated with a few major applications. Polycarbonate has evolved very differently. Polycarbonate is really an in-betweener. Polycarbonate, co-polycarbonates, and polycarbonate blends are essentially moderate-volume specialty thermoplastics that have filled a broad array of niche markets. No single application accounts for more than 10% of market volume. This unusual situation has evolved in part because of the broad palette of properties offered by polycarbonate and its capability to be extensively modified and tailored to meet demanding market applications in many arenas. Most major manufacturers of polycarbonate offer at least 500 grades of polycarbonate commercially. In essence, polycarbonate is a specialty engineering thermoplastic that has found many fits and niches in a wide variety of commercial markets. Because polycarbonate has a special status of a broadly based specialty polymer, it enjoys a much lower cost and price position than could normally be expected of specialty materials. Yet, as in many properties, it is intermediate

between the large-volume commodity polymers and the low-volume specialty polymers.

Polycarbonate is thus very difficult to explain in a commercial sense. Many of the applications are highly technically focused in a small niche. Nonetheless, it is possible to broadly describe the market so that a general understanding is possible. Although polycarbonate can do many things in many areas, it is not capable of solving all issues or fitting in all areas. Thermoplastics are most broadly divided into amorphous and crystalline. Each has its own strengths and weaknesses. Some applications could potentially be served by either an amorphous or a crystalline polymer. Most commercial applications really fit into one of the two categories. Polycarbonate is an amorphous thermoplastic. Polycarbonate is also used in many blends, some of which are blends with crystalline materials.

Describing the commercial utilization of polycarbonate requires an understanding of the useful properties of polycarbonate that result in successful commercial applications. A listing of the top 10 polymer attributes for polycarbonate would probably look like the following:

Transparent
Tough
Strong and stiff
Dimensionally stable
Easy to mold
Easy to paint/decorate/finish (secondary operations)
Excellent aesthetics
Flame resistance
Heat resistance
Safe (medical and food contact)

Each of these attributes can, of course, be achieved by another polymer system. However, many times the unique combination of attributes makes polycarbonate the obvious material of choice. However, not all of these are of equivalent importance. Transparency is the single most important attribute of polycarbonate. Transparency is so important because there are really very few transparent polymers, when compared to opaque or translucent polymers. This is not to say that polycarbonate is only of interest in transparent applications. In fact, about half of all polycarbonate is used in applications that are transparent and about half in opaque applications.

In order to better understand some of these effects, we will utilize combinations of these attributes to demonstrate why polycarbonate is the material of choice for many given applications. We will subdivide the discussion into three areas: transparents, opaques, and blends.

I. TRANSPARENTS

The most obvious property combination to consider first for polycarbonate is toughness and transparency. The number of plastics that are both tough and transparent is relatively small. Compact disks, CD-ROMs, refrigerator crisper trays, lighting fixtures, automotive head lamps, prescription eyeglasses, safety face shields, aircraft windows, bullet-resistant glass, architectural window glazing, automotive moon roofs, automotive side window glazing, and aircraft canopies are examples of applications in which polycarbonate is used for transparency and toughness. Each of these applications has competitive materials to some extent. Sometimes the competitive material is inorganic glass, sometimes it is a thermoset plastic, and sometimes it is another thermoplastic that is deficient in one or more properties when compared to polycarbonate. Let's look at each of these in detail.

Compact disks and CD-ROMs have become a large market for polycarbonate. In simplest terms, these devices store information in a series of pits that can be read by a laser beam. Ease of molding is very important because billions of pits must be replicated by a molten thermoplastic. The polycarbonate disk is molded against a "master" that has a defined topography on a micrometer scale. The polycarbonate must be capable of conforming to the surface of this intricate information pattern yet must also be capable of releasing from the surface after molding. Since the laser reads the information through the thickness of the polycarbonate, clarity and cleanliness are critical. Any particulate matter, down to sizes comparable to laser light wavelengths, can cause scattering of the beam, with resultant loss of information. In order to achieve the level of cleanliness required, melt filtering must be used to physically filter out objectionable particles. These products must be very low viscosity in order to clearly define and replicate the pits. Melt flow is typically about 66 g/10 min at 300°C. Polycarbonate also has an advantage in cycle time over many materials.

During the injection molding process the molten plastic must set up in the mold so that it is sufficiently rigid as to not deform when removed from the mold. Polycarbonate is one of the best, if not the best, for this. This translates commercially into reduced cycle time. Polycarbonate is capable of being molded into compact disks during a cycle time of less than 5 s. This 5 s includes closing of the mold, injection of the molten polycarbonate, solidification of the molten polycarbonate, opening of the mold, and robotic removal of the molded part. Polycarbonate also provides dimensional stability down to the wavelength of light that is required to maintain the integrity of the data. Secondary finishing operations such as aluminum coating and ink printing are also required for a finished product. Today virtually all compact disks and CD-ROMs are made using a polycarbonate-based material. Sufficient ductility is maintained to resist normal abuse, even at these very low molecular weights.

Refrigerator crisper trays at various times have been made from metal as well as lower impact performance thermoplastics. These trays require excellent aesthetics as well as Food and Drug Administration (FDA) food contact approval. As refrigerators and their crisper trays have become larger the demand for higher performance has increased. Most refrigerator crisper trays are now made from polycarbonate.

Architectural glazing made of polycarbonate is an area in which inorganic glass is slowly being replaced. The rate of replacement is accelerating. The design flexibility inherent with thermoplastic polymers leads to many design opportunities that simply would be too difficult or too expensive to attain in inorganic glass. Curved and bubble-shaped three-dimensional structures have become very commonplace when designing with polycarbonate. Not too many years ago, only very-high-volume applications, such as automotive windshields, could be economically made with inorganic glass. Today high-performance systems can be made with thermoplastics, particularly polycarbonate. In fact, when toughness is absolutely required, as seems to become more commonplace every day, then polycarbonate architectural glazing is really the only material of choice. Many of these architectural glazing applications have coatings that provide additional weathering protection, scratch resistance, and chemical resistance. The architectural applications of polycarbonate now extend into many flat panel applications, as well as the curved applications mentioned above. In particular, applications requiring security and protection from vandalism and graffiti have become primarily polycarbonate. All of these types of products are made by continuous extrusion of sheet that can subsequently be thermoformed. These extrusions may be very thick, such as those used to make fighter aircraft canopies, or they may be very thin, such as those used to make graphic arts film.

A significant change has occurred in the materials and methods used for switches and displays for electronic equipment both in the home and in industry. Many displays are now made of polycarbonate films. Switches are commonly built into these displays by locating sensors under the polycarbonate film. Printing can be done so that it either is always visible or is only visible when backlit. Most printing is done in reverse on the back side of the film so that it is much more durable. These films may be textured in many different ways to achieve many different appearance effects. These displays have become common in appliances such as dishwashers, devices such as medical diagnostic equipment, and hermetically sealed equipment such as factory rugged data input panels. But probably the most common application of these displays is in backlit automotive instrument panels.

Moving down to another level of thickness brings us to cast films. Many properties of polycarbonate, such as chemical resistance and fatigue resistance, are highly dependent on molecular weight. Unfortunately, melt processing has a limit in terms of how high a molecular weight that can be processed. Large in-

creases in certain properties, such as chemical resistance, can be attained at molecular weights that are too high for melt processing. Commonly these materials are not polycarbonate homopolymers, but rather are polycarbonate copolymers, in which a small amount of a compatible comonomer is added during polymerization to prevent solvent-induced crystallization. These types of products are primarily used in areas where they have significant chemical exposure or in high-fatigue applications.

A large group of commercial products are created by laminating various types of polycarbonate sheet together with soft bonding inner layers. These create assemblies that display properties that cannot be attained by one solid piece of polycarbonate. The soft inner layers help decouple applied stresses between layers. This is the fundamental technology used to create bullet-resistant glazing that has become so popular in banks. These types of products are also often used in security cases and security shields. These products are created by hot pressing of extruded sheets. The soft inner layer that bonds together the various layers may be acrylic, urethane, or a polycarbonate-siloxane copolymer. Silicone-based systems have the lowest glass transition temperatures and typically are used for the most premium products.

Fixed window glazing is used for windows that do not move, open, or shut. Polycarbonate is becoming common for these types of windows. These fixed windows may be used in aircraft, buses, or automobiles. Most polycarbonate used in fixed window glazing has a protective coating to improve weatherability, scratch resistance, and chemical resistance. The exact type of coating that is used depends on the application. Depending on the volume of the application, these fixed glazings may be made either by sheet extrusion and thermoforming or by injection molding. Some of these parts are not totally fixed but may be removable. An example would be the Corvette moon roof, which is injection-molded from polycarbonate. This product is coated with a silicone hard coat to enhance weatherability, chemical resistance, and scratch resistance. In this case, weight is also very important because this is an owner-removable product. When this part is removed the vehicle has an open top. Weight reduction of these large panels is over 50% with polycarbonate, when compared to inorganic glass.

There are also many other areas in which high clarity and toughness is required. A major area is in safety protective devices. Nonprescription safety glasses are usually made of plastic. Most are made from polycarbonate for premium performance. Polycarbonate is also used extensively for safety visors, face shields, goggles, masks, and so forth.

A higher level of clarity and toughness is needed for ophthalmic lenses, used in prescription eyeglasses. Polycarbonate has become the premium material for these applications because polycarbonate makes the thinnest, lightest eyeglasses that provide the proscribed level of protection. Many eyeglass designers use polycarbonate because of the greater freedom they have in design. For oph-

thalmic lenses dimensional stability and grinding/polishing performance are also very critical to producing a final product. Prescription safety glasses are hybrids that use thicker sections to attain the higher level of protection.

Another application area where clarity and toughness is mandated is in lighting devices. Lighting devices also require high heat resistance, dimensional stability, and ultraviolet (UV) stability. These devices are usually transparent but are sometimes translucent. Translucents are used so that light, but not a distinct image, is transmitted. Inorganic glass is still prevalent in home usage, but polycarbonate is becoming increasingly common in commercial applications. The slightly higher initial cost is more than recovered through the longer lifetime in commercial applications. Some lighting devices have additional requirements related to flammability resistance. Polycarbonate has a very high oxygen index, which implies an inherent tendency to resist burning. Although polycarbonate is not very flame-resistant by itself, it can easily be made flame-resistant. Polycarbonate can be made flame-resistant very easily, when compared to many polymers. Depending on specific application needs, transparent flame-retardant systems can be used to produce materials that have excellent optical properties. Transparent flame-retardant polycarbonates can be achieved by the addition of flame-retardant salts of matching refractive index and/or miscible bromine sources. The miscible bromine sources are usually low molecular weight oligomers of tetrabromo-bisphenal A (BPA) or copolycarbonates of BPA and tetrabromo-BPA. The end-product is transparent and can have various levels of flammability resistance, as recognized by independent agencies, such as Underwriters Laboratory.

Many other applications exist for flame-retardant transparent polycarbonate. Usually these are devices in which it is considered desirable to see electrical connections or in which transparency makes the appearance less obtrusive to the aesthetics of the device. Probably the most common application is in telephone jack connectors. Other applications are commonly where a window is desired to see what is happening inside of an enclosure, but where a flame-retardant product is required. Years ago, this always meant inorganic glass. Today there are many more options available, particularly when toughness is an essential requirement.

Lighting devices can have other types of regulatory requirements besides the Underwriters Laboratory, mentioned above. Automotive lighting is regulated by the Federal Motor Vehicle Safety Standards (FMVSS) #108. In the United States, this is issued by the National Highway Traffic Safety Association (NHTSA). These regulations are based on modifications of testing standard J576 promulgated by the Society of Automotive Engineers (SAE). For lighting these standards require 3-year outdoor weathering in both Florida and Arizona, with strict limits on the allowable amount of color shift and haze after weathering. The actual limits depend on whether the lighting is forward lighting, reflex reflectors, or standard tail lights. For example, forward lighting and reflex reflectors have much tighter haze requirements after weathering. In addition, forward light-

ing requires greater abrasion resistance because it is used on the front on automobiles and is constantly impacted by grit, dirt, and pebbles. Polycarbonate products have performed well for over 25 years in these applications. The transition from inorganic glass is nearly complete in the United States and well underway globally.

Literally thousands of medical devices are made from polycarbonate. Most of these utilize polycarbonate for its clarity, heat resistance to steam sterilization, chemical resistance to ethylene oxide (EtO) sterilization, dimensional stability, strength, and ductility. Leur fittings, valves, blood bowls, dialysis tube holders, bottles, and containers of various sizes and shapes are typical medical applications of polycarbonate. Polycarbonate is primarily used in disposable medical applications. Polycarbonate is not recommended for long-term contact with body tissues or fluids, nor is it suitable for implantation in the human body. Medical devices are some of the most highly regulated plastic applications. In the United States medical devices are regulated by the medical device division of the FDA. Materials must be compliant with the appropriate section of the United States Pharmacopeia (USP). Tests for medical devices are based on biological nonreactivity. Medical grades of polycarbonate are usually recognized as USP Class VI.

Medical devices are one of the most global of all plastics markets. Regulations are also becoming more globally based. The United States, Canada, and Great Britain have created a joint set of test protocols that are a superset of the USP protocols. Starting in 1992, medical device product introductions in these three geographies require compliance to these tripartite guidelines. Compliance to tripartite guidelines has become nearly a global requirement. A superset of the tripartite guidelines is currently under revision by the International Standards Organization (ISO). All of these standards are based on biological nonreactivity. Polycarbonate grades designed for medical applications generally perform very well in meeting these standards. Designing for medical products means that many restrictions exist in terms of types and levels of stabilizers, additives, and colorants that may be used. Although medical products have similar performance to standard grades of polycarbonate, quite often one or more properties are lower because of the restrictions imposed by these requirements. Usually medical grade stabilizers, additives, and colorants are more expensive than standard grades. This also means that many standard grades of polycarbonate are not suitable for medical applications because they use stabilizers, additives, or colorants that are not approved for medical applications.

A special subsection of medical grades of polycarbonate is that of products designed to be resistant to γ irradiation. γ Irradiation is of such a high energy that essentially all bonds in the molecule are affected. Many different pathways must exist to dissipate all of this absorbed energy. First-generation γ-resistant products were introduced during the 1980s, based on various low molecular weight radical–scavenging stabilizers. Second-generation γ-resistant products

were introduced during the 1990s. These second-generation products are much more complex. They usually incorporate high levels of multiple additives and/or miscible polymer blends.

Food contact is an area that is similar in some ways to the medical market, but in other ways it is very different. Food contact applications of plastics must also be approved by the FDA, although in this case it is the food additives division of the FDA. This is different from the medical devices division of the FDA. Food contact regulations govern the type and amount of low molecular weight species that can be extracted by tests that simulate food contact situations. Materials are approved for contact with certain classes of foods under defined temperature ranges and use conditions. Polycarbonate generally does very well on tests under the majority of use conditions. In contrast to medical applications, almost all uses of polycarbonate in food contact applications are permanent, not disposable. Typical applications of transparent polycarbonate would be measuring cups, salt and pepper shakers, bowls, dispensers, containers, glasses, and goblets. Virtually anything made of glass that does not have a heat requirement over 250°F can be made of polycarbonate. Food contact applications also have restrictions on the allowable stabilizers, additives, and colorants that can be used, similar to medical plastics. In fact, cross-qualification of the same polycarbonate grade for both medical and food contact applications is very common.

A specialization of the food contact area is for bottled water containers. This is a very major global application for polycarbonate. This is discussed separately because it is such a large market with very specific requirements. Containers for bottled water not only require FDA food contact approval but also require compliance with the International Bottled Water Association (IBWA). Particular emphasis is placed on taste and ingredients that could leach out and affect taste. Small bottled water containers are made from many types of plastics, but the larger 5-gallon containers are almost all made from polycarbonate. The high strength of polycarbonate allows for lighter containers. Normal linear polycarbonate homopolymer does not have enough melt strength to blow-mold these large containers. A branched polycarbonate is used in these applications to increase melt strength and processibility of these 5-gallon water bottles. Branching provides sufficient melt fluidity at high shear rates that a parrison can be extruded or injection-molded but minimal melt fluidity at low shear rates, so that the parrison will maintain dimensions while hanging but still can be blown out to its correct dimensions.

II. OPAQUE

There are many applications for opaque polycarbonates. Up to this point we have discussed applications that have involved transparency as a critical requirement.

The same properties that make polycarbonate an excellent transparent material also make it a very good choice as an opaque material. Since most polymers are opaque, there are potentially many more viable competitors in each and every opaque application. Nonetheless, there are still very large areas in which polycarbonate is the material of choice.

Probably the most recognized applications of opaque polycarbonate are in the impact-modified products area. Polycarbonate intrinsically has a very high ductility. Thus, it is easier to make polycarbonate even better. High ductility can be extended to thicker sections, lower temperatures, and higher strain rates by the use of impact modifiers. Because the starting matrix has such a high initial ductility, the levels of impact modifier needed are usually at 20–40% of the levels utilized in competitive impact-modified products. Being able to attain similar performance levels at a lower level of additives is a distinct advantage because this means that many of the engineering trade-offs associated with impact modification can be minimized. Since impact modifiers are typically low glass transition, rubbery material, some of the engineering trade-offs that must be made when impact modifying are low strength, low modulus, and low hardness. Other engineering trade-offs are increased viscosity, melt fracture, poorer high-temperature melt stability, poorer surface appearance, greater shear sensitivity, poorer colorability, and more difficulty with secondary finishing operations. Depending on the type of impact modifier used, there may be deleterious effects on other properties, such as weatherability and flammability.

Commercial applications of impact-modified polycarbonate span a wide range of areas. The primary areas are automotive products, safety products, athletic products, communication devices, and chemically resistant products.

Although many automotive products are made of impact-modified polycarbonate, instrument panels are probably the largest area. Instrument panels not only must manage the energy dissipation of vehicle occupants in a crash situation, but they must also handle the high heat loads encountered in highly raked windshields in tropical climates, maintain dimensional rigidity and stability during both arctic cold and desert heat, and meet the stresses imposed by explosively inflated airbags. Depending on the specific application requirements and automotive design, many impact-modified products may be used. Instrument panels tend to either be soft and vinyl covered, used in cars, or hard and painted, used in trucks. Polycarbonate is reserved for the most demanding applications, such as pickup truck instrument panels and air bag deployment covers. Air bag deployment causes a very-high-energy impulse to be applied to the surrounding material. Polycarbonate is the material of choice to handle these impulse loads.

Safety products made from impact-modified polycarbonate are exemplified by hard hats. The light weight and comfort obtained using polycarbonate hard hats is achieved with no loss in safety impact performance. Impact coupled with its nonelectrical conductivity makes polycarbonate hard hats a natural. Other

safety products, such as ear muffs, commonly use impact-modified polycarbonate.

Two athletic products that use impact-modified polycarbonate are well known to just about everyone who follows sports: football helmets and baseball batting helmets. A variety of other types of pad reinforcements, supports, and braces are made with impact-modified polycarbonate. A variety of impact modifiers are utilized, depending on the requirements of the application, particularly low temperatures and the speed of impact expected. The impact needs of less demanding applications, such as biking helmets, are quite often satisfied with lower cost/lower performance plastics. Youth baseball and youth football helmets, in which impact velocities and energy absorption needs are moderate, quite often use impact-modified polycarbonates based on saturated organic impact modifiers. As impact velocities become higher and energy absorption needs are greater, other impact modifiers are used. These premium products are prevalent in professional sports. They are also used for motorcycle helmets. Sporting helmets commonly display a wide variety of decorations. The excellent paintability of polycarbonate ensures that your favorite football or baseball team will have a logo that looks great.

Communication devices are almost always made from an impact-modified plastic. An increasing trend in communication devices has been portability. Two of the major considerations for portability are light weighting and greater impact abuse due to product mobility. Although stationary devices commonly use lower cost polymers, they must be made in thicker wall sections to provide impact protection. Premium stationary applications, such as pay telephones, utilize impact-modified polycarbonate. Most portable communication devices require this premium level of performance. In many cases, a better flow/impact balance is required in these applications than can even be attained with premium grades of impact-modified polycarbonate homopolymer. In these cases an impact-modified polycarbonate copolymer is required. A substantial incorporation of olefinic short blocks into the polycarbonate chain backbone allows for greater flow without loss of impact. This allows thinner wall parts to be easily molded while device impact protection is maintained. Portable computer housings are also becoming common application areas, particularly where higher heat resistance is needed.

Chemically resistant polycarbonate products often use impact modifiers to improve chemical resistance. Impact modifiers lower the yield stress of the polymer, thus allowing ductile yielding to occur, rather than crazing or brittle crack propagation, due to chemical attack. These products have a tendency for delamination; hence they are usually restricted to extruded and thermoformed products or low-shear-rate injection molding conditions. These are commonly used to make food service trays and containers for commercial food operations for hospitals, airplanes, hotels, prisons, and schools. An even higher level of chemical resistance is possible using products that are based on miscible blends. These

are commonly used in the housewares industry to make many food preparation utensils and containers.

Another significant application of opaque polycarbonate is in the area of housings. These are almost always glass-filled for dimensional stability and rigidity and flame-retarded. These are used commercially for small-equipment housings, hand-held power tools, alignment holders, electric motor housings, and small appliances. Two general groups of products exist. Low glass concentrations are used to obtain higher impact capability with some increase in stiffness. At higher glass levels there is more loss in impact and greater increase in stiffness. Glass-filled polycarbonate typically gives much higher impact capability than other glass-filled plastics. In many cases, a better flow/impact balance is required in this application than can be attained with normal grades of glass-filled polycarbonate homopolymer. In these cases a glass-filled polycarbonate copolymer is required. A substantial incorporation of olefinic short blocks allows for greater flow without loss of impact. These products also show dramatically better surface appearance, due to the polycarbonate copolymer preventing glass fibers from being forced to the surface of the polymer melt during injection molding. A specialty application of glass-filled polycarbonate is in the area of foamed products. Foaming is a low-pressure process that is capable of making very large parts with very thick walls, using economical processing equipment. These products are used for making items that must be very strong and very tough. An example of this type of application is automated bank teller machines housings.

Excellent aesthetics is another area in which opaque polycarbonate is commonly used. Since polycarbonate has no significant base color or opacity itself, it can be colored to just about any possible endpoint. This allows colors to be produced that can only be obtained in clear, glassy polymers. Bright, high-chroma colors quite often cannot be made with other opaque polymers. Polycarbonate has the same competitive advantages in this market as it does in transparent markets. Many outdoor signs, such as the red and yellow McDonald's Restaurant signs, are made from polycarbonate in order to attain an excellent visual appearance, coupled with high toughness. Polycarbonate is made into thousands of custom colors every year, just to take advantage of the excellent aesthetics while maintaining impact. A derivative of this is the high-gloss black exterior automotive appliqués made of polycarbonate. These are commonly used for pillar covers between various windows in automobiles. Some of these products are coated with UV filtering hardcoats to improve long-term weathering.

Flame-retarded transparent grades of polycarbonate were mentioned earlier; flame-retarded opaque grades are also very common. A wider variety of flame retardants may be used when the final plastic is to be opaque. Greater flame retardant capability can be built into these opaque systems. These tend to be used in three main areas: business equipment, aircraft interiors, and electrical connectors and housings. The business equipment grades are primarily injection-

molded. Normally polycarbonate is used when heat requirements or dimensional stability requirements are high enough to preclude the use of lower cost materials. Business machine applications commonly would be items like keyboard bases and portable equipment. Aircraft interior polycarbonates are usually made by sheet extrusion and thermoforming of highly flame-retarded polycarbonate. Common applications would be aircraft interior wall and ceiling panels for the aircraft retrofit aftermarket. Usually a protective film is applied to the polycarbonate panels. These types of applications have stringent flammability requirements set by the Federal Aviation Administration. Polycarbonate is chosen for its flammability, ductility, heat resistance, and low cost when compared to competitive systems. Electrical connectors and housings encompass a wide variety of many small parts. They are chosen for high impact, flammability, weatherability, and heat resistance. Network interface devices (NIDs), which are small boxes outside a home that shelter electrical connections, particularly telephone wiring, are commonly made of polycarbonate.

Wear-resistant grades of polycarbonate are used in specialty applications in which a high heat resistance is needed in conjunction with a low coefficient of friction. A major application area is in computer keyboards. It used to be that a computer keyboard would comprise in excess of 600 parts. Newer designs utilize a wear-resistant polycarbonate to mold one piece that provides bearing surfaces for each of the keys to slide against. By changing the design and incorporation of wear-resistant polycarbonate, a 101-key keyboard can be made with fewer than 110 parts. The most critical property is dimensional stability over a wide temperature range.

Certain applications of opaque polycarbonate require higher heat resistance than can be obtained from polycarbonate homopolymer. A polyester carbonate copolymer has been developed with a heat distortion temperature about 50°F higher than polycarbonate homopolymer. The most common utilization for these higher heat polycarbonates is in automotive lighting reflectors. Most times they are metallized for these applications. Another use is in animal cages that require repeated autoclave sterilization.

III. POLYMER BLENDS

Polymer blends are a major area in which polycarbonate is used. The primary commercial blend types are polycarbonate-polyester blends, polycarbonate-ABS (acrylonitrile-butadiene-styrene) blends, polycarbonate-ASA (acrylic-styrene-acrylonitrile) blends, and polycarbonate-imide blends. Each of these has been created to fill areas around polycarbonate performance that are better filled through a polymer blend approach.

Polycarbonate is blended with partly miscible crystallizable polyesters,

such as polybutylene terephthalate and polyethylene terephthalate, to create alloys that feature improved chemical resistance. These products are heavily oriented to the automotive market areas in which gasoline resistance is required. The largest volume applications have been in bumper systems. Injection molded polycarbonate/polybutylene terephthalate Xenoy 1102 bumpers have been used on Ford automobiles in the United States. Similar weatherable molded-in color bumpers are made for Ford automobiles in Europe. Blow-molded polycarbonate/polybutylene terephthalate Xenoy 1402B bumper beams with injection-molded Xenoy 1102 fascias have been used on many Hyundai automobiles. Other polycarbonate/polyester blends are utilized in lawn and garden equipment and automotive weatherable exterior components, such as mirror housings.

Polycarbonate-ABS blends are used as a lower cost, slightly lower performance option in very cost-sensitive markets that do not need the full heat performance of polycarbonate. Two basic types of polycarbonate-ABS blends are utilized: flame-retarded (FR) and non-flame-retarded standard grades. These FR PC-ABS blends are widely used for computer and business machine housings, and portable computer housings. Flame retardant systems are usually nonhalogenated low molecular weight systems that provide dramatically increased flow. Significant reductions in heat distortion temperature are observed in these blends. Standard grades of polycarbonate-ABS are used primarily in automotive products. The market fit for these products are in areas in which lower cost ductile polymers, such as ABS, have insufficient heat resistance but the high-heat properties of polycarbonate are not required. Primary applications are in interior trim pieces, knee bolster panels, instrument panel fillers, and center consoles.

Polycarbonate-ASA blends are utilized to make a product that has better weatherability than polycarbonate yet better physical properties than ASA. Primary application areas are in automotive and construction, particularly ones with reduced gloss. Automotive components are almost exclusively exterior components that need exceptional weatherability. Common applications would be trim pieces and mirror housings. Construction applications would be premium window lineals, particularly ones made with dark colors or high-chroma colors that need higher heat resistance. The addition of polycarbonate to the ASA gives dramatically better strength and physical properties to these blends.

Polycarbonate-polyetherimide blends are used in application areas in which polycarbonate homopolymer or copolymers do not have sufficient heat resistance. The most common applications are higher heat automotive reflectors and in food contact applications. Some of these blends are based on polycarbonate and polyetherimide and some are based on polycarbonate copolymers and polyetherimide. Another common application area is for aircraft interiors, particularly wall and ceiling panels, where the excellent flammability and low smoke generation makes these alloys the premium material of choice.

15
Part Assembly

Andrew J. Poslinski
General Electric Company, Schenectady, New York

I. INTRODUCTION

In most applications, additional manufacturing steps are often required after part fabrication. These may include joining of components through mechanical fastening, bonding, or welding. Although such secondary operations occur toward the end of the development cycle, they should be considered early in the design planning stage. This chapter reviews several functional assembly methods and provides recommendations for optimizing the assembly performance of parts fabricated with polycarbonate resins and their blends [1–3].

II. FASTENING AND BONDING

Joining of polycarbonate components to various materials such as plastic, metal, and wood can be achieved through mechanical fastening or bonding with adhesives and solvents, as shown in Fig. 1. Mechanical fastening and adhesive bonding are used for joining all materials, whereas solvent bonding, which requires softening of the joint interfaces, is only applicable to thermoplastics. In the case of mechanical fastening, preparation of the part surfaces after fabrication is generally not required; however, assembly stress and clearance, thermal expansion and contraction of the materials, and long-term effects due to stress relaxation, creep rupture, chemical attack, and joint fatigue are important design considerations. Although adhesive bonding does require surface cleaning, it facilitates joining to brittle materials such as glass and ceramic, distributing stresses over the entire

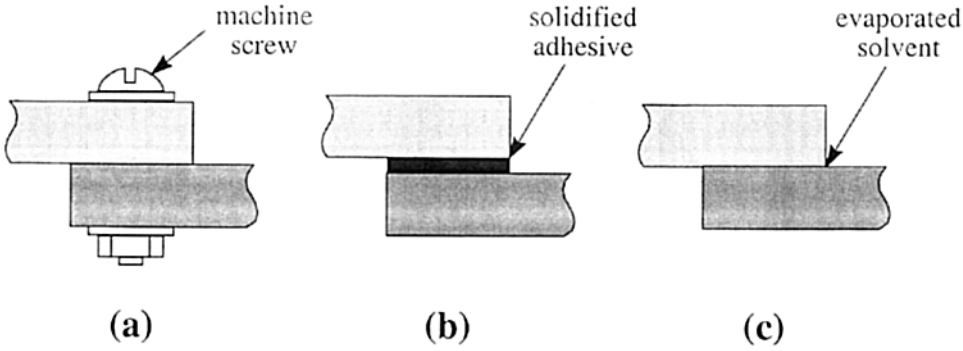

Figure 1 Mechanical fastening (a) and adhesive bonding (b) can be used to join all materials, whereas solvent bonding (c), which requires softening of the joint interfaces, is only applicable to thermoplastics.

bond area and providing a hermetic seal if needed. Solvent bonding eliminates the need for additional hardware like metal fasteners and adhesive pastes; but the joint interfaces must fit precisely and be softened with the appropriate chemicals, requiring that the part halves be molded dimensionally well and possess low residual stresses. The best-suited assembly method depends on cost, environmental and structural requirements, ease of assembly and disassembly, and aesthetic appearance [4].

A. Mechanical Fastening

Attachment by mechanical means can be either permanent or designed for disassembly. Permanent joints can be achieved with ultrasonic staking, metal rivets, and press fits, as shown in Fig. 2. Components fabricated from polycarbonate resins—which exhibit high rigidity in the glassy state—are excellent candidates for ultrasonic staking, allowing high transmission of the vibrational energy. The size and shape of the staking region is usually determined by a trade-off between aesthetic appearance and strength requirements of the resulting joint. When riveting polycarbonate parts, the buildup of high stresses should be avoided by using shoulder designs, inserting washers on the flared ends, and allowing for ample clearance. In contrast, a tight clearance is required in press fits to provide adequate resistance against torsional and axial movement, while maintaining stress levels within acceptable limits. Figure 3 shows the theoretical diametrical interference between hubs and shafts, recommended for polycarbonate blends at room temperature and based on an allowable long-term stress set to 25% of the short-term

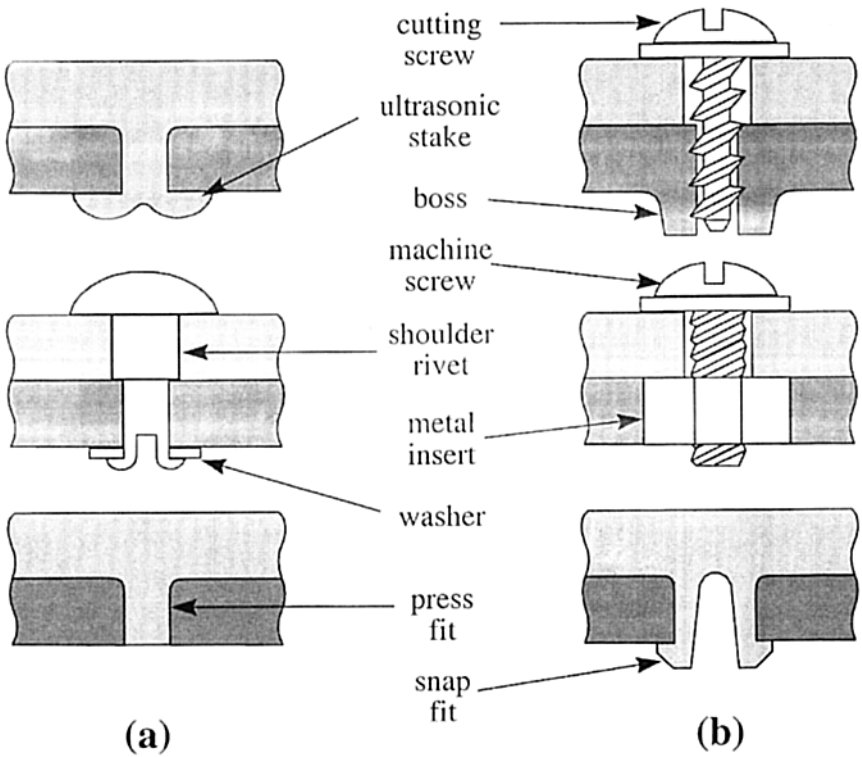

Figure 2 Permanent joints (a) can be achieved with ultrasonic staking, metal rivets, and press fits, whereas operable joints (b), allowing for part disassembly, can be obtained with screws, metal inserts, and snap fits.

tensile yield stress [4]. For glass-filled grades, the diametrical interference is reduced roughly by the weight fraction of the matrix material.

Operable joints, also shown in Fig. 2, allow for part disassembly and can be obtained with screws, metal inserts, and snap fits. Screw fastening is usually performed by using self-threading screws with plastic bosses, machine screws with metal inserts, or machine screws with bolts; the former provides the easiest method of attachment, whereas the latter two provide the best performance during repeated assembly. Metal inserts are not recommended for use with unreinforced polycarbonate resins, particularly in applications exposed to thermal cycling; instead, adequate joint performance may be obtained with glass-reinforced grades due to lower coefficients of thermal expansion and higher design stress limits. Similar to the guidelines for rivets, stresses should be minimized in the vicinity

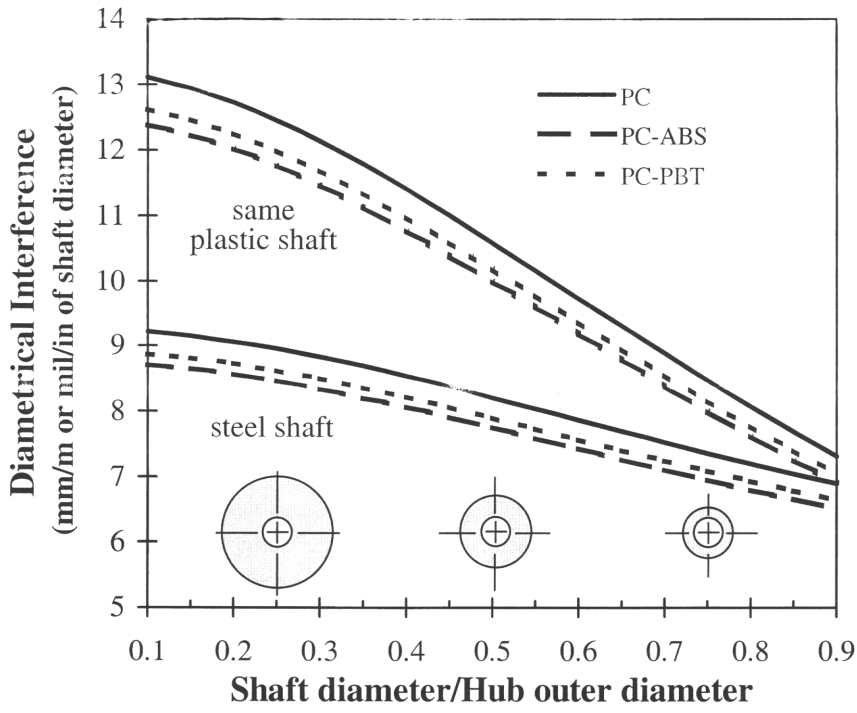

Figure 3 Theoretical diametrical interference in press fits recommended for polycarbonate blends at room temperature and based on an allowable long-term stress set to 25% of the short-term tensile yield stress.

of the screw, especially for the self-threading type. To this end, thread-cutting screws are predominantly used in polycarbonate parts because they cleanly cut through the material with negligible deformation. In order to withstand the hoop stresses developed by screw insertion and to provide enough travel for thread engagement, the outside diameter and length of the mating boss should be at least twice the major diameter of the screw. An alternative and very versatile fastening mechanism that is ideally suited to the ease with which geometrical complexity can be molded into plastic parts can be achieved through snap fits. The design details can be analyzed with standard cantilever beam equations, which require permissible strain and secant modulus properties as inputs. Because good material recovery is critical to ensure that the snap fit will function properly by returning to engage, the permissible strain is usually determined by loading and unloading tensile test specimens to various strain levels. Table 1 lists typical values of permissible strains and secant moduli for unfilled polycarbonate blends that can be used for preliminary snap-fit design [1].

Table 1 Typical Polycarbonate Blend Properties Required for Snap-Fit Design

Blend	Permissible strain (%)	Secant modulus (MPa/ksi)
PC	8	776 (112.5)
PC-ABS	6	977 (141.7)
PC-PBT	6	908 (131.7)

PC, polycarbonate; ABS, acryonitide-butadiene-stynene; PBT, polybutylene terephthalate.

B. Adhesive Bonding

Adhesives can be classified into single- or two-component systems. The most commonly used single-component systems include anaerobics, which cure by oxygen deprivation, and cyanoacrylates, which cure rapidly at room temperature. Two-component systems are mixed just prior to use and react chemically during the cure cycle, examples being epoxies, urethanes, and acrylics. Table 2 lists the performance characteristics for both types of adhesive families. In adhesive

Table 2 Performance Characteristics of Common Polycarbonate Adhesive Families

Family	Cure time (min)	Shear strength (MPa/ksi)	Temperature limit (°C/°F)	Features	Issues
Epoxy	5+	≤69 (10)	≤232 (≤450)	• Good adhesion • High heat tolerance • Good rigidity	• Poor peel strength • Brittle and low impact • High cost
Urethane	5+	≤55 (8)	≤149 (≤300)	• High peel strength • Tough and flexible • Good impact strength	• Excessive creep • Chemical-sensitive • Moisture-sensitive
Acrylic	2+	≤41 (6)	≤177 (≤350)	• High peel strength • Superior toughness • Fast curing	• Poor gap filling
Anaerobic	~0.2	≤34 (5)	≤204 (≤400)	• High peel strength • Solvent resistance • Good impact strength	• Poor gap filling
Cyanoacrylate	~0.2	≤34 (5)	≤82 (≤180)	• High tensile strength	• Brittle and low impact • Moisture-sensitive • Poor gap filling

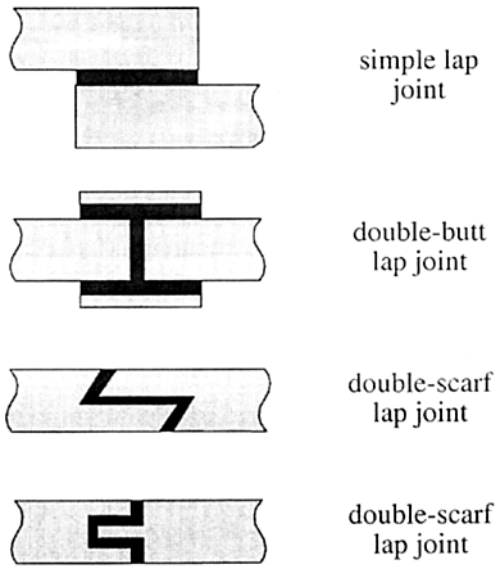

Figure 4 Several joint designs for adhesive bonding of polycarbonate parts. Simple lap joints are less favorable because tensile and shear stresses in line with the adherents cannot be accommodated.

bonding, the part surfaces to be joined are called *adherents*. Pretreatment of the adherents prior to application of the adhesives, such as a degreasing step, is crucial for joint strength and reliability. For further information on surface treatment and specific adhesive systems, see Chapter 17.

Because joints are subjected to several types of stresses, correct joint design is very important to the secondary performance of polycarbonate parts. Examples of joint designs are illustrated in Fig. 4. In tensile-loaded joints, forces are perpendicular to the plane of the joint; in shear-loaded joints, forces are parallel to the plane of the joint. Simple lap joints fall into the latter category and can be used for adhesive bonding; however, tensile and shear stresses in line with the adherents cannot be accommodated. On the other hand, double-butt lap joints, double-scarf lap joints, tongue-and-groove joints, and similar variations combine both types of stresses in line and are preferred for use with polycarbonate parts.

C. Solvent Bonding

In this process, the plastic surfaces to be joined are softened by use of a layer of chemical solvent. The parts are then clamped together under pressure, allowing

the polymer chains to diffuse across the joint interface. Evaporation of the solvent results in the desired bond and the cycle time is governed by the rate of solvent evaporation, which can be shortened by using heat. Methylene chloride, which has a low boiling point of 40.1°C (104°F) and an extremely fast evaporation rate, is one solvent that can be used for assembling polycarbonate parts [2]. When perfectly mated bonding areas are impossible to obtain, perhaps due to molding variations, a 1–5% solution of polycarbonate resin in methylene chloride can be prepared to obtain smooth, completely filled joints. Recommendations for joint designs are similar to those shown in Fig. 4 for adhesive bonding, but with the adhesive layer eliminated.

III. THERMOPLASTIC WELDING

Because welding requires melting and subsequent freezing of the materials to be joined at the weld interface, it is only applicable to thermoplastics such as polycarbonate resins. Depending on how the heat for melting is supplied, welding can be broadly classified into thermal, frictional, and electromagnetic bonding [5]. A common thermal technique for parts molded from polycarbonate resins is hot-tool welding, in which complex geometries such as doubly curved automotive headlamps and rear lights can be joined at the expense of longer cycle times. Two effective frictional techniques that provide good bond strength at short cycle times include vibrational and ultrasonic welding; however, both methods are ideally suited to the welding of smaller thermoplastic parts along seams with minimum out-of-plane curvature. Both the thermal and frictional approaches are generally considered to be irreversible. An alternative electromagnetic method that can be used to produce a reversible assembly is induction welding, combining the hot-tool advantages of joining complex geometries and the vibrational and ultrasonic advantages of short cycle times, but usually with a higher overall cost. Selection of the appropriate welding method is usually determined by aesthetic appearance requirements, part geometry and size, dimensional tolerances, and process economics. Figure 5 illustrates the four welding techniques suitable for joining polycarbonate parts.

A. Hot-Tool Welding

In this process, the surfaces to be joined are brought to the softening temperature by direct contact with the matching surfaces of a heated metallic tool. Upon removal of the tool, the molten surfaces are then brought together, and the common interface is allowed to cool and solidify under controlled pressure, resulting in a weld. Stops on the metallic tool and the fixtures that hold the parts determine the depth of the melt displacement and the overall dimensions of the welded

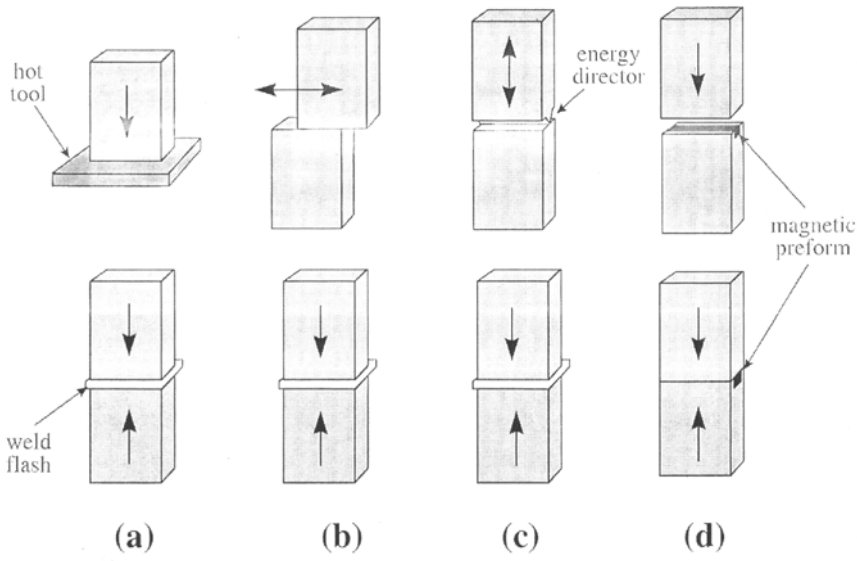

Figure 5 The most effective welding techniques for joining parts molded from polycarbonate resins include (a) hot-tool, (b) vibrational, (c) ultrasonic, and (d) induction bonding.

parts. The initial contact produces a good mating surface, as both ends are made level by the hot tool. A total meltdown of 0.5–0.8 mm (0.02–0.03 in.) on each side is usually recommended for obtaining good weld strength between polycarbonate components. Numerical analysis [6] has shown that the film thickness and material flow is strongly affected by the temperature dependence of the melt viscosity. For example, Fig. 6 shows that with increasing viscosity temperature sensitivity the film thickness increases significantly, whereas the flow is reduced and confined in a narrow channel near the hot-tool surface. To overcome such inhibiting viscous effects, the hot tool is typically set at 100–150°C (180–270°F) above T_g, the glass transition point of amorphous polycarbonate resins. By using different surface temperatures it is also possible to weld dissimilar materials.

The hold time after the stops between the hot tool and part fixtures are engaged determines the depth of secondary softening. Additional melting is often desired to provide enough molten film for subsequent joining of the part halves. Transient calculations [7] suggest that the contact time during melting should be on the order of 10–15 s, whereas the switchover phase, during which the metallic tool is removed and the part halves are brought together, should occur within several seconds to prevent solidification of the joint interfaces due to convective

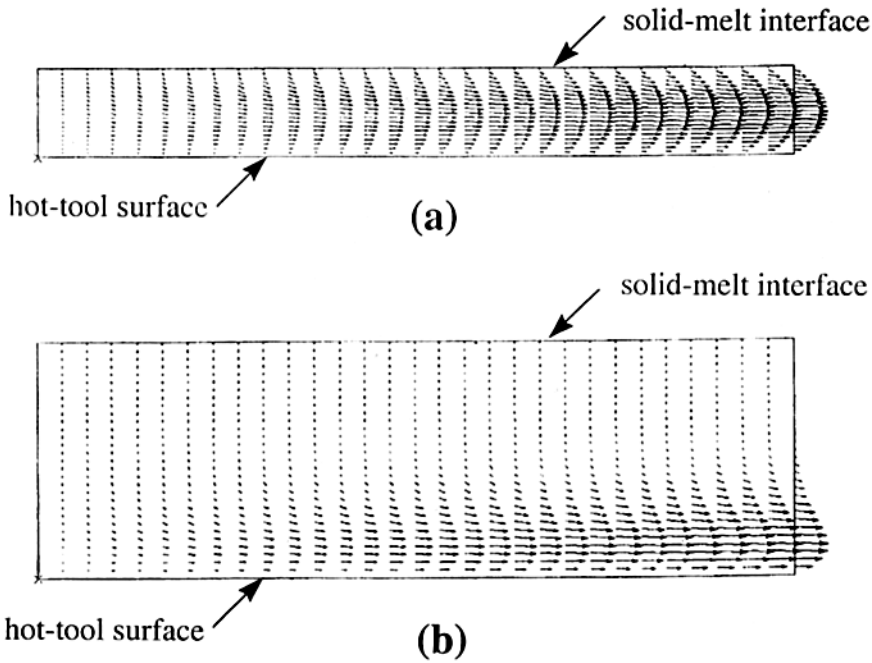

Figure 6 Predictions for the velocity distribution in the molten film for a constant (a) and a temperature-dependent (b) viscosity during hot-tool welding.

cooling. The duration of the joining and melting phases are similar, so that the entire hot-tool welding cycle is usually completed in 20–30 s. During the final joining phase, an additional amount of molten material is displaced until engagement of the stops on the part fixtures occurs. As a result, the applied pressure only affects the rate of displacement and has little effect on the ultimate weld strength. If stops are not used, the applied pressure becomes an important variable in optimizing the process. Weld strengths equal to that of the base polycarbonate material can be achieved at the recommended welding conditions [8]. Poor performance is typically obtained for temperatures between $T_g < T \leq T_g + 100°C$ (180°F) and $T \geq T_g + 150°C$ (270°F) due to insufficient melting and material degradation, respectively. High weld strengths can be attained for both undried and dried specimens of polycarbonate; however, the range of optimum hot-tool temperatures is quite narrow for the undried specimens [9]. In addition, the thickness of the part does have a small effect—with increasing part thickness, the process window shifts to higher temperatures.

B. Vibrational Welding

The phenomenology of this process is best described by weld penetration, i.e., the decrease in the distance between the parts being joined together. Extensive experimentation with several thermoplastic resins has shown that the weld process can be divided into the four phases shown schematically in Fig. 7 [10]. During the first phase, the penetration is zero as Coulomb friction causes the solid interface to heat up and melt under applied pressure. Heat continues to be generated during the second phase by viscous dissipation in the molten film as the penetration increases from zero and the melted material begins to flow outward in a direction lateral to the vibrational motion. A steady state characterized by a linear increase in the weld penetration with time is achieved in the third phase. Finally, phase 4 starts when the vibrational motion is stopped and the molten material solidifies completely, resulting in a weld at the interface.

The key process and geometry variables for vibration welding are welding frequency, amplitude of the vibrational motion, applied pressure, welding time, weld penetration, and part thickness. Experiments have shown that the weld per-

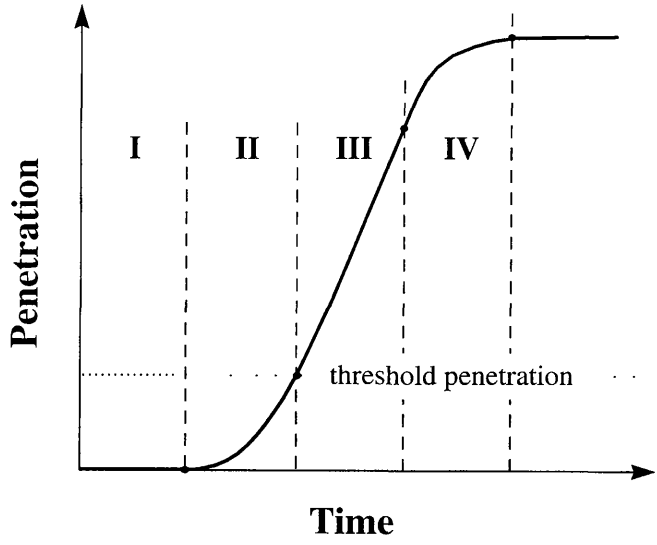

Figure 7 Schematic penetration curve as a function of time showing four phases of the vibration welding process.

formance, measured by means of tensile strength and failure strain, improves with increased penetration; the best performance is obtained when the steady-state phase is achieved [11]. For this reason, penetration curves such as that shown in Fig. 7 are important because they determine the threshold penetration at which the steady state is attained. Depending on the process conditions and part geometry, the threshold penetration for polycarbonate resins varies between 0.05 and 0.25 mm, and the time to reach this threshold limit varies anywhere from fractions of a second up to 10 s [10]. In particular, both the threshold penetration and time decrease at higher values of the frequency, amplitude, and applied pressure, whereas they increase for thicker part cross-sections. Polycarbonate welds extremely well, with a very wide processing window of frequencies ranging from 120 to 400 Hz, amplitudes ranging from 0.3 to 3 mm, and applied pressures ranging from 0.9 to 6.9 MPa. Optimum combination of the variables can be determined through modeling of the welding process [12], although further work is required to account for the temperature and shear rate dependence of polycarbonate melt viscosity as it has been done in the case of the more recent developments in hot-tool welding [6,7].

Similar to hot-tool welding, joining of dissimilar materials can also be obtained with vibration welding. High weld strengths—as high as the strength of the weaker of the two materials—can be attained. However, the conditions for achieving high strengths (threshold penetration) are different from vibration welding of similar resins. For example, in the welding of polycarbonate to polyetherimide specimens [13], the apparent steady-state conditions indicated by penetration–time curves are deceptive because of differences in the glass transition temperatures and melt viscosities. The process is dominated by the high melting and flow rates of the polycarbonate material, which mask the melting and flow of its polyetherimide counterpart. Because of this effect, it is more difficult to optimize vibration welds between dissimilar materials.

The ultimate goal of any joining method is to achieve the best possible joint performance. In the case of vibration welding, one measure of weld performance is the ratio of the tensile strength for the weld divided by the tensile strength of the virgin material in the same test—a relative strength. Another measure of weld performance is to compare the failure strain for the weld with that for the virgin material—a relative ductility. Table 3 lists the relative strength and relative ductility of polycarbonate welds obtained with polycarbonate and several other dissimilar thermoplastic resins [14]. Under the resin headings, the first number indicates the tensile strength σ_y of the virgin resin, and the second number gives the failure strain ε_f. The weld performance is listed as the percent strength followed by the percent failure strain in parentheses. Relatively good performance can be achieved with most dissimilar polycarbonate welds with the exception being the polyethylene oxide materials.

Table 3 Relative Strengths and Failure Strains for Polycarbonate Vibration Welds

Resin	ABS	PPO	PPO/PA	PC	PBT	PC/ABS	PC/PBT	PEI
σ_y(Mpa)	44	45.5	58	68	65	60	50	119
ε_f(%)	2.2	2.5	>18	6	3.5	4.5	—	6
PC								
68	0.83	0.24	0.29	1.0	1.0	0.7	1.0	0.95
6	(1.7)	(0.4)	(0.75)	(6)	(1.7)	(1.8)	(4.9)	(2.75)

PC, polycarbonate; ABS, acrylonitide-polybutadiene-styrene; PPO, polypropylene oxide; PA, polyamide; PBT, polybutylene terephthalate; PEI, polyetherimide.

C. Ultrasonic Welding

Similar to ultrasonic staking, the ultrasonic welding process is used to join small and medium-size thermoplastic components when high bond strengths are desired at very fast cycle times. As shown in Fig. 5, one of the two parts is fixed during welding while the other is subjected to sinusoidal ultrasonic vibration normal to the contact area. The low-amplitude, high-frequency vibrational energy is transmitted through the thermoplastic solid and concentrated at the weld interface through an energy director, generating surface and intermolecular friction that locally heats and melts the material under applied pressure. Once the appropriate weld penetration has been achieved, the vibrational motion is stopped, and the interface is allowed to cool and solidify typically resulting in 0.5–1.5 s of total cycle time [4]. High frequencies ranging from 20 to 50 kHz and low amplitudes ranging from 15 to 60 μm are typically available in ultrasonic equipment [5]. Optimum energy transmission and control is obtained when the signal source is closer to the weld interface, often referred to as *near-field* welding if the transmission distance is within 6 mm. For greater distances, *far-field* welding can be much less effective.

Ultrasonic welding can be effectively utilized when polycarbonate parts are to be joined with each other or with components fabricated from many polycarbonate/ABS blends and some polyphenylene oxide grades. The key element in designing polycarbonate parts for ultrasonic welding is the joint design. Figure 8 illustrates the two most common types of joints. In both cases, weldability is dependent on the concentration of the vibrational energy per unit contact area. Since polycarbonate resins have a higher melting point than many other thermoplastics, more energy is required to cause the material at the joint to melt and flow. Therefore, the energy director in the butt design should be triangular in shape, approximately 0.5–0.6 mm tall, with an apex angle of 75–90°; in the case of the shear design, the edge should be as sharp as possible, making an angle with the shearing surface of 30–45° [2]. Experience has shown that these

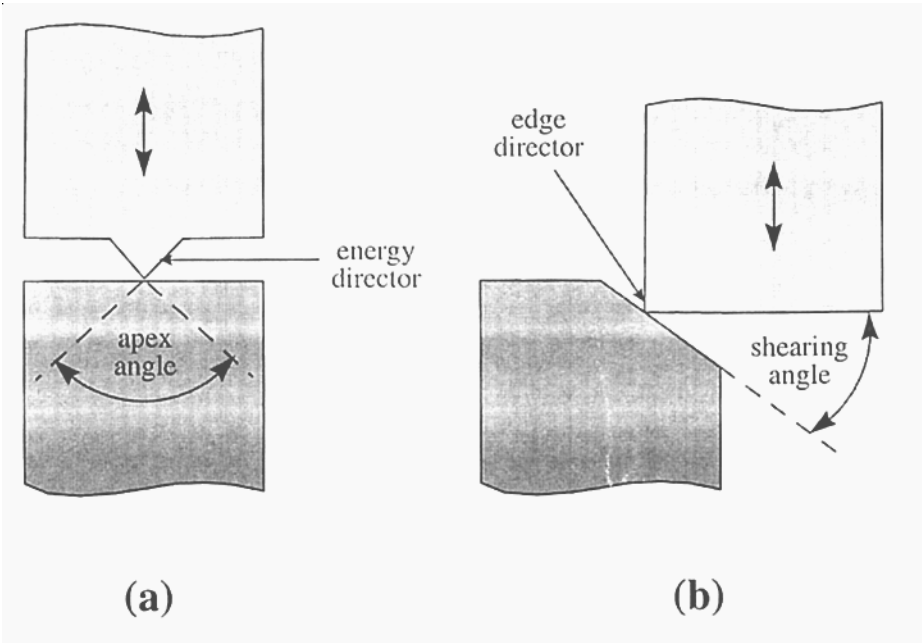

Figure 8 Common ultrasonic joints for polycarbonate parts include (a) energy-directed butt designs and (b) edge-directed shear designs.

angles allow for easier flow of the polycarbonate melt during welding. Recent joint design efforts have shown that by molding textured joint surfaces, the tensile strength and hermetic seal integrity of the ultrasonic welds can be greatly improved with less energy input than that required for untreated surfaces [15].

D. Induction Welding

This reversible welding process is based on the principles of induction heating. Specifically, a 3- to 10-MHz oscillating current is used to set up an electromagnetic field in the vicinity of the weld interface and to heat a ferromagnetic implant above the melting temperature of the thermoplastic parts [5]. Because most plastics, including polycarbonate resins, are not affected by the electromagnetic field at such high frequencies, melting and subsequent solidification of only the material in contact with the implant results in the weld. The ferromagnetic implant is generally composed of a matrix from the same or compatible polymer as that of the parts and finely dispersed micrometer-sized particles of iron, iron oxide, stainless steel, or other magnetic fillers compounded with loadings less than 15% by volume [4]. Cycle times can range from 3 to 10 s depending on the part size,

on the same order as vibrational welding. In addition, parts composed of similar as well as dissimilar materials can be joined with low sensitivity to poor tolerances, part warpage, and type of material filler package.

REFERENCES

1. *Lexan®, Cycoloy®, Xenoy® Design and Molding Guides*, Publications No. CDC-536H & 500, CLY-400 & 425A, X-106B, GE Plastics Technical Support and Sales, Pittsfield, MA 1992.
2. *Lexan® Resin Secondary Operations Guide*, Publication No. CDC-538F, GE Plastics Technical Support and Sales, Pittsfield, MA, 1992.
3. *Engineering Thermoplastics Design Guide*, Publication No. PBG-130, GE Plastics Technical Support and Sales, Pittsfield, MA, 1997.
4. R. A. Malloy, *Plastic Part Design for Injection Molding: An Introduction*, Hanser, New York, 1994.
5. V. K. Stokes, Joining methods for plastics and plastic composites: an overview, *Polym. Eng. Sci. 29*:1310 (1989).
6. A. J. Poslinski and V. K. Stokes, Steady melting of rectangular thermoplastic bars induced by hot contacting surfaces, *Polym. Eng. Sci. 32*:1147 (1992).
7. A. J. Poslinski and V. K. Stokes, Analysis of the hot-tool welding process, *SPE Tech. Papers 38*:1228 (1992).
8. K. R. Conway, Hot-tool welding of thermoplastic parts, prepared under NIST ATP Program No. 70NANB3H1375 Funding, GE Corporate R&D, Schenectady, NY, 1997.
9. V. K. Stokes, Experiments on the hot-tool welding of polycarbonate, *SPE Tech. Papers 41*:1229 (1995).
10. V. K. Stokes, Vibration welding of thermoplastics. I. Phenomenology of the welding process, *Polym. Eng. Sci. 28*:718 (1988).
11. V. K. Stokes, Vibration welding of thermoplastics. III. Strength of polycarbonate butt welds, *Polym. Eng. Sci. 28*:989 (1988).
12. V. K. Stokes, Vibration welding of thermoplastics. II. Analysis of the welding process, *Polym. Eng. Sci. 28*:728 (1988).
13. V. K. Stokes and S. Y. Hobbs, Strength and bonding mechanisms in vibration-welded polycarbonate to polyetherimide joints, *Polym. Eng. Sci. 29*:1667 (1989).
14. V. K. Stokes, Assembly of thermoplastic parts: a vibration welding guide, Prepared Under NIST ATP Program No. 70NANB3H1375 Funding, GE Corporate R&D, Schenectady, NY, 1997.
15. G. R. Smoluk, Why it's time to take another look at ultrasonic welding, *Mod. Plastics 51* (November 1990).

16
Secondary Finishing

Herbert S.-I. Chao and Michael C. Burrell
General Electric Company, Schenectady, New York

I. INTRODUCTION

Numerous secondary finishing operations have been developed for manufactured polycarbonate articles. Polycarbonate responds well to many of those secondary operations [1], such as painting, printing, and metallizing. Also, adhesive bonding and scratch-resistant coatings can be applied to polycarbonate.

II. SURFACE TREATMENTS

The surface tension of polycarbonate is measured to be 42 mN m^{-1}. For successful painting, printing, and adhesive bonding on polycarbonate surfaces, the coating must have a lower surface tension than the polycarbonate surface to ensure wetting and adhesion between the coating and polycarbonate. To merely clean the polycarbonate surface, washing with methanol, isopropanol, heptane, or petroleum ether is adequate. For more demanding operations, the polycarbonate surface can be vapor-polished by using methylene chloride. An exposure time to methylene chloride vapor of 5–10 s is sufficient, and longer exposure times might be detrimental [2]. Plasma [3–8], flame [9], corona discharge, ultraviolet (UV) radiation [10–12], and abrasive [9] treatments are also sometimes applied to polycarbonate to increase the surface wettability.

III. PAINTING AND PRINTING

In general, polycarbonate is not solvent-resistant because quite a few solvents can attack polycarbonate [13]. Thus, the solvent-based paints or inks usually do not have any difficulties in adhering to the material. The solvents help attack the polycarbonate surface, resulting in improved adhesion through mechanical interlocking or interdiffusion with the film former, if the film former has a certain compatibility with polycarbonate.

Application of printing inks, usually by screen printing, is a common finishing operation for a variety of polycarbonate products. For example, labels and backgrounds are printed on polycarbonate films used as membrane switch overlays, automotive instrument clusters, and graphic arts. Labels and decorative printing are also applied to injection-molded articles such as compact disks, and onto blow-molded products including beverage containers and baby bottles. For these and other applications, thermally cured (solvent-based) or UV-cured inks are typically applied.

Surface pretreatments are generally not required to achieve wetting and adhesion of the ink. Many ink formulations contain solvents that swell or partially dissolve polycarbonate, and good adhesion is acquired through mechanical interlocking or interdiffusion. For certain UV-cured inks that contain little or no added solvents, the monomers themselves can be selected to provide suitable interaction with the polycarbonate [14,15], and several manufacturers provide inks specifically for these applications. However, the adhesion of the ink to the polycarbonate substrate is influenced by a number of variables, including the type of ink, printing and processing conditions, and the substrate surface condition.

Ink adhesion is generally measured using the cross-hatch tape test (ASTM D-3359-87). The nature of polycarbonate or modified polycarbonate surfaces has been measured in a number of instances by techniques such as x-ray photoelectron spectroscopy (XPS) and static secondary ion mass spectrometry (SSIMS) [16,17]. These methods are useful for identifying surface contaminants, quantifying the extent of surface oxidation, or identifying reaction products. If ink delamination is occurring, analysis of the opposing sides of the interface pinpoints the locus of failure.

Environmental concerns about solvent emissions are causing an increase in the use of UV-cured inks. Curing the ink exposes not only the ink but also the adjacent unprinted areas to UV light. In many applications, the final product requires a combination of numerous colors and textures, applied in successive processes. Ink applied in the later passes are deposited onto regions of the polycarbonate surface already exposed to the total UV dosages required to cure the inks used in the previous passes. In some cases, a lower level of adhesion between the UV-exposed PC and the ink is observed [17–19]. This effect is due to the UV-induced chemical changes in the (unprinted) polycarbonate surface which

make the subsequent interaction with the ink less favorable. Previous studies have shown that the photochemistry of polycarbonate exposed to UV light and O_2 involves multiple reaction pathways, generally classified as the photo-Fries reaction, and photooxidation. The net result is the formation of numerous oxidized products, surface yellowing, and surface crosslinking or molecular weight degradation, depending on the UV wavelength. The formation of these products on the surface of the polycarbonate prior to ink application may result in less penetration and hence poor adhesion of the ink. The photoproducts may also form a weak boundary layer, again resulting in lower ink adhesion.

Riding and Lilly [19] have reported the practical effects of exposing polycarbonate film to different types of UV lamps commonly employed to cure printing inks. In general, longer wavelength ($\lambda > 400$ nm) UV lamps permit more preexposures of the polycarbonate before the onset of ink delamination is observed. However, the lamp must have sufficient intensity in the range necessary to excite the photoinitiator employed to cure the ink, typically in the range 365–380 nm for acrylic-based inks. Use of the longer wavelength lamps also reduces the amount of film yellowing that can develop after multiple UV exposures. Microwave-excited or "doped" arc lamps are recommended over conventional mercury arc sources.

It has also been observed [20] that other operations such as flaming (used, for example, to smooth sharp seams on injection-molded bottles) can adversely affect subsequent printing of the polycarbonate surface. In those cases, surface analysis measurements show that the degree of surface oxidation and type of oxidation products observed on flamed surfaces were similar to those observed on surfaces overexposed to UV lamps (see above).

Another concern in printing polycarbonate is the possible chemical interactions of the ink components with the polycarbonate. Amine cure accelerators found in some inks can lead to breakdown of the polycarbonate molecular weight at the interface, due to their ability to directly react or catalyze hydrolysis of the carbonate linkages.

In some cases, poor ink adhesion or delamination might develop over time as the reaction results in the formation of a weak boundary layer. This effect may be exacerbated by accelerated heat and/or humidity. SSIMS has been applied to detect the formation of polycarbonate degradation products at delaminated interfaces to verify this mode of interaction [20]. The use of inks containing amine curing agents are therefore not recommended for polycarbonate application.

IV. METALLIZATION

In the metallization of polycarbonate, a number of approaches have been explored to modify the surface of the plastics. Many approaches are aimed at increasing

the physical adhesion of the metal to the polymer [21]. For example, one method employs the radiation of polycarbonate with heavy ions that are produced through radiation of uranium with neutrons. As a result of this treatment, the structure of the polycarbonate molecules near the surface is altered. A subsequent etching step, such as a NaOH treatment process, leads to the formation of exactly defined depressions (cavities) in the surface. By means of this defined surface roughening, the adhesion of the deposited metal is substantially improved [22]. A method of improving the metal adhesion to glass-filled polycarbonate resin through mechanical adhesion was also developed. The surface of the substrate is treated initially through contacting with an alkaline conditioner, followed by an aqueous acid fluoride etch solution [23]. The initial base hydrolysis attacks the polycarbonate–glass interface preferentially to loosen the dispersed glass from the plastic. The glass is further removed by acid fluoride etching to create crevices for metal deposition. More prevalent has been the technique of swelling the polymer with an organic solvent, such as water-compatible halogenated compounds [24] including dichloropropanol, dichloroacetone, dichloroacetic acid and trichloroacetic acid, and glycol ethers [25] including dimethoxydiethylene glycol, dimethoxytriethylene glycol, ethylene glycol dimethyl ether, and dimethoxytetraethylene glycol. Other glycol ether esters such as diethylene glycol monobutyl ether acetate, diethylene glycol monoethyl ether acetate, and mixtures of them are also reported to be effective [26]. The swelled polycarbonate is then etched to create pits in the surface with strong oxidants, such as chromic acid, permanganate, or alkali metal hydroxide. Chromic compounds, especially those containing Cr(VI), are quite toxic [27]. Swell and etch techniques have been found to adversely affect the bulk physical properties, especially the impact property of the polycarbonate.

Another method of obtaining metal adhesion with polycarbonate substrate is based on application of a more easily metallizable polymeric primer layer comprising a fluid organic binder containing a dispersion of active metal particles dispersed therein to the plastic [28,29]. Electroless deposition of metals is then carried out on the primer and anchored by the exposed metal particles in the primer layer.

In addition to employing physical adhesion between polycarbonate and metals, chemical modification of the polycarbonate surface is also a favorable approach. The advantage of chemical bonding is to have a rather smooth metal–plastic interface that presumably will retain the impact property of the polycarbonate. The disadvantage of the approach is that creation of the functionalities sometimes involves multistep surface treatments. Moreover, the final chemical bond formation might require an extra heating/oxidation step at the interface. Polymers such as polyetherimide can be chemically modified to enhance metal adhesion without affecting the bulk properties of the substrate [30,31]. It is believed that the chemical portion of adhesion is increased with little contribution from mechanical adhesion [32,33]. However, a heating step in the presence of

air, i.e., oxidation of the metal interface, at the end of metallization is essential to build the chemical bonding between the polyetherimide surface and metal oxides. A method for chemically pretreating a polycarbonate surface for increased metal adhesion was recently revealed [34]. This process involves nitration of the polycarbonate surface. The nitration predominantly occurs on the aromatic ring carbon which is ortho to the oxygen substituent. After a mild base treatment, the resulting surface is enriched with *o*-nitrophenol functionality and the surface becomes water-wettable. The electrolessly deposited nickel has excellent adhesion with the nitrophenol functionality without further heat treatment. The chemical bonding in this case is established through the electron transfer process that occurs between nickel and the nitrophenol group. However, once the modified polycarbonate surface is completely dried, the nitrophenol surface functionality is rearranged under the surface to render the surface nonwettable by water. As a result, the nickel/polycarbonate adhesion can no longer be achieved. The nitration of polycarbonate suffered a serious setback during a scale-up owing to the continuous loss of the anhydrous nitric acid, which is the active nitration component, to the air through azeotropic evaporation. Thus, a freshly prepared nitration bath loses its nitration ability quickly. Surface modification of polycarbonate with an ion-free, low-pressure, high-frequency plasma of an oxidizing gas containing a halogen compound has been found to improve metal adhesion [35,36].

Another method of improving metal adhesion to polycarbonate is to use chemically and physically modified polycarbonate. The surface is first rendered hydrophilic by exposure to UV light, then impregnated with HCl before being etched with KOH. Finally, the surface is cleaned with an oxidizing agent such as potassium permanganate [37].

In addition to electroless metallization, vacuum deposition of aluminum on polycarbonate is widely used in producing compact disks. The deposited aluminum serves as a reflective layer for the player's laser beam. Magnetron sputtering and wet silvering have also been used on polycarbonate to implement the metal reflective layer [38].

V. POLYURETHANE FOAM ADHESION

Polycarbonate is used as a retainer, or skeleton, in an automotive instrument panel application that has a skin-foam layer on top of the retainer. The polycarbonate was chosen for its desirable physical properties, especially its ductility at low temperature or high strain rate. However, the polycarbonate, with its fully capped end-groups, had poor adhesion to the polyurethane foam [39–41] used in the instrument panel production. The polycarbonate/foam adhesion is improved by using partially OH-terminated or surface-hydrolyzed polycarbonate to promote the covalent bond formation between the polycarbonate surface and the isocya-

nate functionality in the foam components [42]. When the weight ratio of polyisocyanate to polyol is increased in the preparation of polyurethane foam, the foam adhesion to polycarbonate is boosted. In this case, the foam adhesion passes even for capped polycarbonate with inert end-groups. The improved adhesion can be attributed to the chemical reaction occurring between the excess amino group in the newly formulated foam and the carbonate linkage in the polycarbonate backbone. However, the foam adhesion to polycarbonate through modification of either polycarbonate or foam composition deteriorates gradually under the heat/humidity test condition. The decomposition of the polycarbonate top surface is suspected to be the culprit. Application of a primer to the polycarbonate surface for improving foam adhesion is an alternative with one extra step.

VI. ADHESIVE BONDING

Acrylics, such as cyanoacrylate, have been found to have excellent bonding results with polycarbonate [43]. A solventless, UV-curable acrylate adhesive was developed [56] to bind glass to polycarbonate in order to improve the scratch resistance of polycarbonate. Similarly, a glass-polycarbonate laminate, used as structural windshields in motor vehicles, has been developed in which an adhesive of poly(ethylene-co-vinyl acetate) and an adhesion-promoting silane primer was used [59]. A tie layer containing an 80:20 blend of poly(ethylene-co-ethyl acrylate) and poly(4-methyl-1-pentene) was reported to tie polycarbonate and polypropylene together to form a laminate [57]. Other adhesives that have been used are polyurethane and epoxy types to bind polycarbonate to metals [44–46]. However, in one report based on studies of surface preparation and surface exposure time, a urethane adhesive is preferable to a two-component epoxy adhesive for bonding Lexan at room temperature and in an adverse environment [58].

VII. ABRASION-RESISTANT COATINGS

Polycarbonate surfaces are prone to be damaged by scratching. Commercial film or sheet products are usually protected by radiation-curable or thermally cured coatings. Fast-curing radiation curable coatings, such as acrylates, have gradually gained acceptance in industry [2,47,48]. Thermally cured coatings include melamine resins, acrylic coatings, polyurethanes, and especially polysiloxane hard coatings [49,50]. A typical polysiloxane hard coat contains an acidic dispersion of colloidal silica and hydroxylated silsesquioxane in an alcohol-water medium [51]. In addition to the organic coatings, inorganic coatings on polycarbonate have also been developed. Coatings prepared by a plasma-enhanced chemical vapor deposition (PECVD) method have been reported. These coatings are char-

acterized by a gradual transition from a composition consisting essentially of an interfacial material, such as polyacrylate or organosilicone material, to a composition consisting essentially of an abrasion-resistant material, such as silicon carbide, silicon dioxide, silicon nitride, silicon oxynitride, and their mixtures. The transition is achieved by gradually changing the feed composition of the coating material precursors [52,53]. Another method of producing transparent, abrasion-resistant coatings onto the surface of polycarbonate consists of plasma polymerizing the organosilicone monomer in the presence of excess oxygen by employing PECVD [54]. A novel hybrid inorganic-organic coating, prepared by a sol-gel process, was reported recently [55]. It involves the sol-gel reactions of Ti or Zr alkoxides with $(EtO)_3Si$-terminated organic compounds. The resulting materials are spin-coated on polycarbonate, giving abrasion-resistant coatings several micrometers thick.

REFERENCES

1. J. Bucher, *Plastics World*, January 1996, p. 65.
2. D. Satas, in *Plastics Finishing and Decoration* (D. Satas, ed.), Van Nostrand Reinhold, New York, 1986, p. 442.
3. L. J. Gerenser, *Polym. Mater. Sci. Eng. 62*:125 (1990).
4. E. Occheillo, M. Morra, and F. Garbassi, *Angew. Makromol. Chem. 173*:183 (1989).
5. D. T. Clark and R. J. Wilson, *Polym. Sci.; Polym. Chem. Ed. 21*(3):837 (1983).
6. L. J. Gerenser, *J. Adhes. Sci. Technol. 7*(10):1019 (1993).
7. S. L. Kaplan and P. W. Rose, *Plastics Eng. 44*(5):77 (1988).
8. J. R. Hall, C. A. L. Westerdahl, A. T. Devine, and M. J. Bodnar, *J. Appl. Polym. Sci. 13*:2085 (1969).
9. R. F. Wegman, *Surface Preparation Techniques for Adhesive Bonding*, Noyes Publications, Park Ridge, NJ, 1989, p. 119.
10. M. R. Adams and A. Garton, *Polym. Degrad. Stab. 42*(2):145 (1993).
11. M. R. Adams and A. Garton, *Polym. Degrad. Stab. 41*(3):265 (1993).
12. H. van der Wel, F. C. B. M. van Vroonhoven, and J. Lub, *Polymer 34*(10):2065 (1993).
13. H. L. Heiss, *Polym. Eng. Sci. 19*(9):625 (1979).
14. P. May, *Polym. Paint Col. J. 183*:S5 (1993).
15. D. Katsamberis and D. W. Rueger, *RadTech '92 North Am. UV/EB Conf. Expo., Conf. Proc.*, RadTech Int. North Am., Northbrook, IL, 1992, Vol. 1, pp. 564–571.
16. M. C. Burrell and M. G. Tilley, *J. Vac. Sci. Technol. A12*:2507 (1994).
17. J. Lub and G. H. W. Buning, *Polymer 31*(6):1009 (1990).
18. S. Duccilli, *Screen Printing 83* (10):128 (1993).
19. K. D. Riding and K. L. Lilly, UV processing effects on polycarbonate, unpublished results (presented at RadTech '96).
20. M. C. Burrell, J. J. Chera, and M. J. Suchocki, unpublished results.
21. K. Yoshino and N. Ebina, in *Proc. Symp. Electroless Deposition of Metals and*

Alloys (M. Paunovic and I. Ohno, eds.), Electrochemical Society, Pennington, NJ, 1988, p. 268.
22. R. Gliem and R. Brandt, U.S. Pat. 4,364,792 (1982).
23. L. P. Donovan III, E. Maguire, and D. A. Dillard, U.S. Pat. 4,325,992 (1982).
24. L. P. Donovan, E. Maguire, and L. A. Kadison, U.S. Pat. 4,125,649 (1978).
25. E. W. Bastenbeck, J. Haydu, and R. A. Bellemare, Jr., U.S. Pat. 4,775,557 (1988).
26. B. S. James, U.S. Pat. 5,308,387 (1994).
27. J. O. Nriagu and E. Nieboer (eds.), Chromium in the Natural and Human Environments, John Wiley and Sons, New York, 1988.
28. J. B. Hajdu and E. W. Bastenbeck, U.S. Pat. 4,663,240 (1987).
29. G. J. Shawhan and B. R. Chuba, "Electroless metallized conductive coatings for protection of composites and/or thermoplastics" SAMPE, 33rd International Symposium, Anaheim, CA, March 7–10, 1988, p. 1617–1631.
30. D. F. Foust and W. V. Dumas, in *Metallization of Polymers* (E. Sacher, J.-J. Pireaux, and S. P. Kowalczyk, eds.), ACS Symposium Series 440, American Chemical Society, Washington, DC, 1990, Chap. 35.
31. B. R. Karas, D. F. Foust, W. V. Dumas, and E. J. Lamby, in *Metallized Plastics*, Vol. 2 (K. L. Mittal, ed.), Plenum Press, New York, 1991: pp. 387–403.
32. K. L. Mittal, *J. Vac. Sci. Technol. 13*:19 (1976).
33. B. R. Karas and D. F. Foust, *Met. Plast. 3*:319 (1992).
34. K. P. Zarnoch, *J. Adhes. Sci. Technol. 8*(5):501 (1994).
35. M. H. Bernier, J. E. Klemberg-Sapieha, L. Martinu, and M. R. Wertheimer, in *Metallization of Polymers*, (E. Sacher, J.-J. Pireaux, and S. P. Kowalczyk, eds.), ACS Symposium Series 440, American Chemical Society, Washington, DC, 1990, Chap. 10.
36. T. H. Martens and F. H. Sanders, U.S. Pat. 4,536,415 (1985).
37. D. F. Foust and L. B. Bernstein, U.S. Pat. 5,198,096 (1993).
38. K. C. Pohlmann, *The Compact Disk Handbook*, 2nd ed., A-R Editions, Inc. Madison, WI, 1992, pp. 299–301.
39. F. E. Bailey, Jr., in *Handbook of Polymeric Foams and Foam Technology* (D. Klempner, and K. C. Frisch, ed.), Hanser Publishers, New York, 1991, Chap. 4.
40. J. K. Backus, in *Handbook of Polymeric Foams and Foam Technology* (D. Klempner and K. Frisch, eds.), Hanser Publishers, New York, 1991, Chap. 5.
41. L. D. Artavia and C. W. Macosko, in *Low Density Cellular Plastics: Physical Basis of Behaviour* (N. C. Hilyard and A. Cunningham, eds.), Chapman and Hall, London, 1994, Chap. 2.
42. H. S.-I. Chao, unpublished results.
43. P. J. C. Counsell, in *Plastics: Surface and Finish*, 2nd ed. (W. G. Simpson, ed.), Royal Society of Chemistry, 1993, pp. 102 and 106.
44. L. Dorn, *DECHEMA-Monogr. 108*:13 (1987).
45. J. Wank, J. C. Burkhardt, and H. W. Schmoranzer, Eur. Pat. Appl. EP 248310 (1987).
46. M. C. Ross, E. McAbee, and M. J. Bodnar, *SAMPE J. 12*(3):15 (1976).
47. J. E. Pickett and G. A. Patel, U.S. Pat. 5,318,850 (1994).
48. G. A. Patel and M. A. Trapp, U. S. Pat. 5,214,085 (1993).
49. E. A. Bernheim, in *Coatings Technology Handbook* (D. Satas, ed.), Marcel Dekker, New York, 1991, pp. 633–636.

50. G. A. Patel, U.S. Pat. 5,041,313 (1991).
51. H. A. Clark, U.S. Pat. 3,986,997 (1976).
52. C. W. Reed, S. J. Rzad, and J. C. Devins, U.S. Pat. 5,051,308 (1991).
53. C. W. Reed, S. J. Rzad, and J. C. Devins, U.S. Pat. 4,927,704 (1990).
54. I.-F. Hu and J. C. Tou, U.S. Pat. 5,320,875 (1994).
55. B. Wang and G. L. Wilkes, *J. Macromol. Sci., Pure Appl. Chem. A31*(2):1994, 249–260.
56. (a) F. F. Holub and D. R. Olson, WO 8601153 (1986); (b) D. R. Olson, U.S. Pat. 4,600,640 (1986).
57. H. F. Giles, Jr., U.S. Pat. 4,567,105 (1986).
58. M. C. Ross, E. McAbee, and M. J. Bodnar, *SAMPE J 12*(3):15 (1976).
59. R. H. Snedeker, K. T. Garty, and F. J. Skiermont, U.S. Pat. 3,666,614 (1972).

17

Current Applications of Polycarbonates

Lorene Erb Baccaro
General Electric Plastics, Pittsfield, Massachusetts

Patricia Keenan
General Electric Plastics, Atlanta, Georgia

I. MEDICAL APPLICATIONS

Medical devices are some of the most demanding applications for polycarbonate. The properties of polycarbonate that make it desirable for use in medical devices include its transparency to light and x-rays, light weight, heat resistance, toughness, impact strength and high elongation, dimensional stability, biocompatibility, and sterilizable by conventional methods. A disadvantage to be considered is that polycarbonate is chemically attacked by alkalis, amines, and ketones.

Typical applications of polycarbonate in medical appliances and devices are connectors; pumps; housings and reservoirs that require transmittance; thermoformed trays; blood oxygenators; fluid administration applications such as luers, connectors, valves, controls, stopcocks, catheters; intravenous (IV) devices such as manifolds used in coronary arteriography; syringes; blood heat exchangers; and kidney dialyzers.

Syringes: A small amount of polycarbonate is used in syringes for enhanced clarity and strength for high-pressure syringes when polypropylene cannot meet the specifications. Also, polycarbonate is used in safety lock devices within the syringes to prevent accidental needle sticks of medical personnel.

Cardiovascular Devices: Polycarbonate is used in blood oxygenator components such as reservoirs, housing, manifolds, and other parts because of its sterilizability, clarity, high impact strength, efficiency, and reliability during open heart surgery or similar procedures.

Catheters: Catheters are used in cardiopulmonary, diagnostic, urological, and all suction applications. They are used for direct examination, monitoring, and therapy of body cavities, especially the urinary tract and cardiovascular system for removal of fluids, blood clots, and extraneous matter from vessels, organs, and wounds. More recently, these devices have been employed for the direct delivery of drugs to organic tissue locations, such as in delivering a chemotherapeutic agent to a cancerous organ. Requirements for plastics in catheters are low extractables, biocompatibility, rigidity, and flexibility (i.e., sufficient rigidity for insertion into the body, but sufficient flexibility to be manipulated within the body without causing damage.) Polycarbonate is used when performance in higher pressures is required. It can be constructed to withstand up to 1000 psi in connectors and valves. Such pressures are never encountered in diagnostic procedures, but product suppliers and physicians favor the safety factor to avoid catastrophic failures during these procedures.

Solution Delivery Devices: Valves, controls, stopcocks, insertion spikes, and drip chambers are primarily made of polycarbonate and polyvinyl chloride (PVC). In-line IV filters are used in long-term (i.e., more than 24 h) fluid administration applications. These filters are bacteriaretentive and prevent accidental contamination of the patient by fluid-borne microorganisms. They are primarily cellulosic membranes contained in polycarbonate housings, connected to PVC tubing and incorporating polycarbonate or polystyrene clamps, flow controllers, and Y-shaped injection sites. This includes such products as disposable pumps and administration sets, which included drip chambers, clamps, valves, connectors, spikes, and flanges. The material requirements are inertness, solvent bondability (plastic to plastic), chemical resistance, physical strength, and clarity. Although PVC is used in the largest volume due to its cost effectiveness, polycarbonate or other engineering resins are used for applications requiring greater physical strength.

Luers: Tapered luer connectors are used to attach IV lines and connect needles. The female component of luers has been known to fail due to hoop stress. This stress is frequently compounded by the presence of alcohol or fat emulsions (lipids), which can craze polycarbonate. The male or inner component, subject only to compressive force, seldom fails because plastics tolerate compression loading well. Therapeutic equipment such as housings and end-caps on dialysis equipment are applications that benefit from the clarity, toughness, dimensional stability, and biocompatibility.

Surgical Instruments: Although most surgical instruments are reusable and manufactured in stainless steel or titanium, some of these instruments have been substituted by polycarbonate. Polycarbonate handles provide the tactile feel, instrument balance, sterilizability, and durability required by surgeons. Polycarbonate is used in forceps, retractors, and dental surgical instruments.

Bottles and Jars: Polycarbonate growth in this market is driven by plastics

replacement of glass. Plastics offer the advantages of unbreakability, lower weight, and greater flexibility in product design. For ampoules and vials, glass provides inertness, rigidity, and a lower penalty for the weight differential with plastics since the container sizes are so small. For containers of medical products, the shelf life must be considered to assure adequate product protection. Polycarbonate must be used in conjunction with other materials to enhance barrier to oxygen or water.

Polycarbonate is used in medical packaging such as blister packaging, kits, and trays. Polycarbonate offers high clarity and has wide sealing temperature range. It has good resistance to puncture, even in thinner gauges, and is not affected by sterilization by γ irradiation.

A. Effects of Medical Sterilization Techniques on Polycarbonate

Most medical devices are sterilized prior to shipping to users. Polycarbonate withstands all commonly used forms of sterilization. For single-use medical devices, ethylene oxide has 50% market share, γ radiation 45%, and electron (E-beam) radiation 5% market share worldwide [1].

B. Ethylene Oxide

A device sterilization method, gas fumigation using ethylene Oxide (EtO), has been the most widely used method for disposable medical devices. It generally provides an economical, convenient method of sterilization for heat-sensitive and delicate medical instruments. Exposure to high levels of EtO has been recognized as a health hazard due to its toxic and carcinogenic characteristics. Devices must be aerated to allow gas dissipation, which makes EtO a more lengthy method of sterilization. Polycarbonate maintains greater than 95% of its mechanical properties after repeated cycles of EtO sterilization with no visual defects. One concern with EtO appears to be the degassing or dissipation of residuals during the post-sterilization process. Table 1 contains data on residual levels of EtO, ECh (ethylene chlorohydrin), and EGly (ethylene glycol), at 1, 7, and 14 days after sterilization. Desired standard residual levels are EtO $<$ 25 ppm, ECh $<$ 25 ppm, and EGly $<$ 250 ppm.

C. Gamma and Electron Beam Sterilization

The use of radiation to sterilize disposable plastic medical devices has grown considerably over the past 20 years. One early impediment to growth was the lack of radiation-sterilizable plastic materials, but today many of the common medical polymers are radiation-stable. The major problems were discoloration

Table 1 Ethylene Oxide Sterilization Aeration Residual Values

Polycarbonate	EtO (ppm) 1 day	EtO (ppm) 7 days	EtO (ppm) 14 days	ECh (ppm) 1 day	EGly (ppm) 1 day	EGly (ppm) 14 days
Mechanical aeration[a]	177	54	39	ND	30	ND
Ambient aeration	360	128	111	ND	76	31

[a]Conditions: Aeration was conducted at ambient conditions and mechanically with a fan in a 120°F chamber. After aeration, the samples were exhaustively extracted with acetone for 24 h for EtO residual determination, and with water for 72 h for ECh (ethylene chlorohydrin) and EGly (ethylene glycol) residual determination.

and modified physical properties. Polycarbonates are the engineering resin of choice for many critical medical components. Although its physical properties are essentially unaffected by the normal sterilizing doses, it does tend to yellow when irradiated. The yellowness index is a function of dose, and most users could not tolerate the discoloration in vital applications such as blood-handling components.

Radiation interacts with polymers in two basic ways: chain scission, which results in decreased molecular weight and possibly embrittlement, and crosslinking, which results in higher molecular weight. A standard grade of polycarbonate is resistant to radiation effects although it will typically turn yellow-green after γ exposure and about 60% of the color will fade with time. Tinting and blend technologies have been developed to reduce the perceptible amount of color shift of parts that have been sterilized (Table 2). Electron beam radiation, with its low capital costs and high operating costs, is used by small companies and some hospitals to sterilize certain medical devices. It is a sterilization technique that is particularly effective for thin parts.

Table 2 Retention of Tensile and Impact Properties of Polycarbonate Through Gamma Radiation Sterilization

Radiation dose	Modulus (kpsi)	Stress @ yield (psi)	Elongation @ break (%)	Peak load (lb)	Energy @ max. load (ft-lb)	Break
Control	328	8900	230	1520	57	Ductile
2.5 Mrads	342	8900	230	1510	53	Ductile
5.0 Mrads	346	8900	230	1490	52	Ductile
10 Mrads	340	8600	240	1430	52	Ductile

Dynatup conditions: 72°F, 7.5 MPH, 5-in. Tup, 3-in. Ring.

D. Steam Sterilization

Steam autoclaving, a popular sterilization method for reusable devices, is conducted in a pressurized vessel that allows the presence of saturated steam or moisture. Steam is used if a high processing temperature does not affect the product. Polycarbonate can be sterilized for limited reuse applications (fewer than 10 cycles) where the autoclave temperature doesn't exceed 250°F (121°C). The number of sterilization cycles depends on the type of reusable application, i.e., limited or multiple reuse. Repeated sterilization at high exposure temperatures can severely affect the performance of polycarbonate.

Polycarbonate devices may be sterilized in one 20-min cycle at 250°F (121°C) up to 10 cycles at highest molecular weight grades. The number of cycles may vary depending on the design of the part and the stress level. The higher the stress level in a part, the more susceptible it is to cracking or crazing due to the high exposure temperatures found in autoclaving. Sometimes substances such as alkaline corrosion inhibitor added to boiler feed water will cause damage to the polycarbonate parts. Designing and processing parts to minimize stress is crucial. The stress level in a part can build up through design, assembly or molding.

Polycarbonate retains its visual appearance. Yellowness index increases from approximately 0.2 to 0.35 after 10 autoclave cycles at 250°F. There is no significant change in the impact strength through 10 autoclave cycles at 250°F (Table 3).

Table 3 Retention of Impact Properties of Polycarbonate Through Steam Autoclaving

Polycarbonate	Peak load (lb)	Energy @ max. load (ft-lb)	Break
Control	1310	45	Ductile
1 Cycle	1305	41	Ductile
2 Cycles	1268	40	Ductile
4 Cycles	1255	40	Ductile
10 Cycles	1276	40	Ductile

Conditions: Gravity displacement cycle at 250°F: Pressure equilibrium cycle: 4 min; sterilization time: 20 min; dry time 5 min, reset between cycles: 1 min; total cycle time: 30 min. Dynatup conditions: 72°F, 7.5 MPH, 5-in. Tup, 3-in. Ring.

E. Biocompatibility

Medical devices and their component materials are potential sources of toxins that may produce undesirable effects when used clinically. The selection and

evaluation of materials and devices intended for use in humans requires a structured program of assessment to establish biocompatibility and safety. To serve as a guide, it is strongly recommended that only those plastic materials (including any additives, stabilizers, and colorants) that comply with appropriate food additive regulations for use in medical devices be used.

Polycarbonate grades for the medical device industry have been tested for biocompatibility standards outlined by tripartite agreements and modified ISO 10993-1, as well as USP Class VI.

For those grades recommended and sold for use as a component of a medical device application, they comply with all applicable requirements of the U.S. Food, Drug and Cosmetic Act as amended, and these resins will meet the criteria for a USP Class VI (121C) plastic. Typical production lots of polycarbonate resin have been subjected to the battery of biological tests specified by the U.S. Pharmacopeia to judge the suitability of plastic material intended for use as containers or accessories for parenteral perpetration. Additionally, these resins are tested under tripartite guidelines for medical devices, which include such biological tests as (a) acute systemic toxicity, (b) intracutaneous toxicity, (c) implantation, (d) cytotoxicity, (e) hemolysis, (f) Ames mutagenicity, (g) pyrogenicity, (h) sensitization, (i) subchronic toxicity (14-day implantation test with histopathology test).

The medical device manufacturer and the drug packager are in the best position to know the details of the intended conditions of use. It is incumbent on the device manufacturer or drug packager to carry out the appropriate biocompatibility test to assure safety, efficacy, and regulatory compliance. Because of the potential for chemical incompatibility between components of the materials in an overall use system and polycarbonate resin, it is recommended that appropriate chemical compatibility be conducted with all components under intended conditions of use and reasonably foreseeable misuse [2].

F. Cleaning

If the plastic components of medical devices need to be cleaned prior to sterilization due to the production process, typical solvents that may be used as cleaning agents are isopropyl alcohol, *n*-propyl alcohol, ethyl alcohol, and butyl alcohol. Manufacturers are advised to test cleaning agents carefully with their application before using any solvent to clean a part prior to sterilization.

G. Disinfectants

Care must be exercised when using disinfectants which contain aldehydes or phenols as the active ingredient. A large number of commercially available disinfectants have been used on polycarbonate. Chemical compatibility of thermoplas-

Table 4 Tensile Property Retention in Sterilants

Chemical agent	Tensile strength	Tensile elongation
0.9% saline solution	>90% property retention at 1.5% strain	>90% property retention at 0.5% strain
70% ethanol	>90% property retention at 1.5% strain	>90% property retention at 0.5% strain
91% isopropanol	>90% property retention at 1.5% strain	>90% property retention at 1.0% strain
Freon TF	>90% property retention at 1.5% strain	>90% property retention at 1.0% strain
Betadyne	>90% property retention at 1.5% strain	>90% property retention at 1.5% strain
10% chlorine bleach	>90% property retention at 1.5% strain	>90% property retention at 1.0% strain

tics is dependent on the contact agent, time, temperature, stress, and length of exposure. Chemical exposure may result in a softening effect, or cracking and crazing of the thermoplastic. As softening occurs, tensile strength decreases, whereas percent tensile elongation increases. As cracking and/or crazing occurs, the percent elongation decreases and the tensile strength may decrease. Due to the number of parameters that must be considered, the compatibility of any thermoplastic resin should always be evaluated in the actual end-use environment (Table 4).

Conditions: Tensile bars were strained and exposed for 24 h at room temperature. Chemical was wiped on five times at 1 h intervals and allowed to dry for the remainder of 24 h. In Table 2, the tensile strength and elongation retentions of polycarbonate resins after exposure to some chemicals that may be seen in a medical environment are given. The percent elongation or the elongation retention can be related to the ductility of the material. Polycarbonate is inherently ductile, based on typical tensile percent elongation values. For this reason even a decrease in elongation might still provide a ductile end-product.

H. Assembly Methods

Bond strength after sterilization is one area of interest in the medical market. Solvent bonding and UV-curable adhesives are effective in securing polycarbonate to itself. After extremely high doses of γ radiation, the bond strength was not compromised. In all cases, the mode of failure was within the substrate indicating that the material broke, not the bond joint. For IV applications, bonding polycarbonate to flexible PVC can be done with a methylene chloride/cyclohexa-

Table 5 Bonding of Polycarbonate to PVC

Type of bond	Tensile lap shear strength (psi)
Methylene chloride/cyclohexanone (50:50)	230
Cyclohexanone	220
Methylene ethyl ketone/cyclohexanone (50:50)	190
UV-curable adhesive	600

none blend for the highest bond strength. UV-curable adhesives tend to produce an even stronger bond joint, causing the PVC to yield before the adhesive (Table 5).

II. USE OF POLYCARBONATE IN CDS, DVDS AND MOS

As discussed in an earlier section, polycarbonate is an excellent material for impact strength and clarity. These happened to be two of the key properties that Sony and Philips were looking for when they invented compact disk (CD) technology in 1980. Probably the most significant aspect of this new technology was that the information (or music) was stored by digital encoding vs. traditional analog storage. By definition, digital information is stored as discrete numbers, in this case 111's and 000's. Analog, on the other hand, stores continuously, or "analogously," which tends to limit its accuracy and introduce more "noise" in the process. The more times an analog tape is recorded, the more the quality diminishes. With a CD, noise can be eliminated through the digital encoding process. The primary reason for the tremendous success of the audio CD was the sound quality improvement it brought to the consumer through the magic of digital technology.

Since improved sound quality was the most important selling point of the new technology, it was critical that the process for making the disks be highly consistent and reproducible. The CD needed to contain vast amounts of information—the amount of storage needed to record even one song on any type of medium is truly amazing—and data integrity was of utmost importance. The data, or music, on this new medium was to be stored on microscopic "pits." The laser must read through a clear substrate that contained the pits. On the opposite side of the disk would be a thin film of highly reflective metal (aluminum or gold), which would then be covered by a protective lacquer.

The very first disks were made from the most transparent material available,

which was glass. However, this proved to be impractical from both an impact strength and cost perspective. Glass disks simply could not be mass-produced cost-effectively.

The engineers identified the following key needs for a substrate:

High transparency: A red laser must be readable through the substrate, with minimum optical distortion or birefringence.

Dimensional stability: It was necessary to avoid the issue of "tilt," which could cause problems in disk playability.

Purity: The disks had to be free of impurities to ensure that the laser could read accurately.

Accurate reproduction of the "pits" on the molded surface: Since the pits hold the information, 100% accuracy is vital. A high-flow material would be required to ensure that the pits were filled accurately.

Ability to be mass produced: It was determined that injection molding would be an optimum method of producing disks and that material with easy flow would help keep molding cycle times low.

Minimum water absorption: The disks had to be as tough or tougher than cassette tapes, i.e., able to withstand high humidity, such as when stored in an automobile in Florida.

Good impact resistance: It should be possible to handle the disks in much the same way as cassette tapes are handled, i.e., dropped on the floor or treated roughly.

In addition, one of the most important aspects of their new product was that there be a standard format, i.e., that it could be read by any CD player. This standardization was achieved by the industry, and with it came an extra, vital demand on the substrate, i.e., *consistency* of the material.

Polycarbonate was chosen as the material of choice after Sony and Philips completed a series of tests on materials ranging from glass to acrylic to styrene to amorphous polyolefins. Polycarbonate had the best overall property profile for this stringent application.

In 1994, audio CD sales surpassed cassette tape sales for the first time, and along with that came an associated surge in polycarbonate use for the shiny disks. However, another revolution was well underway. In the late 1980s to early 1990s, the computer had progressed out of the office and into the home. The term "multimedia" was on everyone's lips, even those who weren't sure what it was! What audio CD did to cassettes, CD-ROM (compact disk, read-only memory) was getting ready to do to 3.5-in. diskettes.

There was a key barrier to the multimedia age. Computers that could provide information, play music, show color graphics, and be completely interactive required storage, and lots of it. The standard 3.5-in. diskette could only hold 2 megabytes (Mb) of information. This was a perfect fit for CD-ROM, a technology

that the software engineers already knew well. A current CD-ROM can hold 680 Mb of information, i.e., more than 300 times that of the 3.5-in. diskette! The industry challenge was to invent the most interesting and exciting text, sound, and graphics possible using all of the storage available to them in ways that never would have been possible on a diskette.

The year 1993 was when the CD-ROM took the United States by storm. Computer games led the charge, followed closely by home education and, later, business applications. Games were the best example of using CD-ROM technology to its fullest, i.e., incorporating sound and graphics into text. More recently, home and business applications have been developed to make better use of these features, such as real estate CD-ROMs that offer guided tours through homes, or interactive plant tours of a company's manufacturing facility.

Now that CD-ROM is more mainstream, users are looking for even more from their computer and media. For example, although CD-ROM can store graphics and video, it is not currently capable of storing more than 2 minutes of full-motion video, which is what consumers are accustomed to seeing on television, video tapes, or in a movie theater.

In 1996 the first digital video disk player was introduced. For the first time, a 12-cm "CD size" disk could hold a full-length, 133-min motion picture with better than laser disk quality on one side of the disk! This required seven times the storage capacity of a current CD-ROM, or 4.7 Gb worth of storage. The microscopic "pits" that hold the information are even smaller and closer together to allow for more storage. The industry requires higher purity, better dimensional stability, and easier processability in their polycarbonate than ever.

The next hurdle for the CD industry will be to move both CD-R (CD-recordable and CD-E (CD-erasable or rewritable) into more mainstream use. Though CDs that can record and erase information already exist, they have been too expensive to gain widespread acceptance. The substrate requirements for these disks is more stringent, i.e., higher purity and better hydrolytic stability are required. Rewritable disks open up another potentially huge market for polycarbonate provided the material continues to show improvement as the technology changes.

Future optical storage requirements will demand lower birefringence, higher purity, better dimensional and hydrolytic stability. Polycarbonate and its blends will still be the products of choice, but materials technology must continue to advance with the industry.

A thought on the optical disk or compact disc industry, as we live now in the "Information Age." At least for the next 10 years, if the information is digitally encoded, the best place to store it will be on a CD. Even with the "information superhighway" era approaching, all of those data must be stored somewhere; they cannot just clog up the telephone lines. The logical storage space is a CD.

This technology is viable for years to come, and polycarbonate is best positioned to grow with it over the next decade.

REFERENCES

1. R. M. Brinston, *Medical Device Technology*, Nordion International, Ontario, Canada, June 1995.
2. P. Surana, Selection criteria for the use of plastics in medical application, in *Proceedings of the Medical Plastics Industry at the Dawn of the 21st Century*, October 25, 1994, RETEC SPE and SPI.

Index